

August 31st – September 5th 2008 | Opatija, Croatia



EUCMOS 2008

XXIX European Congress on Molecular Spectroscopy

BOOK OF ABSTRACTS

Edited by: Svetozar Musić, Mira Ristić, Stjepko Krehula





EUCMOS 2008

XXIXTH EUROPEAN CONGRESS ON

MOLECULAR SPECTROSCOPY

OPATIJA, CROATIA

BOOK OF ABSTRACTS

Edited By:

**Svetozar Musić
Mira Ristić
Stjepko Krehula**



**August 31st – September 5th 2008
Grand Hotel Adriatic
Opatija, Croatia**

ORGANIZATION AND SPONSORSHIP

EUCMOS 2008 is being organized by the Ruđer Bošković Institute with assistance from:

- ✚ Ministry of Science, Education and Sports of the Republic of Croatia
- ✚ Croatian National Tourist Board
- ✚ Government of the Town of Opatija

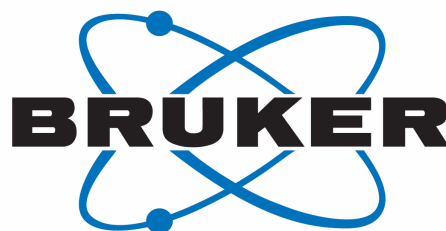
The Congress is organized under auspices of:

- ✚ Croatian Academy of Sciences and Arts, The Department of Mathematical, Physical and Chemical Sciences
- ✚ University of Zagreb
- ✚ University of Rijeka
- ✚ Croatian Chemical Society
- ✚ Croatian Physical Society



The Congress organizers gratefully acknowledge the sponsorship of the following companies:

- ✚ PLIVA d.d., Zagreb, Croatia
- ✚ HORIBA Jobin Yvon, Lille, France
- ✚ JEOL (Europe) SAS, Paris, France
- ✚ Bruker Optik GmbH, Ettlingen, Germany
- ✚ Shimadzu, Duisburg, Germany & Shimadzu d.o.o., Zagreb, Croatia
- ✚ PerkinElmer, Wiesbaden, Germany
- ✚ Hebe d.o.o, Zagreb, Croatia
- ✚ Coca Cola Beverages Hrvatska d.d., Zagreb, Croatia



HORIBA JOBIN YVON

 **SHIMADZU**

JEOL

WELCOME TO EUCMOS 2008

On behalf of the International Committee, Scientific Program Committee, Local Scientific Committee and Local Organizing Committee, I wish to welcome all participants to the XXIX European Congress on Molecular Spectroscopy in Opatija, Croatia from 31 August to 5 September 2008.

European congresses on molecular spectroscopy have a long tradition, starting soon after World War II. From the first of the EUCMOS series held in Basel in 1951, to the Istanbul congress held in 2006, this has been an excellent venue to present results of spectroscopic investigations, to exchange new ideas, and to encourage collaboration among molecular spectroscopists. The topics at EUCMOS congresses have always been in line with current scientific interests in physics and chemistry, and other branches of science. The contributions to the twelve scientific topics of EUCMOS 2008 are the state of the art in molecular spectroscopy, alone or in combination with other methods.

The Congress Centre at the Grand Hotel Adriatic Opatija will play host to the XXIX European Congress of Molecular Spectroscopy. Opatija is an elegant tourist destination with the longest tourism tradition in Croatia. The very attractive geographic position, warm sea, lush green scenery and pleasant climate were the dominant factors for the development of its tourism in the 19th century. Mostly constructed at the turn of the 20th century, Opatija has remained in complete harmony with nature right up until the present day. Many famous persons of the 19th and 20th centuries left their traces in the history of Opatija. During the EUCMOS excursion, participants will have the opportunity to see a part of the history of the Istria region, and to experience the every day life of the locals.

The XXIX European Congress on Molecular Spectroscopy is organized by the Ruđer Bošković Institute, Croatia's largest institute, under the auspices of the Croatian Academy of Science and Arts, University of Zagreb, University of Rijeka, Croatian Physics Society and Croatian Chemical Society.

I wish that all the participants of EUCMOS 2008 have a fruitful meeting, as well as enjoyable and relaxing time in Opatija.

Welcome to Opatija and Croatia!

Dr. Svetozar Musić



Chairman of EUCMOS 2008

SCIENTIFIC TOPICS

1. Molecular structure
2. Biospectroscopy
3. Nanostructured materials
4. Spectroscopy of macromolecules
5. Optoelectronics and semiconductor materials
6. Spectroscopy in chemical, pharmaceutical and environmental analyses
7. Spectroscopy applied to archaeology, arts, geology and mineralogy
8. Chemical dynamics
9. Theoretical spectroscopy and computer methods
10. Surface spectroscopies
11. Time resolved spectroscopy
12. New instrumentation

The participants represent the following countries:

Argentina		Lithuania	
Australia		Macedonia	
Austria		Palestine	
Belgium		Poland	
Brazil		Portugal	
Bulgaria		Romania	
Canada		Russia	
Croatia		Serbia	
Czech Republic		Slovakia	
Finland		Slovenia	
France		South Africa	
Germany		Spain	
Hungary		Sweden	
India		Switzerland	
Ireland		Turkey	
Israel		Ukraine	
Italy		United Kingdom	
Japan		USA	

COMMITTEES

INTERNATIONAL COMMITTEE

W.J. Orville Thomas (Salford UK)
- Honorary Life President
A.J. Barnes (Salford UK) - President
R. Fausto (Coimbra, Portugal) - Vice-President
H. Ratajczak (Wroclaw, Poland) - Vice-President

Members:

S. Akyüz (Istanbul, Turkey)
J. Bellanato (Madrid, Spain)
J.R. Durig (Kansas City, MO, USA)
T.A. Ford (Durban, S.Africa)
K. Furić (Zagreb, Croatia)
M. Handke (Krakow, Poland)
J. Laane (College Station, TX, USA)
H.H. Mantsch (Winnipeg, Canada)
S. Musić (Zagreb, Croatia)
M. Tasumi (Tokyo, Japan)
S. Turrell (Villeneuve d'Ascq, France)
G. Zerbi (Milan, Italy)

LOCAL SCIENTIFIC COMMITTEE

G. Baranović
A. Dulčić
K. Furić
M. Gotić
T. Hrenar
M. Ivanda
L. Klasinc
Z. Maksić
Z. Meić
V. Mohaček Grošev
S. Musić
P. Novak
G. Pichler
M. Ristić
D. Smith
V. Smrečki
G. Štefanić
S. Valić
D. Vikić-Topić
V. Volovšek

SCIENTIFIC PROGRAM COMMITTEE

S. Musić, K. Furić - Chairpersons
S. Akyüz (Turkey)
A.J. Barnes (UK)
J. Bellanato (Spain)
F.J. Berry (UK)
E. De Grave (Belgium)
J.R. Durig (USA)
H.G.M. Edwards (UK)
R. Fausto (Portugal)
T.A. Ford (South Africa)
M. Handke (Poland)
Z. Homonnay (Hungary)
L. Klasinc (Croatia)
J. Laane (USA)
A. Loewenschuss (Israel)
Z. Maksić (Croatia)
H.H. Mantsch (Canada)
Z. Meić (Croatia)
M.I. Oshtrakh (Russia)
H. Ratajczak (Poland)
M. Tasumi (Japan)
S. Turrell (France)
G. Zerbi (Italy)

LOCAL ORGANIZING COMMITTEE

S. Musić, K. Furić - Chairpersons
M. Ristić - Conference Secretary
N. Biliškov
M. Gotić
M. Ivanda
D. Jozić
S. Krehula
S. Miļjanić
V. Mohaček Grošev
P. Novak
D. Ristić
D. Smith
V. Smrečki
G. Štefanić
S. Valić
M. Žic

LIST OF ABSTRACTS

PLENARY LECTURES

PL-1	<u>Austin Barnes</u> EUCMOS - Past, Present and Future	1
PL-2	<u>Vincenzo Schettino</u> Spectroscopy and Monitoring of High Pressure Phenomena	2
PL-3	<u>Philip Güthlich</u> Mössbauer Spectroscopy - A Powerful Tool In Molecular Magnetism	3
PL-4	<u>Eddy De Grave, V.G. de Resende, C. Van Cromphaut, Ch. Laurent, L. Presmanes, R.E. Vandenberghe</u> Integral Low-Energy Electron Mössbauer Spectroscopy (ILEEMS): Methodology and Recent Applications in Material Research	4
PL-5	<u>Mile Ivanda, D. Ristić, K. Furić, S. Musić, M. Ristić, M. Gotić, G. Štefanić, Z. Crnjak Orel, M. Bitenc, M. Montagna, M. Ferrari, A. Chisaera, Y. Jestin</u> Low-Frequency Raman Scattering in Materials Research	5
PL-6	<u>Hiro-o Hamaguchi</u> Time- and Space-Resolved Raman Spectroscopy of Single Living Cells	6
PL-7	<u>Rui Fausto</u> Search for Missing Conformers: Matrix-Isolation SWAT	7
PL-8	<u>Halina Abramczyk, I. Placek, B. Brożek-Pluska, J. Surmacki, Z. Morawiec, M. Tazbir</u> From Femtosecond Dynamics to Breast Tissue Diagnosis by Raman Spectroscopy	8
PL-9	<u>Dieter Naumann, H. Fabian, P. Lasch</u> FT-IR Spectroscopy of Cells and Tissues	9
PL-10	<u>Thomas Bally</u> Electronic and Vibrational Spectroscopy of Radical Cations in Argon Matrices	10
PL-11	<u>Boris Galabov</u> Spectroscopic and Theoretical Parameters In Predicting Hydrogen Bond Strength, Conformational Stability and Chemical Reactivity	11
PL-12	<u>Henry H. Mantsch</u> The Globalization of Science and its Impact on the Transition Countries in Europe	12

INVITED LECTURES

IL-1	<u>Z. Meić, T. Hrenar</u> Vibrational Assignment of 1,4-(<i>E,E</i>)-Distyrylbenzene Supported by Isotopic Shifts and DFT Calculations	13
IL-2	<u>Nada Došlić</u> Multidimensional Quantum Dynamics of Large Amplitude Motion	14
IL-3	<u>Ruth Signorell</u> Intrinsic Particle Properties in Infrared Spectra of Aerosols	15
IL-4	<u>Gaetano Granozzi</u> TiO _x Nanostructures on Metallic Substrates: A Combined Spectroscopic and Theoretical Investigation	16
IL-5	<u>Michael Oshtrakh, V.A. Semionkin, O.B. Milder, E.G. Novikov</u> Mössbauer Spectroscopy with High Velocity Resolution: New Possibilities in Biomedical Research	17
IL-6	<u>Markku Räsänen</u> Advances in Noble Gas Chemistry	18

ORAL & POSTER CONTRIBUTIONS

1. MOLECULAR STRUCTURE

ORAL PRESENTATIONS

- O1-1** N. Biliškov, G. Baranović
Infrared Spectroscopy of Liquid Water-*N,N*-dimethylformamide Mixtures 19
- O1-2** D.K. Breiting, G. Brehm, M. Weil, S. Baumann
Vibrational Spectra of $K_2[O(HgSO_3)_3]$ Containing a New Anionic Metallo-Oxonium Complex with a OHg_3 Core 20
- O1-3** P. Drożdżewski, M. Kubiak
Crystal Structure and Vibrational Spectroscopy of Mixed-valence $[Cu(biz)_2][Cu_2Br_4]$ Complex Formed After *In Situ* Oxidation of 2-Hydrazino-2-Imidazoline to Bisimidazoline (biz) by Copper(II) Ions 21
- O1-4** Y. Kawashima, Y. Tanaka, A. Sato, E. Hirota
Fourier Transform Microwave Spectra of Isobutylmercaptan and Normal Butylmercaptan 22
- O1-5** G. Keresztury, M. Rogojerov, T. Sundius
Polarized IR Spectroscopy and Transition Dipole Moment Determinations in Structural Studies 23
- O1-6** E. Kleinpeter, A. Koch
Spatial Magnetic Properties of Trisannellated Benzenes and Cyclobutadiene Dianion Derivatives Subjected to Aromaticity 24
- O1-7** L. Krim, N. Dozova, E. Alikhani, N. Lacombe
Infrared Spectra of $CH_3Cl + H_2O$ and $NO + H_2O$ Isolated in Solid Neon at 5 K 25
- O1-8** G.S. Kürkcüoğlu, S. Aksay, I. Kavlak
FT-IR and FT-Raman Spectroscopic Studies of 2-Methylpyrazine Tetracyanonickelate Benzene Clathrates: $M(C_5H_6N_2)Ni(CN)_4 \cdot C_6H_6$ ($M = Mn, Cd, Co$ or Ni) 26
- O1-9** J. Laane, P. Boopalachandran, K. McCann, M. Wagner
Spectroscopic Studies of the Electronic Excited States of Pyridine- d_0 and - d_5 , 2-Fluoro- and 3-Fluoropyridine, and 1,3-Benzodioxan 27
- O1-10** D. Michalska, K. Hernik, R. Wysokiński, W. Zierkiewicz, A. Pietraszko
Structures of Vitamin B_{13} Complexes with Transition Metal Ions. The Role of Unusual $Cu(II) \cdots \pi$ Interaction and Hydrogen Bonds. 28
- O1-11** C. Öğretir
The Hydrogen Bonding in Life and Society 29
- O1-12** B. Tolnai, J.T. Kiss, K. Felföldi, I. Pálinkó
 $C-H \cdots F$ Hydrogen Bonds as the Organising Force in F-substituted α -phenyl Cinnamic Acid Aggregates Studied by the Combination of FTIR Spectroscopy and Computations 30
- O1-13** J.G. Philis
UV R2PI Spectra of p-difluorobenzene van der Waals Complexes 31
- O1-14** A.K. Singh, V. Mukherjee, V.B. Singh, B. Singh, A.N. Singh
Spectroscopic Investigation of the Vibrational Spectra of the Benzoxazine 32
- O1-15** R. Singh, M. Kumar, R.A. Yadav
Theoretical Study of IR and Raman Spectra of 5-Hydroxy Uracil 33
- O1-16** M. Szafran, I. Kowalczyk, E. Bartoszak-Adamska, Z. Dega-Szafran
X-Ray diffraction, FTIR and NMR Spectra, and DFT Calculations of 2-Aminopyridine Betaine and 1-*H*-2-oxo-2,3-dihydroimidazo[1,2-*a*] Pyridinium Chloride, Bromide and Perchlorate 34
- O1-17** A. Viridi
X-ray crystallographic, spectroscopy and quantum chemical studies on 3, 3, 6-trimethyl-3, 4-dihydroiso-coumarin 35

POSTER PRESENTATIONS

P1-1	<u>S. Akyuz, T. Akyuz</u> Vibrational Spectroscopic Study of 4-Aminopyrimidine Complexes	36
P1-2	<u>L. Andreeva, F. Trajkovic, J. Petreska</u> Investigation of the Vibrational Spectra of Some Partially Deuterated Cd(NH ₃) ₂ Cl ₂ , Hg(NH ₃) ₂ Cl ₂ , Pd(NH ₃) ₄ Cl ₂ Complexes	37
P1-3	<u>L.M. Babkov, N.A. Davydova, K.E. Uspenskiy</u> 2-Biphenylmethanol Vibrational Spectra and Their Interpretation Using Structural-Dynamical Model in Anharmonic Approximation	38
P1-4	<u>L.M. Babkov, I.I. Gnatyuk, G.A. Puchkovska, S.V. Truckhachev</u> The Investigation of 4-n-butyl-4'-cyanobiphenyl Conformational Mobility by IR Spectroscopy Methods	39
P1-5	<u>L.M. Babkov, I.I. Gnatyuk, G.O. Puchkovska, K.E. Uspenskiy</u> The Appearance of Conformational Mobility of Behenic Acid in IR Spectra	40
P1-6	<u>K. Balci, Y. Akkaya, S. Akyuz</u> A Theoretical Conformational Analysis and Vibrational Spectroscopic Investigation on Niflumic Acid	41
P1-7	<u>Gonul Basar, S. Akyuz, Gunay Basar, S. Kröger</u> Studies on Kyotorphin and D-Kyotorphin in Aqueous Solution by Raman Spectroscopy	42
P1-8	<u>C. Bayrak</u> Vibrational Spectroscopic Studies on the T _d -Type Clathrates: M(N,N'-Dimethylethylenediamine)M'(CN) ₄ .C ₆ H ₆ (M = Mn, M' = Zn, Cd or Hg; M = Cd, M' = Cd or Hg)	43
P1-9	<u>I. Iriepa, J. Bellanato, E. Gálvez, A.I. Madrid</u> Synthesis, Structural and Conformational Study of Some Esters Derived from 3-Methyl-3-azabicyclo[3.2.1]octan-8 α -ol	44
P1-10	<u>M.E. Defonsi Lestard, M.E. Tuttolomondo, E.L. Varetti, D.A. Wann, H.E. Robertson, D.W.H. Rankin, A. Ben Altabef</u> Experimental Structure of CF ₃ CO ₂ CH ₂ CF ₃ from Electron Diffraction Data, Infrared Spectra and Quantum Chemical Calculation of Vibrational Properties	45
P1-11	<u>E. Benassi, I. Baraldi, S. Ciorba, I. Škorić, M. Šindler-Kulyk, A. Spalletti</u> New Organic Fluorophores for Optical and Spectroscopic Applications: 2,3- and 2,5-Distyrylfuran	46
P1-12	<u>E. Benassi, P.S. Sherin</u> Combined Experimental and Theoretical Study on the Kynurenine	47
P1-13	<u>A. Borba, A. Gómez-Zavaglia, R. Fausto</u> Photochemistry and Vibrational Spectra of Matrix-Isolated Isoniazid	48
P1-14	<u>D.K. Bretinger, G. Brehm, J. Zürlbig, M. Weil, S. Baumann</u> Bis(sulfito)mercurates M ₂ [Hg(SO ₃) ₂].xH ₂ O (M = NH ₄ , Na, K; x = 0, 1, 2.25). Vibrational Spectra of the Solids and of Aqueous Solutions.	49
P1-15	<u>D.K. Bretinger, M. Moll, G. Brehm</u> Sulfito Mercurate Complexes in Solution Studied by ¹⁹⁹ Hg NMR Spectrometry	50
P1-16	<u>J. Ceponkus, D. Lesciute, V. Sablinskas</u> Association of Water with Small Monocarboxylic Acids. Matrix Isolation Infrared Absorption Study.	51
P1-17	<u>V. Chiş, R. Ştiufiuc, N. Leopold</u> Molecular and Electronic Structure of PTCDI and Melamine-PTCDI Complex	52

- P1-18** K. Cholewa-Kowalska, M. Laczka, Z. Olejniczak
Effect of Organic Modifiers on the Solution Viscosity, Gelation Time and Progress of Hydrolysis/Condensation Reactions during Hybrid Gels Formation 53
- P1-19** A. Nikolić, B. Jović, E. Davidović, S. Petrović
N–H···O Hydrogen Bonding. FT-IR and NIR Study of N-Methylformamide-Ether Systems. 54
- P1-20** Z. Dega-Szafran, M. Szafran
Experimental and Theoretical Vibrational Spectra of Piperidine-2-carboxylic Acid 55
- P1-21** Z. Dega-Szafran, A. Katrusiak, M. Szafran
Molecular Structure of the Hydrated Complex of 1,4-dimethylpiperazine di-betaine with L-tartaric Acid Studied by X-ray Diffraction and FTIR 56
- P1-22** I. Despotović, Z.B. Maksić
Towards Organic Conductors - the Structure and Stability of Cyano-[n]-Radialenes and Their Dianions 57
- P1-23** M.E. Jamróz, M.H. Jamróz, J.E. Rode, J.Cz. Dobrowolski
Interpretation of Vibrational Spectra of Allyl Acrylate 58
- P1-24** K. Furić, B.-M. Kukovec, Z. Popović
Raman Study of Nickel(II) Complexes with 6-Methylpicolinic Acid 59
- P1-25** J. Polovková, A. Gatial, M. Gróf, J. Kožíšek, V. Milata, N. Prónayová, P. Matějka
Isomerizational and Conformational Study of 3-Cyclopropylamino-2-Acetyl Propenenitrile (CpAAP) and 3-Cyclopropylamino-2-Methylsulfonyl Propenenitrile (CpASP) 60
- P1-26** I. Gocan, C. Nagy, M.M. Venter, V. Bercean, L. David
Spectral Investigations on Metal Complexes of Heterocyclic N,S-Donors 61
- P1-27** M. Gróf, A. Gatial, J. Kožíšek, V. Milata, P. Matějka
Conformational Analysis of Aminomethylene- and Methylaminomethylene-Malonic Acid Dimethylester 62
- P1-28** M. Gróf, A. Gatial, J. Kožíšek, V. Milata, P. Matějka
Conformational Analysis of Dimethylaminomethylene-Malonic Acid Dimethyl Ester 63
- P1-29** L. Hetmańczyk, J. Hetmańczyk, A. Migdał-Mikuli, E. Mikuli
Phase transition and H₂O motions in [Ba(H₂O)₄](ClO₄)₂ studied by differential scanning calorimetry, infrared spectroscopy and inelastic/quasielastic incoherent neutron scattering 64
- P1-30** I. Jelovica Badovinac, N. Orlić, C. Gellini, L. Moroni, P.R. Salvi
Micro-Raman and Computational Study of the Azoxybenzene Photorearrangement to 2-Hydroxybenzene 65
- P1-31** M. Juribašić, L. Stella, Ž. Marinić, M. Vinković, Lj. Tušek-Božić
Microwave Synthesis and Spectroscopic Study of 3-Quinoline-substituted α -Aminophosphonates 66
- P1-32** M. Jurić, P. Planinić, D. Žilić, B. Rakvin, B. Prugovečki
A New Heterometallic (Ni²⁺ and Cr³⁺) Complex – Crystal Structure and Spectroscopic Characterization 67
- P1-33** A. Kocot, K. Merkel, J. Ziolo
Investigation of Liquid-Liquid Phase Transition for Trans-1,2 dichlorethylene 68
- P1-34** N. Kuş, S. Breda, E.M.S. Eusébio, T.M.R. Estronca, R. Fausto
Matrix Isolation Spectrum, UV-Induced Photochemistry ($\lambda > 215$ nm) and Differential Scanning Calorimetry Analysis of 3-(N-Acetamide)-Coumarin 69
- P1-35** S. Lopes, A. Gómez-Zavaglia, C. M. Nunes, T.M.V.D. Pinho e Melo, R. Fausto
Photochemistry and Vibrational Spectra of Matrix Isolated Methyl 4-Chloro-5-Phenylisoxazole-3-Carboxylate 70

P1-36	<u>L. Macalik, M. Maćzka, J. Hanuza, A.A. Kaminskii</u> Polarized Raman and IR spectra of the orthorhombic $\text{CaNb}_2\text{O}_6:\text{Pr}^{3+}$ single crystal	71
P1-37	<u>W. Makulski, A. Wikiel</u> Nuclear Magnetic Shielding and Spin-spin Coupling Constants for Acetaldehyde from Gas-phase NMR Spectroscopy	72
P1-38	<u>K.M. Marzec, K. Malek, B. Gawel, W. Lasocha, L.M. Proniewicz</u> Structure Determination of Ag(I) Ion Complex of Rhodanine	73
P1-39	<u>K. Malek, M. Makowski, L.M. Proniewicz</u> Raman Spectroscopy in Studies on the Selected Dehydropeptides	74
P1-40	<u>K.M. Marzec, K. Malek, A. Kaczor, L.M. Proniewicz</u> Conformational and Vibrational Analysis of Selected Monoterpenoids by Using Density Functional Theory	75
P1-41	<u>S. Miljanić, Z. Meić, G. Keresztury</u> Polarized Vibrational Spectra of <i>p</i> -Substituted Nitro and Dinitro <i>cis</i> - and <i>trans</i> -Stilbenes	76
P1-42	<u>I. Movre Šapić, L. Bistričić, V. Volovšek, V. Dananić</u> DFT Study of Molecular Structure and Vibrations of 3-Glycidoxypropyltrimethoxysilane	77
P1-43	<u>P. Novak, K. Pičuljan, T. Hrenar, M. Rubčić, M. Cindrić</u> Solution State Structure of Methoxysalicylaldehyde Thiosemicarbazone Derivatives by NMR and DFT Methods	78
P1-44	<u>P. Forgó, G. Dombi, K. Felföldi, I. Pálinkó</u> Conformations of <i>Z</i> -2-(3'-pyridyl)-3-phenyl Propenoic Acid in Various Solvents - an NMR Study Supplemented with Computations	79
P1-45	<u>I. Pálinkó, J. Mink</u> Determining the Positions of Aromatic Hydrogens in (ar)C-H...X (X = O or F) Hydrogen Bonded Assemblies of Phenyl-phenyl, Phenyl-furyl Substituted Propenoic Acids and Esters from Their FTIR Spectra	80
P1-46	<u>N. Peran, Z.B. Maksić</u> Calculating pK_a of Some α -Aminoacids Using Cluster-Continuum Model	81
P1-47	<u>G. Petruševski, P. Naumov, G. Jovanovski</u> Fourier Transform Infrared Spectroscopic Analysis of the Solvates and Polymorphs of Sodium Valproate, Active Component of the Anticonvulsant Drug Epilim [®]	82
P1-48	<u>K. Pičuljan, P. Novak, K. Užarević, M. Cindrić, T. Hrenar, T. Jednačak</u> Hydrogen Bonding and Deuterium Isotope Effects in ¹³ C NMR Spectra of Phenylene Enaminones Derived from Dehydracetic Acid	83
P1-49	<u>M. Randić, K. Mehulić, D. Vukičević, T. Pisanski, D. Vikić-Topić, D. Plavšić</u> Graphical Representation of Proteins as Four-Color Maps and Their Numerical Characterization	84
P1-50	<u>S. Rada, V. Maties, M. Rada, L. Pop, E. Culea</u> The Local Structure of Europium Lead-Borate Glasses and Glass Ceramics	85
P1-51	<u>S. Rada, M. Barlea, D. Chicea, E. Culea</u> Structural properties of Gadolinium Borate-Tellurate Glasses and Glass Ceramics Inferred from FTIR spectroscopy and DFT Studies	86
P1-52	<u>M. Ristova, G. Petruševski, A. Raškowska, B. Šoptrajanov</u> Vibrational Spectra of Hydrates of Some Metal(II) Malonates	87
P1-53	<u>J.Cz. Dobrowolski, M.H. Jamróz, R. Kolos, J.E. Rode, J. Sadlej</u> IR Low-temperature Matrix and <i>Ab Initio</i> Study on β -Alanine Conformers	88
P1-54	<u>D. Rusu, O. Baban, I. Hauer, L. David, M. Rusu</u> Synthesis and Physical Chemical Characterization of The Potassium 11-Tungstovanado(IV) Phosphate Anion	89

P1-55	<u>S.G. Sagdinc</u>, B. Köksoy, F. Kandemirli, S.H. Bayari Spectroscopic and Theoretical Studies of 5-Fluoro-isatin-3-(N-cyclohexylthiosemi-carbazone) and Its Metal Complexes	90
P1-56	<u>M. Saldyka</u>, B. Golec, Z. Mielke Spectroscopy and Photochemistry of Glyoxal-Hydroxylamine Complexes. Matrix Isolation and Theoretical Study	91
P1-57	<u>M. Sitarz</u>, Z. Fojud, Z. Olejniczak Submicroheterogenous Structure of Silico-Phosphate Glasses Studied by ²³ Na, ²⁷ Al, ³¹ P NMR and FTIR	92
P1-58	<u>V. Smrečki</u>, P. Novak, D. Vikić-Topić, Z. Meić Deuterium Isotope Effects in ¹³ C NMR Spectra of <i>ortho</i> -, <i>meta</i> - and <i>para</i> -Deuterium Labelled Mono- and Binuclear Aromatic Compounds	93
P1-59	<u>İ. Sıdır</u>, E. Taşal, Y. Gülseven, R. Fausto, T. Önkol Molecular Structure, Infrared Spectra and Some Molecular Properties of 5-Chloro-6-(4-chlorobenzoyl)-2-benzothiazolinone	94
P1-60	<u>D. Vojta</u>, G. Baranović Raman Study of Anharmonic Effects in Vibrational Spectra of Acetylenic Compounds ...	95
P1-61	<u>S.X. Zhou</u>, D.T. Durig, J.R. Durig Vibrational Spectra and Structural Parameter of Methyl and Ethyl Isocyanate	96
P1-62	<u>D. Vojta</u>, B. Zimmermann, G. Baranović Vibrational Analysis of Diacetylenic Aromatic Compounds	97
P1-63	<u>S. Rada</u>, P. Pascuta, M. Culea, M. Pica, E. Culea Vibrational Spectroscopic and DFT Studies of Gadolinium Vanado-Tellurite Glasses and Glass Ceramics	97a
P1-64	V. Stefov, A. Cahil, <u>B. Šoptrajanov</u>, M. Najdoski, F. Spirovski, B. Engelen, H.D. Lutz, V. Koleva Fourier Transform Infrared and Raman Spectra of Hexagonal MgCsPO ₄ ·6H ₂ O	97b

2. BIOSPECTROSCOPY

ORAL PRESENTATIONS

O2-1	<u>A. Barth</u> Ligand Binding to Proteins Studied by Infrared Spectroscopy	98
O2-2	<u>M. Di Foggia</u>, C. Fagnano, P. Taddei, A. Torreggiani, M. Dettin, S. Sanchez-Cortes, A. Tinti Vibrational Characterization of Self-Assembling Oligopeptides for Tissue Engineering on TiO ₂ Surfaces	99
O2-3	<u>S. Madathil</u>, <u>K. Fahmy</u> Cross-Correlation of Fluorescence-Quenching and Infrared Absorption in the Study of Protein Ligand Binding Sites	100
O2-4	<u>J. Grdadolnik</u> Preferential Conformations of Blocked Amino Acids in Water	101
O2-5	<u>H.M. Heise</u>, U. Damm, V.R. Kondepati, J.K. Mader, F. Feichtner, M. Ellmerer Infrared Spectroscopy in Clinical Chemistry: From Lab to Bed-Side Applications	102
O2-6	<u>P. Heraud</u>, E. Ng, B. Wood, T. Frosch, D. McNaughton, E. Stanley, A. Elefanty Early Stages of Human Embryonic Stem Cell (HESC) Differentiation Characterized by FT-IR Spectroscopy	103
O2-7	<u>Y. Ike</u>, Y. Seshimo, S. Kojima Crystallization and Vitrification of Cryoprotectants Studied by Raman Scattering, Brillouin Scattering and THz-TDS	104

P2-6	<u>G. Doyle, D. Zerulla</u> Investigating the Kinetic Interactions between Protein and Nanoparticles via Mie Scattering Spectroscopy and Optical Trapping	122
P2-7	<u>A.V. Glushkov, S.V. Malinovskaya, S.V. Ambrosov, O.Yu. Khetselius</u> Spectroscopy and Structural Properties of Biogene Amines (Serotonine, Histamine, γ -amino oil acid) and Account for Laser and Neutron Capture Effects	123
P2-8	<u>V. Gombás, J. Mink</u> Chemometrics Methods Used by Spectroscopic of Biological Samples	124
P2-9	<u>A. Gómez-Zavaglia, A. Kaczor, R. Almeida, M.L.S. Cristiano, R. Fausto</u> Different Conformational Ground States of a <i>Pseudosaccharin</i> Ether in the Gaseous Phase and in Solid Krypton	125
P2-10	<u>R. Dědic, V. Vyklický, A. Svoboda, J. Hála</u> Phosphorescence of Singlet Oxygen and 5,10,15,20-tetrakis(1-methyl-4-pyridinio)porphyrin: Time and Spectral Resolved Study	126
P2-11	<u>Y. Ike, E. Hashimoto, S. Kojima</u> Micro-Brillouin Scattering Study of Low Temperature Elastic Properties of Protein Crystals	127
P2-12	<u>G. Keresztury, T. Sundius, T. Lóránd</u> Vibrational Spectroscopic Investigation of Bioactive Aminoalcohols	128
P2-13	<u>S. Kumar, A. Barth</u> Ligand induced conformational change of pyruvate kinase studied by ATR-FTIR spectroscopy	129
P2-14	<u>Z. Tarle, D. Škrtić, A. Knežević, D. Matošević, M. Ristić, K. Prskalo, S. Musić</u> Degree of Vinyl Conversion in Experimental ACP Composites	130
P2-15	<u>K. Merkel, A. Kocot, W. Pluskiewicz, A. Pyrkosz</u> Raman and FTIR Spectroscopy of the Keratin as a Potential Tool for Probing Bone Health	131
P2-16	<u>V. Mohaček Grošev, J. Grdadolnik, J. Stare, D. Hadži</u> Hydrogen Bonding in $(\text{COOH})_2 \cdot 2\text{H}_2\text{O}$ and $(\text{COOD})_2 \cdot 2\text{D}_2\text{O}$	132
P2-17	<u>A. Aranyi, Z. Csendes, J.T. Kiss, I. Pálinkó</u> Covalently Grafted, Silica Gel Supported C-protected Cysteine or Cystine Copper Complexes – Syntheses, Structure and Possible Surface Reaction Studied by FT-IR Spectroscopy	133
P2-18	<u>M. Lasalvia, N. L'Abbate, G. Perna, E. Mezzenga, V. Capozzi</u> Raman Spectroscopy Study of Cellular Damage in Human Keratinocytes Treated with Organophosphate Compounds	134
P2-19	<u>D.R. Gauger, E. Mrazkova, P. Hobza, W. Pohle</u> Disentangling Infrared CH Bands Arising from Polar and Apolar Domains of Phospholipids: Headgroup CH Moieties are Involved in Water Binding	135
P2-20	<u>O. Ryazanova, I. Voloshin, I. Dubey, L. Dubey, V. Zozulya</u> Spectroscopic Studies on Binding of Cationic Pheophorbide-a Derivative to Double-stranded and Quadruplex Polynucleotides	136
P2-21	<u>M. Rokita, M. Sitarz</u> Phosphate Layers on Titanium and Ti6Al4V Titanium Alloy – Comparison of Hydroxyapatite Layers Obtained During SBF Soaking	137
P2-22	<u>M. Śmiechowski, E. Gojło, J. Stangret</u> Systematic Study of Hydration Patterns of Phosphoric (V) Acid and Its Mono-, Di- and Tripotassium Salts in Aqueous Solution	138

P2-23	J. Surmacki, B. Brożek-Pluska, H. Abramczyk, Z. Morawiec, M. Tazbir Application of Raman Spectroscopy for Breast Cancer Diagnosis	139
P2-24	R. Tamaian, I. Ștefănescu, R. Ionete Investigations on Deuterium's Grade of Substitution in the Swiss Mice's Body at the Administration of Deuterium Depleted Mediums	140
P2-25	A. Tinti, J. Domènech, S. Atrian, M. Capdevila, A. Torreggiani Raman Spectroscopy Investigation on Metal-Metallothionein Complexes	141

3. NANOSTRUCTURED MATERIALS

ORAL PRESENTATIONS

O3-1	M. Darányi, Á. Kukovecz, Z. Kónya, I. Kiricsi Characterization of Carbon Thin Films Prepared by the Thermal Decomposition of Spin Coated PAN Films	142
O3-2	A. Gajović, I. Friščić, M. Plodinec, D. Iveković High Temperature Raman Spectroscopy of Titanate Nanotubes	143
O3-3	M. Galvin, G. Doyle, B. Ashall, D. Zerulla Raman Spectroscopy: Close to the Laser Line	144
O3-4	S.K. Gupta, P.K. Jha Vibrational Quantization in Semiconductor Nanocomposites	145
O3-5	V.A. Karachevtsev Spectroscopy of Nanohybrids Formed by Carbon Nanotubes and Biomolecules	146
O3-6	V. Ličina, A. Moguš-Milanković, Ž. Skoko, S. Musić, M. Ivanda Influence of Crystallization on the Electronic Conductivity of Iron Phosphate Glasses	147
O3-7	R. Holomb, V. Mitsa Ring-, Branchy-, and Cage-Like As_nS_m Nanoclusters in the Structure of Amorphous Semiconductors: <i>ab initio</i> and Raman Study	148
O3-8	K. Raulin, O. Cristini, P. Baldeck, S. Turrell, B. Capoen, M. Bouazaoui Spectroscopic Characterization of Two-photon Generated CdS Nanoparticles in Sol-gel Zirconia Thin Films	149
O3-9	O. Robbe-Cristini, K. Raulin, B. Capoen, M. Bouazaoui, S. Turrell Spectroscopic Studies of Energy Transfer between Semiconductor Nanoparticles and Eu^{3+} Ions in Silica Gels	150
O3-10	I. P. Suzdalev, Yu.V. Maksimov Magnetic Phase Transitions in Nanoclusters and Nanostructures	151
O3-11	S.N.B. Bhaktha, O. Robbe-Cristini, K. Raulin, B. Capoen, M. Bouazaoui, S. Turrell, J. Habinshuti, B. Grandidier, C. Kinowski Use of Spectroscopic Techniques for Synthesis Optimisation and for the Characterisation of Optical Properties of Semiconductor Nanoparticles	152
O3-12	D. Gracin, A. Gajović, M. Ceh, K. Juraić, D. Meljanac, P. Dubček, S. Bernstorff Structural Analysis of Thin Amorphous- Nano-Crystalline Thin Films by HRTEM, GISAXS and Raman Spectroscopy	153

POSTER PRESENTATIONS

P3-1	<u>M. Barczak, A. Dąbrowski</u> Spectroscopic Characterization of Polysiloxane and Bridged Polysilsesquioxane Xerogels	154
P3-2	<u>L. Bistričić, M. Leskovac, G. Baranović, E. Govorčin Bajsić</u> Linear IR dichroism of polyether-based polyurethane-silica nanocomposites	155
P3-3	<u>V. Canpean, S. Astilean</u> Subwavelength Metallic Nanohole Arrays as Multifunctional Plasmonic Substrates for SPR and SERS Sensors	156
P3-4	<u>E. Culea, L. Pop, M. Bosca</u> Novel Bismuth-Lead-Silver Glasses Doped with Neodymium Ions	157
P3-5	<u>V.G. de Resende, E. De Grave, A. Cordier, C. Laurent, A. Peigney, A. Weibel</u> Carbon Nanotube-Fe/Al ₂ O ₃ Nanocomposites by CCVD Method: Formation of CNTs from α -(Al _{1-x} Fe _x) ₂ O ₃ Oxide Powders that were Prepared by Oxinate Route	158
P3-6	<u>M. Didović, S. Valić, D. Klepac, A.P. Meera, S. Thomas</u> ESR Study of NR/Montmorillonite Nanocomposites	159
P3-7	<u>A. Fraczek, C. Paluszkiwicz, A. Weselucha-Birczynska, S. Blazewicz</u> The Influence of Carbon Nanotubes on PAN-based Fibers Properties	160
P3-8	<u>A. Gajović, S. Šturm, B. Jančar, M. Čeh</u> The Mechanism of BiFeO ₃ Hydrothermal Synthesis	161
P3-9	<u>A.V. Glushkov, S.V. Malinovskaya, S.V. Ambrosov, O.Yu. Khetselius</u> Spectroscopy and Structural Properties of Biogene Amines (Serotonine, Histamine, γ -Amino Oil Acid) and Account for Laser and Neutron Capture Effects	162
P3-10	<u>T. Gumula, C. Paluszkiwicz, S. Blazewicz</u> Study on Thermal Decomposition Processes of Polysiloxane Polymers – from Polymer to Nanosized Silicon Carbide	163
P3-11	<u>M. Iosin, F. Toderas, P. Baldeck S. Astilean</u> Study of Protein-Gold Nanoparticle Conjugates by Fluorescence and Surface Enhanced Raman Scattering	164
P3-12	<u>M.S. Sytnyk, Yu.B. Khalavka, O.V. Jovtiuk, O.O. Korovyanko</u> Morphological Dependence of Magnetite Nanocrystals under Different Growth Conditions	165
P3-13	<u>S. Krehula, S. Musić</u> Formation of Iron Oxides in a Highly Alkaline Medium in the Presence of Palladium Ions	166
P3-14	<u>D. Mikociak, C. Paluszkiwicz, R. Słowiak, M. Blazewicz</u> Vibrational Spectroscopy Applications to Study Carbonization Process of Fibrous Materials	167
P3-15	<u>E. Stodolak, C. Paluszkiwicz, M. Bogun, M. Blazewicz</u> Nanocomposite Fibres for Medical Applications	168
P3-16	<u>D. Mikociak, C. Paluszkiwicz, T. Gumula, J. Michałowski, S. Błażewicz</u> FTIR Studies of Carbon Matrices Modified with Nanosized Hydroxyapatite	169
P3-17	<u>P. Pascuta, S. Rada, G. Borodi, M. Bosca, L. Pop, E. Culea</u> Influence of Europium Ions on Structure and Crystallization Properties of Bismuth-Alumino-Borate Glasses and Glass Ceramics	170
P3-18	<u>V. Pashynska, A. Glamazda, A. Plokhotnichenko, E. Karpenko, T. Pokynbroda, V. Karachevtsev</u> Spectroscopic Investigations of Carbon Nanotubes in Aqueous Suspensions with Biosurfactants	171

P3-19	<u>R. Rémiás, A. Kukovecz, Z. Kónya, I. Kiricsi</u> A Spectroscopic Study on Noble Metal Nanoparticle Embedding into a SBA-15 Catalyst System	172
P3-20	<u>S. Musić, M. Ristić, S. Popović</u> Synthesis and Microstructure of Porous Mn-Oxides	173
P3-21	<u>S. Musić, A. Šarić, S. Popović, M. Ivanda</u> Formation and Characterization of Nanosize α -Rh ₂ O ₃	174
P3-22	<u>Ž. Skoko, S. Popović, G. Štefanić</u> Thermal Behaviour of Al-Zn and Zn-Al Alloys	175
P3-23	<u>D. Sović, D. Iveković, B. Zimmermann</u> Modification of Titanate Nanotubes with Transition Metals and Transition Metal-1,10-phenanthroline Complexes	176
P3-24	<u>G. Štefanić, S. Musić, M. Ivanda</u> The Influence of Thermal Treatment on the Phase Development of ZrO ₂ -ZnO Precursors	177
P3-25	<u>D.S. Su, J. Zhang, X. Liu, J. Delgado, A. Gajović</u> Raman Spectroscopy of Nanocarbon Catalyst for Oxidative Dehydrogenation Reactions	178
P3-26	<u>F. Toderas, M. Baia, L. Baia, S. Astilean</u> Investigation of Annealed Gold Nanoparticles Self-Assembled on Solid Surface for Surface-Enhanced Raman Spectroscopy	179
P3-27	<u>V. Vogel, T. Pisternik, M. Holzer, K. Langer, W. Mäntele</u> Study of Controlled Release of Model Proteins from Poly (D,L lactic-co-glycolic) Acid Nanoparticles by Fluorimetry and Analytical Ultracentrifugation	180
P3-28	<u>K. Žagar, A. Gajović, S. Šturm, M. Čeh</u> BaTiO ₃ Nanorods: New Insight by Raman Spectroscopy	181
P3-29	<u>M. Žic, M. Ristić, S. Musić</u> Precipitation of hematite from dense β -FeOOH suspensions with ammonium amidosulfonate adding	182

4. SPECTROSCOPY OF MACROMOLECULES

ORAL PRESENTATIONS

O4-1	<u>T. Burova, G. Ten, A. Anashkin</u> Quantum-Mechanical Analysis of Intensity Distribution in Resonance Raman and Two-Photon Absorption Spectra of Nucleic Acid Base Pairs	184
O4-2	<u>Olesya V. Stepanenko, I.M. Kuznetsova, V.V. Verkhusha, V.N. Uversky, K.K. Turoverov</u> The Structural Changes of Green Fluorescent Protein Induced by Small Guanidine Hydrochloride Concentrations	185
O4-3	<u>Olga V. Stepanenko, I.M. Kuznetsova, K.K. Turoverov, V. Scognamiglio, M. Staiano, S. D'Auria</u> The Structural Changes of D-Galactose/D-Glucose-Binding Protein Induced by Calcium Depletion	186
O4-4	<u>M.M. Vorob'ev</u> Microwave Hydration Measurements in Aqueous Systems of Proteins and Synthetic Polymers	187

 POSTER PRESENTATIONS

- P4-1** **S. İde, A.B. Arıĝ, T. Trkeř, O. Mergen, S.H. Bayarı, . elik**
Structural Investigation on Some Silk (Dragline, Hiding and Egg Coccon) Samples Weaved by Different Species Living in Turkey 188
- P4-2** **L. Bistrii, V. Volovřek, V. Danani, I. Movre řapi, M. Leskovac**
DFT Vibrational Study of Organic-Inorganic Hybrid Polymers Based on 3-Glicidoxy-propyltrimethoxysilane 189
- P4-3** **T. Burova, G. Ten, A. Anashkin**
Quantum-Mechanical Calculation of the Intensity Distribution in Resonance Raman Spectra of Derivatives of Uracil 190
- P4-4** **E. Dřafi, O. Klein, W. Mntele**
Monitoring of Hydrogen-Deuterium Exchange in Membrane Proteins using Attenuated Total Reflection Infrared (ATR-IR) Spectroscopy and a Microdialysis Perfusion-Cell 191
- P4-5** **M. Handke, A. Kowalewska, W. Mozgawa**
Spectroscopic Study of Preceramic Polymers Obtained by Hydrolytic Condensation of Ethoxycyclosiloxanes 192
- P4-6** **M. Handke, A. Kowalewska**
New POSS-Siloxane Materials of Ladder-Like Structure 193
- P4-7** **S. Ili, R. Setnescu**
Characterization of Some Irradiated Materials Using Spectroscopic and Related Methods 194
- P4-8** **D. Krilov, M. Balarin, M. Kosovi, O. Gamulin, J. Brnjas-Kraljevi**
FTIR Spectroscopy of Lipoproteins - A Comparative Study 195
- P4-9** **E.A. Minakova, E.B. Kruglova**
Different Interaction Models for Explanation of Optical Properties of Ligand-Polynucleotides Systems 196
- P4-10** **ř. Miti, G.S. Nikoli, M. Caki, P. Premovi, Lj. Ili**
FTIR Spectroscopic Characterization of Cu(II) Coordination Compounds with Exopolysaccharide Pullulan and its Derivatives 197
- P4-11** **I. Puci, B. Mihaljevi, M. Jakři**
Concentration of Vapor Phase Corrosion Inhibitor in Anticorrosion Polymer Films – Correlation of Ion-Beam Analysis Results and UV-Vis Spectrophotometry 198
- P4-12** **I. Puci, T. Jurkin**
 γ -Irradiated Poly(Ethylene Oxide): Spectroscopic and Thermal Analysis 199
- P4-13** **J. Striova, M. Camaiti, A. Sansonetti, A. deCruz, R. Palmer, E.M. Castellucci**
Spectroscopic Study of Ablated Organic Substances by a Pulsed Er:YAG Laser 200
- P4-14** **F. Torrens, G. Castellano**
Binding of Water-Soluble, Globular Proteins to Anionic Model Membranes 201
- P4-15** **V. Volovřek, K. Furi, L. Bistrii**
Raman Spectroscopic Study of Siloxane Structures Developed Under Low Pressure 202
-

5. OPTOELECTRONICS AND SEMICONDUCTOR MATERIALS

ORAL PRESENTATIONS

- O5-1** Z. Gyóri, D. Tátrai, F. Sarlós, G. Szabó, A. Kukovecz, Z. Kónya, I. Kiricsi
Laser-induced Fluorescence Measurements On CdSe Quantum Dots 203
- O5-2** G. Kozma, Á. Kukovecz, Z. Kónya
Spectroscopic Characterization of Mechanochemically Synthesized Cr/SnO_x Nanocomposites 204

POSTER PRESENTATIONS

- P5-1** B. Altioikka, S. Aksay, G.S. K rk u glu
FT-Raman and X-ray Diffraction Spectra of CuInS₂ Films by the Spray Pyrolysis at Different Substrate Temperatures 205
- P5-2** M. Balarin, O. Gamulin, M. Ivanda, M. Kosovi , D. Risti , M. Risti , S. Musi ,
K. Furi , D. Krilov, J. Brnjas-Kraljevi 
Structural, Optical and Electrical Characterization of Porous Silicon Prepared on Thin Epitaxial Layer 206
- P5-3** M. Fridrichov , I. N mec, P. N mec
Guanylurea(1+) Hydrogenphosphite – A New Material for Non-Linear Optics 207
- P5-4** T.M. Hammad
The Effect of Annealing on Electrical, Structural and Optical Properties of Sol Gel ITO Thin Films 208
- P5-5** I. Kavlak, G.S. K rk u glu, T. Arslan
Theoretical and Experimental Investigation of Vibrational (FT-IR and Raman) Spectra and Electronic Transitions of Di-p-tolylamine 209
- P5-6** D. Risti , M. Ivanda, K. Furi 
Application of the Phonon Confinement Model on the Optical Phonon Mode of Silicon Nanoparticles 210
- P5-7** N. Vedeanu, D.A. Magdas, O. Cozar, I. Ardelean
EPR Structural Investigation of CuO-V₂O₅-P₂O₅-CaO Glass System for Optoelectronic Applications 211
- P5-8** D.A. Magdas, N. Vedeanu, O. Cozar, I. Ardelean
The Structural Changes Induced in Lead-Phosphate Glasses by Addition of Cooper Oxide 212
- P5-9** E. Wolarz, E. Mykowska, T. Martyński, R. Stolarski
Spectral Properties of New Tetrafluoro-pentenyl-perylene in Isotropic Solvents, Liquid Crystal Layers, and LB Films 213

6. SPECTROSCOPY IN CHEMICAL, PHARMACEUTICAL AND ENVIRONMENTAL ANALYSES

ORAL PRESENTATIONS

- O6-1** O. Abbas, R. Codony, C. von Holst, V. Baeten
Assessment of the Discrimination of Animal Fat by FT-Raman Spectroscopy 214
- O6-2** J. Barbillat, S. Sobanska, J. Rimetz, S. Scolaro, J. Laureyns, D. Petitprez, C. Brémard
Raman and AFM Imaging of Marine Aerosol Particles 215
- O6-3** T. Frosch, J. Popp
Vibrational Spectroscopic Investigation of Drug-Target-Interactions in Malaria Research 216
- O6-4** G. Trettenhahn
In situ FTIR Spectroelectrochemical Investigations and two-dimensional Correlation Spectroscopy of the Hexacyanoferrate-II/-III Redox Couple 217
- O6-5** M. Watanabe, T. Kurabayashi, T. Tanno, N. Kikuchi
Significance of Terahertz Spectrometry for Detecting Molecular States of Chemicals 218

POSTER PRESENTATIONS

- P6-1** Y. Akkaya, K. Balci, S. Akyuz
IR and Raman and Density Functional Theory Studies on a Non-Steroidal Anti-Inflammatory Drug, Naproxen 219
- P6-2** B. Minčeva-Šukarova, L. Andreeva, O. Magdenovska, V. Manevska, N. Anevsk-Stojanovska
Raman and Infrared Spectroscopic Study of Pharmaceutical Tablets *DIPROL* and *CAFETINE COLD*, Products of *ALKALOID AD SKOPJE* (Republic of Macedonia) 220
- P6-3** K. Chruszcz-Lipska, M. Baranska, L.M. Proniewicz
Binding Ability of Fosfomycin towards Sodium and Calcium Ions 221
- P6-4** A. Baran, M. Baranska
Vibrational spectroscopy analysis of the anthraquinone pigment alizarin 222
- P6-5** M. Bartoszek, J. Polak, A. Kos, W.W. Sulkowski
Spectroscopic Study of Humic Substances Extracted From Bottom Sediment and Water 223
- P6-6** J. Polak, M. Bartoszek, M. Kantor, W.W. Sulkowski
Spectroscopic Comparison of the Physico-Chemical Properties of Humic Acids Extracted from Sewage Sludge and Bottom Sediment 224
- P6-7** A.E. Yavuz, S.H. Bayar, N. Kazancı
Structural and Vibrational Study of Maprotiline 225
- P6-8** A.E. Ledesma, J. Zinzuk, J.J. López González, A. Ben Altabef, S.A. Brandán
Structural and Vibrational Study of 4-(2'-Furyl)-1-Methylimidazole 226
- P6-9** B. Bojko, A. Sulowska, M. Maciążek-Jurczyk, J. Równicka, D. Pentak, W.W. Sulkowski
Comparison of the Influence of Myristic Acid on Acetaminophen and Acetylsalicylic Acid Binding with Serum Albumin 227

P6-10	<u>P.Ciacka, A. Jarota, B. Brożek-Pluska, H. Abramczyk</u> Transient Absorption, Low-Temperature Raman, Fluorescence Quantum Yield and Stationary Absorption Studies of Various Metal Phthalocyanines and Their Sulfonated Derivatives	228
P6-11	<u>O. Cozar, F. Drăgan, C. Jelic, V. Chiş, N. Leopold, L. Szabó</u> Spectroscopic Investigation of Some Cu(II) Cardiovascular Complexes	229
P6-12	<u>M. Culea, O. Cozar, E. Culea</u> GC/MS as a Tool for Non-Invasive Diagnosis	230
P6-13	<u>M. Culea, S. Neamtu</u> Study of Amino Acid Transmembranar Transport	231
P6-14	<u>T. Dziembowska, Z. Rozwadowski, M. Szafran</u> NMR and DFT Study of the Enol Imine \leftrightarrow Enaminone Tautomeric Equilibrium in Schiff Bases in Some Organic Solvents	232
P6-15	<u>C. Farcau, S. Astilean</u> Single-Molecule Surface Enhanced Raman Scattering on Periodically Nanostructured Gold Films	233
P6-16	<u>M. Gotić, G. Koščec, S. Musić</u> A Study of the Reduction and Reoxidation of Substoichiometric Magnetite	234
P6-17	<u>A. Hacura, M. Jadamus-Hacura</u> Classification of Polish Honeys by Mid-Infrared Spectroscopy and Multivariate Statistical Analysis	235
P6-18	<u>I. Hannus, Sz. Mészáros, M. Búza, J. Halász</u> IR Spectroscopic Study of the Hydrodechlorination of Chlorobenzenes and Chlorophenols over Nobel Metal Containing Zeolites	236
P6-19	<u>I. Hannus, M. Búza, A. Beck, L. Guzzi</u> Catalytic Activity of Bimetallic Gold Containing Nanoparticles on Different Supports Investigated by IR Spectroscopy	237
P6-20	<u>A. Iordache, M. Culea, O. Cozar</u> Characterization of Allergens in Different Perfumes and Herbs	238
P6-21	<u>O. Klein, I. Klein, G. Oremek, W. Mäntele</u> Clinical Chemistry without Reagents? An Infrared Spectroscopic Technique for Determination of Clinically Relevant Constituents of Body Fluids	239
P6-22	<u>E. Kucharska, W. Sasiadek, H. Ban-Oganowska, M. Mączka, J. Hanuza</u> Synthesis, Molecular Structure, IR and Raman Spectra as well as DFT Quantum Chemical Calculations for N-thiocynoacetyl piperidine and its Methyl Derivatives	240
P6-23	<u>L. Kukoč Modun, Nj. Radić</u> Kinetic Spectrophotometric Determination of N-(2-Mercaptopropionyl)-glycine in Pharmaceuticals	241
P6-24	<u>J. Lorenc, B. Palasek, J. Hanuza, M. Mączka, A. Waškowska</u> Rotational Disorder in 2-Piperidyl-5-nitro-6-methylpyridine: Structural Phase Transition and its Vibrational Characteristics	242
P6-25	<u>Ž. Marinić, P. Trošelj, M. Eckert-Maksić, D. Margetić</u> Spectroscopic and Quantum-Chemical Assignments of Stereochemistry of Products Obtained by 1,3-dipolar Cycloaddition Reactions of Substituted 1,3,4-oxadiazoles With Norbornenes	243
P6-26	<u>M. Marković, T. Biljan, D. Škalec Šamec</u> Entacapone Isomer Quantification Using Raman Spectroscopy	244

P6-27	J. Maurer, V. Vogel, W. Mäntele Study of Heparin/Protamine Complexation by Means of Fluorescence Spectroscopy, Light Scattering and Analytical Ultracentrifugation	245
P6-28	V. Pandurić, Z. Tarle, Z. Hameršak, I. Stipetić, D. Matošević, K. Prskalo, V. Negovetić-Mandić Detection of HEMA in Self-etching Adhesive Systems Using High Performance Liquid Chromatography	246
P6-29	A. Pîrnău, V. Chiş, L. Szabo, O. Cozar, M. Vasilescu, O. Oniga, R.A. Varga Experimental and Theoretical Investigation of 5-para-nitro-benzylidene-thiazolidine-2-thione-4-one Molecule	247
P6-30	J. Równicka, A. Sulowska, M. Maciążek-Jurczyk, B. Bojko, J. Pożycka, W.W. Sulkowski Fluorescence Analysis of Sulfasalazine Bound to Defatted Serum Albumin in the Presence of Denaturing Factors	248
P6-31	M. Maciążek-Jurczyk, A. Sulowska, B. Bojko, J. Równicka, W.W. Sulkowski Fluorescence Analysis of Interaction of Phenylbutazone and Methotrexate in Binding to Serum Albumin in Combination Treatment in Rheumatology	249
P6-32	V. Balevicius, Z. Gdaniec, V. Sablinskas 2D NMR Study of Media Effects of Ionic Liquids on Hydrogen Bonding	250
P6-33	S. Strazdaite, J. Ceponkus, V. Aleksa, V. Sablinskas Structures of 1-Butene and 1-Heptene Primary Ozonides as Studied by Means of Matrix Isolation FTIR Spectroscopy	251
P6-34	L. Szabó, V. Chiş, A. Pîrnău, N. Leopold, O. Cozar, Sz. Orosz Vibrational, NMR and DFT Investigations of Amlodipine Molecule	252
P6-35	L. Szabó, A. Pîrnău, N. Leopold, V. Chiş, O. Cozar Vibrational, NMR and DFT Investigations of Ethylenediaminetetraacetic acid	253
P6-36	A. Terczynska, K. Cholewa-Kowalska, M. Laczka The Effect of Silicate Network Modifiers on Colour and Electron Spectra of Transition Metal Ions	254
P6-37	V. Toteva, A. Georgiev, L. Topalova, S. Andreev Estimation of the Desulphurization Degree in Light Cycle Oil Using FTIR Spectroscopy	255
P6-38	N.U. Perišić-Janjić, Gy.Gy. Vastag, J.D. Janjić, B.Ž. Jovanović Organic Solvents Influence on Electronic Absorption Spectra of 4-R-phenyl-5-carboxyethyl-6-methyl-3,4-dihydropyrimidine-2-tione Derivatives. Ionization Constants Determination	256
P6-39	G. Schäfer, W. Mäntele, G. Wille Carboxylation Reactions Studied Using <i>Caged</i> CO ₂	257
P6-40	K. Vranić, V. Vojković Spectrophotometric Studies of the Interaction of Ruthenium with Hesperetin	258
P6-41	A. Zając, M. Wandas, J. Hanuza Synthesis, Molecular Structure and Vibrational Spectra of Bioactive Hybrid Materials Composed on Chitosan, Sodium Alginate and 1,6-Hexamethylene-di(aminocarboxy-sulfonate)	259
P6-42	J. Zhang, A. Gajović, D. Su, R. Schlögl Molecular Spectroscopy in Coke-free Carbon Catalysis	260
P6-43	B. Trzcińska, J. Zięba-Palus, P. Kościelniak Application of Microspectrometry in Visible Range to Differentiation of Car Solid Paints for Forensic Purposes	261

7. SPECTROSCOPY APPLIED TO ARCHAEOLOGY, ARTS, GEOLOGY AND MINERALOGY

ORAL PRESENTATIONS

- O7-1 B. Davarcioglu**
Spectral Characterization of Kolsuz Area (Ulukisla-Nigde) Clays, Central Anatolian Region, Turkey 262

POSTER PRESENTATIONS

- P7-1 S. Akyuz, T. Akyuz, S. Basaran, I. Kocabas, A. Gulec, H. Cesmeli**
FT-IR and EDXRF Analysis of Wall Paintings of Ancient Ainos Hagia Sophia Church 263
- P7-2 L. Darchuk, Z. Tsybriy, E.A. Stefaniak, C. Vazquez, O.M. Palacios, A. Worobiec, F. Sizov, R. Van Grieken**
Application of Molecular Spectroscopy to Study the Composition of Prehistoric Pigments from Excavations (Argentina) 264
- P7-3 E. del Puerto, Z. Jurasekova, S. Sánchez-Cortés, J.V. García-Ramos, C. Domingo, A. Roquero**
Towards a Surface-Enhanced Raman Spectra Database of Dyed Textiles 265
- P7-4 M.L. Franquelo, A. Duran, L.K. Herrera, M.C. Jimenez de Haro, J.L. Perez-Rodriguez**
Comparison between Two Molecular Spectroscopy Techniques as Analytical Tools in the Characterization of Pigments in Southern Spain Cultural Heritage: Micro Raman and Micro-FTIR Spectroscopy 266
- P7-5 N. Tomašić, A. Gajović, V. Bermanec**
Raman Spectra and Luminescence of the Minerals with Aeschnite and Euxenite Crystal Structure 267
- P7-6 S. Gosav, M. Praisler, D.O. Dorohoi**
Expert Systems Built for the Modeling of Small Molecular Structures Using a Concatenated Spectral Database 268
- P7-7 S. Gosav, M. Praisler**
Optimisation of the Performances of a Hybrid Expert System Designed for the Elucidation of Molecular Structures 269
- P7-8 P. Makreski, G. Jovanovski, B. Kaitner**
Minerals from Macedonia. XXIV. Spectroscopic and Structural Characterization of Tectosilicates 270
- P7-9 N.F.C. Mendes, I. Osticioli, C. Lofrumento, A. Zoppi, E.M. Castellucci**
Combined Fluorescence-LIBS and Raman Spectroscopy Setup for Applications in the Field of Cultural Heritage 271
- P7-10 J. Mihály, J. Mink, V.T. Dobosi, S.F. Parker, J. Tomkinson**
FTIR and INS Study of Lower Palaeolithic Burned Animal Bones from Vértesszőlős (Hungary) 272
- P7-11 W. Mozgawa, W. Jastrzębski**
Vibrational Spectra of β -Cage Units in Different Silicate Structures 273
- P7-12 W. Mozgawa, M. Król**
Application of IR Spectra in the Studies Heavy Metal Cations Immobilization on Natural Sorbents 274
- P7-13 A. Adamczyk, W. Mozgawa, M. Handke, E. Długoń, A. Ferensowicz**
The FTIR Studies of Influence of Different Al_2O_3 and SiO_2 Precursors on Structure of Alumina-Silica Gels and Coatings 275

- P7-14** W. Mozgawa, J. Deja
The IR Spectroscopy Studies of Alkaline Activated Slag Geopolymers 276
- P7-15** L.A. Pérez-Maqueda, A. Duran, P.E. Sánchez Jiménez, M.L. Franquelo, J.L. Perez-Rodríguez
Study of the Dehydroxylation-Rehydroxylation of Pyrophyllite by Spectrometric and Thermal Analysis Methods 277
- P7-16** M. Łodziński, M. Sitarz
Chemical and Spectroscopic Characterization of Some Phosphates Accessory Minerals from Pegmatites of the Sowie Mts (Owles Mts), SW Poland 278
- P7-17** A. Van Alboom, V.G. De Resende, E. De Grave, M.D. Dyar, J.A.M. Gómez
Low Temperature Mössbauer Spectra of Rozenite and Szomolnokite 279

8. CHEMICAL DYNAMICS

ORAL PRESENTATIONS

- O8-1** M. Pasquini, N. Schiccheri, G. Piani, G. Pietraperzia, E. Castellucci, M. Becucci
Studies on Microsolvation in the Gas Phase by HR-LIF and REMPI-TOF Spectroscopy 280
- O8-2** M. Ceppatelli, A. Serdyukov, R. Bini, H.J. Jodl
FTIR Study of the Reactivity of Solid CO at High Pressure 281
- O8-3** V.I. Tomin, R. Jaworski
ESIPT from the S₂ Singlet State in the 3-Hydroxyflavone 282
- O8-4** A.S. Bali, A. Viridi
Kinetics and Mechanistic Studies of the Dissociation of Anthranilic-diacetato-2,2'-dipyridyl Chromium (III) Dihydrated in Acidic Media 283

POSTER PRESENTATIONS

- P8-1** L.M. Babkov, N.A. Davydova, K.E. Uspenskiy
Vibrational Spectra of the 2-, 4-Bromo- and 4,4'-Chlorobenzophenones and Their Interpretation Using Structural-dynamical Models 284
- P8-2** C. Carmona, J. Hidalgo, A. Sánchez-Coronilla, M.A. Muñoz, M. Balón
Betacarboline Tautomerism Induced by Temperature. Dual Emission of Betacarboline Self-Associated Hydrogen Bond Aggregates. 285
- P8-3** E. García-Fernández, M.A. Muñoz, C. Carmona, M. Balón
Ground state Isomerism and Dual Fluorescence of 2-Methylharmine Anhydronium Base (7-Methoxy-1, 2-dimethyl-2H-pyrido[3,4-b]indole) in Aprotic Solvents 286
- P8-4** J. Hetmańczyk, Ł. Hetmańczyk, E. Mikuli, A. Migdał-Mikuli
Phase Transition and NH₃ Motions in Polycrystalline [Ca(NH₃)₆](ClO₄)₂ Studied by Infrared Spectroscopy and Inelastic/Quasielastic Incoherent Neutron Scattering 287
- P8-5** O.Yu. Khetselius
Laser Photo-Ionization (Dissociation) of Molecules in the Isotopes Separation and Relativistic Calculating the Hyperfine Structure Parameters in Heavy-Element Chemistry and Spectroscopy 288
- P8-6** M. Rudbeck, S. Kumar, M. Blomberg, M-A. Mroginski, A. Barth
PEP Vibrations from DFT 289
- P8-7** V.I. Tomin, S. Oncul, G. Smolarczyk, A.P. Demchenko
Dynamic Quenching as a Simple Test for the Mechanism of Excited-State Reaction 290

9. THEORETICAL SPECTROSCOPY AND COMPUTER METHODS

ORAL PRESENTATIONS

- O9-1** E. Benassi
New Features in Theoretical Description of Electronic Energy Transfer: Mechanisms and Matrix Element Calculation 291
- O9-2** T.A. Ford
Ab initio Molecular Orbital Calculations of the Structures and Vibrational Spectra of Some Molecular Complexes Containing Sulphur Dioxide 292
- O9-3** A.V. Glushkov
Raman Scattering of the Light on Metastable Levels of Diatomics: Consistent Energy Approach 293
- O9-4** S. Lebernegg, G. Amthauer, M. Grodzicki
Single-centre Molecular Orbital Theory of Transition Metal Complexes 294
- O9-5** V. Mukherjee, N.P. Singh, R.A. Yadav
FTIR and Raman Spectra of Some Tetra Substituted Benzenes 295
- O9-6** S. Rashev, D.C. Moule
Theoretical Study of a Combined Electronic + Vibrational Relaxation Process in Thiophosgene SCCl_2 296
- O9-7** T.P. Živković
Vibrational Isotope Effect by the Low Rank Perturbation Method 297

POSTER PRESENTATIONS

- P9-1** G.A. Akverdieva, N.M. Godjayev, S. Akyuz, N.E. Dogan, T. Akyuz
Molecular Mechanics Study of Antihypertensive Val-Tyr Dipeptide 298
- P9-2** S. Aydemir, M. Duran, E. Tasal, Halil Berber, C. Öğretir, M.S. Kılıckaya
Ab Initio Calculations of pK_a Values for Some 6-Methyl-2-Pyridine Carboxaldehyde Derivatives 299
- P9-3** S. Aydemir, M. Duran, E. Tasal, Halil Berber, C. Öğretir, M.S. Kılıckaya
Ab Initio Calculations of pK_a Values for 7-Acetylcoumarin-3-Carboxylic Acid 300
- P9-4** P. Borowski, M. Fernández-Gómez, M.-P. Fernández-Liencres, T.P. Ruiz
An Effective Scaling Frequency Factor Method (ESFF) for Scaling of Harmonic Vibrational Frequencies 301
- P9-5** M.Q. Rincón, M. Fernández-Gómez, M.P. Fernández-Liencres, T.P. Ruiz, P. Borowski
Analysis of the Vibrational Spectrum of P-Methyl Styrene Based on IR, Raman and INS Data and *Ab Initio* and DFT Calculations 302
- P9-6** O. Gamulin, M. Kosović, M. Balarin, D. Krilov, J. Brnjas-Kraljević
Denoising Raman Spectra of Biological Samples Using Wavelets 303
- P9-7** A.V. Glushkov, S.V. Malinovskaya, O.Yu. Khetselius
New Laser-Electron Nuclear Effects in the Nuclear γ Transition Spectra of Molecular Systems 304
- P9-8** O.Yu. Khetselius, A.V. Glushkov, E.P. Gurnitskaya, A.V. Loboda
Spectroscopy of Hadronic Molecules and Molecules with Superheavy Elements: Spectra, Energy Shifts and Widths for Different Nuclear Models 305
- P9-9** D. Kirin, I. Lukačević, S.K. Gupta, P.K. Jha
Density Functional Calculation of Raman Intensity in High Pressure Phases of TiO_2 crystal 306
- P9-10** M. Szafarska, M. Woźniakiewicz, M. Pilch, J. Zięba-Palus, P. Kościelniak
Computer Analysis of ATR-FTIR Spectra of Paint Samples for Forensic purposes 307

- P9-11 J. Lamouroux, VI.G. Tyuterev, L. Régalia-Jarlot, S.A. Tashkun**
Comparison of Theoretical Intensity Calculations and Experimental Intensities Measurements for Non Linear Triatomic Molecules 308
- P9-12 I. López-Tocón, J.F. Arenas, S.P. Centeno, D. Pelaez, J.C. Otero**
Correlating the Force Fields of Methylpyrazines: Vibrational Spectrum of Tetramethylpyrazine 309
- P9-13 C.M. Nunes, S. Lopes, T.M.V.D. Pinho e Melo, R. Fausto**
Matrix Isolation FTIR Spectroscopic and Theoretical Study of Dimethyl 2,2-Dioxo-1*H*,3*H*-Pyrazolo[1,5-*c*][1,3]Thiazole-6,7-Dicarboxylate 310
- P9-14 G. Ogruc-Ildiz, S. Akyuz, A.E. Ozel**
Experimental, Ab Initio and Density Functional Theory Studies on Sulfadiazine 311
- P9-15 R. Keça, M. Ostrowska-Kopec**
New Spectroscopic Studies of the Fourth-Positive ($A^1\Pi \rightarrow X^1\Sigma^+$) System Bands in $^{13}\text{C}^{16}\text{O}$ 312
- P9-16 A.E. Ozel, S. Celik, S. Akyuz**
Vibrational Spectroscopic Investigation of Free and Coordinated 5-Aminoquinoline: The IR, Raman and DFT Studies 313
- P9-17 A. Padilla, J. Pérez**
Hindered Rotation in the Infrared Spectra of HCl in Liquefied Rare Gases 314
- P9-18 R. Keça, I. Piotrowska**
New Analysis of the Comet-Tail ($A^2\Pi_r \rightarrow X^2\Sigma^+$) System Bands in $^{12}\text{C}^{18}\text{O}^+$ 315
- P9-19 V.H. Rusu, J.B.P. da Silva, M.N. Ramos**
A Theoretical Study of the Hydrogen Bonding between vic-, cis- and trans- $\text{C}_2\text{H}_2\text{F}_2$ Isomers and Hydrogen Fluoride 316
- P9-20 M.N. Ramos, K.C. Lopes, V.H. Rusu, R.C.M.U. Araújo**
Effects of Wave Function Modifications on Calculated HC and CC Stretching Frequencies in $\text{H}_2\text{C}=\text{CHX}$ and $\text{HC}\equiv\text{CHX}$ Molecules 317
- P9-21 P. Singh, S. Jaiswal, G. Srivastav, R.A. Yadav**
Vibrational Spectroscopic Investigation on Vitamin P Using Ab Initio and DFT Method: Theoretical Study 318
- P9-22 E. Taşal, Y. Gülseven, İ. Sıdır, T. Önkol, C. Öğretir, M.S. Kılıçkaya**
Experimental and Theoretical Studies on ^{13}C and ^1H NMR Spectra of 6-(2-fluorobenzoyl)-3-(2-(4-(4-fluorophenyl) piperazin-1-yl)-2-oxoethyl)benzo[d]thiazol-2(3*H*)-one 319
- P9-23 E. Taşal, Y. Gülseven, İ. Sıdır, T. Önkol**
Theoretical Studies on Molecular Structure and Some Molecular Properties of 6-(2-fluorobenzoyl)-3-(2-(4-(4-fluorophenyl)piperazin-1-yl)-2-oxoethyl)benzo[d]thiazol-2(3*H*)-one 320
- P9-24 Y. Gülseven, E. Taşal, İ. Sıdır, C. Öğretir**
Quantum Chemical Studies on Tautomerism and Acidity-Basicity Behaviours of Some 1,2,4-triazole Derivates 321
- P9-25 T. Wróblewski**
DFT and Ab Initio Computational Study of Structural Properties and Vibrational Spectra for Protonated Water Clusters 322
- P9-26 G. Yapar, K. Balci**
A Theoretical IR and Raman Spectroscopic Study on 1,2-Bis(o-carboxyphenoxy) ethane molecule 323
- P9-27 H. Yurtseven**
Pippard Relations Modified by the Raman Frequency Shifts for the Phases I and II in NH_4I 324
- P9-28 H. Yurtseven**
Calculation of the Raman Frequencies Using Volume Data Close to the Tricritical and Second Order Phase Transitions in NH_4Cl 325

10. SURFACE SPECTROSCOPIES

ORAL PRESENTATIONS

- O10-1** S. Astilean, M. Baia, D. Maniu, F. Toderas, C. Farcau, M. Iosin, V. Canpean
Multifunctional Plasmonic Nanostructures for Surface-Enhanced Spectroscopies 326
- O10-2** M. Nullmeier, I. Zawisza, S.E. Pust, R. Boukherroub, S. Szunerits, G. Wittstock
Structural Studies of Lipid Bilayers on Titania Surfaces by Means of Polarization
Modulation Infrared Reflection Absorption Spectroscopy 327
- O10-3** P. Taddei, A. Tinti, M.G. Gandolfi, F. Siboni, C. Prati
Vibrational Study on the Bioactivity of Portland Cement-Based Materials for Endodontic
Use 328
- O10-4** B. Vlckova, K. Siskova, M. Prochazka, J. Stepanek, P. Smejkal, P.-Y. Turpin
Surface-enhanced Resonance Raman Scattering of Free-base Porphyrins for
Ultrasensitive Spectral Detection and Surface Probing 329

POSTER PRESENTATIONS

- P10-1** E. Akalin, S. Akyuz, T. Akyuz
Adsorption of Isoniazid onto Sepiolite-Palygorskite Group of Clays: An IR and DFT Study 330
- P10-2** S. Aksay, G.S. Kürkçüoğlu, A.Ş. Aybek, M. Kul, E. Turan, T. Özer, Hüseyin
Berber, Halil Berber, M. Zor
FT-IR and FT-Raman Spectra of SnS Film Deposited by Chemical Bath Deposition
Method 331
- P10-3** S. Bonora, M. Di Foggia, A. Maris
Surface Enhanced Raman Spectroscopy (SERS) Study of Diluted Solutions of
Cimetidine and Some of its Metallocomplexes 332
- P10-4** C. Domingo, L. Guerrini, S. Sánchez-Cortés, J.V. García-Ramos
Fabrication and Functionalization of Core-Shell Au/Ag Nanoparticles with Advanced
Physico-Chemical Properties: Application to the Detection of Pollutants by Surface-
Enhanced Raman Scattering 333
- P10-5** J.V. García-Ramos, L. Guerrini, I. Izquierdo, C. Domingo, S. Sánchez-Cortés
Building Highly Selective Hot Spots in Ag Nanoparticles Using Bifunctional Diamines
with Variable Length: Application to the Detection of Pollutants by Surface-Enhanced
Raman Scattering 334
- P10-6** M.R. Lopez-Ramirez, L. Roldán, J.V. Garcia-Ramos, S. Sanchez-Cortes
SERS Analysis of Herbicide Diquat on Nanostructured Metal Electrodes 335
- P10-7** M. Muniz-Miranda, E. Giorgetti, G. Margheri, S. Sottini, A. Giusti, G. Dellepiane
SERS Study of Self-Assembled Carbazolyl-Diacetylene Monolayers Chemisorbed on
Gold Surfaces 336
- P10-8** M. Muniz-Miranda, B. Pergolese, A. Bigotto
Study of the Adsorption of 2-Mercaptobenzoxazole on Gold Colloidal Nanoparticles by
Means of Surface Enhanced Raman Scattering 337
- P10-9** E. Stodolak, C. Paluszkiwicz, M. Błażewicz
In vitro Biofilms Formation on Polymer Matrix Composites 338
- P10-10** C. Paluszkiwicz, W.M. Kwiatek, E. Długoń, A. Weselucha-Birczyńska, M. Piccinini
IR Mapping of Bio-Ceramic Layers on Titanium Substrate 339
- P10-11** M. Sladkova, B. Vlckova, K. Siskova, I. Pavel, M. Moskovits, M. Slouf
Surface-enhanced Raman Scattering from a Single Molecularly-bridged Silver
Nanoparticle Aggregate 340

11. TIME RESOLVED SPECTROSCOPY

ORAL PRESENTATIONS

- O11-1** **C. Niezborala, F. Hache**
Ultrafast Conformational Dynamics of (R) - 1,1'-Bi-2-naphthol Measured with Time-Resolved Circular Dichroism 341
- O11-2** **C. Krejtschi, O. Ridderbusch, R. Huang, T.A. Keiderling, K. Hauser**
Site-Specific Folding Dynamics of Peptides Studied by Time-Resolved Infrared-Spectroscopy 342
- O11-3** **I.P. Pozdnyakov, A. Pigliucci, N. Tkachenko, V.F. Plyusnin, E. Vauthey, H. Lemmetyinen**
Time-Resolved Study of Photophysics of SAD (Salicylic Acid Derivatives) in Aqueous Solution 343

POSTER PRESENTATIONS

- P11-1** **V. Dananić, K. Košutić, B. Kunst, D. Bosnar**
Pore Size Distribution of NF/RO Composite Membranes by Positron Annihilation Lifetime Spectroscopy 344
- P11-2** **A. Krzysztofowicz, V.I. Tomin**
The Temporal Dipole Moment of the Solutes Undergoing Charge Transfer in the Excited State 345

12. NEW INSTRUMENTATION

ORAL PRESENTATIONS

- O12-1** **D. McNaughton, R. Tuckermann, L. Puskar, B. Wood, J. Popp, T. Frosch**
Raman Spectroscopic Analysis in Acoustically Levitated Drops 346
- O12-2** **J. Mink, J. Mihály, Z. Bacsik, V. Gombás, X. Zhou**
New Application of Infrared Microscopy and Imaging in Difficult Sample Analysis 347

POSTER PRESENTATIONS

- P12-1** **V. Ivanovski, T.G. Mayerhöfer, J. Popp**
Employing Polyethylene as Contacting Agent Between ATR-crystals and Solid Samples with Hard Surfaces 348

WORKSHOP & EXHIBITION

- W-1** **Horiba Jobin Yvon S.A.S.**
Latest Innovations in Raman Microscopy for Ultra Fast Raman Imaging and Macro-mapping 349
- E-1** **J. Sikola, G. Zachmann, M. Huber (Bruker Optik GmbH)**
The New Vacuum FT-IR Spectrometer: Design Advances and Research Application 350
- E-2** **Marion Egelkraut-Holtus, Uwe Oppermann (Shimadzu)**
"State of the Art" Spectroscopy in Food Analysis 351
- E-3** **PerkinElmer**
..... 352

LAST MINUTE ABSTARCTS

- O1-18** **S. Mishra, D. Chaturvedi, P. Tandon, V.P. Gupta, A.P. Ayala, S.B. Honorato, H.W. Siesler**
Molecular Structure and Vibrational Spectroscopy investigation of Secnidazole using Density-Functional Theory 353

PLENARY LECTURES

EUCMOS – Past, Present and Future

Austin J. Barnes

Institute for Materials Research, University of Salford, Salford M5 4WT, Great Britain

The European Molecular Spectroscopy Group, which was constituted informally after the Second World War to bring together spectroscopists from across Europe, met for the first time in Konstanz in 1947. Reinhard Mecke was at the time working in temporary accommodation at Wallhausen, a small village on the shores of Lake Constance, and the meeting (initiated by invitation of Professors Lecomte and Kastler from Paris) was attended by French, German and Austrian spectroscopists. However, the meeting which has since become regarded as the first of the EUCMOS series was organised under the auspices of Ernst Miescher in Basel in 1951.

This talk by the current President of the EUCMOS International Committee will provide an illustrated overview of EUCMOS meetings from these early beginnings to the present time, with pictures of many of the prominent spectroscopists who have presented lectures at EUCMOS meetings. The manner in which the organisational structure evolved as the political climate in Europe changed will be discussed. Finally, some thoughts will be offered on the future of EUCMOS meetings.

Spectroscopy and Monitoring of High Pressure Phenomena

Vincenzo Schettino

*Department of Chemistry
and*

*LENS (European Laboratory of Non linear Spectroscopy)
University of Florence – Italy*

Physical and chemical transformations of matter at very high pressures are of interest in many areas of research including geochemistry and planetary science, synthesis of novel materials of technological interest to be quenched at normal conditions, basic understanding of electronic properties, and behaviour of biomolecules in extreme and hostile environments. With the advent in high pressure science of the diamond anvil cell and the use of appropriately selected diamonds that are transparent in most of the optical region between the far infrared and the visible-UV, spectroscopic methods have become techniques of election, and in many instances unparalleled, to study properties and transformations of materials at very high pressures. The information obtained by optical spectroscopic techniques on materials in extreme conditions of pressure are fundamental and unique.

The purpose of this contribution is to report on studies of the mechanisms of chemical reactions and phase transformations of molecular systems at pressures above 1 GPa, using infrared, Raman and electronic spectroscopy and two-photon absorption and fluorescence methods. It will be shown that by the combined use of high pressure and photochemical activation highly selective reaction pathways (dimerization vs. polymerization) can be induced in liquid and solid butadiene and isoprene. From the time evolution of the spectral profiles of reactants and products the activation volumes can be obtained as a function of pressure and from these important information on the reaction mechanisms can be sorted out. The formation at ultrahigh pressures of polymeric materials with interesting structural and mechanical properties will be illustrated with reference to the ethylene polymerization. Infrared spectroscopy and two-photon absorption and fluorescence, in conjunction with x-ray diffraction using synchrotron radiation, have allowed to unveil the role of the changes in the electronic configurations, of the structural reorganization and of the phonon modulation of the interatomic distances as precursors of the benzene amorphization to produce an amorphous hydrogenated carbon. The microscopic counterpart (interatomic distances and molecular orientations) of the high pressure-high temperature reaction thresholds will also be discussed. Finally, the subtleties of conformational and phase transformations at very high pressure, up to the reaction threshold, will be illustrated with reference to the nitromethane crystal, a prototype system for many explosive materials.

Mössbauer Spectroscopy – A Powerful Tool in Molecular Magnetism

Philipp Gütlich

*Institut für Anorganische Chemie und Analytische Chemie,
Johannes Gutenberg-Universität Mainz,
Staudingerweg 9, D-55099 Mainz, Germany
e-mail: guetlich@uni-mainz.de
<http://ak-guetlich.chemie.uni-mainz.de>*

Molecular magnetism with all its fascinating facets like spin crossover, intramolecular magnetic interactions, valence tautomerism, mixed valency has gained increasing interest in recent years among chemists and physicists due to their potential towards applications in devices and sensors. Particularly iron(II) coordination compounds exhibiting thermal, optical and pressured-induced spin state switching properties have been subject to extensive studies. Among the various physical techniques that are commonly employed to investigate such coordination compounds, like magnetic susceptibility measurements, optical and vibrational spectroscopy, X-ray and neutron diffraction techniques, thermodynamic analysis, Mössbauer spectroscopy has developed to an extremely powerful tool in following the phase transitions initiated by external perturbations like variation of temperature, light irradiation or application of pressure. The hyperfine interactions that can be extracted from a Mössbauer spectrum yields information on electronic and molecular structure, valence state and magnetic properties. This will be demonstrated on selected examples exhibiting

- thermal spin crossover in iron coordination compounds,
- light-induced creation of long-lived metastable spin states (LIESST effect),
- spin crossover under applied pressure,
- interplay of spin crossover and antiferromagnetic coupling in dinuclear iron complexes,
- mixed-valency, transition between “trapped” and “delocalized” states,
- ferromagnetic coupling in large-spin clusters,
- electron transfer, magnetic transition and photomagnetism in Prussian Blue analogue systems.

Suggested reading may be found in:

- [1] P.Gütlich, A. Hauser, and H. Spiering, *Angew. Chem.Int. Ed. Engl.* 33 (1994) 2024.
- [2] P. Gütlich, A. Hauser, H. Spiering in: *Inorganic Electronic Structure and Spectroscopy Vol. II*, A.B.P. Lever, E.I. Solomon eds., John Wiley & Sons, 1999, pp. 575.
- [3] P. Gütlich, Y. Garcia, H. Spiering, in: “Magnetism: Molecules to Materials IV“, J.S. Miller, M. Drillon (eds.), Wiley-VCH, Weinheim/Germany, 2003.
- [4] P. Gütlich, H.A. Goodwin (eds.), “Spin Crossover in Transition Metal Compounds”, *Topics in Current Chemistry*, Volumes 233, 234, 235, Springer, Heidelberg, Berlin, 2004.
- [5] V. Ksenofontov, G. Levchenko, S. Reiman, P. Gütlich, A. Bleuzen, V. Escax and M. Verdaguer, *Phys. Rev. B* 68 (2003) 024415.
- [6] A.B. Gaspar, V. Ksenofontov, M. Seredyuk, P. Gütlich, *Coord. Chem. Rev.* 249 (2005) 2661.
- [7] P. Gütlich, A. B. Gaspar, Y. Garcia, V. Ksenofontov, *Comptes Rendus Chimie* 10 (2007) 21.



Integral Low-Energy Electron Mössbauer Spectroscopy (ILEEMS): Methodology and Recent Applications in Material Research

E. De Grave¹, V.G. de Resende¹, C. Van Cromphaut¹, Ch. Laurent², L. Presmanes² and R.E. Vandenberghe¹

¹*Department of Subatomic and Radiation Physics, University of Gent, Proeftuinstraat 86, B-9000Gent, Belgium*

²*CIRIMAT, CNRS/UPS/INPT, LCMIE, Université Paul-Sabatier, Bât. 2R1, 118 route de Narbonne, 31062 Toulouse cedex 9, France*

ILEEMS is a variant of Mössbauer spectroscopy (MS) in which predominantly the low-energy electrons, $E < \sim 10$ eV, emitted by the probe nuclei in the absorber are counted as a function of source velocity. These low-energy electrons are, among others, Auger and “shake-off” electrons that are created in the decay process of the probe nucleus immediately after resonant absorption and excitation by an incident γ -quantum. As a consequence of their low energy, these electrons’ origin lies within a very thin surface layer with thickness of an estimated five nanometers. ILEEMS using ^{57}Fe is as sensitive as transmission MS and the more common emission variants such as CEMS. Consequently, ILEEMS, in combination with conventional transmission MS, is a technique that provides information about the surface of Fe-containing substances.

In a first part of this contribution, we describe the design of a home-made ILEEMS instrument allowing the temperature of the investigated sample to be varied continuously between 77 K and room temperature. In essence, the instrument is the same as a spectrometer for transmission, except that detector and “absorber” are contained within a same vacuum ($\sim 5 \cdot 10^{-5}$ mbar) chamber. The electrons are counted by a single channel electron multiplier (“channeltron”). The efficiency for detecting the low-energy electrons is optimized by applying a bias voltage of ~ 150 V between the sample and the detector input. The ILEEMS instrument has been successfully applied in a few earlier studies reported by the present authors.

The second part of this contribution will deal with a selection of results obtained recently. In particular, the following items will be covered:

- Thin films of hematite, $\alpha\text{-Fe}_2\text{O}_3$, grown by RF sputtering on glass substrates in Ar plasma; ILEEMS measurements, carried out in the temperature range between 80 to 330 K for a number of $\alpha\text{-Fe}_2\text{O}_3$ films with different thickness, will be presented and discussed; this research is focussed on the behaviour of the Morin transition, *i.e.*, the reorientation of the Fe^{3+} spins from the [111] crystallographic direction at low temperature, to the (111) basal plane at high temperature; the influence of thickness, sputtering parameters and of post-deposition annealing is being examined.
- Carbon nanotubes grown by CCVD method in various Fe-containing oxide matrices; the results have shown that the characteristics of the top surface layers as far as the presence of $\alpha\text{-Fe}$, $\gamma\text{-Fe-C}$ and Fe_3C nanoparticles is concerned, are very often significantly different as compared to what is observed for the bulk by transmission MS.
- Freshly synthesized 2 XRD-line and 6 XRD-line ferrihydrite, $5\text{Fe}_2\text{O}_3 \cdot 9\text{H}_2\text{O}$, to compare the results with those obtained earlier for similar samples that had aged for a very long time.

Interesting findings concerning the surface properties of mentioned systems were obtained. ILEEMS studies so far have remained of a rather exploring nature, but the results encourage more systematic research in this and related fields.

Low-Frequency Raman Scattering in Materials Research

M. Ivanda¹, D. Ristić¹, K. Furić¹, S. Musić¹, M. Ristić¹, M. Gotić¹, G. Štefanić¹, Z. Crnjak Orel², M. Bitenc², M. Montagna³, M. Ferrari⁴, A. Chisaera⁴, Y. Jestin⁴

¹Ruđer Bošković Institute, Bijenicka 54, 10000 Zagreb, Croatia, ²National Institute of Chemistry, Hajdrihova 19, SI-1001 Ljubljana, Slovenia, ³Dipartimento di Fisica, Università di Trento, CSMFO group, via Sommarive 14, I-38050 Povo, Trento, Italy, ⁴CNR-IFN Istituto di Fotonica e Nanotecnologie, CSMFO group, via Sommarive 14, I-38050 Povo, Trento, Italy

The intention of this talk is to describe non-specialists with a basic understanding of the information low-frequency Raman Spectroscopy (LFRS) may provide when this characterization tool is applied to nanomaterials like oxide and semiconductor nanoparticles, nanoceramics and nanocomposite glassy materials. A short theoretical introduction of the Lamb theory on the vibrations of elastic spheres will be described for the free nanoparticles as well as for the nanoparticles embedded in matrix where the proper account on the boundary conditions should be taken.

The spherical case is well understood – the normal modes of the sphere are divided into torsional and spheroidal and, experimentally, have been measured in various situations, from very small structures like globular proteins or inorganic nanoparticles to very large structures like planets. Surprisingly the Lamb theory explains the observed results with reasonable agreement. The application of the Lamb theory will be illustrated by the LFRS measurements on different powder samples: TiO₂, SnO₂, ZnO and CdS. The effects of sintering of nanoparticles will be described with the ZrO₂ nanoparticles doped with Sn.

For the nanoparticles embedded in matrix a theoretical treatment of polarization-dependent low-frequency off-resonant Raman scattering which establishes a relation between the particle size, the frequencies, and the widths of various phonons, taking into account the matrix influence on the vibrational spectrum and on its damping, will be presented. In order to distinguish the confined acoustic phonons from the glass background, the spectra have been compared with those obtained from the base material, which does not contain nanoparticles. Polarized and depolarized scattering from confined acoustic phonons was distinctly resolved near the laser line and polarized inner particle modes were observed. The material-dependent generalized form of this analysis enables one to use it for any given combination of particle and matrix materials. A good agreement between the experimental and the theoretical results will be illustrated by TiO₂, CdS_xSe_{1-x}, and HfO₂ nanoparticles in glass matrix. The nanoparticle sizes and even sizes distribution obtained from Raman scattering agree well with those obtained from transmission electron microscope proving the LFRS to be a simple, fast and reliable method for the size distribution measurements. By inverse procedure, starting from the Raman spectra and known particles size distribution, the mean sound velocities of longitudinal and transverse phonons of nanoparticles could be deduced, providing LFRS to be unique technique for determination of the sound velocities in nanoparticles.

[1] H. Lamb, Proc. London Math. Soc. 13 (1882) 189.

Raman Spectroscopy and Molecular Imaging of Living Cells

Hiro-o Hamaguchi

Department of Chemistry, School of Science, The University of Tokyo, Bunkyo-ku, Tokyo 113-0033, Japan
E-mail: hhamai@chem.s.u-tokyo.ac.jp

Recent developments of Raman microspectroscopy have enabled *in vivo* imaging of living cells with high time, space and molecular specificity. We have recently discovered in a living fission yeast (*S. Pombe*) cell a Raman band that sharply reflects the metabolic activity of mitochondria. We called it the “Raman spectroscopic signature of life” [1, 2]. We have also found [3] that this signature disappears concomitantly with a sudden appearance of a particle called “dancing body” in a vacuole of a budding yeast (*S. cerevisiae*) cell and that the appearance of the dancing body inevitably results in an eventual cell death. Changes in organelles accompanying this spontaneous cell death process have been traced with excellent molecular specificity by time-resolved Raman imaging (Figure 1). We are now able to discuss the bio-activities of a single living cell from the viewpoint of structural chemistry.

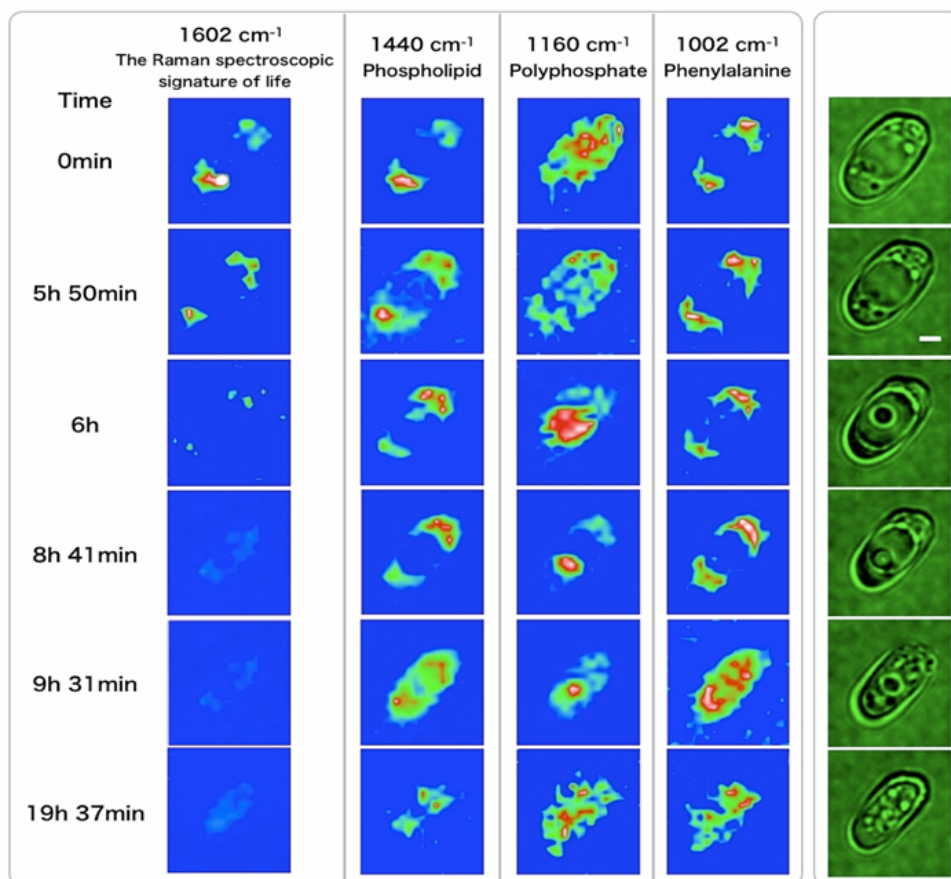


Figure 1: Raman-image tracing of cell death

- [1] Y.-S. Huang, T. Karashima, M. Yamamoto, T. Ogura, H. Hamaguchi, *J. Raman Spectrosc.* 35 (2004) 525-527.
 [2] Y.-S. Huang, T. Karashima, M. Yamamoto, H. Hamaguchi, *Biochemistry* 44 (2005) 10009-10019.
 [3] Y. Naito, A. To-e, H. Hamaguchi, *J. Raman Spectrosc.* 36 (2005) 837-839.

Search for Missing Conformers: Matrix-Isolation SWAT

R. Fausto

*Department of Chemistry, University of Coimbra
P-3004-535 Coimbra, Portugal*

Spatial arrangements of atoms in a molecule, in particular molecular conformations and conformational flexibility, are the ultimate factor determining the qualities of the substances, from physical properties to chemical reactivity and biological activity. For substances where different conformational states may exist in equilibrium, the composition of the conformational mixture must then be precisely known in order to understand and predict their physicochemical behavior. On the other hand, since the chemistry of different conformers can be quite distinct (for instance, even simple molecules like formic acid, which has just two conformers, can react very differently depending on the conformation adopted by the molecule: the *cis* conformer photolyses preferentially to $\text{CO}_2 + \text{H}_2$, whereas the *trans* isomer reacts to yield mainly $\text{CO} + \text{H}_2\text{O}$ [1]), the possibility of changing, in an efficient and simple way, the conformational composition of a given chemical species, appears as a powerful tool to its fundamental study and can be forecast to have many possible practical uses.

Matrix-isolation FTIR spectroscopy has been shown to be one of the most powerful techniques to study molecular conformational preferences and also the specific properties of the different conformational forms. Different methods and strategies have been developed that give this technique nowadays unique capabilities for the conformational study of a substance. These include, for instance, the possibility of isolating a single conformer of a molecule which has several dozens of states significantly populated in the gas phase, and, contrarily to what happens if we try to achieve a similar result by crystallizing the compound, the unique conformer isolated in the cryogenic inert matrix and made available for spectroscopic examination is free of any strong intermolecular interaction [2]. Or, alternatively, the possibility of creating new conformational states, whose observation in other experimental conditions is practically impossible or extremely difficult to achieve [3,4].

In this lecture, I shall discuss some of the most effective approaches used in matrix-isolation FTIR spectroscopy to access elusive conformational species (Matrix-Isolation Special Weapons And Tactics, ☺) and provide several illustrative examples resulting from our own experience in this field of research.

- [1] L. Khriachtchev, E.M.S. Maçôas, M. Pettersson and M. Räsänen, *J. Am. Chem. Soc.* 124 (2002) 10994.
- [2] I.D. Reva, A.J. Lopes Jesus, M.T.S. Rosado, R. Fausto, M.E. Eusébio and J.S. Redinha, *Phys. Chem. Chem. Phys.* 8 (2006) 5339.
- [3] I.D. Reva, S.G. Stepanian, L. Adamowicz and R. Fausto, *Chem. Phys. Lett.* 374 (2003) 631.
- [4] S. Breda, I.D. Reva, L. Lapinski and R. Fausto, *Phys. Chem. Chem. Phys.* 6 (2004) 929.

From Femtosecond Dynamics at the Molecular Level to Breast Tissue Diagnosis by Raman Spectroscopy

H. Abramczyk^{1,2}, I. Placek¹, B. Brożek-Pluska¹, J. Surmacki¹, Z. Morawiec³, M. Tazbir³

¹*Institute of Applied Radiation Chemistry, Laboratory of Laser Molecular Spectroscopy, Technical University of Łódź, The Faculty of Chemistry, Poland, 93-590 Łódź, Wroblewskiego 15, phone: (+ 48 42) 631-31-88, 631-31-75, email: abramczyk@mitr.p.lodz.pl,* ²*Max-Born-Institute, Max-Born-Str. 2A, 12489 Berlin, Germany email: abramczyk@mbi-berlin.de,* ³*Kopernik Hospital, Oncology Ward, Łódź, Poland*

Life and disease are incredibly complex biochemical processes that occur in molecules, macromolecular structures, cells, and tissues. On the molecular level one can notice, however, that the basic mechanisms of living matter are a manifestation of just a few essential factors. One of them is the mechanism of photostability. Moreover, there is a common agreement that photoselection is one of the most important factors determining the evolution of life on the Earth at the early stages of high exposure to harmful UV radiation due to lack of the protective ozone layer. The same factors seem to decide about the health-disease balance in living creatures. Molecular structures responsible for harvesting of the solar energy must be photostable and resistant to photo-induced chemical changes. If the photostability protection and reparation mechanisms fail to any reason the processes that drive the normal tissue into abnormal one are strongly enhanced leading to the symptoms of disease. To answer the questions about the photostability we have to understand mechanisms of energy dissipation upon an optical excitation. There is a common agreement that such channels are provided by special features of the potential energy surfaces called sometimes the conical intersections. Some time ago we proposed the mechanism that leads to intersection (or decrease in the energy difference) of excited-state potential energy surface with the ground state. The mechanism is related to the coupling between the excited state (electronic or vibrational) and the vibrational modes. This mechanism leads to very fast and effective channel of radiationless energy dissipation of optical excitation. We provided spectroscopic evidence that the proposed mechanism seems to be universal both for simple species such as solvated electrons, H-bond systems, and biologically important proteins such as bacteriorhodopsin [1] as well as for electron transfer processes in photodynamic photosensitizers. Recently we have presented the results on the normal and malignant breast tissue by Raman spectroscopy. The results support the importance of photostability for the health-disease processes [2]. This paper presents new biological tissue results based on Raman spectroscopy and demonstrates its power as diagnostic tool with the key advantage in breast cancer research. The results presented here demonstrate the ability of Raman spectroscopy to accurately characterize cancer tissue and distinguish between normal, malignant and benign types. To the best of our knowledge, this paper is one of the most statistically reliable reports (70 patients) on Raman spectroscopy-based diagnosis of breast cancers among the world women population.

[1] H. Abramczyk, *Femtosecond primary events in bacteriorhodopsin*, J. Chem. Phys. 120 (2004) 11120-11132.

[2] H. Abramczyk, B. Brożek-Pluska, K. Kurczewski, Z. Morawiec, M. Tazbir, *From femtosecond dynamics to breast tissue diagnosis by Raman spectroscopy and Raman Imaging*, ISRPS Bulletin 20 (2008) 37.

Acknowledgment

The support from MEXC-CT-2006-042630 and Nr3 T11E 04729 projects are acknowledged.

FT-IR Spectroscopy of Cells, Tissues, and Body Fluids

D. Naumann, H. Fabian, P. Lasch

Robert Koch-Institute, Nordufer 20, 13353 Berlin, Germany, naumannD@rki.de

The last 15 years have witnessed the development of modern infrared spectroscopy into a useful biodiagnostic tool for the analysis of cells, tissues, and body fluids. Dedicated technologies have evolved for rapidly discriminating between diverse microbial species and strains, testing single cells, and identifying various disease states in humans and animals, to give some examples.

Particularly interesting applications came up by means of light microscopes coupled to infrared spectrometers and the advent of dedicated infrared spectroscopic imaging instrumentation. Infrared microscopes equipped with modern focal plane array detectors allow nowadays routinely the parallel collection of thousands of pixel spectra across microscopic areas of biological samples. This imaging technology can be used for routine automatic histological segmentation and imaging of tissue structures without any requirement of dyes or molecular probes. Recent biomedical studies have proven that FT-IR imaging can be used to objectively differentiate benign from malignant histopathological structures in various tissues. Basically the same experimental set-up is also well suited to integrate the fundamental tasks of microbiological analysis, namely detection, enumeration, and differentiation of micro-organisms in one single apparatus.

Due to its high brilliance, IR-synchrotron light coupled into high-quality FT-IR microscopes has been used for spectral mapping of single cells at a spatial resolution near the diffraction limit of mid-infrared light. Using this technology, the accumulation of the pathogenic prion protein (PrP^{Sc}) in neuronal cells, to give an example, could be traced *in situ* by detecting deposition areas of the misfolded prion protein.

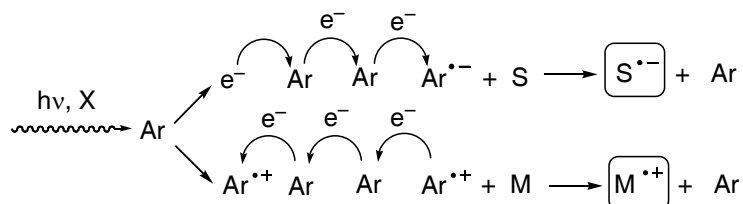
The problem of extracting the characteristic information from the typically very complex, fingerprint-like infrared signatures of biological samples is generally addressed by applying bioinformatic techniques such as factor-, cluster-, linear discriminant analysis, and artificial neural networks together with so-called "feature extraction" algorithms. Examples will be given on the characterization of micro-organisms, analysis of single eukaryotic cells, imaging of diseased human tissues, and disease recognition from body fluids that highlight the new possibilities of modern biomedical infrared spectroscopy.

Electronic and Vibrational Spectroscopy of Radical Ions in Matrices

T. Bally

Department of Chemistry, University of Fribourg, Chemin du Musée 9, CH-1700 Fribourg, Switzerland.

Exposing Ar matrices to X-irradiation leads to the creation of electron-hole pairs of which a few always manage to separate and migrate through the matrix, presumably in the form of polarons, until they are scavenged by added guest molecules that have a lower ionization potential (M) or a higher electron affinity than Ar (S), respectively



The above represents a generally applicable strategy to generate radical cations and (in some cases) radical anions of precursors S or M that can be evaporated without decomposition in Ar which is transparent from ca 180 nm to 100 cm^{-1} [1]. The electronic and vibrational spectra that can be recorded from such samples contain much valuable information that allows to draw conclusions about their electronic and molecular structure.

Among the recent examples from our work that will be discussed are the radical ions of carbon chains $\text{R}-(\text{C}\equiv\text{C})-\text{R}$ which show very rich and interesting spectra, the radical cations and anions of p-benzoquinone, and some surprising rearrangements of hydrocarbons on oxidation.

I will also discuss the role of quantum chemistry, on the one hand as a spectroscopic modelling tool and on the other hand as a tool to understand the reactivity of radical ions, to elucidate and complement the results from the above experiments.

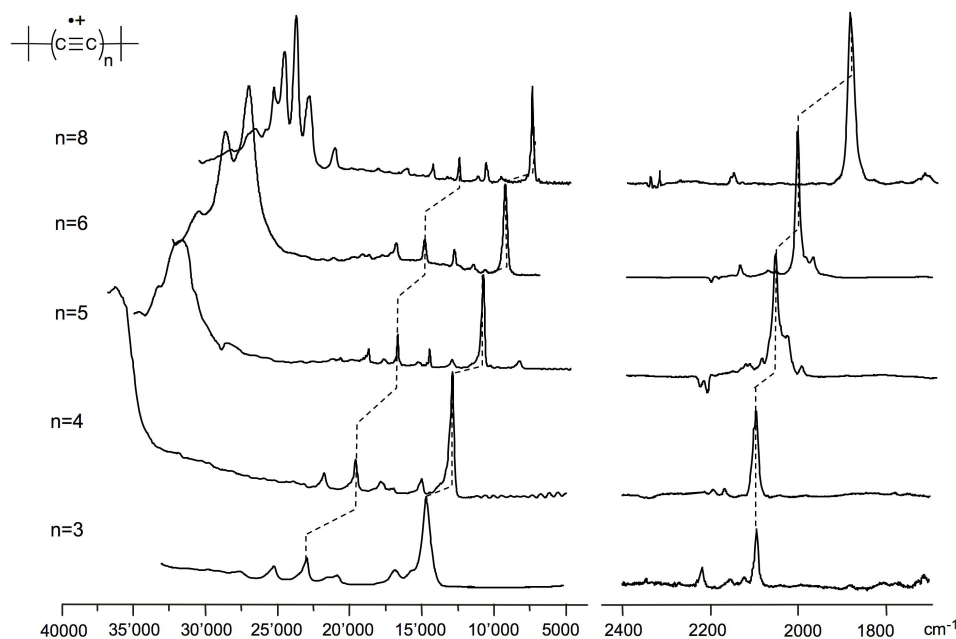


Figure 1: Electronic and vibrational spectra of polyene radical cations in Ar.

[1] T. Bally "Matrix Isolation" in "Reactive Intermediate Chemistry" R.A. Moss, M.S. Platz and M. Jones eds; Wiley-Interscience Hoboken, N.J. 2004.

Spectroscopic and Theoretical Parameters in Predicting Hydrogen Bond Strength, Conformational Stability and Chemical Reactivity

B. Galabov

*Department of Chemistry, University of Sofia,
Sofia 1164, Bulgaria*

Molecular parameters derived from theoretical computations as well as characteristic vibrational group frequencies were employed to quantify the reactivity of molecules for the process of hydrogen bonding and for reactions of organic compounds. The theoretical quantities include: atomic charges derived using different approaches, the Parr electrophilicity index, and the atomic electrostatic potential. The predictive power of these theoretical parameters is compared with the performance of experimental indices and quantities, such as the Hammett constants and shifts in vibrational group frequencies. A number of relationships are derived between the energies of hydrogen bond formation as well as the activation energies of chemical reactions and some of the quantities considered. It is shown for the first time that the atomic electrostatic potential can be employed as a reliable local reactivity index. A number of interactions are studied: hydrogen bonding of aliphatic carbonyl and nitrile derivatives, solvolitic reactions of amides and esters, S_N2 reaction in aliphatic systems, hydrogen transfer reaction in phenols. It is shown that the variations of the carbonyl stretching frequency in amides and esters are linearly linked to theoretically estimated activation energies for reactions of these systems. Such relationships are in some cases absent if higher order effects (such as Fermi resonance) are present in the spectra. It is found that vibrational frequency shifts upon complexation correlate excellently with theoretically estimated energies of hydrogen bonding in series of structurally related molecules.

The conformational stabilities of aromatic amides and thioamides are rationalized in terms of fluctuations of atomic charges as well as variations in characteristic group frequencies. A perfect linear dependence is found between the magnitudes of rotational barriers in series of acetanilides and the $\nu(C=O)$ frequency shifts. The origin of the higher barriers of rotation in thioamides than in amides is definitively established.

- [1] B. Galabov, P. Bobadova-Parvanova, *J. Phys. Chem. A* 103 (1999) 6793.
- [2] B. Galabov, S. Ilieva, B. Hadjieva, E. Dincheva, *J. Phys. Chem. A* 107 (2003) 5854.
- [3] B. Galabov, D. Cheshmedzhieva, S. Ilieva, B. Hadjieva, *J. Phys. Chem. A* 108 (2004) 11457.
- [4] B. Galabov, S. Ilieva, H. F. Schaefer III, *J. Org. Chem.* 71 (2006) 6382.

The Globalization of Science and its Impact on the Transition Countries in Europe

Henry H. Mantsch

Science Advisor, Department of Foreign Affairs, Global Partnership Program, Ottawa, K1A 0G2, Canada

I am pleased to address a subject here that is generally not given a lot of room at molecular spectroscopy meetings, which, however, does greatly affect the spectroscopists themselves.

There is no doubt that the globalization of science breaks up all national borders. In the new, knowledge-based society, the international pool of scientists provides the basis for our economic well-being. However, no single country, large or small, has a monopoly on new ideas. The mobility of scientists, which is a consequence of the globalization of science, requires that we replace the old expressions of “brain drain” and “brain gain” with that of “brain circulation”. Yet, in today’s world the international science community faces a dichotomy: The creation of new knowledge is international and done by individuals (the Nobel Prize being the ultimate recognition), whereas the translation of intellectual goods into material products and the generation of new consumer goods is national. This means that international cooperation in science and competition in the global marketplace is a delicate balancing act.

Coming from someone who has played 40+ years in the “molecular spectroscopy” sandbox and now is acting as Senior Science Advisor to the Canadian Government, this talk aims to stimulate scientists from so called “emerging countries” to seek an active role on the world stage of science, and particularly encourage young scientists to embark upon a career in molecular spectroscopy, an enabling modality that cuts across the traditional fields of physics, chemistry, biology or medicine.

INVITED LECTURES

Vibrational Assignment of 1,4-(*E,E*)-Distyrylbenzene Supported by Isotopic Shifts and DFT Calculations

Z. Meić and T. Hrenar

Department of Chemistry, Faculty of Science, University of Zagreb, Horvatovac 102A, HR-10000 Zagreb, Croatia

Isotopic substitution is taking for decades a crucial role in assigning vibrational spectra. Among various possible isotopic substitutions, by far the most important one for vibrational analysis is the substitution of hydrogen (H) by deuterium (D). Theoretical values of vibrational frequencies depend upon force constants determined at the minimum of the adiabatic potential energy surface but this leads to a theoretical ratio of frequencies of XH and XD normal modes that always exceed experimental values, anharmonicity being responsible for a lower value of this ratio.

A model molecule of 1,4-(*E,E*)-distyrylbenzene (DSB, Figure 1.) was chosen to make a rather complex but reliable vibrational analysis. In order to make a thorough assignment of its infrared and Raman spectra, isotopic shifts in vibrational spectra of its isotopologues were investigated.

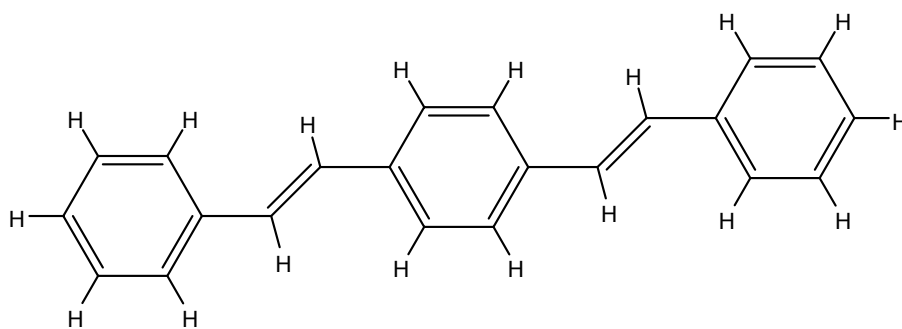


Figure 1: 1,4-(*E,E*)-distyrylbenzene (DSB)

Experimental trends were endorsed by DFT calculations coupled with the Pulay's scaling scheme and using vibrational perturbation theory. Further investigation of potential energy distribution among the normal modes is presented and comparison is made with the spectra of *trans*-stilbene, the precursor of the *para*-phenylenevinylene (PPV) series [1].

[1] T. Hrenar, R. Mitrić, Z. Meić, H. Meier, and U. Stalmach, *J. Mol. Struct.* 661-662 (2003) 33-40.

Multidimensional Quantum Dynamics of Large Amplitude Motion

Nađa Došlić

Department of Physical Chemistry, Ruđer Bošković Institute, 10000 Zagreb, Croatia

The permanent interest for hydrogen bonds and hydrogen-bond dynamics that has been present in the molecular science community for many decades is motivated both by fundamental questions regarding the quantum tunneling phenomenon and by practical questions concerning dynamical and structural properties of H-bonded systems.

In terms of theory, the quantum nature of the hydrogen and the strong coupling between its motion and that of the molecular framework lead to multidimensional quantum dynamics. In this lecture various aspects of the theoretical simulation of vibrational, vibrational-rotational-tunneling, and ultrafast IR spectra will be discussed. First, on the specific example of carboxylic acid dimers we will show how the broad stationary absorption OH-stretching bands can be understood in terms of multidimensional anharmonic vibrational dynamics [1]. Next, the focus will be on the hydrogen tunneling motion and methods capable of predicting ground and vibrationally excited states tunneling splittings will be presented [2, 3]. We will address questions such as: Does vibrational excitation promotes H-tunneling? Which molecular motions are important for the understanding tunneling motion in the formic acid dimer? At the end ultrafast IR-laser driven H-bonds dynamics will be addressed and simulations of vibrational energy redistributions will be presented.

- [1] I. Matanović, N. Došlić, *Chem. Phys* 338 (2007) 121-126.
- [2] I. Matanović, N. Došlić, O. Kühn, *J. Chem. Phys.* 127 (2007) 014309.
- [3] I. Matanović, N. Došlić, B. R. Johnson, *J. Chem. Phys.* in print.

Intrinsic Particle Properties in Infrared Spectra of Aerosols

Ruth Signorell

*Department of Chemistry, University of British Columbia, 2036 Main Mall,
Vancouver, BC V6T 1Z1, Canada*

The study of icy aerosol particles with sizes in the submicron range is a highly interdisciplinary subject at the junction of nanosciences, atmospheric physics, and astrophysics. The microphysics of aerosol clouds in the atmospheres of planets and their moons, such as ammonia clouds on Jupiter and Saturn or methane aerosols on Titan, is currently very much in the focus of the scientific community. Particularly broad interest has been sparked by the recent Cassini-Huygens mission to Saturn's moon Titan, which has illuminated the importance of methane clouds for Titan's weather and their analogy to the role of water ice clouds in Earth's atmosphere.

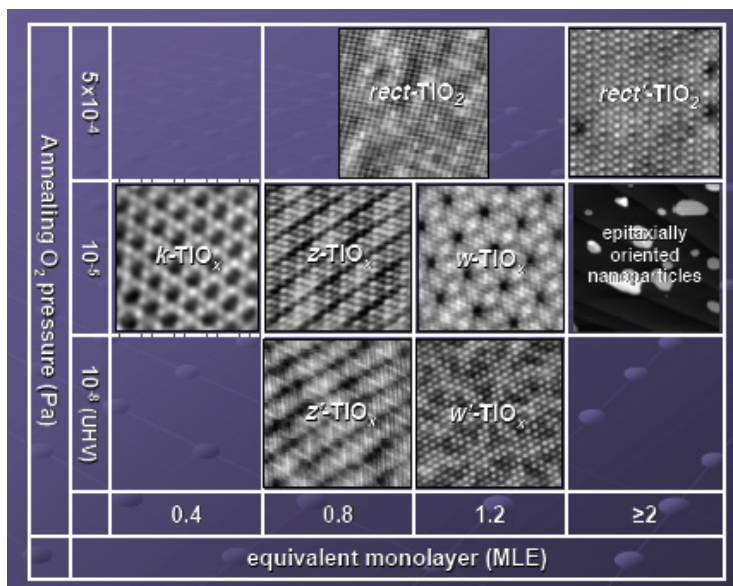
The present contribution focuses on the influence of intrinsic particle properties, such as shape, size or architecture, on infrared optical properties of icy aerosol particles. Intrinsic particle properties manifest themselves in mid-infrared extinction spectra by modifying the structure of vibrational bands. We ultimately aim at unravelling the microscopic origin of the characteristic patterns found in the spectra of these weakly bound molecular aggregates. To this end we compare our experimental results with different model calculations combining molecular dynamics simulations with vibrational quantum dynamics.

TiO_x Nanostructures on Metallic Substrates: a Combined Spectroscopic and Theoretical Investigation

Gaetano Granozzi

Department of Chemical Sciences and CNR-INFN Research Unit, University of Padova, Padova, Italy

Nanolayers of ordered TiO_x films on Pt(111) and Pt(110) surface are prepared by reactive evaporation of Ti in oxygen. In the case of the Pt(111) substrate, varying the Ti dose and the annealing conditions (i.e. temperature and oxygen pressure), several different long-range ordered phases were obtained (see Table below) [1]. They were characterized by means of LEED, synchrotron based valence and core photoemission experiments and STM [1-4].



The experimental analysis show that these wide range of structures can be rationalized in two main groups i.e. three stoichiometric phases with an O-Pt interface and four substoichiometric one-monolayer phases, with Ti at the interface with the substrate. For six of these seven phases a structural model, in agreement with the experimental result and supported by DFT calculation, has been proposed [5-7].

In the case of the Pt(110) substrate, a stoichiometric TiO₂ nanolayer has been prepared and it has been found that the model which best fits all the experimental LEED, XPD and STM data can be obtained from an anatase (001) bilayer by sliding the upper monolayer by half a unit cell along the [1-10] substrate direction. The principal interest of stoichiometric phases is related to their structure that is the same of some TiO₂ nanosheets obtained by exfoliation of 3D stacked titanates. These nanosheets show innovative properties and are presumably the building blocks of titania nanotubes [8].

On the other hand three different substoichiometric TiO_x phases have been used as templates for growing ordered and monodispersed Au nanocluster arrays [9].

- [1] F. Sedona, G.A. Rizzi, S. Agnoli, F.X. Llabrés i Xamena, A. Papageorgiou, D. Ostermann, M. Sambì, P. Finetti, K. Schierbaum and G. Granozzi, *J. Phys. Chem. B* 109 (2005) 24411.
- [2] F. Sedona, S. Agnoli and G. Granozzi, *J. Phys. Chem. B* 110 (2006) 15359.
- [3] P. Finetti, F. Sedona, G.A. Rizzi, U. Mick, F. Sutara, M. Svec, V. Matolin, K. Schierbaum and G. Granozzi, *J. Phys. Chem. C* 111 (2007) 869.
- [4] F. Sedona, M. Sambì, L. Artiglia, G.A. Rizzi, A. Vittadini, A. Fortunelli, G. Granozzi, *J. Phys. Chem. C* 112 (2008) 3189.
- [5] G. Barcaro, F. Sedona, A. Fortunelli and G. Granozzi, *J. Phys. Chem. C* 111 (2007) 6095.
- [6] F. Sedona, G. Granozzi, G. Barcaro and A. Fortunelli, *Phys. Rev. B* 77 (2008) 115417.
- [7] Y. Zhang, L. Giordano, G. Pacchioni, A. Vittadini, F. Sedona, P. Finetti, G. Granozzi, *Surf. Sci.* 601(2007)3488.
- [8] T. Sasaki et al., *J. Am. Chem. Soc.* 118 (1996) 8329.
- [9] F. Sedona, S. Agnoli, M. Fanetti, I. Kholmanov, E. Cavaliere, L. Gavioli and G. Granozzi, *J. Phys. Chem. C* 111 (2007) 8024.

Mössbauer Spectroscopy with High Velocity Resolution: New Possibilities in Biomedical Research

M.I. Oshtrakh¹, V.A. Semionkin², O.B. Milder³, E.G. Novikov²

¹Faculty of Physical Techniques and Devices for Quality Control and ²Faculty of Experimental Physics, Physical-Technical Department and ³Radio-Technical Department, Ural State Technical University – UPI, Ekaterinburg, 620002, Russian Federation

Mössbauer spectroscopy is a useful technique for biomedical research [1–4]. Majority of previous Mössbauer spectra of various samples including biological subjects were measured in 512 channels or less. However, biomedical applications of Mössbauer spectroscopy need the high quality measurement using high stable and precise spectrometer with higher velocity resolution. This requirement is determined in part by importance of Mössbauer study of small variations of hyperfine parameters of iron-containing biomolecules in normal and pathological cases (see [5]), by necessity to decrease experimental error in determination of Mössbauer hyperfine parameters and to reach more reliable fit of complicated Mössbauer spectra. In the present work we consider preliminary results of some biomedical applications of Mössbauer spectroscopy with high velocity resolution.

Study of iron-containing proteins, ferritin and its pharmaceutically important model compound Imferon, chicken liver and spleen tissues and iron-containing pharmaceutical products was made using high precision, sensitive and stable spectrometer SM-2201 with the saw-tooth velocity reference signal. Mössbauer spectra were measured in transmission geometry with moving absorber and registration in 4096 channels with further presentation in 1024 and 2048 channels by consequent summation of four or two neighboring channels, respectively, and in 4096 channels. Improvement of velocity resolution, for instance, revealed clear differences of hyperfine parameters for Imferon and ferritin (Fig. 1). Different fit of ferritin Mössbauer spectra measured with various velocity resolutions using superposition of four quadrupole doublets was shown (Fig. 2). Obtained results demonstrate that increase of velocity resolution in Mössbauer spectroscopy raises spectra quality and possibilities of this technique in biomedical research.

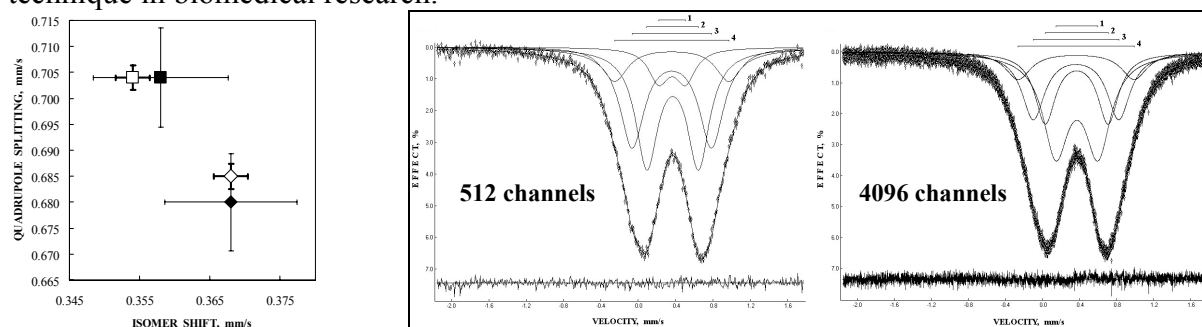


Fig. 1 (left): Differences of the hyperfine parameters for one quadrupole doublet fit of Mössbauer spectra of Imferon (\square) and ferritin (\diamond) presented in 2048 channels (experimental error is ± 0.0024 mm/s) in comparison with those presented in 512 channels (\blacksquare and \blacklozenge , respectively; experimental error is ± 0.0096 mm/s).

Fig. 2 (right): Comparison of four doublets fit for Mössbauer spectra of ferritin measured in 512 and 4096 channels with the same statistics. $T = 295$ K.

[1] M.I. Oshtrakh, *Hyperfine Interact.* 66 (1991) 127–140.

[2] M.I. Oshtrakh, *J. Mol. Struct.* 480-481 (1999) 109-120.

[3] M.I. Oshtrakh, *Hyperfine Interact.* 165 (2005) 313–320.

[4] M.I. Oshtrakh, *J. Radioanal. Nucl. Chem.* 269 (2006) 407–415.

[5] M.I. Oshtrakh, *Spectrochim. Acta, Part A: Molec. and Biomolec. Spectroscopy* 60 (2004) 217–234.

Acknowledgment

This work was supported in part by the Russian Foundation for Basic Research (grant No 06–08–00677-a).

Advances in Noble Gas Chemistry

M. Räsänen

Laboratory of Physical Chemistry, Department of Chemistry, PO Box55, FIN-00014 University of Helsinki, Finland

The family of noble-gas containing hydrides of common structure HNgY amounts 23, including the first argon molecule, HArF [1]. Both inorganic and organic Y fragments are involved in such molecules, the organic acetylenic and diacetylenic species being recently synthesized [2-5]. These examples suggest that new such molecules will be found in future. The HNgY molecules have very characteristic properties as suggested by computational methods: linear bonding is involved around the noble gas atom, the (HNg)⁺Y⁻ structure plays a central role in bonding, and they possess very high dipole moments. The practical consequences of the properties of these molecules are versatile, and will be discussed. First, the H-Ng stretching absorption intensity is quite large, and the formation of the HNgY molecules upon hydrogen atom mobilisation can be monitored with great sensitivity yielding reliable measures for the H/D mobility [6]. Secondly, exceptionally large matrix site effects due to their large dipoles are found for these molecules, giving tools to probe experimentally the local environments of the embedded molecules [7]. Selective and reversible light control of formation of HXeCC radical will be discussed [8].

- [1] L. Khriachtchev, M. Pettersson, N. Runeberg, J. Lundell, and M. Räsänen, *Nature (London)* 406 (2000) 874.
- [2] L. Khriachtchev, H. Tanskanen, J. Lundell, M. Pettersson, H. Kiljunen, and M. Räsänen, *J. Am. Chem. Soc.* 125 (2003) 4696.
- [3] V. I. Feldman, F. F. Sukhov, A. Y. Orlov, and I. V. Tyulpina, *J. Am. Chem. Soc.* 125 (2003) 4698.
- [4] H. Tanskanen, L. Khriachtchev, J. Lundell and M. Räsänen, *J. Chem. Phys.* 125 (2006) 074501.
- [5] L. Khriachtchev, A. Lignell, H. Tanskanen, J. Lundell, H. Kiljunen and M. Räsänen, *J. Phys. Chem. A* 110 (2006) 11876-11885.
- [6] L. Khriachtchev, H. Tanskanen, M. Pettersson, M. Räsänen, V. Feldman, F. Sukhov, A. Orlov, and A. F. Shestakov, *J. Chem. Phys.* 116 (2002) 5708.
- [7] L. Khriachtchev, M. Pettersson, A. Lignell, and M. Räsänen, *J. Am. Chem. Soc.* 123 (2001) 8610.
- [8] L. Khriachtchev, H. Tanskanen and M. Räsänen, *J. Chem. Phys.* 124 (2006) 181101.

ORAL & POSTER CONTRIBUTIONS

1. MOLECULAR STRUCTURE

Infrared Spectroscopy of Liquid Water-*N,N*-dimethylformamide Mixtures

Nikola Biliškov, Goran Baranović

Department of Organic Chemistry and Biochemistry, Ruđer Bošković Institute, Bijenička c. 54, HR-10002 Zagreb, Croatia; e-mail: nbilis@irb.hr

The imaginary molar polarisability spectra, $\alpha_m''(\tilde{\nu})$, of mixtures of water with *N,N*-dimethylformamide (DMF) over the entire composition range ($0 \leq x_{DMF} \leq 1$) at 25 °C were obtained between 4000 and 700 cm^{-1} by use of calibrated multiple reflection attenuated total reflection (ATR) technique [1]. The composition dependent molar fractions of water bonded and DMF bonded OH groups, together with water bonded and free carbonyl groups, were determined from the integral intensities C_{OH} , C_{CO} , C_{NCO} , the areas under the $\nu(OH)$, $\nu(CO)$ and $\delta(NCO)$ bands, respectively, in the $\tilde{\nu}\alpha_m''(\tilde{\nu})$ spectra. The obtained results are compared with thermodynamic properties of the system [2], and with results of molecular dynamics simulations [3, 4].

Behaviour of molar fraction of OH species indicates presence of stable aggregates of H₂O molecules over the large composition interval, $0.2 < x_{DMF} < 0.9$. Aggregates of DMF, in which methyl groups are placed apart from surrounding water, are established in the interval $x_{DMF} < 0.2$. For higher x_{DMF} , DMF molecules orient in random orientation, giving rise to dipole-dipole pairs. Only in the interval $x_{DMF} > 0.9$ water is dispersed into small clusters of water surrounded by DMF molecules.

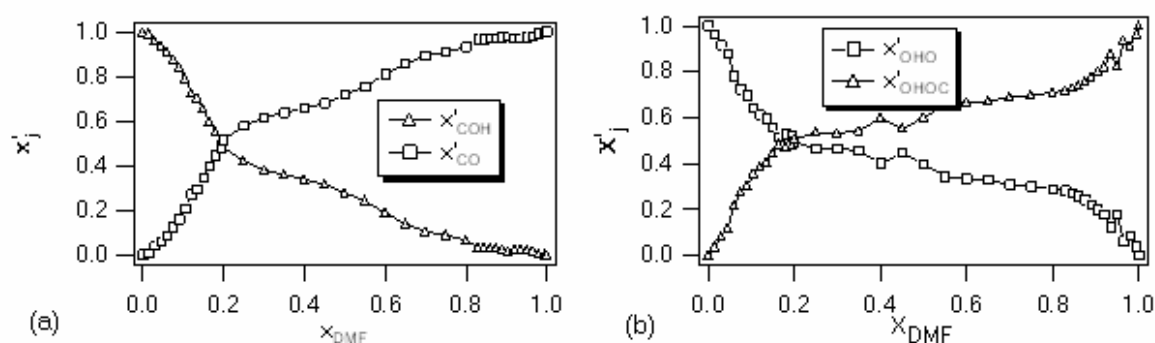


Fig. 1: (a) Fraction of DMF CO oscillators which are free, x'_{CO} , and hydrogen bonded with water molecule, x'_{COH} , against molar fraction of DMF, x_{DMF} . (b) Fraction of water OH oscillators which are hydrogen bonded with another water molecule, x'_{OHO} , and with DMF, x'_{OHOC} , against molar fraction of DMF, x_{DMF} .

- [1] J.E. Bertie, Z. Lan, J. Phys. Chem. B 101 (1997) 4111.
 [2] M. Cilense, A.V. Benedetti, D.R. Vollet, Thermochim. Acta 63 (1983) 151.
 [3] L. Zoranić, R. Mazighi, F. Sokolić, A. Perera, J. Phys. Chem. C 111 (2007) 15586.
 [4] Y. Lei, H. Li, H. Pan, S. Han, J. Phys. Chem. A 107 (2003) 1574.

Vibrational Spectra of $K_2[O(HgSO_3)_3]$ Containing a New Anionic Metallo-Oxonium Complex with a OHg_3 Core

D.K. Breiting¹, G. Brehm², M. Weil³, S. Baumann³

¹*Institute of Inorganic Chemistry, University of Erlangen-Nürnberg, Egerlandstr. 1, D-91058 Erlangen, Germany,*

²*Institute of Physical Chemistry, University of Erlangen-Nürnberg,*

³*Institute of Chemical Technologies and Analytics, Vienna University of Technology, A-91060 Vienna, Austria*

Continuing recent work on sulfite complexes of mercury [1] we studied the systems HgX_2/K_2SO_3 and HgO/K_2SO_3 in aqueous solutions and the solid phases formed therein. In the latter case after dissolution of HgO in hot K_2SO_3 solution and cooling crystals of the new compound $K_2[O(HgSO_3)_3]$ were obtained. This compound crystallises in $Pnma$ with $Z = 4$, with arrangement of both cations and anions into alternating layers parallel to (010) [2]. The distance between equivalent layers along the stacking direction b is about 10 Å. The anionic layers adopt the symmetry $(a:c) \cdot m \cdot 2_1 - p2_1ma$ (cf. [2]), $i e$ a two-dimensional non-centrosymmetric subgroup of $Pnma$, which is isomorphic to point group $C_{2v} - mm2$. The flat pyramidal anions $[O(HgSO_3)_3]^{2-}$ with a central OHg_3 core occupy crystallographic sites with symmetry $C_s - m$, but they are close to $C_{3v} - 3m$.

A factor group/unit-cell group analysis (UGA) for the whole cell-content was performed, also partly in internal coordinates. The UGA predicts much more species of specific vibrations, e.g. $\nu_s(SO_3)$ or $\delta_s(SO_3)$, than found in both IR and Raman spectra. Further, most of the IR and Raman bands show near-coincidence of the wavenumbers and complementary intensities. The conclusion is that correlation coupling between the anionic layers and splitting of their vibrations does not take place anymore, due to the large inter-layer distance. Therefore, the symmetry analysis can be restricted to one of the two layers in the unit-cell. This means that only correlation coupling between two anions within one layer is still considered. Because of the non-centrosymmetry of the layers the mutual exclusion rule is no longer valid.

Assignment of the vibrations $\nu_{as}(SO_3)$ (at least six components around 1150 cm^{-1} in both spectra), $\nu_s(SO_3)$ (quartet in IR around 994 cm^{-1}), $\delta_s(SO_3)$ and $\delta_{as}(SO_3)$ of the S-coordinated sulfite ligands is straightforward. As for the vibrations of the OHg_3 core data for the mercurio-oxonium cations $[O(HgCl)_3]^+$ [4], $[O(HgCH_3)_3]^+$ [5] and $[O(HgOH)(HgI)_2]^+$ [6] are of limited value as these are planar, in contrast to the pyramidal anion under discussion (average angle $\alpha_{av}(Hg-O-Hg)$ 110.8°). Isolated medium to strong bands at 560 cm^{-1} in both spectra are to be assigned to $\nu_{as}(OHg_3)$, without doubt, but the position of $\nu_s(OHg_3)$ in the low-frequency part of the Raman spectrum, dominated by the very strong $\nu(Hg-S)$ bands around 230 cm^{-1} , is less evident. An approximate calculation of $\nu_s(OHg_3)$ using $\nu_{as}(OHg_3)$ and the above average bond angle in OHg_3 gives 285 cm^{-1} . In fact, there is an appropriate medium-to-weak, sharp band at 267 cm^{-1} . But one has to be aware that $\nu_s(OHg_3)$ (species A_1 under idealised symmetry $C_{3v} - 3m$) strongly mixes with $\nu(Hg-S)$, the bending mode $\delta(O-Hg-S)$ (about 100 cm^{-1}), and even the rocking mode $\rho(SO_3)$ (318 cm^{-1}) of the same symmetry species.

[1] M. Weil, D.K. Breiting, G. Liehr, J. Zürgb, Z. Anorg. Allg. Chem. 633 (2007) 429-434.

[2] M. Weil, S. Baumann, D.K. Breiting, Acta Crystallogr. C64 (2008) i35-i37.

[3] A.V. Shubnikov, V.A. Koptsik, Symmetry in Science and Art, Plenum Press, New York-London, 1974, p. 195.

[4] W.P. Griffith, J. Chem. Soc. A 1969, 2270.

[5] J.H.R. Clarke, L.A. Woodward, Spectrochim. Acta 23 A (1967) 2077-2087.

[6] K. Köhler, G. Thiele, D.K. Breiting, Z. Anorg. Allg. Chem. 418 (1975) 79-87.

Acknowledgment

Thanks to S. Hofmann, Institute of Inorganic Chemistry, Erlangen, for measuring IR spectra.

Crystal Structure and Vibrational Spectroscopy of Mixed-valence $[\text{Cu}(\text{biz})_2][\text{Cu}_2\text{Br}_4]$ Complex Formed After *In Situ* Oxidation of 2-Hydrazino-2-Imidazoline to Bisimidazoline (biz) by Copper(II) Ions

Piotr Drożdżewski¹, Maria Kubiak²

¹ Faculty of Chemistry, Wrocław University of Technology, Norwida 4/6, 50-373 Wrocław, Poland

² Faculty of Chemistry, University of Wrocław, F. Joliot-Curie 14, 50-383 Wrocław, Poland

An attempt to obtain the copper(II) complex with 2-hydrazino-2-imidazoline resulted in unexpected, mixed valence $[\text{Cu}(\text{biz})_2][\text{Cu}_2\text{Br}_4]$ complex, where biz denotes *in situ* formed bisimidazoline (biz). The presence of the last compound and copper(I) definitely suggests the redox reaction between 2-hydrazino-2-imidazoline and copper(II) ions.

The X-ray investigation of the obtained complex shows that both ions are centrosymmetric and nearly flat. In the $[\text{Cu}(\text{biz})_2]^{2+}$ cation, all copper(II)-nitrogen bonds are equal making the metal coordination environment as a regular rectangle. In the complex anion, the copper(I) is bonded to two bridging and one terminal Br atoms located close to positions characteristic for sp^2 hybridization of the metal atom. The electrostatic interactions between both complex ions are enhanced by $\text{N}-\text{H}\cdots\text{Br}$ hydrogen bonds which arrange the crystal building units in two sets of ribbons expanding along the (111) and (1-11) directions (Fig. 1).

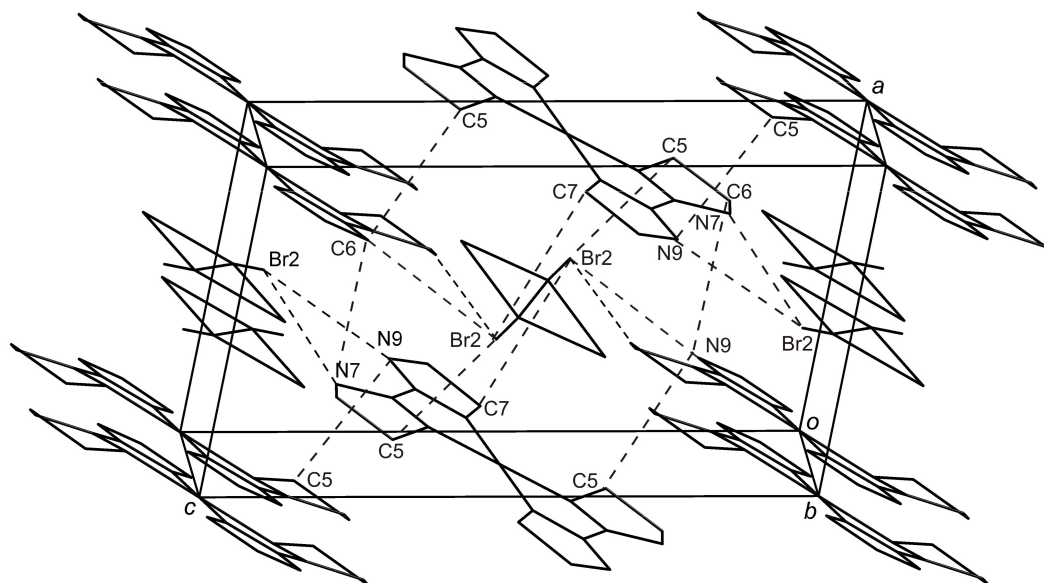


Fig. 1: Crystal packing and hydrogen bonding system in the $[\text{Cu}(\text{biz})_2][\text{Cu}_2\text{Br}_4]$ complex.

Special attention has been focused on the vibrational spectra of the obtained complex, especially on the far-IR region where the metal-ligand vibrations are expected. For the unambiguous detection of the IR bands resulting from mentioned vibrations, the metal isotope ($^{63}\text{Cu} - ^{65}\text{Cu}$) band shifts were measured. Similar shifts were reproduced in theoretical, DFT calculated spectra and applied as an additional criterion in the correlation between observed bands and computed normal vibrations. Full assignment of $[\text{Cu}(\text{biz})_2]^{2+}$ and $[\text{Cu}_2\text{Br}_4]^{2-}$ normal vibrations and corresponding IR and Raman bands was made in terms of potential energy distribution.

Fourier Transform Microwave Spectra of Isobutylmercaptan and Normal Butylmercaptan

Yoshiyuki Kawashima¹, Yugo Tanaka¹, Akinori Sato¹, Eizi Hirota²

¹Department of Applied Chemistry, Faculty of Engineering, Kanagawa Institute of Technology, Atsugi, Kanagawa 243-0292, JAPAN,

²The Graduate University for Advanced Studies, Hayama, Kanagawa 240-0193, JAPAN

In order to obtain information on stable conformations and internal motions of isobutylmercaptan (2-methyl-1-propanethiol) and normal butylmercaptan, we have analyzed their rotational spectra observed by Fourier transform microwave spectroscopy. We may expect that isobutylmercaptan exists in five stable rotational isomers, that is, there are two configurations around the $\text{CH}(\text{CH}_3)_2 - \text{CH}_2\text{SH}$ bond referred to as *gauche* and *trans* and more than two minima on the internal rotation of the SH group, whereas more than ten stable conformations will be present in normal butylmercaptan.

We scanned the frequency region from 3.7 to 25 GHz using a sample of isobutylmercaptan diluted in Ar to 0.5%. We assigned the observed spectra to two *gauche* forms, G_1 and G_2 , and one *trans* form T_1 : *a*-, *b*-, and *c*-type transitions for the G_1 and *a*- and *c*-type transitions for the G_2 , whereas no *b*-type transitions were observed for G_2 . The G_1 spectra were found stronger than those of G_2 . These observations could be explained by the S-H and C-S bond moments. All the three types of transitions were detected for T_1 , of which all *b*-type lines appeared as doublets with the spacing of about 13 MHz. This splitting was ascribed to the tunneling of the SH group through a potential barrier on the *a*-*c* plane between two equivalent minima.

Ab initio calculations at the MP2/6-311++G(*d*, *p*) level demonstrated that for isobutylmercaptan there were two minima for the *gauche* form at the CCSH dihedral angle of 72.2° and 298.1°, which corresponded to G_1 and G_2 , as observed, whereas two equivalent minima at the CCSH dihedral angles of either 73.8° or 286.2° were for the *trans* form, in good accord with the experimental observations.

For normal butylmercaptan we scanned the frequency region from 5 to 20 GHz. We assigned *a*-type transitions from $J = 2 \leftarrow 1$ to $J = 7 \leftarrow 6$ to four conformers and *b*- and *c*-type transitions to two of the four conformers. The spectra of these two were of second and third strongest among others. The rotational constants and inertial defects, $I_{cc} - I_{aa} - I_{bb}$, which were derived from the observed spectra, indicated that the conformer with the strongest spectra had a planar *trans* heavy-atom skeleton, but perhaps the SH hydrogen out of the skeletal plane. Most of the *a*-type $K = 1$ transitions of this species were found split into doublets. The second and third conformers probably take *gauche* conformations with respect to the $\text{CH}_2 - \text{CH}_2\text{SH}$ bond and the fourth again a *gauche* one to the $\text{CH}_2 - \text{CH}_2\text{CH}_2\text{SH}$ bond.

Polarized IR Spectroscopy and Transition Dipole Moment Determinations in Structural Studies

G. Keresztury¹, M. Rogojerov², T. Sundius³

¹Chemical Research Center, HAS, P.O. Box 17, H-1525 Budapest, Hungary, kergabor@chemres.hu;

²Institute of Organic Chemistry, Bulgarian Academy of Sciences, 1113 Sofia, Bulgaria;

³Department of Physical Sciences, University of Helsinki, P.O. Box 64, FIN-00014 Helsinki, Finland

The measurement of transition dipole orientation of IR active vibrations is known to be a very efficient tool for enhancing the reliability of vibrational assignments. Such information can be extracted from polarized IR spectra of oriented samples, i.e. from infrared linear dichroism (IR-LD) measurements. Spectral studies of oriented single crystals are met with a number of technical difficulties. In contrast, solute alignment in a nematic liquid crystal as anisotropic solvent has made the method applicable to a wide range of compounds. In this case the measured dichroic ratios (R_i) of IR absorption bands can be converted to orientational parameters (K_i) that can be used for the calculation of the absolute value of the angles that the transition moments (TMs) make with the preferred direction of molecular orientation called “long molecular axis”. There is a sign ambiguity in this determination, that can be lifted by joint evaluation of experimental and theoretically predicted, calculated spectral parameters.

Several examples of the application of this approach will be given demonstrating its effectiveness in elucidating some details of band assignment and in making structural inferences in molecules with *planar* (C_s) symmetry [1-4]. Determination of the average orientation of such molecules and their experimental transition moment directions is facilitated by corrections introduced through comparison with quantum chemically calculated vibrational transition moments of two strong absorption bands. According to the accumulated evidence, TM directions calculated by DFT (B3LYP/6-31G* or higher level) for medium intense or stronger bands agree with experimental data within 5-10°, i.e. they are much more reliable than what can be anticipated from simple structural considerations.

Further improvement in performance of the method is expected from DFT calculations using the Integral Equation Formalism - Polarizable Continuum Model (IEF PCM) taking into account the effect of anisotropic medium on the solute molecules. This is being tested by asymmetric deuteration of naphthalene (1-D and 2-D-derivatives), where the D_{2h} symmetry of the force field is retained and the observed and calculated changes in TM directions are due to the mass effects alone.

The proposed IR spectroscopic methodology may provide helpful reference data to increase the accuracy of determination of the direction of electronic transitions in a number of dye molecules used in liquid crystal display technology. Finally, other experimental IR-LD approaches encountered in spectroscopic literature (alignment of molecules in stretched polymers; alignment of crystallites in LC suspension; and alignment of biomolecules in helium nanodroplets by strong electric field) will be shortly described and characterized concerning their usefulness in studies of molecular structure.

[1] G. Keresztury, F. Billes, M. Kubinyi and T. Sundius, *J. Phys. Chem. A* 102 (1998) 1371-1380.

[2] M. Rogojerov, G. Keresztury and B. Jordanov, *J. Mol. Structure* 661-662 (2003) 227-234.

[3] M. Rogojerov, G. Keresztury and B. Jordanov, *Spectrochim. Acta Part A* 61 (2005) 1661-1670.

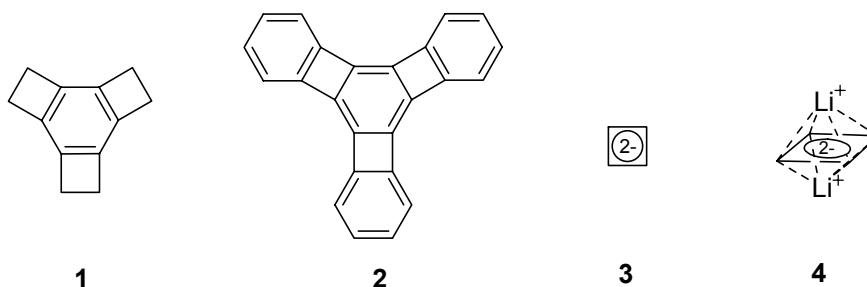
[4] G. Keresztury and M. Rogojerov, *Bulgarian Chem. Comm.* 37/4 (2005) 327-331.

Spatial Magnetic Properties of Trisannelated Benzenes and Cyclobutadiene Dianion Derivatives Subjected to Aromaticity

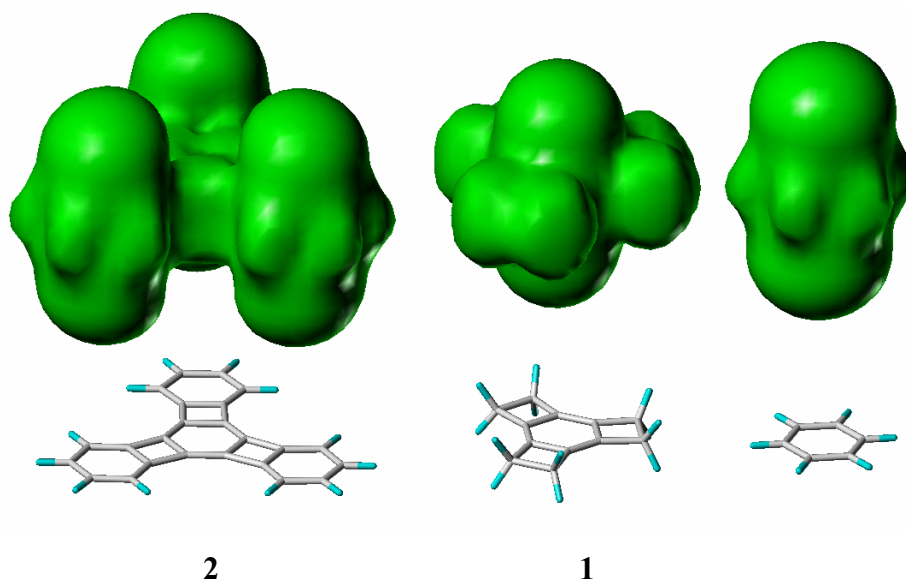
Erich Kleinpeter and Andreas Koch

Universität Potsdam, Chemisches Institut, Karl-Liebknecht-Str. 24-25, D-14476 Potsdam (Golm), FR Germany
e-mail: kp@chem.uni-potsdam.de

The spatial magnetic properties (Through Space NMR Shieldings - *TSNMRS*) of tricyclobutabenzene (*TCBB*) **1**, of $[4n]$ annuleno $[4n+2]$ annulene **2**, of the cyclobutadiene dianion **3** and of the corresponding 2Li^+ complex **4** have been *ab initio* calculated by the GIAO perturbation method employing the Nucleus Independent Chemical Shift (*NICS*) concept of Paul von Ragué Schleyer [1], and visualized as Iso-Chemical Shielding Surfaces (*ICSS*) of various size and direction.



TSNMRS values can be successfully employed to quantify and visualize the (anti)aromaticity of the compounds studied and to discuss the influence of Li^+ complexation to cyclobutadiene dianion **4** on *planar 4c,6e* or *three-dimensional 6c-6e* aromaticity.



[1] P. von R. Schleyer, C. Maerker, A. Dransfeld, H. Jiao, N.J.R. von E. Hommes, *J. Am. Chem. Soc.* 118 (1996) 6317.

Infrared Spectra of $\text{CH}_3\text{Cl} + \text{H}_2\text{O}$ and $\text{NO} + \text{H}_2\text{O}$ Isolated in Solid Neon at 5 K

Lahouari Krim, Nadia Dozova, Esmail Alikhani and Nelly Lacombe

LADIR, UMR 7075, Bat F74, Case 49, Université Pierre et Marie Curie, 4, Place Jussieu, F-75252 Paris Cedex 05, France

The infrared spectra of $\text{H}_2\text{O} + \text{X}$ ($\text{X} = \text{NO}, \text{CH}_3\text{Cl}$) isolated in solid neon at low temperature have been investigated. The $\text{H}_2\text{O} + \text{NO}$ and $\text{H}_2\text{O} + \text{CH}_3\text{Cl}$ systems are remarkable due to its propensity to form $\text{X-H}_2\text{O}$, $(\text{X})_2\text{-H}_2\text{O}$, $\text{X-(H}_2\text{O)}_2$ and $\text{X-(H}_2\text{O)}_n$, and IR spectroscopy reveals a variety of phenomena far from being fully understood.

$\text{CH}_3\text{Cl} + \text{H}_2\text{O}$

Detailed vibrational assignments are made on the observed spectra of water and deuterated water engaged in the $\text{CH}_3\text{Cl:H}_2\text{O}$ and $\text{CH}_3\text{Cl:(H}_2\text{O)}_2$ complexes. With the use of MP2 calculations, geometrical and vibrational properties of each complex have been estimated.

The $\text{CH}_3\text{Cl:H}_2\text{O}$ complex is found to have a cyclic structure, where the chlorine atom is weakly bonded to one of the hydrogen atoms of water, while oxygen atom is weakly bonded to one of the hydrogen atoms of CH_3Cl . The calculated and observed vibrational frequencies of partially deuterated complex established that only $\text{CH}_3\text{Cl:DOH}$ species is formed with hydrogen bonding to D. This is a consequence of the preference for HDO to form a deuterium bonding rather than a hydrogen bonding complex.

High concentration studies of water and subsequent annealing leads to formation of the 1:2 $\text{CH}_3\text{Cl:H}_2\text{O}$ complex. The complex has a cyclic form with two hydrogen-bonds: first between the chlorine atom and one of the hydrogens of H_2O PA of water dimer, and second between the oxygen atom of the H_2O PD of water dimer and one hydrogen of CH_3Cl . Each molecule of H_2O and CH_3Cl acts as a proton acceptor and as proton donor. The binding energy of $\text{CH}_3\text{Cl:(H}_2\text{O)}_2$ is 49.2 kJ/mol while that of water dimer is 19.9 kJ/mol and that of $\text{CH}_3\text{Cl:H}_2\text{O}$ is only 12.7 kJ/mol.

$\text{NO} + \text{H}_2\text{O}$

Low concentration studies (0.01 % - 0.2 %), H/D isotopic substitution and subsequent annealing leads to the formation of $\text{NO-H}_2\text{O}$, $\text{NO-D}_2\text{O}$ and NO-HDO complexes. A detailed vibrational analysis of the deuterated species shows two sets of 1:1 molecular complexes labelled α and β . Only the structure of the $\text{NO-D}_2\text{O}(\beta)$, $\text{NO-HDO}(\beta)$ species where the water deuterium and the NO nitrogen are weakly bonded, has been predicted by DFT calculations. While in the $\text{NO-H}_2\text{O}(\alpha)$, $\text{NO-HDO}(\alpha)$ and $\text{NO-D}_2\text{O}(\alpha)$ case, the potential surface has been explored systematically at the B3LYP level but no stable species reproducing the experimental data is found. This shows that the structure of the observed $\text{NO-H}_2\text{O}(\alpha)$ and $\text{NO-D}_2\text{O}(\alpha)$ complexes results from columbic attractions between the water and NO and is stabilized only in neon matrix.

FT-IR and FT-Raman Spectroscopic Studies of 2-Methylpyrazine Tetracyanonickelate Benzene Clathrates: $M(C_5H_6N_2)Ni(CN)_4 \cdot C_6H_6$ ($M = Mn, Cd, Co$ or Ni)

G.S. Kürkcüoğlu¹, S. Aksay², I. Kavlak³

¹Eskişehir Osmangazi University, Faculty of Arts and Science, Department of Physics, 26480 Eskişehir, Turkey

²Anadolu University University, Faculty of Science, Department of Physics, 26470 Eskişehir, Turkey

³Eskişehir Osmangazi University, Graduate School of Sciences, 26480 Eskişehir, Turkey,

In this study, four new metal (II) 2-methylpyrazine tetracyanonickelate benzene clathrates, $M(C_5H_6N_2)Ni(CN)_4 \cdot G$ (where $C_5H_6N_2 = 2$ -methylpyrazine; $M = Mn, Cd, Co$ or Ni ; $G = \text{benzene}$) are synthesized and characterized by elemental analysis, FT-IR, FT-Raman spectroscopy and thermal analysis techniques. The FT-IR and FT-Raman spectra of $Cd(C_5H_6N_2)Ni(CN)_4 \cdot C_6H_6$ are given in Fig. 1a and 1b, respectively. The spectral features suggest that the compounds are similar in structure to the Hofmann-type two dimensional coordination polymer compounds, formed with $Ni(CN)_4^{2-}$ ions bridged by $M(2mpz)^{2+}$ cations. Several polynuclear $Ni(CN)_4^{2-}$ compounds have been reported, however to our knowledge, no tetracyanonickelate (II) compound with 2-methylpyrazine ligand has been reported. The spectral data show that the positions of almost all bands due to the guest molecule remain practically unchanged on enclathration. The C, H, N analyses were carried out for all the compounds were found to fit the proposed formulae well. The experimental results are in agreement with the proposed formulae (Table 1). Thermal behaviours of these compounds are followed using TG and DTA techniques. TG, DTG and DTA curves of one of the studied compounds, $Cd(C_5H_6N_2)Ni(CN)_4 \cdot C_6H_6$, is shown in Fig. 1c. The first decomposition stage corresponds to benzene molecule, subsequently, release of ligand molecule takes place to form bimetallic cyanides as intermediates and the final decomposition stage is the decomposition of cyanide to yield the respective metals. On the basis of the FT-IR, FT-Raman spectroscopic, thermal and elemental analysis results, we propose that in the case of the $M-Ni-2mpz-Bz$ clathrates, the 2mpz molecules are bound to metal atoms of the adjacent layers of $[M-Ni(CN)_4]_{\infty}$ as bidentate ligand, depending on the coordination properties of the acceptor side.

Table 1: Elemental Analyses of the $M(C_5H_6N_2)Ni(CN)_4 \cdot C_6H_6$

Compounds	Found (Calc.) %		
	C	H	N
$M(C_5H_6N_2)Ni(CN)_4 \cdot C_6H_6$	41.43 (41.01)	3.28 (3.10)	23.58 (23.95)
$Cd(C_5H_6N_2)Ni(CN)_4 \cdot C_6H_6$	39.92 (39.34)	3.16 (3.30)	20.03 (19.12)
$Co(C_5H_6N_2)Ni(CN)_4 \cdot C_6H_6$	42.93 (42.79)	2.68 (2.77)	22.66 (22.68)
$Ni(C_5H_6N_2)Ni(CN)_4 \cdot C_6H_6$	41.95 (40.64)	2.81 (2.55)	23.45 (23.69)

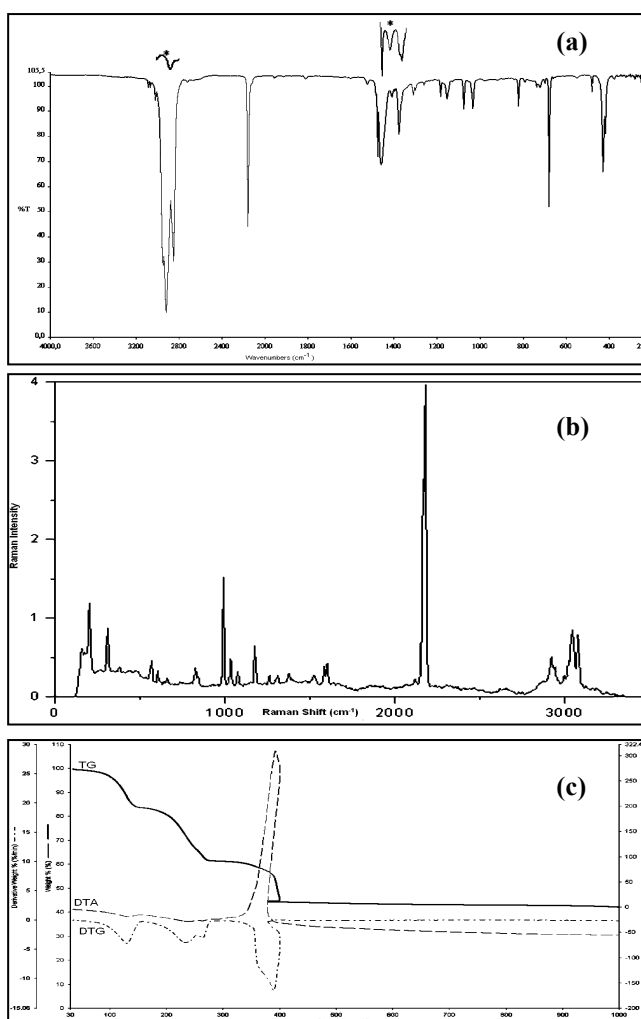


Fig. 1: FT-IR (a) FT-Raman (b) spectra and TG, DTG and DTA curves (c) of the $Cd(C_5H_6N_2)Ni(CN)_4 \cdot C_6H_6$.

Spectroscopic Studies of the Electronic Excited States of Pyridine-d₀ and -d₅, 2-Fluoro- and 3-Fluoropyridine, and 1,3-Benzodioxan

Jaan Laane, Praveen Boopalachandran, Kathleen McCann, and Martin Wagner

Department of Chemistry, Texas A&M University, College Station, TX 77843-3255;

E-mail: laane@mail.chem.tamu.edu

The infrared and ultraviolet absorption spectra and the Raman spectra of vapor-phase pyridine, pyridine-d₅, 2-fluoropyridine, and 3-fluoropyridine have been recorded and analyzed. The UV spectrum of pyridine is shown below. DFT calculations for each molecule have also been carried out for both the ground and S₁(n,π*) electronic excited states. Vibrational assignments for the S₁(n,π*) states have been made and compared to the ground state. In the electronic excited state the molecules become much less rigid and floppy. Investigation of the ν₁₈ out-of-plane ring-bending mode for pyridine-d₀ and -d₅ allowed their potential energy function to be determined, and this demonstrated that pyridine is quasi-planar with a barrier to planarity of 3 cm⁻¹ in the S₁(n,π*) state. The decrease from 403 cm⁻¹ (S₀) to 59.5 cm⁻¹ (S₁) for the ν₁₈ vibration of pyridine reflects the decreased rigidity in the excited state.

The jet-cooled laser induced fluorescence and UV absorption spectra of 1,3-benzodioxan have also been analyzed. Many of the vibronic levels in the S₁(π,π*) state were assigned for the three low-frequency out-of-plane ring motions, and these were used to better understand the structure in the electronic excited state. Theoretical calculations predict barriers to planarity of 9.3 kcal/mole and 8.0 kcal/mole for the S₀ and S₁(π,π*) states, respectively, and the experimental data are consistent with these values.

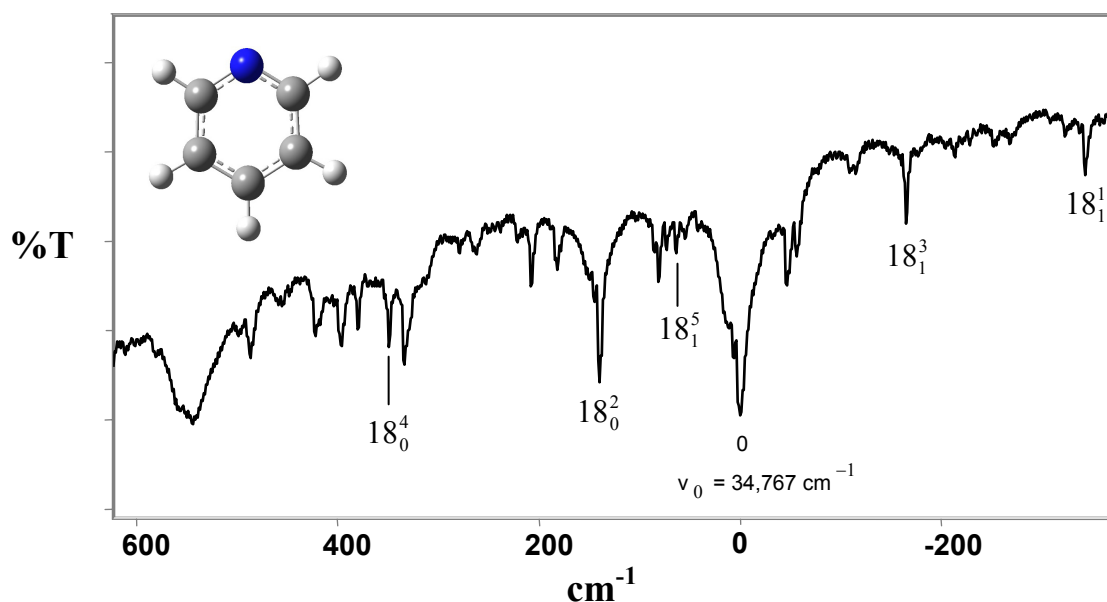


Fig. 1: The UV spectrum of pyridine.

Structures of Vitamin B₁₃ Complexes with Transition Metal Ions. The Role of Unusual Cu(II)··· π Interaction and Hydrogen Bonds.

Danuta Michalska¹, K. Hernik¹, R. Wysokiński¹, W. Zierkiewicz¹, A. Pietraszko²

¹Faculty of Chemistry, Wrocław University of Technology, Wybrzeże Wyspiańskiego 27, 50-370 Wrocław,
²Institute of Low Temperature and Structural Research, Polish Academy of Science, Okólna 2, 50-950 Wrocław,
Poland

Vitamin B₁₃ (orotic acid, 6-carboxyuracil) is indispensable in biological systems as a key precursor in the biosynthesis of pyrimidine nucleotides of nucleic acids. Recently, this compound has attracted growing attention in medicine as the carrier for certain metal ions. Metal orotates can be used in curing syndromes related with metal ion deficiencies and also as promising therapeutic agents for cancer and heart diseases. Vitamin B₁₃ is also interesting multidentate ligand. The coordination chemistry of orotic acid was investigated in numerous papers, however our studies with single crystal X-ray diffraction, vibrational spectroscopy and quantum chemistry methods have provided new insights into the binding properties of this ligand [1,2].

The recently reported crystal structure of *cis*-[Cu(orotate)(NH₃)₂] has revealed the presence of the unusual Cu²⁺··· π binding force, in this complex [1]. The coordination sphere of the Cu²⁺ ion can be described as a (4+1+1) geometry, where one axial position is occupied by the carbonyl oxygen atom of the neighboring uracil ring, but the other axial site, surprisingly, is located at the C=C double bond of another uracil ring. This is the first case, where the π -type interaction between the chelated Cu²⁺ ion and the C=C bond is clearly demonstrated. Thus far, only the Cu⁺-benzene complex has been detected [3]. In this work, we have explored the nature of this interaction by the spectroscopic and theoretical studies using the *ab initio* second-order Moller-Plesset perturbation (MP2) and density functional (B3LYP) methods with several basis sets. According to our results, the dispersion energy is very important in this non-covalent Cu²⁺··· π binding interaction.

The role of hydrogen bonds has also been investigated. In *cis*-[Pt(orotate)(NH₃)₂], a new cisplatin analogue, strong intramolecular N-H···O hydrogen bond may have significant influence on the biological activity of this compound. In [Ni(H₂O)₆][Horotate]₂·2H₂O, the [Ni(H₂O)₆]²⁺ cation is associated with two trans-related [Horotate]⁻ anions only *via* hydrogen bonds between the oxygen carboxylate atoms and the water molecules coordinated to the metal cation. In all these complexes, the orotate ligands are also engaged in “base-pairing” hydrogen bonds between the planar uracil rings. This indicates that Vitamin B₁₃ can form complementary hydrogen bonds with the adenine residues in many biological molecules, and it may serve as the carrier molecule, which transports metal ions through the cell membranes.

[1] D. Michalska, K. Hernik, R. Wysokiński, B. Morzyk-Ociepa, A. Pietraszko, *Polyhedron* 26 (2007) 4303.

[2] R. Wysokiński, K. Hernik, R. Szostak, D. Michalska, *Chem. Phys.* 333 (2007) 37.

[3] F. Meyer, F.A. Khan, P.B.J. Armentrout, *J. Am. Chem. Soc.* 117 (1995) 9740.

The Hydrogen Bonding in Life and Society

Cemil Öğretir

*Eskişehir Osmangazi University, Faculty of Arts & Sciences, Chemistry Department,
Meşelik Campus, Eskişehir, Turkey
E-mail: cogretir@ogu.edu.tr*

After giving a brief historical review on hydrogen bonding some hydrogen bonding controlled phenomena of life and society will be summarized. The importance and inevitability of H-bonding processes will be stressed on. The strength and the length of intermolecular and intramolecular hydrogen bonding which are measured experimentally and/or calculated theoretically will be discussed. The differences between nitrogen, oxygen, sulfur and halogen hydrogen bonding will be covered. Some selected cases of our work will be presented [1].

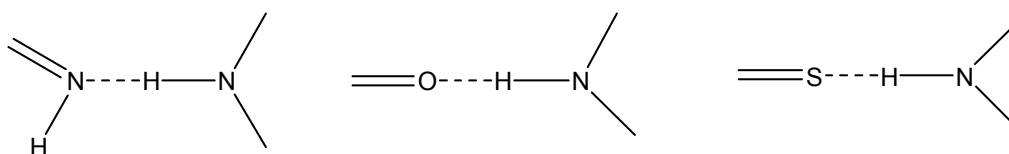


Figure 1: Some representative hydrogen bonding examples

[1] A.R. Katritzky, A.T. Soldatenkov, A.F. Pozharskii: *Heterocycles in life and society*, John Wiley & Sons, New York, 1997, England.

C-H...F Hydrogen Bonds as the Organising Force in F-substituted α -phenyl Cinnamic Acid Aggregates Studied by the Combination of FTIR Spectroscopy and Computations

B. Tolnai, J.T. Kiss, K. Felföldi, I. Pálinkó

Department of Organic Chemistry, University of Szeged, Dóm tér 8, Szeged, H-6720 Hungary

It has been found previously that short-range ordering prevails in α -phenyl cinnamic acid (*E*- or *Z*-2,3-diphenyl propenoic acid) solutions (the organising force is strong O-H...O hydrogen bonds), while weak (aromatic)C-H...O hydrogen bonds are responsible for long-range ordering in the solid state [1]. If substituents are present in the molecules that are capable to act as hydrogen bond donors and acceptors (the oxygen of the methoxy group on the aromatic rings [2] or the fluorine in the CF₃ group in position 3 – substituting the olefinic hydrogen [3]), they take part in forming extended aggregates, but only in the solid state. In this contribution the scope is further extended, experimental and computational results concerning the aggregate-forming properties of *E*- α -phenyl cinnamic acid molecules having one or two fluorine substituents on the phenyl rings and in some cases methoxy substituent as well are communicated.

Six molecules have been synthesized and used for exploring all possible hydrogen bonding interactions in solution and the solid state too. They are the *E* isomers of 2-phenyl-3-(4'F-phenyl), 2-(4'F-phenyl)-3-(4'F-phenyl), 2-(2'methoxyphenyl)-3-(4'F-phenyl), 2-(4'methoxyphenyl)-3-(4'F-phenyl), 2-(4'F-phenyl)-3-(2'methoxyphenyl), 2-(4'F-phenyl)-3-(4'methoxyphenyl) propenoic acid molecules. In the experimental part of the work FTIR spectroscopy (BIORAD FTS 65/896 spectrophotometer, 4000–400 cm⁻¹ range) was the tool of structural investigation. For the solution-phase studies CCl₄ was chosen as the solvent and the 10⁻²-10⁻⁴ mol/dm³ concentration range was investigated. For measurements in the solid-state the KBr technique was applied. Molecular modelling was performed with semiempirical and *ab initio* codes included in the *HyperChem* package [4].

The combination of experimental and computational approaches proved to be powerful in exploring hydrogen bonding possibilities. It was found that large aggregates were formed, but again only in the solid state. They were kept together by hydrogen bonds. The major organising force was C-H...F hydrogen bonding. It connected the acid dimers (which were the basic unit of the hydrogen-bonded aggregates). All forms that could be envisaged were identified indeed. Beside the expected (aromatic)C-H...F hydrogen bonds, the scarcer (olefinic)C-H...F bonds also proved to be major structure-organising forces. When methoxy substituent was present even (aliphatic)C-H...F bonds could be identified. Although the various forms of the C-H...F interactions were crucial in forming extended structures even in these molecules, (aromatic)C-H...O and even (aliphatic)C-H...O hydrogen bonds contributed, too. Fluorine is so much involved in hydrogen bonding that a model with nine dimers kept together by (olefinic)C-H...F only could be built easily, forecasting that modelling even 3-dimensional structure is within reach.

- [1] I. Pálinkó, B. Török, M. Rózsa-Tarjányi, J.T. Kiss, Gy. Tasi, *J. Mol. Struct.* 348 (1995) 57-60; (b) I. Pálinkó, J.T. Kiss, *Mikrochim. Acta [Suppl.]* 14 (1997) 253-255.
[2] J.T. Kiss, K. Felföldi, I. Hannus, I. Pálinkó, *J. Mol. Struct.* 565/566 (2001) 463-468.
[3] J.T. Kiss, K. Felföldi, I. Pálinkó, *J. Mol. Struct.* 744-747 (2005) 207-210.
[4] *Hyperchem 8.0*, Hypercube, Inc., Gainesville, Florida, 2007.

UV R2PI Spectra of p-difluorobenzene van der Waals Complexes

John G. Philis

Department of Physics, University of Ioannina, GR45110 Ioannina, Greece

The real world generally involves systems of great complexity. The study of molecular dimers and clusters (produced in a supersonic molecular jet) provides an important link with condensed phase behavior. The structure, energetics and intramolecular dynamics of van der Waals clusters are of considerable importance for the basic understanding of intermolecular interactions. There have been extensive spectroscopic studies involving aromatic molecules [1, 2, 3, 4, 5]. Here we study the dimers with p-C₆H₄F₂ and other molecules (see Fig. 1), applying the combination of resonant two-photon ionization spectroscopy (R2PI) with a time-of-flight mass spectrometer. The broadening of the spectral bands is due to the coexistence of two or more conformations.

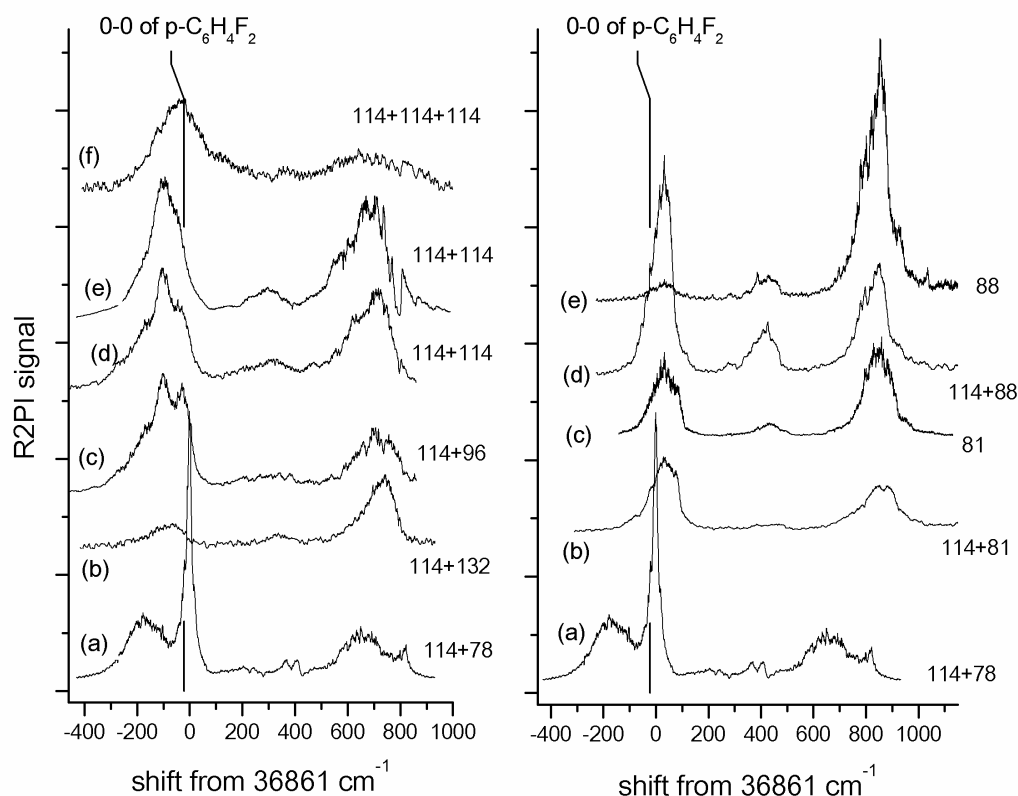


Fig. 1: Mass selected 1C-R2PI $S_1 \leftarrow S_0$ spectra of p-C₆H₄F₂ with various clustered molecules. Left side: (a) with benzene, (b) with 1,3,5-trifluorobenzene, (c) with fluorobenzene, (d) and (e) homodimer, (f) homotrimer. Right side: (a) with benzene, (b) and (c) with N-methylpyrrole, (d) and (e) with p-dioxane. The origin band of bare p-C₆H₄F₂ is at 36839 cm⁻¹.

- [1] K. Rademann, B. Brutschy, H. Baumgartel, Chem. Phys. 80 (1983) 129-145.
- [2] B. Ernstberger, H. Krause, A. Kiermeier, H.J. Neusser, J. Chem. Phys. 92 (1990) 5285-5296.
- [3] Y. Numata, Y. Ishii, M. Watahiki, I. Suzuka, M. Ito, J. Phys. Chem. 97 (1993) 4930-4935.
- [4] K. Buchhold *et al.*, J. Chem. Phys. 112 (2000) 1844-1858.
- [5] A. Musgrave, T.G. Wright, J. Chem. Phys. 122 (2005) 074312.

Spectroscopic Investigation of the Vibrational Spectra of the Benzoxazine

Arvind K. Singh¹, V. Mukherjee¹, V.B. Singh¹, B. Singh¹ and A.N. Singh²

¹Department of Physics, Udai Pratap Autonomous College, Varanasi, India

²Department of Physics, BHU, Varanasi, India

E-mail: nps_physics@rediffmail.com

Vibrational spectrum of the benzoxazine molecule has been systematically investigated by combined approach of infrared spectrum, *ab initio* and density functional theory (DFT) calculations. Infrared spectrum of the benzoxazine molecule in KBr pellet has been recorded in the wavenumber region 400-4000 cm⁻¹. Optimized geometries, harmonic vibrational wavenumbers and the intensities of the vibrational bands have been calculated at the RHF/6-311++g** and B3LYP/6-311++g** levels. Some appropriate scale factors have also been considered to scale the calculated frequencies. The scaled values have been compared with experimental frequencies observed in infrared spectrum. The molecule benzoxazine consists of 16 atoms and thus it possesses 42 normal modes of vibrations. Each vibrational frequency has been assigned to their corresponding normal mode with the help of band intensities and vector displacements. The vibrational frequencies and infrared intensities so obtained have been discussed.

Theoretical Study of IR and Raman Spectra of 5-Hydroxy Uracil

Rashmi Singh, M. Kumar and R.A Yadav

*Laser and Spectroscopy Lab, Department of Physics, Banaras Hindu University,
Varanasi-221005, India*

Ab initio calculations were used to investigate the interactions of nucleosides with 5-hydroxy uracil. 5-hydroxy uracil could form a stable base pair. Quantum chemical methods have been employed to carry out vibrational frequencies for 5-hydroxy uracil. The assignment of each calculated fundamental has been assigned using band intensities and depolarization ratios for the Raman lines. We have calculated optimized geometrical parameters, atomic charges, fundamental frequencies and their corresponding IR and Raman intensities and Raman depolarization ratios. The influences of the presence of the OH group in 5-hydroxy uracil molecule on the geometries and normal modes of the parent molecule (Uracil) have been differentiated.

- [1] H. Susi, J.S. Ard, *Spectrochim. Acta A* 27 (1971) 1549.
- [2] V. Krishnakumar, R. Ramasamy, *Spectrochim. Acta A* 66 (2007) 503.
- [3] V. Thivyanathan, A. Somasunderam, D.E. Volk and D.G. Gorenstein, *Chem. Commun.* 401 (2005) 400.
- [4] G. Fogarasi, P. Pulay, *Ann. Rev. Phys. Chem.* 35 (1982) 191.
- [5] G. Fogarasi, P. Pulay, in: J.R. Durig (Ed.), *Vibrational Spectra and Structure* 14 (1985) 125.
- [6] B.A. Hess Jr., L.J. Schaad, P. Carsky, R. Zahradnik, *Chem. Rev.* 86 (1986) 706.

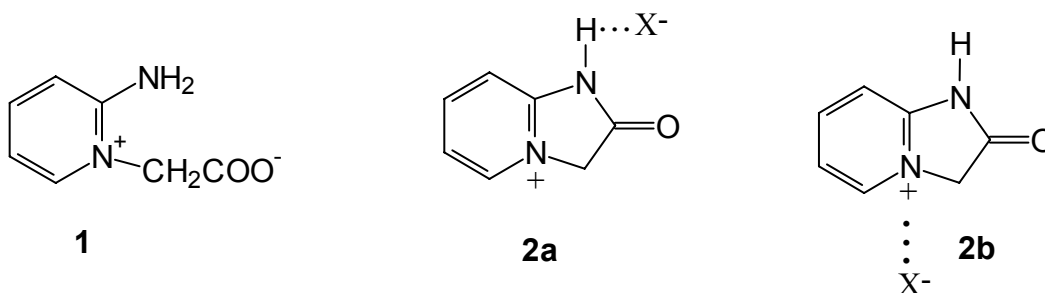
X-Ray diffraction, FTIR and NMR Spectra, and DFT Calculations of 2-Aminopyridine Betaine and 1-*H*-2-oxo-2,3-dihydroimidazo[1,2-*a*] Pyridinium Chloride, Bromide and Perchlorate

Mirosław Szafran, Iwona Kowalczyk, Elżbieta Bartoszak-Adamska, Zofia Dega-Szafran

*Faculty of Chemistry, Adam Mickiewicz University, ul. Grunwaldzka 6, 60-780 Poznań, Poland
szafran@amu.edu.pl*

Betaines make a special class of zwitterions, in which net uncharged molecules have separate cationic and anionic sites [1]. The positive charge is localized on N^+ , S^+ or P^+ atoms which have no hydrogen atom, but the negative charge is on COO^- , O^- , SO_2O^- or $R-P=OO^-$ groups. Betaines have a variety of applications in medicine, pharmacy, biology and other scientific fields [2]. An interesting group of betaines are those containing pyridine rings, which are easily obtained by quaternization of pyridines with halogenoacetic acids as well as their salts and esters. Quaternization of 2-amino-pyridine with $X-CH_2-COOH$ ($X = Cl$ or Br) is more complex, because it depends on reaction temperature.

This contribution reports the crystal and molecular structure and spectroscopic properties of 2-amino-pyridine betaine (1-carboxymethyl-2-amino-pyridinium inner salt) (**1**) and its complexes with HCl, HBr and $HClO_4$. These complexes on boiling in ethanol cyclize to 1-*H*-2-oxo-imidazo[1,2-*a*]pyridinium salts (chloride, bromide and perchlorate). Two types of cyclic molecules, one with $N(1)-H \cdots X^-$ hydrogen bonds (type **2a**) and the second with the electrostatic interactions (type **2b**) between the positively charged nitrogen atom ($N^+(4)$) and the counter anions ($X^- = Cl^-$, Br^- and ClO_4^-) have been optimized by the B3LYP/6-31G(d,p) level of theory. Molecules of type **2b** have slightly higher energy than type **2a**. Both type of interactions are responsible for the structures of the above mentioned molecules. Structures of 2-amino-pyridine betaine complexes and 1-*H*-2-oxo-imidazo[1,2-*a*] pyridinium salts have been confirmed by the FTIR, 1H and ^{13}C NMR spectra.



[1] M. Milton, R.S. Macomber, A.R. Pinhas, R.M. Wilson, *The Vocabulary and Concepts of Organic Chemistry*, J. Wiley & Sons, New Jersey, 2005, pp. 529 and 772.

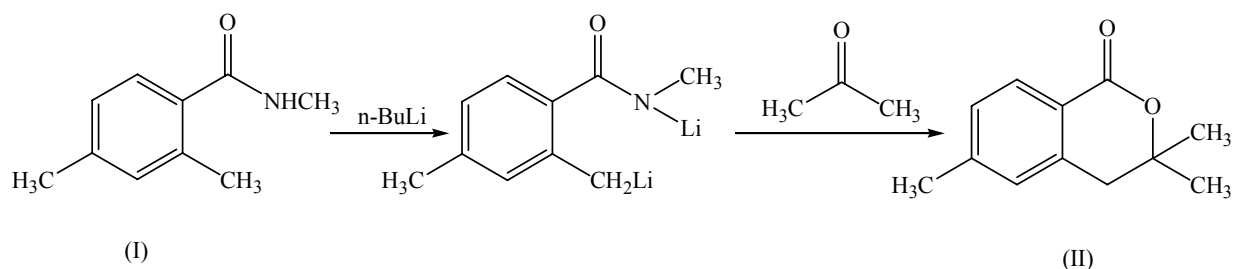
[2] E.G. Lombax, X. Domingo (Eds) *Amphoteric Surfactants*, Marcel Dekker, New York, 1996, pp. 75-190.

X-ray crystallographic, spectroscopy and quantum chemical studies on 3,3,6-trimethyl-3,4-dihydroiso-coumarin

Ajit Viridi

Department of Engineering Physics, Model Institute of Engineering & Technology, Jammu, India

Structural and spectral characteristics of 3,3,6-trimethyl-3,4-dihydroiso-coumarin have been studied by methods of X-ray crystallography, infrared spectroscopy and quantum chemistry. The reaction mechanism of the compound crystallization is given below:



An irregular shaped crystal of dimensions 0.3 x 0.2 x 0.2 mm was selected for intensity data collection and the unit cell parameters were determined by least-squares fit of setting angles of 1880 reflections (θ range 2.71-24.46°). The intensities were measured by the ϕ and ω scan method. The space group was determined to be $P2_1/c$ from the systematic absences $h0l: l = 2n + 1, 0k0: k = 2n + 1$. Data were corrected for Lorentz-and polarization corrections. The structure was solved by direct methods using SHELXS86 software. The structure contains three crystallographically independent molecules, in the asymmetric unit. R-factor based on E-values, $R_E = 0.217$. The optimized geometry of the three molecules has been obtained by quantum chemical calculations by using DFT and RHF methods by using 6-311++G** basis set. The optimized molecular geometries are in good agreement with the X-ray analysis. The geometry of all the three asymmetric molecules indicates similarity in terms of their bond distances and bond angles. However, pronounced differences are observed in the values of torsion angles. Based on the suitable scaled DFT/6-311G** calculation, assignments have been provided to the fundamental vibrational bands of these molecules in terms of frequency, form and intensity of vibrations and potential energy distribution across the symmetry coordinates in the ground state.

Vibrational Spectroscopic Study of 4-Aminopyrimidine Complexes

Sevim Akyuz and Tanil Akyuz

Istanbul Kultur University, Science and Letters Faculty, Department of Physics, Atakoy Campus, 34156, Istanbul, Turkey

Pyrimidine derivatives display a class of heterocycles of great importance. Many pyrimidine derivatives possess remarkable biological activity and have been widely used in fields ranging from the medicinal to industrial applications. Pyrimidine ring system provides a potential binding site for metals and so any information on their coordinating properties are important for understanding the role of metal ions in biological system.

4-aminopyrimidine tetracyanometallate, $M(4APM)_2M'(CN)_4$ {where $M = Mn$ or Zn ; $M' = Pd$ or Pt ; 4APM = 4-aminopyrimidine}, coordination polymer compounds are prepared for the first time and their FT-IR ($400-4000\text{ cm}^{-1}$) and FT-Raman ($70-4000\text{ cm}^{-1}$) spectra are reported. 4APM is coordinated to $M(II)$ through one of the pyrimidine ring nitrogen atom as monodentate ligand; the amino group is not involved in the complex formation. Comparison of the Raman wavenumbers of tetracyanometallate sheet of the isostructural compounds lead us to express a tentative assignment for $\nu(M-N)_{4APM}$, $\nu(M-NC)$ and $\delta(NMN)_{4APM}$ vibrations. Coordination effect on 4APM vibrational wavenumbers is analysed.

Investigation of the Vibrational Spectra of Some Partially Deuterated $\text{Cd}(\text{NH}_3)_2\text{Cl}_2$, $\text{Hg}(\text{NH}_3)_2\text{Cl}_2$, $\text{Pd}(\text{NH}_3)_4\text{Cl}_2$ Complexes

L. Andreeva, F. Trajkovic and J. Petreska

Institute of Chemistry, Faculty of science, University St. Cyril and Melody
Skopje, Macedonia, e-mail: lilea@iunona.pmf.ukim.edu.mk

Due to the exchange of hydrogen by deuterium in ammonia, four types of isotopic species (NH_3 , NH_2D , NHD_2 , ND_3) are present in the structure of the investigated complexes. Since chemical isolation of the mixed isotopic parent is not possible, it is expected that in the IR spectra of partially deuterated analogues, bands would appear due to vibrations of all isotopic species. In order to obtain information on the bands due to vibrations of different types of isotopomers of coordinated ammonia, the FT-IR spectra of a series partially deuterated $\text{Cd}(\text{NH}_3)_2\text{Cl}_2$, $\text{Hg}(\text{NH}_3)_2\text{Cl}_2$ and $\text{Pd}(\text{NH}_3)_4\text{Cl}_2$ complexes, were recorded and studied. The spectra were recorded in the region between 400 and 4000 cm^{-1} , at room temperature and at liquid nitrogen boiling temperature. The corresponding bands due to vibration of all isotopic species of coordinated ammonia were studied. The bands originating from the deformation NH_2D and NHD_2 vibrations appear in the region below 1600 cm^{-1} and the shifting towards lower frequencies varies with the different types of isotopomers.

Along with the experimental studies, quantum chemical studies of several model systems mimicking the title complexes were also carried out. The B3LYP and mPW1PW91 density functional levels of theory were employed, with the 6-31++G(*d,p*) basic sets on all atoms except metal-atom, for which various effective core potentials were used. Theoretical studies included full geometry optimizations of the mentioned species, followed by subsequent harmonic vibrational analyses of all possible isotopomers. The shifting of the band due to different types of $(\text{NH},\text{D})_3$ groups towards low frequencies is in good agreement with the theoretical predictions, but it is different for different types of isotopic species.

2-Biphenylmethanol Vibrational Spectra and Their Interpretation Using Structural-Dynamical Model in Anharmonic Approximation

L.M. Babkov¹, N.A. Davydova², K.E. Uspenskiy¹

¹Saratov State University, Moskovskaya st, 155, Saratov, 410012, Russia E-mail: babkov@sgu.ru

²Institute of Physics of NAS of Ukraine, 46 Nauki prosp., Kyiv, 03022, Ukraine E-mail: davydova@iop.kiev.ua

Vibrational spectra of 2-biphenylmethanol were measured at room temperature in 400-4000 cm^{-1} (IR spectra) and 0-3500 cm^{-1} (Raman spectra) regions.

In previous works [1-3] the structure-dynamical model of 2-biphenylmethanol was built using harmonic approximation.

In present work, using B3LYP/6-31G (d) method [4], the energy minimization, structure optimization, dipole moment and polarizabilities calculations for the 2-biphenylmethanol (2BPM) molecule were performed. The force field was built and the frequencies of the normal modes with their overtones and combinational frequencies were calculated using anharmonic approximation. It is known, that in the investigated crystal 2BPM sample [3] the triclinic modification is realized. In this modification the four molecules in unit cell are joined into H-bond complex. The shifts and splitting of the frequencies of fundamental vibrations at the H-complex formation. With the anharmonicity taken into account the agreement between the calculated and measured frequencies was considerably better than in the case of using harmonic approximation. This approach allows avoiding the scaling procedure for the calculated force constants and vibrational frequencies. At the dynamics description of the H-bond complex core the low frequencies (under 400 cm^{-1}) corresponding to the deformational vibrations and valence stretch of the hydrogen bond $\nu(\text{O}\cdots\text{H})$ are in worth agreement with the measured IR spectrum.

On the basis of the modeling results obtained by authors in their previous experimental and theoretical investigations of the 2 BPM crystalline sample structure in stable triclinic modification and its vibrational spectra, a full interpretation of the measured IR and Raman spectra was given.

[1] L.M. Babkov, J. Baran, N.A. Davydova, S.V. Trukhachev, J. Mol. Struct. 700/1-3 (2004) 55-59.

[2] L.M. Babkov, J. Baran, N.A. Davydova, A. Pietraszko, K. E. Uspenskiy, J. Mol. Struct. 744-747 (2005) 433-438.

[3] L.M. Babkov, J. Baran, N.A. Davydova, K.E. Uspenskiy, J. Mol. Struct. (792-793) 2006 68-72.

[4] J. Frisch, G.W. Trucks, H.B. Schlegel et al., Gaussian03, Revision B.03; Gaussian, Inc., Pittsburgh PA, 2003.

The Investigation of 4-n-butyl-4'-cyanobiphenyl Conformational Mobility by IR Spectroscopy Methods

L.M. Babkov¹, I.I. Gnatyuk², G.A. Puchkovska², S.V. Truckhachev¹

¹Saratov State University, Moskovskaya st, 155, Saratov, 410012, Russia E-mail: babkov@sgu.ru

²Institute of Physics of NAS of Ukraine, 46 Nauki prosp., Kyiv, 03022, Ukraine E-mail: puchkov@iop.kiev.ua

Using theoretical and experimental IR spectroscopy methods the appearance of conformational mobility in 4-n-butyl-4'-cyanobiphenyl (4CB) IR spectra was investigated.

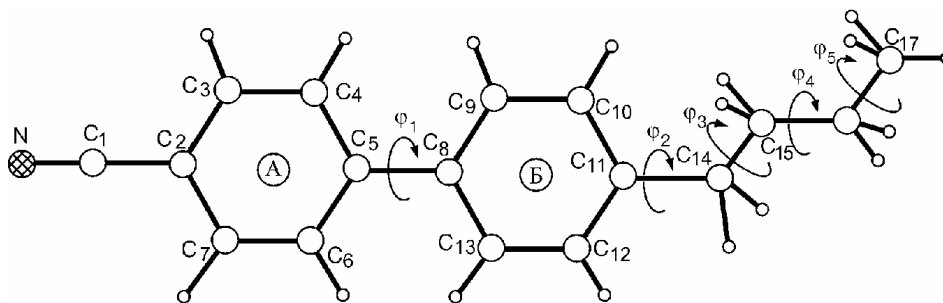


Fig. 1: 4CB molecule plane conformer ($\varphi_1, \dots, \varphi_5 = 0^\circ$).

IR absorption spectra of the 4CB samples in 400-4000 cm^{-1} region were measured in 28-70 $^\circ\text{C}$ temperature interval for solid crystal and liquid phases. Calculation of the 4CB conformers was performed on the basis of theoretical methods of molecular spectroscopy using LEV-100 software, in which the method of fragments implemented [1].

On the basis of the calculation results a full assignment of the experimental bands was given. Bands, that were sensitive to the conformational changes in the molecule, were found in the spectra. From the investigation performed a few conclusions made by the authors:

- in considered temperature interval (28-70 $^\circ\text{C}$) the conformational composition of 4CB is inhomogeneous
- at the heating from 28 to 50 $^\circ\text{C}$ in solid crystal and liquid (46.5-50 $^\circ\text{C}$) states of 4CB the conformational composition of the sample is not changed
- conformational mobility that concerned with rotations around the single bonds in the temperature interval 46.5-50 is restricted for the liquid and solid crystal states of 4CB
- in liquid state at the temperatures 55-70 $^\circ\text{C}$ possible conformers are the following
1 - $\varphi_1 = 40.5^\circ$, $\varphi_2 = -8^\circ$, $\varphi_3 = -5^\circ$, $\varphi_4 = -41^\circ$, $\varphi_5 = 0^\circ$; 2 - $\varphi_1 = 70^\circ$, $\varphi_2 = \varphi_3 = \varphi_4 = \varphi_5 = 0^\circ$;
- at the heating from 50 to 55 $^\circ\text{C}$ of the liquid 4CB a conformational mobility was found, determined by the 5-10 $^\circ$ turning of the propyl fragment relatively of the trans form
- in solid crystal state of 4CB the conformers differed by the orientation of the ethyl group (φ_4) are presented. The existence of the conformers in which $\varphi_4 = 0^\circ$ and -41° is most probable.

[1] L.A. Gribov, V.A. Dement'ev, Modelirovanie kolebatelnykh spektrov slojnykh soedinenij na EVM. Nauka, Moscow, 1989, p.160. (in Russian).

The Appearance of Conformational Mobility of Behenic Acid in IR Spectra

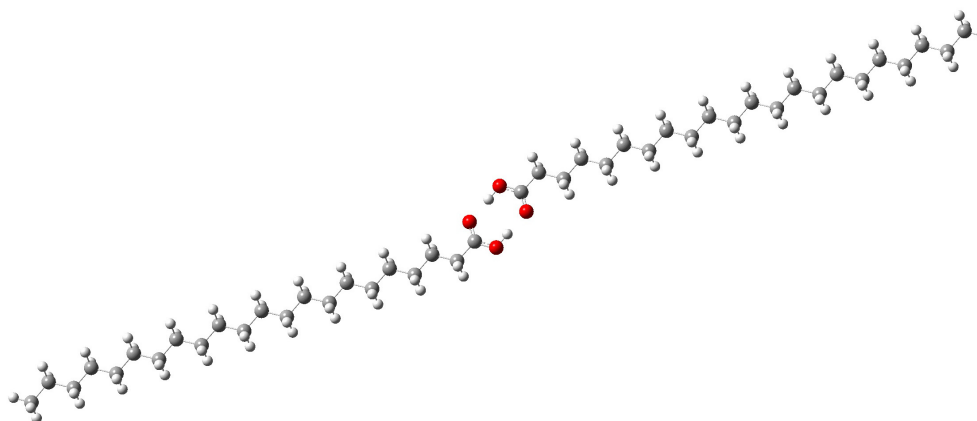
L.M. Babkov¹, Ivan I. Gnatyuk², Galina O. Puchkovska², Kirill E. Uspenskiy¹

¹Saratov State University, Moskovskaya st, 155, Saratov, 410012, Russia E-mail: babkov@sgu.ru

²Institute of Physics of NAS of Ukraine, 46 Nauki prosp., Kyiv, 03022, Ukraine E-mail: puchkov@iop.kiev.ua

In the last time the interest in investigation of structure and dynamics of the long chain aliphatic compounds (of the highest members of homologous series, particularly) appeared again [1].

In wide temperature interval (11-330 K) IR absorption spectra of the carbonic acid $\text{CH}_3(\text{CH}_2)_{20}\text{COOH}$ (behenic acid, kC_{22}) were measured. The changes revealed in the spectra at the temperature increasing can be explained by the assumption about the conformational mobility of the molecules in the sample. The modeling of the structure and vibrational spectra of conformers of $\text{CH}_3(\text{CH}_2)_{20}\text{COOH}$ molecule have been carried out to confirm this assumption. These conformers were differed by the orientation of carboxylic group and by the orientation of fragment including carboxylic group and the closest CH_2 group relatively to the remaining part of the plane carbonic frame of alkyl radical (AR). Also the modeling of the $\text{CH}_3(\text{CH}_2)_{20}\text{COOH}$ molecules H-bond dimer, in which the AR carbonic frames and dimer ring are lying in the same plane, was performed.



Using density functional method (B3LYP/6-31G) [2] the energies, structures, dipole moments and polarizabilities of conformers of the $\text{CH}_3(\text{CH}_2)_{20}\text{COOH}$ molecule with different orientation angles and of the H-bond dimer were calculated. The force fields were built and the frequencies of normal vibrations with intensities in IR spectra were calculated for all mentioned above quantum molecular systems. On the basis of the analysis of the calculated and measured IR spectra the authors made a conclusion about the conformational mobility of the molecules in $\text{CH}_3(\text{CH}_2)_{20}\text{COOH}$ carbonic acid sample.

[1] H-W. Li, H.L. Strauss, R.G. Snyder. J. Phys. Chem. A 108 (2004) 6629-6642.

[2] Frisch J., Trucks G.W., Schlegel H.B. et al., Gaussian03, Revision B.03; Gaussian, Inc., Pittsburgh PA, 2003.

A Theoretical Conformational Analysis and Vibrational Spectroscopic Investigation on Niflumic Acid

K. Balci¹, Y. Akkaya¹, S. Akyuz²

¹ Istanbul University, Faculty of Science, Department of Physics, Vezneciler, 34134, Istanbul, Turkey, ² Istanbul Kultur University, Faculty of Science and Letters, Department of Physics, Atakoy Campus, Istanbul, Turkey

Niflumic acid is a selective inhibitor of COX-2 enzyme. It provides potent analgesic and anti-pyretic properties and is widely used as a drug for joint and muscular pain. Theoretically possible stable conformers of niflumic acid molecule in electronic ground state were carefully examined by means of both molecular dynamics calculations using molecular mechanics AMBER force field and potential energy surface scan calculations carried out at B3LYP/3-21g(d) level of theory. The equilibrium geometrical parameters for the determined stable conformers of the free molecule were obtained through geometry optimizations carried out using B3LYP hybrid DFT and MP2 ab-initio methods with 6-31G(d), 6-31++G(d,p), 6-311++G(d,p) and aug-cc-pvTZ basis sets. The vibrational normal modes and corresponding frequencies, IR and Raman intensities of each determined stable conformers of the molecule were obtained through frequency calculations performed at the same levels of theory as used in the geometry optimizations in both “harmonic oscillator” and “anharmonic oscillator” approaches, separately.

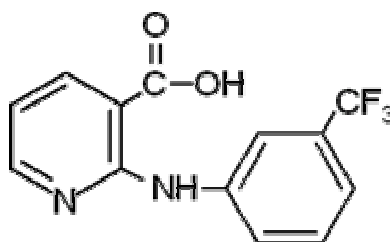


Fig. 1: Chemical structure of niflumic acid molecule.

In fitting of the calculated harmonic wavenumbers to the experimental ones, two different scaling procedures referred to as “Scaled Quantum Mechanical Force Field (SQM FF) methodology” [1, 2] and “Scaling wavenumbers with dual scale factors” [3] were proceeded, independently. The frequencies and associated Raman and IR intensities calculated for each normal mode of the molecule were compared with the corresponding experimental data ; the theoretical results have been found to be in rather good agreement with our experimental assignments proposed as the fundamental bands of the molecule.

[1] G. Rauhut, P. Pulay, J. Phys. Chem. 99 (1995) 3093.

[2] G. Rauhut, P. Pulay, J. Phys. Chem. 99 (1995) 14572.

[3] M.D. Halls, J. Velkovski, H.B. Schlegel, Theor. Chem. Acc. 105 (2001) 413.

Studies on Kyotorphin and D-Kyotorphin in Aqueous Solution by Raman Spectroscopy

Gonul Basar¹, Sevim Akyuz², Gunay Basar³ and Sophie Kröger⁴

¹Istanbul University, Science Faculty, Physics Department, Vezneciler 34134, Istanbul Turkey, ²Istanbul Kultur University, Science and Letters Faculty, Physics Department, Atakoy Campus, 34156 Bakirkoy, Istanbul,

³Istanbul Technical University, Science and Letters Faculty, Physics Department, Ayazaga Campus, Istanbul, Turkey, ⁴Technische Universität Berlin, Institut für Atomare und Analytische Physik, Hardenbergstr. 36, 10623 Berlin, Germany

Kyotorphin (L-Tyr-L-Arg) is an analgesic dipeptide. It displays opioid type actions, including analgesic effects by releasing opioid pentapeptide Met-enkephalin from slices of the brain and spinal cord [1]. The analogue D-kyotorphin [L-Tyr-D-Arg] also produces analgesic effects by the introduction of Met-enkephalin release [1]. In this study Raman spectra of L-Tyr-L-Arg and L-Tyr-D-Arg dipeptides in water and heavy water solutions are reported for the first time in the 1800-100 cm⁻¹ range. Vibrational assignments have been made for all observed frequencies. Hydrogen bonded state of the tyrosine phenoxyl group was found to change depending on the concentration of the kyotorphin solution. On the other hand amide I and amide III bands are also found to altered depending on the concentration of the solution which indicates conformational alterations.

[1] A. Kawabata, S. Manabe and H. Takagi, Br. J. Pharmacol. 112 (1994) 817.

Vibrational Spectroscopic Studies on the T_d -Type Clathrates: $M(N,N'$ -Dimethylethylenediamine) $M'(CN)_4.C_6H_6$ ($M = Mn, M' = Zn, Cd$ or $Hg; M = Cd, M' = Cd$ or Hg)

C. Bayrak

Department of Physics Education, Hacettepe University, 06800 Beytepe, /Ankara, Turkey
cbayrak@hacettepe.edu.tr

In this study, the $M(N,N'$ -dimethylethylenediamine) $M'(CN)_4.C_6H_6$ ($M = Mn, M' = Zn, Cd$ or $Hg; M = Cd, M' = Cd$ or Hg) clathrates of N,N' -dimethylethylenediamine (DMEDA) were prepared for the first time and their FT-IR and FT-Raman spectra were investigated. The infrared spectra of the clathrates were recorded in the range $4000-500\text{ cm}^{-1}$ and FT-Raman spectra of the clathrates (Cd-DMEDA-Cd-Bz and Cd-DMEDA-Hg-Bz) were recorded $4000-700\text{ cm}^{-1}$ and its fundamental vibrational wavenumbers were obtained (Fig. 1). All the vibrational modes of coordinated DMEDA were characterised. Several modes of coordinated DMEDA have upward shifts in frequencies compared to those in the free molecule, these shifts being metal dependent.

The assigned wavenumbers for the $M(CN)_4$ group in the compounds studies appeared to be much higher than those for the $M(CN)_4$ ion $K_2M(CN)_4$ ($M = Zn, Cd$ or Hg) salts. The CH out-of-plane mode (A_{2U}) of benzene in the infrared spectra of the clathrates was located at ca. 693 cm^{-1} and observed as a very intense single band. This band in the spectra of the clathrates was found shifting to higher frequency (693 cm^{-1}) from that of liquid benzene (670 cm^{-1}). Similar positive frequency shifts were observed for Hofmann- T_d -type and Hofmann-type clathrates.

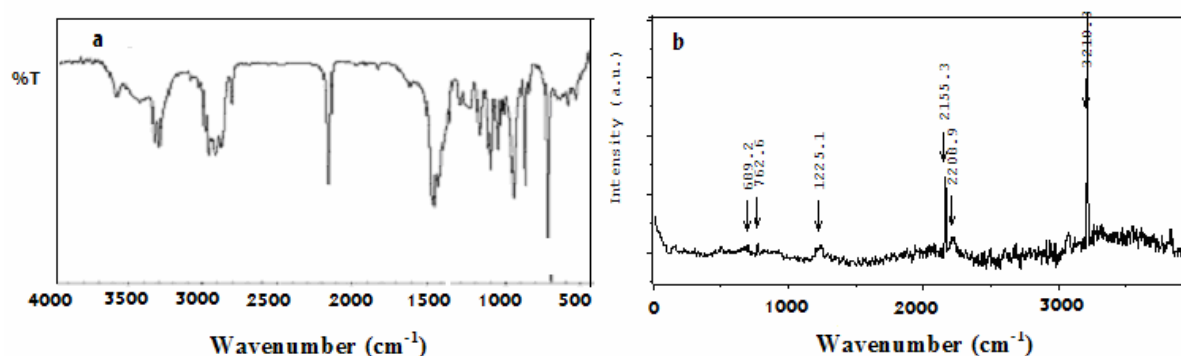


Fig. 1: FT-IR (in KBr) (a) and FT-Raman spectra (b) of Cd-DMEDA-Cd-Bz clathrate.

Synthesis, Structural and Conformational Study of Some Esters Derived from 3-Methyl-3-azabicyclo[3.2.1]octan-8 α -ol

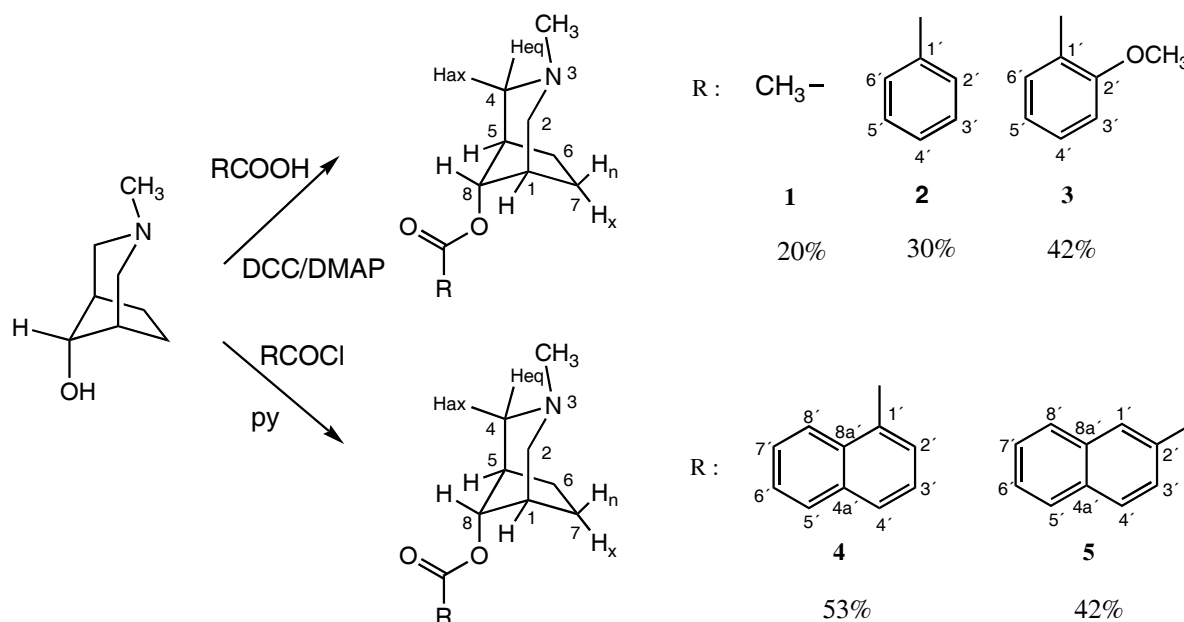
I. Iriepa¹, J. Bellanato², E. Gálvez¹ and A.I. Madrid¹

¹Departamento de Química Orgánica, Universidad de Alcalá, Madrid, Spain

²Instituto de Estructura de la Materia, C.S.I.C., Madrid, Spain

isabel.iriepa@uah.es

As a part of a research program related to the synthesis and structural study of potential pharmacologically interesting compounds we have focused our attention on the preparation of some esters derived from 3-methyl-3-azabicyclo[3.2.1]octan-8 α -ol.



For compounds **1**, **2** and **3** higher yields have been obtained starting from the alcohol and the corresponding acid, whereas the reaction between the alcohol and the acyl chloride is the best method to obtain the compounds **4** and **5**.

A detailed study by ¹H and ¹³C NMR has been done to determine the preferred conformations in solution. The assignments of proton and carbon resonances have been made on the basis of the literature data for related systems and double resonance experiments for compound **2**.

The α esters (**1-5**) adopt in CDCl₃ solution a chair envelope conformation with the N-CH₃ group in equatorial position. ³JH₂(4)_{ec}-H₈ > ³JH₂(4)_{ax}-H₈; therefore, the piperidine ring adopts a non-flattened chair conformation. The shape of the signals corresponding to the aromatic protons accounts for a free rotation of the acloxy group around the C-O bond.

Finally, although compounds **2** and **3** showed analgesics properties, they are much less active than the reference compound (morphine). Compound **2** shows higher potency than compound **3**; therefore, the introduction of the *o*-OCH₃ substituent in the aromatic ring produces a decreasing of the analgesic activity.

Experimental Structure of $\text{CF}_3\text{CO}_2\text{CH}_2\text{CF}_3$ from Electron Diffraction Data, Infrared Spectra and Quantum Chemical Calculation of Vibrational Properties

M.E. Defonsi Lestard¹, M.E. Tuttolomondo¹, E.L. Varetti², D.A. Wann³, H.E. Robertson³,
D.W.H. Rankin³ and A. Ben Altabef¹

¹ Instituto de Química Física, Facultad de Bioquímica, Química y Farmacia, Universidad Nacional de Tucumán, San Lorenzo 456, 4000 Tucumán, R. Argentina.

E-mail: altabef@fbqf.unt.edu.ar

² CEQUINOR, Departamento de Química, Facultad de Ciencias Exactas, Universidad Nacional de La Plata, C. Correo 962, 1900 La Plata, R. Argentina

³ School of Chemistry, University of Edinburgh, West Mains Road, Edinburgh, UK EH9 3JJ.

E-mail: d.w.h.rankin@ed.ac.uk

The molecular structure of 2,2,2-trifluoroethyl trifluoroacetate, $\text{CF}_3\text{CO}_2\text{CH}_2\text{CF}_3$, was determined in the gas phase from electron-diffraction data supplemented by ab initio (HF, MP2) and DFT calculations using 6-31G(d), 6-311++G(d,p) and 6-311G(3df,3pd) basis sets¹. The experimental and theoretical data indicate that, although both *trans* and *gauche* conformers are possible by rotation about the O-CH₂ bond, the preferred conformation is *trans*. To explain this fact, the total energy of each conformation and the natural bond orbital (NBO) partition schemes were considered. In addition, the total potential energy was deconvoluted using a Fourier-type expansion with six terms. The infrared spectra of the substance in the gaseous, liquid and solid states as well as the Raman spectrum of the liquid were also obtained. These spectra show the presence of both *trans* and *gauche* conformers by the components of some fundamental mode bands. The harmonic vibrational frequencies and the force field were calculated² using the above-mentioned techniques. The force constants were adjusted by scaling to achieve a final root-mean-square deviation of 10 cm⁻¹ between calculated and experimental frequencies.

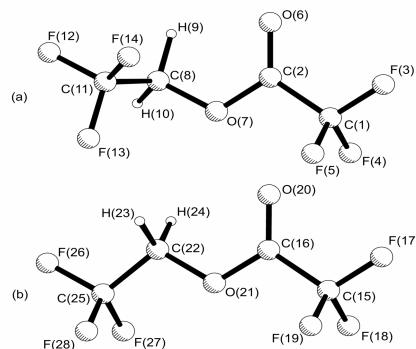


Figure 1: Molecular structure, including numbering scheme, for (a) *gauche* conformer, and (b) *trans* conformer of $\text{CF}_3\text{CO}_2\text{CH}_2\text{CF}_3$.

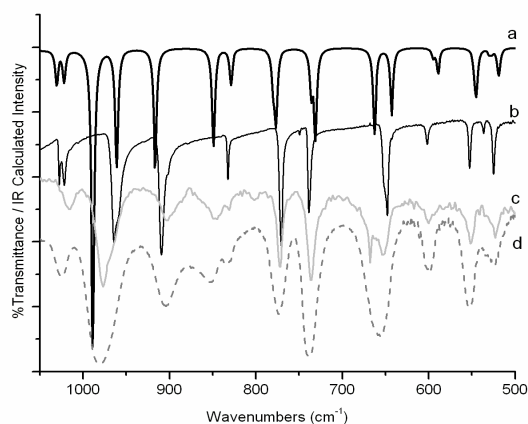


Figure 2: Infrared spectra of $\text{CF}_3\text{CO}_2\text{CH}_2\text{CF}_3$. a) calculated with B3LYP/6-311++G** for the mixture of conformers; b) solid (-160°C); c) liquid (room T); d) gas.

[1] *Gaussian 03*, Revision B.02, Gaussian, Inc., Pittsburgh PA, 2003.

[2] P. Pulay, G. Fogarasi, G. Pongor, J.E. Boggs, A. Vargha, *J. Am. Chem. Soc.* 105 (1983) 7037.

New Organic Fluorophores for Optical and Spectroscopic Applications: 2,3- and 2,5-Distyrylfuran

E. Benassi¹, I. Baraldi¹, S. Ciorba², I. Škorić³, M. Šindler-Kulyk³ and A. Spalletti²

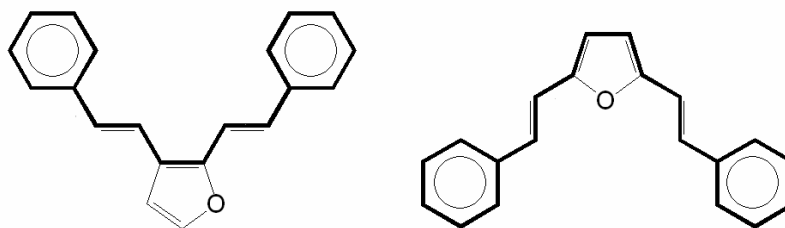
¹*Dipartimento di Chimica, Università di Modena e Reggio Emilia, Modena, Italy*

²*Dipartimento di Chimica e Centro di Eccellenza Materiali Innovativi Nanostrutturati (CEMIN),
Università di Perugia, 06123 Perugia, Italy*

³*Department of Organic Chemistry, Faculty of Chemical Engineering and Technology,
University of Zagreb, 10000 Zagreb, Croatia*

baraldi.ivan@unimore.it ; enrico.benassi@libero.it ; faby@unipg.it (Anna Spalletti); marija.sindler@fkit.hr

The 2,3- and 2,5-distyrylfuran were found very stable compounds [1] that show a strong and structured fluorescence, and therefore may be used as fluorescence probes, dye laser media, scintillators and as π -core for new push-pull polyenes. The spectroscopic behaviour is similar to that of *cis*- α,ω -diphenylpolyenes, as shown in Scheme 1 and underlined in refs. [2] and [3].



Scheme 1

In this work we investigated, from a theoretical and experimental points of view, the rotational isomerism, absorption and emission spectra, photophysics and electric properties of 2,3- and 2,5-distyrylfuran. The conformers of the ground electronic state have been studied by Hartree-Fock *ab initio* methods and Density Functional Theory. The electronic spectra have been calculated with the CS INDO S-CI and SDT-CI procedures. The spectral and photophysical behaviour was investigated by stationary and time-resolved techniques [4].

We are going to investigate distyrylfuran positional isomers bearing the two styryl groups in 2,4- and 3,4- positions of furan. These conjugated molecular systems are expected to display strong differences in their electronic properties.

[1] I. Škorić, I. Flegar, Ž. Marinić, M. Šindler-Kulyk, *Tetrahedron* 62 (2006) 7396.

[2] I. Baraldi, G. Ginocchetti, U. Mazzucato, A. Spalletti, *Chem. Phys.* 337 (2007) 168.

[3] I. Baraldi, E. Benassi, A. Spalletti, *Spectrochim. Acta A* (2008) in press.

[4] I. Baraldi, E. Benassi, S. Ciorba, M. Šindler-Kulyk, I. Škorić, A. Spalletti, in preparation.

Combined Experimental and Theoretical Study on the Kynurenine

E. Benassi¹ and P.S. Sherin²

¹*Dipartimento di Chimica, Università di Modena e Reggio Emilia, Modena, Italy*

²*ITC SB RAS, Novosibirsk, Russia*

e-mail: enrico.benassi@libero.it, sherin@tomo.nsc.ru

Kynurenine (KN) (Figure 1) and its derivatives act an important biological rule as UV-filters in the human lens. They absorb UV light in 300-400 nm wavelength region and protect the eye tissues from the harmful sun irradiation. This behaviour is due to the fast deactivation of the excited state; in fact, these molecules exhibit short fluorescence lifetimes and small fluorescence quantum yields. The nature of the deactivation processes is actually unknown.

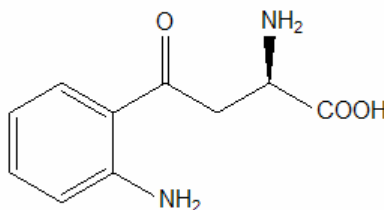


Figure 1: Structural formula of kynurenine.

The main aim of the present work is to study the energy gap between ground state and the first two singlet excited states, electronic spectra and to investigate solvent effects, both from an experimental and theoretical point of view.

Photochemistry and Vibrational Spectra of Matrix-Isolated Isoniazid

Ana Borba¹, Andrea Gómez-Zavaglia^{1,2} and Rui Fausto¹

¹Department of Chemistry, Coimbra University, P3004-535 Coimbra, PORTUGAL

²Facultad de Farmacia y Bioquímica, Buenos Aires University, RA-1113 Buenos Aires, ARGENTINA
anaborba@ci.uc.pt

Tuberculosis is still one of the most infectious diseases in the world [1]. At present, the accepted treatment of tuberculosis is achieved by drugs involving a combination of several molecules, including isoniazid, pyrazinamide, ethambutal and rifampicin. There are three main properties of antituberculosis drugs: bactericidal activity, sterilizing activity and the ability to prevent resistance [2]. Isoniazid (INH) is known to act as a bacteriostatic or bactericidal drug (depending on the concentration of the drug attained at the site of infection) against *Mycobacterium tuberculosis*. Being active only during bacterial cell division, it is still the most widely used drug in antituberculous regimens [1, 2].

In this study, INH was studied by matrix isolation infrared spectroscopy and DFT(B3LYP) and MP2 calculations. In the matrix isolation experiments, samples were prepared by co-deposition of INH (placed in a specially designed temperature variable mini-oven assembled inside the cryostat) and the inert gas, onto a cooled (10 K) CsI substrate. Irradiation of the matrices was carried out with a Hg(Xe) lamp at $\lambda > 235$ nm.

According to calculations at the DFT(B3LYP)/6-311G(d,p) level of theory, three minima were found on the potential energy surface, *Tsk*, *CSk* and *TC*, with relative energies of 0.0, 20.4 and 22.6 kJ mol⁻¹, respectively (see figure 1). In consonance with the theoretical results, only the *Tsk* form could be isolated in both argon and xenon matrices. Assignment of the observed bands was carried out on the basis of the comparison with the theoretically predicted spectra and annealing experiments. After UV irradiation, the intensities of the bands corresponding to INH decreased significantly while new bands appeared in the spectrum, indicating that INH had been photolysed to several photoproducts, whose structures are discussed in this study. The knowledge of the photochemistry of the compound may help to develop better strategies for its management, preventing undesirable losses during its industrial production and processing.



Fig. 1: Conformers of isoniazid.

[1] G. Klopman, D. Fercu, J. Jacob, *Chem. Phys.* 204 (1996) 181.

[2] F.P. Silva, J. Ellena, M. de Lima Ferreira, et al., *J. Mol. Struct.* 788 (2006) 63.

Acknowledgements

This work was supported by FCT (Projects POCTI/QUI/59019/2004 and POCTI/QUI/58937/2004), and the Instituto de Investigação Interdisciplinar of the University of Coimbra (Project III/BIO/40/2005). A.B. acknowledges FCT a Ph.D. grant (SFRH/BD/21543/2005).

Bis(sulfito)mercurates $M_2[Hg(SO_3)_2] \cdot x H_2O$ ($M = NH_4, Na, K; x = 0, 1, 2.25$) Vibrational Spectra of the Solids and of Aqueous Solutions

D.K. Breiting¹, G. Brehm², J. Züribig¹, M. Weil³, S. Baumann³

¹Institute of Inorganic Chemistry, University of Erlangen-Nürnberg, Egerlandstr.1, D-91058 Erlangen, Germany,

²Institute of Physical Chemistry, University of Erlangen-Nürnberg,

³Institute of Chemical Technologies and Analytics, Vienna University of Technology, A-91060 Vienna, Austria

As part of our recent studies of sulfito complexes of mercury [1, 2] we reacted $HgCl_2$ or HgO with sulfites M_2SO_3 ($M = NH_4, Na, K$) (molar ratio 1:2, partly with excess of sulfite) in aqueous solutions. The resulting solutions were studied by Raman spectrometry. The structures of crystalline reaction products from these solutions were determined some time ago ($Na_2[Hg(SO_3)_2] \cdot H_2O$ (2) [3]) or recently ($(NH_4)_2[Hg(SO_3)_2] \cdot (1)$ [1], $K_2[Hg(SO_3)_2] \cdot 2.25 H_2O$ (3) [4]). Common to all of these structures are $[Hg(SO_3)_2]^{2-}$ anions with slightly bent S-Hg-S units. Further, these anions are linked through extended intermolecular donor-acceptor interactions $S-O \rightarrow Hg$ leading to a three-dimensional network in (1), or to layered assemblies with (2) and (3).– Optical vibrational spectra (IR, Raman) of the crystalline solids were measured and discussed considering the respective structures.

In Raman spectra of the solutions (measured unpolarised and with two polarisation directions) the higher wavenumbers of the valence vibrations $\nu_{as}(SO_3)$ and $\nu_s(SO_3)$ of the SO_3 ligands (with reference to free SO_3^{2-}) indicate S-coordination. Then, the strong, structured and partly polarised band peaked at 185 cm^{-1} , besides rocking modes $\rho(SO_3)$, should contain the symmetric valence vibration $\nu_s(HgS_2)$ of the S–Hg–S fragment, probably linear in solution.

This vibration is also the dominating feature in the Raman spectra of the solid compounds (1), (2) and (3) (210 to 190 cm^{-1}). Further details in both Raman and IR spectra, *e.g.* partially multiple splitting of the $\nu_{as}(SO_3)$ (about 1100 to 1200 cm^{-1}), and even of $\nu_s(SO_3)$ (~ 1010 to 970 cm^{-1}), as well as of $\delta_s(SO_3)$ (around 650 cm^{-1}) and of $\delta_{as}(SO_3)$ ($\sim 500\text{ cm}^{-1}$) are due to the general positions of the anions $[Hg(SO_3)_2]^{2-}$ in all of the structures, the occurrence of two independent anions in (3), and possibly restricted and/or selective correlation coupling between the anions. This latter point has to be considered with the layered compounds (2) and (3), with distances between the anionic layers of ~ 5.1 and $\sim 9.0\text{ \AA}$, respectively. As a consequence, correlation coupling should mainly occur within and vanish between the layers with increasing distance. Weakening or loss of interlayer correlation coupling is the probable reason for the deceptively simple Raman and IR spectra of compound (3), despite the rather complex crystal structure (space group $C2/c$, cell content $Z = 16$, and $Z' = 8$ in the reduced primitive unit-cell).

Note: A few earlier IR data of (1) and their interpretation [5] differ from ours, whereas IR bands given for the internal vibrations of the SO_3 ligands in (2) [6] also appear in our otherwise more detailed IR spectrum.

[1] M. Weil, D.K. Breiting, G. Liehr, J. Züribig, *Z. Anorg. Allg. Chem.* 633 (2007) 429-434.

[2] M. Weil, S. Baumann, D.K. Breiting, *Acta Crystallogr.* C64 (2008) i35-i37.

[3] B. Nyberg, I. Cynkier, *Acta Chem. Scand.* 26 (1972) 4175-4176.

[4] M. Weil, S. Baumann, D.K. Breiting, to be published.

[5] J.I. Bullock, D.G. Tuck, *J. Chem. Soc.* (1965) 1877-1881.

[6] B. Nyberg, R. Larsson, *Acta Chem. Scand.* 27 (1973) 63-70.

Acknowledgment

Thanks to S. Hoffmann, Institute of Inorganic Chemistry, Erlangen, for running IR spectra.

Sulfito Mercurate Complexes in Solution Studied by ^{199}Hg NMR Spectrometry

D.K. Breitinger¹, M. Moll¹, G. Brehm²

¹*Institute of Inorganic Chemistry, University of Erlangen-Nürnberg, Egerlandstr. 1, D-91058 Erlangen, Germany,*

²*Institute of Physical Chemistry, University of Erlangen-Nürnberg,*

Recently, several crystalline sulfito complexes of mercury appropriate for X-ray structure analyses were obtained upon reaction of HgX_2 ($X = \text{Cl}, \text{Br}$) or HgO with sulfites M_2SO_3 ($M = \text{NH}_4, \text{Na}, \text{K}$) in aqueous solutions [1-3]. Some of these complexes in solution were already studied by Raman spectrometry. In order to get more insight into the composition of the solutions prior to crystallisation of solid reaction products we started ^{199}Hg NMR studies, also of redissolved crystalline reaction products. To our knowledge no pertinent ^{199}Hg NMR data have been published up to now.

In the chosen systems only atoms without magnetically active nuclei or with quadrupole nuclei (Cl, Br) are bound to mercury; thus, because of lack or suppression of heteronuclear coupling very simple single-line ^{199}Hg NMR spectra are expected.

First, solid $\text{K}_2[\text{Hg}(\text{SO}_3)_2] \cdot 2.25 \text{H}_2\text{O}$ (**1**) contains $[\text{Hg}(\text{SO}_3)_2]^{2-}$ anions (X-ray structure analysis [4]) which are still present after dissolution in H_2O (Raman spectrometry). The ^{199}Hg NMR spectrum of a solution of (**1**) in D_2O displays one single resonance at $\delta = -2152$ ppm *re neat* $\text{Hg}(\text{CH}_3)_2$; the very narrow NMR signal of HgCl_2 in D_2O appears at $\delta = -1556$ ppm. This means that the Hg nuclei in the anion are much more shielded than in solvated HgCl_2 . Further, the solution of HgCl_2 and $(\text{NH}_4)_2\text{SO}_3$ (molar ratio 1:1), from which $(\text{NH}_4)[\text{ClHgSO}_3]$ crystallises after some time (crystal structure in [1]), gives one NMR signal (-1550 ppm) close to that of HgCl_2 , but asymmetric and much broader than that of HgCl_2 . This signal is attributed to the polar $[\text{ClHgSO}_3]^-$ anions (probably linear Cl-Hg-S skeleton) with shielding of the Hg nuclei similar as in HgCl_2 , but with faster (spin-lattice) relaxation.

Finally, for the D_2O solution obtained upon reaction of HgO and K_2SO_3 in the heat, analogous to the preparation of the compound $\text{K}_2[\text{O}(\text{HgSO}_3)_3]$ with a new anionic metalloonium complex [2], a single signal is observed at $\delta = -1999$ ppm. This signal is appropriate and reasonable for the $[\text{O}(\text{HgSO}_3)_3]^{2-}$ anion, as shielding is expected to be lower with reference to $[\text{Hg}(\text{SO}_3)_2]^{2-}$ for the following reasons: The average negative charge in one Hg- SO_3 fragment is lower than in $[\text{Hg}(\text{SO}_3)_2]^{2-}$, the charge tends to shift to the periphery, and Hg is bound to the electronegative and formally positive central oxygen atom.

As a general result, in each of the solutions studied seemingly only one mercury-containing complex species is present.

[1] M. Weil, D.K. Breitinger, G. Liehr, J. Zürlbig, *Z. Anorg. Allg. Chem.* 633 (2007) 429-434.

[2] M. Weil, S. Baumann, D.K. Breitinger, *Acta Crystallogr. C* 64 (2008) i35-i37.

[3] M. Weil, S. Baumann, D.K. Breitinger, *Z. Anorg. Allg. Chem.*, in press.

[4] M. Weil, S. Baumann, D.K. Breitinger, to be published.

Acknowledgment

Thanks to Mrs S.-E. Tschech, Institute of Inorganic Chemistry, Erlangen, for assistance.

Association of Water with Small Monocarboxylic Acids. Matrix Isolation Infrared Absorption Study.

J. Ceponkus, D. Lesciute, V. Sablinskas

*Department of General Physics and Spectroscopy, Vilnius University
Universiteto str. 3 Vilnius, LT-01513, Lithuania*

Water is very important in many chemical, physical and biological processes. Single water molecule is rather simple system, consisting from three atoms. Nevertheless, due to its structure water molecules are able to form hydrogen bonds. Thus water molecules could form very complicated associates with organic and inorganic substances.

There are a number of reasons to study hydrogen bond complexes between water and carboxylic acids. Small carboxylic acids are abundant in the environment therefore it is important to know how water changes the properties of such substances. On the other hand carboxylic acids are one of the smallest organic compounds capable of forming hydrogen bonds therefore they could serve as very good model compounds for the understanding of more complicated systems in biology and biochemistry.

There only two attempts experimentally characterize structure of formic acid and water complexes [1-2]. Due to the complicity of the system there are no experimental studies on the complexes of water with higher carboxylic acids. In order to have full picture of hydrogen bonding between water and organic compounds it is very important to understand how this interaction is influenced by the length of the radical chain of the substance under study.

Infrared absorption spectroscopy is one of the most suitable methods to study molecular systems. From the structure of vibrational and rotational bands one can obtain direct information about molecules and molecular clusters. Matrix isolation technique extends possibility of the infrared spectroscopy, to study isolated molecules and molecular complexes.

Vapor of carboxylic acid and water were mixed in the vacuum system using standard manometric technique. Such mixtures afterwards were diluted with argon (matrix gas). In order to identify spectral bands associated with different possible clusters a wide number of ratios carboxylic acid:water:argon was used. Matrix mixtures were deposited on the spectroscopic window cooled down to 10 K, in the close cycle helium cryostat. Approximately 2 moles of the matrix mixture were deposited in all experiments.

Quantum chemistry calculations of possible water carboxylic acid complexes were performed at HF 6-311++(3df, 3pd) and B3LYP 6-311++(3df, 3pd) calculation levels. Based on theoretical calculations and experimental observations C=O stretch vibrations are the most sensitive to the formation of the hydrogen bond, therefore spectral region corresponding to those vibrations were chosen for the detail examination.

Spectral bands were attributed to the water carboxylic acid complexes based on results of experiments performed using different acid:water:argon ratios and matrix annealing experiments. Our theoretical calculations support such assignment. Strength of the hydrogen bond and the structure of the most stable complexes between water and carboxylic acid were estimated from the theoretical and experimental data. In this work structural and energetic parameters of acetic acid – water, propionic acid – water and butyric acid – water were obtained for the first time.

- [1] D. Priem, T.-K. Ha, and A. Bauder, *The Journal of Chemical Physics* 113 (2000) 169-175.
[2] L. George, W. Sander, *Spectrochimica Acta A* 60 (2004) 3225–3232.

Molecular and Electronic Structure of PTCDI and Melamine-PTCDI Complex

V. Chiş, R. Ştiufluic, N. Leopold

Babeş-Bolyai University, Faculty of Physics, Kogalniceanu 1, RO-400084, Cluj-Napoca, Romania

Perylene derivatives received great scientific interest in the last years due to their potential applications in molecular electronics. Particularly, 3,4,9,10-perylene-tetracarboxylic diimide (PTCDI) and the anhydride analogue (PTCDA) were the subject of studies aiming to elucidate their absorption mechanism on different substrates [1]. Recent studies are reported on the hydrogen-bonding guided assembling by co-adsorption of PTCDI and melamine (1,3,5-triazine-2,4,6-triamine) on silver terminated silicon [2] or gold surfaces [3].

In this work we will report on the molecular and electronic structure of PTCDI, melamine and melamine-3PTCDI complex (Fig.1). The complex is stabilized by strong intermolecular hydrogen bonds whose calculated lengths at B3LYP/6-31G level of theory are 2.914 Å and 2.888Å for NH...O and N...HN bonds, respectively. The calculated center-to-center spacing of PTCDI-melamine (9.972 Å) pair is in excellent agreement with the observed separation of 9.98Å [2].

Infrared and Raman spectra of PTCDI and melamine-3PTCDI complex were calculated and the experimentally observed spectra were safely assigned based on theoretical data. Important shifts are observed for the imide groups whose $\nu(\text{NH})$ wavenumbers are 3583cm^{-1} in free PTCDI and 2790cm^{-1} in melamine-3PTCDI complex.

Molecular orbitals energies of the PTCDI molecule are calculated at different levels of theory, using DFT methods. The influence of an external electrostatic field on the shape and energies of the frontier orbitals and HOMO-LUMO gap is investigated. The field shifts both the HOMO and LUMO energy levels and their spatial distribution. The gap decreases drastically by increasing the strength of the applied external field parallel to the molecular plane and it remains almost insensitive when the external field is applied perpendicular to the molecular plane.

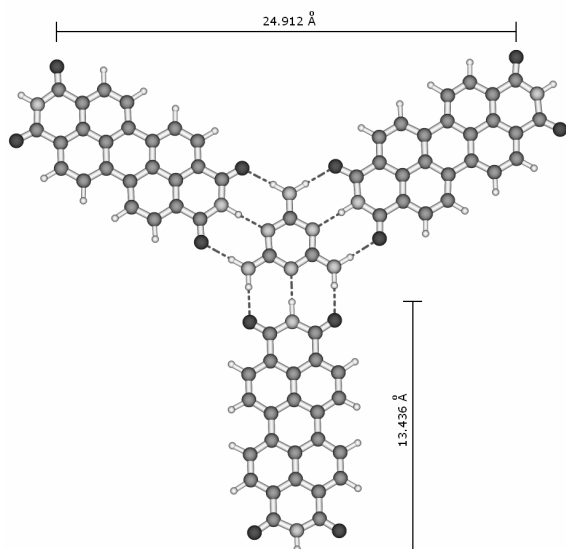


Fig. 1: B3LYP/6-31G optimized geometry of the melamine-3PTCDI molecular complex

- [1] D.R.T. Zahn, G. Salvan, B.A. Paez, R. Scholz, J. Vac. Sci. Technol. A 22 (2004) 1482-1487.
- [2] J.A. Theobald, N.S. Oxtoby, M.A. Phillips, N.R. Champness, P.H. Beton, Nature 424 (2003) 1029-1031.
- [3] F. Silly, A.Q. Shaw, K. Porfyrakis, G.A.D. Briggs, M.R. Castell, Appl. Phys. Lett. 91 (2007) 253109.

Effect of Organic Modifiers on the Solution Viscosity, Gelation Time and Progress of Hydrolysis/Condensation Reactions during Hybrid Gels Formation

K. Cholewa-Kowalska¹, M. Laczka¹, Z. Olejniczak²

¹*AGH-University of Science and Technology, Faculty of Materials Science and Ceramics, Department of Glass Technology and Amorphous Coating, Al. Mickiewicza 30, 30-059 Krakow, Poland*

²*Institute of Nuclear Physics, ul. Radzikowskiego 152, 31-342 Krakow, Poland*

Inorganic-organic hybrid gels are new nanometric materials where coexistence, on molecular scale, inorganic structures in the form of silica-oxide network and organic structures basing on carbon links. Properties of these hybrids are intermediate between inorganic glasses and organic polymers and depend on the kind and amount of units, building their structure. Moreover, the structure and properties of hybrids are determined by the progress of hydrolysis and polycondensation reactions during gel formation.

The objective of this work is to study the effect of the type of organic modifiers on the rheological property of the alkoxide solution and structure of the obtained organic –inorganic gels.

Five different kinds of hybrid materials produced by sol-gel method, all identical in terms of production procedure, but differing in terms of organic modifiers, have been examined. Tetraethoxysilane was used as the inorganic precursor and methyltrimethoxysilane (MTMS), vinyltriethoxysilane (VTES), phenyltriethoxysilane (PhTES), diethoxydimethylsilane (DEDMS), diethoxymethylvinylsilane (DEMVS) as organic modifiers.

The viscosity of the solutions was measured at 20 °C using a Brookfield viscometer. The gelation time was recorded for each of the sols. The progress of hydrolysis and polycondensation reactions was examined for wet gels, gels dried at ambient conditions and gels after treatment at 40 and 100 °C. As a method of examinations FTIR spectroscopy and ²⁹Si MAS NMR spectroscopy were used.

From our result it follows that the introduction of unhydrolysable organic groups retards the sol-gel process (longer gelation time) and act as fillers in the silica network, leading to the condensation of the obtained gels. It has been also found that hydrolysis reaction of hybrid gels proceeds mainly in solutions and polycondensation of gels, in the presence of organic modifiers, is more advanced than in the case of TEOS without addition of modifiers. Moreover, copolymers are formed between structural units of Si atoms in TEOS (Q) and in organic modifiers (T, D).

N–H···O Hydrogen Bonding. FT-IR and NIR Study of N-Methylformamide-Ether Systems.

A. Nikolić¹, B. Jović¹, E. Davidović² and S. Petrović³

¹Department of Chemistry, Faculty of Sciences, University of Novi Sad, 21000 Novi Sad, Serbia

²"Lavoslav Ružička" Polytechnic of Vukovar, 32000 Vukovar, Croatia

³Faculty of Technology and Metallurgy, University of Belgrade, 11000 Belgrade, Serbia

The paper reports the results of FT-IR and NIR study of N-methylformamide in carbon tetrachloride solution and in presence of ethers as the O-electron donors. The spectroscopic characteristics for N-H···O hydrogen bonded complexes are given. Also, the equilibrium constants for 1:1 complex formation, at 25 °C were determined using IR and NIR measurements.

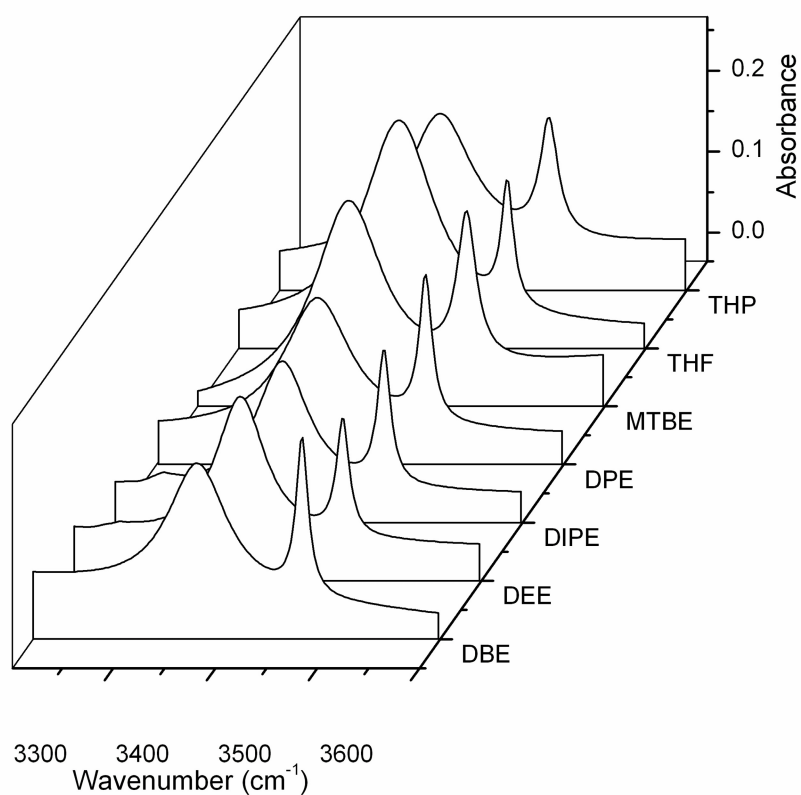


Figure 1: IR spectra of N-methylformamide, in the presence of seven different ethers with same concentration.

[1] A. Nikolić, B. Jović, V. Krstić, J. Tričković, *J. Mol. Liquids* 133 (2007) 39.

[2] A. Nikolić, B. Jović, S. Csanady, S. Petrović, *J. Mol. Structure* 834 (2007) 249.

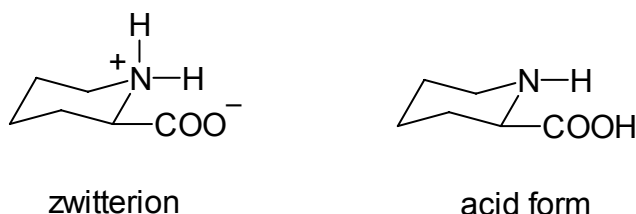
Experimental and Theoretical Vibrational Spectra of Piperidine-2-carboxylic Acid

Zofia Dega-Szafran, Mirosław Szafran,

*Faculty of Chemistry, Adam Mickiewicz University, 60-780 Poznań, Poland
degasz@amu.edu.pl*

Piperidine-2-carboxylic acid, P2C (pipecolic acid, homoproline) is a widespread, naturally occurring nonproteinogenic α -amino acid found in many plants e.g. beans, mushrooms, potatoes, green pepper, tulip, celery, barley and coconut milk [1].

P2C crystallizes from water as tetrahydrate [2, 3], however the commercially available product (Sigma, Aldrich) is anhydrous [4]. P2C exists in crystals as a zwitterion with the carbonyl group in the equatorial position. P2C molecules interact by the N-H \cdots OOC intermolecular hydrogen bond of 2.767 Å [4].



In this contribution we investigate the FTIR, Raman and NMR spectra of P2C. To get detailed information on the nature of normal modes, the potential energy distributions (PED) were calculated at the B3LYP/6-31G(d,p) level of theory. Spectroscopic and theoretical investigations allowed unequivocal and complete vibrational assignments of the FTIR spectrum of P2C. In the optimized structure P2C exists in its acid form.

- [1] N. Grobbelaar, R.M. Zacharius, F.C. Steward, *J. Am. Chem. Soc.* 76 (1954) 2912.
- [2] S.K. Bhattacharjee, K.K. Chacko, *Acta Crystallogr.* B35 (1979) 396.
- [3] K.L. Lyssenko, Y.V. Nelyubina, R.G. Kostyanovsky, M.Yu. Antipin, *Chem. Phys. Chem.* 7 (2006) 2453.
- [4] C.P.D. Stapleton, E.R.T. Tiekink, *Acta Crystallogr.* E57 (2001) 75.

Molecular Structure of the Hydrated Complex of 1,4-dimethylpiperazine di-betaine with L-tartaric Acid Studied by X-ray Diffraction and FTIR

Zofia Dega-Szafran, Andrzej Katrusiak, Mirosław Szafran

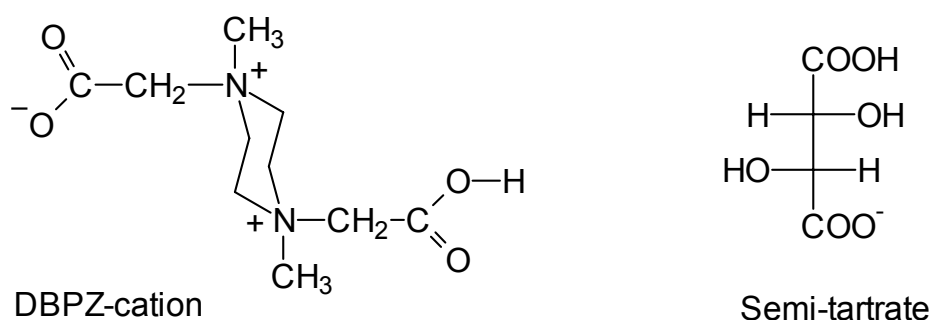
Faculty of Chemistry, Adam Mickiewicz University, 60-780 Poznań, Poland
degasz@amu.edu.pl

1,4-Dimethylpiperazine di-betaine (1,4-dicarboxymethyl-1,4-dimethylpiperazinium inner salt, DBPZ) forms two kinds of 1:1 complexes with L-tartaric acid (TA), anhydrous DBPZ·TA and hydrated DBPZ·TA·2.5H₂O.

In the first one, DBPZ·TA, DBPZ and TA molecules are linked into infinite chains by two asymmetric hydrogen bonds of 2.485(3) and 2.566(3) Å, the carboxylic group of TA and the carboxylate group of DBPZ, without the proton transfer. The piperidine ring has a chair conformation with the methyl groups in the axial positions and the CH₂COO substituents equatorial [1].

In this contribution we report the molecular structure and spectroscopic properties of the DBPZ·TA·2.5H₂O complex studied by the X-ray diffraction, FTIR and Raman spectroscopies and optimized by at the B3LYP/6-31G(d,p) level of theory.

In the complex investigated the piperazine ring has a chair conformation, however the substituents assume the opposite orientations than in the DBPZ·TA complex, e.g. the methyl groups are equatorial and the CH₂COO substituents are axial. One proton from the carboxylic group of TA is transferred to the carboxylate group of DBPZ. The DBPZ cations are linked by the asymmetric, short COOH···OOC hydrogen bonds of 2.476(3) Å into chains, while the semi-tartrate anions are linked by the short and symmetric COO·H·OOC hydrogen bonds of 2.464(3) Å into separate chains. The chains of the positively charged, DBPZ⁺, and negatively charged, TA⁻, molecules are joined together only by a weak O-H···O=C hydrogen bond of 3.230(4) Å, into layers. Water molecules are involved in the hydrogen bonds with the TA chains.



The solid-state FTIR spectrum is consistent with the crystal structure. The broad band, attributed to the ν_{OH} vibration, appears in the 3600-3100 cm⁻¹ region. A broad absorption in the 1500-400 cm⁻¹ region is characteristic of the short OHO hydrogen bonds.

[1] Z. Dega-Szafran, A. Katrusiak, M. Szafran, J. Mol. Struct. (2008) in press.

Towards Organic Conductors - the Structure and Stability of Cyano-[n]-Radialenes and Their Dianions

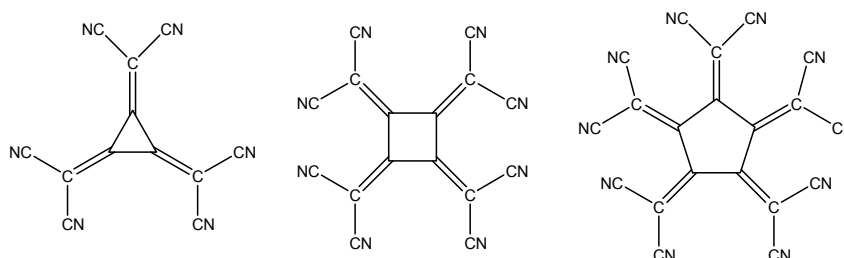
I. Despotović¹, Z.B. Maksić²

¹*Quantum Organic Chemistry Group, Division of Organic Chemistry and Biochemistry, Ruđer Bošković Institute, Bijenička 54, 10000 Zagreb, Croatia; e-mail: idespoto@irb.hr*

²*Faculty of Science, Department of Physical Chemistry, The University of Zagreb, Horvatovac 102A, 10000 Zagreb, Croatia*

It is well known that molecular anions play important role in organic chemistry and biochemistry. Special attention has been focused on dianions and higher anions lately, because they might prove very useful in storage and transport of electrons in the fields of photo-and/or electrically conducting polymers [1]. It follows that anions are likely to provide a bridge between organic chemistry and material science. It is therefore very important to get insight into the structure, stability and reactivity of mono- and higher anions.

In the present work we consider the structure and energetic properties of some neutral [n]-radialenes (n = 3, 4, 5) substituted by various groups and their mono- and dianions utilizing B3LYP/6-311+G* computational scheme [2]. It is found that cyano substitution enables efficient stabilization of dianions, which is higher the greater number of the CN groups is present. Hexacyano-[3]-radialene dianion is by 126 kcal mol⁻¹ more stable than the initial



neutral compound, and by 13.3 kcal mol⁻¹ than its monoanion. Other examined [3]-radialene dianions dissociate to monoanions, which are significantly more stable. The underlying principle governing strong stabilization of hexacyano-[3]-radialene dianion is highly effective anionic resonance, which distributes the excessive negative charge predominantly on the peripheral parts of the dianions. The latter is corroborated by examination of the bond lengths and redistribution of the electron density upon reduction and by calculation of the perpendicular NICS(1)_{zz} component of the magnetic shielding tensor calculated 1 Å above the center of the three-membered ring. Higher [n]-radialenes (n = 4, 5) involving larger number of CN substituents provide even more stable dianions [3], giving excellent candidates for polyanions which could make strong complexes with the electron accepting system and eventually yielding strong organic conductors or perhaps the organic “metals”. It is shown that hexacyano-[3]-radialene is strong oxidant in MeCN.

[1] M. Baumgarten, U. Müller, *Synth. Met.* 57 (1993) 4755-4761.

[2] I. Despotović, Z.B. Maksić, *J. Mol. Struct. THEOCHEM* 811 (2007) 313-322.

[3] To be published.

Interpretation of Vibrational Spectra of Allyl Acrylate

Małgorzata E. Jamróz¹, Michał H. Jamróz¹, Joanna E. Rode¹, Jan Cz. Dobrowolski^{1,2}

¹Industrial Chemistry Research Institute, 8 Rydygiera Street, 01-793 Warsaw, Poland, ²National Medicines Institute, 30/34 Chelmska Street, 00-725 Warsaw, Poland,

Esters of acrylic acid are widely used as monomers for acrylic polymers, which are further used for production of dyes, paper, textiles, glues, adhesives, paints etc. Demand for acrylic acid was estimated in 2005 to increase ca. 4.2 percent a year [1]. More than half of the world production of acrylic acid is used to synthesize various acrylic acid esters: mainly methyl, ethyl, n-butyl, and 2-ethylhexyl acrylates. Since few years we are developing a technology for production of acrylates from waste glycerol, therefore, we are also involved in a deeper characterization of particular products such as allyl acrylate. Allyl acrylate is used for curing polymeric materials, such as those utilized in dentistry.

The vibrational spectra of allyl acrylate (Fig. 1) were not interpreted in details, so far. This is a laborious task because of numerous conformations that the allyl acrylate molecule can adopt (Fig. 2). Our population analysis and IR and Raman spectra calculations of the allyl acrylate conformers were performed at the B3LYP/aug-cc-pVDZ level. Based on these calculations, there are seven conformers which are less stable than the most stable one by less than 1.0 kcal/mol, only. To interpret the experimental spectra, the calculations were followed by the potential energy distribution analysis.

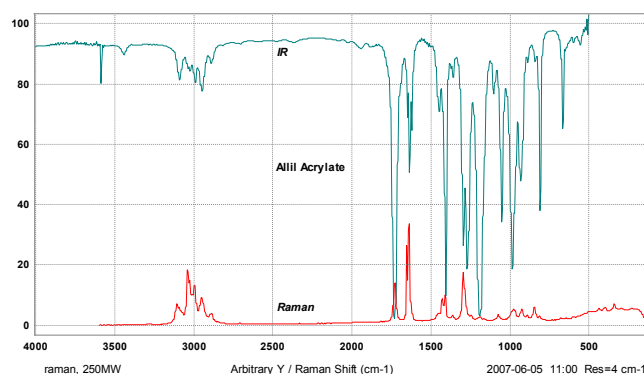


Fig. 1: The IR and Raman spectra of allyl acrylate.

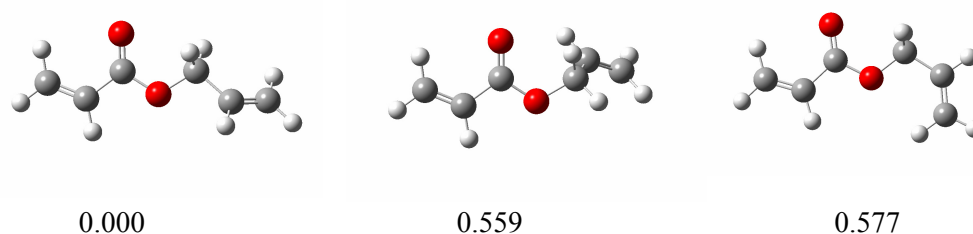


Fig. 2: The most stable three conformers of allyl acrylate calculated at the B3LYP/aug-cc-pVDZ level accompanied with the Gibbs free energy differences in kcal/mol.

[1] Acrylic Acid & Derivatives to 2005 - Market Size, Market Share, Market Leaders, Demand Forecast and Sales, © Copyright 2006 The Freedonia Group, Inc. 767 Beta Drive Cleveland, Ohio 44143.

Raman Study of Nickel(II) Complexes with 6-Methylpicolinic Acid

Krešimir Furić¹, Boris-Marko Kukovec² and Zora Popović²

¹Molecular Physics Laboratory, Division for Material Physics, Ruđer Bošković Institute, POB 180, Bijenička cesta 54, HR-10002 Zagreb, Croatia, kfuric@irb.hr

²Laboratory of General and Inorganic Chemistry, Department of Chemistry, Faculty of Science, University of Zagreb, Horvatovac 102a, HR-10000 Zagreb, Croatia, bkukovec@chem.pmf.hr

The first **(1)** nickel(II) complex with 6-methylpicolinic acid was prepared by mixing of 6-methylpicolinic acid and nickel(II) nitrate hexahydrate solutions, while the second **(2)** complex was prepared by recrystallization of **(1)** from DMF solution [1]. Pseudopolymorphism of these two complexes was identified and characterized by means of X-ray, Raman, IR, calorimetric and DFT methods. X-ray diffraction study discovered two structures differing mainly in crystal packing due to the presence **(1)** or absence **(2)** of hydrated water molecules (see Fig. 1; **(2)** is isostructural with Co(II) complex [2]).

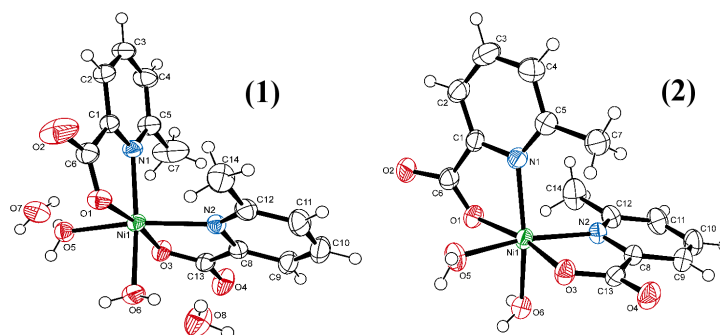


Fig. 1: ORTEP-3 drawings of $[\text{Ni}(6\text{-Mepic})_2(\text{H}_2\text{O})_2]\cdot 2\text{H}_2\text{O}$ **(1)** and $[\text{Ni}(6\text{-Mepic})_2(\text{H}_2\text{O})_2]$ **(2)**.

Raman spectroscopy of both $[\text{Ni}(6\text{-Mepic})_2]$ complexes confirmed that difference of two structures is correlated with the presence of water molecule that appears incorporated in the solid structure across two different hydrogen bonds of weak and medium strengths.

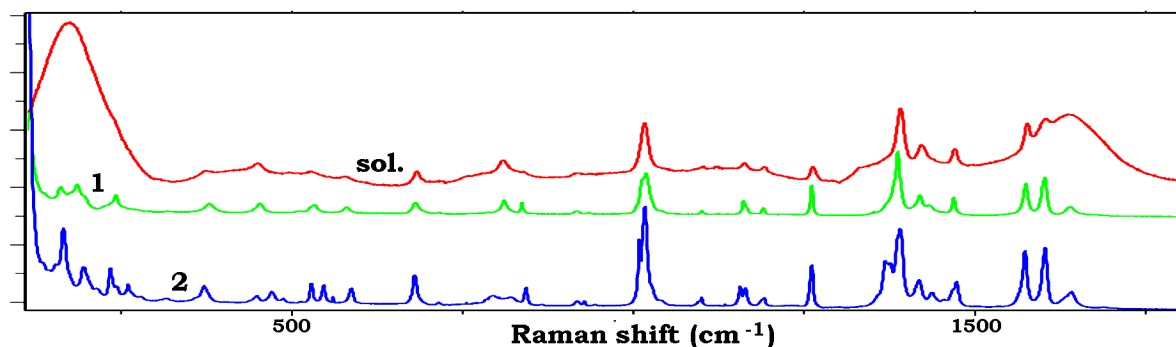


Fig. 2: Fingerprint region of Raman spectra of the solution and both Ni complexes **(1)** and **(2)**.

All bands observed for crystalline matter and for the solution, together with the assignment based on other similar complexes and methylpyridine [3], verify X-ray study results.

[1] B.M. Kukovec *et al*, International School of Crystallography, 39th Course, Erice, Italy, 2007, Lecture Notes and Poster Abstracts, Part 2, p. 626.

[2] R. March *et al*, Inorg. Chim. Acta 353 (2003) 129-138.

[3] J.F. Arenas, I. López Tocón, J.C. Otero, J.I. Marcos, J. Mol. Struct. 476 (1999) 139.

Isomerizational and Conformational Study of 3-Cyclopropylamino-2-Acetyl Propenenitrile (CpAAP) and 3-Cyclopropylamino-2-Methylsulfonyl Propenenitrile (CpASP)

J. Polovková¹, A. Gatial¹, M. Gróf¹, J. Kožíšek¹, V. Milata², N. Prónayová³, P. Matějka⁴

¹Department of Physical Chemistry, ²Department of Organic Chemistry, ³Central Laboratories, Faculty of Chemical and Food Technology, Slovak University of Technology, SK-81237 Bratislava, Slovakia

⁴Department of Analytical Chemistry, Institute of Chemical Technology, CZ-16628 Prague, Czech Republic

(H₅C₃)-NH-CH=C(CN)(COCH₃) (CpAAP) and (H₅C₃)-NH-CH=C(CN)(SO₂CH₃) (CpASP) belong to the push-pull ethylenes intensively used in synthetic organic chemistry. The electron donor cyclopropylamino group in the investigated compounds seems to have a special influence on their conformational and configurational equilibria perhaps due to the possibility to create an intramolecular hydrogen bond.

Using *ab initio* MP2 and DFT B3LYP calculations in 6-31G** basis set seven conformers of CpAAP have been found, three for *Z*-isomer and four for *E*-isomer (the first letter denotes *cis* and *trans* position of cyclopropylamino and acetyl groups, the second *Z* or *E* and the third *s* or *a* letters denote the conformational orientation of carbonyl oxygen and cyclopropylamino group towards or from double C=C bond, respectively). However, as shown by calculations, they significantly differ in energy. The most stable conformer is the *ZZa* one that enables an intramolecular hydrogen bond. This conformer has been synthesized and confirmed by NMR in chloroform. *ZZa* cannot pass to other *Z*-isomer conformers. Nevertheless, in more polar DMSO only the process of isomerization takes place and the next two conformers of *E*-isomer with *anti* and *syn* orientation of cyclopropylamino group have been confirmed.

In the case of CpASP, there are only four possibilities from the conformational point of view because sulfonyl group can exist only in a single orientation towards the double C=C bond (one S=O bond coplanar with C=C bond, the second S=O bond and methyl group above and below this plane). Therefore we can consider for both *E* and *Z* isomers only the *anti* (*a*) or *syn* (*s*) conformational positions of cyclopropylamino group (second letter). Because the cyclopropylamino group is also oriented out of the plane of olefinic skeleton, its position toward the methyl group is given by the third letter *a* or *s* (on the opposite or the same side of this plane). Analogously to CpAAP we have found by *ab initio* MP2 calculations that the most stable conformer is the *Zaa* one. However, in the synthetic process the pure *E*-isomer has been obtained. In DMSO the presence of both *E*-isomer conformers has been proven both by NMR and vibrational spectroscopy with *Eaa* conformer as the more stable one. Additionally, in less polar chloroform an isomerization process occurred and the *Z*-isomer has been detected as well. In order to explain such behavior, solvent effect calculations using PCM model have been done.

Table 1: MP2/6-31G** calculated *ab initio* relative energies ΔE of CpAAP and CpASP conformers.

CpAAP	<i>EZa</i>	<i>EZs</i>	<i>EEa</i>	<i>EEs</i>	<i>ZZa</i>	<i>ZZs</i>	<i>ZEa</i>
$\Delta E(\text{kJ/mol})$	14.93	19.68	28.09	37.65	0.00	40.77	49.86
CpASP	<i>Eaa</i>	<i>Eas</i>	<i>Esa</i>	<i>Ess</i>	<i>Zaa</i>	<i>Zas</i>	<i>Zsa</i>
$\Delta E(\text{kJ/mol})$	4.28	4.58	6.17	7.08	0.00	0.60	28.73

Acknowledgement

This work has been supported by Slovak Grant Agency VEGA (Projects No. 1/3566/06 and 1/0225/08).

Spectral Investigations on Metal Complexes of Heterocyclic N,S-Donors

I. Gocan¹, C. Nagy¹, M.M. Venter², V. Bercean³, L. David¹

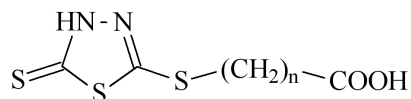
¹"Babes-Bolyai" Univ., Faculty of Physics, Kogalniceanu 1, RO- 400084 Cluj-Napoca, Romania
leodavid@phys.ubbcluj.ro

²"Babes-Bolyai" University, Faculty of Chemistry and Chemical Engineering, Arany Janos 11, RO- 400028 Cluj-Napoca, Romania

³"Politehnica" University, Faculty of Industrial Chemistry and Environment Engineering, Pt. Victoriei 2, 300006 Timisoara, Romania.

The heterocyclic N,S-donors were successfully used in the design of supramolecular structures revealing nanometric cavities. Some of these derivatives (i.e. trithiocyanuric acid) revealed outstanding catalytic and separation properties. The design of such non-conventional microporous materials involves molecular self-assembly through E-H...E (E = N, S) and/or S...S interactions [1, 2].

In view of recent interest in this field, we initiated the vibrational characterization of new 5-mercapto-1,3,4-thiadiazole-2-yl carboxylic acids, C₂N₂HS₃(CH₂)_nCOOH, *n* = 1 – 3 (Scheme I) [3]. Furthermore, the first homologue (*n* = 1) was used in its monodeprotonated form in the synthesis of some s and d metal complexes [4]. The preliminary spectral investigations encouraged the extension of our work on a larger range of coordination compounds, including: (i) paramagnetic metal centers, (ii) completely deprotonated donor species and (iii) various homologue ligands.



Scheme I

The reaction of mono- and di-deprotonated precursors [ex. Na(HL) and Na₂L, L = C₂N₂S₃(CH₂)_nCOO²⁻] with d metal salts (ex. Cr³⁺, Mn²⁺, Fe²⁺, Fe³⁺, Co²⁺, Ni²⁺, Cu²⁺, etc.) produced a series of metal complexes. FT-IR, Raman, UV-VIS and RES spectral methods were used to suggest the most probable coordination sites of the ligands and coordination geometries around the metal centers. For example, the powder ESR spectra of the majority of paramagnetic complexes are typically for monomeric species with octahedral local symmetry around the metallic ions.

The FT-IR and Raman spectra were of great help in elucidating the thione tautomer of the 5-mercapto-1,3,4-thiadiazole-2-yl carboxylic donors in their monodeprotonated form. Moreover, the spectra revealed that the deprotonation of the ligand occurs first at the carboxylic group.

- [1] V. Bercean, C. Crainic, I. Haiduc, M.F. Mahon, K.C. Molloy, M.M. Venter, P.J. Wilson, J. Chem. Soc., Dalton Trans. (2002) 1036.
- [2] C.N.R. Rao et al, J. Amer. Chem. Soc. 119 (1997) 10867; J. Mater. Chem. 9 (1999) 2407; J. Amer. Chem. Soc. 121 (1999) 1752.
- [3] M.M. Venter, S. Cinta-Pinzaru, I. Haiduc, V. Bercean, Studia Univ. Babes-Bolyai, Physica XLYX(3) (2004) 285.
- [4] M.M. Venter et al, Rev. Roum. Chim. 52(1-2) (2007) 75; Studia Univ. Babes-Bolyai, Ser. Chem. LII(1) (2007) 55; Studia Univ. Babes-Bolyai, Ser. Chem. LI(2) (2006) 65.

Conformational Analysis of Aminomethylene- and Methylaminomethylene-Malonic Acid Dimethylester

M. Gróf¹, A. Gatiaľ¹, J. Kožíšek¹, V. Milata², P. Matějka³

¹Department of Physical Chemistry, Faculty of Chemical and Food Technology, Slovak University of Technology, SK-81237 Bratislava, Slovakia

²Department of Organic Chemistry, Faculty of Chemical and Food Technology, Slovak University of Technology, SK-81237 Bratislava, Slovakia

³Department of Analytical Chemistry, Institute of Chemical Technology, CZ-16628 Prague, Czech Republic

The aim of this work is the conformational study and interpretation of vibrational spectra of aminomethylene-malonic acid dimethylester [H₂N-CH=C(COOCH₃)₂, AMDME] and methylaminomethylene-malonic acid dimethylester [H₃C-NH-CH=C(COOCH₃)₂, MAMDME]. These compounds belong to the so-called push-pull olefines which are often used as starting reactants or intermediates for a lot of pharmaceutical, dye, polymer and other syntheses [1]. The polar character of push-pull ethylenes, the electronic interactions between substituents and the double bond are responsible for their non-linear optical properties [2].

Both compounds can exist in four *ZZ*, *EZ*, *ZE* and *EE* conformations with regard to the orientation of both methylester groups where the first and second letters express the orientation of the carbonyl oxygen to the C=C bond for *trans* and *cis* methylester group, respectively. In addition, for MAMDME the next conformational possibility due to the *anti* and *syn* orientation of the methylamino group to the C=C bond exists. Previous study of such aminodiesteres revealed that *EZ* conformation of these compounds exists in solid phase. In a nonpolar solvent the next *ZZ* conformer is present and in a polar solvent even the third one, probably *ZE*, was observed, too [3, 4]. This work contains theoretical calculations and X-ray, vibrational and NMR study as well. The solid phase X-ray study revealed *EZ* conformer of AMDME but *ZZa* conformer of MAMDME. Though, MP2 and DFT calculations in 6-31G** basis set predict for both compounds the conformer with *ZZ* orientation of both methylester groups as the most stable one followed by the *EZ* one (Table 1). These differences are explained by the influence of environment polarity on the conformational equilibrium and are discussed with respect to the SCRF solvent effect calculations using PCM model.

Table 1: Calculated MP2 and DFT relative energies ΔE and dipole moments μ of AMDME and MAMDME conformers.

AM DME	$\Delta E(\text{MP2})$ (kJ/mol)	$\Delta E(\text{DFT})$ (kJ/mol)	$\mu(\text{MP2})$ (D)	MAM DME	$\Delta E(\text{MP2})$ (kJ/mol)	$\Delta E(\text{DFT})$ (kJ/mol)	$\mu(\text{MP2})$ (D)
<i>ZZ</i>	0.00	0.00	1.50	<i>ZZa</i>	0.00	0.00	2.01
<i>EZ</i>	3.08	4.51	3.36	<i>EZa</i>	3.39	4.78	3.91
<i>ZE</i>	13.51	16.51	4.17	<i>ZEa</i>	15.17	18.04	4.66
<i>EE</i>	19.24	25.63	5.85	<i>EEa</i>	21.29	27.40	6.41

[1] S.F. Dyke, *The Chemistry of Enamines*; Cambridge University Press: London 1973.

[2] D. Chemla, J. Zyss, *Nonlinear Optical Properties of Organic Molecules and Crystals*, vol. 1, Academic Press, New York, 1987, pp. 23-187.

[3] D. Smith, P.J. Taylor, *J. Chem. Soc., Perkin Trans. II* (1979) 1376.

[4] A. Gomez-Sanchez, E. Sempere, J. Bellanato, *J. Chem. Soc., Perkin Trans. II* (1981) 561.

Acknowledgement

This work has been supported by Slovak Grant Agency VEGA (Projects No. 1/3566/06 and 1/0225/08).

Conformational Analysis of Dimethylaminomethylene-Malonic Acid Dimethyl Ester

M. Gróf¹, A. Gatiaľ, J. Kožíšek¹, V. Milata², P. Matějka³

¹Department of Physical Chemistry, Faculty of Chemical and Food Technology, Slovak University of Technology, SK-81237 Bratislava, Slovakia

²Department of Organic Chemistry, Faculty of Chemical and Food Technology, Slovak University of Technology, SK-81237 Bratislava, Slovakia

³Department of Analytical Chemistry, Institute of Chemical Technology, CZ-16628 Prague, Czech Republic

The aim of this work is the conformational study and interpretation of vibrational spectra of the title compound [(H₃C)₂N-CH=C(COOCH₃)₂, DMAMDME]. This compound belongs to the family of so-called push-pull ethylenes containing electron-donor groups at one end and electron-acceptor groups at the other end. Despite the large interest in organic synthesis [1] the theoretical and experimental study of their conformers with the interpretation of vibrational spectra has not yet been carried out for many of them.

DMAMDME can exist in four *ZZ*, *EZ*, *ZE* and *EE* conformations with regard to the orientation of both methylester groups where the first and second letters express the orientation of the carbonyl oxygen to the C=C bond for *trans* and *cis* methylester group, respectively. Previous study of DMAMDME revealed that this compound exists in solid phase in *ZE* conformation with the carbonyl of *cis* methylester twisted by 68° to the plane formed by the other double bonds [2] and in nonpolar solvents no next conformers were reported [2, 3]. This work contains theoretical calculations and vibrational and NMR study as well. Theoretical calculations were carried out at the *ab initio* MP2 and DFT B3LYP level in 6-31G** basis set. According to the theoretical calculations, the *ZZ* conformer is most stable followed by *EZ* and *ZE* conformers (Table 1). Vibrational spectra in polar solvents indicate the presence of the next conformer. These experimental results are explained by the influence of environment polarity on the conformational equilibrium and are discussed with respect to the SCRF solvent effect calculations using PCM model.

Table 1: Calculated MP2 and DFT relative energies ΔE and dipole moments μ of DMAMDME conformers and their relative energies in solvents (CHCl₃, CH₃CN) using PCM model.

DMAM DME	ΔE (MP2) (kJ/mol)	ΔE (DFT) (kJ/mol)	μ (MP2) (D)	ΔE (MP2) (kJ/mol) (CHCl ₃)	ΔE (MP2) (kJ/mol) (CH ₃ CN)	ΔE (DFT) (kJ/mol) (CHCl ₃)	ΔE (DFT) (kJ/mol) (CH ₃ CN)
<i>ZZ</i>	0.00	0.00	2.56	0.00	0.00	0.00	0.00
<i>EZ</i>	4.49	5.53	4.22	4.23	3.15	4.25	3.36
<i>ZE</i>	5.11	7.12	4.22	2.72	1.52	3.14	1.83
<i>EE</i>	11.32	15.40	5.69	6.47	3.58	7.78	4.64

[1] S.F. Dyke, *The Chemistry of Enamines*; Cambridge University Press: London 1973

[2] U. Shmureli, H. Shanan-Atidi, H. Horwitz, Y. Shvo, *J. Chem. Soc., Perkin Trans. II* (1973) 657

[3] D. Smith, P.J. Taylor, *J. Chem. Soc., Perkin Trans. II* (1979) 1376

Acknowledgement

This work has been supported by Slovak Grant Agency VEGA (Projects No. 1/3566/06 and 1/0225/08).

Phase Transition and H₂O Motions in [Ba(H₂O)₄](ClO₄)₂ Studied by Differential Scanning Calorimetry, Infrared Spectroscopy and Inelastic/Quasielastic Incoherent Neutron Scattering

Ł. Hetmańczyk, J. Hetmańczyk, A. Migdał-Mikuli and E. Mikuli

*Department of Chemical Physics, Faculty of Chemistry, Jagiellonian University,
ul. Ingardena 3, 30-060 Kraków, Poland*

Compounds of the type: [M(H₂O)_x](ClO₄)₂ ($x = 4-6$) are particularly interesting molecular materials because of the occurrence of different reorientational motions of the complex cations, H₂O ligands and ClO₄⁻ anions. Polymorphism of several similar (M = Ni, Mg, Mn, Co, Fe, Cr) compounds have been investigated up to now [1-5].

One phase transition at: $T_c^h = 210.6$ K (onset on heating) and $T_c^c = 204.6$ K (onset on cooling) was determined for [Ba(H₂O)₄](ClO₄)₂ in the temperature range of 90–300 K by means of differential scanning calorimetry (DSC). The thermal hysteresis of the phase transition temperature T_c equal to ca. 6 K and the heat flow anomaly sharpness suggest that the detected phase transition is a first-order one. The relatively high entropy change ($\Delta S \approx 16.8$ J·mol⁻¹·K⁻¹) connected with observed phase transition indicates high degree of dynamical disorder. We have performed infrared (FT-MIR) and neutron scattering (IINS/QENS) measurements in order to establish relationship between the observed phase transition and reorientational motions of the H₂O ligands. Fourier transform middle infrared spectra were measured in the temperature range of 16–295 K. On cooling the sample no characteristic changes in the FT-MIR spectra are observed till 220 K, where the splitting of the band connected with $\rho(\text{H}_2\text{O})$ mode at ca. 720 cm⁻¹, can be distinctly seen. In addition to this at ca. 200 K a new weak shoulder band at ca. 1652 cm⁻¹ starts to appear. It suggests that in the vicinity of the phase transitions at T_c the crystal symmetry is reduced. On the other hand we can not see any narrowing of the bands during cooling. In the high temperature phase the bands are not broadened. It means that particular groups (H₂O and/or ClO₄⁻) do not perform fast ($\tau_R \approx 10^{-12}$ s) stochastic reorientational motion (even in high temperature phase) at least from point of view of infrared spectroscopy and correlation time characteristic for this method. Moreover, from our infrared measurements one can conclude that in the investigated compound there exist hydrogen bonds. The neutron scattering (IINS, QENS) studies performed with NERA time of flight spectrometer (Dubna in Russia) in the temperature range of 20–270 K did not give the evidence of fast (correlation time $\tau \approx 10^{-11}-10^{-12}$ s) stochastic reorientational motions of H₂O (180° flips) ligands in high and low temperature phases. The QENS maximum does not show any broadening (characteristic for the so called ODDIC crystals) above the phase transition temperature. This conclusion, consistent with infrared measurements, is also supported by the proton-weighted phonon density functions $G(\nu)$ calculated in one phonon harmonic approximation from the time-of-flight IINS spectra. The $G(\nu)$ spectra obtained at temperatures 20, 175, 200, 225, 270 K show some separate peaks characteristic for ordered phase. Concluding the H₂O groups do not perform fast stochastic reorientation (within picoseconds time scale) in the temperature range of 20–270 K. There are possible much slower reorientations ($\tau_R \approx 10^{-4}-10^{-5}$ s) of the whole complex cation [Ba(H₂O)₄]²⁺.

- [1] E. Mikuli, A. Migdał-Mikuli, M. Rachwalska, T. Stanek, *Physica B* 104 (1981) 326.
- [2] M. Rachwalska, T. Stanek, *Phys. Stat. Sol. A* 48 (1978) 297.
- [3] E. Mikuli, A. Migdał-Mikuli, I. Natkaniec, J. Mayer, *Z. Naturforsch. A* 55 (2000) 759.
- [4] E. Mikuli, A. Migdał-Mikuli, I. Natkaniec, B. Grad, *Z. Naturforsch. A* 56 (2001) 244.
- [5] E. Mikuli, B. Grad, K. Zaremba, S. Wróbel, *J. Thermal Anal. Calor.* 76 (2004) 719.

Micro-Raman and Computational Study of the Azoxybenzene Photorearrangement to 2-Hydroxybenzene

I. Jelovica Badovinac¹, N. Orlić¹, C. Gellini², L. Moroni², P.R. Salvi²

¹Department of Physics, University of Rijeka, Omladinska 14, Rijeka, Croatia, ²Department of Chemistry, University of Florence, via della Lastruccia 3, 50019 Sesto Fiorentino, Italy

When azoxybenzene (**1**) is irradiated by light with wavelength less than 400 nm, the molecule undergoes an intramolecular rearrangement to yield 2-hydroxyazobenzene (**2**) as photoproduct with a quantum yield of formation of ~ 0.020 , independent of temperature, concentration and wavelength in the range 250 – 400 nm [1]. As shown in Fig. 1, left, the lowest absorption region of (**2**) is red-shifted with respect to that of the reactant azoxybenzene, in particular in alkaline ethanolic solution.

The micro-Raman spectroscopy [2] can afford to characterize the vibrational properties of the photoproduct due to the possibility of focusing the exciting radiation on the tiny microcrystals of (**2**) obtained by slow evaporation of the solvent. This application of the technique is appealing when only minute amounts of the reaction product are available. In our case, the Raman spectrum of (**2**) of Fig. 1, right lower, has been measured on fibrous microcrystals $\sim 150 \mu\text{m}$ long by examination with the focusing microscope.

The combination of the experimental results with *ab initio* DFT calculations of vibrational frequencies and Raman intensities further helps to identify the crystalline photoproduct. Calculated data for (**2**) and for the tautomeric imino molecule confirm that (**2**) has been obtained during the irradiation.

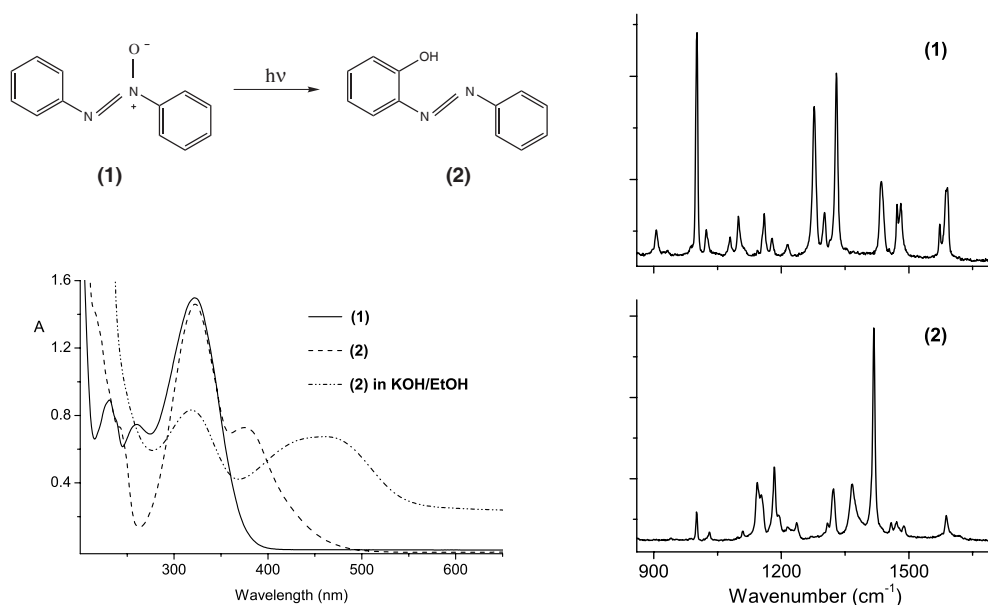


Fig. 1: Left, upper: the photochemical rearrangement of (**1**) to (**2**); lower: absorption spectra of $\sim 10^{-4}$ M solution of (**1**) in ethanol before and after (**2**) irradiation. Right: micro-Raman spectra of (**1**) and (**2**) microcrystals at room temperature exciting at 785 nm.

[1] N.J. Bunce, J. LaMarre, S.P. Vaish, Photochem. Photobiol. 39 (1984) 531-533.

[2] *Modern Techniques in Raman Spectroscopy*, J.J. Laserna ed., Wiley, Chichester (England), 1996.

A New Heterometallic (Ni^{2+} and Cr^{3+}) Complex – Crystal Structure and Spectroscopic Characterization

M. Jurić¹, P. Planinić¹, D. Žilić¹, B. Rakvin¹, B. Prugovečki²

¹Ruđer Bošković Institute, Bijenička cesta 54, 10000 Zagreb, Croatia, ²Department of Chemistry, Faculty of Science, University of Zagreb, Horvatovac 102a, 10000 Zagreb, Croatia

The design of new molecular solids with desirable physical properties is often based on the controlled supramolecular aggregation of molecular entities. In molecular solids with localized paramagnetic centres, supramolecular aggregates often serve as pathways for the magnetic exchange interactions. In a complete characterization of these systems (besides crystal structure analysis), various spectroscopic methods take a very important part. The first idea on coordination geometry is often obtained by UV/Vis spectroscopy, whereas the evidences on magnetic properties of individual metal centres of these species, provided by the EPR measurements have an exceptionally significant role for a better understanding of their magnetic behaviour.

As a continuation of our research work on polynuclear transition metal complexes, a new heterometallic complex of the composition $[\text{Ni}(\text{bpy})_3]_2[\text{Cr}(\text{C}_2\text{O}_4)_3]\text{NO}_3 \cdot 10\text{H}_2\text{O}$ (bpy = 2,2'-bipyridine) has been synthesized. The prepared compound has been characterized by means of chemical and TG/DTA analysis, IR, UV/Vis and EPR spectroscopy and by single crystal X-ray diffraction method. Due to the rigidity of the didendate bipyridine and oxalate ligands, two symmetry independent $[\text{Ni}(\text{bpy})_3]^{2+}$ cations as well as the $[\text{Cr}(\text{C}_2\text{O}_4)_3]^{3-}$ anion possess a trigonally distorted octahedral geometry. Analysis of crystal packing reveals a specific type of supramolecular contact comprising four bipyridine ligands from two neighbouring $[\text{Ni}(\text{bpy})_3]^{2+}$ cations – quadruple aryl embrace (QAE) contact [1]. The electronic spectrum has shown the superposition of bands characteristic for both the nickel(II) and chromium(III) six-coordinated ions. The EPR spectra have been recorded on a single crystal as well as on a powdered sample of the prepared complex. During the measurements the crystal was rotated round three arbitrary, mutually perpendicular axes. In the complex investigated, two kinds of paramagnetic species are present: Ni^{2+} with a spin $S = 1$ and Cr^{3+} with $S = 3/2$. In the frequency range examined, from the room to the liquid helium temperature, Ni^{2+} has been EPR silent and only the transition $M_S = -1/2 \leftrightarrow M_S = 1/2$ for Cr^{3+} has been observed.

[1] M. Jurić, B. Perić, N. Brničević, P. Planinić, D. Pajić, K. Zadro, G. Giester, B. Kaitner, Dalton Trans. (2008) 742-754.

Investigation of Liquid-Liquid Phase Transition for *Trans*-1,2 dichloroethylene

A. Kocot, K. Merkel and J. Ziolo

University of Silesia, Institute of Physics, Katowice, Poland

A single component liquid, contrary to common belief, may have more than one kind of isotropic liquid state, and the transition between these states is called the liquid-liquid phase transition (LLPT). Evidence of such a transition in *trans*-1,2-dichloroethylene (TDCE) has already been reported by Kawanishi et al. [1, 2]. By applying the NMR technique they found that temperature dependences of spin-lattice relaxation times (T_1) exhibited a "jump" at -16 °C which indicated the presence of the liquid-liquid phase transition. Specific volume measurements showed a change in V-T curve at the singular point of -16 °C.

IR vibrational spectroscopy has been employed to study liquid-liquid phase transitions of *trans*-1,2-dichloroethylene (TDCE). Temperature dependence of the vibrational frequency, band absorbance and band broadening has been analyzed in the temperature range 293 K to 237 K. All peaks show distinct increases of their absorbancies at the temperature 246.7 K accompanied by frequency shift and bandwidth changes. Weak H...Cl hydrogen bonding is suggested as the explanation of the overall behavior in a wide temperature range, whereas the significant changes of the spectrum at 246.7 K are probably due to molecular ordering originating from electrostatic interactions. The transition is regarded as a nucleation growth-type and is well described by the model of the cooperative formation of locally favored structures.

The TDCE molecule is non polar itself therefore no dipolar distribution of charge is expected for dimers. However, for one configuration of dimers structure, the resultant dipole moments is about 0.25 D. Recent our measurements of the non-linear dielectric effect (NDE) for TDCE strongly support such a concept. They show a positive sign of the NDE signal that dramatically increases on approaching 247 K. This is most probably due to the increase of the local polarity of the system.

[1] S. Kawanishi, T. Sasuga, M. Takehisa, J. Phys. Soc. Jpn. 48 (1980) 1307.

[2] S. Kawanishi, T. Sasuga, M. Takehisa, J. Phys. Soc. Jpn. 50 (1981) 3080.

Matrix Isolation Spectrum, UV-Induced Photochemistry ($\lambda > 215$ nm) and Differential Scanning Calorimetry Analysis of 3-(*N*-Acetamide)-Coumarin

N. Kuş^{1,2}, S. Breda¹, E.M.S. Eusébio¹, T.M.R. Estronca¹ and R. Fausto¹

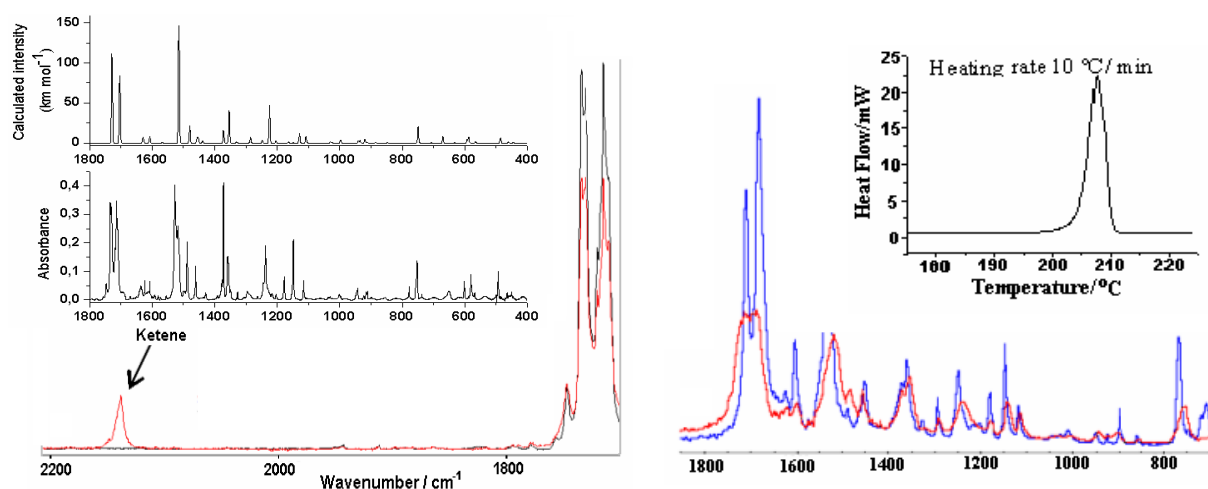
¹Department of Chemistry, University of Coimbra, 3004-535 Coimbra, Portugal

²Department of Physics, Anadolu University, 26470 Eskişehir, Turkey

Coumarins are biologically relevant compounds and they also receive industrial application as dyes. From a structural point of view, these molecules can be considered substituted benzoderivatives of α -pyrones, a family of compounds that have been studied thoroughly in our laboratories [1-3]. As a general rule, matrix-isolated α -pyrones undergo easy photolysis upon *in situ* irradiation, with the two fundamental processes being ring-opening to ketenes and ring-contraction to their Dewar analogues.

Following the same lines of our previous studies on α -pyrones and related compounds, in the present study we considered 3-(*N*-acetamide)-coumarin (3NAC). Like for 3-methyl coumalate [4], UV ($\lambda > 215$ nm) irradiation of matrix-isolated 3NAC appears to lead exclusively to the ring-opening ketene photoproduct, as testified by observation of the characteristic ketene band around 2130 cm^{-1} in the IR spectra of the irradiated 3NAC matrices and absence of any bands ascribable to other possible photoproducts (Figure 1).

In addition to the matrix-isolation spectra of 3NAC, IR spectra of the pure compound in its neat condensed phases were recorded as a function of temperature (in the range 20-225 °C). The observed spectra were correlated with results obtained by differential scanning calorimetry (DSC) (Figure 2). All spectroscopic data were rationalized with help of extensive theoretical DFT calculations on 3NAC and its possible photoproducts.



Figures: 1 (Left panel) - Calculated vs. experimental IR spectra of matrix-isolated 3NAC and results of *in situ* UV irradiation of the matrix-isolated compound (showing the characteristic band of the C=C=O asymmetric stretching of the photoproduct ketene). **2 (Right panel)** - DSC profile of the exothermic peak around 208 °C (melting) and IR spectra of crystal (room temperature; 20 °C - blue line) and melted phase (210 °C - red line).

- [1] N. Kuş, S. Breda, I. Reva, E. Tasal, C. Öğretir and R. Fausto, *Photochem. Photobiol.*, 83 (2007) 1237.
 [2] S. Breda, I. Reva, L. Lapinski and R. Fausto, *PCCP* 6 (2004) 929.
 [3] S. Breda, L. Lapinski, I. Reva and R. Fausto, *J. Photochem. Photobiol. A*, 162 (2004) 139.
 [4] I. Reva, M. Nowak, L. Lapinski and R. Fausto, *Chem. Phys. Lett.* 452 (2008) 20.

Acknowledgements:

This work was supported by the Portuguese FCT (Project POCI/QUI/58937/2004) and Eskişehir Osmangazi University (Project 200519010). SB also thanks to the Portuguese FCT for the Ph.D. grant ref. SFRH/BD/16119/2004.

Photochemistry and Vibrational Spectra of Matrix Isolated Methyl 4-Chloro-5-Phenylisoxazole-3-Carboxylate

S. Lopes¹, A. Gómez-Zavaglia^{1,2}, C. M. Nunes¹, T.M.V.D. Pinho e Melo¹ and R. Fausto¹

¹Department of Chemistry, University of Coimbra, P-3004-535 Coimbra, Portugal.

²Facultad de Farmacia y Bioquímica, Universidad de Buenos Aires, Junín 956, 1113 Buenos Aires, Argentina.

Heterocyclic compounds such as isoxazoles and its derivatives are important building blocks of many compounds of biological interest. These heterocycles are involved directly or as intermediates in the synthesis of new compounds that are potentially useful in a variety of fields, with pharmaceutical and medicinal applications. On the other hand, the agricultural uses of isoxazole derivatives include herbicidal, insecticidal and soil fungicidal activities. Isoxazoles have also been used as semiconductors, as corrosion inhibitors in fuels and lubricants and in the production of photographic and liquid crystalline materials [1].

In this study, methyl 4-chloro-5-phenylisoxazole-3-carboxylate (MCPIC) has been synthesized and its monomeric structure studied by DFT(B3LYP)/6-311++G(d,p) calculations. The DFT calculations predicted the existence of three different conformers with small energy differences in the ground state potential energy surface.

The compound has also been studied by Matrix Isolation FTIR spectroscopy (in both argon and xenon matrices) and in the condensed phases: neat amorphous and crystalline solid states. Finally, the photochemical behaviour of the matrix isolated MCPIC monomer was investigated through *in situ* broadband irradiation using a standard Hg(Xe) lamp as UV-light ($\lambda > 235$ nm) source. The interpretation of the IR spectra of the compound isolated in the different matrices investigated and of those of the resulting photoproducts were supported by theoretical calculations undertaken at the DFT(B3LYP)/6-311++G(d,p) level of theory.

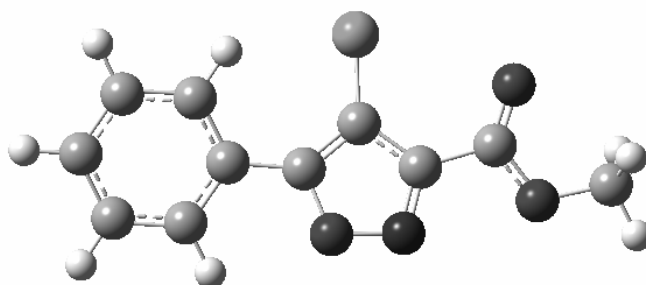


Fig. 1: Structure of the most stable conformer of MCPIC.

- [1] S.A. Lang, Jr. and Y-I Lin, in A.R. Katritzky, C.W. Rees, (series Eds.), K.T. Potts (Ed.), *Comprehensive Heterocyclic Chemistry*, Vol. 6 Part 4B Pergamon, Oxford, 1984 (Chapter 4.16) page 1.

Acknowledgements

This work was funded by FCT (Projects POCTI/QUI/59019/2004 and POCTI/QUI/58937/2004), and the Instituto de Investigação Interdisciplinar of the University of Coimbra (Project III/BIO/40/2005). S.L. acknowledges FCT the Ph.D. grant (SFRH/BD/29698/2006).

Polarized Raman and IR spectra of the orthorhombic $\text{CaNb}_2\text{O}_6:\text{Pr}^{3+}$ single crystal

L. Macalik¹, M. Mączka¹, J. Hanuza^{1,2} and A.A. Kaminski³

¹*Institute of Low Temperature and Structure Research, Polish Academy of Sciences P.O. Box 1410, 50-950 Wrocław, Poland,* ²*Department of Bioorganic Chemistry, Faculty of Engineering and Economics, Wrocław University of Economics, 118/120 Komandorska str., 53-345 Wrocław, Poland,* ³*Joint Open Laboratory for Laser Crystals and Precise Laser Systems, Institute of Crystallography, Russian Academy of Sciences, Moscow, Russia l.macalik@int.pan.wroc.pl*

A high optical quality columbite $\text{CaNb}_2\text{O}_6:\text{Pr}$ single crystal doped with 0.5 at. % of Pr^{3+} ions has been grown by Czochralski method. The orientation of the crystallographic axes has been done using X-ray method. The orientation of the $x \parallel \mathbf{a}$, $y \parallel \mathbf{b}$ and $z \parallel \mathbf{c}$ axes has been used for the unit cell Pbcn with lattice parameters: $\mathbf{a} = 14.926 \text{ \AA}$, $\mathbf{b} = 5.752 \text{ \AA}$ and $\mathbf{c} = 5.204 \text{ \AA}$ and $\alpha = \beta = \gamma = 90^\circ$ [1].

The polarized Raman spectra of this crystal in the $z(xx)-z$, $z(yy)-z$ and $y(zz)-y$ geometry for A_g , $z(yx)-z$ for B_{1g} , $y(zx)-y$ for B_{2g} and $x(yz)-x$ for B_{3g} have been measured. Polarized IR spectra of the single crystal have been measured in the $E \parallel y$ and $E \parallel z$ geometry using a fixed-angle specular reflectance accessory. The discussion of the results has been based on the factor group approach for the orthorhombic Pbcn (D_{2h}^{14}) space group with $Z = 4$. The analysis of the vibrational characteristics of the NbO_6 distorted octahedra and CaO_6 units has been made on the basis of the literature data [2].

The columbite crystal is a prospective Raman laser. The results obtained for the spontaneous Raman scattering have been used in the discussion of the stimulated Raman spectra of the material studied. Among the modes observed in the fully symmetric A_g Raman spectra the strongest line appears at 904 cm^{-1} that corresponds to the symmetric $\nu_s(\text{NbO}_6)$ mode. This mode is expected to participate in the stimulated Raman effect as the promoting vibration.

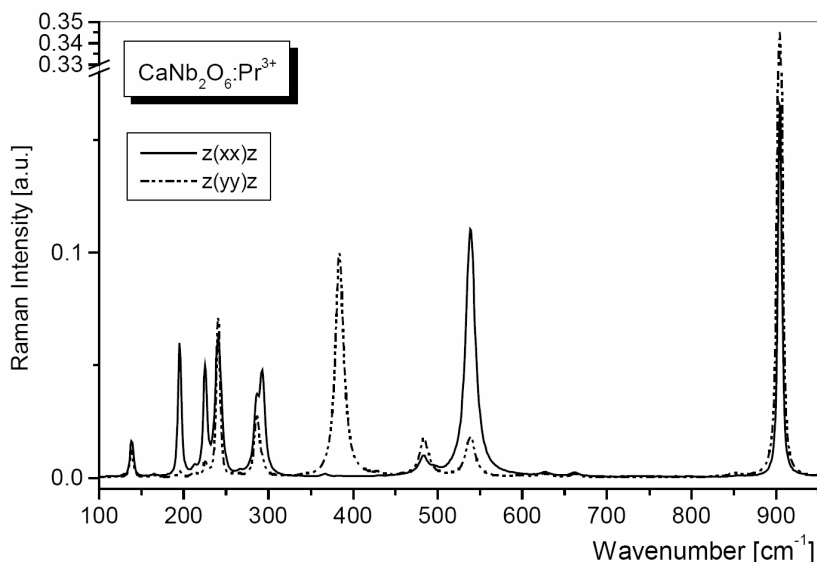


Fig. 1: A_g Raman spectra of $\text{CaNb}_2\text{O}_6:\text{Pr}$ single crystal.

[1] J.P. Cummings, S.H. Simonsen, *American Mineralogist* 55 (1970) 90.

[2] E. Hudson, Y. Repelin, N.Q. Dao, H. Brusset, *J. Chem. Phys.* 66 (1977) 5173.

Nuclear Magnetic Shielding and Spin-spin Coupling Constants for Acetaldehyde from Gas-phase NMR Spectroscopy

W. Makulski, A. Wikieł

Laboratory of NMR Spectroscopy, Department of Chemistry, Warsaw University
Pasteura 1, 02-093 Warsaw, Poland

Experimental NMR spectrum of a measured substance provides valuable information on the chemical environment of the NMR-active nuclei in the molecule. The chemical shift observed reflects not only the nucleus position in a given molecule but also the solvent effects. In addition, the coupling constants determined from the spectra reveal information on the spatial structure of the molecule. Gaseous systems are studied in relatively "isolated" environments, where the effects due to solvent interactions can be restricted or completely eliminated [1]. It is obvious that gas-phase NMR spectra prove useful when parameters independent of intermolecular interactions are of interest [2]. These can be used as verification of *ab initio* calculations [3,4]. Recently we provide those kind of measurements on volatile organic substances like: CH₃F, CH₃OCH₃, CH₃CN, CH₃NH₂ and CH₃OH.

This work is concerned with acetaldehyde molecule. Acetaldehyde was studied by high-precision ¹H and ¹³C NMR spectroscopy in liquid and gaseous states at 300K. The gas pressure at room temperature of pure compound reached about 1 atm value but very effective relaxation processes in this conditions lead to relatively wide signals. The same signal can be substantially narrower when another component is used as a solvent to increase significantly the total pressure of the sample. To achieve this effect, approximately 0.1 mg of acetaldehyde was introduced into the buffer gases: CO₂, Xe and SF₆ taken at 0.2 – 1.3 mol/L densities. Extrapolation of the gas-phase chemical shifts to the zero-density limit permitted the determinations of ¹H and ¹³C absolute nuclear magnetic shieldings of an isolated acetaldehyde molecule. The values found are shown in Table 1; additionally previously measured ¹⁷O data is included [5].

Table 1: ¹H, ¹³C and ¹⁷O nuclear magnetic shielding constants for acetaldehyde from gas phase measurements at 300K [ppm]

Group	¹ H	¹³ C	¹⁷ O
-CH ₃	28.82	156.7	
-CHO	21.03	- 7.6	- 340.0

These new experimental results are necessary in a correct verification of *ab initio* calculations of proton and carbon nuclear magnetic shieldings in the molecule under study. The indirect spin-spin coupling constants were extracted from experimental spectra and compared with the values previously reported in the literature. Intermolecular effects in the gaseous state as well as in passing from gas to liquid are also found. The gas-to-liquid shifts measured are negative both for proton and carbon nuclei showing the deshielding effect.

[1] C. Suarez, The Chemical Educator 3 (1998) 1.

[2] K. Jackowski, J. Mol. Struct. 786 (2006) 215.

[3] D. Zaccari, V. Barone, J.E. Peralta, R.H. Contreras, O.E. Taurian, E. Díez, A. Esteban, Int. J. Mol. Sci. 4 (2003) 93.

[4] A.A. Auer, J. Gauss, J.F. Stanton, J. Chem. Phys. 118 (2003) 10407.

[5] W. Makulski, K. Jackowski, J. Mol. Struct. 651-653 (2003) 265.

Structure Determination of Ag(I) Ion Complex of Rhodanine

K.M. Marzec, K. Malek, B. Gawel, W. Lasocha, L.M. Proniewicz

Faculty of Chemistry, Jagiellonian University, 3 Ingardena Str., 30-060 Kraków, Poland.

4-thiazolidinone (rhodanine) and its derivatives are known to possess biological activities such as antimiotic, antidiabetic, antibacterial, hypocholesterolemic, antiperlipemic [1] and others. The pharmacological properties of rhodanine are connected with its high ability of coordination towards metal ions. Until now, studies on complexes of rhodanine have been focused on structure determination of coordination compounds with Ag(I), Cu(I), Hg(I), Pt(II) and Pd(II) by analytical methods, e.g. potentiometric techniques [2-3]. However, these results only suggest possible coordination models of the rhodanine complexes.

As the extension of these studies, we present here systematic studies on the molecular structure of the silver(I) complex of rhodanine. Synthesis of the complex was carried out for various metal:ligand ratio (M:L) at different pH values. However, the elemental analysis and IR results showed clearly that M:L is 1:1 only and all the complexes are isostructural. Molecular structure of the complex in solid state was determined by vibrational spectroscopy (FT-IR, FT-Raman) and confirmed by X-ray powder diffraction. Additionally, DFT calculations allowed us to perform clear-cut assignment of the experimental vibrational bands.

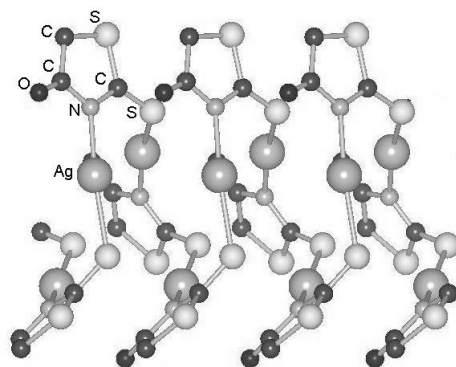


Fig. 1: Crystallographic structure of the silver complex of rhodanine.

The comparison of IR and Raman spectra of rhodanine and its complex with Ag(I) ion indicate as follows: the NH group is deprotonated, the stretching mode of C=O is red-shifted by 27 cm⁻¹ in IR and 14 cm⁻¹ in Raman, the stretching mode of C=S is red-shifted by 60 cm⁻¹ in IR and 31 cm⁻¹ in Raman, and the stretching mode of CH₂ is observed. It clearly implies that the metal ion is coordinated by the exocyclic S and O atoms, and the ring N atom. The detailed structure of the complex was obtained from crystallographic measurements (Fig. 1) that showed the presence of the hexagonal unit cell with parameters: $a = 28.056(2)$ Å, $b = 28.056(2)$ Å, $c = 3.993(4)$ Å, $\alpha = 90.0^\circ$, $\beta = 90.00^\circ$, $\gamma = 120.00^\circ$, $V = 2722.0(4)$ Å³, $F_{20} = 16.4$ (the PROSZKI package [4]).

[1] V. Enchev, S. Chorbadjiev, B. Jordanov, *Chem. Heterocycl. Comp.* 38 (2002) 9–19.

[2] P.M. Arena, M.D. Porter, J.S. Fritz, *Analytica Chimica Acta* 482 (2003) 197–207.

[3] E.S. Raper, *Coord. Chem. Rev.* 61 (1985) 165–166.

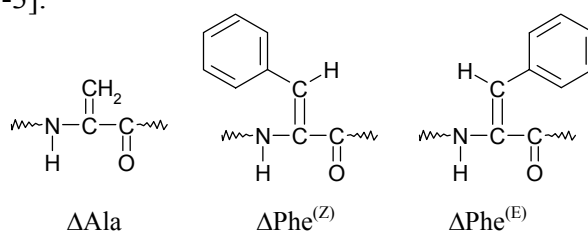
[4] W. Lasocha, K. Lewinski *J. Appl. Cryst.* 27 (1994) 437.

Raman Spectroscopy in Studies on the Selected Dehydropeptides

K. Malek¹, M. Makowski², L.M. Proniewicz¹

¹Faculty of Chemistry, Jagiellonian Chemistry, 3 Ingarden Str., 30-060 Krakow, Poland, ²Institute of Chemistry, University of Opole, 48 Oleska Str., 45-052 Opole, Poland

α,β -dehydroamino acid moiety contains a double carbon-carbon bond between α and β carbon atoms. The presence of this bond decreases conformational flexibility of proteins, and thus can lead to specific biochemical properties, e.g. a different enzymatic activity. These amino acids are natural and non-coded. For instance, dehydroalanine is active in the catalytic site of the ammonia lyase. They are synthesized in ribosome via a precursor peptide due to enzymatic modification. The conformational analysis of these derivatives of peptides as well as their inhibition potency into the active sites of some receptors have been previously reported [1-3].



Scheme 1

The conformational preferences of amino acids are of crucial importance in determining interactions that govern the favored orientation of polypeptides and proteins. In case of dehydropeptides, two parameters are important in determination of their geometrical features, i.e. the degree of flatness and the size and shape of its side chain.

In this work, we present three dipeptides containing glycine and the unsaturated alanine or phenylalanine in the E and Z forms (Scheme 1). Additionally, the glycine molecule is blocked with *t*-butoxycarbonyl group. Δ Ala and Δ Phe have been selected on the basis of their different steric constraints while the E and Z isomerism of dehydrophenylalanine allows determining their spectral features. Our goal is to investigate structural properties of these molecules in terms of Raman scattering spectroscopies, i.e. normal (Fig. 1) and surface enhancement Raman effects on the silver colloid. The spectroscopic analysis is supported by the DFT calculations.

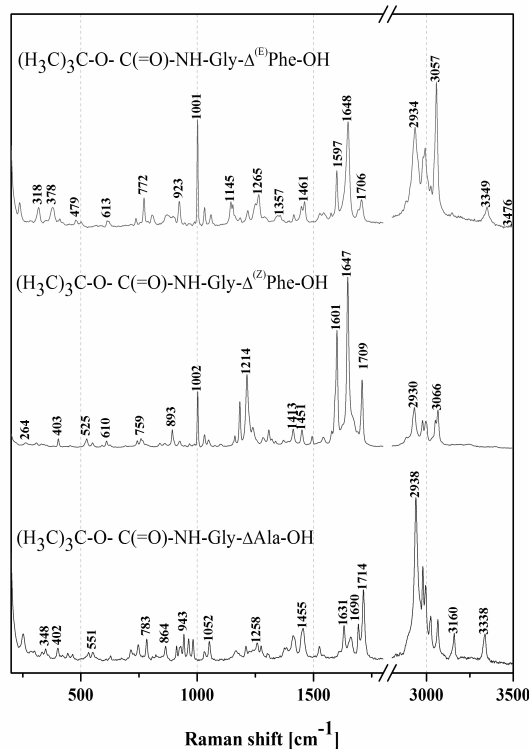


Fig. 1: FT-Raman spectra of solid samples.

[1] D. Siodlak, M.A. Broda, B. Rzeszutarska, J. Mol. Struct. (Teochem) 668 (2004) 75-85.

[2] T.P. Singh, P. Kaur, Prog. Biophys. Molec. Biol. 66 (1996) 141-165.

[3] M. Makowski, M. Pawelczak, R. Latarka, K. Nowal, P. Kafarski, J. Peptide Sci. 7 (2001) 141-145.

Conformational and Vibrational Analysis of Selected Monoterpenoids by Using Density Functional Theory

K.M. Marzec, K. Malek, A. Kaczor, L.M. Proniewicz

Faculty of Chemistry, Jagiellonian University, 3 Ingardena Str., 30-060 Krakow, Poland

Monoterpenes are built from two isoprenoid units and represent the most abundant group of terpenoids. Here, we present systematic studies on conformational and vibrational analysis of monocyclic monoterpenoids (Fig. 1).

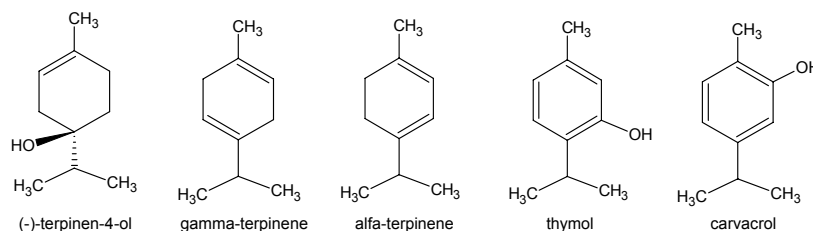


Fig. 1: Structures of the selected monoterpenoids

Until now, studies of the above-mentioned monoterpenes have been focused on identification, quantitative and qualitative analysis of these substances in chemical composition of the plant essential oils. This analysis has been carried out by using GC-MS, [1-3], ^1H and ^{13}C NMR, [2, 4], NIR-FT-Raman, and ATR/FT-IR spectroscopies [2, 5, 6,]. Moreover, inhibitory effects and pharmacological properties (e.g. antibacterial, anti-inflammatory, and anti-cancer action) of these substances have been studied.

To this point, there have been very few papers about molecular structures of the selected monoterpenoids. Crystallographic data concern only metal complexes of thymol [4] and carvacrol [7]. To the best of our knowledge, there is no information about the molecular structures of liquid terpinolene, p-cymene, α -terpinene, and solid state of terpinen-4-ol.

Firstly, the DFT/B3LYP method with a 6-31G(d,p) basis set was used to determine conformational population for each of the terpenoid in respect of dihedral angles of the exocyclic groups. Then, the rotamers of the lowest energy were selected for the further calculations of frequencies of normal modes, and their IR and Raman intensities. The presence/absence of the studied molecular structures was confirmed by comparison of the theoretical vibrational spectra with FT-IR and FT-Raman spectra. Finally, an assignment of the normal vibrations of the molecules presented here was carried out on the basis of potential energy distribution (PED) of normal modes.

- [1] F. Sefidkon, Z. Jamzad, M. Mirza, *Food Chem.* 88 (2004) 325-328.
- [2] S.K.S. Al-Burtamani, M.O. Fatope, R.G. Marwah, A.K. Onifade, A.S.H. Al-Saidi, *J. Ethnopharma.* 96 (2005) 107-112.
- [3] Cheng, J. Liu, Y. Hsui, S. Chang, *Biores. Tech.* 97 (2006) 306-312.
- [4] A.A. Mahmoud, A.A. Ahmed, *Phytochem.* 67 (2006) 2103-2109.
- [5] H. Schultz, M. Barańska, *Vib. Spectrosc.* 43 (2007) 13-25.
- [6] H. Schulz, G. Ozkan, M. Barańska, H. Kruger, M. Ozcan, *Vib. Spectrosc.* 39 (2005) 249-259.
- [7] H. Schulz, R. Quilitzsch, H. Kruger, *J. Mol. Struct.* 661-662 (2003) 299-306.

Polarized Vibrational Spectra of *p*-Substituted Nitro and Dinitro *cis*- and *trans*-Stilbenes

S. Miljanić¹, Z. Meić¹, G. Keresztury²

¹Laboratory of Analytical Chemistry, Department of Chemistry, Faculty of Science, University of Zagreb, Horvatovac 102a, HR-10000 Zagreb, Croatia, ²Institute of Structural Chemistry, Chemical Research Center, Hungarian Academy of Sciences, P.O. Box 17, H-1525 Budapest, Hungary

Polarized IR spectra of *p*-nitro and *p,p'*-dinitro derivatives of stilbene were measured in anisotropic (nematic liquid crystalline) solvent. Using the Thulstrup-Eggers stepwise reduction procedure, based on the interactive subtraction of the two polarized IR spectra $A_{||}(\nu)$ and $A_{\perp}(\nu)$, orientational parameters of nearly planar, low symmetry stilbene molecules were determined [1]. Dichroic ratios (subtraction factors), R_u ($u = x, y, z$), of observed vibrational transitions were evaluated and orientational parameters along the out-of-plane axis, K_x , the short in-plane axis, K_y , and the long in-plane axis, K_z , were calculated.

Since the rotation around the double bond changes the molecular geometry, different set of orientation parameters were determined for each molecule (Table 1). The K_z values indicate, as expected, that the *trans*-isomers are better oriented along the long in-plane axis than the *cis*-isomers. In addition, the K_z value for the mono substituted *trans*-stilbene, which is higher than the one for the disubstituted *trans*-stilbene, implies a possible involvement of the nitro groups in dipole-dipole interactions responsible for orientational mechanism of solute molecules in nematic solvent.

Table 1: Orientational parameters of *p*-nitro and *p,p'*-dinitro *cis*- and *trans*-stilbenes.

Compound	K_x	K_y	K_z
<i>p</i> -nitro- <i>trans</i> -stilbene	0.139	0.287	0.574
<i>p</i> -nitro- <i>cis</i> -stilbene	0.192	0.384	0.424
<i>p,p'</i> -dinitro- <i>trans</i> -stilbene	0.150	0.383	0.467
<i>p,p'</i> -dinitro- <i>cis</i> -stilbene	0.196	0.362	0.442

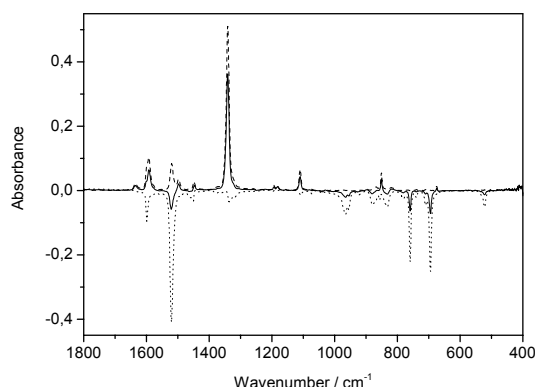


Fig. 1: Polarized IR spectra of *p*-nitro-*trans*-stilbene after reduction by subtraction factors of 0,32 (dashed curve), 1,00 (solid curve) and 2,70 (dotted curve).

Finally, polarized Raman spectra of crystalline stilbene substances were measured and depolarization ratios of selected vibration modes calculated. The values will be compared with those of the parent *trans*-stilbene molecule [2].

[1] M. Rogojerov, G. Keresztury, B. Jordanov, Spectrochim. Acta A 61 (2005) 1661-1670.

[2] G. Baranović, Z. Meić, A.H. Maulitz, Spectrochim. Acta A 54 (1998) 1017-1039.

DFT Study of Molecular Structure and Vibrations of 3-Glycidoxypropyltrimethoxysilane

I. Movre Šapić¹, L. Bistričić², V. Volovšek¹, V. Dananić¹

¹Faculty of Chemical Engineering and Technology, University of Zagreb, Marulićev trg 19, Zagreb, Croatia, e-mail: imovre@fkit.hr

²Faculty of Electrical Engineering and Computing, University of Zagreb, Unska 3, Zagreb, Croatia

Organofunctional alkoxy silanes have a widespread application in the polymer industries. Possessing both organic and inorganic properties, these chemicals react with organic polymers and with inorganic substrates, pigments or fillers, forming durable covalent bonds across the interface. 3-glycidoxypropyltrimethoxysilane (GPTMS) is one of the most widely applied organofunctional alkoxy silanes. It has two functional groups on the opposite sites of the molecule. Methoxy groups, at one end of the molecule, are transformed through hydrolysis into silanol groups which can interact and form a silicate network during the condensation process. On the other side, by using curing agents at room temperature, epoxy ring opening and organic network formation can be achieved.

Changes in the vibrational spectra of GPTMS during these processes are frequently used for monitoring the relevant dynamics. The knowledge and assignment of the vibrational spectra of individual GPTMS molecule may be helpful in understanding the nature of the interactions involved. Therefore, we have investigated molecular structure and vibrational frequencies of GPTMS by density functional theory (DFT) calculations using Becke's three-parameter exchange functional combined with Lee-Young-Parr correlation functional (B3-LYP) and standard basis set 6-311++G(d,p). In order to reveal all possible conformations of GPTMS, potential energy scan has been performed in three dihedral angles SiCCC, CCCO and OCCO. The calculations predict the existence of seven different conformations: 1-*ttg*, 2-*gtg*, 3-*gtg*, 4-*tgg*, 5-*tgg*, 6-*ttg* and 7-*ttt*. Mostly, they have negligible differences in their calculated vibrational spectra. The lowest energy conformer according to our calculations is 6-*ttg*. The complete assignment of the measured vibrational spectra is given for this most stable molecule using the correspondence of observed and calculated frequencies, calculated Raman activities and IR intensities, characteristic group frequencies and comparison with aminopropylsilanetriol [1] and gamma-aminopropyltriethoxysilane [2]. Comparing the results of spectroscopic measurements (Raman and IR spectra of liquid sample were recorded) and DFT calculations it was possible to distinguish four pairs of corresponding vibrational bands characteristic for three different groups of conformers. Bands at 1480 cm⁻¹, 1441 cm⁻¹ and 1313 cm⁻¹ are ascribed to 6-*ttg* and 7-*ttt* conformers. Corresponding normal modes in the remaining five conformers generate the same bands at 1466 cm⁻¹, 1414 cm⁻¹ and 1341 cm⁻¹. Strong Raman band at 612 cm⁻¹ is attributed to SiO stretching vibration in molecules 2-*gtg* and 3-*gtg*, while the similar normal mode in other five conformers gives rise to the strong Raman band at 642 cm⁻¹.

A comparison of experimental and calculated results points to the possible co-existence of all conformers in the liquid GPTMS.

[1] L. Bistričić, V. Volovšek, V. Dananić, I. Movre Šapić, *Spectrochim. Acta A* 64 (2006) 327-337

[2] L. Bistričić, V. Volovšek, V. Dananić, *J. Mol. Struct.* 834-836 (2006) 355-363

Solution State Structure of Methoxysalicylaldehyde Thiosemicarbazone Derivatives by NMR and DFT Methods

P. Novak, K. Pičuljan, T. Hrenar, M. Rubčić, M. Cindrić

Faculty of Science, Department of Chemistry, Horvatovac 102a, Zagreb, Croatia

Salicylaldehyde thiosemicarbazones and their metal complexes belong to an important class of biologically active compounds (anticancer, antiviral, antibacterial, antiinflammatory and antifungal activity) [1]. They can exist in several tautomeric forms (hydroxy-thione, hydroxy-thiol, keto-thione and keto-thiol) with both intra- and intermolecular hydrogen bonds (Fig. 1). X-ray structural analysis has confirmed the existence of intramolecular hydrogen bonds in different salicylaldehyde thiosemicarbazone derivatives [2, 3]. Bioactivity is closely related to molecular structure which is governed by the presence of hydrogen bonds. Therefore, the aim of our study was to investigate the solvent influence on molecular conformation and structure of hydrogen bonds in methoxysalicylaldehyde thiosemicarbazones by combining NMR and DFT methods. Solvents of different polarities, *i. e.* of different proton donor and acceptor abilities were used (chloroform, acetone, methanol, dimethyl sulfoxide).

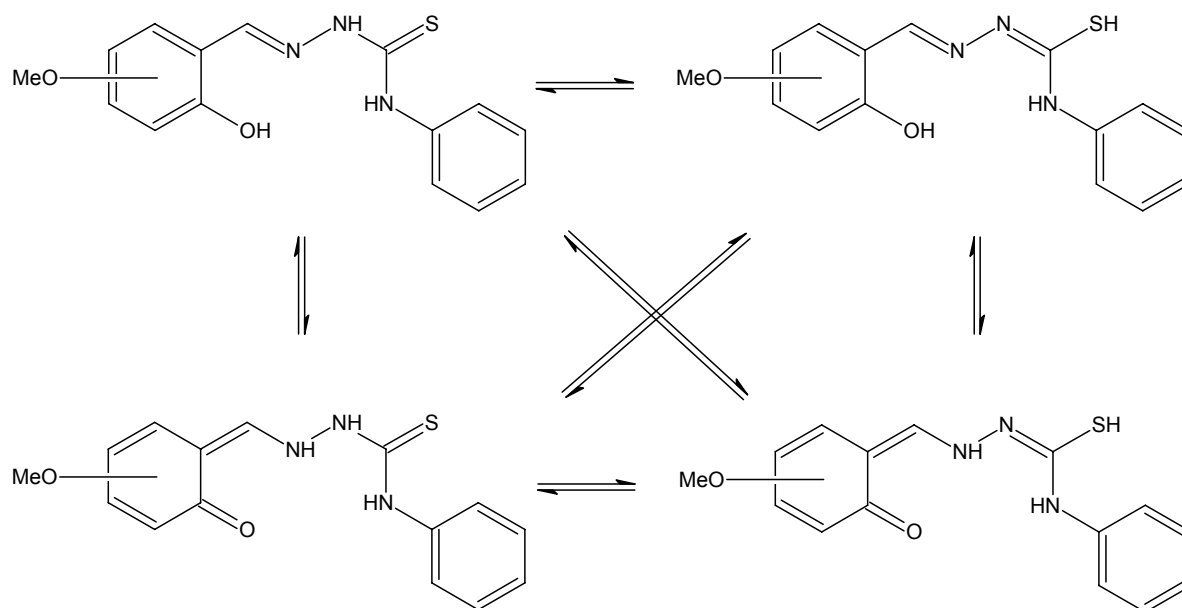


Fig. 1: Tautomerism in methoxysalicylaldehyde thiosemicarbazones.

- [1] W.X. Hu, W. Zhou, C.N. Xia, X. Wen, *Bioorg. Med. Chem. Lett.* 16 (2006) 2213–2218.
 [2] V. Vrdoljak, M. Cindrić, D. Milić, D. Matković-Čalogović, P. Novak, B. Kamenar, *Polyhedron* 24 (2005) 1717–1726.
 [3] P. Novak, K. Pičuljan, T. Biljan, T. Hrenar, M. Cindrić, M. Rubčić, Z. Meić, *Croat. Chem. Acta* 80 (2007) 575-581.

Conformations of Z-2(3'-pyridyl)-3-phenyl Propenoic Acid in Various Solvents - an NMR Study Supplemented with Computations

P. Forgó¹, G. Dombi¹, K. Felföldi², I. Pálinkó²

¹Institute of Pharmaceutical Analysis, University of Szeged, Somogyi u. 4, H-6720 Szeged, Hungary

²Department of Organic Chemistry, University of Szeged, Dóm tér 8, Szeged, H-6720 Hungary

In order to study the conformational properties of Z-2(3'-pyridyl)-3-phenyl propenoic acid (**1**) in solvent a comprehensive NMR study was undertaken, supplemented with computations using the PM3 semiempirical as well as *ab initio* codes implemented in the Hyperchem 8.0 molecular modelling package [1]. Details of the experiments and the computations and the results obtained are detailed in this work.

The model compound was synthesized with modified Perkin condensation [2] and was purified with column chromatography and recrystallization until reaching constant melting point. Its NMR parameters were obtained in three solvents of significantly altering characteristics (DMSO(d₆) – dipolar aprotic solvent, methanol(d₄) – polar, protic solvent and chloroform(d) – apolar, aprotic solvent) on a Bruker DRX 500 instrument. ¹³C NMR spectrum was not possible to get collected in chloroform due to poor solubility. The ¹H NMR spectrum in all solvents displayed signals only at the high chemical shift region, in dms(d₆) even the proton signal of the carboxylic function appeared at 12.96 ppm. The aromatic and olefinic protons resonated in a narrow (approximately 2ppm wide) chemical shift region at the low-field end of the spectrum. Although, the ¹H NMR spectrum and coupling constant modulated ¹³C NMR spectrum (JMOD) revealed the chemical shift of some characteristic functionalities (carboxylic, non-protonated aromatic resonances), one-dimensional NMR spectra did not provide enough evidence to make unambiguous assignment because of the severe overlap of resonances in certain cases. Two-dimensional chemical shift correlation spectra were used to assign resonances. Homonuclear COSY spectrum was used to identify the proton resonances in isolated spin systems (phenyl, pyridyl); moreover, the olefin proton appeared as a singlet in the aromatic region. The ¹³C NMR signals were assigned with the use of heteronuclear chemical shift correlation spectrum on the basis of the known ¹H NMR chemical shifts. Furthermore, two dimensional heteronuclear multiple bond experiment (HMBC) provided the connectivity information between different functionalities within the molecule.

The solution state conformation was monitored with the two-dimensional NOESY experiment. The solvent change introduced very small, but significant chemical shift changes in both ¹H, and ¹³C NMR spectra for all resonance lines. It became clear that the properties of the solvents influenced the conformational preferences of the aromatic rings and the carboxylic group too. In accordance with experiments, computations revealed that even though there were many feasible conformers (calculations were performed on carboxylic acid dimers as fundamental units [3]) they occupied certain segments of the conformational space. Modelling in the gas-phase showed that the aromatic rings sterically hindered the (virtually) free rotation of the carboxylic groups.

[1] Hyperchem 8.0, Hypercube, Inc., Gainesville, Florida, 2007.

[2] I. Pálinkó, Á. Kukovecz, B. Török, T. Körtvélyesi, Monatsh. Chem. 131 (2000) 1097-1104.

[3] I. Pálinkó, B. Török, M. Rózsa-Tarjányi, J.T. Kiss, Gy. Tasi, J. Mol. Struct. 348 (1995) 57-60; (b) I. Pálinkó, J.T. Kiss, Mikrochim. Acta [Suppl.] 14 (1997) 253-255.

Determining the Positions of Aromatic Hydrogens in (ar)C-H...X (X = O or F) Hydrogen Bonded Assemblies of Phenyl-phenyl, Phenyl-furyl Substituted Propenoic Acids and Esters from Their FTIR Spectra

I. Pálinkó¹, J. Mink^{2,3}

¹Department of Organic Chemistry, University of Szeged, Dóm tér 8, Szeged, H-6720 Hungary

²Institute of Structural Chemistry, Chemical Research Center of the Hungarian Academy of Sciences, PoBox 17, Budapest H-1525 Hungary

³Faculty of Information Technology, Research Institute of Chemical and Process Engineering, University of Pannonia, Egyetem u. 10, Veszprém H-8200 Hungary

In the last couple of years the structure forming properties of various cinnamic acid and ester derivatives have been studied mostly with the combination of spectroscopic (mainly IR spectroscopy was applied) and computational methods (PM3 semiempirical method was used chiefly; originally the available computer power imposed us to use this level of theory, later the studied structures were extended to the size when this method could only be used even with increased computer power). As work went on even though the core structure was kept (propenoic acid that is), but the family of molecules has been largely extended. Phenyl (with occasionally, methoxy substituents) [1-3] and furyl [4] substituents were built into the unsaturated acid or methyl ester structure and, occasionally, the olefinic proton was also substituted for CF₃ group [5]. It has been found that short-range ordering (it was found in solutions) was originated in strong O-H...O hydrogen bonds for the acids, while weak (aromatic) C-H...O hydrogen bonds were responsible for long-range ordering only found in the solid state for the acids as well as the esters. These observations could be unequivocally stated, however, designating the positions of aromatic protons has not been attempted. Since in the meantime the variety of structures has been increased considerably enough data have been accumulated to assign now the aromatic protons to positions on the phenyl ring. This assignation is reported in this contribution.

The aggregating properties of a large variety of compounds have been studied. They were 2,3-phenyl or methoxy-substituted phenyl groups, 2,3-phenyl groups and a CF₃ group in position 3, 3,2-phenyl and furyl- substituted derivatives (acids as well as esters). Since each molecule contained at least one phenyl group collecting the normal modes of the phenyl groups was the first step. From this first step the assignment of vibrations to the protons in various positions followed. Fortunately, the bands belonging to the different (ar)C-H stretching vibrations could be separated in most cases, and thus, the work could be done.

The shifts in the relevant C-H stretching vibrations and the distances between the pillar atoms of the corresponding (aromatic)C-H...X hydrogen bonds have also been correlated.

- [1] I. Pálinkó, B. Török, M. Rózsa-Tarjányi, J.T. Kiss, Gy. Tasi, J. Mol. Struct. 348 (1995) 57-60; (b) I. Pálinkó, J.T. Kiss, Mikrochim. Acta [Supp.] 14 (1997) 253-255.
[2] J.T. Kiss, K. Felföldi, I. Hannus, I. Pálinkó, J. Mol. Struct. 565/566 (2001) 463-468.
[3] J.T. Kiss, K. Felföldi, T. Körtvélyesi, I. Pálinkó, Vib. Spectr. 22 (2000) 63-73.
[4] J.T. Kiss, K. Felföldi, Z. Paksi, I. Pálinkó, J. Mol. Struct. 651-653 (2003) 253-258.
[5] J.T. Kiss, K. Felföldi, I. Pálinkó, J. Mol. Struct. 744-747 (2005) 207-210.

Acknowledgement

This work was supported by the National Science Fund of Hungary through grant K62288. The financial help is highly appreciated.

Calculating pK_a of Some α -Aminoacids Using Cluster-Continuum Model

Nena Peran¹ and Zvonimir B. Maksić^{1,2}

¹Quantum Organic Chemistry Group, Division of Organic Chemistry and Biochemistry, Ruđer Bošković Institute, Bijenička 54, 10 000 Zagreb, Croatia, e-mail: nena@spider.irb.hr

²Faculty of Science, Department of Physical Chemistry, University of Zagreb, Horvatovac 102A, 10 000 Zagreb, Croatia

Aminoacids have several stable forms in water solutions, depending on the pH. The form in neutral solutions is zwitterionic possessing COO^- and NH_3^+ charged groups as a rule. However, all attempts to obtain aminoacids' pK_a s by theoretical methods using common thermodynamic cycles that include gas phase structures and energies of zwitterionic forms fail, because of the instability of such structures. It was found, on the other hand, that complexation with a few water molecules can stabilize zwitterionic structures [1], thus enabling use of cluster-continuum model [2] in calculating pK_a of some α -aminoacids which is a goal of our investigations.

In the present work we introduce a new approach in modelling standard reaction of solvation based on the assumption that microstructure of water solutions can be described as appropriate water clusters immersed in a dielectric continuum. These clusters of water molecules encompass solvated aminoacid as well as the H^+ and OH^- ions.

The calculations of pK_a values of the α -aminoacids require identification of the most stable conformers of water clusters formed around zwitterions and their (de)protonated structures. Reactions necessary for the calculations of basic and acidic pK_a values of some α -aminoacids selected for illustrative purposes will be discussed in detail, as well as some similarities in the cluster geometries of the most stable conformers.

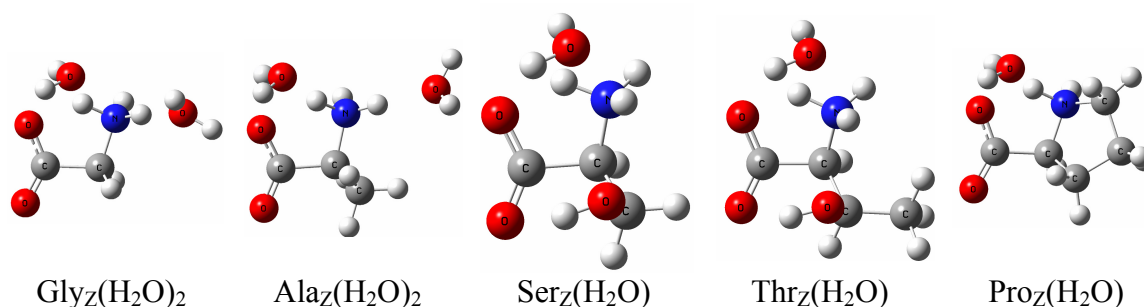


Figure 1: Most stable conformers for zwitterionic structures with minimal number of water molecules needed to stabilize zwitterionic form.

[1] J.H. Jensen, M.S. Gordon, J. Am. Chem. Soc. 117 (1995) 8159-8170.

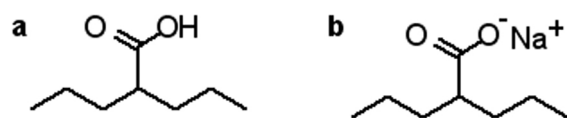
[2] J.R. Pliego, J.H. Riveros, J. Phys. Chem. A 105 (2001) 7241-7247.

Fourier Transform Infrared Spectroscopic Analysis of the Solvates and Polymorphs of Sodium Valproate, Active Component of the Anticonvulsant Drug Epilim®

G. Petruševski¹, P. Naumov^{1,2}, G. Jovanovski^{1,3}

¹Institute of Chemistry, Faculty of Science, SS. Cyril and Methodius University, POB 162, MK-1001 Skopje, Macedonia, ²Graduate School of Engineering, Osaka University, 2-1 Yamada-oka, Osaka, Suita 565-0871, Japan, ³Macedonian Academy of Sciences and Arts, POB 428, MK-1001, Skopje, Macedonia

2-Propylvaleric (valproic) acid and its sodium salts (Scheme 1) have been extensively clinically used as anticonvulsants and mood-stabilizing drugs to treat cases of epilepsy and bipolar disorders, diseases which affect approximately 1% of the human population. Although sodium valproate has been used as medicine for more than fifty years, until recently [1,2], no detailed studies of the polymorphism and crystal structure of this compound were performed. Here, we report the first systematic study of the solid state solvates and polymorphs of sodium valproate, as studied with Fourier transform infrared (FTIR) spectroscopy. Using wet and dry methods, as many as seven solid forms and one thermal intermediate (denoted forms A, B, C, D, E, F, G and H) were prepared. Three compounds (forms A, B and D) are extremely hygroscopic polycrystalline hydrates, three compounds (forms C, E and F) are stoichiometric solvates of sodium valproate with valproic acid, and one compound is an anhydrous salt (form H). Forms A, B and C are unstable upon evacuation and pressing with KBr, and under such treatment they are converted into form D. On the contrary, forms E and F are stable under ambient conditions.



Scheme 1: Formulas of valproic acid (a) and sodium valproate (b).

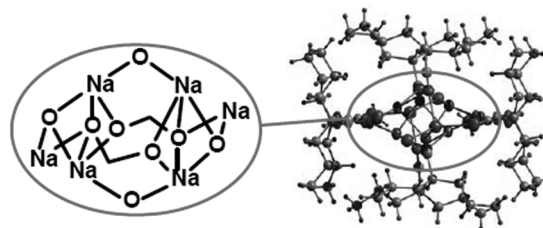


Figure 1: Crystal structure of form C, trisodium hydrogentetravalproate monohydrate.

It is concluded that the spectra recorded from milled samples are sufficiently descriptive to distinct among different polymorphic forms of sodium valproate. Most useful band in the infrared spectra is the antisymmetric carboxylate stretching vibration (1552–1570 cm^{-1}). The frequency split between the antisymmetric and symmetric carbonyl stretches (1413–1441 cm^{-1}), combined with the molecular geometry as determined for the crystal of the form C [1] (Fig. 1), was used to correlate the structural preferences of the carboxylate ion in the other forms of unknown structure. Theoretical calculations were also performed in order to assign the characteristic IR bands, to correlate the spectral appearance with the structural data, and to predict structural features of the sodium valproate forms of unknown structure.

[1] G. Petruševski, P. Naumov, G. Jovanovski, S.W. Ng, *Inorg. Chem. Commun.* 11 (2008) 81–84.

[2] G. Petruševski, P. Naumov, G. Jovanovski, G. Bogoeva-Gaceva, S.W. Ng, submitted for publication.

Hydrogen Bonding and Deuterium Isotope Effects in ^{13}C NMR Spectra of Phenylene Enaminones Derived from Dehydracetic Acid

K. Pičuljan, P. Novak, K. Užarević, M. Cindrić, T. Hrenar, T. Jednačak

Faculty of Science, Department of Chemistry, Horvatovac 102a, Zagreb, Croatia

Enaminones have been recently a subject of comprehensive studies due to their wide applications in organic synthesis [1] and coordination chemistry, as well as their potential pharmacological importance. Studies have shown that enaminone derivatives possess anti-inflammatory, anticonvulsant, antimalarial and cardiovascular activities.

Hydrogen bonds are an important structure and reactivity factor, and also a bioactivity modulator. The aim of this work is to investigate the intra- and intermolecular hydrogen bonding structure in solution of enaminones derived from dehydracetic acid by employing NMR and DFT methods. X-ray structural analysis has confirmed the existence of the keto-amine form (**1a**) in the solid state, stabilized by formation of intramolecular H-bonds [2]. However, the fundamental question is whether the nature of the intramolecular H-bond $\text{N}-\text{H}\cdots\text{O}$ and the proton transfer (Fig. 1) will be affected by solvents of different proton donor and acceptor abilities and the substitution pattern (*ortho*, *meta*, *para*) of enaminone isomers. In order to get further insight into these interactions secondary deuterium isotope effects on ^{13}C chemical shifts have been measured and analyzed.

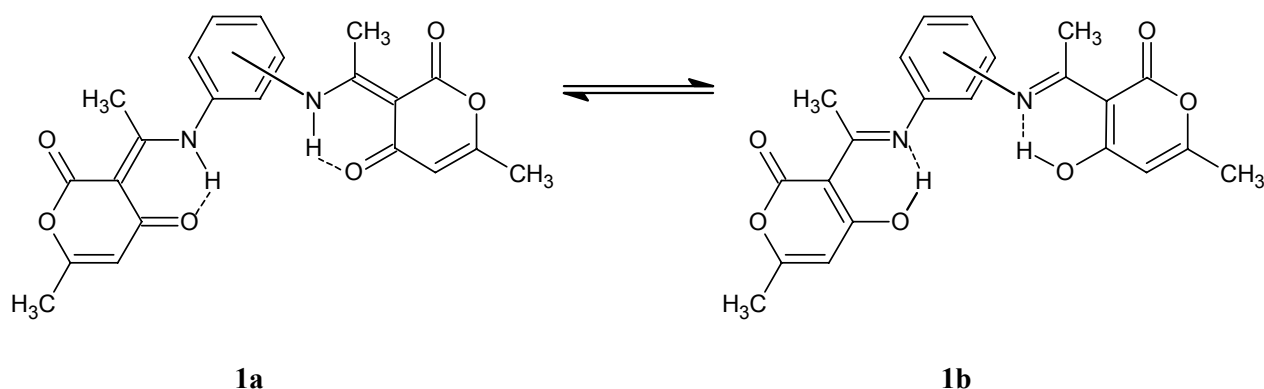


Fig. 1: Tautomerism in phenylene enaminones derived from dehydracetic acid (1a = keto-amine form, 1b = hydroxy-imine form).

[1] A.Z.A. Elassar, A.A. El-Khair, Tetrahedron 59 (2003) 8463-8480.

[2] M. Cindrić, T. Kajfež Novak, K. Užarević, J. Mol. Struct. 750 (2005) 135-141.

Graphical Representation of Proteins as Four-Color Maps and Their Numerical Characterization

Milan Randić¹, Ketij Mehulić², Damir Vukičević³, Tomaž Pisanski⁴,
Dražen Vikić-Topić⁵, Dejan Plavšić⁵

¹National Institute of Chemistry, P.O. Box 3430, 1001 Ljubljana, Slovenia, ²School of Dental Medicine, University of Zagreb, Gundulićeva 5, 10000 Zagreb, Croatia, ³Department of Mathematics, University of Split, Nikole Tesle 12, 21000 Split, Croatia, ⁴IMFM, Department of Theoretical Computer Science, University of Ljubljana, Jadranska 19, 1000 Ljubljana, Slovenia, ⁵Ruđer Bošković Institute, NMR Center, P.O.Box 180, HR-10002 Zagreb, Croatia

We put forward a novel compact 2-D graphical representation of proteins based on the concept of virtual genetic code and a four-color map. The novel graphical representation uniquely represents proteins and allows one to easily and quickly visually observe and inspect similarity/dissimilarity between them. It also leads to a novel protein descriptor being a 10-vector derived from a novel structure matrix \mathbf{S} associated with the map. The approach is illustrated with the A-chain of human insulin and the A-chain of human insulin analogue glargine.

The Local Structure of Europium Lead-Borate Glasses and Glass Ceramics

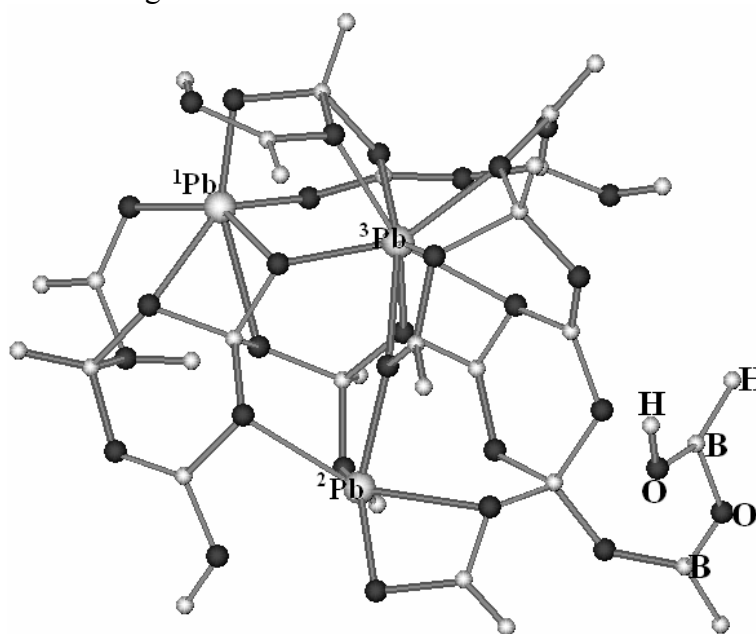
S. Rada, V. Maties¹, M. Rada¹, L. Pop, E. Culea

Department of Physics, Technical University of Cluj-Napoca, 400641 Cluj-Napoca, Romania

¹Department of Mechatronics, Technical University of Cluj-Napoca, 400641 Cluj-Napoca, Romania

Glasses in the system $x\text{Eu}_2\text{O}_3 \cdot (100-x)[3\text{B}_2\text{O}_3 \cdot \text{PbO}]$ with $0 \leq x \leq 70$ mol% have been prepared from melt quenching method. Influence of europium ions on structural behavior in lead-borate glasses has been investigated using infrared spectroscopy and DFT calculations. The structural changes have been analyzed with increasing rare earth concentration.

Structural changes, as recognized by analyzing band shapes of IR spectra, revealed that Eu_2O_3 causes a change from the continuous borate network to the continuous lead-borate network with interconnected through Pb-O-B and B-O-B bridges. In addition, the gradual increase of europium oxide in the glass up to 35 mol% results to transformation of some tetrahedral $[\text{BO}_4]$ units into trigonal $[\text{BO}_3]$ units, a reduction of the proportion of the tetrahedral $[\text{BO}_4]$, in place of which pyroborate, orthoborate groups and chains or metaborate rings are formed and disintegration of some boroxol units.



DFT calculations show that lead atoms occupy three different sites in the proposed model. The first are coordinated with six oxygen atoms forming distorted octahedral geometries. The second lead atom has an octahedral oxygen environment and the five longer Pb-O bonds are considered as participating in the metal coordination scheme. The third lead atom has ionic character.

Structural properties of Gadolinium Borate-Tellurate Glasses and Glass Ceramics Inferred from FTIR spectroscopy and DFT Studies

S. Rada, M. Barlea, D. Chicea¹ and E. Culea

Technical University of Cluj-Napoca, 400020 Cluj-Napoca, Romania

¹University Lucian Blaga of Sibiu, 550012 Sibiu, Romania

The structure of tellurate-borate glasses is of great interest due to at least two motives: (i) adding a network modifier oxide breaks the Te-O-Te network bridges (the process is accompanied by the formation of non-bridging oxygen sites) and (ii) the different nature of the oxygen polyhedra surrounding the boron atoms.

The purpose of this paper was to approach the structure of gadolinium borate-tellurate glasses using the infrared spectroscopy investigation and the DFT calculations.

First, we attempt to develop a structural model for the binary $0.6\text{TeO}_2\cdot 0.4\text{B}_2\text{O}_3$ borate-tellurate glass paying a special attention to the coordination state of tellurium and boron atoms.

As recognized by X-ray diffraction and FTIR analysis, the addition of Gd_2O_3 to the $0.6\text{TeO}_2\cdot 0.4\text{B}_2\text{O}_3$ host glass matrix causes important structural modifications. Thus, up to a content of 25% Gd_2O_3 a higher extent of network polymerization occurs. After that, increasing the Gd_2O_3 content up to 50 mole% occur the transformation of the $[\text{BO}_4]$ units into the $[\text{BO}_3]$ units from boroxol rings and into $[\text{BO}_3]$ units with varied types of borate groups and also, the coordination of the tellurium atom should be changed progressively from 4 though 3+1 to 3.

Heat treated samples were also investigated. The FTIR data show that these samples consist mainly of $[\text{TeO}_3]$, $[\text{TeO}_4]$, $[\text{BO}_4]$ and $[\text{BO}_3]$ structural units. The DFT calculations show that the increase in the number of non-bridging oxygen atoms would decrease the connectivity of the glass network and would necessitate quite a radical rearrangement of the network formed by the $[\text{TeO}_6]$ octahedron.

Vibrational Spectra of Hydrates of Some Metal(II) Malonates

Mirjana Ristova¹, Gorgi Petruševski, Aleksandra Raškavska, Bojan Šoptrajanov^{1,2}

¹*Institute of Chemistry, Faculty of Science, SS. Cyril and Methodius University, Arhimedova 5, 1000 Skopje, Republic of Macedonia,*

²*Macedonian Academy of Sciences and Arts, Bul. Krste Misirkov 2, 1000 Skopje, Republic of Macedonia*

Interest in the synthesis and studies of metal(II) malonates crystalhydrates M(Co, Ni, Cu and Cd)^{1,2} steams from the extensive use of malonato ion in controlled assembly of molecules and ions into strategies for supramolecular synthesis and crystal engineering purposes.

In the course of vibrational spectroscopic investigations of crystalline hydrates of salts of malonic acid, the FTIR spectra were recorded at room temperature and the boiling temperature of liquid nitrogen (RT and LNT, respectively) and studied together with its RT Raman spectrum. The regions of the COO stretchings are discussed in more detail, and the appearance of the characteristic bands is correlated with the available structural data.

- [1] P. Naumov, M. Ristova, B. Šoptrajanov, M.G.B. Drew, S. Weng Ng, *Croat. Chem. Acta* 75 (2002) 707.
- [2] P. Naumov, M. Ristova, B. Šoptrajanov, K. Moon-Jib., Han-Jun L., S. Weng Ng, *Acta Cryst.* E57 (2001) m14.
- [3] H.-Y. Shen, W.-M. Bu, D.-Z. Liao, J.-H. Jiang, S. P. Yan, G.-L. Wang, *Inorg. Chem. Commun.* 3 (2000) 497-500.
- [4] Y. Rodriguez-Martin, C.Ruiz-Pérez, J. Sanchiz, F. Lloret, M. Julve, *Inorg. Chim. Acta* 318 (2001) 159-165.

IR Low-temperature Matrix and *Ab Initio* Study on β -Alanine Conformers

J.Cz. Dobrowolski^{1,2}, M.H. Jamróz², R. Kołos³, J.E. Rode², J. Sadlej^{1,4}

¹National Medicines Institute, 30/34 Chełmska Street, 00-725 Warsaw, Poland, ²Industrial Chemistry Research Institute, 8 Rydygiera Street, 01-793 Warsaw, Poland, ³Institute of Physical Chemistry, PAS, Kasprzaka 44, 01-224 Warsaw, Poland, ⁴Faculty of Chemistry, Warsaw University, 1 Pasteura Street, 02-093 Warsaw, Poland

Synthetic β -aminoacids are used to synthesize β -peptides which are not recognized and decomposed by majority of enzymes. Therefore, the β -peptides are desired and requested candidates for new antibacterial drugs. In contrast to α -aminoacids, the β -aminoacids have so far been little looked into. Conformation of β -alanine in the gas phase was studied by using FTMW method [1, 2] and two and four conformers was identified, respectively.

To interpret our Ar and N₂ low-temperature IR matrix spectra of β -alanine (Fig. 1), the B3LYP/aug-cc-pVDZ anharmonic IR spectra of the probable 10 conformers were calculated. For the most stable three conformers, the anharmonic spectra were recalculated by using aug-cc-pVTZ basis set. The theoretical spectra were then interpreted by means of the potential energy distribution analysis. The DFT energies taken as the only source for estimation of conformer population may lead to misinterpretations, therefore the conformer population calculations were also performed at the MP2/aug-cc-pVDZ and QCISD/aug-cc-pVDZ levels.

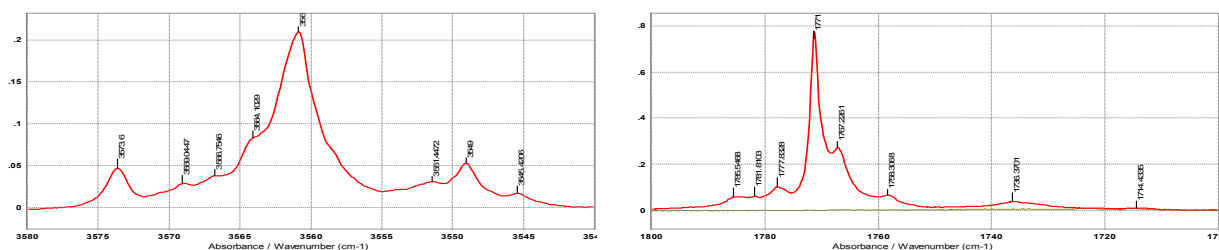


Fig. 1: Low temperature Ar-matrix IR spectra of β -alanine on the $\nu(\text{OH})$ and $\nu(\text{C}=\text{O})$ regions revealing strong evidence of three, weak evidence of the other two, and supposition of presence of another two conformers.

Based on a detailed analysis of the whole mid-IR Ar and N₂ matrix spectra we claimed to the conclusion that there is strong evidence for the presence of the conformer **1** (Fig. 2), some evidence of the **2** and **3** β -alanine conformers (Fig. 2), a weak evidence for the other two conformers, and a supposition of presence of another two conformers. The difference between our low temperature matrix data and those found in the gas phase [1, 2], is an absence, or only supposed presence, of the conformer with the internal $\text{COOH}\dots\text{NH}_2$ hydrogen bond.

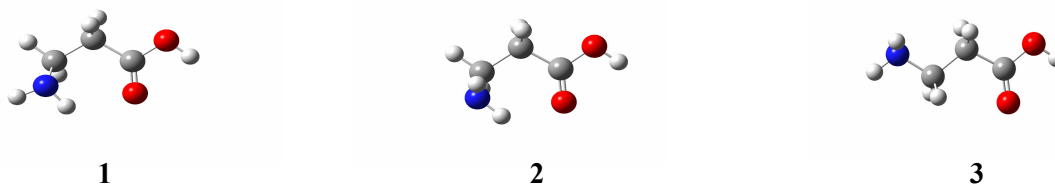


Fig. 2: Three of β -alanine conformers identified in the Ar-matrix IR spectra.

- [1] S.J. McGlone, P.D. Godfrey: *Rotational Spectrum of a Neurohormone: β -Alanine*. J. Am. Chem. Soc. 117 (1995) 1043-1048.
 [2] M.E. Sanz, A. Lesarri, M.I. Peña, V. Vaquero, V. Cortijo, J.C. López, J. L. Alonso: *The Shape of β -Alanine*. J. Am. Chem. Soc. 128 (2006) 3812-3817.

Synthesis and Physical Chemical Characterization of The Potassium 11-Tungstovanado(IV) Phosphate Anion

D. Rusu¹, O. Baban², I. Hauer³, L. David³, M. Rusu²

¹"Iuliu Hatieganu" Univ. of Medicine and Pharmacy, Str. Emil Isac nr.13, 400023 Cluj-Napoca, Romania

²"Babes-Bolyai" Univ., Faculty of Chemistry, Str. Arany Janos nr. 11, 400028 Cluj-Napoca, Romania

³"Babes-Bolyai" Univ., Faculty of Physics, Str. M. Kogalniceanu nr. 1, 400084 Cluj-Napoca, Romania

Polyoxometalates constitute a large class of compounds that are remarkable for their molecular and structural versatility as well as their interesting and diverse properties, which makes them more and more popular in many fields such as catalysis, biology, medicine, magnetism, photochemistry and material science [1, 2].

The new $K_5[(VO)PW_{11}O_{39}].10H_2O$ complex was synthesized by alternative methods and investigated by chemical and thermogravimetric analysis, X-ray diffraction and spectroscopic (FT-IR, UV-Vis, ESR) methods.

The FT-IR spectrum in KBr pellets shows the following vibration bands: 1622 cm^{-1} (δ_{H-O-H}), 1089 and 1063 cm^{-1} ($\nu_{as}P-O_i$), 964 cm^{-1} ($\nu_{as}W-O_t + \nu_{as}V-O$), 889 cm^{-1} ($\nu_{as}W-O_c-W$), 798 and 735 cm^{-1} ($\nu_{as}W-O_e-W$), 679 and 594 cm^{-1} ($\delta_{W-O_c,e-W}$), which are characteristic for polyoxometalates.

The two absorption bands in the electronic spectrum at 13500 and 15500 cm^{-1} are due to d-d transitions and correspond to so-called bands I and II in normal oxovanadium complexes. The absorption bands at 20000 and 25000 cm^{-1} which are responsible for the intense color of the anion are assigned to the heteronuclear intervalence charge-transfer transitions $V(IV) \rightarrow W(VI)$.

The powder EPR spectrum (Fig. 1) of the complex obtained in the X band at room temperature contains eight hyperfine components, both in the perpendicular and parallel bands.

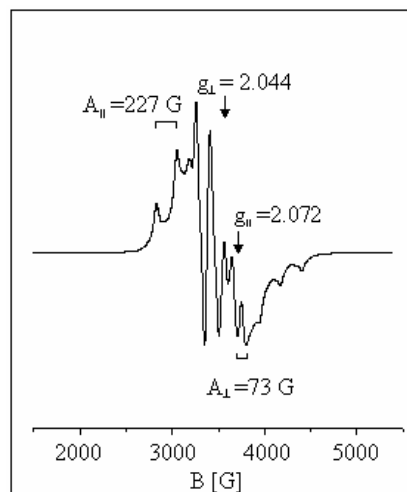


Fig. 1: The EPR spectrum of the $K_5[(VO)PW_{11}O_{39}].10H_2O$ complex

Single-crystal X-ray diffraction shows that the complex crystallizes in the triclinic system and belongs to the $P3(2)$ 21 space group with two molecules per cell.

[1] M.T. Pope, A. Müller, *Angew. Chem. Int. Ed. Engl.* 30 (1991) 34.

[2] A. Müller, F. Peters, M.T. Pope, D. Gatteschi, *Chem. Rev.* 98 (1998) 238.

Spectroscopic and Theoretical Studies of 5-Fluoro-isatin-3-(N-cyclohexylthiosemicarbazone) and Its Metal Complexes

S. Gunesdogdu Sagdinc¹, B. Köksoy², F. Kandemirli² and S. Haman Bayari³

¹ University of Kocaeli, Faculty of Science, Dept. of Physics, Kocaeli, Turkey,

² University of Kocaeli, Faculty of Science, Dept. of Chemistry, Kocaeli, Turkey

³ University of Hacettepe, Faculty of Education, Dept. of Physics, Ankara, Turkey

The isatin-3-thiosemicarbazones and their metal complexes have been studied by several researchers because of important biological activities [1, 2]. Transition metal ions Zn(II) and Ni(II) complexes with 5-Fluoro-1*H*-indole-3-dione-3-[-(N-cyclohexylthiosemicarbazone)](HFIC) was synthesized. Zn(II) complex takes a distorted tetrahedral geometry in which two nitrogens and two sulphur donors coordinate to Zn(II). Ni complex takes also a distorted octahedral coordination with the monodeprotonated ligand that behaves as an O,N,S terdentate.

The compounds Zn(HFIC)₂ and Ni(HFIC)₂ has been characterized using elemental analysis, Fourier transform infrared spectroscopy (FT-IR), UV spectroscopy and ¹H-NMR spectroscopy. Theoretical calculations have been also performed by HF method using 6-31G(d,p) and LanL2DZ basis sets. The normal mode calculations and the assignments of bands observed in FT-IR spectrum for H₂FIC and its metal complexes have been made using *ab initio* and DFT methods. Some significant differences in vibrational structures between ligand and its complexes have been observed and discussed.

The molecular parameters (bond lengths, bond angles, the highest occupied molecular orbital energy (E_{HOMO}), lowest unoccupied molecular orbital energy (E_{LUMO}), the energy gap between E_{HOMO} and E_{LUMO} (ΔE_{HOMO-LUMO}), dipole moment, charges on the atoms of 5-Fluoro-1*H*-indole-3-dione-3-[-(N-cyclohexylthiosemicarbazone)] was studied by HF, and B3LYP methods using several basis sets.

[1] A. Rai, S.K. Sengupta, O.P. Pandey, Spectrochim. Acta A 61 (2005) 2761-2765.

[2] G. Vatsa, O.P. Pandey and S.K. Sengupta, Bioinorg. Chem. Appl. 3 (2005) 3.

Acknowledgment

We would like to thank TUBITAK for partial support through the project 106T465(TBAG-HD/199).

Spectroscopy and Photochemistry of Glyoxal-Hydroxylamine Complexes. Matrix Isolation and Theoretical Study

M. Sałdyka, B. Golec, Z. Mielke

Faculty of Chemistry, University of Wrocław, Joliot-Curie 14, 50-383 Wrocław, Poland

Glyoxal is formed in the atmosphere during the oxidation of hydrocarbons, which are emitted by biogenic and anthropogenic sources. In particular, glyoxal is an important ring-cleavage product in the OH radical initiated oxidation of aromatic hydrocarbons, and is also formed in the reaction of ozone and OH radicals with some alkenes and unsaturated aliphatic oxygenated hydrocarbons [1]. The photolysis is the most important removal process for glyoxal in the troposphere, which can lead to the formation of H₂, CO, HCHO, and HCO species [2]. In spite of the fact that the spectroscopy and photochemistry of glyoxal has been extensively studied [3], the less attention has been devoted to the molecular interactions of this molecule.

In this work we present the results of the infrared matrix isolation and theoretical studies of the glyoxal-hydroxylamine complexes. The comparison of the theoretical and experimental spectra allowed us to determine the structures of the complexes present in the matrixes. The MP2(6-311++G(2d,2p)) calculations resulted in seven stable structures of the glyoxal-hydroxylamine system. Six planar complexes are stabilized by various types of hydrogen bonds and one non-hydrogen bonding structure is stabilized by a dipole-quadrupole interaction. In argon and nitrogen matrixes three most stable complexes were identified: the non-hydrogen bonding system and two complexes where the OH...O or CH...N hydrogen bonds are formed.

The UV-VIS photolysis with a medium-pressure mercury lamp of the matrix isolated complexes led to the appearance of a number of bands in the OH, C=O stretching and CH bending regions of the spectra. In addition, a strong band due to the C=C=O asymmetric stretching mode was also identified. On the basis of different growth rates during photolysis and different response to matrix annealing the absorptions appearing after photolysis are assigned to various conformers of carbinolamine and to hydroxyketene. The identification of the photolysis products was confirmed by the isotopic studies with deuterated hydroxylamine ND₂OD and MP2 simulations of the IR spectra of the possible photolysis products.

- [1] R. Volkamer, P. Spietz, J. Burrows, U. Platt, J. Photochem. Photobiol. A 172 (2005) 35-46.
- [2] L. Zhu, D. Kellis, Ch. Ding, Chem. Phys. Lett. 257 (1996) 487-491.
- [3] B. Klotz, F. Graedler, S. Sørensen, I. Barnes, K.H. Becker, Int. J. Chem. Kinet. 33 (2001) 9-20 and references therein.

Submicroheterogenous Structure of Silico-Phosphate Glasses Studied by ^{23}Na , ^{27}Al , ^{31}P NMR and FTIR

Maciej Sitarz¹, Zbigniew Fojud², Zbigniew Olejniczak³

¹ Faculty of Materials Science and Ceramics, AGH University of Science and Technology, Al. Mickiewicza 30, 30-059 Kraków, Poland

² Institute of Physics, Adam Mickiewicz University, Poznań, Poland

³ Institute of Nuclear Physics PAN, Kraków, Poland

Silico-phosphate glasses of $\text{NaCaPO}_4\text{-SiO}_2$ and $\text{NaCaPO}_4\text{-AlPO}_4\text{-SiO}_2$ system have been the subject of the presented investigations. Glasses of these systems are the basis for the preparation of glassy-crystalline biomaterials [1]. Detailed knowledge of the precursor glass structure is necessary for proper design of the glassy-crystalline biomaterials preparation procedure. Since there is no long-range ordering in glasses, spectroscopic methods which make it possible to study the short range ordering should be applied.

MIR studies carried out in the work have allowed to establish that the glasses of the systems studied show domain composition [2, 3]. Detailed ^{31}P , ^{23}Na , ^{27}Al and ^{29}Si NMR as well as Raman investigations have confirmed existence of domains. Domain structure is close to that of the corresponding crystalline phases. It has been shown that even small amount of aluminum in the glass (5 mol. % of AlPO_4) significantly influences both, its texture (microscopic and EDX studies) and its structure (spectroscopic studies). ^{27}Al NMR investigations have made it possible to unequivocally that aluminum occurs exclusively in tetrahedral coordination, i.e. it is involved in the formation of glass framework. Presence of aluminum results in significant changes in the $[\text{SiO}_4]^{4-}$ i $[\text{PO}_4]^{3-}$ tetrahedra environment which is reflected in ^{31}P and ^{29}Si NMR spectra. Changes in the shapes and positions of the bands in the NMR spectra of glasses belonging to the $\text{NaCaPO}_4\text{-AlPO}_4\text{-SiO}_2$ system confirm great influence of aluminum on silico-phosphate glasses structure.

[1] R.D. Rawlings, Clinical Materials 14 (1993) 155.

[2] M. Sitarz, M. Rokita, M. Handke, E. Galuskin, J. Molec. Struc. 651-653 (2003) 489.

[3] M. Handke, M. Sitarz, M. Rokita, E. Galuskin, J. Molec. Struc. 651-653 (2003) 39.

Acknowledgment

This work is supported by Polish Committee for Scientific Research under grant no. 3T08D 033 27.

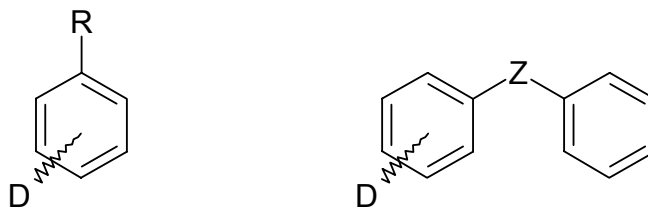
Deuterium Isotope Effects in ^{13}C NMR Spectra of *ortho*-, *meta*- and *para*-Deuterium Labelled Mono- and Binuclear Aromatic Compounds

Vilko Smrečki¹, Predrag Novak², Dražen Vikić-Topić¹ and Zlatko Meić²

¹Ruder Bošković Institute, NMR Center, Bijenička 54, HR-10000 Zagreb, Croatia

²Faculty of Science, University of Zagreb, Dept. Anal. Chem., Horvaćanska bb, HR-10000 Zagreb, Croatia

Differently deuterium labelled isotopomers of mono- and binuclear aromatic compounds (aniline, *trans*-azobenzene, benzaldehyde, benzoic acid, benzonitrile, benzophenone, *trans*-N-benzylideneaniline, *trans*-N-salicylideneaniline, *cis*-stilbene, *trans*-stilbene and toluene) were studied by ^{13}C NMR spectroscopy. A number of deuterium isotope effects (DIE) on ^{13}C chemical shifts have been observed.



$\mathbf{R} = -\text{CH}_3, -\text{CHO}, -\text{COOH}, -\text{NH}_2, -\text{CN}$ $\mathbf{Z} = -\text{C}=\text{N}-, -\text{N}=\text{C}-, -\text{C}=\text{C}-, -\text{N}=\text{N}-,$

The changes of magnitude, sign and extent of isotope effects in studied isotopomers of aforementioned compounds are quite different. The range of isotope effects, sign alterations, and magnitude variations will be discussed in terms of steric effects, planarity, symmetry, lone-pair interactions and charge redistribution.

Molecular Structure, Infrared Spectra and Some Molecular Properties of 5-Chloro-6-(4-chlorobenzoyl)-2-benzothiazolinone

İsa Sıdır¹, Erol Taşal¹, Yadigar Gülseven¹, Rui Fausto², Tijen Önkol³

¹Department of Physics, Faculty of Arts & Sciences, Eskişehir Osmangazi University, 26480 Eskişehir, Turkey

²Department of Chemistry, University of Coimbra, 3004-535 Coimbra, Portugal

³Department of Pharmaceutical Chemistry, Faculty of Pharmacy, Gazi University, 06330 Ankara, Turkey

The molecular structure, vibrational frequencies and infrared intensities of 5-chloro-6-(4-chlorobenzoyl)-2-benzothiazolinone (abbreviated as CCB) molecule in the ground state were calculated by HF and DFT (B3LYP and BLYP) methods using 6-311++G(d,p), 6-31G(d), 3-21G and STO-3G basis sets. The FT-IR spectra have been measured for the title compound in the solid state. In this molecule, we obtained 2 different stable conformers for the title compound. It is shown that in the most conformer $\alpha = -59.6$ and $\beta = -14.5$, with α and β being the C9-C8-C12-C18 and C8-C12-C18-C17 dihedral angles, respectively. The comparison of the theoretical and experimental geometry of the title compound shows that the X-ray parameters of a similar molecule to CCB [1] fairly well agree with the corresponding ones obtained theoretically for the most stable conformer of the molecule studied in the present work. The calculated vibrational data are also in a good agreement with the experimental results.

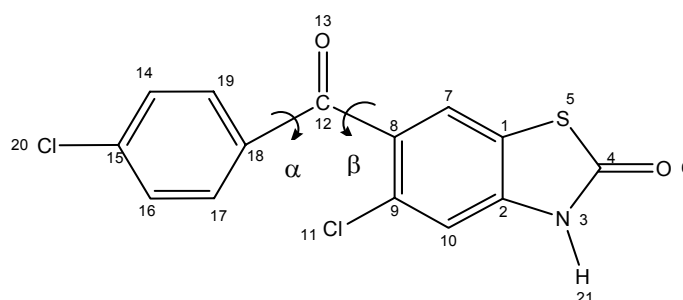


Fig. 1: Molecular structure and atoms numbering scheme for CCB.

[1] Hakan Arslan, Öztekin Algül, Tijen Önkol, *Spectrochimica Acta Part A* (2007) in press.

Acknowledgements

We are grateful to ESOGU for financial support through Research Project No: 200519010 and ESOGU Research Project No: 200819XXX. RF thanks FCT for financial support (POCI/QUI/59019/2004).

Raman Study of Anharmonic Effects in Vibrational Spectra of Acetylenic Compounds

D. Vojta, G. Baranović

Department of Organic Chemistry and Biochemistry, Ruđer Bošković Institute,
Bijenička 54, 10002 Zagreb, Croatia, dvojta@irb.hr

The π -conjugated compounds consisting of an acetylenic chain $[-(C\equiv C)_n-]$ are calculated to be one-dimensional conductors and could be utilized as molecular electronic devices. The variation of the functional groups attached to the terminal carbon atoms and the length of the acetylenic chain can be the test for the molecular ability to serve as a molecular wire [1].

During spectroscopic investigations of acetylenic compounds with phenyl and trimethylsilyl terminal group(s) (Fig. 1), an unusual and hitherto unexplained phenomenon has been observed in their Raman spectra. The band that originates from the acetylenic stretching has pronounced asymmetry on the low-frequency side (Fig. 2). The asymmetry is most probably a consequence of the unresolved hot band sequence that occurs due to the coupling between the acetylenic stretching at $(2130 \pm 100) \text{ cm}^{-1}$ and the linear bending at around $(200 \pm 100) \text{ cm}^{-1}$. The hypothesis is based on the existence of such a sequence in gas and liquid phase spectra of halogeno substituted acetylenes [2] and also on the experimental results that have already been obtained for **DPA** and **PA** under different conditions [3].

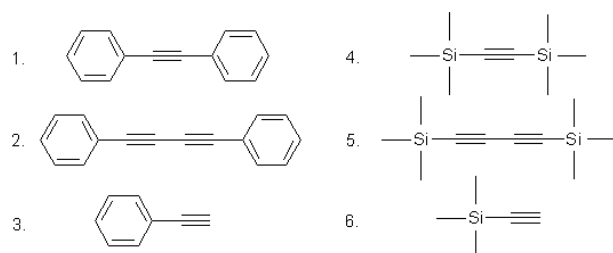


Figure 1:

1. Diphenylacetylene (**DPA**),
2. Diphenyldiacetylene (**DPDA**),
3. Phenylacetylene (**PA**),
4. Di(trimethylsilyl)acetylene (**DTMSA**),
5. Di(trimethylsilyl)diacetylene (**DTMSDA**),
6. Trimethylsilylacetylene (**TMSA**)

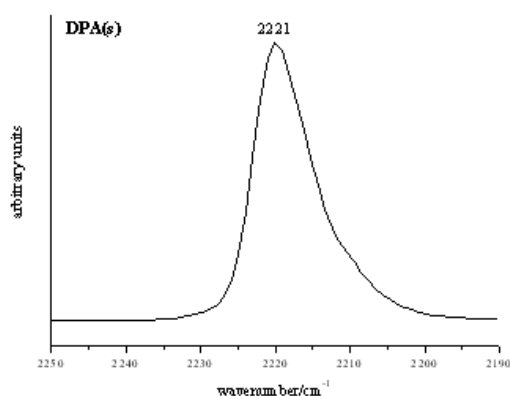


Figure 2: FT Raman spectrum of **DPA(s)**

The asymmetry of this feature is present in Raman spectra of all the studied molecules regardless of the phase. However, the splitting of the bands seems to be at the resolution limit and therefore, it had to be quantified as the skewness with an error defined as the skewness of the perfectly symmetric Raman band of $\text{KMnO}_4(\text{s})$ at 350 cm^{-1} . The asymmetry is more pronounced for compounds with phenyl terminal groups than for those with trimethylsilyl terminal groups, and, additionally, it is the most pronounced in Raman spectra of **DPDA** and **DTMSDA** that have the longest acetylenic chain.

[1] R.L. Carrol, C.B. Gorman, *Ang. Chem. Int. Ed.* 41 (2002) 4378.

[2] J.K. Brown, N. Sheppard, *Spectrochim. Acta* 23A (1967) 129.

[3] (a) H. Abramczyk, M. Kolodziejski, G. Waliszewska, *Chem. Phys.* 228 (1998) 313; (b) H. Abramczyk, G. Waliszewska, M. Kolodziejski, *J. Phys. Chem. A* 102 (1998) 7765.

Vibrational Spectra and Structural Parameter of Methyl and Ethyl Isocyanate

Sarah Xiaohua Zhou¹, Douglas T. Durig², James R. Durig¹

¹University of Missouri-Kansas City, Kansas City, MO, 64110 USA, ²College of the South, Sewanee, TN, 37383 USA

The infrared and Raman spectra of methyl and ethyl isocyanate have been investigated from 50-4000 cm^{-1} additionally the infrared spectra of xenon and krypton solutions have been recorded from 100-4000 cm^{-1} . Analysis of the vibrational data of methyl isocyanate shows the molecule has a very low barrier to internal rotation of the methyl group. The fine structures on the pseudo degenerate vibrational modes of the methyl group have been analyzed. Support for the vibrational assignments is provided by *ab initio* and density functional theory calculations. The vibrational spectrum of the ethyl isocyanate has also been obtained similarly to that for the methyl compound. The Raman spectra [1] of ethyl isocyanate clearly show that the fluid phases have two conformers (Figure 1) which convert to a single conformer on annealing. The potential for different conformation has been evaluated and the data clearly show that the most stable conformer is the *cis* form. This is in agreement with the microwave data but is at variance with proposed conclusion obtained from *ab initio* calculation.

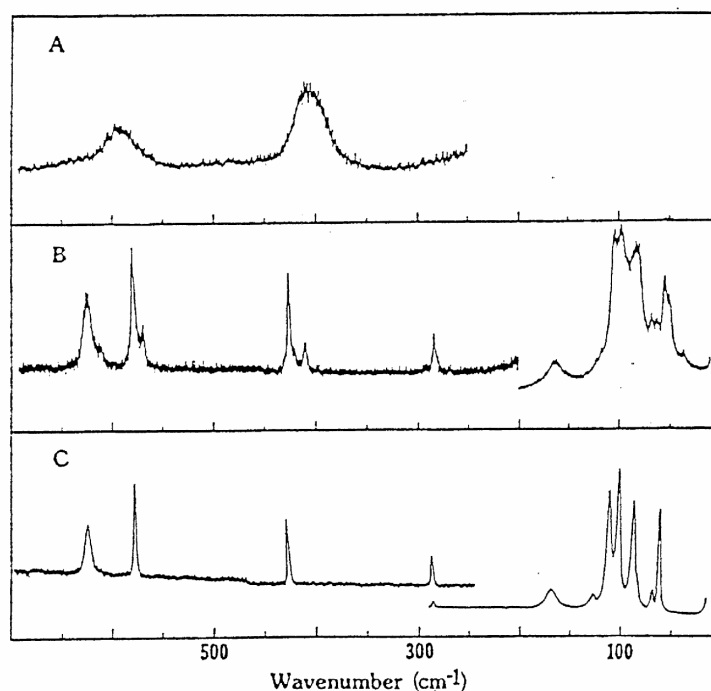


Fig. 1: Low-frequency Raman spectra of ethyl isocyanate: (A) liquid, (B) amorphous solid, and (C) annealed solid.

Structural parameters of both methyl and ethyl isocyanate have been obtained and the result will be presented and the differences among the various possible structures will be compared along with those for similar molecules with the isothiocyanate group.

[1] J.F. Sullivan, D.T. Durig, J.R. Durig, S. Cradock, J. Phys. Chem. 91(7) (1987) 1770-1778.

Vibrational Analysis of Diacetylenic Aromatic Compounds

D. Vojta, B. Zimmermann, G. Baranović

Department of Organic Chemistry and Biochemistry, Ruđer Bošković Institute,
Bijenička 54, 10002 Zagreb, Croatia, e-mail: zimmer@irb.hr

Carbon rich compounds such as polyynes, $[-(C\equiv C)_n-]$, are currently an area of great interest and research. They are major building-blocks in constitution of most fundamental class of carbon-based molecular wires. Phenyl substitution into the terminals of the polyyn chain reduces the isomerization and the chemical reactivity of polyynes, at the same time improving conducting and optical properties. Conjugation can also be improved by inclusion of more than one acetylenic bridge in molecule, hence creating cyclic analogs i.e. dehydrobenzoannulenes. Besides the phenyl groups, a special attention has been given to the pyridine as a terminal group because of opening a possibility of complexation with metal atoms [1].

Spectroscopic measurements of aromatic acetylenic and diacetylenic compounds show that in IR spectral region $2300-2000\text{ cm}^{-1}$ only one band (at $\sim 2105\text{ cm}^{-1}$) corresponding to the acetylenic stretching is observed. However, in IR spectra of solid 2,6-diethynylpyridine and 1,2-diethynyl-4,5-dimethoxybenzene, the mentioned region is rich with bands (Figure 1.).

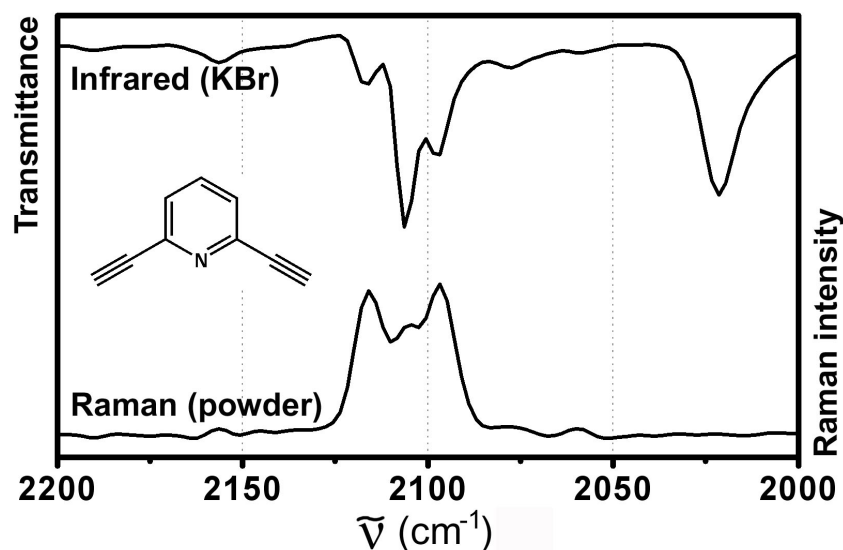


Figure 1: IR and Raman spectra of 2,6-diethynylpyridine.

It is reasonable to assume that additional bands are a consequence of a crystal packing, namely, non-specific and directional intermolecular interactions. In order to investigate these phenomena, we conducted vibrational measurements (IR and Raman) in solid state at different temperatures and in solutions with solvents of different polarities.

[1] F. Diedrich, P.J. Stang, R.R. Tykwinski, Eds.: *Acetylene Chemistry*, Wiley-WCH, Weinheim, Germany, 2005.

Vibrational Spectroscopic and DFT Studies of Gadolinium Vanado-Tellurite Glasses and Glass Ceramics

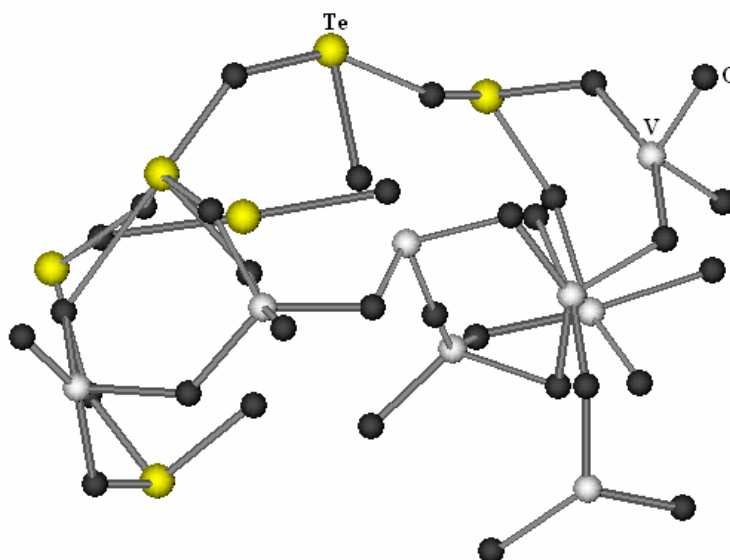
S. Rada, P. Pascuta, M. Culea¹, M. Pica, E. Culea

Department of Physics, Technical University of Cluj-Napoca, 400641 Cluj-Napoca, Romania

¹Faculty of Physics, Babes-Bolyai University of Cluj-Napoca, 400084 Cluj-Napoca, Romania

The structure of $\text{TeO}_2\text{-V}_2\text{O}_5$ glasses is still subject to discussion from two motives: (i) adding to the network modifier oxides occur the broken Te-O-Te network bridges accompanied by the formation of non-bridging oxygen sites, and (ii) the structure of vanadate glasses remains a subject of interest because there is no clear picture as to the exact nature of the oxygen polyhedra surrounding the vanadium atoms or of the role played by the other glass components. Moreover, the structure of the vanadate glasses can be related to the nature of the network formers as well as on the network modifiers.

The purpose of this paper was to approach the structure of gadolinium vanado-tellurite glasses using the infrared spectroscopy and DFT calculations. We attempt to develop such a model for binary vanado-tellurite glasses. Special attention was paid to the coordination state of tellurium and vanadium atoms.



Structural changes, as recognized by analyzing band shapes of X-ray diffraction and FTIR spectra, revealed that Gd_2O_3 causes a higher extent of network polymerization as far as 40 mol%, after that between 40 and 50 mol% reveal a drastic structural modification which lead to the forming of the GdVO_4 crystalline phase.

Then, the present study provides interesting information concerning devitrification behavior of the gadolinium vanado-tellurite vitreous system which occur $\text{Te}_2\text{V}_2\text{O}_9$ and GdVO_4 crystalline phases. Surface of the heat-treated glasses was found to consist mainly of rings containing $[\text{TeO}_3]$, $[\text{TeO}_4]$, $[\text{VO}_4]$ and some $[\text{VO}_5]$ structural units.

The DFT calculations show that the $[\text{VO}_4]$ tetrahedrons are easy distorted whereas the $[\text{VO}_5]$ square pyramids are considerably distorted around vanadium center.

Fourier Transform Infrared and Raman Spectra of Hexagonal $\text{MgCsPO}_4 \cdot 6\text{H}_2\text{O}$

V. Stefov¹, A. Cahil¹, B. Šoptrajanov^{1,2}, M. Najdoski¹, F. Spirovski¹, B. Engelen³,
H.D. Lutz³, V. Koleva⁴

¹*Institut za hemija, PMF, Univerzitet "Sv. Kiril i Metodij", P.O. Box 162, 1001 Skopje, R. Macedonia*

²*Makedonska akademija na naukite i umetnostite, Skopje, Republic of Macedonia*

³*Anorganische Chemie, Universität Siegen, 57068 Siegen, Deutschland*

⁴*Institut po obšta i neorganična himija, Blgarska akademija na naukite, 1113 Sofija, R. Bulgaria*

The Fourier transform infrared and Raman spectra of a struvite analogue, hexagonal magnesium caesium phosphate hexahydrate, $\text{MgCsPO}_4 \cdot 6\text{H}_2\text{O}$ and of its partially deuterated analogues were recorded from room temperature (RT) down to the boiling temperature of liquid nitrogen (LNT).

The crystal structure of hexagonal $\text{MgCsPO}_4 \cdot 6\text{H}_2\text{O}$ has been solved by X-ray diffraction [1]. According to the crystallographic results, it crystallizes in the hexagonal space group $P6_3mc$ (C_{6v}^4) with $Z = 2$. It was found that Mg^{2+} , Cs^+ and PO_4^{3-} occupy special positions with C_{3v} symmetry, while the two types of water molecules are situated on positions with C_s symmetry.

The existence of strong hydrogen bonds formed by the water molecules is supported by the appearance of a broad band from 3600 to 2200 cm^{-1} in the O–H stretching region of the vibrational spectra. In the difference LNT infrared spectrum of the analogue with a small deuterium content ($\approx 5\%$ D), in the region of the OD stretching vibrations of isotopically isolated HDO molecules, at least two bands (from the expected three) at 2255 and 2180 cm^{-1} are observed.

In the infrared region of the $\nu_3(\text{PO}_4)$ modes, a broad and asymmetric band at around 1000 cm^{-1} is found, while in the region of the $\nu_4(\text{PO}_4)$ bending vibrations and of the external modes of the water molecules, several bands can be seen. The intense band at 945 cm^{-1} in the Raman spectra can be attributed with certainty to the components of the $\nu_1(\text{PO}_4)$ mode. On the basis of a careful analysis of the RT and LNT spectra of the protiated compound, as well as those of its partially deuterated analogues, the asymmetric band at around 550 cm^{-1} was assigned to the $\nu_4(\text{PO}_4)$ modes, the bands between 470 and 430 cm^{-1} to the $\nu_2(\text{PO}_4)$ vibrations and the remaining ones to librational and translational modes of the water molecules.

[1] A. Ferrari, L. Cavalca, M. Nardelli, *Gazz. Chim. Ital.* 85 (1955) 1232.

2. BIOSPECTROSCOPY

Ligand Binding to Proteins Studied by Infrared Spectroscopy

A. Barth

*Department of Biochemistry and Biophysics, The Arrhenius Laboratories for Natural Sciences,
Stockholm University, SE – 10691 Stockholm, Sweden
e-mail: barth@dbb.su.se*

Infrared spectroscopy provides a highly detailed look into working enzymes: conformational changes of the polypeptide backbone as well as environmental changes of side chains and bound ligands can be followed at the level of individual groups. Here, three aspects of our recent work on the binding of molecules to proteins will be presented:

(I) Binding of the substrate ATP to the Ca^{2+} -ATPase has been studied with infrared spectroscopy. Using a special technique based on the photolytic release of ATP from a blocked precursor (caged ATP), the very small conformational changes of the protein were detected. They depend in a characteristic way on the structure of the molecule, as shown for several ATP analogues (ADP, ITP, 2'-dATP, 3'-dATP). This mapping of the binding site identified those groups of ATP that interact with the protein. Binding can be described by an induced fit mechanism where the extent of conformational change depends *drastically* on individual interactions between substrate and protein. There is no simple link between the extent of conformational change induced by a ligand and its ability to function as a substrate (J. Biol. Chem. 278, 10112-10118).

(II) The infrared absorbance of a single, functionally important group that is transiently present in a large protein has been observed. The isotope exchange experiment observed 3 out of 50 000 protein vibrations. The experiment revealed that the covalent bond between phosphate group and Ca^{2+} -ATPase is weakened by the protein environment in the ground state which accounts for the fast dephosphorylation rate (J. Biol. Chem. 279, 51888-51896).

(III) Binding of phosphoenol pyruvate to pyruvate kinase has been studied by an approach that couples a dialysis accessory to an attenuated total reflection setup. This enables the addition of a ligand to a protein sample and the sensitive detection of very small absorbance changes. The results indicate a small structural change of the protein. The interactions of the ligand with the protein seem to be different than with water.

Vibrational Characterization of Self-Assembling Oligopeptides for Tissue Engineering on TiO₂ Surfaces

M. Di Foggia¹, C. Fagnano¹, P. Taddei¹, A. Torreggiani², M. Dettin³, S. Sanchez-Cortes⁴, A. Tinti¹

¹Dipartimento di Biochimica "G. Moruzzi", Università di Bologna, via Belmeloro 8/2, 40126 Bologna (Italy)

²ISOF, Consiglio Nazionale delle Ricerche, via P. Gobetti 101, 40129 Bologna (Italy)

³Dipartimento di Processi Chimici dell'Ingegneria, Università di Padova, via Marzolo 9, 35131 Padova (Italy)

⁴Instituto de Estructura de la Materia, CSIC, Serrano 121, 28006 Madrid, Spain

In the emerging field of tissue engineering, the development of synthetic materials promoting cells growth has led to the study of functionalised biomimetic materials and in particular to investigations on regular alternating polar/non-polar oligopeptides such as EAK-16, AEAEAKAKAEAEAKAK, first synthesised by Zhang et al. The characteristic of EAK-16 is to have a preferential β -sheet structure, to be resistant to proteolytic cleavage and to self-assemble into an insoluble macroscopic membrane. Its ability to create stable self-assembling layers derives from hydrophobic interactions between the $-\text{CH}$ groups of non-ionic residues and complementary ionic bonds between acidic and basic amino acids: this stability can be enhanced by the regulation of pH and the presence of monovalent metallic ions. In order to evaluate the ability to form self-assembled layers on oxidised titanium surfaces, we investigated 7 different oligopeptides (16 to 19 residues) derived from EAK-16 but modified in their sequence by substitution of acid, basic and neutral amino acid or by the addition at the N-terminus of the RGD sequence, able to control osteoblast adhesion.

The techniques used to determine the structure of the oligopeptides were IR and Raman vibrational spectroscopies, which can provide useful information on the secondary structure of the peptides, both on the qualitative and the quantitative aspect, by the help of different amide stretching modes. The peptides were examined as synthesised and after deposition on oxidised titanium substrates.

A quantitative evaluation of the secondary structure of the oligopeptides was obtained by fitting the Raman amide I band. Almost all the peptides showed a preferential beta-sheet structure, as revealed by the position of the amide I band at 1670-1673 cm^{-1} in their Raman spectra and at 1694-1697 cm^{-1} and 1620-1626 cm^{-1} in the IR ones. The substitution of the non polar amino acid (A \rightarrow α -aminobutyrric acid and A \rightarrow Y) induced in the first case an increase of alpha-helix conformation while in the second one allowed a higher order of the hydrophobic component. Mainly alpha-helix or mixed content was found in the peptides containing the RGD head, as revealed by the presence of Raman and IR bands at 1659 and 1640 cm^{-1} , respectively.

Micro Raman and micro ATR/FT-IR techniques were used to study the conformational changes of the peptides deposited on oxidised porous titanium plates under physiological conditions (pH 7.4, in phosphate buffer). From a macroscopic point of view, some peptides formed a very ordered and homogeneous layer covering the entire metallic surface, while other peptides formed clusters of crystalline aggregates. However, vibrational analysis pointed out that all peptides, regardless of their macroscopic disposition on the surface, showed the typical amide I and ν NH bands of beta-sheet. Another major feature of micro-IR and Raman spectra was the increase in intensity of the $\nu_{\text{sym}} \text{COO}^-$ band at 1400 cm^{-1} , indicating that the peptides interact with the surface by means of their carboxylic groups. The importance of COO^- was focussed by a further study with the SERS technique on silver colloids: the interaction with Ag particles is mediated by carboxylic groups and by aromatic groups when tyrosine is present in the primary structure of the peptides.

Cross-Correlation of Fluorescence-Quenching and Infrared Absorption in the Study of Protein Ligand Binding Sites

S. Madathil and K. Fahmy

*Institute of Radiochemistry, PF 510119, Research Centre Dresden-Rossendorf
Dresden, D-01314, Germany, k.fahmy@fzd.de*

The allosteric regulation of biomolecules such as enzymes or receptors is based on structural changes that are initiated at a ligand-binding site and become transmitted to a "distant" active site where enzymatic efficiency or interaction with effectors is altered. Understanding the molecular mechanisms of this long range coupling between distinct protein domains is crucial for many pharmacologically relevant systems where the conformation of a target molecule has to be specifically affected by a designed ligand. We have developed a generalized multidimensional spectroscopic approach to investigate long range conformational coupling in proteins. It employs the integration of fluorescence emission and infrared absorption data recorded simultaneously from the same protein sample that undergoes conformational transitions in response to an external perturbation. Using attenuated total reflectance (ATR) Fourier-transform infrared (FTIR) difference spectroscopy, additional channels for excitation and detection of fluorescence were established by light guides positioned above the sample on the ATR crystal. Long range coupling in the signal transfer through rhodopsin has recently been identified by Fluorescence-IR-cross-correlation [1]. Using 2D-cross-correlation techniques, the kinetic asynchronicity of the emission from natural or artificial site-specific fluorophores relative to the secondary structure-sensitive IR-absorption bands can be determined. Thereby, IR absorptions can be identified in a model-free and unbiased way that can be assigned to secondary-structural elements that become specifically stabilized by ligand interactions. Here, we demonstrate in a cytoskeletal protein the correlation of the loss of ligand-dependent static quenching of intrinsic tryptophan emission during thermal unfolding with the loss of structure monitored by FTIR spectroscopy. The high signal to noise ratio in 2D-correlation and the "synchronicity tagging" of the IR bands through their correlation with an independent monitor of ligand dissociation allows detecting ligand protein interactions with an accuracy that is not achieved by FTIR-spectroscopy alone. In addition, topological information can be obtained from the emission wavelength of the tryptophans that become gradually unquenched during temperature-induced ligand dissociation. Fluorescence-IR-cross-correlation spectroscopy thus extends the IR-based conformational analysis by the inclusion of site-specific information on local physical parameters (polarity, electrostatics, etc.) specifically affecting the emission of fluorophores. We show how this approach provides structural information on flavonoid binding to actin, a cytoskeletal and nuclear protein that has recently been shown to respond to the binding of these natural compounds by flavonoid-specific conformational changes [2].

[1] N. Lehmann, U. Alexiev, K. Fahmy, *J. Mol. Biol.* 336 (2007) 1129–1141.

[2] M. Boehl, S. Tietze, A. Sokoll, S. Madathil, F. Pfennig, J. Apostolakis, K. Fahmy, H.-O. Gutzeit, *Biophys. J.* 93 (2007) 2767-2780.

Acknowledgement

We acknowledge financial support by the Deutsche Forschungsgemeinschaft to KF (grant 248/4)

Preferential Conformations of Blocked Amino Acids in Water

J. Grdadolnik

National Institute of Chemistry, Hajdrihova 19, Ljubljana, SI-1000, Slovenia, joze.grdadolnik@ki.si

Determination of the preferential amino acid conformations and understanding the physical basis of intrinsic preferences of amino acid residues in water are crucial for solving the protein folding problem. Dipeptides of type Ac-X-NHMe, (X is an amino acid) represent an ideal system for studying the intrinsic conformational preferences of residues. They are the smallest fragments that preserve the main characteristic of the individual amino acids within the host molecules. Moreover, the effects of neighbouring residues are absent.

Conformational behaviour of 19 dipeptides has been studied using infrared and Raman spectroscopy. Previously, we showed by applying $^3J(H^\alpha, H^N)$ coupling constants [1] that the distribution of amino acid conformations depends on the type of the side chain. However, by applying these coupling constants and Karplus equation we can distinguish only between conformations with similar ψ and different ϕ angles. The difficulty occurs when we try to determine the conformations with different ψ angles (P_{II} and α_R). Namely, the largeness of coupling constant for α_R structure is comparable to those characteristic for P_{II} structure. Therefore, we apply the vibration spectroscopy. We have utilized three distinct indicator vibrations sensitive to values of ψ and ϕ angles: infrared Amide I and Amide III vibrations and skeletal Raman vibration. Applying those vibrations we had the opportunity to unambiguously determine the existence of α_R conformation [2]. Experimental results from the vibrational spectroscopy correlates with NMR coupling constants. Taking into account experimental results from the vibrational study the main conformations of amino acids remain P_{II} and β . The α_R structure represents the minor contribution to distribution of amino acid conformations in water. The distribution of these conformations strongly depends on the type of side chain. Thus the prevailing conformation of His, Thr, Cys, Ile and Val dipeptides is β (57%, 55%, 55%, 52% and 49% respectively), while dipeptides such as Ala, Trp, Lys, Arg, Met and Leu adopt predominately P_{II} conformation (62%, 54%, 53%, 53%, and 50% respectively). The part of α_R conformation varies between 1% and 10%, except for Gly dipeptide where a population of α_R conformers rises up to 51%.

The experimental results are explained by the electrostatic screening model [3, 4]. The model is based on a hypothesis that the peptide conformations are affected by electrostatic dipole-dipole interactions in the peptide backbone and by screening of these interactions with surrounded water molecules. The extent of screening effect depends on nearby side chains.

- [1] F. Avbelj, S. Golič Grdadolnik, J. Grdadolnik, R.L. Baldwin: *Intrinsic Backbone Preferences are Fully Present in Blocked Amino Acids*. Proc. Natl. Acad. Sci. U.S.A. 103 (2006) 1272-1277.
- [2] J. Grdadolnik, S. Golič Grdadolnik, F. Avbelj: *Determination of Conformational Preferences of Dipeptides Using Vibrational Spectroscopy*. J. Phys. Chem. B112 (2008) 2712-2718.
- [3] F. Avbelj, R.L. Baldwin: *Role of Backbone Solvation in Determining Thermodynamic beta-Propensities of the Amino Acids*. Proc. Natl. Acad. Sci. USA 99 (2002) 1309-1313.
- [4] F. Avbelj, R.L. Baldwin: *Role of Backbone Solvation and Electrostatics in Generating Preferred Peptide Backbone Conformations: Distributions of phi*. Proc. Natl. Acad. Sci. USA 100 (2003) 5742-5747.

Infrared Spectroscopy in Clinical Chemistry: From Lab to Bed-Side Applications

H.M. Heise¹, U. Damm¹, V.R. Kondepoti¹, J.K. Mader², F. Feichtner³ and M. Ellmerer³

¹ ISAS – Institute for Analytical Sciences at Dortmund University of Technology, Bunsen-Kirchhoff-Str. 11, D-44139 Dortmund, Germany

² Department of Internal Medicine, Division of Diabetes and Metabolism, Medical University Graz, Auenbruggerplatz 15, A-8036 Graz, Austria.

³ Joanneum Research Forschungsgesellschaft mbH, Institute of Medical Technologies and Health Management, Elisabethstrasse 11A, A-8010 Graz, Austria

Infrared spectroscopy is a powerful method for the study of various biomedical tissue or biofluid samples [1]. The analysis takes advantage of the fact that a multitude of analytes can be quantified simultaneously and rapidly without the need for reagents. Our recent findings with dry film attenuated total reflection (ATR) measurements of nanoliter sample volumes [2] and continuous aqueous transmission measurements of sub-microliter volumes could revolutionise the analytical assays in clinical laboratory. Further applications were possible with our recent developments in silver halide fibres used for the construction of fibre-optic probes for remote measurement of small biosamples.

A hot topic is the development of glucose monitoring technology for diabetic and critically ill patients as part of an artificial pancreas system. Infrared spectroscopy with a micro-cell of sub-microliter internal volume can be used for drift-free patient monitoring. Results from continuous measurements with whole blood show the needs for improving the biocompatibility of cell window materials to avoid the adsorption of cellular blood components for long-term usage. On the other hand - without any complications arising from the missing bio-compatibility of the cell windows for blood, transmission spectroscopy can be reliably applied for patient monitoring using biofluid harvesting by means of a subcutaneously implanted micro-dialysis catheter [3] or by dialysis of continuously sampled whole blood [4]. Using this approach, the biofluid matrix can be significantly simplified, since large molecular components such as proteins can be separated from the sample to be analyzed. The method also allows the determination of metabolites such as urea, lactate and others based on multivariate calibrations. The assessment of dialysis recovery rates renders possible an accurate quantification of subcutaneous interstitial concentrations. As a result of our research, an automated, long-term reliable bed-side device has been developed for continuous monitoring of blood glucose with application to intensive care patients, replacing less efficient electrochemical biosensors designed for single-component monitoring. The device performance has been tested in many clinical measurement campaigns. Prospects for spectrometer miniaturization are promising and will enable even for wearable devices applicable for diabetic patient self-monitoring of blood glucose.

- [1] H.M. Heise, Biomedical Vibrational Spectroscopy - Technical Advances, in: *Biomedical Vibrational Spectroscopy*, P. Lasch and J. Kneipp (Eds.), Wiley (2008), 9-37.
- [2] E. Diessel, P. Kamphaus, K. Grothe, R. Kurte, U. Damm, H.M. Heise, *Appl. Spectrosc.* 59 (2005) 442
- [3] H.M. Heise, U. Damm, M. Bodenlenz, V.R. Kondepoti, G. Köhler, M. Ellmerer, *J. Biomed. Optics* 12 (2007) 024004.
- [4] H.M. Heise, V.R. Kondepoti, U. Damm, M. Licht, F. Feichtner et al., *Proc. SPIE* 6863 (2008) 686309.

Acknowledgment

Financial support from the European Commission with the CLINICIP project (contract no. 506965, 6th Framework Programme) is gratefully acknowledged.

Early Stages of Human Embryonic Stem Cell (HESC) Differentiation Characterized by FT-IR Spectroscopy

P. Heraud^{1,2}, E. Ng¹, B. Wood², T. Frosch², D. McNaughton², E. Stanley¹, A. Elefanty¹

¹Monash Immunology and Stem Cell Laboratories, ²Centre for Biospectroscopy, Monash University, Wellington Road, Clayton, Victoria, Australia.

It should be possible to reproducibly and efficiently direct the differentiation of HESCs towards specific lineages of interest. The achievement of this goal will have significant therapeutic implications for many human illnesses. For example, it may be possible to provide normal cells differentiated from HESCs to replace those damaged through disease. It is anticipated that cells prepared for clinical use will need to be differentiated towards the lineage of interest in order to maximise the chance of therapeutic benefit. Therefore, it will be necessary to have accurate and reproducible assays that could be rapidly performed to validate the efficacy and safety of the HESC differentiation process and to 'certify' each batch of differentiated cells prior to transplantation.

To determine whether FT-IR spectroscopy could be used to classify early stages of HESCs differentiation, analyses were performed on replicate cultures of undifferentiated HESCs and HESCs differentiated towards ectodermal lineages by culture in serum free medium supplemented with FGF2 or towards mesendodermal precursors by a combination of BMP4 and Activin A [1,2]. The HESCs were cytopspun to produce monolayers of cells on low-E slides and infrared images acquired with a Varian focal plane array (FPA) microspectrometer. Spectra extracted from the FPA images were pre-processed using a second derivative, normalized using Extended Multiplicative Signal Correction, then outliers removed by minimizing the residual variance using Principal Component Analysis (PCA) [3]. In total, 141 HESC, 97 BMP4/Activin A-treated and 149 FGF2-treated spectra were used in the final analysis.

PCA was used to examine the variability of the IR spectra. The first two PCs explained over 70% of the variance in the dataset with PC1 versus PC2 scores plots revealing distinct clustering of spectra from the three treatment groups. Spectra from the replicate samples co-located within each respective cluster grouping, indicating the reproducibility of this result. The HESC spectra were separated from the other spectra along PC1, whereas BMP4/Activin A and FGF2 spectra were clustered along PC2. PC1 and PC2 loadings plots showed that lipid bands (3000-2800 and 1740 cm^{-1}) were heavily weighted, indicating large differences in lipid absorbance between the three treatment groups. Loadings for protein bands (1700-1500 cm^{-1}) indicated differences in protein secondary structure, whereas complex changes in many bands associated with nucleic acids and carbohydrates (1500-900 cm^{-1}) appeared to be involved in both the PC1 and PC2 clustering of the spectral groups.

The spectral dataset was randomly divided into two classes consisting of one third and two thirds of the total, to test the hypothesis that early stages of HESC differentiation could be reliably classified using FT-IR spectra. The larger subset was used for training and the smaller for validation testing. Partial Least Squares Discriminant Analysis (PLS-DA) and Artificial Neural Network (ANN) analysis classification methods were compared. The ANN correctly classified all 149 spectra in the independent validation set, whereas PLS-DA classified 147 out of 149 spectra correctly with two FGF2 spectra classified incorrectly as HESC.

[1] R. Davis, E. Ng, M. Costa, A. Mossman, K. Sourris, A. Elefanty, E. Stanley, *Blood* 111 (2008) 1876-1884.

[2] E. Ng, R. Davis, E. Stanley, A. Elefanty, *Nature Protocols*, 2008 in press. (accepted 5 Feb. 2008).

[3] P. Heraud, J. Beardall, B. Wood, D. McNaughton, *J. Chemometrics* 20 (2006) 193-197

Crystallization and Vitrification of Cryoprotectants Studied by Raman Scattering, Brillouin Scattering and THz-TDS

Yuji Ike, Yuichi Seshimo and Seiji Kojima

Graduate School of Pure and Applied Sciences, University of Tsukuba, Tsukuba, Ibaraki 305-8573, Japan

The vitrifying tendency of cryoprotective solutions on cooling is the important factor for successful cryopreservation of biological substances. The tendency of crystallization or vitrification is closely related to the cooperative motion, steric hindrance, intermolecular and intramolecular interactions of molecules in solution. In the case of propylene glycol, well known glass forming liquid, undergoes a glass transition without crystallization even in slow cooling. It is interesting that the tendency of crystallization or vitrification is affected by not only intermolecular bonding but also the available conformational structure of molecules. In the present study, we examine one of the best candidates of cryoprotectant, ethylene glycol (HO-CH₂-CH₂-OH, EG) aqueous solutions by using light scattering technique. EG has a three-dimensional network of hydrogen bonded molecules and it is possible to view as being similar to water. Several studies have been done on EG aqueous solutions and they show good ability to use as ice crystallization inhibitors [1]. The microscopic nature of molecules can be determined by Raman scattering. The Raman scattering measurements provides the information on internal vibrational modes of molecules. The Raman scattering of EG aqueous solutions were investigated to characterize the conformations of molecular structure. The intermediate concentrations of EG solutions easily undergo glass transitions, while the crystallization occurs in the solutions of low and high concentrations of EG. The structural configuration of EG in crystalline phase in pure liquid shows only *gauche* OCCO form of EG which is the lowest energy conformers, while *gauche* and *trans* forms exist in the liquid phase. EG can exhibit stabilization in the lowest energy form of the *gauche* conformers owing to the intramolecular hydrogen bond [2]. The tendency of crystallization and vitrification in EG is related to its capability of forming intermolecular and intramolecular hydrogen bonding. Further dynamical properties from gigahertz to terahertz frequency range are investigated by using Raman scattering, Brillouin scattering and terahertz time domain spectroscopy (THz-TDS).

[1] Y. Seshimo, S. Kojima, Jpn. J. Appl. Phys. (in press).

[2] O.V. Oliveira, L.C.G. Freitas, J. Mol. Struct. Theochem. 728 (2005) 179.

Application of Mössbauer and FTIR Spectroscopic Techniques in Structural Research Related to Microbial Signalling and Cellular Responses to Environmental Factors

Alexander A. Kamnev

Institute of Biochemistry and Physiology of Plants and Microorganisms, Russian Academy of Sciences, Prosp. Entuziastov 13, Saratov, 410049, Russia (E-mail: aakamnev@ibppm.sgu.ru)

Processes of microbial intercellular communication, exchange of molecular signals between microbial cells and their host macroorganisms, involving specific low-MW diffusible substances (used as a 'chemical language'), and cellular responses are at the peak of current research in biosciences [1, 2]. This fundamental interest is due to the unique possibility of controlling the microbial behaviour and metabolism by influencing their signalling pathways. On the other hand, abiotic impact of the environment (medium) on extracellular molecular signals is also of great importance, as any of their chemical interactions (e.g., complexation or oxidation) represent direct interferences in the process of 'signal delivery' [3].

In this work, chemical interaction of microbial extracellular molecular signals (indolic derivatives – auxin phytohormones [1, 4]; alkylresorcinols – chemical analogues of microbial autoregulators [3]) with iron(III) was monitored using ^{57}Fe Mössbauer spectroscopy in rapidly frozen aqueous solutions and in dry solids. The conditions applied were designed to simulate possible processes occurring in soils, where ferric iron is commonly ubiquitous. In moderately acidic media, gradual reduction of iron(III) was observed coupled to oxidative degradation of the organics. Some alkylresorcinols were found to be significantly more rapidly oxidised by iron(III) than indole-3-acetic acid, exhibiting a notable oxidation rate already within a few minutes; their reducing power was found to be much higher for derivatives with a longer alkyl chain. This finding is yet more interesting, since the non-alkylated analogue (resorcinol) was earlier reported to show no iron(III) reduction (see [3] and references reported therein).

Bacterial cellular responses to host plant-root signal represented by plant lectin [5] were for the first time shown to be nondestructively detectable in whole bacterial cells using FTIR spectroscopy in the diffuse reflectance mode (DRIFT). Some alterations in secondary structure components of cellular proteins were observed as a response both to the host-plant signal and to a nutritional stress (nitrogen deficiency), also with accumulation of intracellular polyester storage compounds in the latter case [5]. In addition, FTIR spectroscopy allowed different responses of endophytic and epiphytic strains of the same bacterial species to heavy-metal stress to be observed [6], with emission ^{57}Co Mössbauer spectroscopy used to monitor metabolic transformations of $^{57}\text{Co}^{\text{II}}$ traces in live cells, as compared with dead biomass.

- [1] S. Spaepen, J. Vanderleyden, R. Remans, *FEMS Microbiol. Rev.* 31 (2007) 425-448.
- [2] B.A. Hense, C. Kuttler, J. Muller, M. Rothballer, A. Hartmann, J.-U. Kreft, *Nature Rev. Microbiol.* 5 (2007) 230-239.
- [3] A.A. Kamnev, K. Kovács, E. Kuzmann, L.A. Kulikov, Yu.D. Perfiliev, B. Biró, A. Vértés, in: *Metal Ions in Biology and Medicine*, Vol. 10, John Libbey Eurotext, Paris, 2008, in press.
- [4] K. Kovács, A.A. Kamnev, J. Mink, Cs. Németh, E. Kuzmann, T. Megyes, T. Grósz, H. Medzihradsky-Schweiger, A. Vértés, *Struct. Chem.* 17 (2006) 105-120.
- [5] A.A. Kamnev, J.N. Sadovnikova, P.A. Tarantilis, M.G. Polissiou, L.P. Antonyuk, *Microb. Ecol.* (2008) in press.
- [6] A.A. Kamnev, A.V. Tugarova, L.P. Antonyuk, P.A. Tarantilis, L.A. Kulikov, Yu.D. Perfiliev, M.G. Polissiou, P.H.E. Gardiner, *Anal. Chim. Acta* 573-574 (2006) 445-452.

Acknowledgment: Supported by NATO, Grants LST.NR.CLG.981092 and ESP.NR.NRCLG 982857, as well as under the Agreement between the Russian and Hungarian Academies of Sciences.

Energy Conversion in Bioluminescent Reactions

N.S. Kudryasheva, N.V. Belogurova

Institute of Biophysics SB RAS, Krasnoyarsk, 660036, Russia
Siberian Federal University, 660041, Krasnoyarsk, Russia

Bioluminescence phenomenon is based on enzymatic reactions transforming chemical energy to visible light with high quantum efficiency (1-100%). There exist several types of bioluminescent reactions corresponding to several types of luminous organisms; they differ in chemical structure of components and enzymes. Purpose of the work was to reveal general similarities and peculiarities of energy conversion in different types of bioluminescent reactions – marine bacteria, coelenteramides, and fireflies. Variation of color of bioluminescence due to energy conversion is a question of special interest in this study.

Among similarities of the bioluminescent reactions are: (1) oxidative type of the reactions (with molecular oxygen included) and (2) type of electronic structure of the emitting molecules: emitters of the bioluminescent reactions are characterized by effective fluorescence of $\pi\pi^*$ - type and upper electron-excited states of $n\pi^*$ - type. The type of electronic structure of the emitters suggests activity of the upper states, which can be formed as primary excited states in the oxidative bioluminescent reactions.

The hypothesis on activity of the upper electron-excited states in bioluminescent process was experimentally verified using fluorescent molecules as energy acceptors. The hypothesis was confirmed experimentally in bacterial and coelenterate bioluminescence. However, activity of the upper electron-excited states was not found in firefly bioluminescence, probably because of highest efficiency of intramolecular energy transfer in the firefly emitter.

The upper excited states can be responsible for blue shifts of the bioluminescence in the presence of proper fluorescent acceptors. Examples of red shifts of the bioluminescence due to Forster energy transfer are discussed.

Another mechanism for variation of bioluminescence color takes place in coelenterate bioluminescence. It deals with chemistry in the fluorescent states of the emitting molecule (coelenteramide). This molecule can change its acidity in the fluorescent states since the lifetime of these states is longer than time of proton transfer. Several fluorescent forms of coelenteramide can be formed depending on its ionization degree. That is why the spectra of coelenterate bioluminescence are broad and complex; they include spectral components of various forms of coelenteramide in a broad spectral region.

The spectral components of coelenterate bioluminescence (from jellyfish *Aequorea victoria* and hydroid *Obelia longissima*) were determined and characterized. The results are discussed taking into consideration the proton transfer in the fluorescent states of the emitting molecule and amino acid surrounding of the emitter in the enzymes.

Near-Infrared Fluorescence in Bioanalytical and Medical Applications

Gabor Patonay, Lucjan Streckowski, Maged Henary, Jun-Kim Seok

Department of Chemistry, Georgia State University, Atlanta, GA 30303, USA

Near-Infrared (NIR) absorbing chromophores have been valuable in several areas of bioanalytical chemistry and in medical applications both *in vitro* and *in vivo*. NIR probes and labels have been used for numerous applications, including solvent polarity, hydrophobicity, DNA sequencing, immunoassays, CE separations, etc. By moving detection from a visible region to the longer wavelengths, the background interference from the complex matrix is greatly lowered, thereby reducing scatter and shifting of the Raman line even further from the spectral region of interest. Our research group pioneered NIR fluorescence spectroscopy and has been active in this area for over twenty years.

Advanced dye synthesis developed in our laboratories has afforded the design of highly stable NIR chromophores. Carbocyanines are especially good candidates for bioanalytical purposes. They are relatively easy to synthesize and variations in their structures allow for designing dyes that fit a particular application. Applications include biomolecule characterizations and quantitative and qualitative determinations of biologically important analyses (e.g., intracellular Ca^{2+} , etc). Recently, our research group introduced bis-cyanines as novel NIR indicators. Depending on their microenvironment, bis-cyanines can exist as an intramolecular dimer with the two cyanines either in a stacked form or in a linear conformation in which the two subunits do not interact with each other. In this intramolecular H-aggregate, the chromophore has a low extinction coefficient and low fluorescence quantum yield. Upon addition of biomolecules the H- and D- bands are decreased and the monomeric band is increased, with concomitant increase in fluorescence intensity, suggesting that clamshell H-aggregates open up.

These dyes can be used as effective non-covalent labels in complex CE separations of biomolecules, or just simply as reporters for the presence of biological materials including whole cells on solid surfaces or in solutions. For example, these are suitable for visualizing latent fingerprints or bacterial contamination on surfaces with virtually no interference from the background. NIR chromophores that do not possess chirality can exhibit induced circular dichroism (CD) upon binding to biomolecules. CD and fluorescence detected CD can be used to study the structure of native biomolecules because induced CD of NIR chromophores is characteristic to the different protein secondary structures and it is useful for deducing information about the biomolecule and its binding properties. One application of NIR dyes developed in our laboratories is for characterizing amyloid fibrils that are associated with several diseases, e.g., Alzheimer's disease, Parkinson's disease, spongiform encephalopathies, and type II diabetes.

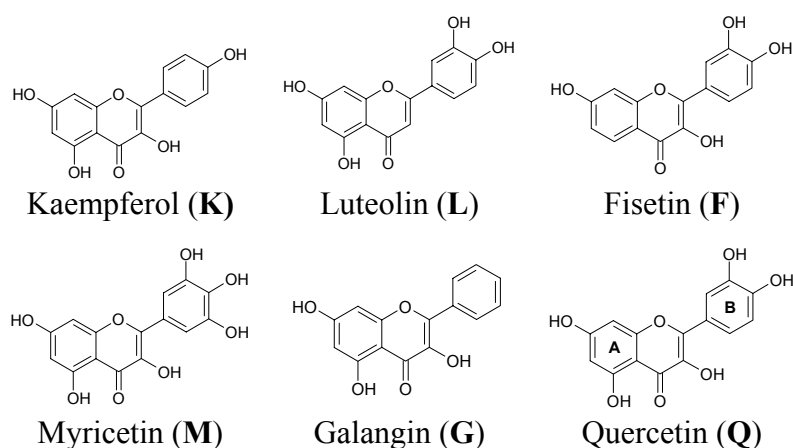
Carbocyanines recently moved into medical applications and to a degree much wider in scope than was possible with the original cardiogreen (or ICG). Another potentially extremely important use of NIR dyes developed in our laboratories is NIR imaging of tumors. Our dyes have been tested in several medical laboratories we cooperated with and were found to be very effective *in vivo* markers. This presentation will focus on new data that we obtained in biomolecule characterization using NIR dyes *in vitro* including data utilizing bis-carbocyanines for protein binding site characterization, induced NIR CD for determining amyloid fibrils and detecting conformational changes leading to misfolded proteins forming β secondary structures. We also present data showing the effectiveness of our NIR dyes for imaging organs and neoplasm. Detailed chemistry of dye development will also be discussed.

Structure-Activity Relationship in Interactions of Quercetin and its Analogues with Double Stranded DNA/RNA and Single Stranded RNA

Ivo Piantanida¹, Lozika Mašić¹, Gordana Rusak²

¹ Laboratory for Supramolecular and Nucleoside Chemistry, Ruđer Bošković Institute, P.O.B. 180, 10002 Zagreb, Croatia, ² Department of Biology, Faculty of Science, University of Zagreb, P.O.B. 163, 10001 Zagreb, Croatia

Flavonoids are ubiquitous in all vascular plants and important constituents of human diet. Molecular targets of flavonoids relevant for their broad spectrum of biological activities are not systematically identified and characterized [1]. Particularly interesting is usage of flavonoids as promising anticancer agents [2]. Our recent studies of interactions of quercetin with double stranded DNA / RNA and single stranded RNA revealed among other interesting results that addition of poly G yielded more than order of magnitude stronger changes in UV/vis and fluorescence spectrum of quercetin compared to the changes upon addition of poly A and poly U, revealing possible usage of quercetin as a powerful spectroscopic probe for poly G sequences [3]. In order to investigate the role of -OH substituents of quercetin in binding and spectroscopic recognition of DNA/RNA, we have studied interactions of DNA/RNA with five close analogues of quercetin (Scheme 1).



Scheme 1: Studied flavonoids.

The studies were performed by UV/vis titrations of flavonoids with *calf thymus* (ct) DNA, synthetic double stranded RNA (poly A- poly U, poly G- poly C) and single stranded RNA (poly A, poly G, poly C, poly U). Obtained results revealed significance of a number and distribution of -OH groups within phenylbenzopyrane core on the affinity of the particular flavonoid toward specific DNA / RNA. Moreover, the intensity of the observed changes in the UV/vis spectra of flavonoids upon addition of studied DNA/RNA is also dependent on a number and distribution of -OH groups within phenylbenzopyrane core as well as on the nucleobase constitution of the polynucleotide. Exclusively poly G caused significant bathochromic shift of the UV/vis maxima of all studied flavonoids, whereby the intensity of bathochromic shift can be lined as follows: **Q**>>>**K**>**L**>**F**>**G**, the tendency nicely corresponding to the number of OH groups attached to the phenylbenzopyrane core.

[1] Bent H. Havsteen, *Pharmacology & Therapeutics* 96 (2002) 67– 202.

[2] W. Ren, Z. Qiao, H. Wang, L. Zhu, L. Zhang, *Med. Res. Rev.* 23 (2003) 519-534.

[3] M. Marinić, I. Piantanida, G. Rusak, M. Žinić, *J. Inorg. Biochem.* 100 (2006) 288–298.

New Insights into the Structural Biophysical Chemistry of Amphiphiles with 18-Carbon Chain Length as Provided by FTIR Spectroscopy

W. Pohle¹, D.R. Gauger¹, V. Andrushchenko², P. Bour², H. Boehlig³

¹*Institute of Biochemistry and Biophysics, Friedrich-Schiller University, Philosophenweg 12, D-07743 Jena, Germany, e-mail: walter.pohle@uni-jena.de*

²*Institute of Organic and Biochemistry, Academy of Sciences, Flemingovo nam. 2, Prague 16610, Czech Republic*

³*Wilhelm Ostwald Institute of Physical and Theoretical Chemistry, University of Leipzig, Linnéstr. 2, D-04103 Leipzig, Germany*

An experimental algorithm comprising FTIR spectroscopic measurements of the hydration of oriented films [1] was used to explore structural and phase properties of a series of amphiphiles which are inter-related by having the same chain length of 18 carbon atoms. The set of compounds involved the surfactants stearyltrimethylammonium chloride (STMAC), stearylamine and stearylalcohol as well as the biologically relevant phospholipids distearoylphosphatidylcholine (DSPC), dioleoyl-PC or DOPC and DOPE (E=ethanolamine) so that the structure varied gradually in both headgroup and chain regions. Considerable differences in the overall water uptake (estimated at 98 % relative humidity) were observed, from practically none in stearylalcohol and stearylamine via a moderate one in DOPE, STMAC and DSPC up to a strong uptake in DOPC. This was primarily explained by the diversity of different phases adopted under the sample preparation conditions [1], reaching from crystalline lamellae in stearylalcohol and stearylamine to fluid aggregates in DOPC and DOPE. In the latter, the hydration is restricted due to a strong hydrogen-bonded network in the headgroup domain. Peculiar behavior was found for STMAC and DOPE. The former undergoes a novel lyotropic transition between interdigitated crystalline and gel phases which is accompanied by a number of spectral features not observed so far. DOPE exhibits a hydration-driven transition from a nonlamellar fluid ribbon phase to an inverted hexagonal phase [2,3]. These interpretations are supported by complementary X-ray diffraction measurements using synchrotron radiation performed according to our recently described protocol [4] and, for STMAC, also by theoretical calculations. IR spectra of stearylamine reveal the presence of NH and NH₃⁺ groups instead of the NH₂ groups normally expected for a primary amine and, thus, appear to indicate a proton transfer occurring under the applied experimental conditions [1]. Stearylalcohol forms a particularly rigid crystalline lamellar phase with densely packed tilted hydrocarbon chains and hydroxyl groups involved in a tight hydrogen-bonding network totally preventing any water uptake.

Despite the similar chemical composition of the amphiphile monomers, the data show dramatic differences in the structural and physical properties of the resulting aggregates.

[1] W. Pohle, C. Selle, H. Fritzsche, H. Binder, *Biospectroscopy* 4 (1998) 267-280.

[2] W. Pohle, C. Selle, *Chem. Phys. Lipids* 82 (1996) 191-198.

[3] H. Binder, W. Pohle, *J. Phys. Chem. B* 104 (2000) 12039-12048.

[4] W. Pohle, C. Selle, D.R. Gauger, K. Brandenburg, *J. Biomol. Struct. & Dynam.* 19 (2001) 351-364.

The New Infrared Beamline: Australian Synchrotron Infrared Microscopy at the Single Cell Level

L. Puskar¹, M. Tobin¹, P. Heraud², B. Wood³

¹ Australian Synchrotron Company, 800 Blackburn Rd., Clayton, VIC 3168 Australia, ² Monash Immunology and Stem Cell Laboratories, STRIP1, Monash University, VIC 3800 Australia, ³ Centre for Biospectroscopy and School of Chemistry, Monash University, Vic 3800 Australia

Infrared Microspectroscopy is increasingly revealing chemical information of biological systems beyond the tissue level at the single cell level. Due to the brightness of a synchrotron source, high spatial resolution (diffraction limited) and good signal to noise ratios have been achieved on single living cells in cell culture, under aqueous media. Results from these studies at the new infrared microspectroscopy beamline at the Australian Synchrotron operating since May 2007 are presented. Some biological applications include diagnosing malaria at different stages of the parasite intra-erythrocytic development within single fixed and live malaria infected cells, detection of live Human Mesenchymal Stem Cells and monitoring the changes in the IR spectra of single living algal cells subjected to environmental change.

Use of micro ATR mapping in forensic applications and grazing angle objective for thin polymer films have also verified outstanding performance of the beamline in terms of both the instrumentation and the stability of the synchrotron beam. Future plans and developments would be presented.

The microscope beamline comprises the Hyperion 2000 IR microscope (Bruker Optics Inc., Billerica, MA) coupled to a Bruker Vertex 80v spectrometer. Chemical mapping of the samples is allowed by motorised microscope stage in the mid Infrared range using either Narrow-Band D* 4×10^{10} (Cut-off 750 cm^{-1}) or Wide-Band MCT D* 5×10^9 (Cut-off 420 cm^{-1}) single point detector. For 5×5 microns aperture setting in the $2550\text{-}2450 \text{ cm}^{-1}$ spectral region typical noise (RMS%) measured in transmission is in the order of 0.02-0.04 (128 scans) and 0.05-0.1 (16 scans) using standard collection conditions.

Low Temperature FTIR Difference Spectroscopy Reveals New Insights on the Proton Pathway of Proteorhodopsin at Different pH Values

G. Schäfer¹, M.-K. Verhoeven², S. Shastri³, I. Weber³, C. Glaubitz³,
J. Wachtveitl^{1,2}, W. Mäntele¹

¹Institute of Biophysics, Max von Laue-Str.1, Johann Wolfgang Goethe-University Frankfurt, 60438 Frankfurt, Germany, ²Institute of Physical and Theoretical Chemistry, Johann Wolfgang Goethe-University Frankfurt, Max von Laue-Str.7, 60438 Frankfurt, Germany, ³Institute of Biophysical Chemistry and Center of Biomolecular Magnetic Resonance, Johann Wolfgang Goethe-University Frankfurt, Max von Laue-Str.9, 60438 Frankfurt, Germany

Proteorhodopsin (PR) discovered in the γ -proteobacterium SAR86 is believed to be a lightdriven proton pump [1] Since the first description of PR several studies have uncovered evidence of intermediates comparable to the photoproducts of the BR photocycle. However, there is an ongoing discussion about the inversion of the proton pumping direction due to pH-change and the general function of PR. Until now, no M intermediate could be detected kinetically at acidic pH [2, 3], but recently low temperature visible spectroscopy demonstrated the existence of a band typical for the M state at pH 4 [4].

To further investigate the photocycle of PR, we have used FTIR difference spectroscopy at low temperature between 77 and 250 K. Low-temperature spectroscopy has widely been used to trap and investigate intermediates in the photocycle of proteins. In combination with FTIR spectroscopy, it is a powerful tool to gather information about the involvement of amino acids and about structural changes of the chromophore concomitant with the light reaction. Until now, only the K intermediate of the PR photocycle has been characterized using this technique [5].

We have used various samples ranging from PR reconstituted with lipids to PR 2Dcrystals. Each sample provides different advantages, such as high concentration and stability in the case of the crystals or the observable lipid-protein interactions in reconstituted samples.

We started our experiments with a comparison of the K-state at 77 K for our samples at pH 9, 8.5, 5.5 and 5. For pH 8.5 and 5.5 an increased amount of L-intermediate was monitored, which was absent in the spectra at pH 9 and 5. This hints to lowered reaction barriers for PR between pH 5.5 and 8.5. In agreement with this finding the samples at pH 5.5 and pH 8.5 show a similar kinetic behavior and identical spectral characteristics differing from either higher or lower pH values at higher temperatures. They both lack the characteristic positive band at 1755 cm^{-1} indicative for protonation of Asp-97. This band in combination with amid II changes was clearly observable at 242 K, showing M state formation for pH 9. However, the pH 5 sample showed an M-like state at 227 K, which involves aspartic or glutamic acid side chain modes at 1726 cm^{-1} and 1730 cm^{-1} .

Our results hint at different proton translocation pathways at pH 9, pH 8.5 to 5.5 and pH 5. This finding further supports the assumption of variable vectoriality proposed by Friedrich et al. [2].

- [1] O. Béjà et al., Science 289 (2000) 1902.
- [2] T. Friedrich et al., J. Mol. Biol. 321 (2002) 821.
- [3] A.K. Dioumaev et al., Biochemistry 42 (2003) 6582.
- [4] É. Lőrinczi, M.-K. Verhoeven, to be submitted.
- [5] V. Bergo et al., Biochemistry 43 (2004) 9075.

The Excited-State Dynamics of Kynurenine – UV Filter of the Human Eye

P.S. Sherin¹, O.A. Snytnikova¹, Yu.P. Tsentalovich¹, E. Vauthey²

¹*International Tomography Center SB RAS (Institutskaya str. 3A, 630090, Novosibirsk, Russia),*

²*Dpt. of physical chemistry, University of Geneva (quai Ernest-Ansermet 30, 1211, Geneva, Switzerland)*

Kynurenine (KN) and its derivatives act as UV-filters in the human lens. They absorb UV light in 300–400 nm spectral region and protect the eye tissues from the harmful sun irradiation. Kynurenines are weak photosensitizers and redirect the absorbed light energy into benign channels. They are characterized by a low fluorescence quantum yield and a short fluorescence lifetime, a low triplet yield and a high photochemical stability. These observations indicate the existence of a fast process deactivating the excited states of KN; the nature of this process is still unknown.

Here we report on the detailed study of the primary photoprocesses occurring in KN molecule after UV excitation. The main goals of this work are: (i) to understand the photophysical properties of the lowest excited state of KN, (ii) to establish the origin of the effective deactivation of this state and (iii) to determine the precursor of KN photoionization. The measurements were performed with the use of femtosecond and nanosecond resolved optical spectroscopy.

In aqueous solutions KN demonstrates a short fluorescence lifetime of about 30 ps which increases by more than one order of magnitude in alcohols and exceed 1 ns in aprotic solvents like DMF and DMSO. Internal conversion is shown to be the main channel of the lowest excited state of KN. The rate constant of IC is pH independent but it depends on temperature with a weakly solvent-dependent activation energy about 7 kJ/mol. The observation of a deuterium effect indicates that the hydrogen bonds are involved in the rapid decay of fluorescence in protic solvents. The nature of ultrafast deactivation is discussed in terms of a tight hydrogen-bonded complex and proton transfer from KN molecule to solvent. The obtained results show the crucial role of intramolecular charge transfer interactions in the fast IC.

The high density of UV irradiation results in the formation of KN cation radical and solvated electron. The measurements of the ionization quantum yield at different laser energies and at different excitation wavelengths show that the photoionization of KN proceeds by a biphotonic mechanism. Our experimental data speak in favor of triplet state as a precursor for KN biphotonic ionization.

Acknowledgment

This work was supported by ESF DYNA Exchange Grant №1325, SNSF grant 200020-115942, FASI state contract 02.512.11.2166, by RFBR Projects 07-03-00253 and 08-03-00539, by Grant of President RF Scientific School 3604.2008.3, by Program of Division of Chemistry and Material Sciences RAS.

The FeCO Unit Vibrations as a Probe of the Structure of the Active Site of Heme Proteins: Combined Quantum Chemical, Vibronic and Spectroscopic Study

Solomon S. Stavrov

Sackler Institute of Molecular Medicine, Department of Human Molecular Genetics and Biochemistry, Sackler Faculty of Medicine, Tel Aviv University, Ramat Aviv, P.O.B.39040, Tel Aviv 69978, Israel, stavrov@post.tau.ac.il

Heme proteins (HPs) play central roles in the life of organisms. The major classes of heme proteins share the same prosthetic group, heme IX, but differ in the axial coordination of the iron and the distal environment of the heme. In myoglobin (Mb), hemoglobin (Hb), peroxidases (including horse radish peroxidase, HRP) and b- and c- cytochromes, imidazole (Im) is one of the iron axial ligands. In Mb, Hb and HRP the sixth coordination position is empty or weakly ligated by the solvent. Therefore these HPs can coordinate different diatomic molecules (XY).

The nature of the proximal iron ligand, hydrogen bonds, steric and electrostatic environment of the heme in HP(XY)s and the XY coordination geometry, are the essential factors through which the protein regulates the XY storage, transport, or activation (change of interatomic distance, force field constant and activation barrier of dissociation). One major problem is that of discriminating between the different factors affecting these properties of HP(XY)s.

The vibronic theory of activation and quantum chemical INDO calculations were used to study the CO activation by the heme-Im complex in dependence on the distortion of the porphyrin ring, geometry of the CO coordination, Fe-C and Fe-N_{Im} distances, and presence of the charged groups in the heme environment [1, 2]. It was shown that the main contribution to the CO activation stems from the change in the σ -donation from the 5σ CO orbital to iron, and back-bonding from the iron to the $2\pi^*$ orbital of CO. It follows from the results that none of the studied distortions can explain by itself wide variation of the C-O vibrational frequency in the experimentally studied model compounds and heme proteins.

On contrary, the results showed that charged groups can strongly affect the FeC and CO vibrational frequencies (ν_{CO} and ν_{FeC}) both in the same and in opposite directions, the type of the correlation between ν_{CO} and ν_{FeC} depends on the charged groups position [1, 2].

The developed theory was applied to the study of the effect of the heme environment on ν_{CO} in Mb(CO), Hb(CO) and HRP(CO) [2, 3]. In particular, it was revealed that the A₀ and A₁ conformational substates of Mb(CO) and Hb(CO) corresponded to the substates with the distal histidine located out of and in the heme pocket, respectively; that the A₃ substate corresponded to the conformation with the histidine located in the pocket and hydrogen bonded to the solvent water molecule; and that the considerably lower ν_{CO} of HRP(CO) was caused by the strong hydrogen bond of the proximal histidine with the protein globule.

In conclusion, the study shows that position of the CO infrared band of HP(CO)s can be considered as a probe of the structure of the heme environment, whereas the width of this band provides a researcher with information of water population of the heme pocket [4].

[1] B. Kushkuley, S. S. Stavrov, *Biophys. J.* 70 (1996) 1214-29.

[2] B. Kushkuley, S. S. Stavrov, *Biophys. J.* 72 (1997) 899-912.

[3] A. D. Kaposi, W. W. Wright, J. Fidy, S. S. Stavrov, J. M. Vanderkooi, I. Rasnik, *Biochemistry* 40 (2001) 3483-91.

[4] A. D. Kaposi, J. M. Vanderkooi, S. S. Stavrov, *Biophys. J.* 91 (2006) 4191-200.

Synchrotron FTIR Spectroscopy Reveals New Insights into Mouse Oocyte Maturation

B.R. Wood¹, T. Chenenko², U. Bernhard¹, C. Jayne¹, A. Bramble¹, A.O. Trounson³,
D. McNaughton¹ and O. Lacham-Kaplan³

¹Centre for Biospectroscopy, Monash University, Victoria, 3800, Australia, ²Dept. of Chemistry & Chemical Biology, 316 Hurtig Hall, Northeastern University, Boston, MA 02115, ³Monash Immunological Stem Cell Laboratories, Monash University, Victoria, 3800, Australia

Synchrotron Fourier transform infrared (FTIR) spectroscopy was applied to investigate mouse oocyte maturation *in vivo* and *in vitro*. FTIR maps of entire intact immature Germinal Vesicle (GV) and mature (MII) mouse oocytes matured *in vivo* are compared with *in vitro* matured oocytes (IVM) and *in vivo* matured oocytes aged in culture for 13 hours (designated Aged). False-colour univariate and multivariate maps show distinct lipid regions within the oocytes that vary in size and composition between the different maturation states. GV oocytes show a small intranuclear lipid deposit and another deposit located at the periphery of the egg. MII oocytes have large centrally located lipid deposits that are predominantly composed of long chain saturated fatty acids. To assess inter-oocyte variability line scans were recorded across the diameter of the oocytes from the four groups and added together from 3 independent trials (GV oocytes n = 91, MII n = 172, IVM n = 95 and Aged n = 58). The average spectra show distinct and reproducible changes in the CH stretching region and ester carbonyl region for the different oocyte types. Aged oocytes have a pronounced band at 1120 cm⁻¹ assigned to the RNA ribose skeletal vibration, which is indicative of an increase in RNA synthesis in response to repair. MII and IVM cells have very similar averaged spectra that differ significantly to the Aged and GV oocytes. The results are corroborated by performing a Principal Components Analysis on the CH stretching region, which show distinct groupings of the GV and Aged oocyte spectra but a mixed group of IVM and MII oocyte spectra. An artificial neural network (ANN) could correctly classify all spectra using absorbance values from the CH stretching region as inputs. The technique paves the way for developing an independent assay to assess oocyte maturation status and provides new insight into lipid distribution at the single oocyte level.

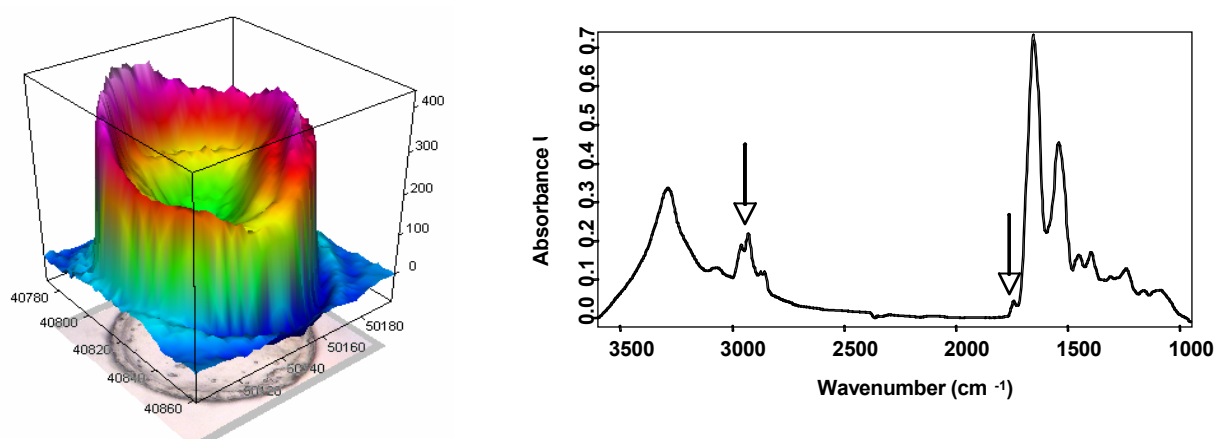


Figure 1: A. Total absorbance map of a GV oocyte showing the variable thickness of the zona pellucida and low absorbance in the nucleus. B. Mean spectra of an MII oocyte (light) and a GV oocyte (dark). Note the lipid contribution to the MII oocyte highlighted by the arrows.

Identification of Drug Resistant Melanoma Cell Lines Using Vibrational Spectroscopy

A. Zwielly¹, J. Gopas^{2,3}, G. Brkic², S. Mordechai¹

¹Department of Physics Ben-Gurion University (BGU), Beer-Sheva, 84105, Israel; ²Department of Microbiology and Immunology, Faculty of Health Sciences, Ben Gurion University, Beer-Sheva, Israel; ³Department of Oncology, Soroka Medical Center, Beer-Sheva, Israel

The major limitation to the successful treatment of malignancies is the emergence of drug-resistant tumor cells [1]. We investigated the ability of FTIR-Microscopy to define spectral changes between drug sensitive and drug resistant human melanoma cells. As a model system, a resistant melanoma cell line (GAC) was selected with cisplatin from parental (GA) cells as described by Brkic et al. [2]. By applying the principal component analysis (PCA) model, we reduced the original data size to six principal components. Figure 1 shows a good classification between resistant (red +) and sensitive (blue *) cells. It can be achieved by using PC1 vs. PC3 (a) and 3D plots presenting PC4 in addition to PC1 and PC3, indicating a clear distinction between the two groups (b).

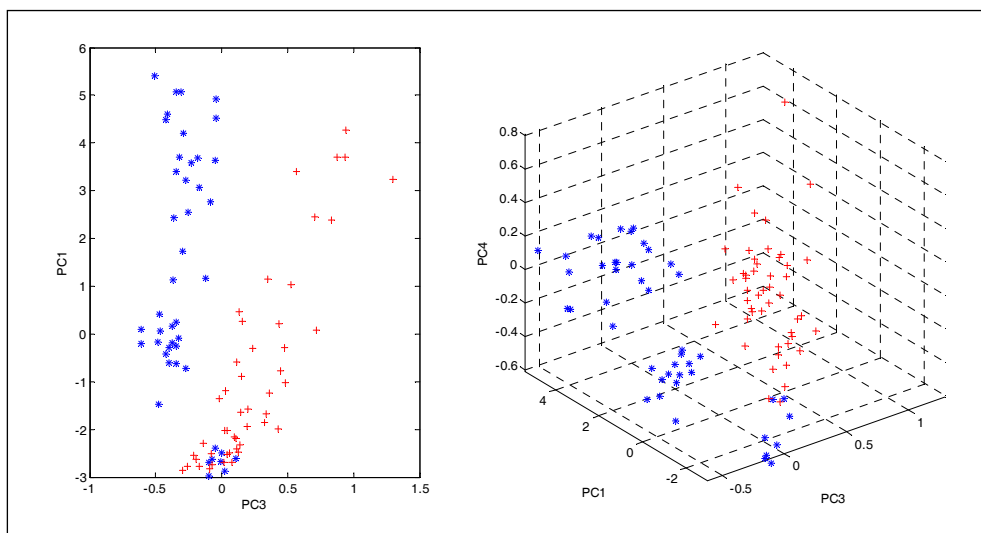


Fig. 1: Principle Component Analysis (PCA) model

Our preliminary results show that it is possible to obtain an estimate of the classification between these two cell lines. Due to its ability to provide detailed information at the molecular level [3] FTIR microspectroscopy has the potential to emerge as a simple, method for the identification of drug-resistant cells. Rapid detection of tumors resistant to a particular drug, should contribute to the ability of the physician to choose an effective treatment protocol.

- [1] P. Pil, S.J. Lippard, In *Encyclopedia of Cancer*, J.R. Bertino, Ed. Academic Press: San Diego, CA, 1997, Vol. 1, pp. 392-410.
- [2] G. Brkic, J. Gopas, N. Tanic, N. Dedovic-Tanik, D. Benharroch, E. Finkelstein-Jaworowsky and B. Dimitrijevic, *Genomic instability in drug resistant human melanoma cell lines detected by Alu-I-arbitrary-primed PCR*, *Anticancer Research* 23 (2003) 2601.
- [3] J. Liquier and E. Taillandier, In *Infrared Spectroscopy of Biomolecules*, (ed. by H. H. Mantsch & D. Chapman). Wiley-Liss, John Wiley & Sons, INC., Publication, NY, 1996, 131-158.

Effect of Different Fungal Associates on the FT Raman Spectral Characteristics of Norway Spruce Needles

P. Matějka¹, L. Mrnka², H. Tokárová¹, M. Vosátka², K. Volka¹

¹Dept. of Analytical Chemistry, Institute of Chemical Technology, Technická 5, CZ 166 28 Prague 6 – Dejvice

²Dept. of Mycorrhizal Symbioses, Institute of Botany ASCR, Zámek 1, Příhonice, CZ 252 43, Czech Republic

Norway spruce (*Picea abies* (L.) Karst.) dominates European forest ecosystems. Survival and performance of spruce trees strongly depend on the belowground fungal web involved in nutrient cycling, rock weathering and multiple trophic chains. Ectomycorrhizal fungi are able to influence levels of photosynthetic pigments and nutrients in needles of coniferous hosts. FT Raman spectroscopy is a method that make possible analyses of Norway spruce needles performed both *in vitro* and *in vivo* [1, 2]. In this study we used FT Raman spectroscopy to evaluate effects of several ecologically relevant groups of fungi on the composition of important compounds of spruce needles (waxes and carotenoids).

Aseptically germinated seedlings were planted in systems containing sterilized litter needles and inoculated with either individual fungi or combination of two fungal strains from different groups. Representatives of three ecological groups of fungi were used: saprotrophic (S, M1), mycorrhizal (M2, E2) and endophytic (E1). The seedlings without inoculation (K) were used as a reference. Systems were cultivated in a growing chamber for six months. Fresh needles were cut from each of the seedlings and two spectra were recorded per needle. 24 spectra represented one group of seedlings. The same number of spectra was collected for needles from natural forest area in Šumava mountains (NPŠ). The spectra were evaluated using principal component analysis (Fig. 1) and SIMCA modeling. Significant differences among models were observed. The effects of individual fungal types and various combinations can be related to contents of carotenoids and waxes in corresponding needles.

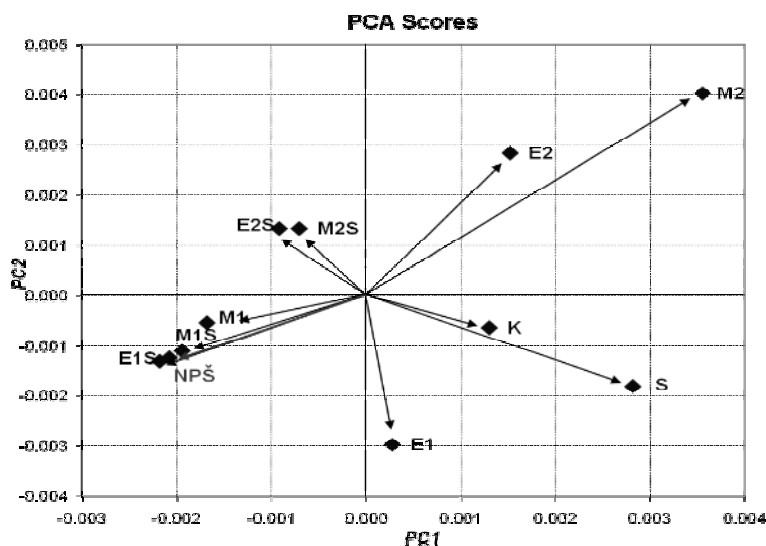


Fig. 1: Comparison of Raman spectral models obtained for individual fungal types

[1] P. Matějka, L. Plešerová, G. Budínová, K. Havířová, X. Mulet, F. Skácel, K. Volka, J. Mol. Struct. 565-566 (2001) 305-310.

[2] P. Matějka, H. Tokárová, T. Pekárek, K. Volka, J. Mol. Struct. 661-662 (2003) 333-345.

Acknowledgment: Financial support from Czech Science Foundation (GA CR 203/05/0697) and from the Ministry of Education of Czech Republic (MSM 6046137307) is gratefully acknowledged.

Interpretation of Vibrational Spectra of DNA Fragments Interacting with Metal Ions

V. Andrushchenko and P. Bour

Institute of Organic Chemistry and Biochemistry, Academy of Sciences, Flemingovo nam. 2, Prague, 16610, Czech Republic

e-mail: andrushchenko@uochb.cas.cz, bour@uochb.cas.cz

Metal ions play an important role in structure and in vivo functioning of nucleic acids. They can stabilize or destabilize native double-helical DNA, participate in replication and transcription as well as metallo-enzymatic and some metabolic processes, mutagenesis, carcinogenesis, and DNA packing in a living cell [1]. Therefore, the interaction with metal ions has been widely studied by a number of techniques, including vibrational spectroscopy [2].

Traditionally, infrared (IR) and Raman vibrational spectra were used for investigating nucleic acid secondary structure. However, recent development of chiral vibrational methods, such as vibrational circular dichroism (VCD) and Raman optical activity (ROA), significantly broadened the structural information, which could be obtained from these experiments. Additionally, due to advances in computer technologies and quantum chemistry tools, it became possible to apply high level calculations to relatively large molecular systems, allowing reasonably accurate simulations and reliable interpretations of the vibrational spectra [3]. However, systems with metals are difficult to model due to the relativistic and spin effects, and the weak metal-DNA bond.

Therefore, we calibrate the methodology on both theoretical and experimental IR analyses of model DNA fragments interacting with metal ions. Complexes of one of the main DNA building blocks, deoxyguanosine monophosphate (dGMP), with various metal ions, such as Cu, Cd, Zn, Ni, Ca, Mg and Na are studied. Owing to the theoretical computations most of the spectral features observed experimentally could be assigned to simulated spectra and explained. In many cases a correlation between the spectral changes occurring upon the dGMP interaction with the metal ions and the geometry of the complexes could be established. Differences in the interactions of alkaline, alkaline earth and transition metal ions with several distinct binding sites of dGMP are analysed.

- [1] A. Sigel, H. Sigel, *Interactions of Metal Ions with Nucleotides, Nucleic Acids and Their Constituents*, Marcel Dekker, New York, 1996; Vol. 32.
- [2] T. Theophanides, H.A. Tajmir-Riahi, In *Spectroscopy of Biological Molecules*, C. Sandorfy, T. Theophanides, (Eds.), Reidel, Dordrecht, Netherlands, 1984, pp. 137-152.
- [3] P. Bour, V. Andrushchenko, M. Kabelac, V. Maharaj, H. Wieser, *J. Phys. Chem. B* 109 (2005) 20579-20587.

Laser Tweezers Raman Spectroscopic Investigation of Geranylgeranyl Pyrophosphate Synthase in Recombinant *Schizosaccharomyces pombe* Cell

G. Basar¹, S. Kin¹, Guler Temizkan^{2,3}, Tuba Gunel^{2,3}, S. Akyuz⁴

¹Istanbul Technical University, Faculty of Sciences and Letters, Physics Engineering Department, 34469, Maslak, İstanbul, Turkey, ²Istanbul University, Faculty of Science, Department of Molecular Biology and Genetics, 34134, Vezneciler, İstanbul, Turkey, ³Istanbul University, Research and Application Center for Biotechnology and Genetic Engineering 34134, Vezneciler, İstanbul, Turkey, ⁴Istanbul Kültür University, Faculty of Sciences and Letters, Physics Department, Bakırköy 34156, İstanbul, Turkey

Carotenoids are the most widespread group of pigments found in nature, synthesized de novo by all photosynthetic organisms and some non-photosynthetic bacteria and fungi [1]. Carotenoids and several classes of economically essential metabolites such as sterols, quinones and rubber are derived from the isoprenoid pathway. The gene encoding geranylgeranyl pyrophosphate synthase (GGPPS) from bell pepper (*Capsicum annuum*) which key enzyme in this pathway was previously cloned and its heterologous expression was analyzed in *Schizosaccharomyces pombe* a suitable model organism for eukaryotes [2]. GGPPS gene was shown to be successfully transcribed by Dot and Northern hybridization. Comparison of the protein profiles from recombinant and host cells by SDS-PAGE revealed that the protein band of recombinant cells similar to GGPPS protein band.

In this study, host cell (leu1-32) and recombinant cell which contained cDNA encoding GGPPS were analyzed with Laser Tweezers Raman Spectroscopy (LTRS). Spectral alterations of the host structure due to cDNA encoding GGPPS were investigated.

- [1] P.C. Lee, C. Schmidt-Dannert: *Metabolic Engineering towards Biotechnological Production of Carotenoids in Microorganisms*. Appl. Microbiol. Biotechnol 60 (2002) 1-11.
- [2] T. Günel, M. Kuntz, N. Arda, S. Ertürk, G. Temizkan: *Metabolic Engineering for Production of Geranylgeranyl Pyrophosphate Synthase in Non-Carotenogenic Yeast Schizosaccharomyces pombe*. Biotechnology and Biotechnological Equipment 20 (2006) 76-82.

Upper Electron-Excited States in Coelenterate Bioluminescence

N.V. Belogurova¹, N.S. Kudryasheva^{1,2}, R.R. Alieva², A.G. Sizykh²

¹Institute of Biophysics SB RAS, Akademgorodok, Krasnoyarsk, 660036, Russia, e-mail: nbelogurova@mail.ru

²Siberian Federal University, Svobodny 79, Krasnoyarsk, 660043, Russia.

Bioluminescence is a result of chemiluminescent oxidative enzymatic reactions. The theories of chemiluminescence and structure of the molecules predict that the process of bioluminescence may involve upper electron-excited states of the bioluminescent emitter molecule. It is believed that organic peroxides decompose to form $n\pi^*$ -states of organic substances located at carbonyl groups. The bioluminescent emitter is supposed to be a heterocyclic compound with high fluorescence yield. It is specified by the upper singlet and triplet excited states of $n\pi^*$ -type (Fig. 1) with excitation located on carbonyl groups. Generation of an excited carbonyl group of the similar compounds is to be followed by population of lower-energy singlet states, e.g. through intramolecular non-radiative transitions $T_{n\pi^*} \rightsquigarrow S_{\pi\pi^*}$. This process is permitted as transition between the levels of different both orbital nature and multiplicity (El Sayed rule). Emission of light is the final stage of the bioluminescent process (Fig. 1).

The hypothesis of activity of upper electron-excited states of the bioluminescent emitter was first proposed by N.S. Kudryasheva and D.N. Shigorin. It was experimentally confirmed for bioluminescent emitter of bacteria. Application of the hypothesis to bioluminescent emitters of other organisms (fireflies, coelenterates, etc.) is of great interest now.

This investigation was aimed to examine activity of upper electron-excited states in coelenterate bioluminescence. Bioluminescent spectra of mutant of obelin F88H in the presence of pyrene were studied. Pyrene is a dye molecule serving as foreign energy acceptors in the bioluminescence system (Fig. 1). The weak sensitized fluorescence of pyrene was found. Since the energy of the fluorescent states of pyrene (28500 cm^{-1}) exceeds that of the bioluminescent emitter (23800 cm^{-1}) and its absorption spectrum does not overlap with the bioluminescence spectrum, the trivial light absorption and intermolecular resonance S-S transfer were excluded. This result confirmed activity of upper electron-excited states in coelenterate bioluminescence.

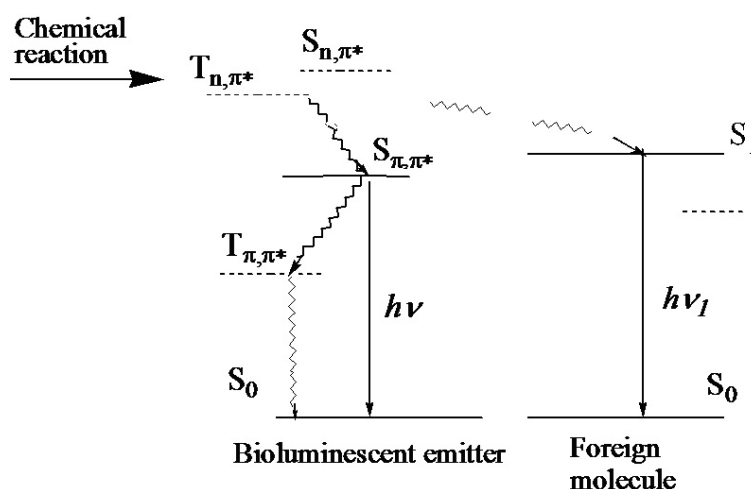


Fig. 1: Yablonski diagram of bioluminescent emitter and exogenous fluorescent compound.

On the Hydrogen-Deuterium Exchange in Proteins and Nucleic Acids Monitored by Vibrational Spectroscopy

P. Carmona¹, M. Molina², A. Rodríguez-Casado³

¹*Instituto de Estructura de la Materia (CSIC), Serrano 121, Madrid 28006 Spain,* ²*Departamento de Química Orgánica I, Escuela Universitaria de Óptica, Arcos de Jalón, s/n, 28037 Madrid, Spain,* ³*Instituto Madrileño de Estudios Avanzados, E.T.S.I. Agrónomos, 2804 Madrid, Spain*

A way of probing the structure and dynamics of proteins and nucleic acids is to monitor hydrogen-deuterium exchange [1, 2]. It is well known that groups exposed to the solvent exchange fastest, and the hydrogens of a structured region exchange more slowly compared with the hydrogens of an unstructured part. This is due to hydrogen bonding, low solvent accessibility, and steric blocking. A protected group can be regarded as “closed” to exchange.

In order to get insights into the structure and interactions between these types of molecules, we have developed an infrared and Raman probe of exchangeable hydrogenic sites in these biomolecules. The method is based upon the measurement in real time of the decay of band intensities associated with specific molecular groups, as these become progressively exchanged by deuterium in heavy water environment. The isotopic exchange measured by infrared spectroscopy has been carried out using a conventional liquid cell containing a thick front plate to fix two cylinders containing heavy water buffer. Two dialysis membranes having an appropriate molecular weight cutoff are placed on the cell filling holes of the front plate. The Raman measurements of the isotopic exchange were carried out using a single fibre of hollow microdialysis tubing with 216 μm diameter and variable molecular weight cutoff, the fibre being maintained within the Raman cell. This cell was either a glass capillary tube of 1 mm diameter or a quartz cell of 40 μl capacity. A constant flow of 4-6 ml/h, which is sufficient to maintain constant D_2O effluent concentration at the tubing boundary, was accomplished with a syringe injection pump. We have optimised the said accessories by changing their geometrical characteristics and reached measurements of exchange rates as fast as 0.4 min^{-1} and 1.5 min^{-1} by infrared and Raman spectroscopy respectively. Applications of these exchange probes to nucleic acid and protein molecules and subsequent treatment of the spectra by principal component analysis and two-dimensional correlation spectroscopy demonstrate the usefulness of this methodology for investigating the structure and dynamics of biological macromolecules.

[1] S.W. Englader, N.R. Kallenbach, *Q. Rev. Biophys.* 16 (1984) 521-655.

[2] T.M. Raschke, S. Marqusee, *Curr. Opin. Biotechnol.* 9 (1998) 80-86.

Dysprosium/Iron Aluminosilicate for Simultaneous Radiotherapy and Hyperthermia: Structural Investigation and Biocompatibility Evaluation

S. Cavalu¹, V. Simon², F. Banica¹

¹University of Oradea, Faculty of Medicine and Pharmacy, P-ta 1 Decembrie 10, Oradea 410087 Romania
e-mail: scavalu@rdslink.ro

²Babes-Bolyai University, Faculty of Physics, Kogalniceanu 1, Cluj-Napoca, Romania

The proposed materials in the present work are of great interest in the treatment of degenerative diseases by internal radiotherapy and hyperthermia. The sol-gel method chosen for the preparation of the materials allows obtaining materials of high purity and homogeneity at lower temperatures than those used in classical melting method. These biomaterials could be used in internal therapy of cancer, by local irradiation of the malignant tumors, with high energy and short range beta radiation, and in the same time heating them by electromagnetically hyperthermia; the concomitant effect of both therapy methods significantly increases the treatment's efficiency. Structural properties of dysprosium/iron aluminosilicate are investigated in this work by FTIR, Raman and EPR spectroscopy. Vibrational spectroscopy reveals the dominant bands around 1080 cm^{-1} assigned to the stretching vibration of Si-O-Si and Al-O-Al bond, and the Al-O stretching vibrations of tetrahedral AlO_4 groups related with the bands at 796 cm^{-1} (fig.1). The EPR spectra indicate the modifications of the environment of Fe^{3+} ($3d^5$, ${}^6\text{S}_{5/2}$) due to different dysprosium concentration. The use of in vivo radiotherapy is drastically limited by the biocompatibility of the materials incorporating radionuclides, the activity of the radionuclides and the chemical stability of the materials in the biological environment. Radiotherapeutic glasses must be biocompatible, insoluble and have high chemical purity as long as they are radioactive. The biocompatibility was evaluated with respect to collagen and fibrinogen adsorption, by analysing the ATR FTIR spectra (Fig. 1). Deconvolution of amide I absorption band (Fig.2) of both proteins is indicative of conformational changes in the secondary structure upon the adsorption. The results are interpreted by correlating the dysprosium concentration with structural properties of adsorbed proteins.

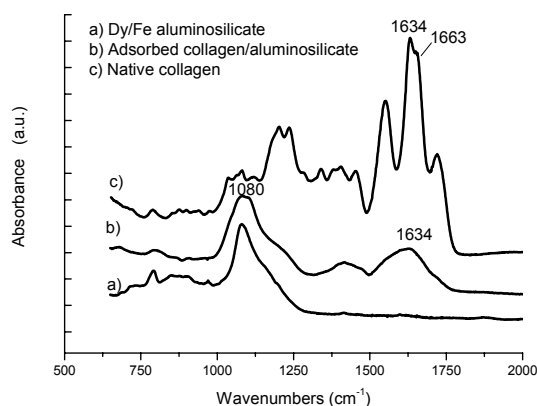


Fig. 1: FTIR spectra of Dy/Fe aluminosilicate.

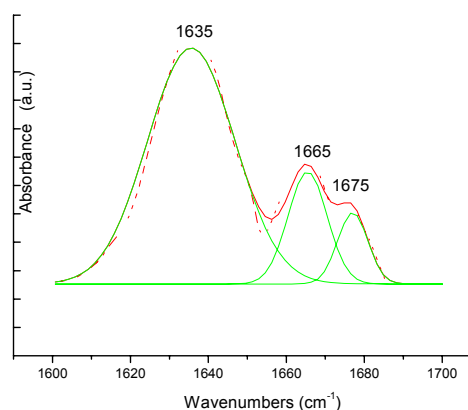


Fig. 2: Deconvolution of amide I band of adsorbed collagen.

Investigating the Kinetic Interactions between Protein and Nanoparticles via Mie Scattering Spectroscopy and Optical Trapping

G. Doyle, D. Zerulla.

Molecular Biophysics, School of Physics, University College Dublin, Belfield, Dublin 4, Ireland

The basis of the research is the kinetic study of the interaction between nanoparticles and protein by means of surface plasmon polariton enhanced scattering spectroscopy. Mie scattering spectroscopy for fast kinetic studies will be employed as the method of measurement. One of the most desirable properties of a surface plasmon is its strong electromagnetic field that is confined and localised near to the metal surface. The evanescent field of the surface plasmon carries the information regarding the molecules within the strong plasmon field. Two approaches are used; the first uses a sample containing a large number of particles [1]. This produces a broad resonance peak in the visible range due the presence of particles of different sizes. The second method uses an optical tweezers setup, for single particle spectroscopy. Although the intensity of the signal is naturally reduced, this technique eliminates broadening of the Surface Plasmon resonance peak due to the absence of size distribution. The interactions between the nanostructures and the protein are powerfully indicated by the corresponding shift in wavelength of the resonance peak as the local refractive index at the surface of the nanoparticles changes with progression of protein binding. This system can be used with a large number of proteins, provided the proteins themselves have an affinity for the metal from which the nanoparticles are constructed.

The methodology also involves using different geometrical formations of the nanostructures for example; rod-shaped and spherical-shaped particles in addition to experimenting with different types of metals. The rod-shaped particles are of particular interest because of their enhanced sensitivity. The presence of two resonance peaks in their spectra allows us to distinguish between the two geometrical axes – the longitudinal and transverse axes. Manipulation of the excitation wavelength offers an opportunity to investigate coupling between the Surface Plasmons excited along their respective axes.

The research ultimately aims to provide a novel method for the detection of conformational changes that occur in molecular systems by the observation and analysis of the SPP enhanced interaction between the nanoparticle and the protein via spectroscopy. This simultaneously provides information regarding the characteristic behaviour exhibited by Surface Plasmons in different geometrical environments.

- [1] G. Doyle, B. Ashall, M. Galvin, M. Berndt, S. Crosbie, D. Zerulla, *Appl. Phys. A* 89 (2007) 351-355.

Spectroscopy and Structural Properties of Biogene Amines (Serotonine, Histamine, γ -amino oil acid) and Account for Laser and Neutron Capture Effects

A.V. Glushkov^{1,2}, S.V. Malinovskaya¹, S.V. Ambrosov¹, O.Yu. Khetselius¹

¹*Odessa University, P.O. Box 24a, Odessa-9, 65009, South-East, Ukraine*

²*Institute of Spectroscopy, Russian Academy of Sciences, Troitsk-Moscow, 142090, Russia*

Paper is devoted to the Monte-Carlo computational studying the structural and spectroscopic properties for the biogene amines: serotonine (ST), histamine (HM), γ -amino oil acid (AC) and the laser and neutron capture action on the indicated properties of studied molecules. The ST (or 5-hydroxitriptamine, 5-HT) is produced by means of the hydroxycilation of essential amine acid of the triptophane [1]. ST influences mainly in a place of its appearance and calls for blood vessel narrowing in places of the trombocytes decay. Probably, serotonine ST is the mediator for transition of the nervous pulses in some branch of the brain. HM is produced in cells (mastocides) from the histidine amino acid. The γ -amino oil acid AC is produced in the brain substance and probably plays a role of the mediator or inhibitor of pulses. Many biomolecules (BM) are composed not only by hydrophilic, but also by hydrophobic groups, in the vicinity of which the water-water (or blood plasma) interaction is expected to be present even in the zeroth approximation. We present results of the Monte-Carlo calculating the cluster consisting of the serotonine ST (histamine HM) molecules and 100 molecules of water. All relevant interaction potentials are obtained by means of quantum calculation [1]. The water-water interaction potential was found by Matsouka etal by CI method. The BM-water interaction potential was obtained in the SCF approximation. Calculation is carried out at T=300K; All molecules are treated as rigid. The results for interaction energies are given below in table:

Potential / $kJmol^{-1}$	Neutral molecule	zwitterion
Water-water	-27.7 ± 0.8	-27.2 ± 0.7
ST-water	-59.5 ± 2.0	-348.5 ± 15.0
HM-water	$-37,8 \pm 2.0$	$-178,4 \pm 15.0$

The zwitterion appears as expected to be strongly favoured with respect to neutral molecule. The HM in the “zwitterion” more intensively (on the order) catalyses the gastric juice secretion and secretion from other endocrine glands. The similar situation is with action of the HM in the inflammatory and allergic reactions with further increasing vessel walls permeability and action of the ST with further blood-vessel narrowing in places of the trombocytes decay. We at first consider the possibilities of laser and neutron capture action on different of molecules, including an analysis of Szilard-Chalmers (n, γ), (n,n), Mössbauer and GM [2] effects. Some new bio-nano-technologies are analysed.

- [1] E. Clementi et al, Gazz. Chim. Ital. 108 (1978) 157-174; J. Am.Chem. Soc. 99 (1977) 5531-42 ; A.Glushkov, Journ.Struct. Chem. 34 (1993) 3-10; 31 (1990) 9-15; 32 (1992) 11-16; Rus. J. Phys. Chem. 66 (1992) 1259-76; 66 (1992) 589-596; A. Glushkov, S.Malinovskaya, Rus. J. Phys. Chem. 62 (1988) 100-106; 65 (1991) 2970-78;
- [2] A. Glushkov, S.Malinovskaya, In: New projects and new lines of research in nuclear physics. Eds. G.Fazio and F.Hanappe, Singapore : World Scientific.-2003.-P.242-250 ; nt.J.Quant.Chem 99 (2004) 889-896 ; 104 (2005) 496-500 ; Mol.Phys. (2008).

Chemometrics Methods Used by Spectroscopic of Biological Samples

Veronika Gombás¹, János Mink^{1,2}

¹*Institute of Analytics, Environmental Science and Limnology, University of Pannonia, H-8201 Veszprém, Pf. 158, Hungary*

²*Chemical Research Center, Hungarian Academy of Sciences, H-1525 Budapest, Pf. 17, Hungary*

The living tissues, like human skin and hair, have very complex biomolecular structures. These structures depend on the general health condition of the patient, and can be influenced by several external effects like stress situation, etc. It was shown in our laboratory that some illnesses can include more significant differences in the hair and skin spectra than other factors.

Due to the extremely complex structure of tissues a complete band assignment is impossible, however, small spectral changes even can be observed in the spectra. To a trustworthy analysis of discrepancies and a significant differentiation of the spectra the use of chemometrics methods like pattern recognition is indispensable.

Cluster analysis has been used for the spectra of healthy and unhealthy (cancerous) human skin (Fig.1). The cluster analysis makes groups, clusters without prior information. The method regards each spectrum as a separate group, then calculate the distance between the groups, and then it makes the two nearest group into a new one. The method iterate these two steps until only one type of group left, then can be seen the result. With this method we can discriminate the healthy and the cancerous human skin.

Cluster analysis has been used for the hair structure determination, too. The upper layer of hair is generally strongly degraded. We can differentiate between the surface degraded (e.g. bleached) features and the “living” layer of hair, so we can perform in an automated way the selection of useful spectra for further analysis to correlate with health condition.

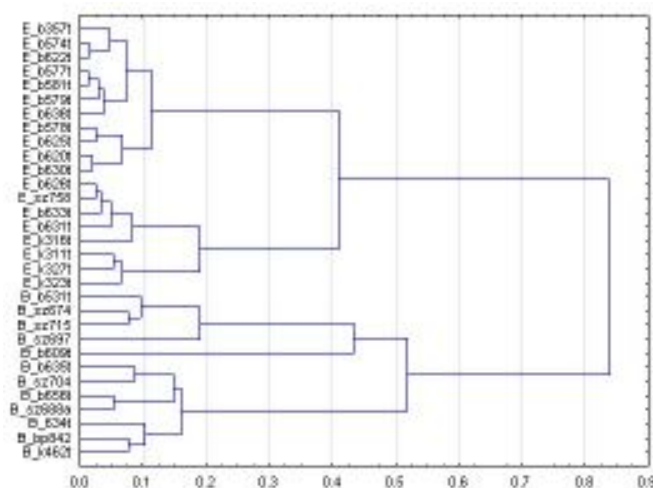


Fig. 1: Cluster analysis result of healthy and unhealthy skin spectra. The upper is the spectra of a healthy human skin (started with “E”), and the lower spectra belong to the cancerous patient (started with “B”).

Acknowledgement

The authors gratefully acknowledge financial support from the Hungarian Research Council (OTKA K-61611).

Different Conformational Ground States of a *Pseudosaccharin Ether* in the Gaseous Phase and in Solid Krypton

Andrea Gómez-Zavaglia^{1,2}, Agnieszka Kaczor^{1,3}, Rui Almeida⁴,
Maria de Lurdes S. Cristiano⁴, Rui Fausto¹

¹Department of Chemistry, Coimbra University, P3004-535 Coimbra, PORTUGAL

²Facultad de Farmacia y Bioquímica, Buenos Aires University, RA-1113 Buenos Aires, ARGENTINA

³Faculty of Chemistry, Jagiellonian University, Ingardena 3, 30-060 Krakow, POLAND

⁴Department of Chemistry and Biochemistry, University of Algarve, Faro, PORTUGAL

e-mail: angoza@qui.uc.pt

Benzisothiazoles are often vital structural units of biologically active systems. In particular, their use as herbicides and antibiotic agents has been extensively described [1]. Benzisothiazoles have also been described as phospholipase inhibitors efficient in the treatment of hepatic diseases [2].

In this work, the conformational space of the *pseudosaccharyl ether* 3-(allyloxy)-1,2-benzisothiazole 1,1-dioxide (ABID) has been studied by means of infrared spectroscopy and density functional theory (DFT) calculations. Five different low energy conformers (*TSk*, *TC*, *GSk*, *GSk'* and *GC*, with relative energies of 0.00, 1.97, 2.00, 3.82 and 6.02 kJ mol⁻¹, respectively) were found on the DFT(B3LYP)/6-311++G(3df,3pd) potential energy surface of the molecule, all of them differing in the conformation of the allyl substituent. According to calculations, in the gaseous phase all conformers are significantly populated *TSk*:*TC*:*GSk*:*GSk'*:*GC* = 47%:16%:18%:12%:7%, at 350 K). However, in the cryogenic matrices only the *TSk* and *TC* conformers exist due to isomerization from the higher energy *gauche* forms to the most stable *trans* isomers during deposition of the matrix (conformational cooling). The observed conformational cooling is in consonance with the low calculated energy barriers for the *GSk*→*TSk*, *GSk'*→*TSk* and *GC*→*TC* isomerization processes. Results from annealing experiments in a krypton matrix doubtlessly show that in this matrix the order of stability of the *TSk* and *TC* conformers is reversed, with the more planar *TC* form becoming the most stable conformer.

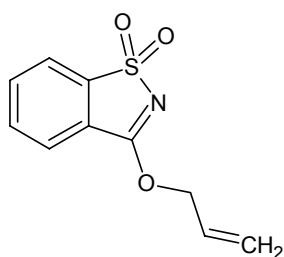


Fig. 1 Structure of ABID.

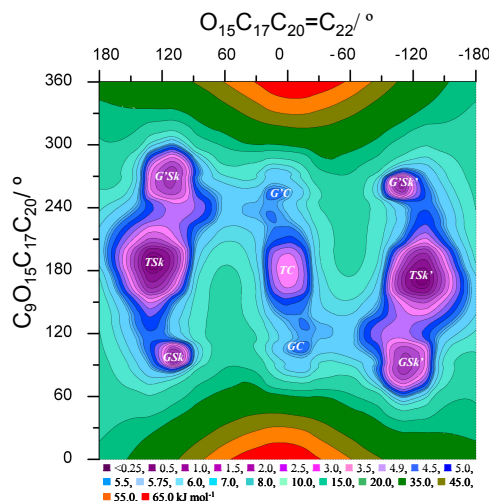


Fig. 2: DFT(B3LYP)/6-311++G(3df,3pd) potential energy (kJ mol⁻¹) contour map for ABID as a function of the C₉O₁₅C₁₇C₂₀ and O₁₅C₁₇C₂₀=C₂₂ dihedral angles.

- [1] M. Otten, W. von Deyn, S. Engel, R. Hill, U. Kardorff, M. Vossen and P. Plath, Patent number WO9719076. Internationale Anmeldung veröffentlicht durch die Weltorganisation für geistiges Eigentum.
- [2] P.I. Eacho, P.S. Foxworthy-Mason, H.S. Lin, J.E. Lopez, M. Mosior and M.E. Richett, (2004) Patent number: WO2004094394. Internationale Anmeldung veröffentlicht durch die Weltorganisation für geistiges Eigentum.

Phosphorescence of Singlet Oxygen and 5,10,15,20-tetrakis(1-methyl-4-pyridinio)porphyrin: Time and Spectral Resolved Study

R. Dědic, V. Vyklický, A. Svoboda, J. Hála

Charles University, Faculty of Mathematics and Physics, Department of Chemical Physics and Optics
Ke Karlovu 3, 121 16 Prague 2, Czech Republic
e-mail: hala@karlov.mff.cuni.cz

Photogeneration of singlet oxygen ($^1\text{O}_2$) via triplet states of water soluble porphyrin photosensitizers is the first step in photodynamic therapy as well as in recent $^1\text{O}_2$ imaging of cells [1]. High sensitive spectroscopic experimental set-up was built to detect time- and spectral- resolved infrared phosphorescence of both photosensitizers and $^1\text{O}_2$ [2]. In this contribution, new data obtained on 5,10,15,20-tetrakis(1-methyl-4-pyridinio)porphyrin (TMPyP) in buffer (pH = 7.4) are presented. TMPyP belongs to cationic photosensitizers which are known to photocleave DNA due to their affinity towards nucleic acids. Using TMPyP phosphorescence around 846 nm, lifetime of the triplet states of $(1.8 \pm 0.1) \mu\text{s}$ was determined for all TMPyP concentrations ($5 \mu\text{M} - 100 \mu\text{M}$). The corresponding rise time of $^1\text{O}_2$ slightly decreases from $(1.8 \pm 0.2) \mu\text{s}$ to $(1.5 \pm 0.2) \mu\text{s}$ with increasing TMPyP concentration. On the other hand, $^1\text{O}_2$ lifetime increases from $(3.7 \pm 0.2) \mu\text{s}$ to $(4.1 \pm 0.2) \mu\text{s}$ with increasing TMPyP concentration. Typical $^1\text{O}_2$ phosphorescence kinetic is shown in Fig. 1 together with its single exponential fit. The obtained results are discussed in the frame of TMPyP aggregation and quenching.

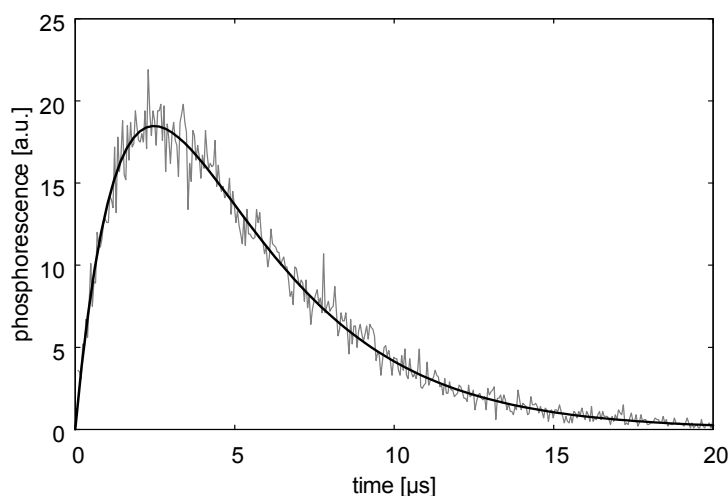


Fig. 1: Time resolved IR luminescence of $^1\text{O}_2$ detected at 1278 nm photogenerated at 420 nm in tetrakis(1-methyl-4-pyridinio)porphyrin tetra(*p*-toluenesulfonate) in buffer (air saturated, $10 \mu\text{M}$, pH = 7.4)

- [1] J.W. Snyder, J.D.C. Lambert, P.R. Ogilby: 5,10,15,20-tetrakis(N-Methyl-4-Pyridyl)-21 H, 23 H-Porphine (TMPyP) as a Sensitizer for Singlet Oxygen Imaging in Cells: *Characterizing the Irradiation-dependent Behavior of TMPyP in a Single Cell*. Photochemistry and Photobiology 82 (2006) 177–184.
- [2] R. Dědic, A. Molnár, M. Kořínek, A. Svoboda, J. Pšenčík, J. Hála: *Spectroscopic study of singlet oxygen photogeneration in meso-tetra-sulphonatophenyl-porphin*. J. Luminescence 108 (2004) 117–119.

Micro-Brillouin Scattering Study of Low Temperature Elastic Properties of Protein Crystals

Yuji Ike, Eiji Hashimoto and Seiji Kojima

Graduate School of Pure and Applied Sciences, University of Tsukuba, Tsukuba, Ibaraki 305-8573, Japan

The analysis of the complete three-dimensional structure of protein requires preparation of a single protein crystal of high quality. The study of protein crystals has wide applications such as, modeling of three dimensional structures, investigating bioactivities, synthesizing new drugs. Since protein crystals contain a large amount of water molecules, the crystals may deform and damage during the dehydration such as, unwanted stresses, cracks, degradations in mosaicity etc. [1]. Special care needs to be taken in handling these crystals from being damaged both mechanically and chemically for any accurate measurements. Generally, protein crystals are cryopreserved for long term preservation. The vitrifying tendency of cryoprotective solutions on cooling is the important factor for successful cryopreservation of biological materials. In the present study, the behavior of elastic properties in hen egg white lysozyme (HEWL) crystals with cryoprotective agents is studied by using micro-Brillouin scattering over a wide temperature range. The micro-Brillouin scattering technique is the best solution for the measurement of the elastic properties in small size crystals [2, 3]. We employed well known glass forming liquid of glycerol which undergoes a glass transition around 185 K without crystallization even in slow cooling. The observed behavior of hypersonic acoustic phonons shows continuous increase of sound velocity with decreasing temperature and no abrupt jump of sound velocity due to crystallization observed.

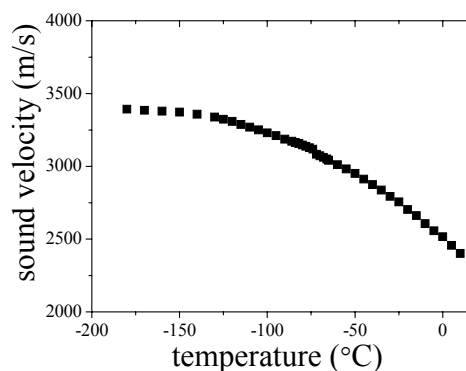
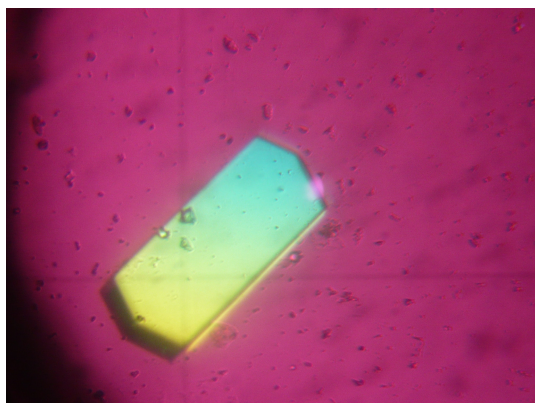


Fig. 1: Optical micrograph of a tetragonal HEWL crystal. **Fig. 2:** Sound velocity in a HEWL crystal in glycerol.

- [1] I. Dobrianov, S. Kriminski, C.L. Caylor, S.G. Lemay, C. Kimmer, A. Kisselev, K.D. Finkelstein, R.E. Thorne, *Acta Cryst. D57* (2001) 61-68.
- [2] E. Hashimoto, Y. Aoki, Y. Seshimo, K. Sasanuma, Y. Ike, and S. Kojima, *AIP Conference Proceedings* 982 (2008) 367-370.
- [3] E. Hashimoto, Y. Aoki, Y. Seshimo, K. Sasanuma, Y. Ike and S. Kojima, *Jpn. J. Appl. Phys.* (in press).

Vibrational Spectroscopic Investigation of Bioactive Aminoalcohols

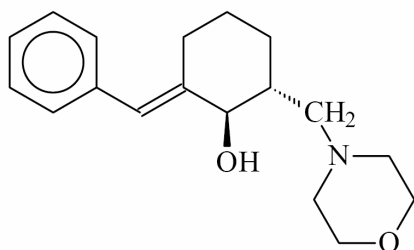
G. Keresztury¹, T. Sundius², T. Lóránd³

¹Chemical Research Center, HAS, P.O. Box 17, H-1525 Budapest, Hungary
e-mail: kergabor@chemres.hu;

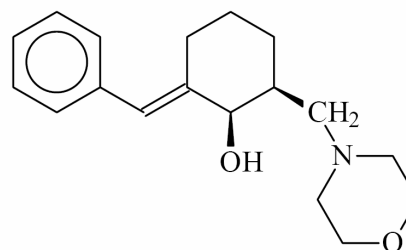
²Department of Physical Sciences, University of Helsinki, P.O. Box 64, FIN-00014 Helsinki, Finland

³Department of Biochemistry and Medical Chemistry, University Medical School of Pécs,
H-7601 Pécs, P.O. Box 99, Hungary

As part of our continued interest in studying the infrared and Raman spectroscopic manifestations of *cis-trans* and conformational isomerism in bioactive polycyclic organic compounds, we have published our studies of isochromanone and coumarin derivatives [1-3]. The present work concerns with similar investigations of bioactive aminoalcohols obtained by reduction of cyclic Mannich ketones. The stereocomposition of the reaction mixtures is influenced by the type of reducing agent applied and the size of the central ring [4]. An increased preference for the *trans* isomer was attributed to a weak intramolecular hydrogen bond between the OH group and the N atom, as demonstrated by X-ray crystallography [4].



MK-O23R *trans*
(main product)



MK-O23R *cis*
(minor product)

The vibrational spectroscopic study consists of measurement of FT-IR and Raman spectra of the reaction products and subsequent DFT quantum mechanical calculations (prediction) of the vibrational spectra for the anticipated structural varieties of the synthesized molecules. Comparison of the measured and computed frequencies as well as the observed and simulated spectra is performed to resolve any uncertainties in identifying the reaction products.

The capabilities of vibrational frequency and normal mode calculations based on scaled quantum mechanical (SQM) force fields performed at the DFT/B3LYP/6-31G* and higher levels of theory to predict the small spectral differences between the stereoisomers are tested in this work.

[1] G. Keresztury, S. Holly, T. Sundius, T. Lóránd: *Vibr. Spectrosc.*, 29 (2002) 53-9.

[2] G. Keresztury, S. Holly, K. István, T. Sundius, T. Lóránd, *J. Biochem. Biophys. Meth.* 61 (2004) 107-18.

[3] G. Keresztury, S. Holly, V. Komlósi, K. István, and T. Lóránd, *J. Biochem. Biophys. Meth.* 69/1-2 (2006) 163-177.

[4] T. Lóránd, E. Ósz, Gy. Kispál, G. Nagy, E. Weckert, D. Luebbert, A. Meents, B. Kocsis and L. Prókai, *ARKIVOC* (2004) (vii) 34-52.

Ligand Induced Conformational Change of Pyruvate Kinase Studied by ATR-FTIR Spectroscopy

S. Kumar, A. Barth

Department of Biochemistry and Biophysics, The Arrhenius Laboratories for Natural Sciences, Stockholm University, SE – 10691 Stockholm, Sweden

Pyruvate kinase (PK) is a key enzyme of the glycolytic pathway that catalyzes the transfer of phosphate from phosphoenol pyruvate (PEP) to adenosine diphosphate (ADP). It requires divalent and monovalent cations for activity. In this study, structural changes induced by ligand binding were studied by attenuated total reflection Fourier transform infrared (ATR-FTIR) spectroscopy in combination with a dialysis accessory [1]. Our experiments probed the effects of PEP, ADP and metal ions on PK. PEP was the most efficient ligand in inducing a change in the PK infrared spectrum. Secondary structure changes and changes of PEP absorption (carboxylate, phosphate) upon binding to PK were monitored successfully and will be discussed.

[1] M. Krasteva, S. Kumar, and A. Barth, *Spectroscopy* 20 (2006) 89-94.

Acknowledgement

This work was supported by Sven och Lilly Lawskis fond för naturvetenskaplig forskning.

Degree of Vinyl Conversion in Experimental ACP Composites

Z. Tarle¹, D. Škrčić², A. Knežević¹, D. Matošević¹, M. Ristić³, K. Prskalo¹, S. Musić³

¹Department of Endodontics and Restorative Dentistry, School of Dental Medicine, University of Zagreb, Gundulićeva 5, 10000 Zagreb, Croatia, ²American Dental Association Foundation, Paffenbarger Research Center, USA, ³Division of Materials Chemistry, Laboratory for Synthesis of New Materials, Ruđer Bošković Institute, Zagreb, Croatia

A unique amorphous calcium phosphate (ACP)-based composite with the potential to arrest caries development and regenerate mineral-deficient tooth structures has recently been developed. When embedded in polymerized methacrylate matrices and exposed to an aqueous environment, ACP releases sufficient levels of remineralizing calcium and phosphate ions in a sustained manner to promote redeposition of apatitic tooth mineral. The aim of this study was to assess the degree of vinyl conversion (DVC) attained in experimental composites based on zirconia-modified ACP and photo-activated resins.

The composites were made from the resins comprising: 1) ethoxylated bisphenol A dimethacrylate (EBPADMA), triethylene glycol dimethacrylate (TEGDMA), 2-hydroxyethyl methacrylate (HEMA) and methacryloxyethyl phthalate (MEP) (ETHM series with varying EBPADMA/TEGDMA molar ratios assigned 0,5 - ETHM I, 0,85 - ETHM II and 1,35 - ETHM III), and 2) 2,2-bis[p-(2'-hydroxy-3'-methacryloxypropoxy)phenyl]-propane (bis-GMA), TEGDMA, HEMA and zirconyl dimethacrylate (BTHZ series). Both ETHM and BTHZ resins were photo-activated by the addition of camphorquinone and ethyl-4-N,N-dimethylaminobenzoate. In order to assess a possible effect of filler particle size on CR, resins (60 mass %) were blended with 40 mass % of either milled ACP (mACP; median diameter $d_m = 0.9 \mu\text{m}$) or coarse ACP (cACP; $d_m = 6.0 \mu\text{m}$). Composite specimens were polymerized by irradiating them for 40 sec with soft start mode (LED curing unit Bluephase; Ivoclar Vivadent, Liechtenstein). The DVC was calculated as the % change in the ratio of the integrated peak areas between the aliphatic and aromatic absorption bands (eight specimens/experimental group) determined by Fourier transform infrared spectroscopy (Perkin Elmer 2000 spectrometer; Perkin Elmer, UK).

One-way ANOVA indicated that the differences in DVC of tested composites are significant ($p < 0,001$). The highest DVCs were attained in mACP-BTHZ, cACP-BTHZ and mACP-ETHMIII formulations (Table 1).

Table 1: Composition of tested materials and the attained DVC.

Material number	Filler type	Resin matrix	Mean	Std. Dev.
1	mACP	ETHM I	73,63	2,00
2	cACP	ETHM I	72,93	1,94
3	mACP	ETHM II	71,90	1,10
4	cACP	ETHM II	74,92	1,69
5	mACP	ETHM III	80,31	2,69
6	cACP	ETHM III	75,43	1,93
7	mACP	BTHZ	82,77	1,46
8	cACP	BTHZ	82,23	0,90

DVC of tested ACP composites (on average $(76,76 \pm 4,43) \%$) compares well with or is even higher than the DVCs reported for the majority of commercial materials. Since the composites with high DVC usually exhibit high polymerization shrinkage, future studies of ACP composites will focus on determining the polymerization shrinkage of these materials.

Raman and FTIR Spectroscopy of the Keratin as a Potential Tool for Probing Bone Health

K. Merkel¹, A. Kocot¹, W. Pluskiewicz² and A. Pyrkosz¹

¹*Institute of Physics, University of Silesia, 40-000 Katowice, Poland*

²*Department and Clinic of Internal Medicine, Silesian Medical University, Zabrze, Poland*

Bone matrix is composed of collagenous and noncollagenous bone proteins. Collagen synthesis, secretions and deposition are coordinated with and dependent on synthesis on the other matrix proteins. The presence of cysteine in forming disulfide bonding is a feature of all noncollagenous bone proteins [1]. It is considerate that cysteine residues within structural proteins and consequent disulfide bonding might result in structure with variable ranges [2, 3]. While the mechanism of the bone formation is not defined yet, the need for cysteine and sulfation of the bone proteins is essential to all. There is an in vivo exchange between inorganic sulphate mainly due to synthesis and decomposition of sulphated glycosaminoglycans, which form the basic body of the bone matrix. Lost of cysteine is expected to influence both indirectly and directly, collagenous and noncollagenous proteins as well. The problem of bone fragility may result from disturbance of metabolism of collagenous and noncollagenous proteins.

Osteoporosis affects the organic and mineral phases of bone resulting in a decrease in resistance to fracture. Patients can suffer osteoporotic fractures despite normal bone mineral density, partly because of unmeasured influences of both the protein and mineral phases of bone that are affected in osteoporosis. There is currently no clinically applicable method of evaluating the health of the protein phase. This work has suggested that changes in the organic phase of bone are reflected in similar proteins, such as keratin, from which fingernails are composed. The proteins in human nail (keratin) and bone (collagen) require sulphation and disulphide bond (S-S) formation, via cysteine, for their structural integrity. A disorder of either process should lead to disordered collagen and keratin synthesis.

We use Raman and FTIR spectroscopy to investigate spectra changes of the nails sourced from osteoporosis patients with respect to those sourced from control group of healthy patients. The method was successful in assessing disulfide bond content of human fingernail. The disulfide bond content of the nails sourced from osteoporosis patients was lower and flatter than that from healthy patient. In protein spectra, the carbon sulphide vibrational band originates from methionine, cysteine and cystine. The content of methionine in human nail is insignificant so the contribution of the C-S and S-S bands must have originated from cysteine and cystine. Therefore, we conclude that reduced cysteine or sulphur's may play a role in nail brittleness and bone fragility. Fluorescence is the phenomena, which make Raman measurements more difficult. In case of nails of osteoporosis patients, the fluorescence is more intensive. So this effect may be another indication of changes in nails and bone structure.

[1] P.G. Robey, *Osteoporosis*, 2nd ed., Lippincott-Raven, Philadelphia, New York, 1995.

[2] L.A. Komarnisky, R.J., Christopherson, T.K. Basu, "Sulfur: Its clinical and toxicologic aspects", *Nutrition*, 19 (2003) 54.

[3] I. Pillay, D. Lyons, M.J. German, N.S. Lawson, H.M. Pollock, J. Saunders, S. Chowdhury, P. Moran, M.R. Towler, *J. Women's Health*. 14 (2005) 339-344.

Hydrogen Bonding in $(\text{COOH})_2 \cdot 2\text{H}_2\text{O}$ and $(\text{COOD})_2 \cdot 2\text{D}_2\text{O}$

V. Mohaček Grošev¹, J. Grdadolnik², J. Stare², D. Hadži²

¹*Ruđer Bošković Institute, Bijenička c. 54, 10002 Zagreb, Croatia*

²*National Institute of Chemistry, Hajdrihova 19, 1000 Ljubljana, Slovenia*

Despite repeated efforts, vibrational spectra of single crystal oxalic acid are still not assigned properly in all spectral intervals studied. Far infrared study of single crystals of $(\text{COOH})_2 \cdot 2\text{H}_2\text{O}$ by Wyncke, Brehat and Hadni gave the assignment of infrared active phonons and internal vibrations with frequencies below 200 cm^{-1} [1], while Villepin and Novak concentrated on vibrations involving hydrogen bond and did not present the list of all observed frequencies [2]. Ebisuzaki and Angel compared Raman bands of two polymorphs of oxalic acid dihydrate, α and β , both belonging to $P2_1/c$ space group and with two molecules per unit cell [3]. Their assignment was empirical and some bands were left unassigned.

We have recorded Raman spectra of single crystals of α $(\text{COOH})_2 \cdot 2\text{H}_2\text{O}$ and α $(\text{COOD})_2 \cdot 2\text{D}_2\text{O}$, including low temperature Raman spectra of α $(\text{COOH})_2 \cdot 2\text{H}_2\text{O}$, and compared the positions of observed bands with the values calculated with CRYSTAL06 and Car-Parrinello molecular dynamics programs. The values given by CRYSTAL06 program altogether are in better agreement with the observed positions of phonons, but the value of carboxyl O-H stretching frequency is still too high (calculated values are 2289 cm^{-1} for A_g and 2543 cm^{-1} for B_g mode respectively, while the observed Raman band is at 1959 cm^{-1}). For deuterated sample, the carboxyl $\nu(\text{O-H})$ appears at practically the same place, at 1938 cm^{-1} , indicating strong hydrogen bond. The other modes relating to OH carboxyl group are attributed to $\gamma(\text{OH})$ at 1265 cm^{-1} (infrared band), while $\delta(\text{COH})$ is strongly mixed with H_2O bending modes (1415 cm^{-1} , 1439 cm^{-1} , 1530 cm^{-1} , 1635 cm^{-1} are observed Raman bands).

Recently, two new crystal forms of sesquihydrates of oxalic acid were reported [4]. One crystal structure belongs to PI^- group with two molecules per unit cell, while the other belongs to $Pnma$ with eight molecules per unit cell. Compared to α $(\text{COOH})_2 \cdot 2\text{H}_2\text{O}$, which has the closest $\text{O} \cdots \text{O}$ distance equal to 2.484 \AA , and that is between $\text{O}(\text{H})$ of carboxyl group and O from water, in the PI^- group the closest $\text{O} \cdots \text{O}$ distance between the same two groups is 2.519 \AA , while the next one is equal to 2.505 \AA and involves the distance between hydroxyl oxygen from COOH group of the first molecule and carbonyl oxygen from the COO^- group of the second molecule. The way water is incorporated between oxalic acid molecules could explain the fact that in some Raman spectra three bands were observed where only two were expected for $\nu(\text{C-C})$ stretching band.

[1] B. Wyncke, F. Brehat, A. Hadni *J.Phys.* 36 (1975) 877–882.

[2] J. De Villepin, A. Novak *Proceedings of the 12th European Congress on Molecular Spectroscopy*, Strasbourg, France, July 1–4 1975, Elsevier, pages 299–302.

[3] Y. Ebisuzaki, S.M. Angel *J. Raman Spectrosc.* 11 (1981) 306–311.

[4] M. Wenger, J. Bernstein *Mol. Pharmaceutics* 4 (2007) 355–359.

Covalently Grafted, Silica Gel Supported C-protected Cysteine or Cystine Copper Complexes – Syntheses, Structure and Possible Surface Reaction Studied by FT-IR Spectroscopy

A. Aranyi, Z. Csendes, J.T. Kiss, I. Pálinkó

Department of Organic Chemistry, University of Szeged, Dóm tér 8, Szeged, H-6720 Hungary

In order to satisfy the need for novel highly active, and, even more importantly, highly selective catalysts various strategies may be followed. One promising way may be to mimic the active sites of enzymes [1]. To ease the work-up procedure as well as facilitating the recovery of the catalyst, immobilising these active site mimics looks advantageous. In this contribution we describe such a biomimetic approach: our work concerns the covalent anchoring of Cu(II)–C-protected L-cysteine or C-protected cystine complexes onto a modified silica gel support. Previously, we applied for anchoring of various copper–amino acid complexes onto silica gel [2] and montmorillonite [2-4] hydrogen bonding and ionic interactions, respectively. Although immobilization was successful, we hoped for a better control of synthesis using covalent grafting. Our initial results with N-protected tyrosine and chloropropylated silica gel were encouraging [5].

The components of the anchored complexes [L-cysteine or L-cystine methylester, Cu(NO₃)₂, chloropropylated silica gel (SG)] and the isopropanol solvent were commercial products. Covalent grafting was performed at the N-terminal of the amino acid (N-alkylation-like transformation) with the chlorine of the chloropropylated SG. Complexation followed the anchoring, applying either ligand-poor conditions (only the immobilised protected amino acids were available for coordination) or circumstances abundant in non-anchored protected amino acid molecules. Structural information on each step of the synthesis procedure was obtained by mid-range infrared spectroscopy, measuring diffuse reflectance (4000–400 cm⁻¹ wavenumber range, BIO-RAD Digilab Division FTS-65 A/896 FT-IR spectrophotometer, 2 cm⁻¹ resolution, 126 scans, the Win-IR package).

It was found that covalent anchoring was successful with both amino acids. The primary coordination site was found to be the thiolate or the disulfide sulphur for cysteine and cystine, respectively. The other site available for coordination is the carbonyl oxygen. The nitrogen was not accessible due to its direct participation in surface grafting. The cysteine methylester acted as bidentate ligand, i.e., two amino acids satisfied the fourfold coordination of the Cu(II) ion under ligand-poor conditions, while one surface-bound cystine could do the same. Ligand excess did not change the coordination mode for cysteine methylester, while for the cystine methylester the sulphur atoms of the excess amino acids molecules expelled the carbonyl oxygens from the coordination sphere. Comparing the spectra of anchored complexes revealed that there was no cysteine → cystine transformation neither under ligand-poor nor ligand-excess conditions.

- [1] A.J. Kirby, *Angew. Chem. Int. Ed. Engl.* 35 (1996) 706-724.
- [2] I. N. Jakab, K. Hernadi D. Méhn, T. Kollár, I. Pálinkó, *J. Mol. Struct.* 651-653 (2003) 109-114.
- [3] K. Hernadi, I. Pálinkó, E. Böngyik, I. Kiricsi, *Stud. Surf. Sci. Catal.* 135, 366; CD-ROM edition 27P10 (2001).
- [4] I. Szilágyi, I. Labádi, K. Hernadi, T. Kiss, I. Pálinkó, *Stud. Surf. Sci. Catal.* 158 (2005) 1011-1018.
- [5] I. N. Jakab, K. Hernadi, J. T. Kiss, I. Pálinkó, *J. Mol. Struct.* 744-747 (2005) 487-494.

Acknowledgement: This work was supported by the National Science Fund of Hungary through grant K62288. The financial help is highly appreciated.

Raman Spectroscopy Study of Cellular Damage in Human Keratinocytes Treated with Organophosphate Compounds

M. Lasalvia¹, N. L'Abbate¹, G. Perna², E. Mezzenga², V. Capozzi²

¹*Dipartimento di Scienze Mediche e del Lavoro, Università di Foggia, Viale Pinto, 71100 Foggia, Italy*

²*Dipartimento di Scienze Biomediche, Università di Foggia, Viale Pinto, 71100 Foggia, Italy*

The environment conditions could have several consequences on the health of the population. In particular, plant protection products, among which a large group is represented by pesticides, have significant toxicological implications. Many pesticides are used for the disinfestations of the crops and for food preservation. In particular, the use of organophosphate compounds, such as malathion, parathion and diazinon is recently grown up. Exposure to pesticides affects a large number of people, because they can be found both in water and food. The effects of such substances on normal human keratinocytes are of considerable interest because the epithelial cells are the first to come into contact with substances in the environment.

Biochemical modifications of single human keratinocytes treated with different organophosphate compounds (diazinon, malathion and parathion) at different concentrations were investigated by Raman microspectroscopy technique. Although the viability assay reveals that the exposure of keratinocytes to organophosphate compounds at low concentration has no cytotoxic effect, structural and biochemical modifications are detected by Raman spectra at such concentration. Such modifications consist of breakdown of both membrane lipidic layers and DNA bonds; fragmentation of DNA bases also occur, whereas proteins concentration and structure are not influenced by organophosphate compounds exposure. These results are promising in view of the possibility to use Raman-microspectroscopy, in combination with a remote optical probe, as a diagnostic tool for early detection of cellular damages induced by chemical stress due to toxic agents exposure.

Disentangling Infrared CH Bands Arising from Polar and Apolar Domains of Phospholipids: Headgroup CH Moieties are Involved in Water Binding

D.R. Gauger¹, E. Mrazkova², P. Hobza², W. Pohle¹

¹*Institute of Biochemistry and Biophysics, Friedrich-Schiller University, Philosophenweg 12, D-07743 Jena, Germany, e-mail: walter.pohle@uni-jena.de*

²*J. Heyrovsky Institute of Physical Chemistry, Academy of Sciences of the Czech Republic and Center for Complex Molecular Systems and Biomolecules, Dolejskova 3, Prague 8, C-18223, Czech Republic*

The polar region of lipid molecules is equipped with sites suitable for electrostatic and hydrogen-bonding interactions that are important for both their propensity to assemble to higher-order structures, usually bilayers, and the binding or embedding of other functional unities, as membrane proteins. Knowing the interaction potency of lipid headgroups is, thus, a prerequisite to understand the pathways related to biomembrane functions.

An ideal probe molecule to explore the binding behavior of lipid aggregates (as of any molecule with polar regions) is water as it combines manifold H bonding potentialities with a small size largely excluding steric problems. We have applied infrared spectroscopy to study the hydration of phosphatidylcholines (PCs) according to a protocol developed in this laboratory [1] in terms of the specific contributions of the different lipid components for water binding. Beside the well known binding centers, as phosphate and carbonyl groups, CH (i.e. methyl, methylene and methine) groups, which are not easily accessible by experimental means, are present in the polar lipid region. To visualize the pertinent CH vibrational bands, which are practically hidden in the spectra of common lipids because of complete overlap by the predominant chain CH bands, a chain-depleted model compound, methyl-PC [2], as well as different specifically deuterated dimyristoyl-PCs as “complete” lipid molecules have been used. Systematic variation of the isotopic-exchange pattern made it possible to disentangle the CH stretches by separating from each other the different molecular regions of a phospholipid, that is headgroup, glycerol backbone and hydrocarbon chains [3]. CH (or CD) stretching vibration bands due to methyl and methylene groups located in methyl-PC or in the polar region of dimyristoyl-PCs surprisingly undergo dramatic hydration-driven wavenumber upshifts by as much as 6-20 cm⁻¹. As these shifts are relatively strong referred to the 2 cm⁻¹ wavenumber increase commonly found for the lipid chain-melting process, which in fact represents a conformationally demanding (i.e. the main) transition, they can be considered as indicating a direct water binding to the CH groups in the polar lipid domain rather than merely conformational changes.

This suggestion is supported and rationalized by theoretical calculations performed for methyl-PC that reveal, among other structural and molecular-physical phenomena, instances of (lipid-)C-H...OH₂ hydrogen bonding to explain the spectroscopic findings [4]. The formation of these weak C-H...O H bonds might be promoted by the presence of the electrophilic substituents located next to the CH groups in the polar lipid domain.

[1] W. Pohle, C. Selle, H. Fritzsche, H. Binder, *Biospectroscopy* 4 (1998) 267-280.

[2] W. Pohle, D.R. Gauger, H. Fritzsche, B. Rattay, C. Selle, H. Binder, H. Böhlig, *J. Mol. Struct.* 563-564 (2001) 463-467.

[3] D.R. Gauger, W. Pohle, *J. Mol. Struct.* 744-747 (2005) 211-215.

[4] E. Mrazkova, P. Hobza, M. Bohl, D.R. Gauger, W. Pohle, *J. Phys. Chem. B* 109 (2005) 15126-15134.

Spectroscopic Studies on Binding of Cationic Pheophorbide-a Derivative to Double-stranded and Quadruplex Polynucleotides

O. Ryazanova¹, I. Voloshin¹, I. Dubey², L. Dubey², V. Zozulya¹

¹*B. Verkin Institute for Low Temperature Physics and Engineering of NAS of Ukraine, 47 Lenin ave., 61103, Kharkov, Ukraine*

²*Institute of Molecular Biology and Genetics of NAS of Ukraine, 150 Zabolotnogo str., 03143, Kyiv, Ukraine
e-mail: ryazanova@ilt.kharkov.ua.*

Pheophorbide-a (Pheo) is an anionic porphyrin derivative. It is widely used as a photosensitizer in photodynamical therapy of tumors because of its high photosensitizing activity in vitro and in vivo [1, 2]. Modification of Pheo with the trimethylammonium group was carried out to obtain a cationic dye derivative (CatPheo) capable of polyanion binding. The interaction of CatPheo with double-stranded poly(A)·poly(U) and poly(G)·poly(C) as well as with four-stranded poly(G) homopolymer was investigated in buffered aqueous solutions (pH6.9) of low ionic strengths (2mM Na⁺) by methods of absorption and polarized fluorescence spectroscopy in a wide range of molar phosphate-to-dye ratios, P/D. Determination of type of the complexes formed by CatPheo with the polynucleotides and definition of binding characteristics were carried out.

It was revealed two mechanisms of CatPheo binding to the polynucleotides: (i) chromophore intercalation between the nucleic bases; (ii) formation of the external complexes via electrostatic attraction of cationic dye to polynucleotide backbones. It was shown that (ii) type is predominant for double-stranded polynucleotides. However, in the case of four-stranded poly(G) containing systems it competes with the intercalation binding mechanism. Fluorescent technique was revealed to be efficient for recognition of the type of complex formed, because of CatPheo emission intensity increases upon its intercalation and quenches strongly upon the external stacking-association. It was established that for poly(G) at low P/D values (P/D < 5) the outside cooperative binding was predominated being accompanied with CatPheo associations due to chromophore stacking; while the P/D increase results in disintegration of these external complexes and prevalence of the intercalative binding mechanism. It was confirmed by rise in fluorescence polarization degree under P/D increase.

Simulation of the external binding to DNA on a system containing the single-stranded polyphosphate was carried out under the same conditions. It was established that at low P/D values CatPheo forms continuous stacking associates on the polyanionic matrix, and at large P/D it binds to polyphosphate in the dimer form. The increase in the solution ionic strength reduces the electrostatic binding efficiency due to CatPheo and Na⁺ ions competition. However, even at the physiological ionic strength this interaction type gives essential contribution into the complex formation. The thermodynamic characteristics of external complex formation were estimated by Schwarz's method [3].

The improved photodynamical activity for CatPheo in comparison with that for Pheo is expected because of a good water solubility of CatPheo and the efficient dye binding with polyanionic biopolymers. Besides, the strong CatPheo binding with nucleic acids probably allows to use this porphyrin derivative in anticancer applications for targeting of G-quadruplexes of telomeric DNA.

[1] B. Roeder, J. Photochem. Photobiol. B 5 (1990) 519-521.

[2] B. Roeder, Lasers Med. Sci. 5 (1990) 99-106.

[3] G. Schwarz, Eur. J. Biochem. 12 (1970) 442-453.

Phosphate Layers on Titanium and Ti6Al4V Titanium Alloy – Comparison of Hydroxyapatite Layers Obtained During SBF Soaking

M. Rokita, M. Sitarz

*Faculty of Materials Science and Ceramics, AGH University of Science and Technology,
Al. Mickiewicza 30, 30-059 Kraków, Poland
e-mail: rokita@agh.edu.pl*

Titanium and its alloy are used for orthopaedic and dental implants preparation despite poor bioactive properties. Covering the metallic base by ceramic phosphate layers is a chance of correction of bioparameters retaining mechanical properties.

The series of phosphate and silica-phosphate layers on the mentioned bases were obtained using sol-gel and electrophoresis methods. The selection of sol/suspension composition, time of depositing and layer heating treatment conditions have the conclusive influence on the layers parameters. The obtained layers are amorphous or nearly amorphous (what was checked using XRD analysis). The chemical composition of the layers was estimated on the base of SEM with EDX measurements.

All the samples were soaked in standard simulated body fluid (SBF) [1]. Amorphous hydroxyapatite growing on the samples surface was expected. FT IR spectroscopy with mathematic treatment of the spectra (BIO-RAD Win IR program, Arithmetic-subtract function) was used to detect the increase or decrease of any phosphate phases. On the base of FT IR results the processes of hydroxyapatite growing or layer solution were estimated.

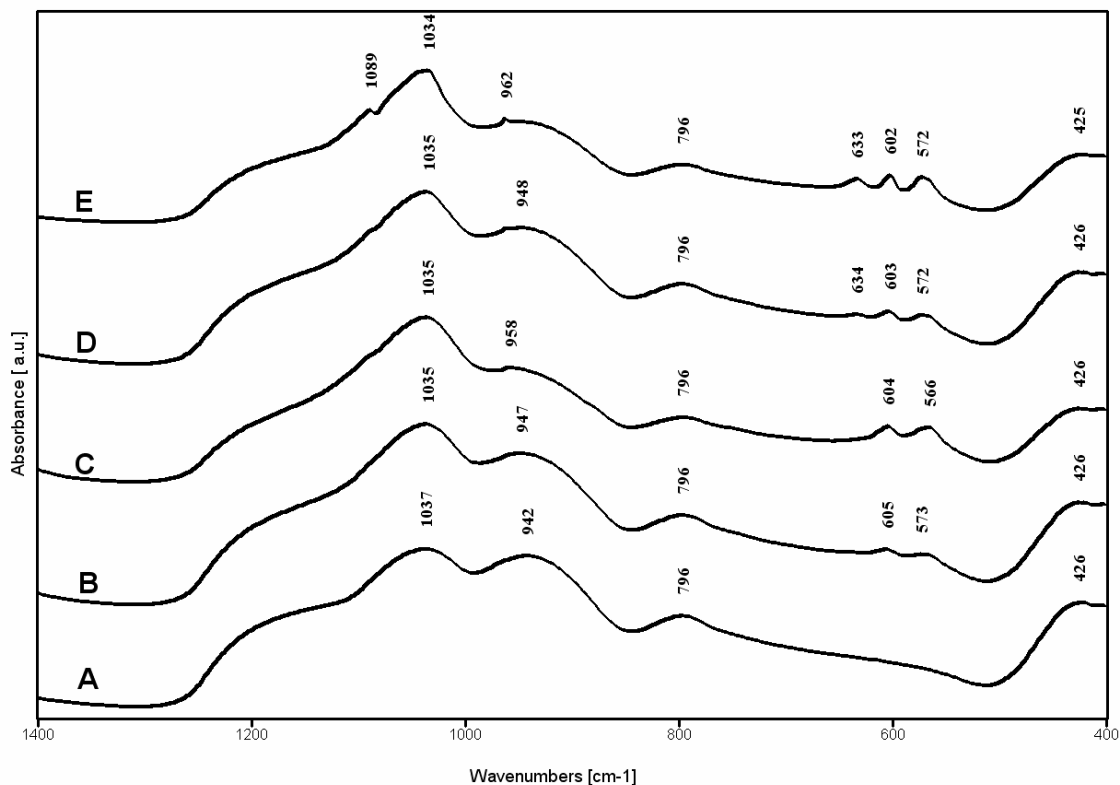


Fig. 1: MIR spectra of samples on titanium base: A) Si-Ti sublayer, B) Si-Ti + electrophoresis HAp (pure base), C) sample B after SBF soaking, D) Si-Ti + electrophoresis HAp (nitriding base), E) sample D after SBF soaking

[1] T. Kokubo: *Novel Bioactive Materials Derived from Glasses*. Proc. Int. Congress Glass, Madrid, 7 (1992) 119.

Systematic Study of Hydration Patterns of Phosphoric (V) Acid and Its Mono-, Di- and Tripotassium Salts in Aqueous Solution

Maciej Śmiechowski, Emilia Gojło, Janusz Stangret

*Department of Physical Chemistry, Chemical Faculty, Gdańsk University of Technology,
Narutowicza 11/12, 80-952 Gdańsk, Poland
e-mail: msmiech@chem.pg.gda.pl*

The phosphate anions are of crucial importance in biological systems. Their universal role in the proper functioning of living organisms cannot be underestimated. Phosphates also find numerous applications in agricultural industry (as fertilizers), food industry (as soft drink additives) and cosmetic industry (as components in detergents and cleaning agents). Particularly, the dihydrogenphosphate anion plays a key role in the metabolic pathways, but all other phosphate forms present at varying acidity of the medium should be taken into account and thoroughly studied. Potassium is the most suitable cation of choice in this study, since its tendency to form ion pairs with phosphate anions appears to be negligible [1].

Ionic equilibria between the phosphate anions are complicated and involve multiple species and complexes [2]. The dihydrogenphosphate and hydrogenphosphate salts yield more than 99% of the principal anionic form, when dissolved in water. However, in the case of the phosphate anion, as well as phosphoric acid, the contribution of different phosphate forms is non-negligible, as predicted by simple balance based on H_3PO_4 dissociation constants [3].

Fourier transform infrared (FTIR) spectroscopy is a useful technique allowing the study of solute hydration. It has been successfully applied to study a wide range of electrolytes. By using isotopic dilution technique, HDO spectra can be obtained that are free from interpretative and experimental difficulties connected with H_2O spectra. The application of the difference spectra method proposed in our laboratory for results' analysis allows separation of the spectra of solute-affected HDO [4]. Here we apply FTIR spectroscopy of the OD band of HDO molecules to perform a systematic study of various phosphate forms in the order of decreasing protonation: $\text{H}_3\text{PO}_4 \rightarrow \text{KH}_2\text{PO}_4 \rightarrow \text{K}_2\text{HPO}_4 \rightarrow \text{K}_3\text{PO}_4$.

The position at maximum of the principal anion-affected HDO band for potassium phosphates moves in the order KH_2PO_4 (2614 cm^{-1}) > K_2HPO_4 (2447 cm^{-1}) > K_3PO_4 (2300 cm^{-1}) and remains in accordance with the previously determined linear dependence of OD band position on the polarizing power of the anion [5]. The number of moles of water affected by one mole of solute (N) equals 11.0, 11.9 and 16.2, respectively. The high coordination number of PO_4^{3-} in water has been recently inferred from neutron scattering studies [6]. Other important finding is that the isotopic substitution occurs also on the phosphate anions and phosphoric acid. The thus formed P-O-D groups interact with water molecules via strong hydrogen bonds and the relative strength of this interaction decreases with increasing anion charge. This and other plausible assignments of OD bands of HDO have been confirmed by calculating equilibrium structures of small aqueous clusters of the studied individuals utilising Density Functional Theory (DFT) with hybrid B3LYP functional and triple-zeta quality 6-311++G(d,p) basis set.

- [1] C.M. Preston, W.A. Adams, *J. Phys. Chem.* 83 (1979) 814-821.
- [2] J. Baril, J.-J. Max, C. Chapados, *Can. J. Chem.* 78 (2000) 490-507.
- [3] D.R. Lide (Ed.), *CRC Handbook of Chemistry and Physics*, 80th ed., CRC Press, Boca Raton, 1999, pp. 8-44-8-48.
- [4] J. Stangret, T. Gampe, *J. Phys. Chem. B* 103 (1999) 3778-3783.
- [5] J. Stangret, T. Gampe, *J. Phys. Chem. A* 106 (2002) 5393-5402.
- [6] P.E. Mason, J.M. Cruickshank, G.W. Neilson, P. Buchanan, *Phys. Chem. Chem. Phys.* 5 (2003) 4686-4690.

Application of Raman Spectroscopy for Breast Cancer Diagnosis

Jakub Surmacki¹, Beata Brożek-Płuska¹,
Halina Abramczyk¹, Zbigniew Morawiec², Marek Tazbir²

¹ Institute of Applied Radiation Chemistry, Laboratory of Laser Molecular Spectroscopy,
Technical University of Lodz, The Faculty of Chemistry, Wroblewskiego 15, 93-590 Lodz, Poland
e-mail: jsurmacki@mitr.p.lodz.pl

²Kopernik Hospital, Oncology Ward, Paderewskiego 4, 93-513 Lodz, Poland

The Raman spectra of normal, malignant and benign lesions tissues obtained from the human breast surgeries have been studied. Raman and fluorescence spectra have been recorded for *ex vivo* samples from 80 patients. Spectra were analyzed using principal component analysis (PCA) and Matlab.

The results demonstrate the ability of Raman spectroscopy to detailed description of cancer tissue and distinguish between normal, malignant and benign types. Our results demonstrate that the spectra of normal tissue are dominated by lipids and carotenoids [Fig. 1]. Moreover, the analysis of the carotenoids bands combined with the auto-fluorescence of the time allows confirming the cancer diagnosis [1-2].

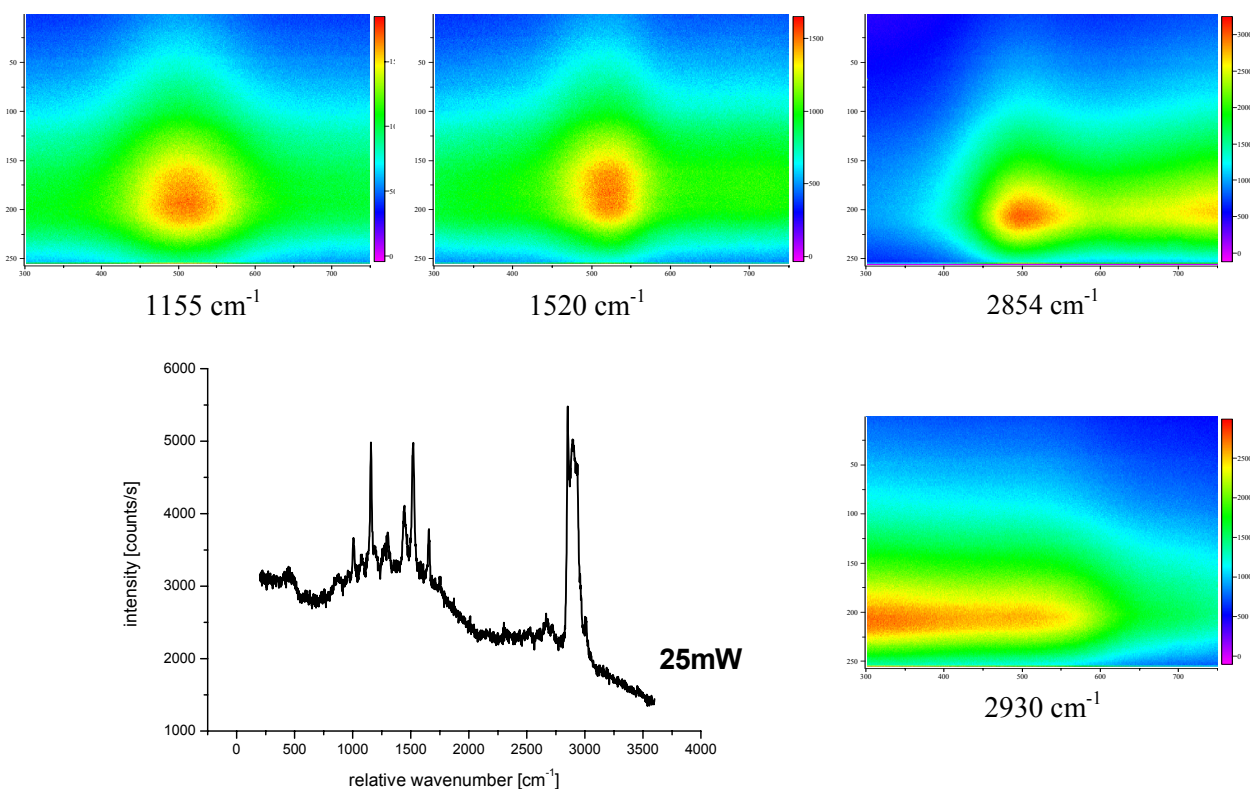


Fig. 1: Raman spectra of healthy tissue

- [1] H. Abramczyk, B. Brożek-Płuska, K. Kurczewski, Z. Morawiec, M. Tazbir: *From femtosecond dynamics to breast tissue diagnosis by Raman spectroscopy and Raman Imaging*. ISRPS Bulletin 20 (2008) 37.
- [2] H. Abramczyk, I. Placek, B. Brożek-Płuska, K. Kurczewski, J. Surmacki, Z. Morawiec, M. Tazbir: *Human breast tissue cancer diagnosis by Raman spectroscopy*. Spectroscopy 2008 in print.

Acknowledgment

The support from MEXC-CT-2006-042630 and Nr3 T11E 04729 projects are acknowledged.

Investigations on Deuterium's Grade of Substitution in the Swiss Mice's Body at the Administration of Deuterium Depleted Mediums

Radu Tamaian, Ioan Ștefănescu, Roxana Ionete

National R & D Institute for Cryogenics and Isotopic Separation – I.C.I.T. Râmnicu Vâlcea
Uzinei Street No. 4, PO 4, BOX 10, Zip Code 240050, Rm. Vâlcea, România
e-mail: tradu@icsi.ro

In over 70 years which have passed since deuterium was discovered in natural water [1] many experiments were made for the statement of its effects on living matter. The replacement of the hydrogen with deuterium represents an environmental alteration at which the organism (*in vivo*), respectively the cells (*in vitro*) if they can't accommodate will disappear. In this way deuterium's isotopical abundance variations can be compared with the environmental stress factors (temperature's variations, nourishment quantity, pollutants, radiations, etc.)

It was demonstrated that while the normal quantities didn't have harmful effects, the increase of ambiental deuterium concentration (in culture mediums, development medium, etc), respectively the increase of deuterium's intrinsic concentration through several methods determines structural, metabolic and functional alterations in different grades [2, 3, 4].

In comparison with the biological modifications produced by the deuterium excess in water, concentration reduction effects are less studied. The few data published concern the fibroblasts' growth rhythm inhibition in the culture and the development of the tumours transplanted at rats [5, 6], the growth of basal tone and of vascular reactivity at rat [7] and the growth of defense capacity of the organism and of rats' resistance at radiations [8]. General aspect of the induced general reactivity modifications at prolonged administration of deuterium depleted water was of stimulation of the general reactivity, reduction of harmful effects of different noxious agents, especially of those which act through the intensification of the oxidative metabolism or through the induction of oxygen's free radicals.

Starting with those observations, it was proposed the study of deuterium's substitution grade by hydrogen at the prolonged administration of water with low content in deuterium at Swiss mice. The results show that in natural conditions, the organism has the tendency to accumulate deuterium; the grade of deuterium depletion seems to be under influence both of specimen genotype and phenotype and behavior, and also of deuterium's depleting medium concentration (which's effect is cumulated in time).

- [1] H.C. Urey, F.G. Brickwedde, G.M. Murphy, Phys. Rev. 39 (1932) 164.
- [2] W. Buzgariu, M. Caloianu, S. Lazăr, Rom. J. Bio. Sci. 1 (1997) 5-6.
- [3] A. Kaneko, K. Moritake, Y. Kimura, Neurol. Res. 27:4 (2005) 446-451.
- [4] D.A. Dufner, I.R. Bederman, D.Z. Brunengraber, N. Rachdaoui, F. Ismail-Beigi, B.A. Siegfried, S.R. Kimball, S.F. Previs, Am. J. Physiol. Endocrinol. Metab. 288:6 (2005) E1277-E1283
- [5] G. Somlyai, G. Jancso, G. Jakli, K. Vass, B. Barna, V. Lackics, T.M. Gaal, FEBS Lett. 317 (1993) 1-4.
- [6] G. Somlyai, G. Laskay, T. Berkenyi, G. Jakli, G. Jancso, Naturally occurring deuterium may have a central role in cell signaling. John Wiley and Sons Ltd., 1997, pp. 137-141.
- [7] I. Hăulică, M. Peculea, I. Ștefănescu, Gh. Tițescu, M. Todiraș, W. Bild, Rom. J. Physiol. 35:1-2 (1998) 25-32.
- [8] W. Bild, I. Ștefănescu, I. Hăulică, C. Lupușoru, Gh. Tițescu, R. Iliescu, V. Năstasă, Rom. J. Physiol. 36:3-4 (1999) 205-218.

Raman Spectroscopy Investigation on Metal-Metallothionein Complexes

A. Tinti¹, J. Domènech^{2,3}, S. Atrian³, M. Capdevila⁴, A. Torreggiani²

¹Dep. Biochemistry, Univ. Bologna, Via Belmeloro 8/2, 40126 Bologna, Italy; ²I.S.O.F., National Council Research, Via P. Gobetti 101, 40129 Bologna, Italy; ³Dep. Genètica, Univ. Barcelona, Av. Diagonal 645, 08028 Barcelona, Spain; ⁴Dep. Química, Universitat Autònoma de Barcelona, 08193 Barcelona (Bellaterra), Spain

Metallothioneins (MTs) are low molecular weight, cysteine-rich proteins with an exceptional heavy metal coordination capacity. Because of their ability to bind metals and to scavenge oxidant radicals, MTs are considered to play a role in metal homeostasis, metal detoxification and control of the oxidative stress. Their high heterogeneity, metal binding abilities and primary structure suggest very diverse functional specializations. Structural and functional studies have been mainly devoted to vertebrate MTs. Participation of metal ligands other than Cys and the presence of secondary structure elements in metal-MT complexes are fairly unknown, especially in non-vertebrate MTs. Recently, it has been shown that other ligands can participate in metal coordination; two main ligand types have been identified: endogenous, as His residues and exogenous, as inorganic ions (i.e. S²⁻ or Cl⁻).

In vivo-synthesized Zn-MTs, representative of different families (mollusc, insect, nematode, echinoderm, vertebrate and plant, enclosing the mammalian MT1 isoform), were heterologously synthesized in *E.coli* and studied by analytic and spectroscopic techniques. The examined MTs (CeMT2, MeMT, SpMTA, MtnB, QsMT and MT1) contain 43-73 a.a., among which at least a 30% are Cys. To evaluate the influence of the metal on the MT structure, also the Cd-QsMT was synthesised and analysed in comparison with Zn-QsMT. Almost all the MTs considered are devoid of aromatic residues (only Phe in SpMTA and QsMT, Tyr in CeMT2, and His in CeMT2 and QsMT) and contain variable amounts of metal and S²⁻ ions, quantitatively evaluated by acid ICP-AES and GC-FPD measurements. The formation of more than one species (S²⁻-containing and S²⁻-devoid complexes), revealed by ESI-MS spectra, was evident for all the MTs.

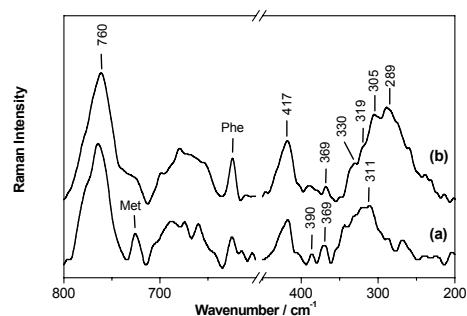


Fig. 1: Raman spectra of (a) Zn-QsMT and (b) Cd-QsMT.

The Raman spectra gave information about the structure of the metal-MT aggregates. In particular, the presence of secondary structure elements was determined: for the examined MTs isoforms, a relevant contribution of β -sheet and β -turns was shown, whereas the α -helix content resulted almost negligible. As regards Cys sulfurs, almost all Cys were involved in the metal coordination, as indicated by several bands attributable to metal-S stretching modes at low wavenumbers ($< 500 \text{ cm}^{-1}$) (Fig. 1). In particular, the high number of ν M-S bands, as well as their broadening, suggest the formation of different metal centres. Raman bands markers of sulfide bridging ligands were also identified. In Zn-

CeMT2 and Zn-QsMT the eventual participation of the His residue in metal binding was evaluated through a curve fitting analysis of the $1630\text{-}1565 \text{ cm}^{-1}$ region (Fig. 2). By considering the integrated intensity of the bands, it can be concluded that His residues are mainly coordinated in Zn-CeMT2 ($\approx 90\%$), whereas in Zn-QsMT His is mainly present as free tautomer ($\approx 90\%$). The combination of analytical and spectroscopic techniques has been highly informative for the analysis of *in vivo*-synthesized metal-MT complexes; Raman studies revealed one of the most promising experimental strategies to provide new data on the knowledge of the metal binding behavior of MTs from the most diverse organisms.

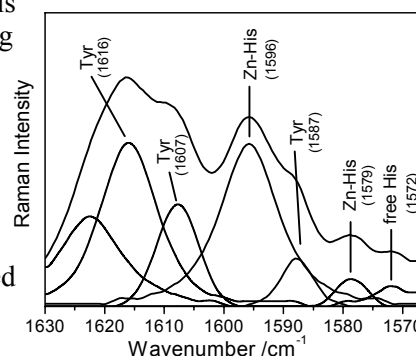


Fig. 2: Curve fitting analysis of His-containing Zn-CeMT.

3. NANOSTRUCTURED MATERIALS

Characterization of Carbon Thin Films Prepared by the Thermal Decomposition of Spin Coated PAN Films

M. Darányi, Á. Kukovecz, Z. Kónya, I. Kiricsi

*Department of Applied and Environmental Chemistry, University of Szeged,
Rerrich B. tér 1, Szeged, H-6720 Hungary*

Carbonaceous thin films are intensely researched today because of their potential applications in e.g. optics, heat transfer and tool coatings. Molecular spectroscopy is well-suited for monitoring the thermal decomposition of polymers. Variations in the intensity and the position of Raman [1] and infrared peaks are correlated with structural changes taking place in polyacrylonitril (PAN) carbon membranes during heat treatment (Table 1).

We built thin films by spin coating glass and quartz substrates with a 10 % PAN solution in N,N-dimethylformamide and carbonizing the layer in N₂ at different temperatures. Carbonization was catalyzed by transition metal ions such as iron, cobalt and nickel. The synthesized films were characterized by IR and Raman spectroscopy (Fig. 1), scanning electron microscopy and ellipsometry.

Table 1: Raman shifts and functional groups.

Raman shift (cm⁻¹)	2936	2245	1455	~1600	1582	1320
Functional group	CH ₂	C≡N	CH ₂	C=C, C=N	G peak	D peak

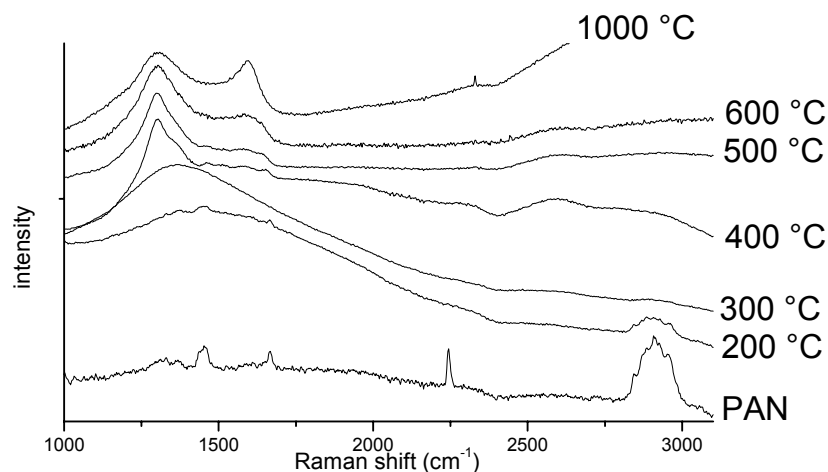


Fig. 1: Raman spectra of the carbonized samples without metal ions.

We report on the effects of carbonization temperature and metal concentration on the morphology, composition and electronic properties of the formed carbon layer. The temperature threshold for PAN decomposition is ~500 °C. Thinner carbon films can be prepared by increasing the Ni²⁺ contents of the precursor solution.

[1] G. Xue, J. Dong, J. Zhang, *Macromolecules* 25 (1992) 5855-5857.

High Temperature Raman Spectroscopy of Titanate Nanotubes

A. Gajović¹, I. Friščić^{1,*}, M. Plodinec^{1,*}, D. Iveković²

¹Ruđer Bošković Institute, Bijenička 54, HR-1002 Zagreb, Croatia, gajovic@irb.hr, ² Faculty of food technology and biotechnology, University of Zagreb, Zagreb, Croatia, *graduate students of Department of Physics, Faculty of Science, University of Zagreb, Bijenička 32, HR-10000 Zagreb, Croatia,

In last few years, properties of titanate nanotubes were extensively studied due to their potential applications in solar cells, electronics, chemical sensors, (photo)catalysis, hydrogen sensing and as mesoporous material for ion exchange. Titanate nanotubes are especially interesting because of their high aspect ratio and high specific surface area. Although there are some ambiguities regarding the exact structure and chemical composition of titanate nanotubes, it is generally accepted that the nanotubes have a layered titanate structure. An interlayer space of about 8 Å is occupied by water molecules and alkali metal cations. However, the mechanism of nanotube formation and growth are still the subject of the numerous studies. In this work the formation of titanate nanotubes are discussed in the view of different TiO₂ precursors. The thermal stability of prepared nanotubes has been studied *in situ* at high temperatures. The influence of Na⁺ content on the thermal stability of titanate nanotubes is also considered in details.

Titanate nanotubes were synthesized by hydrothermally treating the TiO₂ powder with NaOH solution. The starting precursors for nanotube synthesis were anatase or the mixture of anatase, rutile, and high-pressure TiO₂II phase (TiO₂-II) as a major component. The samples with various Na/Ti ratios were prepared by ion-exchange of interlayer Na⁺ cations with H⁺ ions under controlled pH conditions. The structural changes in the nanotubes induced by the thermal treatment were studied *in situ* by Raman spectroscopy (RS) and transmission electron microscopy (TEM). The morphology and the microstructure of the nanotubes before and after the thermal treatment in heating stage for RS were additionally examined by TEM and selected area electron diffraction (SAED).

We found that hydrothermal treatment of mixture of TiO₂ phases (anatase, rutile, and TiO₂-II) leads to the formation of titanate nanotubes with structure and morphology similar to the nanotubes obtained from pure anatase, as observed both by RS and TEM. However, the temperature stability of nanotubes prepared from mixtures containing TiO₂-II was much lower. These nanotubes undergo phase transition to anatase at temperatures lower than 100 °C, while, in the case of nanotubes obtained from anatase precursor, Raman bands characteristic for titanate nanotubes were visible up to 300 °C. At 500 °C titanate nanotubes in H-form were completely transformed to anatase. Furthermore, titanate nanotubes in Na-form showed even better thermal stability – tubular structure was preserved to the temperatures as high as 500 °C. Phase transformation temperatures observed for nanotubes prepared from anatase are in good agreement with X-ray diffraction results reported by E. Morgano Jr. et al. [1].

[1] E. Morgano Jr., M.A.S. de Abreu, O.R.C. Pravia, B.A. Marinkovic, P.M. Jardim, F.C. Rizzo, A.S. Araújo, Solid State Sciences 8 (2006) 888.

Raman Spectroscopy: Close to the Laser Line

M. Galvin, G. Doyle, B. Ashall, D. Zerulla

UCD Dublin, Belfield, Dublin, Ireland

Raman Spectroscopy is a powerful tool for investigation of the vibrational structure of a variety of materials. We have a triple monochromatic system for attaining the Raman spectra of a variety of samples including Single Walled Carbon Nanotubes (SWCNT's) and proteins bound to gold nanoparticles. The value of the triple monochromator system is that we are capable of achieving spectra down to very low energies ($\sim 50\text{cm}^{-1}$). This is due to the subtractive double monochromator which acts as a filter, replacing the standard notch-filter most commonly used in Raman Spectroscopy.

This setup allows us to investigate low frequency vibrations of any Raman active sample to a very high resolution ($\pm 1\text{-}3\text{cm}^{-1}$). Raman spectra of swcnt's in aqueous solution and proteins (achieved using Surface Enhanced Raman Spectroscopy (SERS)) are presented.

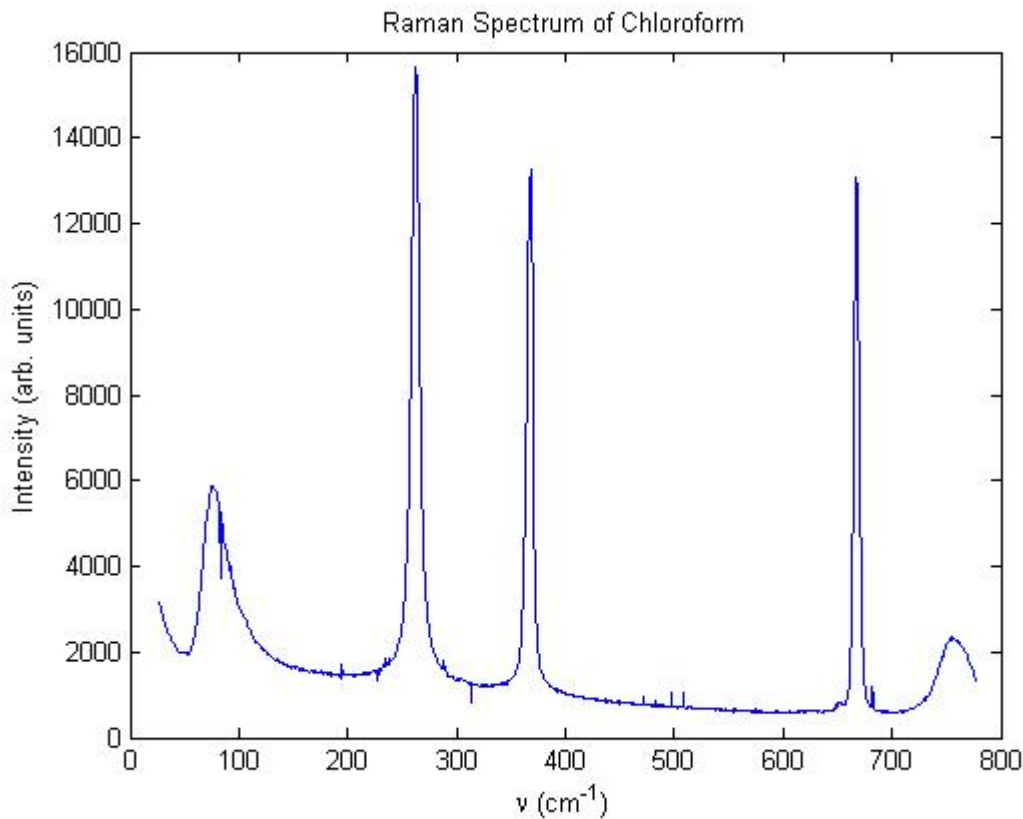


Fig. 1: Raman Spectrum demonstrating the low energy vibrations of chloroform.

- [1] M.J. Longhurst, N. Quirke: *Pressure Dependence of the Radial Breathing Mode of Carbon Nanotubes: The effect of Fluid Adsorption*. PRL 98 (2007) 145503.

Vibrational Quantization in Semiconductor Nanocomposites

Sanjeev K. Gupta, Prafulla K. Jha

Department of Physics, Bhavnagar University, Bhavnagar -364 002, India

Semiconductor nanoparticles embedded in borosilicate glass matrix have generated considerable attention in last few years due to their wide range of applications and an important model system in the study of 3-D quantum confinements. As size is reduced in a nanoparticle; the electronic structure is modified as compared to the bulk with the oscillator strength concentrated into a few discrete transitions. Aside from modifying the electronic structure, confinement also affects coupling to optical and acoustical phonons.

In the present presentation we present a low frequency Raman scattering of $\text{CdS}_x\text{Se}_{1-x}$ and $\text{CdTe}_x\text{Se}_{1-x}$ nanocrystals embedded in borosilicate glass for various compositions and sizes. The peaks obtained in the experimental low frequency Raman spectra have been analysed by three different theoretical models. We have been able to observe the overtone of phonon mode and torsional mode against the selection rule. We attribute the presence of torsional mode to the nonspherical shape of particle confirmed by the HRTEM result.

Spectroscopy of Nanohybrids Formed by Carbon Nanotubes and Biomolecules

V.A. Karachevtsev

B.I. Verkin Institute for Low Temperature Physics and Engineering, 47 Lenin ave., Kharkov 61103, Ukraine

Bionanohybrids based on single-walled carbon nanotubes (SWNT) attract the particular interest of scientists due to their promising application for creating the new generation biosensors. In this report we reviewed our study of the carbon nanotubes and fragmented single- and double-stranded genomic DNA (fss- or fds-DNA) hybrids. We employed near IR luminescence and resonance Raman spectroscopy to control SWNTs as well as the UV absorption spectroscopy to observe DNA behavior [1-4]. As follows from these measurements, thermostability of DNA increased after its adsorption on the nanotube surface. The model of the fds- DNA:SWNT hybrids formation was suggested. It was found that the long single-stranded polymer at high concentration can wrap around the nanotube in several layers forming a strand-like spindle [4]. The hybrids of SWNTs with the biopolymer wrapped around them were simulated by molecular dynamic method and it was shown that such structures are stable.

SWNTs film obtained from deposition of the aqueous suspensions containing fss-DNA and nanotubes was investigated too [1]. SWNT:DNA film yields luminescence which indicates the presence of individual tubes or small bundles in the film. The luminescence bands of SWNTs:DNA film are relatively wider than in the aqueous suspension and is attributed to the increasing interaction of DNA with the nanotube surface in the solid state.

In this report we demonstrated a new approach for immobilization of glucose oxidase (GOX) on DNA-wrapped SWNTs [2, 3]. The DNA interface between the enzyme and nanotube keeps the enzyme activity, which usually decreases when the enzyme is directly bound to the nanotube. The sensing of the glucose concentration in aqueous solution with SWNTs:DNA:GOX hybrids was detected by the luminescence intensity of semiconducting nanotubes.

Hybridization of the free polynucleotide (poly(rU)) with complementary poly(rA) adsorbed to the SWNT surface was studied in the aqueous suspension. The appearance of the double-stranded polymer is confirmed with the characteristic S-like form of its dependence of UV light absorption of polymers on the temperature in the range 20-90 °C (melting curve). However, melting temperature of this polymer is decreased in comparison with the free poly(rA)·poly(rU). In contrast, adsorption of the initial double-stranded poly(rA)·poly(rU) on the nanotube surface leads to thermostabilization of the polymer, at which melting temperature increases (by about 6 °C). This result indicates that poly(rU) hybridization with poly(rA) adsorbed to the SWNT surface occurs with defects because of essential π - π stacking interaction between nitrogen bases and the nanotube surface, which hinders the usual hybridization process. Computer modeling demonstrates different possible structures of hybridized polymers on the nanotube surface. An application of bionanohybrids for development of sensitive biosensors with miniaturized analytical systems is discussed.

- [1] V.A. Karachevtsev, A.Yu. Glamazda, U. Dettlaff-Weglikowska, V.S. Leontiev, P.V. Mateichenko, S. Roth, and A. M. Rao, *Carbon* 44 (2006) 1292-1297.
- [2] V.A. Karachevtsev, A.Yu. Glamazda, V.S. Leontiev, O.S. Lytvyn and U. Dettlaff-Weglikowska, *Chem. Phys. Lett.* 435 (2007) 104-108.
- [3] V.A. Karachevtsev, A.Yu. Glamazda, M.V. Karachevtsev, O.S. Lytvyn, and U. Dettlaff-Weglikowska, *Proc. SPIE* 6796 (2007) 679625 (7 pages).
- [4] M.V. Karachevtsev, O.S. Lytvyn, S.G. Stepanian, V.S. Leontiev, L. Adamowicz, and V.A. Karachevtsev, *J. Nanosci. Nanotechnol.* 8 (2008) 1473-1480.

Influence of Crystallization on the Electronic Conductivity of Iron Phosphate Glasses

V. Ličina¹, A. Moguš-Milanković¹, Ž. Skoko², S. Musić¹, M. Ivanda¹

¹Ruđer Bošković Institute, Bijenička c. 54, 10000 Zagreb, Croatia

²Department of Physics, Faculty of Science, University of Zagreb, Bijenička c. 32, 10000 Zagreb, Croatia

Electronically conducting glasses of the composition $43\text{Fe}_2\text{O}_3\text{-}57\text{P}_2\text{O}_5$ were analyzed by Raman spectroscopy, XRD analysis and scanning electron microscopy (SEM). The main crystalline phases formed during thermal treatments are $\text{Fe}_3(\text{P}_2\text{O}_7)_2$, FePO_4 and $\text{Fe}_4(\text{P}_2\text{O}_7)_3$ [1]. The effects of the annealing of iron phosphate glasses on their electrical conductivity were studied by impedance spectroscopy. The electrical conductivity was measured for as-quenched glass and after thermal treatments up to 804. The presence of crystalline $\text{Fe}_3(\text{P}_2\text{O}_7)_2$ grains formed after thermal treatment at temperature close to the first crystallization temperature, T_{C1} , 590 °C, enhances the electrical conductivity as compared with the as-quenched glass. This conductivity enhancement is related to the conduction at the interfaces between the crystallites and glassy phase [2]. Further thermal treatment at higher temperature, T_{C1} , 724 °C and 804 °C leads to formation of ferric orthophosphate, FePO_4 along with pronounced growth of $\text{Fe}_4(\text{P}_2\text{O}_7)_3$. Electrical conductivity of this glass-ceramics decreases. The decrease in electrical conductivity is explained by a considerable weakening in the interactions between Fe sites in crystalline glasses, caused by poorly defined conduction pathways. This is result of the presence of larger crystalline grains and disappearance of glassy matrix in fully crystallized sample. Formation of microcrystallites causes a drop in conductivity due to the reduction of grain boundary region suggesting that the conductivity depends on the electron hopping in crystalline phases.

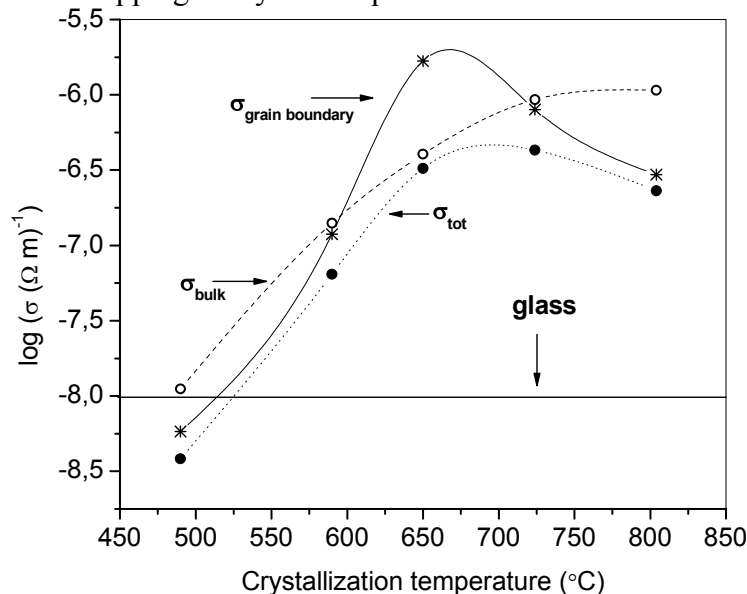


Fig. 1: Dependence of electrical conductivity of the grains, grain boundaries and total electrical conductivity upon the temperature of thermal treatment of the crystallized samples

[1] A. Moguš-Milanković, M. Rajić, A. Drasner, R. Trojko, D.E. Day, *Phys. Chem. Glasses* 39 (1998) 70-75.

[2] B. Roling, S. Murugavel, *Z. Phys. Chem.* 219 (2005) 23-33.

Ring-, Branchy-, and Cage-Like As_nS_m Nanoclusters in the Structure of Amorphous Semiconductors: *ab initio* and Raman Study

R. Holomb, V. Mitsa

Research Institute for Solid State Physics and Chemistry, Uzhhorod National University, Uzhhorod 88000, Ukraine, e-mail: holomb@ukr.net, mitsa@univ.uzhgorod.ua

The conceptual statements of topological-cluster structure of non-crystalline semiconductors related with the change in the connectivity of the structure matrix and physical properties depending on the average coordination number were studied both by experimental and theoretical methods.

We here present a study of different type As_nS_m nanoclusters ($n = 1-6$; $m = 3-6, 8, 10, 12$) which realization in the amorphous structure is possible. The differences in geometry structure and chemical bonds in clusters cause the changes of their physico-chemical properties. Therefore, the formation energy, stability, electronic, optical, and vibrational properties of such clusters were calculated from the first-principles and were analyzed.

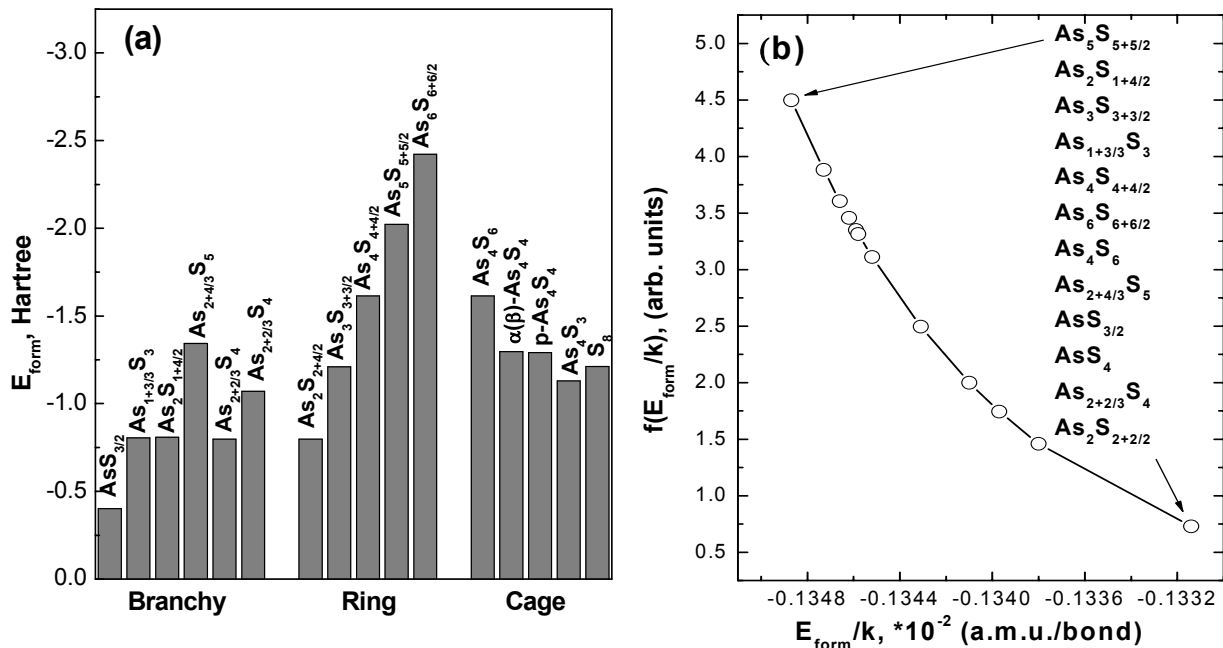


Fig. 1: Formation energy (E_{form}) and Boltzmann distribution of E_{form}/k (k is a number of bonds) values of $As_nS_m(S_8)$ clusters (b).

The physical and technological conditions under which the structure of amorphous film reaches the structure of the corresponding bulk glass or essentially differs from it have been revealed. The experimental spectra of amorphous arsenic sulphides were interpreted by using the results of *ab initio* calculations of the vibration spectra of As_nS_m nanoclusters with taking into account their relative stability.

Spectroscopic Characterization of Two-photon Generated CdS Nanoparticles in Sol-gel Zirconia Thin Films

Katarzyna Raulin¹, Odile Cristini¹, P. Baldeck³, Sylvia Turrell¹, Bruno Capoen² and Mohamed Bouazaoui²

¹Laboratoire de Spectrochimie Infrarouge et Raman (CNRS, UMR 8516), Bât. C-5,

²Laboratoire de Physique des Lasers, Atomes et Molécules (CNRS, UMR 8523), Bât. P-5
Centre d'Etudes et de Recherches Lasers et Applications (CERLA-FR CNRS 2416)

Université des Sciences et Technologies de Lille, 59655 Villeneuve d'Ascq, France, and

³Laboratoire de Spectrométrie Physique (CNRS, UMR 5588), 140 Avenue de la Physique BP 87 – 38402 Saint-Martin d'Hères

Nanostructured materials have many applications in the development of sub-wavelength optical components in the visible and near infrared. Up to now, the structuring of materials on a nano-scale has usually involved methods based on one of the following mechanisms: soft chemical processes for self-organization of nano-structures using the laws of hydrodynamics or random precipitation of nanocrystals during thermal treatment. On the contrary, the present work aims to master the *in situ* creation and the localized organization of CdS nanoparticles (NPs) in a sol-gel matrix by controlling the growth with an optical beam.

The best way to achieve crystal growth on the submicron scale is to avoid any thermal effects which might induce a broad energy dispersion. For this reason, two-photon absorption (TPA) with a focused ultra-short laser beam is particularly adapted. In this communication, we present first results on TPA-assisted organized growth of CdS semiconductor NPs in ZrO₂ sol-gel thin films and on their optical properties.

The ZrO₂ matrix is of particular interest because of its excellent mechanical, thermal and optical properties. Particularly interesting for waveguiding applications are its high refractive index and its low temperature of densification. The films were dip-coated on cover-glass slides using sols containing the CdS precursors and eventually a photo-initiator like carbazole. The NPs were created through TPA dissociation of the precursors and were spectrally analyzed *in situ* using a femtosecond laser ($\lambda_{\text{ex}} = 740$ nm). The formation kinetics of the CdS NPs can be followed using time-resolved photoluminescence spectra (Fig. 1). The systems obtained were also characterized using micro-Raman spectroscopy, a fully suitable tool for verifying the presence of CdS NPs in the matrices, even at low concentrations (Fig. 2).

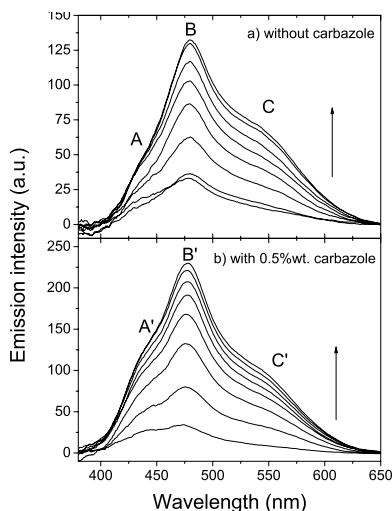


Fig. 1: The PL spectra of ZrO₂:CdS samples ($\lambda_{\text{ex}}=740\text{nm}$, $P=6\text{mW}$), $t_0 : 500\text{ms}$, acquisition each second

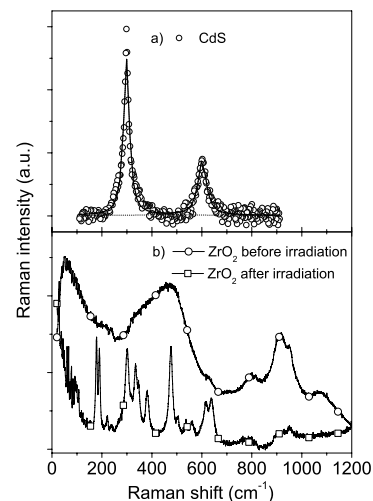


Fig. 2: Raman spectra of a) CdS created by TPA ($\lambda_{\text{ex}}=488$ nm) and of b) ZrO₂ structure transformed by insolation ($\lambda_{\text{ex}}=514$ nm)

Spectroscopic Studies of Energy Transfer between Semiconductor Nanoparticles and Eu^{3+} Ions in Silica Gels

O. Robbe-Cristini¹, K. Raulin¹, B. Capoen², M. Bouazaoui², S. Turrell¹

¹ *Laboratoire de Spectrochimie Infrarouge et Raman (CNRS, UMR 8516), Bât. C-5, and*
² *Laboratoire de Physique des Lasers, Atomes et Molécules (CNRS, UMR 8523), Bât. P-5, Centre d'Etudes et de Recherches Lasers et Applications (CERLA-FR CNRS 2416), Université des Sciences et Technologies de Lille, 59655 Villeneuve d'Ascq, France*

Porous silica-based materials receive widespread attention with much current interest focused on the optical properties of nanoporous sol-gel silica glasses and the potential development of such glasses for photonic applications. The doping of these systems with rare earth ions (RE) or semiconductor nanoparticles (NP) can lead to the development of improved optical amplifiers or displays. The sol-gel technique presents advantages for the preparation of nanoporous vitreous oxides, allowing the control of the transparency and of the nanoporous structure of the derived materials. Adjustment of the composition and of the heat-treatment of the gels can be used to control their porous structure (which can be followed using Raman spectroscopy), thus permitting post-doping with various species like active ions and NP. The pores of the host matrix can also control the NP size, an important factor since the optical properties of semiconductor NPs result from the size-dependant quantum confinement effects of NP clusters.

In the present work, silica xerogels were synthesized using base-catalysis. After a heat treatment at 850°C, the resulting gels were post-doped with NP precursors. Raman and photoluminescence spectroscopic data were correlated with nitrogen adsorption-desorption measurements. With gel pore sizes ranging from 30 to 100 Å, the NP size varied from 25 to 40 Å. Raman spectral changes indicated the structural evolutions responsible for the pore-size changes and the increasing NP size resulted in a red-shift of the NP emission band.

Co-doping SiO_2 gels with semiconductor CdS NPs and Eu^{3+} RE ions can lead to efficient energy transfer from the NPs to the RE ions and a resulting increased RE emission. The changes in gel structure resulting from variations in concentration of doping agents as well as from different heat treatments have distinct effects on the RE emission. The energy-transfer presented in Fig.1, between NC and RE ions, was studied using excitation and emission photoluminescence spectroscopies.

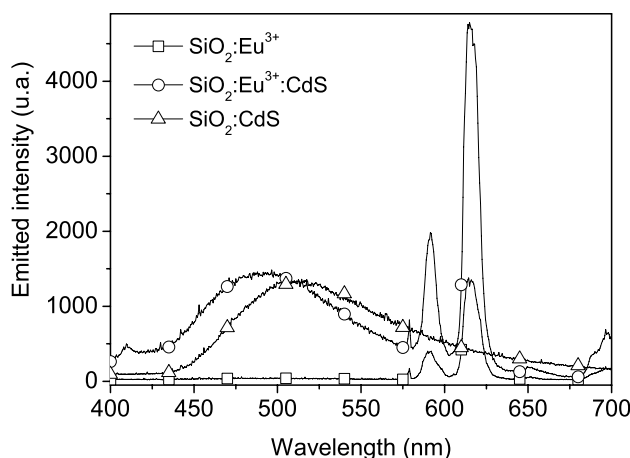


Fig. 1: Luminescence spectra of a 1% Eu^{3+} -1% CdS codoped gel and a 1% Eu^{3+} -doped gel treated at 200 °C ($\lambda_{\text{ex}}=351.1$ nm)

Magnetic Phase Transitions in Nanoclusters and Nanostructures

I.P. Suzdalev, Yu.V. Maksimov

Semenov Institute of Chemical Physics RAS, Moscow, Russian Federation

Nanoclusters and nanostructures possess new magnetic properties when compared to the bulk materials. For example, the critical cluster size exists ensuring the first order magnetic phase transitions (FOMPT) [1, 2] when cluster magnetization disappears by jump. This critical cluster size is analog the critical magnetic points (the Curie or Neel points) for the FOMPT in the bulk magnetic materials that dramatically differ from superparamagnetic behavior. In this work we deal with 3 nanosystems showing FOMPT: 1) 1-3 nm isolated iron oxide clusters localized in (A) copolymer styrene and divinylbenzen and (B) polyacryl acid and polyethylenimide matrixes, 2) 30-50 nm disordered iron oxide nanoclusters obtained at the outset of sintering, 3) 10-15 nm iron oxide nanoclusters prepared from reversed micelle and template-sending showed cluster ordered structure. We discuss thermodynamic models of magnetic phase transitions in nanoclusters taking into consideration the cluster-matrix, cluster-cluster interactions, surface tension, influence of defects and stresses and intercluster ordering.

In the system 1) the FOMPT was observed by Mössbauer spectroscopy and magnetization measurements. For the matrix (A) a weak cluster-matrix interaction was observed and the FOMPT was interpreted in terms of action of surface pressure up to 1GPa and compressibility of iron oxide clusters at the temperature range 4.2-6K. In the matrix (B) the origin of the FOMPT we discuss in terms of strong influence of cluster-matrix interaction and the influence of surface tension and magnetic anisotropy in the vicinity 3K-6K.

Iron oxide nanosystems 2) obtained by thermal decomposition of ferric oxalate showed structure disorder. The FOMPT in these nanosystems was observed at 20 - 300K and was found to be dependent on structure defect density. Shear stress under high pressure action was the reason why a great number of iron oxide clusters have been involved in magnetic phase transition whereby the transition temperature decreased because of severe plastic deformation and structure defect generation. For nanosystem consisting of iron oxide and nanostructured metal europium the effect of plastic deformations of Eu caused first-to-second order change of magnetic phase transition accompanied by an increase in the Neel point.

In the cluster ordered system 3) we observe fivefold increase of magnetization and increase of Curie or Neel temperature than compare with disorder iron oxide nanocluster 2) and with disordered iron oxide nanoclusters obtained by aerosol technique (NaCl-Fe(NO₃)₃ thermal decomposition). The ordered nanosystem 3) again demonstrates the FOMPT. In contrary, the disordered nanoclusters obtained by aerosol technique showed only superparamagnetic behavior. As compared to NaCl-doped iron oxide nanoclusters showing superparamagnetic behavior the cluster organized iron oxide nanosystems showed considerable magnetization and coercitive force. These effects can be interpreted in terms of the FOMPT like in the system 1) and 2). The possible reason in this case is the peculiar nanocluster ordered structure with its specific Curie or Neel temperatures generated by intercluster exchange interaction.

[1] I.P. Suzdalev, V.N. Buravtsev, V.K. Imshennik, Yu.V. Maksimov, V.V. Matveev, S.V. Novichikhin, A.X. Trautwein, H. Winkler, *Z.Phys. D.* 37 (1996) 55-76.

[2] I.P. Suzdalev, V.N. Buravtsev, V.K. Imshennik, Yu.V. Maksimov, *Scripta mater.* 44 (2001) 1937-1941.

Use of Spectroscopic Techniques for Synthesis Optimisation and for the Characterisation of Optical Properties of Semiconductor Nanoparticles

S.N.B. Bhaktha¹, O. Robbe-Cristini¹, K. Raulin¹, B. Capoen², M. Bouazaoui²,
S. Turrell¹, J. Habinshuti^{1,3}, B. Grandidier³, C. Kinowski¹

¹ *Laboratoire de Spectrochimie Infrarouge et Raman (CNRS, UMR 8516), Bât. C-5, and*

² *Laboratoire de Physique des Lasers, Atomes et Molécules (CNRS, UMR 8523), Bât. P-5, Centre d'Etudes et de Recherches Lasers et Applications (CERLA-FR CNRS 2416), Université des Sciences et Technologies de Lille, 59655 Villeneuve d'Ascq, France*

³ *Institut d'Electronique et Microélectronique et de Nanotechnologie (CNRS 8520), BP 60069 Cité Scientifique –avenue Poincaré, Villeneuve d'Ascq, France*

Semiconductor nanocrystals (NCs) are studied because of their unique physical properties which are very different from those of their corresponding bulk materials and lead to strong confinement of the charge carriers and phonons and as a result, the band-gap of such materials can be tuned from the near infrared to the visible simply by changing the NC size, thus making them promising “building blocks” for a wide number of applications in photonics, biophotonics and optoelectronics.

In the first part of the present work, PbSe NCs were synthesized using a colloidal route. The resulting NCs with a narrow size distribution were characterized using TEM, absorption spectroscopic measurements as well as with micro-Raman spectroscopy. The Raman spectrum of Figure 1 shows the first-order longitudinal optical phonon and its first overtone for a NC sample, thus confirming the existence of PbSe. TEM images of the same sample showed quasi-spherical PbSe NCs of about 7 nm. The size-dependence of the position of the two Raman bands has been established and a correlation with TEM data will be presented.

In the second part, semiconductor nanocrystals of SnO₂ were used to transfer energy to rare-earth (RE) ions. In effect, if RE ions are doped into semiconductor nanoclusters with their crystal-like arrangement, then band gap excitation may result in efficient energy transfer thus yielding intense luminescence from the RE ion. In the present work, europium doped tin silicate thin-film samples were fabricated via sol-gel syntheses using the dip-coating technique. Spectroscopic investigations are carried out using mainly Raman and x-ray. Figure 2 shows the Raman spectra collected in the waveguiding configuration for samples heat-treated in air at temperatures ranging from 800 to 1100 °C. The formation and growth of nanocrystals with increasing temperature is evident from the shifts observed in the sharp crystal peak in the low frequency region. Raman data has been used to determine the size and structure of the nanocrystals.

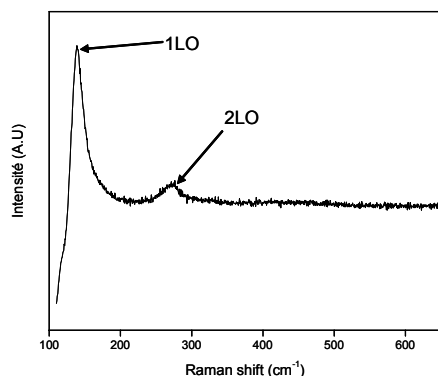


Figure 1: Raman spectrum of 7-nm PbSe NCs

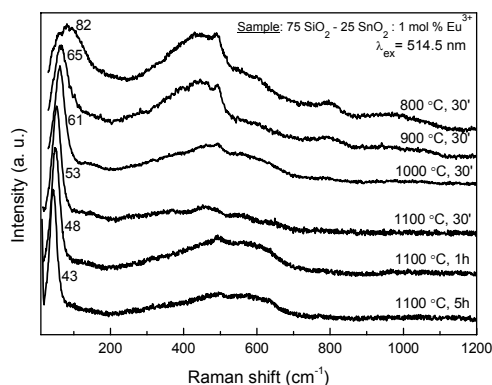


Figure 2: Raman spectra of samples as a function of annealing temperature and time.

Structural Analysis of Thin Amorphous- Nano-Crystalline Thin Films by HRTEM, GISAXS and Raman Spectroscopy

D. Gracin¹, A. Gajović¹, M. Ceh², K. Juračić¹, D. Meljanac¹, P. Dubček¹, S. Bernstorff³

¹ Ruđer Bošković Institute, 10000 Zagreb, Bijenička 54, Croatia, email: gracin@irb.hr

² Institut Jožef Stefan, Ljubljana, Jamova 37, SI1000 Slovenia

³ Sincrotrone Trieste, SS 14, km 163.5, Basovizza (TS), Italy

The series of amorphous- nano-crystalline silicon films, deposited on glass using plasma enhanced chemical vapor deposition (PECVD) method, were analysed by Raman, HRTEM (High Resolution Transmission Electron Microscopy) and GISAXS (Grazing Incidence Small Angle X-ray Scattering) spectroscopy. The crystal to amorphous volume fraction ratios, estimated from the areas under corresponding TO-like (Transversal Optical) phonon bands in Raman, varied from few to 70%. The crystalline TO peak positions were between 500 and 521 cm^{-1} which corresponds to average crystal sizes between 2 and 20 nm, considering only phonon confinement due to nano-size of crystals. However, the TO line was asymmetric and line-width was broad suggesting also the existence of smaller and larger crystals.

The size and size distribution of nano-crystals were estimated from HRTEM and compared with Raman. The results show excellent match in average individual sizes. However, the distribution was slightly different than those obtained by Raman and suggested larger contribution of smaller crystals.

GISAX of deposited samples indicated particles with Gyro radii between 2 and 6 nanometers. Larger particles are present in the samples with higher degree of crystal fraction and larger crystals. However, the samples are porous to certain degree (as concluded from optical measurements) and direct correlation between particles and crystals are not easy to establish. GISAXS obtained under variation in incidence angle allowed estimating in depth distribution of particles. For growing conditions that favor smaller nano-crystals, the individual sizes of particles were uniform going from surface towards depth of the sample and shape was spherically symmetric. For growth that resulted in larger crystals the particles were elongated parallel to the surface and smaller in the "bulk" of the samples. These results were used in discussion of difference in distributions of individual crystal sizes obtained by HRTEM and Raman.

Spectroscopic Characterization of Polysiloxane and Bridged Polysilsesquioxane Xerogels

Mariusz Barczak, Andrzej Dąbrowski

Maria Curie-Skłodowska University, Maria Curie-Skłodowska Sq. 5, 20-031 Lublin, Poland

Bridged polysilsesquioxanes are a class of hybrid organic-inorganic materials, formed by molecular building blocks. Such building units include an organic bridge linking two or more Si atoms by hydrolytically stable Si–C bonds. It is possible to design these materials on a molecular level keeping control over their chemical and physical properties, including structure-adsorption characteristics by choosing the appropriate precursors in the reaction of hydrolytic polycondensation [1]. The possibility of introduction of the organic and inorganic groups into the structure of the final structure by co-condensation of different monomers is also an invaluable advantage of the sol-gel processing of organosilicas [2].

Amino-, thiol-, urea-, phenyl-, vinyl-, isocyano-, cyano- and acetoxy- functionalized polysilsesquioxane xerogels have been obtained by co-condensation of appropriate monomers: organobis(trialkoxysilanes) and trialkoxysilanes (Fig. 1). To investigate the influence of the organic bridge on the structural properties, the polysiloxane xerogels functionalized with the same groups were synthesized by co-condensation of tetraethoxysilane and appropriate trialkoxysilanes.

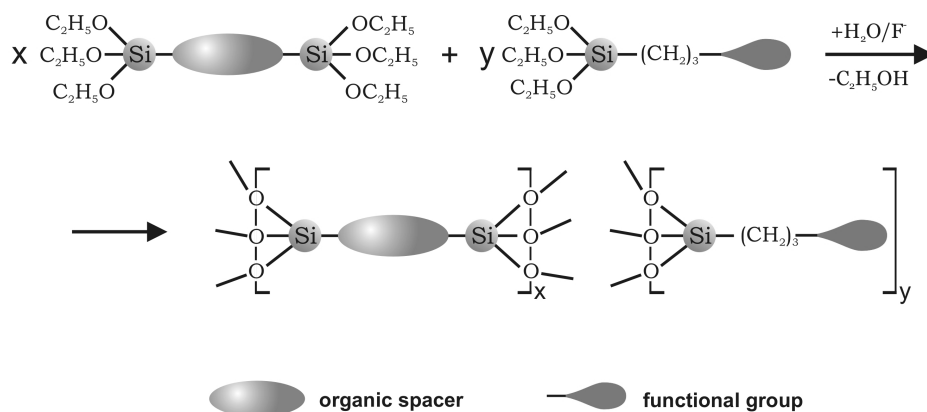


Fig. 1: Co-condensation of organobis(trialkoxysilane) and trialkoxysilane

The structure and composition of the final materials were investigated by several techniques: ^{13}C NMR, ^{29}Si NMR, FTIR and Raman spectroscopy, thermogravimetry, elemental analysis, AFM and TEM microscopy and nitrogen adsorption measurements. All of techniques used to characterize the final materials proved to be efficient and complementary tools to determine a broad spectrum of properties of xerogels studied in the present work. The spectroscopic techniques used during the studies turned out to be particularly useful in the investigation of such complex hybrid structures [2].

- [1] K.J. Shea, J. Moreau, D.A. Loy, R.J.P. Corriu, B. Boury, [in:] P. Gomez-Romero, C. Sanchez, Eds. "Functional Hybrid Materials", Wiley-VCH Verlag GmbH & Co. KGaA, Weinheim 2004.
 [2] A. Dabrowski, M. Barczak, N.V. Stolyarchuk, I.V. Melnyk, Yu.L. Zub, *Adsorption* 11 (2005) 501.

Linear IR dichroism of polyether-based polyurethane-silica nanocomposites

L. Bistričić¹, M. Leskovic², G. Baranović³, E. Govorčin Bajsić²

¹*Department of Applied Physics, Faculty of Electrical Engineering and Computing, University of Zagreb, Unska 3, 10000 Zagreb, Croatia*

²*Faculty of Chemical Engineering and Technology, University of Zagreb, Marulićev trg 19, 10000 Zagreb, Croatia*

³*Ruđer Bošković Institute, P.O.B. 1016, 10001 Zagreb, Croatia
lahorija.bisticic@fer.hr*

Polymer nanocomposites are new class of materials with improved physical (thermal, mechanical, dielectric and magnetic) properties due to the interaction between polymer matrix and nanofillers. In this work, two polyether based polyurethanes (ETPU-1, ETPU-2) with different ratios of hard/soft segment contents have been synthesized using 4,4'-diphenylmethane diisocyanate (MDI), poly(oxytetramethylene) glycol (PTMO) of 1000 molecular weight and 1,4-butane diol as chain extenders. In ETPU-1 and ETPU-2 the molar ratio of NCO to OH groups in prepolymers was kept 4/1 and 2/1, respectively. Two series of ETPU-1 and ETPU-2 silica nanocomposite thin films were also prepared with addition of 0.5, 1 and 3% volume fraction of silica nanoparticles.

Mechanical and FTIR investigations were performed on neat ETPU and ETPU-silica nanocomposite thin films in order to understand how the ratio of hard/soft segment contents and the presence of nanofiller influenced mechanical properties. Introduction of the nanosilica into ETPU matrix changed both tensile strength and elongation at break.

The orientation of hard and soft segments, as well as the phase separation, was studied by FTIR linear dichroic measurements performed on stretched films [1]. The analysis of C=O stretching vibrations yielded information about the hydrogen bonding between different segments in neat ETPU polymers and nanocomposites. The degree of phase domain separation (DPS) was calculated from the integrated intensities of the absorbance bands observed at 1732 and 1703 cm⁻¹, which were attributed to the free and hydrogen bonded carbonyl groups, respectively. The analysis has indicated that DPS depends on the hard/soft segment ratio and inter-segment interactions. In ETPU-1 neat film with higher concentration of hard segments DPS was 69%. The lower concentration of hard segments in ETPU-2 reduced the DPS to 61%. The addition of small amount of nanosilica increased the DPS in thin films of ETPU silica nanocomposites, especially in ETPU-1. This enhancement is an obvious consequence of interactions between polymer chains and nanosilica particles.

[1] L. Bistričić, M. Leskovic, G. Baranović, S. Lučić Blagojević, J. Appl. Polym. Sci. 108 (2008) 791-803.

Subwavelength Metallic Nanohole Arrays as Multifunctional Plasmonic Substrates for SPR and SERS Sensors

V. Canpean, S. Astilean

Nanobiophotonics Laboratory, Institute for Interdisciplinary Experimental Research and Faculty of Physics, Babes-Bolyai University, M. Kogalniceanu 1, 400084 Cluj-Napoca, Romania

In the past years there has been a growing interest in the development of highly sensitive substrates for Surface Plasmon Resonance (SPR) and Surface Enhanced Raman Spectroscopy (SERS). In 1998, Ebbesen and co-workers [1] discovered the extraordinary optical transmission (EOT) through periodic arrays of subwavelength holes in metallic films, an exciting breakthrough for many applications in biophotonics and near-field microscopy, among others. The physical mechanism responsible for the EOT through a metallic film with a periodic array of subwavelength holes is attributed to two different resonances: the localized waveguide resonance and periodic surface plasmon resonance [2]. Surface plasmons excitation leads to a high enhancement of the electromagnetic field close to the metal surface, which corroborated with the high sensitivity of the SPR on the dielectric constant of the surrounding medium make these structures interesting multifunctional plasmonic substrates for SPR and SERS sensors.

In this work we implemented a new variant of classical nanosphere lithography [3] which combines the reactive ion etching (RIE) of self-assembled film of polystyrene nanospheres with metal deposition in order to fabricate gold films with periodic arrays of nanoholes. The film microstructure and morphology was characterized by atomic force microscopy (AFM). The optical and SERS properties as function of metallic hole diameter were measured using an optical fiber microspectrometer and confocal Raman microscope, respectively. Typical AFM image and optical transmission spectra of the fabricated structures are depicted in figure 1.

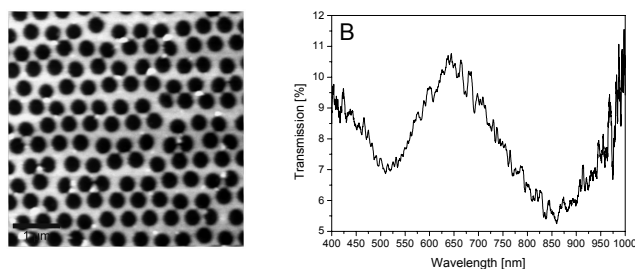


Fig. 1: (A) AFM image of metallic nanohole array; (B) Transmission through the Au film with periodic array of nanohole. The scale bar in the AFM image is 1 μm .

We demonstrated SPR and SERS applicability of fabricated periodic arrays of subwavelength holes by monitoring the changes in dielectric constant of the surrounding medium and ultrasensitive detection of adsorbed molecules.

- [1] T.W. Ebbesen, H.J. Lezec, H.F. Ghaemi, T. Thio and P.A., *Nature* 391 (1998) 667.
- [2] Z. Ruan and M. Qiu, *Phys. Rev. Lett.* 93 (2006) 233901.
- [3] J.C. Hulteen, R. P. Van Duyne, *J. Vac. Sci. Technol. A* 13 (1995) 1553.

Acknowledgments

This work was partially supported by the Romanian National Authority for Research in the frame of the CEEEX program (Project No. 71/ 2006) and by The National University Research Council in the frame of the PN-II program (Project No. TD-28/2007).

Novel Bismuth-Lead-Silver Glasses Doped with Neodymium Ions

E. Culea, L. Pop, M. Bosca

Technical University of Cluj-Napoca, str.C.Daicoviciu nr.15, 400020 Cluj-Napoca, Romania

Vitreous systems containing rare earth ions have received a significant attention due to their interesting applications in the field of telecommunications, laser technology and optics [1].

New bismuth-lead-silver glasses doped with neodymium ions have been obtained. Structural and spectroscopic behaviour of the samples was studied by IR spectroscopy, X-ray diffraction, and magnetic susceptibility and density measurements.

The IR spectra obtained for the bismuth-lead-silver glasses doped with neodymium were analyzed to obtain the deconvolution of the absorption bands [2] in order to realize their correct assignment. The IR data permitted the identification of the main structural units that build up the studied vitreous network. These structural units are based on bismuth ions having the 6+ and 4+ valence states, Bi^{6+} and Bi^{4+} . IR spectroscopic data show that addition of neodymium ions produces changes of the structural units in the studied samples, namely the bismuth ions play a network modifier role in the studied vitreous system. These structural changes are generated by the neodymium ions that modify the $\text{Bi}^{6+} \leftrightarrow \text{Bi}^{4+}$ equilibrium in the host bismuth-lead-silver vitreous matrix.

X ray diffraction investigation show the amorphous nature of the samples and, together with the IR spectroscopy, permits to follow the structural modifications produced by the addition of neodymium ions.

The presence of the neodymium ions in the host vitreous matrix induces the magnetic behaviour of the bismuth-lead-silver glasses. Magnetic susceptibility measurements show an antiferromagnetic interaction between the magnetic neodymium. The analysis of the magnetic data evidences an important clustering tendency of neodymium ions.

[1] A.Pann, A.Ghosh, J.Non-Cryst.Solids 271 (2000) 157.

[2] E.Culea, L. Pop, Bosca, I. Bratu, M. Bogdan, Modern Phys.Let. B 21 (3) (2007) 1-7.

Carbon Nanotube-Fe/Al₂O₃ Nanocomposites by CCVD Method: Formation of CNTs from α -(Al_{1-x}Fe_x)₂O₃ Oxide Powders that were Prepared by Oxinate Route

Valdirene G. de Resende¹, Eddy De Grave¹, Anne Cordier², Christophe Laurent², Alain Peigney² and Alicia Weibel²

¹Department of Subatomic and Radiation Physics, University of Ghent, B-9000 Gent, Belgium
Email: valdirene.gonzaga@ugent.be

²CIRIMAT, CNRS/UPS/INPT, LCMIE, Université Paul-Sabatier, Bât. 2R1, 118 route de Narbonne, 31062 Toulouse cedex 9, France

In this contribution the formation of carbon nanotubes from α -(Al_{1-x}Fe_x)₂O₃ oxide powders containing different amounts of iron is examined. These oxide powders were prepared by combustion of oxinates and characterized in detail in an earlier report. Three different ways of growing CNTs were applied: (i) from the starting solid solutions, α -(Al_{1-x}Fe_x)₂O₃; (ii) from a self-supported solid-solution foam; and (iii) from a self-supported solid-solution foam and using a commercial ceramic foam impregnated by Mo₂O₃. Upon reduction during heating at 5 °C/min up to 1025 °C in H₂/CH₄ of the oxide powders nanometric Fe particles, which are thought to be active for the in-situ nucleation and growth of carbon nanotubes, are formed. The post-reaction phases as identified by Mössbauer spectroscopy (Fig. 1) are α -Fe, Fe₃C, γ -Fe-C, α -(Al,Fe)₂O₃, Fe_{1-y}C_y alloy and Fe²⁺-bearing phase. These two last components are not present in all of the spectra of the CNT-nanocomposite samples. The most important aspect of this series of experiments was that, for each of the applied synthesis routes, almost no undesirable carbon forms were detected in the nanocomposite powders obtained from oxide solid solutions containing more than 2 cat.% Fe. In addition to Mössbauer spectroscopy, the powders were characterized by X-ray diffraction, Raman spectroscopy, carbon analysis and electron microscopy.

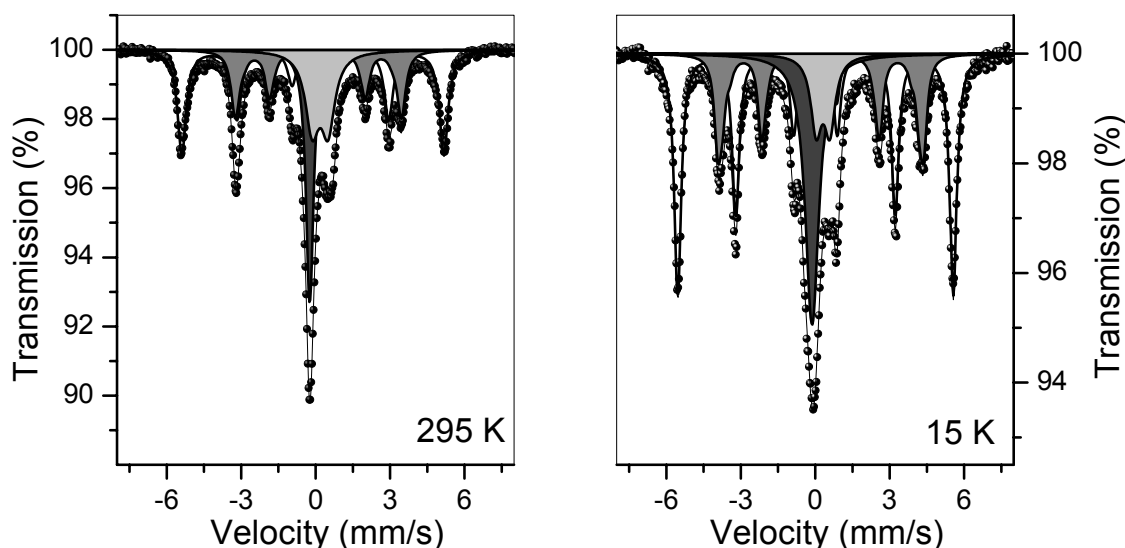


Fig. 1: Typical Mössbauer spectra of the CNTs-Fe/Al₂O₃ nanocomposite powders measured at 295 K and 15 K. α -Fe (white); Fe₃C (gray); γ -Fe-C (dark gray); and α -(Al,Fe)₂O₃ doublet (light gray).

ESR Study of NR/Montmorillonite Nanocomposites

M. Didović¹, S. Valić^{1,2}, D. Klepac¹, A.P. Meera³, S. Thomas³

¹*School of Medicine, University of Rijeka, Braće Branketta 20, HR-51000 Rijeka, Croatia
E-mail: Mirna.Didovic@medri.hr*

²*Rudjer Bošković Institute, Bijenička 54, HR-10000 Zagreb, Croatia*

³*School of Chemical Sciences, Mahatma Gandhi University, Priyadarshini Hills P.O.
Kottayam -686 560, Kerala, India*

Nanocomposites of natural rubber (NR) containing 2, 5 and 10 phr of organically modified clay (montmorillonite) were prepared in order to study the influence of the filler content on the local chain dynamics and motional heterogeneity of the composite system via electron spin resonance (ESR) and to correlate the ESR results with those obtained by other methods.

The dispersion of the clay in the polymer matrix was examined by transmission electron microscopy (TEM), scanning electron microscopy (SEM) and X-ray diffraction (XRD). Thermal behaviour of the composite material, as well as of the pure clay, was investigated by differential scanning calorimetry (DSC). ESR spectra were measured in the temperature range from -100 °C to 130 °C, using the spin probe method.

ESR spectra reflect significant differences in the local chain dynamics and motional heterogeneity of the composite material in comparison with the pristine NR, especially in the higher temperature region. The shape of the spectra varies with the filler content and with the type of distribution of the clay particles, in accordance with SEM results. An increase in the amount of the broad component is observed at the temperatures above 100 °C, indicating hindered motion of the chain segments. DSC results of the composite material indicate that T_g is not affected by addition of the clay; DSC curve of the pure clay shows an endothermic peak around 40 °C, which corresponds to the melting of the clay and is shifted towards higher temperatures when clay is incorporated in the polymer matrix. Hence, hindered motion of the chain segments observed at higher temperatures can be related to the melting of the clay particles.

The Influence of Carbon Nanotubes on PAN-based Fibers Properties

A. Fraczek¹, C. Paluszkiwicz¹, A. Weselucha-Birczynska², S. Blazewicz¹

¹ AGH University of Science and Technology, Faculty of Material Science and Ceramics,
al. Mickiewicza 30, 30-059 Krakow, Poland

² UJ - The Regional Laboratory of Physiocochemical Analyses and Structural Research,
ul Ingardena 3, 30-060 Krakow, Poland

New trends in development of composites technologies are to combine small amount of nanoparticles with polymeric matrix to form nanocomposite fibers. Carbon nanotubes are known to have unusual chemical, physical and mechanical properties, quite different from their bulk and fibrous forms, which make them attractive component for polymers in order to engineer their properties. The presence of carbon nanomaterials in polymer matrix allows for the modification of material properties such as surface charge, mechanical strength, thermal and electrical conductivity etc.

Recently, numerous works on nanocomposites based PAN co-polymers precursors containing carbon nanotubes were published. Introduction of a nanoparticle into polymer fiber precursor may lead to change of susceptibility to plastic deformation during stretching. Effectiveness of reinforcement of polymers by carbon nanotubes may be realized by obtaining uniform dispersion of nanotubes in the matrix and to achieve the interfacial adhesion between the nanotubes and the matrix.

The purpose of this investigation was to determine the effect of carbon nanotubes introduced into PAN solution. Polyacrylonitrile (PAN) fibers were spun from the solution in DMF containing singlewall carbon nanotubes (SWNT). Carbon nanotubes were immersed in DMF and sonicated with ultrasounds for 1 hour at 20 °C. Polyacrylonitrile was separately dissolved in dimethylformamide (DMF), and PAN/DMF solution was added to the SWNT/DMF dispersion and homogenized while stirring. After solidification the fibers were dry-jet wet spun on a laboratory spinning machine. The properties of carbon nanotubes and their influence on polymeric matrix were determined using several methods such as Raman spectroscopy, infrared spectroscopy, and thermal analysis. The Raman spectroscopy allows to displays structural features of the carbonaceous skeleton, whereas FT-IR analysis provides information about the presence of covalent functionalities in carbon materials.

The infrared spectra of SWNT are related to the bands attributed to carbon – oxygen and oxygen-hydrogen bonds existing in the structure of carbon nanotubes. A broad envelope of band in the range of 800-1200 cm⁻¹ is assigned to C-O-H stretching vibration. The presence of hydroxyl groups in this carbon sample is also confirmed by an intensive stretching band at 3300-3500 cm⁻¹. It seems reasonable to conclude that SWNT's contain chemical functionalities such as -OH and -COOH carboxyl groups which could responsible for good interaction between nanoadditives and polymeric matrix. The frequencies of D-band in the Raman spectra indicate high lattice defects in the graphite sheet of SWNT. Raman investigation was also used to ensure the presence of SWNT inside the fibers and check their dispersity inside polymer.

Acknowledgement

This work was financially supported by the Polish Ministry of Science and Higher Education grant No. 3763/T02/2006/31.

The Mechanism of BiFeO₃ Hydrothermal Synthesis

A. Gajović^{1,2}, S. Šturm², B. Jančar², M. Čeh²

¹Ruđer Bošković Institute, Bijenička 54, HR-1002 Zagreb, Croatia

²Jožef Stefan Institute, Jamova 39, SI-1000 Ljubljana, Slovenia

The perovskite bismuth ferrite BiFeO₃ is a multiferroic material – ferroelectric ($T_C = 1103$ K) and antiferromagnetic ($T_N = 643$ K) – exhibiting weak magnetism at room temperature. Since the spins in this material take the form of a long-wavelength (62 nm) the spiral linear magnetoelectric effect averages to zero. One of the ways to recover the linear effect is by thin-film epitaxial constraints [1]; so we expected the same effects in nanostructured BiFeO₃. The phases appearing in the hydrothermal reaction in the Fe–Bi–O system were investigated, with the aim to study the conditions for the synthesis of nanostructural bismuth ferrite.

For the hydrothermal reactions a series of precipitations, with various molar ratios of iron and bismuth ions, were carried out. The solution of iron and bismuth salt was co-precipitated with a strong hydroxide to high pH values. The hydrothermal treatments were performed for 6 h at 200 °C in a stainless-steel Teflon-lined autoclave. The phase composition of the samples was studied by micro-Raman spectroscopy (RS) and was compared with X-ray powder diffraction (XRD) results. To avoid laser-induced thermal effects on the samples during the recording of the Raman spectra the laser power was carefully optimized. The morphologies and nanostructures of the different phases were determined using high-resolution transmission electron microscopy (HRTEM) and/or scanning electron microscopy (SEM). The chemical composition at the nanoscale was determined with energy-dispersive X-ray spectroscopy (EDXS).

BiFeO₃ was detected only in the samples with a higher content of Bi³⁺ ions, while in the case of the lower content of Bi³⁺ ions only the iron oxide and/or the iron-hydroxide phases with different Bi-doping were observed. Raman spectroscopy was used to clarify the possible existence of metastable maghemite or magnetite [2] in the samples with 3.5 and 5 mol% of bismuth, since it is difficult or impossible to distinguish between these two phases just from the XRD results. In the samples with 7.5 and 10 mol% of Bi³⁺ ions in the reactions, the hematite phase dominated. We observed that the bismuth ferrite did not form at these low Bi³⁺ concentrations and was detected only for contents above 30 mol%. However, at 20% of Bi³⁺ content a poorly crystalline, nanosized phase appeared during the sintering. This phase implies a formation step between the doped iron oxide/hydroxide phases and the BiFeO₃. RS, XRD and HRTEM results have to be combined for a proper and complete meaningful evaluation. In spite of the difficulties in synthesizing pure BiFeO₃ [3], this was achieved in a hydrothermal reaction with 50 mol% Bi³⁺. The mechanism of the BiFeO₃ synthesis will be discussed in terms of the observed stable and metastable phases.

[1] W. Eerenstein, N. D. Mathur and J. F. Scott, *Nature* 442 (2006) 759, and the references therein.

[2] D. L. A. de Faria, S. Venancio Silva and M. T. Oliveira *J. Raman Spectrosc.* 28 (1997) 873.

[3] J.-T. Han, Y.-H. Huang, X.-J. Wu, C.-L. Wu, W. Wei, B.o Peng, W. Huang and J. B. Goodenough *Adv. Mater.* 18 (2006) 2145, and the references therein.

Study on Thermal Decomposition Processes of Polysiloxane Polymers – from Polymer to Nanosized Silicon Carbide

Teresa Gumula, Czesława Paluszkiewicz, Stanislaw Blazewicz

*AGH-University of Science and Technology, Faculty of Materials Science and Ceramics, Al. Mickiewicza 30,
30-059 Krakow, Poland*

Controlled heat treatment of organosilicon polymers leads to formation of various ceramic products, depending on the type of polymeric precursor and conditions of heat treatment. This is the way leading to obtaining materials differing with chemical composition, structure and microstructure (e. g. amorphous, nanocrystalline or crystalline). In the literature exist many information about application of polycarbosilanes, that are used in commercial applications e.g. manufacturing of silicon carbide fibres (Nicalon) or silicon carbide matrix composites. However, these polymers are expensive.

In this work polysiloxanes, as an alternative for currently commercially used polycarbosilanes, were investigated. Four types of cheap commercially available polymethylsiloxanes and polymethylphenylsiloxanes produced by Lucebni zavody (Kolin, Czech Republic) were used. The polymers differed in C/Si molar ratio. Structure, microstructure and phase composition of ceramic products of polymers heat treatment were investigated. Also usefulness of polysiloxanes as substrates of composite ceramic matrices were evaluated.

Curing and heat treatment conditions were determined on the basis of thermogravimetric measurements. Ceramic yield (Y_c) after heat treatment in the temperature range from 20 to 1700 °C was calculated. The ceramic samples obtained by heat treatment of polymers were analysed by means of Fourier transform infrared absorption spectroscopy (FTIR) in the range from 4000 to 400 cm^{-1} with 4 cm^{-1} resolution by means of FTS-60 V Bio-Rad spectrometer. A standard KBr pellet technique was used. The structure of ceramic samples was carried out on XRD diffractometer (Cu K_α radiation, Ni-filtered). The average grain size of ceramic products was calculated by using Scherrer's equation. Microstructure of the materials was examined by scanning electron microscopy JEOL 5400.

It was found that during thermal decomposition of polymers up to the temperature of 1000 °C amorphous inorganic Si-C-O ceramics was formed. Between the temperatures 1000 and 1700 °C nanosized 3C and 2 H types of silicon carbide crystalized.

Acknowledgment:

This work was supported by The Ministry of Science and Higher Education, grant No. PBZ-MEiN-2/2/2006.

Study of Protein-Gold Nanoparticle Conjugates by Fluorescence and Surface Enhanced Raman Scattering

Monica Iosin¹, Felicia Toderas¹, Patrice Baldeck² and Simion Astilean¹

¹Babes-Bolyai University, Nanobiophotonics Laboratory, Institute for Interdisciplinary Experimental Research, Treboniu Laurian 42, 400271, Cluj-Napoca, Romania

²Laboratoire de Spectrométrie Physique, Université Joseph Fourier & CNRS UMR5588 Saint Martin d'Hères, France

It is a universal rule of materials in biology that a material is always covered by proteins immediately upon contact with a physiological environment and this phenomenon will also be key to understanding much of the bionanoscience world. Proteins are the important part of the cell's language, machinery and structure and understanding their functionalities is extremely important for further progress in human well being. The protein-nanoparticle interactions has begun to emerge recently with the development of the idea of the nanoparticle-protein “corona” [1] with applications in nanomedicine and nanotoxicity.

Noble-metal nanoparticles open exciting new ways to create efficient optical probes based on the strongly enhanced spectroscopic signals that can occur from molecules in their surface plasmon resonance fields.

In this study, Surface-Enhanced Raman Scattering (SERS) and fluorescence spectroscopy were used to investigate the interaction of well known proteins bovine serum albumin (BSA) and collagen with gold nanoparticles (GNP). While the modification of fluorescence spectra of tryptophan residue in BSA in the presence of GNP was exploited for determining their binding constant (Fig 1A), the SERS indicates the specific binding sites as well as possible modification of protein structure in contact with gold nanoparticles (Fig 1B).

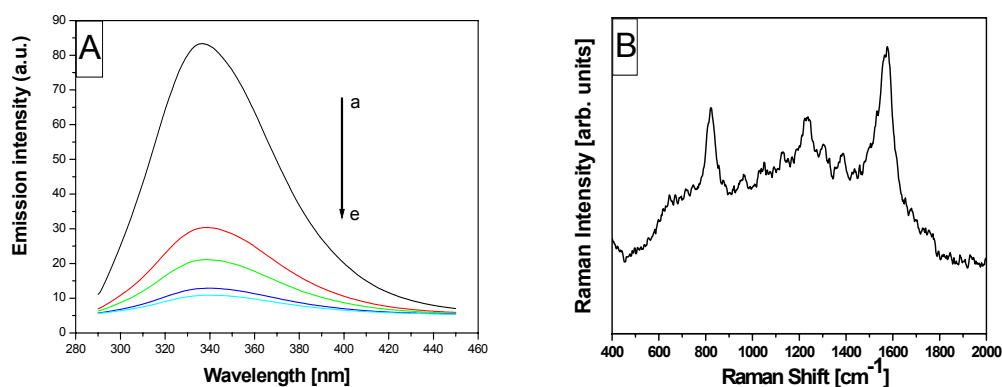


Fig. 1: (A) Fluorescence emission spectra of BSA in the absence (curve a) and presence of GNP (curve b-e); (B) SERS spectrum of bioconjugates gold nanoparticles-BSA;

The protein-conjugated gold nanoparticles could have potential for use for labels for living cells and tissues. While most of the knowledge regarding protein-nanoparticle interactions is from solution and *in vivo* studies, it is clear that future directions will require studies under competitive binding conditions such as occur *in vivo*.

[1] I. Lynch et al., Adv. Colloid Interface Sci. 134-135 (2007) 167.

Acknowledgments

This work was partially supported by the Romanian National Authority for Research in the frame of the CEE program (Project No. 71/ 2006) and by The National University Research Council in the frame of the PN-II program (Project No. TD-65/2007).

Morphological Dependence of Magnetite Nanocrystals under Different Growth Conditions

M.S. Sytnyk¹, Yu.B. Khalavka², O.V. Jovtiuk¹, O.O. Korovyanko¹

¹*Inorganic Chemistry, Chernivtsi National University, 2, Kotsyubynskogo str., 58012, Chernivtsi, Ukraine*
E-mail: o.korovyanko@chnu.edu.ua, ²*Institute for Physical Chemistry, University of Mainz, Jakob-Welderweg 11, 55128 Mainz, Germany*

Control of morphology, orientation and assembly properties of oxide nanostructures are of great importance for their implementation on technological devices. Chemical procedures permit the synthesis of magnetite nanocrystals in fatty acids in different morphologies depending on the number of temporary slowing-down stages.

In this work we are presenting new results concerning the synthesis base modifications for obtain of iron oxide nanocrystals. Magnetite nanocrystals growing inhibition were provided by the several modes: during reaction on the oleic acid – water solution phases (fig. 1 b, c); Fe²⁺ ions supplementary oxidation (fig. 1a); under the undecylenic acid derivatives stabilization (fig. 1d).

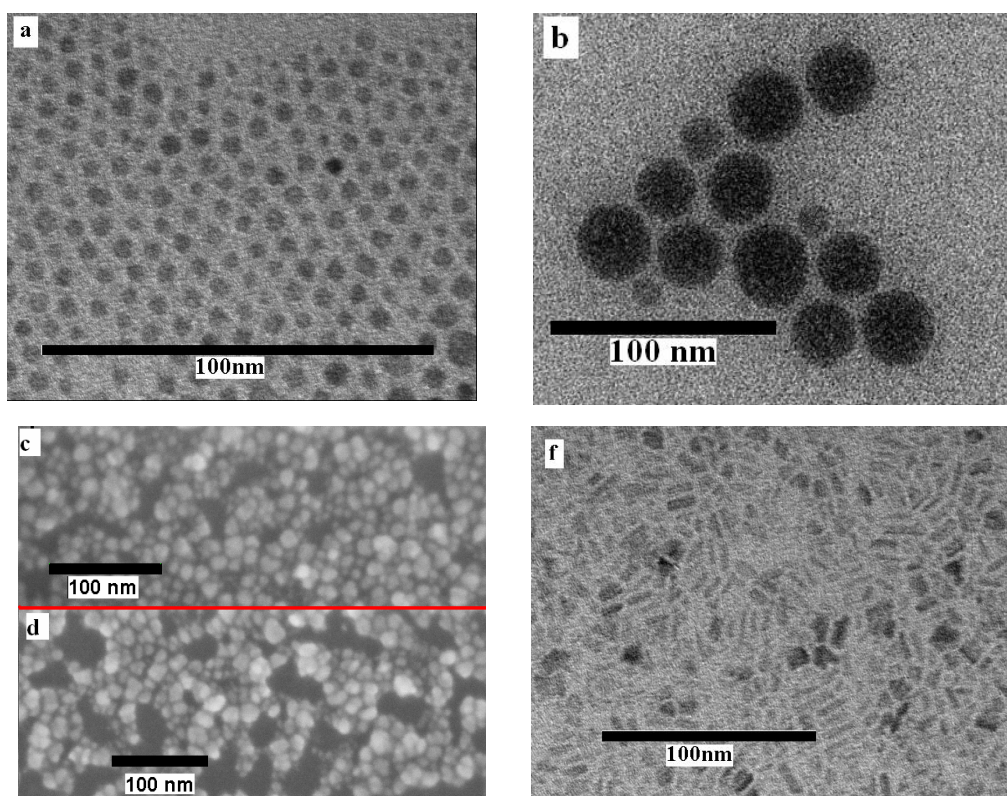


Fig. 1: TEM (a,b,f) and SEM (c,d) images of magnetite (a,b,c,f) and MnO₂ (d) nanocrystals

Crystal structure and morphology of obtained nanocrystals were characterized using TEM and SEM techniques. SEM images of oleic acid stabilized (fig. 1c) and undecylenic acid stabilized (fig. 1d) magnetite nanocrystals were identical. But undecylenic acid stabilization properties can be composed with additional oxidation during the Magnetite nanocrystals growing. Nanoparticles of MnO₂ was obtained by undecylenic acid oxidation of potassium permanganate with reaction product - 10,11 dihydroxy undecylenic acid stabilization. TEM images in fig. 1d shows planes MnO₂ nanocrystals

A reaction path with undecylenic acid derivatives stabilization is proposed which accounts the main experimental features. This leads to a better understanding of key parameters controlling the growing of nanocrystals: surface interaction, temperature variation and speed of interdiffusion.

Formation of Iron Oxides in a Highly Alkaline Medium in the Presence of Palladium Ions

Stjepko Krehula and Svetozar Musić

Division of Materials Chemistry, Ruđer Bošković Institute, P.O. Box 180, HR-10002 Zagreb, Croatia

Iron oxides and oxyhydroxides are common compounds which are widespread in nature and possess properties suitable for a broad range of applications [1]. They are used as pigments (paints, coatings, rubber fillers, construction sealants, cosmetics, ceramic glaze, etc.), catalysts, materials for magnetic recording devices, abrasives, gas sensors, etc. For most of these applications it is very important that a particular iron oxide or oxyhydroxide material has specific characteristics which depend on its microstructural properties (particle size and shape, crystallinity, porosity, etc.). The presence of various additives in the precipitation system has an important influence on the properties of synthetic iron oxides.

The effect of the presence of palladium ions in a highly alkaline precipitation system on the formation of iron oxides was investigated using X-ray powder diffraction (XRD), Mössbauer and FT-IR spectroscopies, field emission scanning electron microscopy (FE-SEM) and energy dispersive X-ray spectroscopy (EDS). Acicular α -FeOOH particles precipitated in a highly alkaline medium with the addition of tetramethylammonium hydroxide (TMAH) were used as reference material. Initial addition of palladium ions to that precipitation system had a major impact on the formation of iron oxide phases and their properties. In the presence of palladium ions, the initially formed α -FeOOH has been transformed into α -Fe₂O₃ crystals in the form of hexagonal bipyramids (Fig. 1) via the dissolution-reprecipitation mechanism with a simultaneous formation of metallic palladium nanoparticles. These palladium nanoparticles acted as a catalyst for the reductive dissolution of α -Fe₂O₃ particles and the formation of Fe₃O₄ crystals in the form of octahedrons. Increase in the initial concentration of palladium ions in the precipitation system accelerated the transformation process α -FeOOH \rightarrow α -Fe₂O₃ \rightarrow Fe₃O₄.

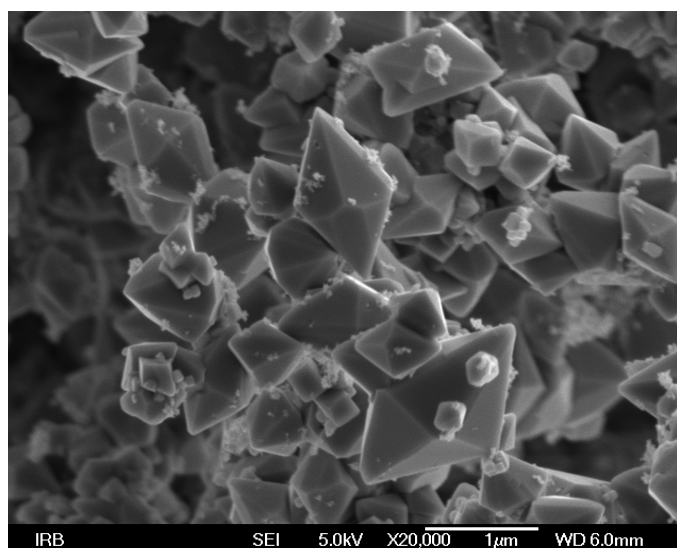


Fig. 1: α -Fe₂O₃ crystals in the form of hexagonal bipyramids along with metallic palladium nanoparticles.

- [1] R.M. Cornell, U. Schwertmann, *The Iron Oxides, Structure, Properties, Reactions, Occurrence and Uses*, Wiley-VCH, Weinheim, 2003, pp. 516-517.
- [2] S. Krehula, S. Musić, *J. Mol. Struct.* 834 (2007) 154-161.

Vibrational Spectroscopy Applications to Study Carbonization Process of Fibrous Materials

D. Mikociak¹, C. Paluszkiewicz², R. Słowiak¹, M. Blazewicz¹

¹AGH – University of Science and Technology, Faculty of Materials Science and Ceramics, Department of Biomaterials, Al. Mickiewicza 30, 30-059 Krakow, Poland

²AGH – University of Science and Technology, Faculty of Materials Science and Ceramics, Department of Silicate Chemistry, Al. Mickiewicza 30, 30-059 Krakow, Poland

Carbon adsorbents have been known and applied for many years. However, the unique properties of low-carbonised carbon related to its surface chemistry and complex porosity make it still attractive especially for medical and environmental applications. Carbon sorbents are porous materials with high surface area, which chemical constitution of the surface allows to selective adsorption from gaseous and liquid phase.

The investigations concerned materials fabricated as a result of carbonisation of precursors containing organic fibres and phenol-formaldehyde resin. The carbon materials were examined using Raman, Infrared Spectroscopy and chemical analysis of the surface groups.

Raman spectroscopy is a suitable method for investigation of carbon structure. Bands near to c.a. 1350 cm^{-1} (defects and disorder mode) and 1590 cm^{-1} (in plane E_{2g} zone – centre mode) allow to determine degree of order of carbon structure as well as the quantity of ordered and amorphous phase. Results of the FT-IR investigations enabled characterisation of bonds present in the amorphous component of the carbon materials.

The FT-IR measurements were carried out in the transmission mode in the mid-infrared range ($400\text{--}4000\text{ cm}^{-1}$). FT-Raman spectra were obtained with Nd-YAG laser system ($\lambda = 1064\text{nm}$). Both FT-IR and FT-Raman spectra were collected with 4 cm^{-1} resolution.

Spectroscopic analysis of the low-carbonised carbons combined with their surface chemistry investigations provided original data related to carbon structure and influence of the carbonisation process parameters on its degree of order and structure of the amorphous phase.

Acknowledgment

The work was financially supported by The Ministry of Science and Education, project No PBZ-MEiN-2/2/2006, Chemistry of prospective processes and conversion products of carbon.

Nanocomposite Fibres for Medical Applications

E. Stodolak¹, C. Paluszkiwicz², M. Bogun³, M. Blazewicz¹

¹AGH – University of Science and Technology, Faculty of Materials Science and Ceramics, Department of Biomaterials, Al. Mickiewicza 30, 30-059 Krakow, Poland

²AGH – University of Science and Technology, Faculty of Materials Science and Ceramics, Department of Silicate Chemistry, Al. Mickiewicza 30, 30-059 Krakow, Poland

³Technical University of Lodz, Faculty of Textile Engineering and Marketing, Department of Man-Made Fibres, 50-952 Lodz, Poland

Polymer nanocomposites can be produced via modification of polymers by introduction and dispersion of nanometric particles into a polymer matrix. Small amount of nanoparticles (up to 10 wt.%) can essentially improve various properties of an initial polymer. Ceramic nanoparticles form chemical bonds with polymer chains which considerably affects its mechanical and thermal properties, as well as its environmental stability.

According to the literature, this perspective group of materials may be applied in biomaterials engineering [1, 2]. Application of the nanocomposites may lead to production of bio-compatible, strong materials which can stimulate reaction of repairing tissue, as well as bio-resorbable implants with controlled resorption time.

In the work nanocomposite alginate fibres ($\text{Ca}(\text{Alg})_2$) were fabricated. A modifying phase consisted of ceramic nanoparticles such as amorphous silica (nSiO_2) and natural hydroxyapatite (nHA). Both nano-fillers were characterised in respect to their size, morphology and specific surface area. Mass fraction of the nano-filler in both produced nanocomposites was 3 wt.%

Process of formation of the fibres from a solution was performed in several stages. The nano-filler particles were introduced into a spinning solution of sodium alginate (NaAlg) and dispersed with ultrasounds then the solution with a suitable viscosity was passed through spinning nozzle and produced fibres were solidified in CaCl_2 baths. Introduction of the nano-filler into the biopolymer matrix modified also its chemical structure.

The degree of dispersion of the nanoparticles in the polymer matrix was investigated using Fourier Transformation Infrared Spectroscopy (FTIR). The measurements were carried out in the transmission mode in the mid-infrared range ($400\text{--}4000\text{ cm}^{-1}$). The bands characteristic for nano-hydroxyapatite (wave number ranges of $470\text{--}600\text{ cm}^{-1}$ and $990\text{--}1090\text{ cm}^{-1}$) were observed in $\text{Ca}(\text{Alg})_2/\text{nHAp}$ nanocomposite fibres. The same effect of nano-filler on chemical structure of the biopolymer was observed in case of the nanosilica. Characteristic bands at c.a. 1050 cm^{-1} related to Si–O bonds vibrations were present in the $\text{Ca}(\text{Alg})_2/\text{nSiO}_2$ nanocomposite FTIR spectrum.

[1] R. Murugan, S. Ramakrishna, *Development of nanocomposite for bone grafting*. Composites Science and Technology 65 (2005) 2385-2406.

[2] Suprakas Sinha Ray, Masami Okamoto, *Layered silicate nanocomposites: a review from preparation to processing*. Progress in Polymer Science 28 (2003) 1539-1641.

Acknowledgment

This work was supported by The Ministry of Science and Education, project No R0804303.

FTIR Studies of Carbon Matrices Modified with Nanosized Hydroxyapatite

Danuta Mikociak¹, Czesława Paluszkiewicz¹, Teresa Gumuła¹, Jerzy Michałowski²,
Stanisław Błazewicz¹

¹ AGH University of Science and Technology, Faculty of Materials Science and Ceramics, Department of Biomaterials, Al. Mickiewicza 30, 30-059 Krakow, POLAND

² IFJ – Institute of Nuclear Physics, Polish Academy of Sciences, ul. Radzikowskiego 152, Kraków, POLAND

Nowadays, high-performance composites are one of the most interesting structural materials which are more and more applied not only in industry but also in medicine. In biomaterials engineering materials exhibiting both biocompatibility and bioactivity play an important role in the case of bone replacement. Such materials are able to form a natural bond with host tissue. Hydroxyapatite (HAp) is known to be bioactive and due to this feature, is widely used as bone tissue replacement. However, its poor mechanical parameters cause difficulties with its application as structural implant. Therefore, we propose to use HAp as a modifier of constructive carbon fibres-based composites.

This work reports the results concerning modification of pitch- based carbon matrices with hydroxyapatite nanoparticles. Isotropic pitch and nanosized HAp mixtures were used as substrates of composite matrices. Concentration of HAp in pitch precursors varied from 1, 5 and 10 wt%. The samples were first oxidized and next subjected to heat treatment at 1000 °C in an inert atmosphere at the mean heating rate of 0.7 °C/min (total time of heating - 24 hour). The study on oxidation and heat treatment products was led by means of FTIR technique in the range from 4000 to 400 cm⁻¹ on FTS-60 V Bio Rad spectrometer. The structure of the samples was carried out on XRD diffractometer (Cu K_α radiation, Ni-filtered). Microstructure of the materials was examined by scanning electron microscopy JEOL 5400 with LINK AN 10000 point microanalyzer of X-ray radiation.

This study of a family pitch – based carbon matrices/HAp provided a basis for selecting an appropriate composition for fabrication of structural carbon composite containing nanosized HAp.

Acknowledgment

This work was supported by The Ministry of Science and Education, **project No PBZ-MEiN-2/2/2006**, Chemistry of prospective processes and conversion products of carbon.

Influence of Europium Ions on Structure and Crystallization Properties of Bismuth-Alumino-Borate Glasses and Glass Ceramics

Petru Pascuta¹, Simona Rada¹, Gheorghe Borodi², Maria Bosca¹, Lidia Pop¹, Eugen Culea¹

¹Physics Department, Technical University, 400641 Cluj-Napoca, Romania

²National Institute for R&D of Isotopic and Molecular Technology, P.O. Box 700, RO-400293 Cluj-Napoca, Romania

e-mail: petru.pascuta@phys.utcluj.ro

Glasses based on heavy metal oxides, such as Bi_2O_3 , are interesting because their properties are exploited in applications such as wave-guides in non-linear optics, radiation shielding windows, scintillation counters, optical transmission devices, thermal and mechanical sensors, as well as optical devices, such as optical fibers, optical switching, optical memory etc. [1-4]. Glasses containing two glass-forming oxides, such as the bismuth borate glasses, which have superior properties, have a wide range of practical applications. B_2O_3 is a typical glass former, while Bi_2O_3 is a conditional glass former. The addition of an extra cation, such as Al_2O_3 , to the bismuth borate glass network exerts an influence on the glass structure, because it directly influences the cross-linking between polyhedra constituting the three-dimensional network [5]. X-ray diffraction and FT-IR spectroscopy measurements have been employed to investigate the $x\text{Gd}_2\text{O}_3 \cdot (100-x)[2\text{Bi}_2\text{O}_3 \cdot \text{B}_2\text{O}_3 \cdot \text{Al}_2\text{O}_3]$ glasses and glass ceramics system, with $0 \leq x \leq 25$ mol%. Melting at 1100 °C for 15 minutes and rapid cooling at room temperature permitted to obtain glass samples. In order to improve the local order and to develop crystalline phases, the glass samples were kept at 550 °C for 24 h. FT-IR spectroscopy data suggest that the europium ions play the network modifier role in the studied glasses. These data show that the glass structure consists of the BiO_3 , BiO_6 , BO_3 , BO_4 and AlO_4 structural units, and the conversion among these units mainly depends on the Eu_2O_3 content. Density functional theory (DFT) calculations were employed to develop a model for ternary bismuth-alumino-borate glasses.

[1] Y. Takahashi, Y. Benino, T. Fujiwara, T. Komatsu, J. Appl. Phys. 95 (2004) 3503.

[2] M. Nocun, W. Mozgawa, J. Jedlinski, J. Najman, J. Mol. Struct. 744-747 (2005) 603.

[3] Y. Cheng, H. Xiao, W. Guo, W. Guo, Thermochim. Acta 444 (2006) 172.

[4] P. Pascuta, L. Pop, S. Rada, M. Bosca, E. Culea, J. Mater. Sci.: Mater. El. 19 (2008) 424-428.

[5] A.B. Corradi, V. Cannillo, M. Montorsi, C. Siligardi, J. Mater. Sci. 41 (2006) 1573-4803.

Spectroscopic Investigations of Carbon Nanotubes in Aqueous Suspensions with Biosurfactants

V. Pashynska¹, A. Glamazda¹, A. Plokhotnichenko¹, E. Karpenko²,
T. Pokynbroda², V. Karachevtsev¹

¹B. Verkin Institute for Low Temperature Physics and Engineering of the National Academy of Sciences of Ukraine, 47, Lenin Ave., Kharkov, 61103, Ukraine, pashynska@ilt.kharkov.ua, ²Lviv Department of Physical-Organic Chemistry Institute, National Academy of Sciences of Ukraine

Application of carbon nanotubes in medicine, pharmacology and biotechnology belongs to the prospective areas of nanoscience and nanotechnology. The ideas of nanotubes utilization for directed transport of medicines in human organism and using nanostructures as parts of bionanosensors are under intensive investigation now. One of the crucial problems limiting nanostructures application for medical purposes is a weak solubility of carbon nanotubes in water and other polar solvents. To solve this problem surfactants of different types are utilized. Application of biosurfactants (natural surfactants) for nanotubes dilution in biorelated experiments has some advantages because of non-toxicity, high efficiency and biodegradability of the biosubstances that allows increasing a nanotubes biocompatibility.

In present work an efficiency of two rhamnolipid biosurfactants for promotion of single-walled nanotubes (SWNT) dilution in water was investigated by spectroscopic methods. These mono- (RL1) and di- (RL2) rhamnolipids were produced naturally by bacterial strain *Pseudomonas sp. PS-17* as extracellular surface-active substances. The biosurfactants were extracted from the bacterial supernatant by the method described in [1].

Steady aqueous suspensions of SWNTs were prepared by sonication of nanotubes bundles with biosurfactants for 40 minutes (1 W, 44 kHz). Then the solutions were centrifuged at 15000 g for 15 min, and the supernatants were decanted and recentrifuged at 60000 g for 40 min. The initial nanotubes concentration was 0.1 mg/mL. Biosurfactants concentration was 1%. After ultracentrifugation the supernatants were decanted and these homogenous suspensions were stable for a month. For reference the nanotubes aqueous suspension with non-biosurfactant (sodium dodecylbenzenesulfonate (SDBS)), which demonstrated high efficiency of individual nanotubes dilution, was prepared too.

The light absorption spectra of SWNT:RL1, SWNT:RL2 and SWNT:SDBS aqueous suspensions in the UV-visible-near infra-red region (300-1500 nm) were obtained. In spite of the lower concentration of SWNTs in the suspensions with biosurfactants in comparison with the SWNT:SDBS suspension the observed spectra of SWNT:RL1, SWNT:PL2 systems testify to a presence in the suspensions individually dissolved nanotubes. Among two biosurfactants RL2 provides higher nanotubes concentration in aqueous suspension that is evidence of the higher RL2 efficiency in the SWNT dilution process in comparison with the RL1 one. Similar results were obtained by the investigation of luminescence spectra of the systems studied. The bands in the spectrum of SWNTs:RL2 shifted to the low energy area in comparison with the SWNTs:SDBS spectrum. This shift can be explained by the less partial covering of the nanotubes surface by RL2 molecules comparing with SDBS ones that results in increase of water-nanotube contact area in SWNT:RL2 system and correspondent spectrum features. The difference in the efficiency of RL1 and RL2 for nanotubes delution is discussed.

[1] E.V. Karpenko, N.B. Martynyuk, A.N. Shulga, Surface active biopreparations, Patent of Ukraine N 71792, Bull.N 12, 2004.

A Spectroscopic Study on Noble Metal Nanoparticle Embedding into a SBA-15 Catalyst System

Róbert Rémiás, Ákos Kukovecz, Zoltán Kónya, Imre Kiricsi

*Department of Applied and Environmental Chemistry, University of Szeged,
Rerrich B. tér 1, Szeged, H-6720 Hungary*

SBA-15 is a promising mesoporous catalyst support material [1] because of its large surface area and good thermal stability. A particularly advantageous property of SBA-15 is that its channels are wide enough to allow the entrance of pre-synthesized metallic nanoparticles. Noble metal nanoparticles are widely used in hydrogenation/dehydrogenation reactions and it is anticipated that by controlling the shape of the nanoparticles it should be possible to improve the selectivity of some processes [1]. We are interested in the development and characterization of model catalyst systems based on SBA-15 supported noble metal nanoparticles. In the present contribution we report on the applicability of various spectroscopic methods for monitoring the physico-chemical properties of these materials.

We successfully embedded Pt, Pd, Ru and Rh nanoparticles into the channels of SBA-15. Samples were characterized at various stages of the synthesis using IR and Raman spectroscopy, XRD, TEM, XPS and dielectric spectroscopy (Fig. 1).

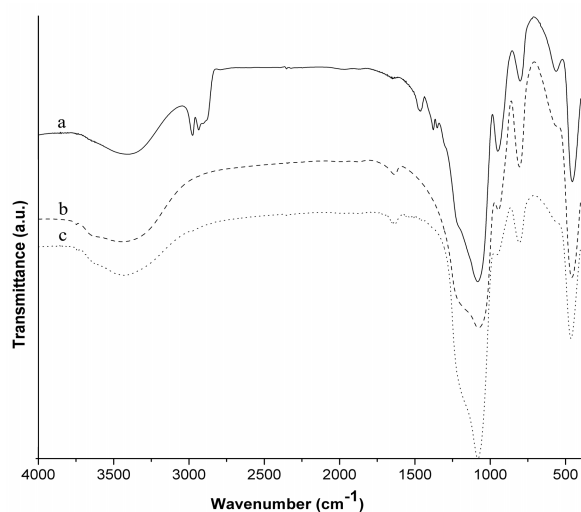


Fig. 1: IR spectra of the pure SBA-15 before calcination (a), after calcination (b) and the 0.1 % Pt/SBA-15 with NIPA capping agent (c)

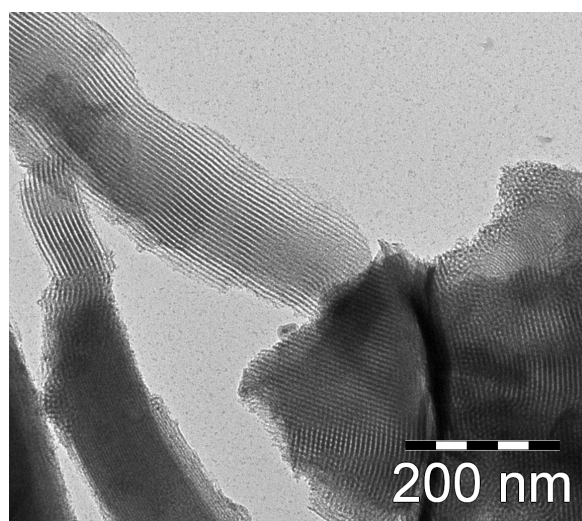


Fig. 2: TEM image of SBA-15 after the calcination

Our results offer insight into the formation mechanism of the working catalyst system, in particular into the interaction of the metal nanoparticle capping agent (NIPA, SPA etc) with the SBA-15 framework. We conclude this report with a comparison between the catalytic performances of the discussed systems in the hydrogenation of cyclohexene.

[1] Éva Molnár, Gyula Tasi, Zoltán Kónya, Imre Kiricsi, *Catalysis Letters* Vol. 101 (2005) 159-167.

Synthesis and Microstructure of Porous Mn-Oxides

Svetozar Musić¹, Mira Ristić¹, Stanko Popović²

¹*Division of Materials Chemistry, Ruđer Bošković Institute, P. O. Box 180, HR-10002 Zagreb, Croatia*

²*Department of Physics, Faculty of Science, University of Zagreb, P.O.Box 331, HR-10002 Zagreb, Croatia*

Generally, porous metal oxides find broad application in catalysis, chromatography, separation, environmental sensing, etc. The investigation of porous metal oxides is also important from an academic standpoint. The relationship between the synthesis and porosity of metal oxides was investigated. Different synthesis routes were used in the preparation of porous metal oxides, for example, sol-gel processing, sonochemistry, water-in-oil microemulsion processing, etc. The influence of various templates on the formation of porous metal oxides was investigated as well. Controlling the porous microstructure (nanostructure) of metal oxides is not an easy task, because this property strongly depends on the synthesis route. Small variations in the synthesis route also change the porosity, as well as the size and geometrical shape of particles. In the present work we are reporting new results in the synthesis of porous α - Mn_2O_3 and Mn_3O_4 particles. The porous Mn-oxide particles were synthesized by urea processing in combination with the thermal treatment of the precursor precipitated. The samples were characterized by XRD, FT-IR, DTA and FE SEM. Upon heating of the precursor at 600 °C, the α - Mn_2O_3 particles containing nanopores (cheese-like) were obtained. Most nanopores varied from ~ 20 to 60 nm, and some were close to ~ 100 nm in size. α - Mn_2O_3 showed a strong twinning effect. At 1100 °C, a single crystal phase Mn_3O_4 particles were forming a 3D structure.

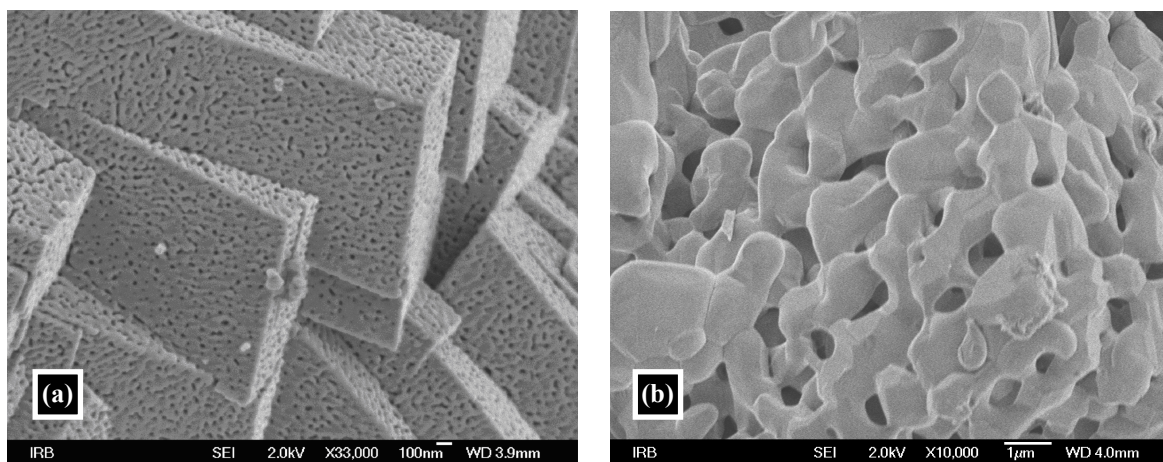


Fig. 1: FE SEM images of (a) nanoporous α - Mn_2O_3 and (b) microporous Mn_3O_4 .

Formation and Characterization of Nanosize α -Rh₂O₃

Svetozar Musić¹, Ankica Šarić¹, Stanko Popović², Mile Ivanda¹

¹*Ruder Bošković Institute, P. O. Box 180, HR-10002 Zagreb, Croatia*

²*Department of Physics, Faculty of Natural Sciences and Mathematics, University of Zagreb, P. O. Box 331, HR-10002 Zagreb, Croatia*

Rhodium and Rh-oxide based catalysts have found important applications, for example, in methanol or methane oxidations, decomposition of NO_x gases to N₂ and O₂ etc. The catalytic chemistry of rhodium involves various redox reactions in which rhodium participates in different Rh-oxide forms. Reference literature demonstrates a high discrepancy between the number of publications about the catalytic activity of Rh-catalyst, on one hand, and, on the other, the redox chemistry of rhodium. For that reason, we have investigated the formation of α -Rh₂O₃ at the laboratory level. We focused on the formation of α -Rh₂O₃ from amorphous rhodium (hydrated)oxide obtained by precipitation from Rh(NO₃)₃ aqueous solution. The isolated precipitate was dried, then heated in air atmosphere up to 650 °C. Samples were characterized by XRD, FT-IR, Raman and FE-SEM. The XRD of sample obtained at 400 °C showed a broad and intensive peak which can be assigned to the amorphous nature of the sample. This peak is positioned at the Bragg angles corresponding to prominent peaks of α -Rh₂O₃. For the same sample, FT-IR spectrum showed one very broad and intensive peak centered at 544 cm⁻¹, while the corresponding Raman spectrum showed broad peaks at 268, 411 and 556 cm⁻¹. The Raman spectrum of the sample obtained at 650 °C showed peaks at 276, 422, 568 and 610 cm⁻¹, which can be attributed to α -Rh₂O₃ in line with XRD. FE-SEM showed a gradual increase in size (in the nanometer range) of rhodium oxide particles with an increase of temperature reaching 650 °C.

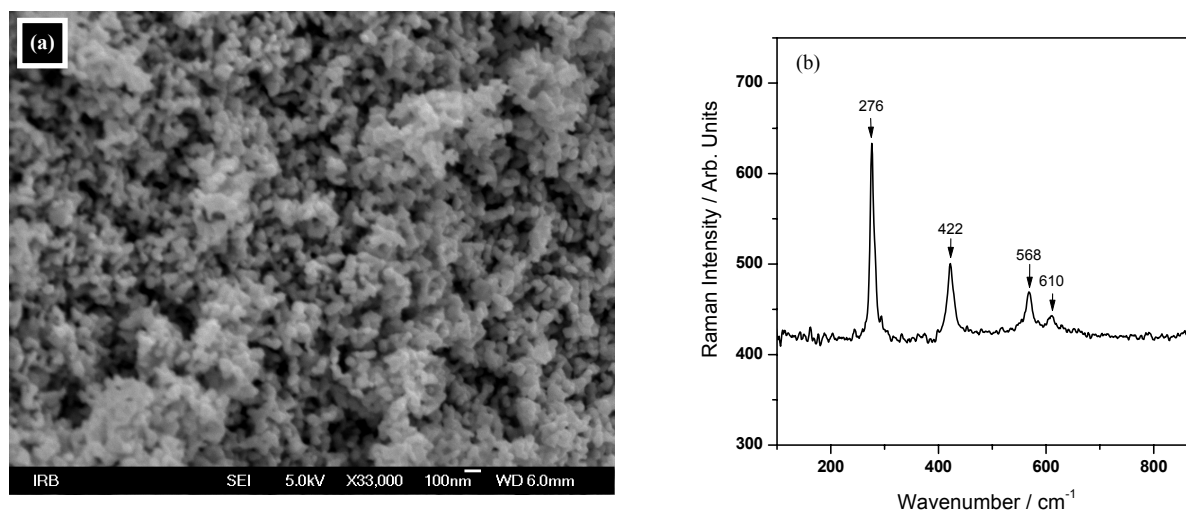


Fig 1: (a) FE-SEM micrograph of α -Rh₂O₃ obtained at 650°C and (b) Raman spectrum of the same sample.

Thermal Behaviour of Al-Zn and Zn-Al Alloys

Željko Skoko¹, Stanko Popović¹ and Goran Štefanić²

¹Physics Department, Faculty of Science, University of Zagreb, POB. 331, 10002 Zagreb, Croatia

²Ruder Bošković Institute, POB. 180, 10002 Zagreb, Croatia

E-mail: zskoko@phy.hr, spopovic@phy.hr, stefanic@irb.hr

Thermal properties of the title alloys, having the Zn atomic fraction, x_{Zn} , from 0.03 to 0.62, have been studied *in situ* by X-ray powder diffraction (XRD) and differential scanning calorimetry (DSC). It has been found that the temperature dependence of microstructure of the alloys, rapidly quenched from the solid-solution temperature, T_{ss} , to room temperature, RT, is quite different from that of the alloys slowly cooled from T_{ss} to RT [1]. The area between two curves showing that dependence during the first heating from RT to T_{ss} and first cooling from T_{ss} to RT is much smaller for the slowly cooled alloys than for the rapidly quenched alloys. That area slightly increases with the increase of the Zn content in the alloys. The temperature dependence of microstructure of the alloys during the second heating from RT to T_{ss} and second cooling from T_{ss} to RT differs little from that during the first cooling from T_{ss} to RT. The ideal equilibrium state cannot be reached either by slow cooling of the alloys from T_{ss} to RT, or by a prolonged ageing at RT of the rapidly quenched alloys. During cooling from T_{ss} to RT, a temperature hysteresis is observed in reversal phase transitions. Several characteristic phenomena were observed during the temperature rise from RT to T_{ss} : a decrease of diffraction line intensities due to enhanced thermal vibrations, anisotropy of thermal expansion, changes in the precipitate shape, partial or complete dissolution of precipitates in the matrix, phase transitions and formation of solid solution.

The phase transitions were also followed by the DSC technique, and confirmed results obtained by XRD studies.

The observed sequence of phase transitions in alloys during heating from RT to T_{ss} is different from that which could be expected according to the phase diagram of the system Al-Zn accepted in the literature [2-4].

[1] S. Popović and B. Gržeta, *Croat. Chem. Acta* 72 (1999) 621-643.

[2] Ž. Skoko and S. Popović, *Fizika A (Zagreb)* 10 (2001) 191-202.

[3] Ž. Skoko and S. Popović, *Fizika A (Zagreb)* 15 (2006) 61-72.

[4] S. Popović and Ž. Skoko, 22nd European Crystallographic Meeting, Budapest, 2004.

Modification of Titanate Nanotubes with Transition Metals and Transition Metal-1,10-phenanthroline Complexes

D. Sović¹, D. Iveković¹, B. Zimmermann²

¹ *Laboratory for General and Inorganic Chemistry and Electroanalysis, Faculty of Food Technology and Biotechnology, University of Zagreb, Pierottijeva 6, HR-10000 Zagreb, Croatia*

² *Ruder Bošković Institute, Bijenička 52, HR-10002 Zagreb, Croatia*

In last few years, titanate nanotubes (TiNT) have attracted a lot of attention as a promising material for application in the field of photocatalysis (e.g. degradation of organic wastes) and photovoltaic's (solar energy conversion). Titanate nanotubes are an n-type semiconductor with band gap of cca. 3.6 eV. Therefore, for photogeneration of electron-hole pairs necessary for photocatalytic action of TiNT, photons with energy greater than 3.6 eV are required. Because photons with that energy correspond to the UV-radiation with wavelength shorter than 340 nm, for efficient use of TiNT as a photocatalyst it is desirable to shift the absorption of TiNT into the visible part of spectrum. In addition, modification of TiNT with transition metal ions is interesting because the incorporation of redox-active centers into the structure of TiNT might improve their catalytic properties.

In this work we investigated spectral properties of TiNT modified with selected transition metal cations (Ru^{3+} , Fe^{2+} , Cu^{2+}), as well as Fe^{2+} and Cu^{2+} -1,10-phenanthroline (Me-Phen) complexes. Titanate nanotubes were prepared by hydrothermal treatment of anatase powder in 10 M NaOH at 120 °C for 24 hours. Obtained TiNT were washed with 0.1 M HCl to convert them into the H-form (H-TiNT). Incorporation of Ru^{3+} , Fe^{2+} and Cu^{2+} cations into the structure of H-TiNT was performed by ion-exchange of H^+ with metal cations in 0.5 M aqueous solution of corresponding metal salts. Spectral properties of transition metal ions-modified TiNT were determined by UV/VIS diffuse reflectance spectroscopy. Broad absorption bands centered at 418 and 585 nm were observed for Ru^{3+} , at 463 nm for Fe^{2+} and at 818 nm for Cu^{2+} -modified TiNT.

For modification of TiNT with Me-Phen complexes three procedures were tested:

- 1) Soaking of Fe^{2+} or Cu^{2+} -modified TiNT in the solution of 1,10-phenanthroline;
- 2) Adsorption of 1,10-phenanthroline onto the surface of H-TiNT, followed by soaking in the solution of metal salt;
- 3) Adsorption of Me-Phen complex on the surface of H-TiNT directly from the aqueous solution of the complex.

In all three cases formation of Me-Phen complexes adsorbed on TiNT was confirmed by UV/VIS diffuse reflectance spectroscopy and FTIR spectroscopy. Absorption bands corresponding to Fe^{2+} and Cu^{2+} -Phen complexes were observed at 514 and 770 nm, respectively.

By monitoring the kinetics of complex formation, it was found that in the case of procedure 1 formation of complex was slow due to the migration of Me^{2+} cations from the interlayer space of TiNT to the surface of nanotubes. Procedure 3 is the simplest and the most convenient way to obtain TiNT modified with surface adsorbed Me-Phen complexes.

The Influence of Thermal Treatment on the Phase Development of ZrO₂-ZnO Precursors

G. Štefanić, S. Musić, M. Ivanda

*Division of Materials Chemistry, Ruđer Bošković Institute,
P.O. Box 180, HR-10002 Zagreb, Croatia
E-mail: stefanic@irb.hr*

The amorphous precursors of the ZrO₂-ZnO system at the ZrO₂-rich side of the concentration range were prepared by co-precipitation from aqueous solutions of the corresponding salts. Structural and microstructural changes during the thermal treatment of the amorphous precursors were examined by differential scanning calorimetry, X-ray powder diffraction, Raman spectroscopy, Fourier transform infrared spectroscopy, field emission scanning electron microscopy and energy dispersive X-ray spectrometry. The crystallization temperature of the amorphous precursors increased with an increase in ZnO content, from 453 °C (0 mol% ZnO) to 551 °C (~25 mol% ZnO). The phase analysis results showed that maximum solubility of Zn²⁺ ions in the ZrO₂ lattice (~25 mol%) occurred in the metastable products obtained after crystallization of the amorphous precursors. The incorporation of Zn²⁺ ions partially stabilized the tetragonal ZrO₂ polymorph. A precise determination of unit-cell parameters using the whole-powder-pattern refinements shows that the unit-cell parameters of the tetragonal ZrO₂ solid solution decrease with an increase in Zn²⁺ content. The increase in zinc content above its solid-solubility limit leads to the appearance of a phase structurally closely related to zincite. Further temperature treatment (up to 1000 °C) leads to an increase in the zincite-type phase followed by the transition of metastable tetragonal ZrO₂ into a thermodynamically stable monoclinic ZrO₂ polymorph.

Raman Spectroscopy of Nanocarbon Catalyst for Oxidative Dehydrogenation Reactions

Dang Sheng Su¹, Jian Zhang¹, Xi Liu¹, Juan Delgado¹, Andreja Gajovic²

¹Fritz Haber Institute of the Max Planck Society, Faradayweg 4-6, D-14195 Berlin, Germany

²Molecular Physics Laboratory, Division of Materials Physics, Rudjer Boskovic Institute, Bijenicka 54, HR-10002 Zagreb, Croatia

We use Raman spectroscopy to study nanocarbon catalyst for the oxidative dehydrogenation of ethyl benzene to styrene. The Raman spectra of lava-CNFs catalyst before and after reaction are shown in Fig 1. The band characteristic to carbon and CNTs are observed at 1344 cm^{-1} (D band), 1584 cm^{-1} (G band), 2688 cm^{-1} (2D; overtone of D band), 2928 cm^{-1} (G+D; combination of G and D bands) and 3168 cm^{-1} (2G; overtone of G band). After the catalytic reaction, all the major Raman features of lava-CNFs composite remain (Fig. 1 (c) and (d)). A slight shoulder at 1612 cm^{-1} , known as D' band appeared (inset in Fig. 1). The D' band is typical for disordered carbon. The Raman studies indicate that, besides the slight carbon deposition, the lava-CNFs are stable catalysts for the tested reactions [1].

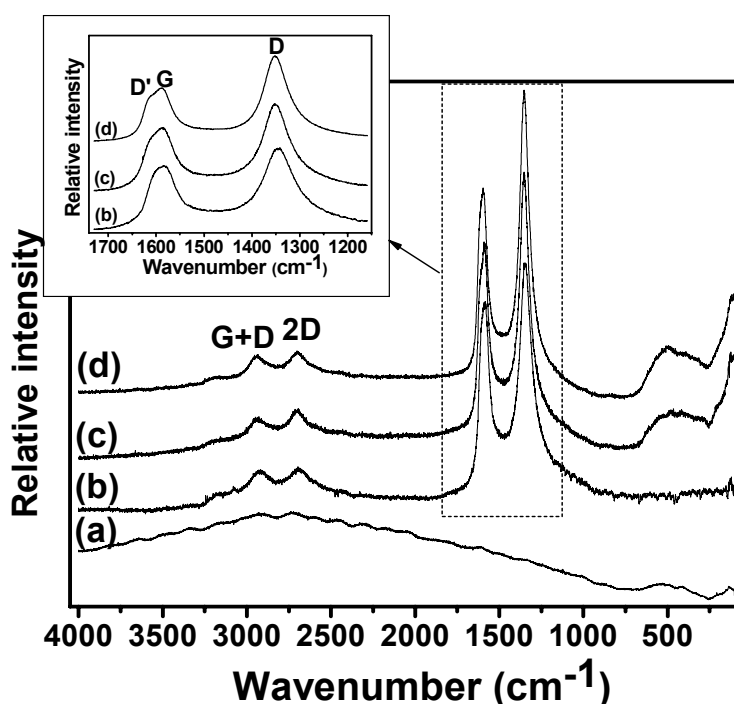


Figure 1: Raman spectra of: (a) lava, (b) lava-CNFs before reaction, (c) lava-CNFs after ODH of ethylbenzene to styrene and (d) lava-CNFs after ODH of butane to butadiene reaction. The inset: Part of the Raman spectra of samples containing CNTs showing D, G and D' bands.

[1] D.S. Su et al, to be published.

Investigation of Annealed Gold Nanoparticles Self-Assembled on Solid Surface for Surface-Enhanced Raman Spectroscopy

F. Toderas, M. Baia, L. Baia, S. Astilean

Nanobiophotonics Laboratory, Institute for Interdisciplinary Experimental Research and Faculty of Physics, Babes-Bolyai University, Treboniu Laurian 42, 400271, Cluj-Napoca, Romania

The control of nanostructure morphology (size and shape) is of great interest in nanotechnology because it can tune the intrinsic chemical and physical properties. Due the unique scattering and absorption properties, gold nanoparticles have many applications in biological sensing [1] and surface-enhanced Raman scattering (SERS) [2, 3].

In this work, we report morphological and size changes induced by annealing gold nanoparticles self-assembled on solid surface and correlate these changes with their surface plasmon and SERS properties. The self-assembled gold nanoparticles were characterized before and after annealing by transmission electron microscopy (see Fig. 1), UV-VIS absorption spectroscopy and X-ray diffraction. We employed the p-aminothiophenol as probe molecule to compare the Raman enhancement factor in visible and near-infrared spectral region of two as prepared samples. The comparison has been done by using 532, 633 and 830 nm laser excitation lines. According to the experimental results, the surface plasmon and SERS properties correlate with the structure of self assembled gold nanoparticles on solid substrate.

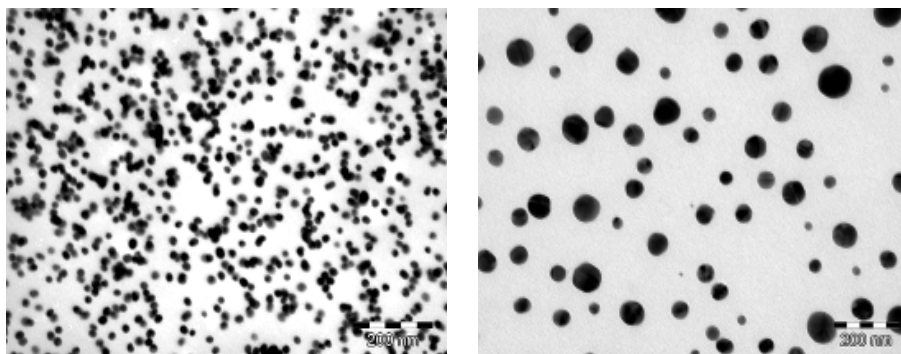


Fig. 1: Transmission Electron Microscopy of self-assembled colloidal gold nanoparticles on solid substrate (a) before annealing and (b) after annealing at 500°C

- [1] R. Elghanian, J.J. Storhoff, R.C. Mucic, R.L. Letsinger and C.A. Mirkin, *Science* 277 (1997) 1078 – 1081.
- [2] N. Felidj, S. Lau Truong, J. Aubard, G. Levi, J.R. Krenn, A. Hohnéau, A. Leitner and F.R. Aussenegg, *J. Vhem. Phys.* 120 (2004) 7141-7146.
- [3] Felicia Toderas, Monica Baia, Lucian Baia and Simion Astilean, *Nanotechnology* 18 (2007) 255702 (6pp).

Acknowledgement

This work is supported by the Romanian Agency for Scientific Research under the project CEE X No 71/2006 (Matnantech).

Study of Controlled Release of Model Proteins from Poly (D,L lactic-co-glycolic) Acid Nanoparticles by Fluorimetry and Analytical Ultracentrifugation

V. Vogel¹, T. Pisternik¹, M. Holzer², K. Langer², W. Mäntele¹

¹*Institute of Biophysics, Johann Wolfgang Goethe-University, D-60438, Frankfurt, Germany*

²*Institute of Pharmaceutical Technology, Johann Wolfgang Goethe-University, D-60438, Frankfurt, Germany*

The development of sustained release systems capable of delivering proteins (peptides) over extended periods of time is an actual problem for a variety of biomedical applications. We presently report the analysis of protein-loaded poly (D,L lactic-co-glycolic) acid nanoparticles as model delivery system. Model proteins (human serum albumin or immunoglobulin IgG) loaded poly(lactic-co-glycolic acid) (PLGA) nanoparticles were prepared by a solvent extraction/evaporation method with polyvinyl alcohol (PVA) as an emulsifier. Protein-loaded nanoparticles were characterized for size and size distribution, surface morphology, protein-encapsulation efficiency, and in vitro drug-release kinetics by fluorimetry and analytical ultracentrifugation. FITC and PromoFluor fluorescence dyes labeled proteins were used for release kinetics measurements. Both types of protein-loaded nanoparticles have similar size ~130 nm and size distribution, surface morphology, and stability. These loaded nanoparticles exhibit sustained protein release profile approximately over a period of 1 month, with typical initial burst-effect within the first five days. Protein-loaded PLGA nanoparticles have great potential for the effective and sustainable delivery of protein.

BaTiO₃ Nanorods: New Insight by Raman Spectroscopy

K. Žagar¹, A. Gajović^{1,2}, S. Šturm¹, M. Čeh¹

¹Jožef Stefan Institute, Jamova cesta 39, SI-1000 Ljubljana, Slovenia

²Ruder Bošković Institute, Bijenička 54, HR-1002 Zagreb, Croatia

In our work we report on the synthesis of BaTiO₃ nanorods by sol-gel electrophoretic deposition into template membranes. As a template we used track-etched hydrophilic polycarbonate (PC) membranes with pore diameters of 200 nm and thickness of 10–25 μm. The template membrane was attached to aluminum working electrode while Pt mesh electrode was used as a counter electrode. For electrophoretic deposition of the sol into porous templates the potential of 30 V was applied between both electrodes for 30 min. After the deposition, the samples were annealed at elevated temperatures. This heating procedure was done in order to burn off the polycarbonate membrane and to make the nanorods dense and crystalline.

Obtained nanorods were characterized by Raman spectroscopy (RS) and X-ray powder diffraction (XRD), while their sizes and the morphology were observed by scanning and transmission electron microscopy (SEM, TEM). RS experiments were made using micro-Raman with 50x LWD objective and 1 mW or 10 mW laser powers at the surface of the sample.

XRD analysis (Fig. 1) indicated that nanorods consist of cubic (space group *m-3m*) BaTiO₃. However, in case of tetragonal *4mm* symmetry with *c/a* axis ratio close to one, it is tedious to distinguish between cubic and tetragonal structure by XRD [1]. This is why we applied RS in order to study tetragonal structure in BaTiO₃ nanorods [1]. Raman spectra from the BaTiO₃ nanorods recorded using 1 mW showed bands of tetragonal structure in samples annealed at 700 and 800 °C (Fig. 2). Additionally in the sample annealed at 700 °C the band corresponding to hexagonal structure was also observed (Fig. 2). Since the laser-induced thermal effects within the samples can induce structural phase transitions in it, the influence of the laser power to the observed structures was also studied. By increasing the laser power in the sample annealed at 800 °C to 10 mW, the phase transition to hexagonal structure was observed (Fig.2).

Based on RS results it was concluded, that BaTiO₃ nanorods exhibit tetragonal structure, contrary to the XRD results.

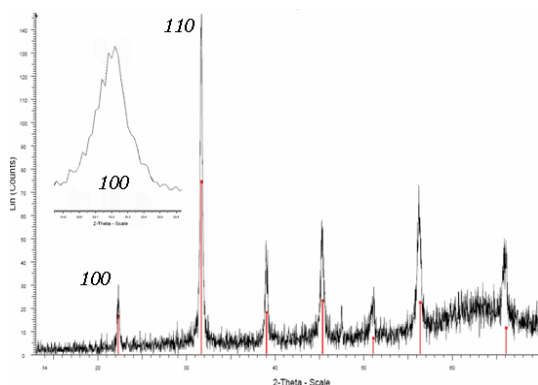


Fig. 1: XRD pattern of the BaTiO₃ nanorods.

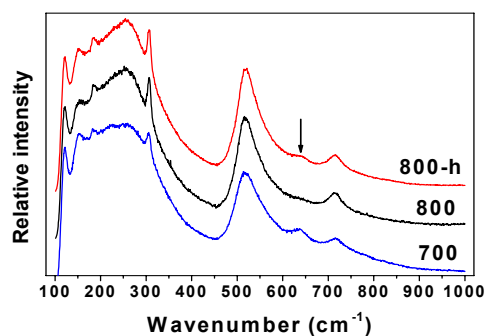


Fig. 2: Raman scattering spectra of BaTiO₃ nanorods.

[1] W. Satoshi et al., Jpn. J. Appl. Phys. 42 (2003) 6188-6195.

Precipitation of Hematite from Dense β -FeOOH Suspensions with Ammonium Amidosulfonate Adding

Mark Žic, Mira Ristić, Svetozar Musić

Division of Materials Chemistry, Ruđer Bošković Institute, P. O. Box 180, HR-10002 Zagreb, Croatia

Precipitation of hematite (α -Fe₂O₃) from aqueous solutions has been the subject of many investigations. The hydrolysis of aqueous Fe(III)-salt solutions, microemulsion hydrolysis, sol-gel or crystallization from ferrihydrite were used in the synthesis of α -Fe₂O₃. Some precipitation methods are limited due to small yield and they can be only of academic interest. On the other hand, the crystallization from concentrated aqueous Fe(III)-salts solutions yields α -Fe₂O₃ in high quantities. However, in the latter case it is more difficult to control the size and shape of α -Fe₂O₃ particles.

In the present work we have investigated the precipitation of α -Fe₂O₃ particles from dense β -FeOOH suspensions in the presence of amidosulfonate anion under hydrothermal conditions at 160 °C. The samples were characterized by ⁵⁷Fe Mössbauer, FT-IR, XRD, FE-SEM and EDS. The crystallization kinetics of α -Fe₂O₃, the geometrical shape and size of α -Fe₂O₃ particles depended on the concentration of ammonium amidosulfonate added at the start of the precipitation process. The aggregation effect plays an important role in the formation of α -Fe₂O₃ particles. It was also concluded that the geometrical shape and size of both primary and secondary particles were impacted by the preferential adsorption of sulfonate groups under acidic conditions in a dense suspension.

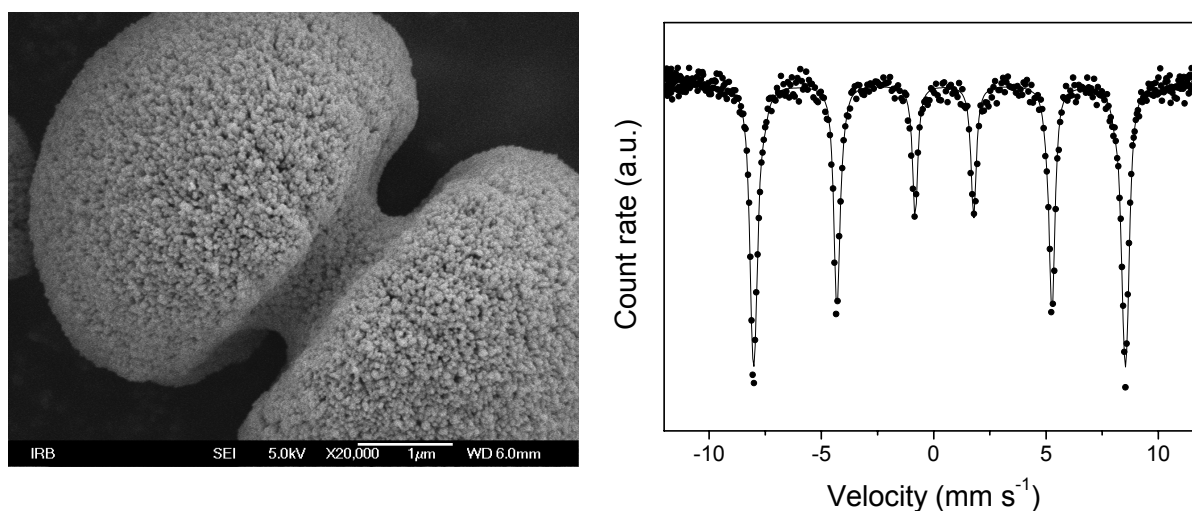


Fig. 1: FE-SEM image of selected sample shows a large α -Fe₂O₃ particle in the form of a double cupola consisting of much smaller particles (left) and the corresponding ⁵⁷Fe Mössbauer spectrum (right).

4. SPECTROSCOPY OF MACROMOLECULES

Quantum-Mechanical Analysis of Intensity Distribution in Resonance Raman and Two-Photon Absorption Spectra of Nucleic Acid Base Pairs

T. Burova, G. Ten, A. Anashkin

*Saratov State University, Astrakhanskaya str. 83, 410026 Saratov, Russia
e-mail: burova2004@inbox.ru*

This study continues the investigation of the resonance Raman (RR) and two-photon absorption (TPA) spectra of nucleic acids by direct calculations of the intensity distribution with the quantum-mechanical method [1] for the adiabatic model in the Herzberg-Teller approximation. In [1] it is suggested that one- and two-photon absorption spectra as well as luminescence and Raman resonance spectra of polyatomic molecules be described using a single approach, in line with the similarity of their physical nature. In one-photon absorption spectra the Herzberg-Teller effect may be quantitatively described with confidence using the procedure [2]. Extension of this procedure to RR and TPA spectra allows one to calculate vibronic coupling and evaluate the relative intensities of lines in these spectra using the same set of initial data. Inclusion of the vibronic term makes it possible to explain the presence of lines corresponding to one-quantum nontotally symmetric vibrations, their odd overtones and combinations. In this study, the method of direct quantum-mechanical calculations is applied to the calculation of the RR and TPA spectra of adenine-thymine (A-T), adenine-uracil (A-U) and guanine-cytosine (G-C) base pairs.

It is shown that the basic features of the intensity distribution in the spectra can be explained only by taking into account the vibronic mixing of electronic states and the contribution to the components of the scattering tensor from excited electronic states located close to the resonance state. Furthermore, it should be noted that the influence of a particular excited electronic state on the intensity distribution in RR spectrum depends not only on the closeness of this state to the resonance state, but also on such factors as the character of the vibronic interaction and the oscillator strength of the corresponding transition. The calculated results agree satisfactorily with experimental RR spectra of A-T, A-U and G-C [3] excited by laser radiation at 266, 240, 218 and 200 nm. The comparative analysis of vibration mode activity was made. A common feature of these spectra is the redistribution of intensity between the bands of two vibrations in passing from the RR spectra corresponding to the resonance with the first two $\pi-\pi^*$ transitions to the spectra corresponding to the resonance with the third and fourth $\pi-\pi^*$ transitions. This feature, which was reflected in our calculations, can be explained by the complexity of intramolecular interactions and by marked changes in the geometrical parameters due to the electronic excitation.

The direct quantum-mechanical calculations of the relative intensities of lines in the TPA spectra of A-T and A-U in the region of the second transition and of G-C in the region of the first $\pi-\pi^*$ transition were also performed. Previously, the method [1] was applied to the description of the RR and TPA spectra of adenine, thymine, uracil and guanine [4-5]. The general and specific features of the intensity distribution in the RR and TPA spectra of nucleic acid base pairs A-T, A-U, G-C and single molecules (adenine, thymine, guanine and cytosine) are compared and discussed.

[1] T. Burova, Zh. Strukt. Khim. 38 (1997) 248-254.

[2] M. Kovner, M. Prijutov, Dokl. Akad. Nauk SSSR 204 (1972) 634-636.

[3] S. Fodor, T. Spiro, J. Amer. Chem. Soc. 108 (1986) 3198-3205.

[4] T. Burova, G. Ten, V. Kucherova, Optics and spectroscopy 95 (2003) 25-29.

[5] T. Burova, G. Ten, V. Kucherova, Optics and spectroscopy 97 (2004) 1-4.

The Structural Changes of Green Fluorescent Protein Induced by Small Guanidine Hydrochloride Concentrations

Olesya V. Stepanenko¹, I.M. Kuznetsova¹, V.V. Verkhusha², V.N. Uversky³, K.K. Turoverov¹

¹ *Institute of Cytology of the Russian Academy of Sciences, Tikhoretsky av. 4, 194064, Saint-Petersburg, Russia,*

² *Albert Einstein College of Medicine, 1300 Morris Park Avenue, 10461, New York, USA,* ³ *Indiana University, 10th Street 410 W, 46202, Indianapolis, USA.*

Green fluorescent protein (EGFP) belongs to a large family of the so-called “fluorescent proteins” or “GFP-like proteins” characterized by the presence of chromophore which able to absorb and in the most cases to emit visible light. A great interest to fluorescent proteins (FPs) is caused by their wide use as biological markers for studying of gene expression and protein localization and tracking in living cells and tissues. In spite of low amino acid homology, all fluorescent proteins have a unique β -can fold which represents an 11 β -stranded cylinder threaded by an α -helix containing the chromophore formed from residues in the position 65-67 through an autocatalytic cyclization. The structure of FPs has been extensively investigated. It has been shown that FPs possess high conformational stability under a variety of denaturing conditions as well as that denaturation process is much slowly as compared to unfolding of proteins having structure of the other topology. This means that native and unfolded states of fluorescent proteins are separated by high energy barrier. In the recent works it is pointed out that the unfolding of GFP is not one-stage process but is accompanied by accumulation of several intermediate states. Existence of intermediate states is thought to be connected with two features of GFP structure. First, the chromophore is slightly twisted in the native protein while it is planar in the unfolded protein. Second, the central helix shows some deviations from optimal geometry. These peculiar properties are supposed to result in hysteresis of unfolding and refolding curves for sfGFP (superfolder).

In this work the effect of small guanidine hydrochloride (GdnHCl) concentrations on the structure of EGFP have been studied. The addition of such denaturant concentrations has been shown to induce no noticeable changes of secondary structure and chromophore microenvironment as can be seen from almost indistinguishable far UV and visible CD spectra; at the same time these GdnHCl concentrations induce just a small tertiary structure distortion recorded by changes in near UV CD spectra and by data of tryptophan fluorescence quenching induced by acryl amide. For all that, the addition of 0.1-0.2 M GdnHCl to EGFP results in approximately 20% increase of “green” fluorescence intensity. Furthermore, experiments on kinetics of EGFP denaturation by GdnHCl have revealed that denaturant addition leads to the sharp increase of chromophore fluorescence intensity which just after GdnHCl addition essentially exceeds the level of native protein intensity.

All experimental data allow us to conclude that both effects have the same nature and caused by the stabilizing action of denaturant. This implies that GdnHCl in small concentrations does not act as denaturant but can stabilize the protein structure through the hydrogen bonds with carbonyl group on the protein surface and through ionic interactions between the denaturant ions and the charged sites on the protein. In the presence of small GdnHCl concentrations the structure of green fluorescent protein becomes less strained. In these conditions, the chromophore being inaccessible to quenching action of water molecules gets less twisted, more planar, configuration. This leads to the increase of the conjugation of a π -electron system that in its turn increases the fluorescence quantum yield of EGFP.

Acknowledgment: This work was supported by Program “Leading Scientific School of Russia” (grant 1961.2008.4) and Russian Science Support Foundation (Stepanenko O.V., 2008).

The Structural Changes of D-Galactose/D-Glucose-Binding Protein Induced by Calcium Depletion

Olga V. Stepanenko¹, I.M. Kuznetsova¹, K.K. Turoverov¹, V. Scognamiglio², M. Staiano², S. D'Auria²

¹ Institute of Cytology of the Russian Academy of Sciences, Tikhoretsky av. 4, 194064, Saint-Petersburg, Russia,

² Institute of Protein Biochemistry CNR, Via Pietro Castellino 111, 80131, Napoli, Italy.

The question of how a protein folds into its unique, compact, highly ordered and functionally active form is one of the most intriguing and perplexing questions of structural and cellular biology. Special attention deserves the role of ligands. The convenient subjects of inquiry to elucidate this problem are the periplasmic ligand binding proteins. This work is focused on investigation of D-galactose/D-glucose-binding protein (GGBP) from *E. coli* belonging to this protein family. GGBP molecule can bind not only one molecule of sugar, but has one calcium localized in the loop of the C-terminal domain and coordinated by oxygen atoms from every second residue of this loop and from Glu 205. The aim of this work is to examine the mutual influence of calcium ion and sugar molecule on GGBP structure. Our investigations have been carried out by intrinsic fluorescence of proteins and far-UV CD.

Kinetics of structural changes of GGBP and its complex with D-glucose (GGBP/Glc) induced by EDTA has been studied. Calcium depletion is shown to result in GGBP structural changes recorded by the increase of intrinsic fluorescence intensity up to 35 % in the first 2 min after EDTA addition to protein solutions. Fluorescence intensity of GGBP achieves its equilibrium value in 4–7 min after mixing of protein and EDTA solutions of different concentrations. Calcium removing finally leads to approximately 20 % increase in fluorescence intensity of GGBP and practically does not affect fluorescence intensity of GGBP/Glc complex. These data apparently indicate that 3D structures of GGBP/Glc with and without calcium are the same which allows us to make conclusion about stabilizing action of D-glucose on the protein structure. Far UV CD experiments reveal that GGBP and GGBP/Glc complex with calcium and calcium free possess the same secondary structure. The denaturation kinetics of GGBP and GGBP/Glc calcium free (GGBP-Ca and GGBP-Ca/Glc, respectively) induced by guanidine hydrochloride (GdnHCl) have been measured by monitoring tryptophan fluorescence intensity and parameter A ($A=I_{320}/I_{365}$ characterizing position and form of fluorescence spectra). It is shown that the rate of denaturation of GGBP with calcium is less than that of GGBP-Ca. Also, denaturation of GGBP-Ca/Glc takes less time compared to that of GGBP/Glc. The value of parameter A recorded after proteins incubation in the presence of 1.0 M GdnHCl during 10 minutes illustrates that according to their resistance to GdnHCl denaturing action, proteins are distributed as follows: GGBP-Ca < GGBP < GGBP-Ca/Glc < GGBP/Glc.

The results of our study prove the stabilizing role of calcium in the structure of GGBP obtained earlier by temperature denaturation [1]. Calcium depletion results in 3D structure changes of GGBP. At the same time, the presence of bounded sugar makes GGBP-Ca/Glc more resistant to structure reorganization induced by calcium removal. Kinetic experiments have revealed that GGBP-Ca is less stable than GGBP while D-glucose binding increases GGBP-Ca/Glc resistance against denaturant.

[1] P. Herman, J. Vecer, I. Barvik Jr., V. Scognamiglio, M. Staiano, M. de Champdore, A. Varriale, M. Rossi, S. D'Auria. *Proteins*. 61 (2005) 184-195.

Acknowledgment

This work was supported by RFBR (№ 06-04-48231), Program “Leading Scientific School of Russia” (№ 1961.2008.4) and Russian Science Support Foundation (Stepanenko Olga V., 2008).

Microwave Hydration Measurements in Aqueous Systems of Proteins and Synthetic Polymers

M.M. Vorob'ev

Institute of Organoelement Compounds, Russian Academy of Sciences, 28 ul. Vavilova, 119991 Moscow, Russia

Microwave treatment at 30 GHz of polymeric aqueous systems was combined with simultaneous hydration measurement by waveguide resonance method. Hydration numbers were estimated from the difference in absorption between undisturbed water and water with solute, as it was attributed to the solute-induced reduction in water mobility. Bound water was shown to be a measure of hydrophobicity allowing to characterize hydrophobically driven processes like temperature-induced coil-globule transition of poly(*N*-isopropylacrylamide) (PNIPA) and gelation of casein micelles at acidification [1, 2].

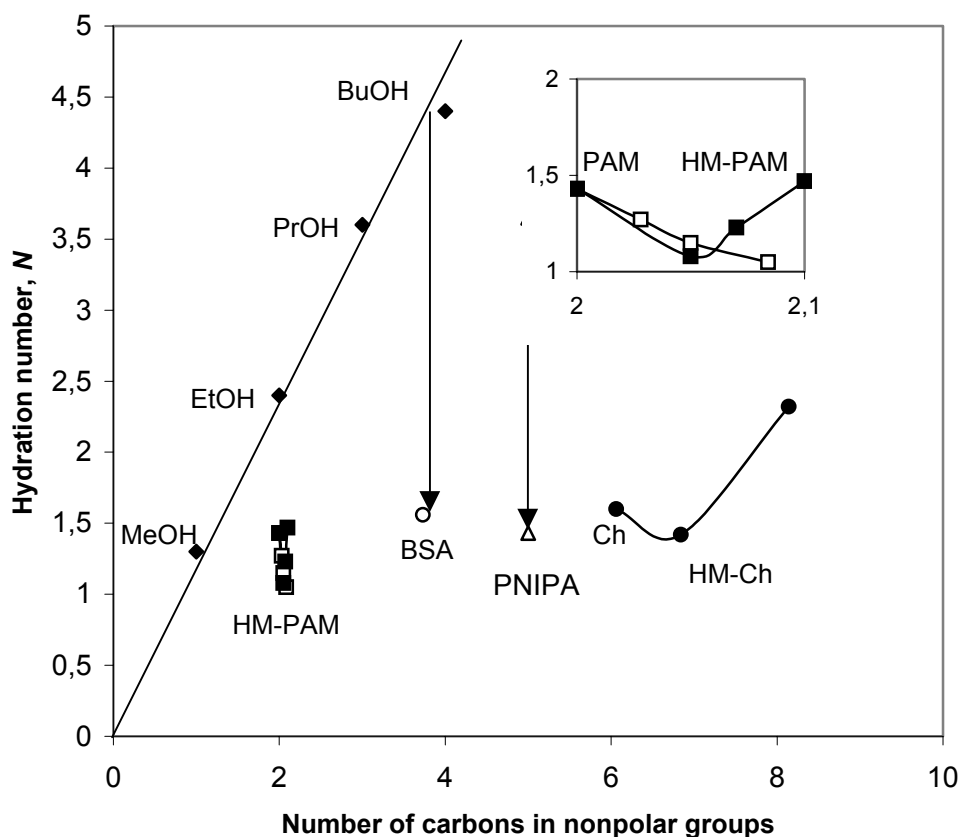


Fig. 1: Dependence of hydration number N on the mean number of carbon atoms in nonpolar groups of hydrophobically modified polyacrylamide (PAM) and chitosan (Ch). PAM and HM-PAM: AM/NMA - ■, AM/DDMA - □; BSA - ○; Ch and HM-Ch - ●; PNIPA(coil) - ▲; PNIPA(globule) - Δ. Straight line corresponds to the aliphatic alcohols (◆).

[1] M.M. Vorob'ev, *Food Hydrocolloids* 21(2007) 309-312.

[2] M. Vorob'ev, N. Churochkina, A. Khokhlov, E. Stepnova, *Macromolecular Bioscience* 7 (2007) 475-481.

Structural Investigation on Some Silk (Dragline, Hiding and Egg Coccon) Samples Weaved by Different Species Living in Turkey

S. İde¹, A.B. Arıĝ¹, T. Trkeŝ², O. Mergen³, S. Haman Bayarı⁴, . elik⁵

¹Hacettepe Univ., Faculty of Eng., Dept. of Physics Eng. 06800 Beytepe-Ankara, Turkey

²Niĝde Univ., Faculty of Science, Dept. of Biology, Niĝde, Turkey

³Hacettepe Uni., Faculty of Science, Dept. of Biology, 06800 Beytepe-Ankara, Turkey

⁴Hacettepe Univ., Faculty of Education, Dept. of Physics Ed. 06800 Beytepe-Ankara, Turkey

⁵Harran Univ., Faculty of Science and Art, Dept. of Physics, Őanlıurfa, Turkey

Spiders produce a variety of high performance structural fibres with mechanical properties unmatched in the native world and comparable with the very best synthetic fibres produced by modern technology [1-2]. X-ray diffraction and FT-IR spectroscopy were used to investigate the molecular structure of spider silks weaved by *Salticidae Heliophonus flavipes*, *Titanocidae nurscia albomaculate*, *Agelera lambrinitica*, *Cheiraconthium erralicum*. Silk samples were collected from the natural habitats of the species (Near Salt Lake / Őereflikoçhisar, İvriz Dam / Ereĝli-Konya, Karataŝ Lake/ Burdur) in Turkey [3]. Egg coccon and hiding silk samples of *Titanocidae Nurscia albomaculate* were investigated separately to find the crystallization difference of alanine and glycine rich regions in these structures. Serine (an amino acid) is also found in the structure of egg coccons.

X-ray diffraction and infrared spectroscopy results indicated that the structural differences exist in the samples. The crystallographic planes in the X-ray patterns were investigated to find the effect of alanine and glycine rich crystalline regions in the structures.

[1] A. Bram, C.I. Branden, C. Craig, I. Snigireva, C.Riekell, J. Appl. Cryst. 30 (1997) 390-392.

[2] J.M. Gosline, P.A. Guerette, C.S. Ortlepp, K.N. Savage, J. Exp. Biol. 202 (1999) 3295-3303.

[3] A.B. Arıĝ, The Report of Advanced Physics Project Laboratory, Advisor: Dr. Semra İde, FIZ 402-22 (2007) 1-51.

Acknowledgment

This work was supported by TUBİTAK (TBAG- 107T017).

DFT Vibrational Study of Organic-Inorganic Hybrid Polymers Based on 3-Glicidoxypropyltrimethoxysilane

L. Bistričić¹, V. Volovšek², V. Dananić², I. Movre Šapić², M. Leskovic²

¹*Department of Applied Physics, Faculty of Electrical Engineering and Computing, University of Zagreb,
Unska 3, 10000 Zagreb, Croatia*

²*Faculty of Chemical Engineering and Technology, University of Zagreb,
Marulićev trg 19, 10000 Zagreb, Croatia
e-mail: lahorija.bisticic@fer.hr*

Organic-inorganic hybrid polymers have recently attracted much attention since they combine the advantages of organic polymers, like toughness and flexibility, with those of inorganic components such as high heat resistance, good optical and mechanical properties. The objective of this research is the characterization of the structure of organic-inorganic hybrid polymers based on 3-glicidoxypropyltrimethoxysilane (GPTMS). GPTMS molecule possesses both epoxy and silicon alkoxide functionality and so interlinked organic-inorganic networks can be formed. Hydrolysis of the methoxy groups gives silanol groups (SiOH) which can condense and form siloxane (SiOSi) bonds. The epoxy ring can be opened and polymerized to form organic network.

In this work polymer with inorganic SiOSi bonds (GPTMS-1) and hybrid polymer obtained from GPTMS/APTES (3-aminopropyltriethoxysilane) system (GPTMS-2) was prepared by a sol-gel process. The structure of polymers was characterized by vibrational spectroscopy (Raman and IR). The interpretation of vibrational spectra is supported by the normal coordinate analysis based on density functional theory (DFT) calculations. A comprehensive conformational and vibrational analysis of expected polymer structures has been carried out by DFT calculations using Becke's three-parameter exchange functional in combination with the Lee-Young-Parr correlation functional (B3-LYP) and standard 6-311+G(d,p) basis set.

The comparison of theoretical spectra with the experimental data enabled us to extract the characteristic vibrational bands of different polymer structures. The free GPTMS molecule has characteristic fundamentals at 1256 cm⁻¹ (mode of epoxy ring) as well as SiO stretching modes at 642 and at 612 cm⁻¹ [1]. The SiO stretching vibrations are not evident in spectra of GPTMS-1 polymer indicating the condensation of methoxy groups and possibility of inorganic SiOSi polymerization. The intense Raman band observed at 1136 cm⁻¹ and assigned to the SiOSi stretching vibrations suggests the ladder-type structure of GPTMS-1 polymer [2]. In vibrational spectra of GPTMS-2 polymer the absence of 1256 cm⁻¹ band and NH₂ stretching modes at ~ 3400 cm⁻¹ from APTES [3] resulted from reaction between primary amine and epoxy ring. The analysis of vibrational spectra has shown that the structure of GPTMS-2 polymer obtained by simultaneous inorganic and organic polymerization depends on the presence of water and solvents.

[1] I. Movre Šapić, L. Bistričić, V. Volovšek, V. Dananić, sent to J. Mol. Struct

[2] L. Bistričić, V. Volovšek, V. Dananić, J. Mol. Struct. 834-836 (2007) 355-363.

[3] V. Volovšek, L. Bistričić, V. Dananić, I. Movre Šapić, J. Mol. Struct. 834-836 (2007) 414-418.

Quantum-Mechanical Calculation of the Intensity Distribution in Resonance Raman Spectra of Derivatives of Uracil

T. Burova, G. Ten, A. Anashkin

Saratov State University, Astrakchanskaya str.83, 410026, Saratov, Russia
e-mail: burova2004@inbox.ru

A quantum-mechanical calculation [1] of the intensity distribution in the resonance Raman (RR) spectra of 2-thiouracil (2-TU), 4-thiouracil (4-TU), 2,4-thiouracil (2,4-TU), F-uracil and Cl-uracil is carried out for exciting laser radiation at different wavelengths (300, 257, 248 nm). It is shown that, for satisfactory agreement between the calculated results and the experimental data, it is necessary to take into account in the calculations of relative intensities of lines the Herzberg-Teller effect and the contribution from excited electronic states adjacent to the resonance state.

In description of the RR spectra of uracil, it was noted that, on going from the spectra corresponding to resonance with the first $\pi\pi^*$ transition to the spectra corresponding to resonances with transitions to highly excited electronic states, the intensity distribution between the lines of the vibrational structure varies. This feature is also observed in the RR spectra of thiosubstituted derivatives of this compound. Common to all these spectra is the very fact of the intensity redistribution, whereas the character of redistribution is specific for each individual spectrum. This is explained by the complexity of interactions in molecules of uracil and derivatives and by the noticeable changes in the geometric parameters of these molecules upon electronic excitation.

Table 1: Calculated and experimental values of the relative intensities of lines in the RR spectra of 2,4-thiouracil excited by laser radiation at 300 nm

Calculated 2,4-TU		Calculated 121(2,4-TU)		Calculated 2141(2,4-TU)		Experiment [2]	
Wave-number (cm ⁻¹)	Relative intensity	Wave-number (cm ⁻¹)	Relative intensity	Wave-number (cm ⁻¹)	Relative intensity	Wave-number (cm ⁻¹)	Relative intensity
1617	1.0	1618	1.0	1634	0.11	1614	0.87
1542	0.16	1558	0.27			1566	0.36
1482	0.42	1510	0.36	1536	0	1494	0.47
1428	0.61	1407	0.56	1431	0.21	1422	0.72
1326	0.05			1373	0.25	1362	0.27
1195	0.28	1201	0.40	1224	1.0	1234	1.0
1149	0.07	1146	0.11	1135	0.59	1128	0.56
1065	0.11			1075	0.31	1086	0.20

For dithiouracil we made calculations not only for stable structure (2,4-TU) but also for two tautomeric forms – 141-TU and 2141-TU. In each case the calculated results for some lines didn't agree with the experimental data. But when we combined the picture of intensity distribution in all these spectra the good qualitative agreement became possible. This fact is illustrated by data of the table 1. Because the experimental data was obtained for water solution of dithiouracil our results showed that of all forms (2,4-TU, 141-TU and 2141-TU) may be presented in the conditions of experiment [2] (water solutions) with the same probability.

[1] T.Burova, Khim. Fiz. 64 (1994) 29.

[2] M.Ghomi, R.Letellier, E.Taillandier, L.Chinsky, A.Laigle, P Turpin, J. Raman Spectr. 17 (1986) 249.

Monitoring of Hydrogen-Deuterium Exchange in Membrane Proteins using Attenuated Total Reflection Infrared (ATR-IR) Spectroscopy and a Microdialysis Perfusion-Cell

E. Džafić, O. Klein, W. Mäntele

*Institut für Biophysik, Johann Wolfgang Goethe-Universität,
Max von Laue-Str. 1, 60438 Frankfurt/Main, Germany
e-mail: dzafic@biophysik.org*

Protein structure and flexibility was studied by probing water accessibility in $^1\text{H}/^2\text{H}$ exchange experiments using ATR-IR spectroscopy and a microdialysis perfusion-cell. The perfusion-cell was developed using a diamond ATR unit with 7 reflections. The solution or suspension of target protein in H_2O buffer contained in a chamber with sample volumes of below $5\ \mu\text{l}$ is in contact with the ATR crystal and separated from the flowing $^2\text{H}_2\text{O}$ by a dialysis membrane (molecular weight cut-off value of 25 kDa). The perfusion ATR unit is characterised by small volumes for the target protein and the buffer solution used for perfusion, by high stability and fast response, and by high sensitivity for the detection of binding-induced conformational changes. Its design is shown in Fig. 1.

As an example, the amide proton exchange of Na^+/H^+ antiporters was followed, NhaA [1] from *Escherichia coli* and MjNhaP1 [2] from *Methanococcus jannaschii*. They are involved in cell energetics, regulation of cytoplasmic Na^+ , alkaline pH homeostasis and cellular volume [3, 4]. Fundamental for cytoplasmic pH regulation is their activity which is strongly regulated by pH. NhaA is inactive at pH 7 and below but highly active at alkaline pH value from above pH 8. The active state of MjNhaP1 is between pH 6 and 6.5, which is identical to the human homologue NHE1, but opposite to NhaA. The analysis of $^1\text{H}/^2\text{H}$ exchange using amide II mode has been carried out for inactive and active state of the protein, respectively. This provides information about accessible fraction of polypeptide chain between these two states. With further study of the exchange amide protons with respect to time, it was possible to distinguish between exchanging rate of amide protons in different regions of the protein. $^1\text{H}/^2\text{H}$ exchange experiments allowed to investigate the flexibility and structural changes between inactive and active state of the protein.

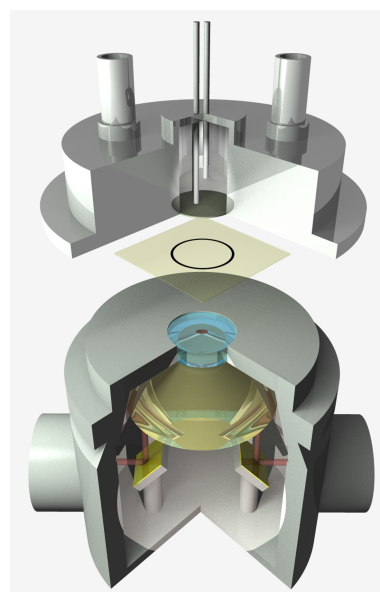


Fig. 1: ATR-IR Microdialysis Perfusion-Cell

- [1] C. Hunte, E. Screpanti, M. Venturi, A. Rimon, E. Padan, H. Michel, *Nature* 435 (2005) 1197-1202.
- [2] K.R. Vinothkumar, S.H.J. Smits, W. Kühlbrandt, *EMBO J.* 24 (2005) 2770-2729.
- [3] E. Padan, N. Maisler, D. Taglicht, R. Karpel, S. Schuldiner, *J. Biol. Chem.* 264 (1989) 20297-20302.
- [4] E. Padan, T. Tzuber, K. Herz, L. Kozachkov, A. Rimon, L. Galili, *BBA* 1658 (2004) 2-13.

Spectroscopic Study of Pre-ceramic Polymers Obtained by Hydrolytic Condensation of Ethoxycyclosiloxanes

M. Handke¹, A. Kowalewska², W. Mozgawa¹

¹*Faculty of Materials Science and Ceramics, AGH University of Science and Technology
Al. Mickiewicza 30, Kraków, POLAND*

²*Centre of Molecular and Macromolecular Studies, Polish Academy of Sciences
Ul. Sienkiewicza 112, Łódź, POLAND
e-mail: mhandke@agh.edu.pl*

Cyclosiloxanes of general formula: $\text{Si}_n\text{O}_n(\text{CH}_3)_n(\text{OEt})_n$ ($n = 4, 5$ and 6) were prepared by controlled hydrolytic condensation of dichloromethylsilane, followed by dehydrogenative coupling with ethanol. Such alkoxy derivatives of cyclic siloxane molecules were subsequently condensed in sol-gel process with the formation of new type xerogels - polymeric precursors for silicon-based modern ceramics. The process undergoes selectively on hydrolysable alkoxy groups.

Composition and structure of the obtained xerogels were studied by FT-IR, CP MAS-NMR and XRD methods. Thermal properties of the samples were determined by DTG measurements. The silsesquioxane structure of the materials obtained in the sol-gel process varied, depending on the size of monomeric cyclosiloxane molecules and the reaction conditions. The shape of starting 4, 5 or 6-membered siloxane rings is preserved in the silsesquioxane macromolecules.

Selected xerogels were heated in the temperature range of 600 °C to 1000 °C both, in air and argon atmospheres. Structure of final ceramic materials was determined by FT-IR, CP MAS-NMR and XRD methods.

Acknowledgment

Financial support for this work was provided by Polish Ministry of Science and Higher Education under grant N507 093 31/2271.

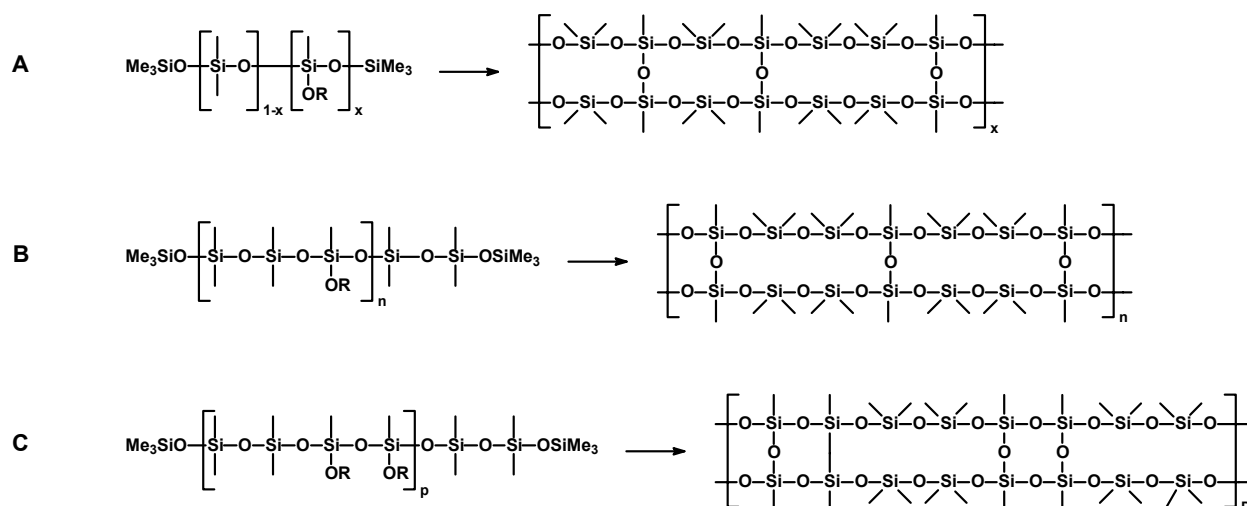
New POSS-Siloxane Materials of Ladder-Like Structure

M. Handke¹, A. Kowalewska²

¹Faculty of Materials Science and Ceramics, AGH University of Science and Technology
Al. Mickiewicza 30, Kraków, POLAND

²Centre of Molecular and Macromolecular Studies, Polish Academy of Sciences
Ul. Sienkiewicza 112, Łódź, POLAND
e-mail: mhandke@agh.edu.pl

A series of POSS-siloxane materials containing ladder-like linkages between siloxane chains was obtained with linear oligosiloxane precursors bearing side alkoxy groups {siloxanes of regular structure A [M(D₂D^{OR})₁₀D₂M] and B [M(D₂D^{OR})₂]₁₀D₂M}, as well as oligomers of random distribution of Si-OR units along the main siloxane chain C [PDMS(1-x)PM(OR)S_x (x = 0.15, 0.3, 0.5, 1.0)]. Alkoxy-functionalized oligosiloxane precursors were cross-linked under hydrolytic condensation conditions. The relationship between the structure of siloxane chain (the amount of Si-OR units and their distribution along the polymer backbone) and the properties of obtained preceramic materials were studied by CP-MAS NMR, DSC, TGA, SEC. The details including analysis of the influence of type-T siloxane linkages distribution on the polymer properties will be described.



Selected POSS-siloxane materials were heated in the temperature range 600 to 1000 °C in both, air and argon atmospheres. The structure of final ceramic materials was determined by FT-IR, CP MAS-NMR and XRD methods.

Acknowledgment

Financial support for this work was provided by Polish Ministry of Science and Higher Education under grant N507 093 31/2271.

Characterization of Some Irradiated Materials Using Spectroscopic and Related Methods

Sorin Ilie, Radu Setnescu

European Organization for Nuclear Research (CERN), CH-1211 Geneva 23, Switzerland

Perfluorohexane coolant and some polymer based electrical insulators used within High Energy Physics Detectors in the Large Hadrons Collider (LHC) at CERN were irradiated in different conditions and were characterized using spectroscopic methods (FT-IR, UV-Vis, chemiluminescence) together with GC and DSC methods. The aim of this work was the assessment of the radiation hardness, thus the service time of such materials. Their various radiation sensitivities during the irradiation process were explained as a function of oxygen together with known impurities presence and the content of specific protective molecules.

FTIR Spectroscopy of Lipoproteins - A Comparative Study

D. Krilov, M. Balarin, M. Kosović, O. Gamulin and J. Brnjac-Kraljević

University of Zagreb School of Medicine, Šalata 3b, Zagreb, Croatia

Lipoproteins are object of extensive research for last 40 years due to their active role in atherogenesis. The spherical particles consist of polar lipid monolayer which encapsulates apolar lipids. The apolipoprotein is mostly embedded in the lipid monolayer.

The presence of external compounds can induce structural changes in lipoproteins which can alter their normal metabolic pathways. These changes will be studied by FTIR and FT-Raman spectroscopy. The first step was to thoroughly describe the spectra of intact particles in all frequency regions. So far the studies on lipoproteins were limited to the amid I band which produces information about the secondary structure of apolipoprotein. The four major classes of lipoproteins were so far studied by FTIR spectroscopy: very low density lipoprotein (VLDL), low density lipoprotein (LDL) and two subclasses of high density lipoproteins (HDL₂ and HDL₃). The different position of amid A band in high frequency region of the spectra of particular lipoproteins reflects the influence of hydrogen bonds in β -sheets in Apo B (LDL and VLDL) on N-H stretching vibration. In fingerprint region (Fig. 1), the composition of amid I band was resolved by curve fitting method. The results are in agreement with the data about the secondary structure of Apo A I and Apo B. The comparison of the intensities of lipid ester bond at 1738 cm⁻¹ and amid I and amid II band give the information about the ratio of lipid and protein content in the particle. There are also some differences in the structure of the two bands, around 1240 cm⁻¹ and 1088 cm⁻¹ from phosphate group of phospholipids. In the region of skeletal modes the CH=CH bending vibration arises from the unsaturated fatty acids and the information about the intensity of this band reflects the ratio of these fatty acids in different lipoproteins. The bands assigned to amide V, amide IV and amide VI are also observed in this region but with low intensity.

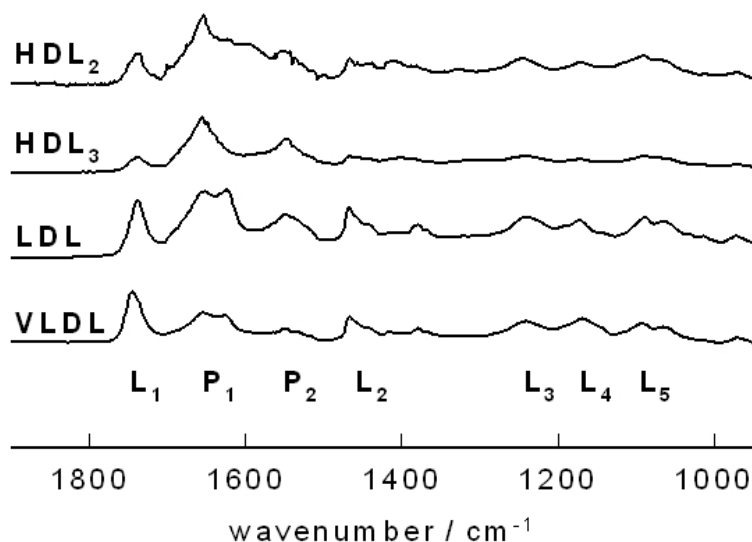


Fig. 1: IR spectra of dried lipoprotein films in fingerprint region. Lipid (L) and protein (P) bands are marked by the letters under the spectra: L₁ - C=O stretch, P₁ - amide I, P₂ - amide II, L₂ - CH₂ bend, L₃ and L₅ - phosphate group vibrations, L₄ - CH₃ rock

Different Interaction Models for Explanation of Optical Properties of Ligand-Polynucleotides Systems

E.A. Minakova, E.B. Kruglova

*Biophysics department, IRE of NAS of Ukraine, 12 Ac. Proskura str., Kharkov 61085, Ukraine
e-mail: evgenia_minakova@mail.ru*

Spectrophotometry in visible region was used to investigate the processes of complexation in a system of ligand-polynucleotide. These investigations were developed in large area of wavelengths and polynucleotide concentrations. But usually not whole set of obtained data is used simultaneously at binding parameters determination especially for Scatchard plot construction and other simple methods.

Many ligands can bind to double stranded matrix forming several types of complexes with different optical parameters. Those binding parameters for each type of complex can be calculated via using optimization programs of optical titration data. So, the influence of different complexes on total optical properties of mixtures at multimodal binding can be found.

Using two kinds of competitive binding models, describing ligands interaction with polyelectrolyte, the equilibrium composition (association constants, stoichiometry and molar extinction coefficients) was calculated by the DALSMOD optimization program of spectrophotometric concentration dependences for Actinomycin D derivatives in the presence of native and denatured DNA samples.

Two binding models for competitive binding with different values of parameters were considered. The first model provides for accounting cooperative effects at interaction on adjacent sites of external binding molecules. And the second model describes the differences in spectral and thermodynamic parameters between monomeric bound intercalated ligands and molecules bound to neighbour site sizes.

Spatially unlocalized monovalent ions added to the system can be competitive ligands at drugs (cations) binding. In consideration of monovalent ions (Na^+ , K^+) influence of as competitors for both external and intercalating binding types and using both models, the accounting of different types of complexes contribution in observable optical absorption were found for different concentration of added ions.

FTIR Spectroscopic Characterization of Cu(II) Coordination Compounds with Exopolysaccharide Pullulan and its Derivatives

Ž. Mitić¹, G.S. Nikolić², M. Cakić², P. Premović³, Lj. Ilić⁴

¹Faculty of Medicine, Department of Pharmacy, Bul. dr Zorana Đinđića 81, 18000 Niš, Serbia
e-mail: zak_chem2001@yahoo.com

²Faculty of Technology, Bul. Oslobođenja 124, 16000 Leskovac, Serbia

³Laboratory for Geochemistry, Cosmochemistry and Astrochemistry, University of Niš, 18000 Niš, Serbia

⁴Pharmaceutical and Chemical Industry "Zdravlje Actavis Co.", 16000 Leskovac, Serbia

Pullulan is a water-soluble, extracellular neutral polysaccharide with a linear flexible chain of α -(1 \rightarrow 6)-linked maltotriose units, whose structure is intermediate between dextran and amylose structures because of the coexistence of both α -(1 \rightarrow 6) and α -(1 \rightarrow 4)-glycosidic linkages in a single compounds. In alkali solutions Cu(II) ion forms complexes with reduced low-molar pullulan (RLMP). The metal content and the solution composition depended on pH. The complexing process begins in weak alkali solution (pH>7), and involves OH groups in C(2) and C(3) or C(6) pullulan monomer units (α -D-glucopyranose). Complexes of Cu(II) ion with reduced low-molar pullulan were synthesized in the water solutions, at the boiling temperature and at different pH values (7.5–12). Fourier-Transform Infrared (FTIR) spectroscopic data of synthesized complexes are rare in literature. FTIR spectroscopic characterization (FTIR, LNT-FTIR, ATR-FTIR, deuterated FTIR and FTIR microspectroscopy) is now widely used to study the composition of complex carbohydrate systems, the molecular interactions, molecular orientation and conformational transitions of polysaccharides [1–4]. FTIR spectroscopic characterization (FTIR-spectrometer Bomem MB-100 (Hartmann&Braun Canada), connected with variable temperature cell Specac P/N-21525 for the LNT measurements), and FTIR microspectroscopy system (ATR-FTIR spectrometer Bruker Hyperion Tensor-27 in conjunction with a FTIR Bruker Hyperion-1000/2000 microspectroscopy attachment equipped with a 15 \times objective and a 250- μ m liquid N₂ cooled MCT detector, ATR objective GMBH, Germany) of Cu(II) ion complexes with RLMP (M_w 6000 g mol⁻¹) was done in this work. Samples of Cu(II) ion complexes with RLMP were deuterated 2 hours at room temperature in vacuum. Investigation of Cu(II) complexes by D₂O isotopic exchange is very sensitive method for OH group coordination, and related to hydrogen bond strength.

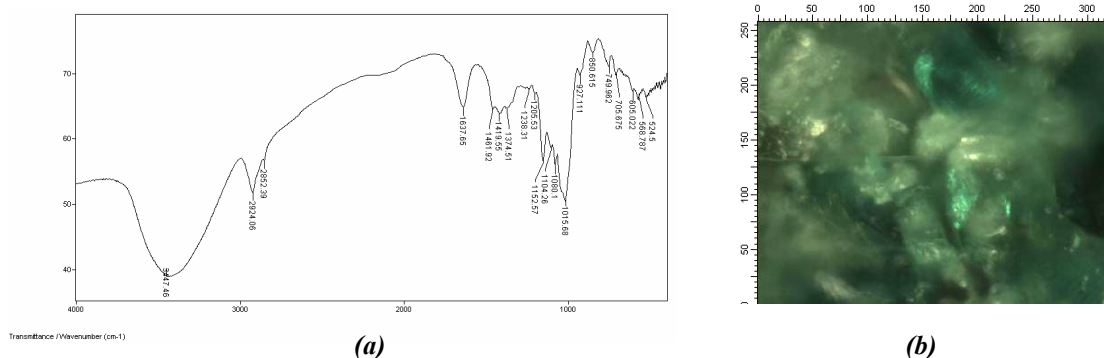


Fig. 1: FTIR spectrum of Cu(II)–RLMP complex synthesized at pH 7.5 (a); and FTIR microscopy image (250 μ m \times 300 μ m) (b)

- [1] G.S. Nikolić, M. Cakić, Ž. Mitić, Lj. Ilić, Russ. J. Coord. Chem. 34(5) (2008) 322–328.
 [2] Ž. Mitić, G.S. Nikolić, M. Cakić, et al., Russ. J. Phys. Chem. 81(9) (2007) 1433–1437.
 [3] M. Cakić, Ž. Mitić, G.S. Nikolić, Lj. Ilić, G.M. Nikolić, Spectrosc.-Int. J. (2008) in press.
 [4] R.G. Zhabankov, V.M. Andrianova, M.K. Marchewka, J. Mol. Struct. 436–437 (1997) 637–654.

Concentration of Vapor Phase Corrosion Inhibitor in Anticorrosion Polymer Films – Correlation of Ion-Beam Analysis Results and UV-Vis Spectrophotometry

I. Pucić, B. Mihaljević, M. Jakšić

*Ruder Bošković Institute, Zagreb, Bijenička 54, Croatia
e-mail: pucic@irb.hr*

Anticorrosion polyolefinic films are being increasingly used in corrosion protection, from packaging of electronic products to protection of firearms of all sizes. Anticorrosion polymer films are produced by coextrusion of polymer and vapor phase corrosion inhibitor (VCI) that slowly diffuses out of the film and forms a protective layer on metal surface. Thereby the concentration of VCI in the film decreases with time what limits duration of anticorrosion protection. Earlier [1] we analyzed a number of such films of various ages, identified polymer carrier as low-density polyethylene and VCI as an organomolybdate salt. We also confirmed that VCI provides protection by migrating out of the film. We determined that the protection last up to 6 or 7 years, depending on initial concentration of VCI in the film. Particle Induced X-Ray Emission spectroscopy, an ion-beam analysis method was necessary both to confirm the nature of VCI and determine its concentration in anticorrosion films. The concentration of molybdenum in the films is very low so the error of classical analytical methods would be greater than the expected concentration change or even concentration itself. In PIXE the X-ray emission characteristic of a particular nuclei produced by, in this case proton impact on a material, is measured so it is possible to identify the nuclei present in the film if corresponding atomic number is higher than 12 and to determine its concentration in the sample if larger than 1 ppm. The drawback of PIXE method is its limited availability. Because of that, a method that provides fast and reliable determination of VCI concentration change with time to detect when the anticorrosion protection ends was needed.

Since UV-VIS spectrophotometers are much more widespread, the goal of this investigation was to determine whether there is a correlation between the concentration of Mo determined by PIXE and UV-VIS absorptions in anticorrosion films. The assumption that the anticorrosion films are of same thickness was checked by FTIR. The UV-VIS spectra of selected anticorrosion films with various concentration of VCI were recorded showing two prominent absorptions at about 710 and 610 nm. In spite of the problems of determination of the molar absorptivities of the VCI, the intensities of both absorptions had excellent correlation to molybdenum concentrations determined by PIXE so it was concluded that UV-VIS spectroscopy could be used to control the decrease of VCI concentration. In that manner control of the properties of anti-corrosion films is possible provided initial concentration of VCI is determined by another method that gives absolute concentration of VCI in the sample.

[1] I. Pucić, T. Madžar, M. Jakšić, Chem. Monthly 137 (2006) 953-961.

γ -Irradiated Poly(Ethylene Oxide): Spectroscopic and Thermal Analysis

I. Pucić, T. Jurkin

*Ruđer Bošković Institute, Zagreb, Bijenička 54, Croatia
e-mail: pucic@irb.hr*

Polymer modification by high energy radiation has many advantages: no catalyst or additives are needed to initiate the reaction and it can be performed at various temperatures. The initiation is homogeneous throughout the system resulting in higher reaction extents and the reaction rate is easily controlled by varying the dose rate. The products are sterile what is important for medical applications. Chemical properties of a particular polymer determine its radiation response: generally crosslinking is the main effect in unsaturated chain polymers while degradation dominates in the polymers with saturated carbon chain,

Poly(ethylene oxide), PEO, is a semicrystalline polymer that is widely used particularly for preparation of polyelectrolytes and hydrogels. PEO mostly degrades if irradiated in air while crosslinks in the inert atmosphere, but numerous factors can influence the outcome, so its radiation chemistry has to be investigated in detail. Infrared spectroscopy combined with thermal analysis is a powerful tool to study corresponding changes, while other experimental techniques can provide additional information.

Ionizing radiation usually reduces the degree of crystallinity of polymers, both because of crosslinking and degradation, but in some cases shorter polymer chains formed on degradation of more radiation-sensitive amorphous part easily crystallize resulting in an increased degree of crystallinity. The changes in the degree of crystallinity are easily and quickly assessed by differential scanning calorimetry (DSC), the shapes of thermograms and heats of phase transformations being very sensitive.

The purpose of this study is to assess the changes brought into PEO by ^{60}Co γ -radiation to selected doses, taking into consideration its properties (molecular mass) whether it was irradiated as powder, pellet or in solution, in air or nitrogen, its postirradiation changes. Thermal analysis showed that the heats of crystallization generally increased at lower doses but then decreased with the dose, the changes being more pronounced at higher dose rate. The peak widths increased and crystallization temperatures decreased reflecting lower quality of crystallites that further decreased during postirradiation period. The molecular mass and sample form had minor effects on thermal properties of irradiated PEO samples. The greatest changes occurred in PEO irradiated as aqueous solution. Thermal analysis cannot offer information on underlying chemical change since both crosslinking and degradation may result in the same type of thermal changes.

To record infrared spectrum each PEO sample type had to be approached differently and appropriate spectral range to be chosen carefully. The most prominent changes in FTIR spectra of PEO on irradiation in solid state are the absorption increases at about 3500 cm^{-1} and 1100 cm^{-1} while some absorptions at 960 cm^{-1} and 842 cm^{-1} somewhat decreased in number of others samples. Carbonyl absorptions appeared in the samples where oxidative degradation occurred due to the irradiation in air while in those irradiated in the inert atmosphere vinyl absorptions appeared. Such changes are mostly due to degradation. The spectra of hydrogels recorded in the NIR region showed significant increases at 7000 cm^{-1} and 5250 cm^{-1} and shifts of those maxima to higher wavenumbers indicating changes in hydrogen bonding implying both crosslinking and structural changes in those samples.

Spectroscopic Study of Ablated Organic Substances by a Pulsed Er:YAG Laser

J. Striova¹, M. Camaiti¹, A. Sansonetti¹, A. deCruz², R. Palmer², E.M. Castellucci³

¹ICVBC-CNR Florence, Via Madonna del Piano 10, Sesto Fiorentino, Italy

²Department of Chemistry, Duke University, Durham, NC, USA

³Lens and Department of Chemistry, via Lastruccia 3, 500 19 Sesto Fiorentino, Italy

The interaction between a pulsed free-running erbium:YAG laser radiation (2940 nm wavelength) and macromolecular materials is examined by means of spectroscopic techniques (infrared and micro-Raman). The Er:YAG laser radiation at 2.94 μm is strongly absorbed by O-H and/or N-H bonds and hence the ablative action is often mediated by means of auxiliary wetting agents containing these groups. Processes activated in polymeric materials, when irradiated by the Er:YAG laser in presence (wet conditions) or absence (dry conditions) of wetting agents, have been studied; this kind of interaction is of interest in studying innovative cleaning methods for cultural heritage. Actually, laser ablation is currently used in cleaning problems on stone, metal and other materials, used as substrates in artistic techniques. Nevertheless, the Nd:YAG laser (1064 nm) has been, till now, the most used and studied source in removing gypsum based black crust, particulate deposits and other kind of soiling from artistic surfaces. The Er:YAG laser source represents an innovative cleaning method, especially in removing polymeric layers.

The polymers under examination had a form of thin films covering a marble substrate. The fresh and the artificially aged (UV) films were irradiated using different laser energies first in dry and then in wet conditions.

In those polymers that do not contain –OH and/or –NH group in their molecular structure (e.g., acrylates, polyvinylacetate) no reaction with respect to the laser radiation has been detected in the range of utilized energies, both in dry and wet conditions. On the other side, materials containing –OH or –NH groups (e.g., proteinaceous polymers) may directly interact with the laser radiation, mainly in dry conditions. This interaction is evidenced, above all, by change in the film color, and also by the variations in the spectral characteristics of irradiated materials. Raman and infrared data proved useful, even though not exhaustive, in characterizing the effects of the erbium:YAG laser radiation on organic materials.

Binding of Water-Soluble, Globular Proteins to Anionic Model Membranes

F. Torrens¹, G. Castellano²

¹*Institut Universitari de Ciència Molecular, Universitat de València, Edifici d'Instituts de Paterna, P. O. Box 22085, 46071-València, Spain,* ²*Instituto Universitario de Medio Ambiente y Ciencias Marinas, Universidad Católica de Valencia San Vicente Mártir, Guillem de Castro-94, 46003-València, Spain*

The role of electrostatics in the adsorption process of proteins to preformed negatively-charged (phosphatidylcholine/phosphatidylglycerol, PC/PG) and neutral (PC) small unilamellar vesicles (SUVs) is studied [1]. The interaction is monitored, at low ionic strength, for a set of model proteins as a function of *pH* [2]. The adsorption behaviour of lysozyme, myoglobin and bovine serum albumin (BSA) with *pI*s = 10.7, 6.9 and 5.5, respectively, with preformed SUVs is investigated, along with changes in the fluorescence emission spectrum of charged proteins, *via* the adsorption on SUVs [3]. Significant adsorption of the proteins to negatively-charged SUVs is only found at *pH* values, where the number of positive charge moieties exceeds the number of negative charge moieties on the protein by at least 3 e.u. Negligible adsorption to SUVs composed of zwitterionic lipids is observed in the tested *pH* range (4–9), except for formally dianionic cardiolipin (CL). The fluorescence emission of positively-charged proteins increases after adsorption on negatively-charged SUVs. With increasing protein to phospholipid ratio, the increase in the fluorescence emission levels off and reaches a plateau; protein adsorption profiles show a similar shape. Analysis of the data demonstrates that neutralization of the SUV charge, due to the adsorption of the positively-charged proteins, is the controlling factor in their adsorption. The reached plateau level depends on the type of protein and the *pH* of the incubation medium. This *pH* dependency can be ascribed to the mean positive charge of the protein. The effective charge of lysozyme, myoglobin and BSA (defined as the number of phosphatidylglycerol groups neutralized by one adsorbed protein molecule) is calculated from the charge differences between empty and protein-coated SUVs, using the Gouy–Chapman theory.

[1] F. Torrens, A. Campos, C. Abad, *Cell. Mol. Biol.* 49 (2003) 991-998.

[2] F. Torrens, C. Abad, A. Codoñer, R. García-Lopera, A. Campos, *Eur. Polym. J.* 41 (2005) 1439-1452.

[3] F. Torrens, G. Castellano, A. Campos and C. Abad, *J. Mol. Struct.* 834-836 (2007) 216-228.

Raman Spectroscopic Study of Siloxane Structures Developed Under Low Pressure

V. Volovšek¹, K. Furić², L. Bistričić³

¹Faculty of Chemical Engineering and Technology, University of Zagreb, Marulićev trg 19, Zagreb, Croatia, e-mail: volovsek@fkit.hr

²Ruder Bošković Institute, Bijenička 54, Zagreb, Croatia, e-mail: kfuric@irb.hr

³Faculty of Electrical Engineering and Computing, University of Zagreb, Unska 3, Zagreb, Croatia, e-mail: lahorija.bisticic@fer.hr

As a part of our study of polymerization process of aminopropylsilanetriol (APST) we investigated the behavior of APST dissolved in water (~25%) under low pressure (~ 5 mbar) by Raman spectroscopy. It has been already noticed that the polymerized structure of APST depends significantly on the temperature at which the condensation took place [1]. At the same time the speed of evaporation of water could also play important role in forming different polymer structures. In order to distinguish between these two influences, the glass tubes with solution were connected to the vacuum pump and exposed to the low pressure of ~5 mbar for one to three hours. The samples with different concentrations of water were then left to polymerize under atmospheric conditions. In order to determine the starting water content, the samples were weighted after being exposed to the low pressure and at the end of the condensation process.

Raman spectra of solutions and of condensed samples were recorded. Structure developments were also monitored under mid-magnification optical microscope.

The spectra of solutions show the change in distribution of water clusters present in different solutions [2]. Concentration of tetramers, pentamers and hexamers is increasing with decreasing content of water. On the other hand, the same condition favors formation of *gauche* conformation of propyl chain in APST molecules [3]. At the same time the accelerated decrease of water contents hinders the formation of siloxane ladder structure [4] in APST polymer.

[1] V. Volovšek, L. Bistričić, K. Furić, V. Dananić, I. Movre Šapić, J. Phys.: Conference Series. 28 (2006) 135-138.

[2] M. Starzak, M. Mathlouthi, Food Chemistry 82 (2003) 3-22.

[3] L. Bistričić, V. Volovšek, V. Dananić, I. Movre Šapić, Spectrochim. Acta A 64 (2006) 327-337.

[4] V. Volovšek, L. Bistričić, K. Furić, V. Dananić, I. Movre Šapić, J. Mol. Struct. 834 (2007) 414-418.

5. OPTOELECTRONICS AND SEMICONDUCTOR MATERIALS

Laser-induced Fluorescence Measurements On CdSe Quantum Dots

Z. Györi¹, D. Tátrai², F. Sarlós², G. Szabó², A. Kukovecz³, Z. Kónya³, I. Kiricsi^{3,1}

¹Bay Zoltan Foundation for Applied Research, Institute for Nanotechnology, H-3515 Miskolc-Egyetemváros Pf. 46, Hungary, ²Department of Optics and Quantum Electronics, University of Szeged, H-6720 Szeged, Rerrich Béla tér 1., Hungary, ³Department of Applied and Environmental Chemistry, University of Szeged, H-6720 Szeged, Rerrich Béla tér 1., Hungary

Quantum dots (QDs) are semiconductor nanocrystals with a typical size smaller than 10 nm in diameter. They are mostly composed of atoms from groups II-VI or III-VI elements of the periodical table. Their properties are between those of bulk semiconductors and discrete atoms, with unique optical and electronic characteristics due to the quantum confinement effect. One of the most important properties of these nanocrystals is the size-tunable fluorescent emission wavelength. For example, CdSe QDs vary in color from yellow to red and their luminescence from blue to red depending on their size.

CdSe nanocrystals in various sizes were synthesized in air by the kinetic growth method which is based on the “greener route” from CdO and elemental Se precursors. The obtained particle size depends on many synthesis parameters such as the temperature of the CdO solution, the injection time of the Se stock solution, the overall solution temperature, the initial concentration of the precursors, and especially, the growing time.

We studied the effects of changing the growth time on the size, emission spectrum and the fluorescence lifetime of the synthesized QDs. The size was determined from the absorption spectrum. The decay time measurements were based on single shot time-resolved laser-induced fluorescence techniques where a third harmonic generated pulsed Nd:YAG laser system was used as source.

Due to the quantum confinement effect and Fermi's golden rule the fluorescence decay times should decrease with size. Two different decay times can be measured on CdSe QDs. Each sample has a fast and a relatively slow decay. The fast one was measured by a streak camera, while the slow one by a PIN diode and oscilloscope. The sum of two exponential decays was fit to the measurement results (Fig. 1). Whereas the slow decay (t_2) show the expected size dependence, the fast one (t_1) appears to be size independent.

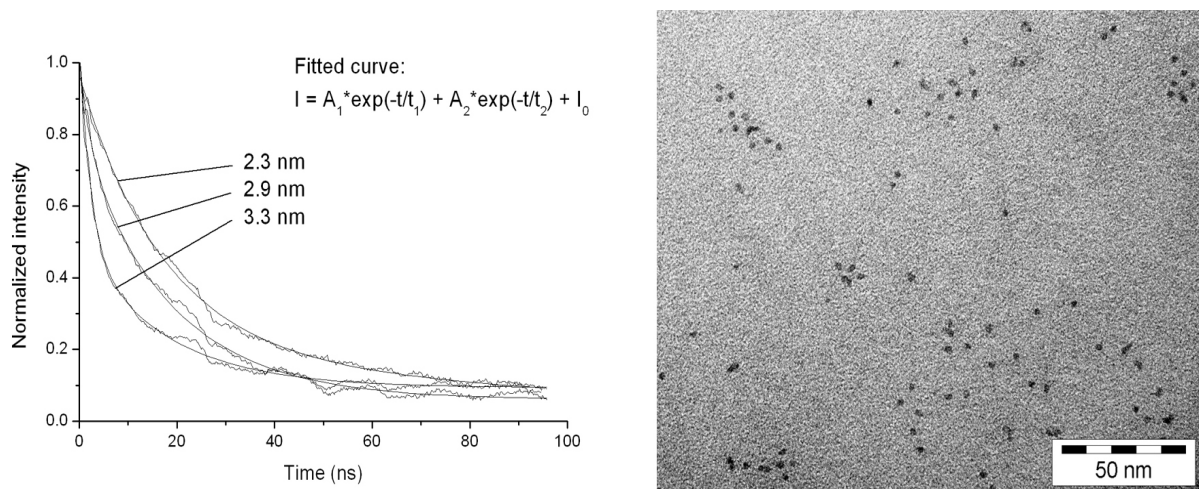


Fig. 1: Decay curves of different size CdSe QDs (left) and TEM image of synthesized CdSe nanocrystals with mean size of 2.9 nm (right)

Spectroscopic Characterization of Mechanochemically Synthesized Cr/SnO_x Nanocomposites

G. Kozma, Á. Kukovecz, Z. Kónya

*Department of Applied and Environmental Chemistry, University of Szeged,
Rerrich B. tér 1, Szeged, H-6720 Hungary*

Gaining control over the morphology and physico-chemical properties of semiconductor oxide nanomaterials is an important field of contemporary materials science research. Their potential applications include e.g. sensors, intelligent coatings and ceramic glazes [1]. We have recently discussed how spectroscopic methods can be applied to uncover the formation kinetics of SnO₂ nanoparticles synthesized in a planetary ball mill [2].

Here we report on the successful mechanochemical synthesis of Cr/SnO_x nanocomposites. Samples were characterized by IR, Raman and diffuse reflectance UV-Vis spectroscopy, X-ray diffraction, atomic force microscopy and scanning electron microscopy (SEM) (Fig. 1).

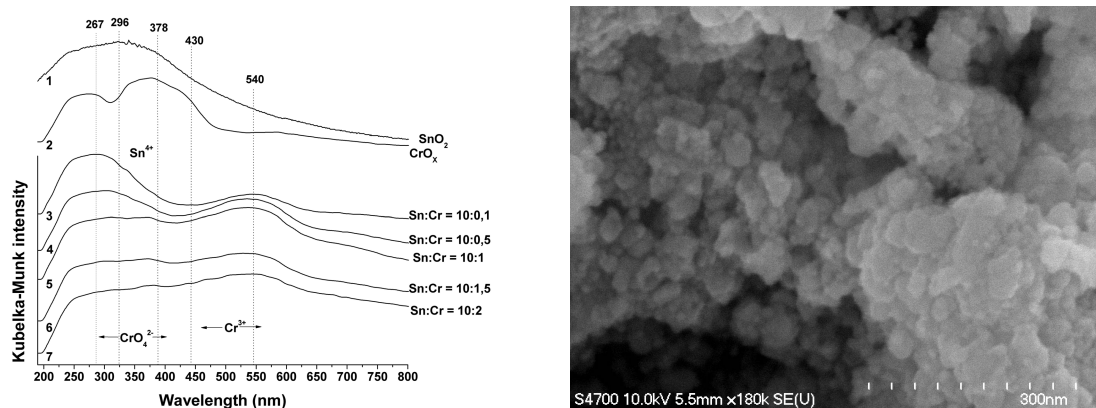


Fig. 1: Diffuse reflectance UV-Vis spectra of mechanochemically synthesized Cr/SnO_x nanocomposites (left) and SEM image of the Sn:Cr=10:1 composite (right)

We have found it possible to control both the chemical properties and the particle size distribution of the composites by varying the Sn:Cr ratio and the calcination temperature. Our results indicate that chromium does not form a separate phase in the samples, but rather, it acts as a dopant of the tin-oxide matrix.

[1] E. López-Navarrete, A.R. González-Elipe, M. Ocaña, *Ceramics International* 29 (2003) 385-392.

[2] G. Kozma, Á. Kukovecz, Z. Kónya, *J. Mol. Struct.* 834-836 (2007) 430-434.

FT-Raman and X-ray Diffraction Spectra of CuInS₂ Films by the Spray Pyrolysis at Different Substrate Temperatures

Bariş Altıokka¹, Sabiha Aksay², Güneş Süheyla Kürkcüoğlu³

¹Bilecik Vocational School, Bilecik University, TR-11100 Bilecik, Turkey

²Faculty of Sciences, Department of Physics, Anadolu University, TR- 26470 Eskisehir, Turkey

³Faculty of Arts and Sciences, Department of Physics, EskişehirOsmangazi University, TR- 26480 Eskisehir, Turkey

We report the structural and Raman properties of CuInS₂ (CIS) polycrystalline films deposited onto corning glass substrates by spray pyrolysis (SP) method. The films were grown at different substrate temperatures in the range, 225–275 °C. The X-ray diffraction (XRD) spectra showed that all of the films are of polycrystalline nature (Fig. 1a). The (112) peak intensity increases with the increase in substrate temperature and the film tends to have a preferential orientation. Texture coefficient (TC), grain size values and lattice constants were calculated. The elemental analysis and surface morphology of the deposited films were investigated by EDX and Scanning electron micrograph (SEM), respectively. The surface morphology is found to be smooth and dense from SEM images for both the films. The optical band gap of the film was found to be substrate temperature dependent [1]. The FT-Raman spectrum of the film is shown in Fig. 1b. It can be seen that there are four Raman peaks at 64.95 (E⁶), 114.07 (E⁴), 299.96(A₁) and 468.59 cm⁻¹ (CuS and/or Cu₂S). The films also present additional modes in the FT-Raman spectra, together with the ones that are chalcopyrite related. The results are agreement with the literature [2-5]. These results point to important photovoltaic applications of this material.

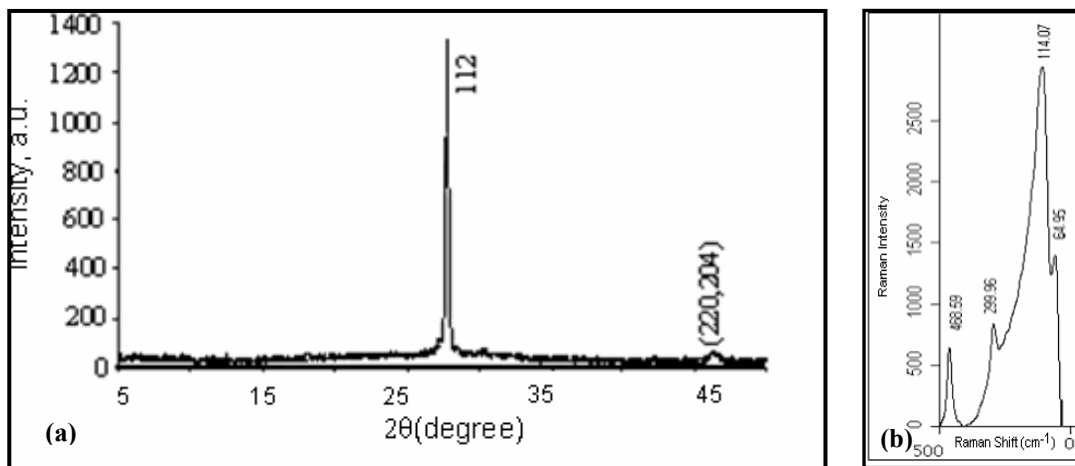


Fig. 1: XRD (a) and FT-Raman spectra (b) of CuInS₂ polycrystalline film at 275 °C substrate temperature.

- [1] S. Aksay and B. Altıokka, Phys. Stat. Sol. (c) 4 (2007) 585-588.
- [2] T. Riedle, Ph. D. Thesis, Technical University of Berlin, 2002.
- [3] E. Rudigier, B. Barcones, I. Luck, T. Jawhari-Colin, A. Perez-Rodriguez, R. Scheer, J. Appl. Phys. 95 (2004) 5153-5158.
- [4] F.W. Ohrendorf, H. Haeuseler, Cryst. Res. Technol. 35 (2000) 569-578.
- [5] J. Alvarez-Garcia, E. Rudigier, N. Rega, B. Barcones, R. Scheer, A. Perez-Rodrigues, A. Romano-Rodriguez, J.R. Morante, Thin Solid Films 431-432 (2003) 122-125.

Structural, Optical and Electrical Characterization of Porous Silicon Prepared on Thin Epitaxial Layer

M. Balarin¹, O. Gamulin¹, M. Ivanda², M. Kosović¹, D. Ristić², M. Ristić², S. Musić²,
K. Furić², D. Krilov¹ and J. Brnjas-Kraljević¹

¹Department of Physics and Biophysics, University of Zagreb, Medical School,
Šalata 3b, 10000, Zagreb, CROATIA

²Rudjer Bošković Institute, P.O. Box 180, 10002 Zagreb, CROATIA ivanda@rudjer.irb.hr

Commercially available silicon-on-insulator wafers, consisting of 22 μm thick p-type silicon epitaxial layer grown on 280 μm thick n-type (111) silicon substrate, were electrochemically etched¹ in hydrofluoric acid (HF) to produce porous silicon (PSi) samples. The pores of different size and different depth were obtained by etching at different time duration, from ten to eighty minutes, using constant concentration of 48% HF in ethanol solution. The structural and the optical properties of prepared samples were investigated by FT-IR, Raman spectroscopy and scanning electron microscopy (SEM).

Current-voltage characteristics² were determined by enhancing the voltage until the current reached 100 mA, which produced 8 mA/cm² current density. Sudden increase of current, after approximately 10 minutes, was observed. That increase might be connected with the etching out of the insulator layer inside the wafer. During the remaining etching time the current was kept constant. In that period, the decrease of voltage was measured. That was explained by the decrease of resistivity caused by etching out the insulator layer.

All samples showed photoluminescence (PL) peak in the visible spectral range. The intensity of the PL peak was increased with the increase of etching time. The exception was the sample in which the whole epitaxial and insulator layers were etched out. It showed the decrease in the PL peak intensity.

There was practically no difference in recorded Raman spectra comparing with the crystal silicon (c-Si) Raman spectrum, indicating that the samples consist mostly of macroporous structures. This statement is consistent with the obtained SEM images.

The appearance of the Si-H_x vibrational bands, ranging from 2000 to 2300 cm⁻¹, observed in the FT-IR spectra, is consistent with the porous silicon etching process.

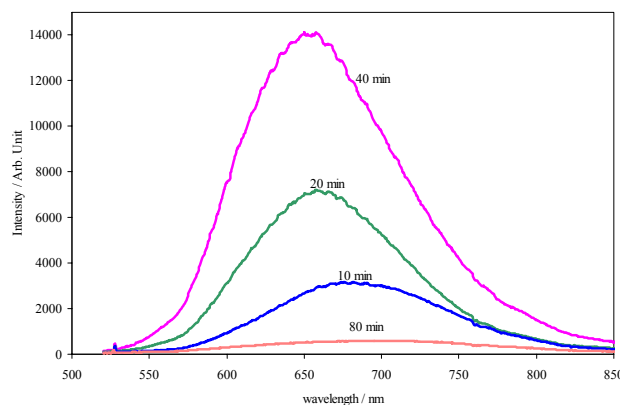


Fig. 1: The PL spectra of samples etched at different time duration

[1] Z. Gaburro, N. Dalbosco, L. Pavesi, Porous Silicon, Encyclopedia of Condensed Matter Physics, in: F. Bassani, J. Liedl, P. Wyder (Eds.), Elsevier, Amsterdam, 2005.

[2] R.L. Smith, S.D. Collins, J. Appl. Phys. 71 (1992) R1-R22.

Guanylurea(1+) Hydrogenphosphite – A New Material for Non-Linear Optics

M. Fridrichová¹, I. Němec¹, P. Němec²

¹Charles University in Prague, Faculty of Science, Department of Inorganic Chemistry, Hlavova 2030, 128 40 Prague 2, Czech Republic

²Charles University in Prague, Faculty of Mathematics and Physics, Department of Chemical Physics and Optics, Ke Karlovu 3, 121 16 Prague 2, Czech Republic

Guanylurea(1+) hydrogenphosphite belongs to the family of salts of nitrogen-containing organic compounds with delocalized π - electrons. This group of compounds has potential to have interesting non-linear optical properties, especially high efficiency of the second harmonic generation (SHG).

In this contribution we are reporting on preparation, crystal structure determination, spectroscopic and optical characterisation of guanylurea(1+) hydrogenphosphite. This salt can be prepared by acid hydrolysis of cyanoguanidine water solutions. It crystallizes as single crystals or more usually as aggregates in good yield from solutions with stoichiometric concentration or even a little excess of phosphorous acid. Its crystals are transparent, relatively hard, non-hygroscopic and resistant. The non-centrosymmetric lay-out of guanylurea(1+) hydrogenphosphite and its laminated structure, assembled by numerous hydrogen bonds (see Fig.1), are essential for optical properties of the compound.

FTIR and FT Raman spectra were recorded and interpreted according to computations based on B3LYP 6-31+G(d,p) (ultrafine grid) method. SHG efficiency of powdered guanylurea(1+) hydrogenphosphite was determined at 800 nm.

Guanylurea(1+) hydrogenphosphite is due to its easy preparation and advantageous physical and optical properties a very promising material for applications in non-linear optics.

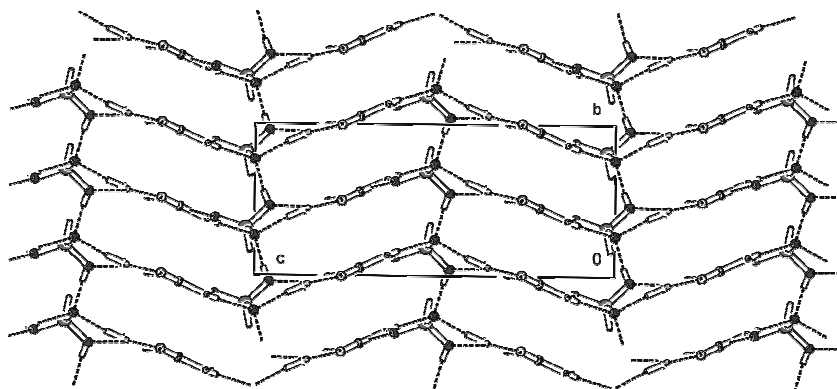


Fig. 1: Guanylurea (1+) hydrogenphosphite structure assembly
(view in crystallographic direction 100)

The Effect of Annealing on Electrical, Structural and Optical Properties of Sol Gel ITO Thin Films

Talaat Moussa Hammad

*Physics Department, Faculty of Science, Al-Azhar University, P.O. Box 1277,
Gaza, Palestine*

The ITO thin films (In : Sn = 90 : 10) were prepared by the sol gel dip-coating process on glass substrates and then were annealed in air at different temperatures from room temperature to 550 °C for 1 h. The electrical resistivity of ITO thin films was decreased by increasing annealing temperature. XRD pattern showed that increasing annealing temperature increased the crystallinity of thin films and at 550 °C high quality crystalline thin films with preferentially oriented in the (111) direction. The UV-Vis transmittance spectra were also confirmed that the annealing temperature has significant effect on the transparency of thin films. The highest transparency at wavelength 520 nm of spectrum 92.3% obtained at 550 °C on annealing temperature. The allowed direct band gap at temperature range RT TO 550 °C was estimated 3.39–4.15 eV. It was observed that the direct energy gap increases as the annealing temperature increases.

Theoretical and Experimental Investigation of Vibrational (FT-IR and Raman) Spectra and Electronic Transitions of Di-p-tolylamine

I. Kavlak¹, G.S. Kürkçüoğlu², T. Arslan³

¹Eskişehir Osmangazi University, Graduate School of Sciences, 26480 Eskişehir, Turkey,

²Eskişehir Osmangazi University, Faculty of Arts and Science, Department of Physics, 26480 Eskişehir, Turkey,

³Eskişehir Osmangazi University, Faculty of Arts and Science Department of Chemistry, 26480 Eskişehir, Turkey

The growing interest in molecular organic materials as the basis for creating optoelectronic devices has led to an increasing interest in the structure and growth dynamics of organic molecular thin films. Molecular organic semiconductors are promising materials for organic light-emitting diodes [1, 2], thin-film transistors [3], and photovoltaic devices [4]. One of the most important molecules is di-p-tolylamine. Therefore, we report a structural and spectroscopic investigation of the di-p-tolylamine molecule. The optimized geometry of this molecule was calculated from *ab-initio* and quantum chemistry density functional theory (B3PW91 and B3LYP methods) with using 6-31+G(d) basis set on the ground state. Vibrational wavenumbers, infrared and Raman intensities and normal mode descriptions were predicted. Calculated wavenumbers and intensities were compared with the FT-IR and Raman spectra of di-p-tolylamine, thus supporting for a general assignment of the recorded spectra. In Fig. 1(a) and (b), FT-IR and Raman spectra of di-p-tolylamine are presented, representively.

Density Functional Theory (DFT) method was used to determine the minimum energy structures of di-p-tolylamine by using B3LYP and B3PW91 functional 6-31+G(d) level. Then, theoretical UV spectrum was obtained by Time-Dependent DFT (TDDFT) and compared to the experimental spectrum (Fig. 1(c)). The singlet and triplet excited states of di-p-tolylamine found by TDDFT calculations. The lowest excited triplet state of di-p-tolylamine almost entirely consists of the single HOMO→LUMO+1 configuration. The excitation energy of 3.47 eV is rather close to the difference in energies of HOMO and LUMO.

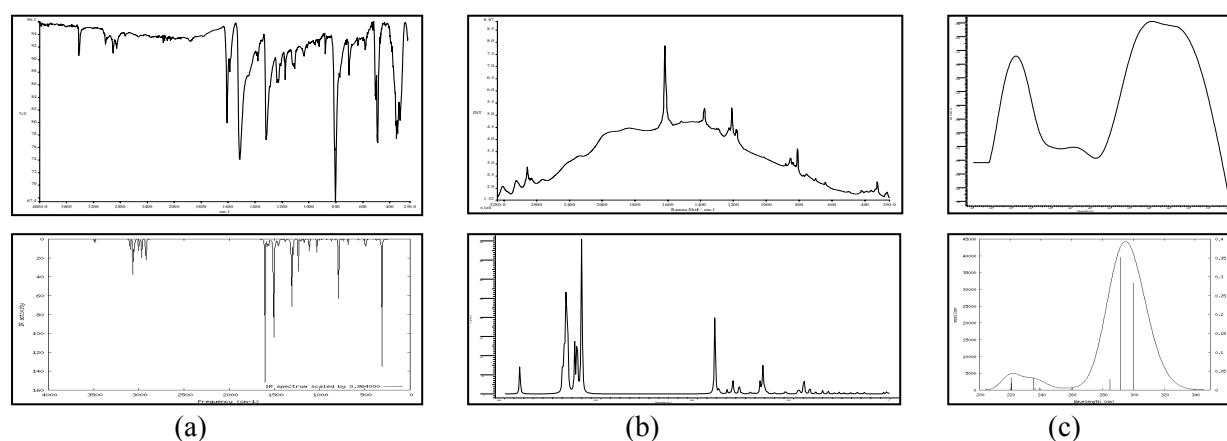


Fig. 1: Experimental and Theoretical Infrared spectra (a) Raman Spectra (b) UV spectra (c) of di-p-tolylamine

[1] W. Brütting, S. Berleb, A.G. Miickl, *Org. Electron.* 2 (2001) 1-36.

[2] S.R. Forrest, *Chem. Rev.* 97 (1997) 1793-1896.

[3] H.E. Katz, *J. Mater. Chem.* 7 (1997) 369-376.

[4] J. Simon and J.J. Andre, *Molecular Semiconductors*, Springer, Berlin, (1985).

Application of the Phonon Confinement Model on the Optical Phonon Mode of Silicon Nanoparticles

D. Ristić, M. Ivanda and K. Furić

Ruder Bošković Institute, P.O.Box 180, 10002 Zagreb, Croatia

The Si-rich silicon oxide (SiO_x) thin films are prepared on silica substrates by low pressure chemical vapor deposition (LPCVD) method and by the physical vapor deposition method (PVD). In order to induce the phase separation to SiO_2 and Si nanostructures the samples are annealed at the temperatures 900-1100 °C. The phonon confinement model is used to calculate the effect of quantum confinement inside the silicon nanoparticle on the optical phonon mode Raman peak. The results are used to determine the size distribution of nanoparticles from the Raman spectrum. The effect of stress on the shift of the optical phonon mode Raman peak is also discussed.

EPR Structural Investigation of CuO-V₂O₅-P₂O₅-CaO Glass System for Optoelectronic Applications

N. Vedeau¹, D.A. Magdas², O. Cozar³, I. Ardelean³

¹ Iuliu Hatieganu University of Medicine and Pharmacy, Department of Biophysics, 400023, Cluj-Napoca, Romania, e-mail: nvedeanu@phys.ubbcluj.ro

² National Institute for Research and Development of Isotopic and Molecular Technologies, 400293, Cluj-Napoca, Romania

³ Babes-Bolyai University, Faculty of Physics, Department of Biomedical Physics, 400084, Cluj-Napoca, Romania

$x(\text{CuO} \cdot \text{V}_2\text{O}_5)(1-x)[\text{P}_2\text{O}_5 \cdot \text{CaO}]$ glass system with $0 \leq x \leq 40$ mol% was investigated using EPR spectroscopy. EPR spectra of the studied glasses did not put in evidence the typical hyperfine structure of copper ions, only the hyperfine structure of vanadium ions. According to the calculated EPR parameters ($g_{\parallel} \sim 1.93$, $g_{\perp} \sim 2.00$ and $A_{\parallel} = 196 \cdot 10^{-4} \text{ cm}^{-1}$) vanadium ions are present in this glasses in a square pyramidal (C_{4v}) site as VO^{2+} ions [1]. The spectra put also in evidence the existence of two sets of hyperfine structures for vanadyl ions, fact that was also evidenced by Hosono et all [2].

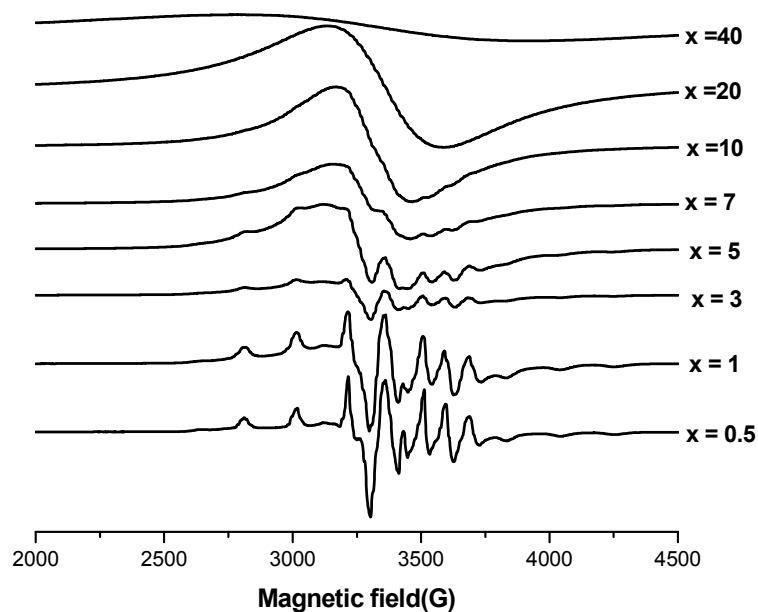


Fig.1: EPR spectra of $x(\text{CuO} \cdot \text{V}_2\text{O}_5) (100-x)[\text{P}_2\text{O}_5 \cdot \text{CaO}]$

The shape of the EPR spectra is modified with the increasing of vanadium and copper ions content. For $x \geq 3$ mol% the appearance of a broad line in the spectrum suggests the formation of ion pairs ($\text{V}^{4+} \cdot \text{V}^{4+}$, $\text{Cu}^{2+} \cdot \text{Cu}^{2+}$ and $\text{V}^{4+} \cdot \text{Cu}^{2+}$) linked through dipole-dipole interactions. For intermediate concentrations ($x > 7$ mol%) the prevalent interactions between ions are the superexchange ones, as the broad line is narrowing [3].

At high content of TM ions ($x > 20$ mol%) the cluster line becomes again larger suggesting a certain degree of ions dispersion in the studied glass system.

[1] O. Cozar, I. Ardelean, V. Simon, L. David, N. Vedeau, V. Mih, Appl. Magn. Reson. 16 (1990) 473.

[2] H. Hosono, H. Kawazoe, T. Kanazawa, J. Non-Cryst. Solids 37 (1980) 427.

[3] V. Ramesh Kumar, R.P.S. Chakradhar, A. Murali, N. O. Gopal, J. Lakshmana Rao, Int. J. Mod. Phys. B 16 (2003) 3033.

The Structural Changes Induced in Lead-Phosphate Glasses by Addition of Cooper Oxide

D.A. Magdas¹, N. Vedeanu², O. Cozar³, I. Ardelean³

¹National Institute for Research and Development of Isotopic and Molecular Technologies, Donath, 71-103, P.O. 700, RO-400293, Cluj-Napoca, Romania, e-mail: amagdas@itim-cj.ro

²Iuliu Hatieganu University of Medicine and Pharmacy, Department of Physics-Biophysics, RO- 400023, Cluj-Napoca, Romania

³Faculty of Physics, Babes-Bolyai University, 400084 Cluj-Napoca, Romania

Cooper-doped phosphate glasses have interesting electrical and optical properties that make them suitable for use as super-ionic conductors, solid state lasers, color filters and non-linear optics. The main advantage of phosphate glass over other oxide glasses (e.g. silicate and borate) is its ability to accommodate to high concentration of transition metal ions and to remain amorphous [1].

The $\text{CuO} \cdot (1-x)[2\text{P}_2\text{O}_5\text{PbO}]$ glass system with $0 \leq x \leq 50$ mol% was prepared and characterized by mean of vibrational spectroscopy in order to understand the role of CuO in the local structure. The aim of this work is to study the compositional dependence of different structural units which appear in these glasses with the increasing of the cooper ions content.

The addition of cooper oxide leads to more P=O bond breakage and the formation of the P-O-Cu bonds. We concluded that at high content of CuO it acts in the structure of glasses as a network former. Similar trend was observed in iron-lead-phosphate glasses with addition of iron oxide [2]. The presence of the Cu-O-P and Fe-O-P bonds for higher content of modifier oxide in these glass systems is consistent with the improving of their chemical durability.

[1] E. Metwalli, M. Karabulut, D.L. Sidebottom, M.M.Morsi, R.K.Brow, J.Non-Cryst. Solids 344 (2004) 128.

[2] D.A. Magdas, O. Cozar, V. Chis, I. Ardelean, N. Vedeanu, Vibrational Spectroscopy (in print).

Spectral Properties of New Tetrafluoro-pentenyl-perylene in Isotropic Solvents, Liquid Crystal Layers, and LB Films

E. Wolarz¹, E. Mykowska¹, T. Martyński¹, R. Stolarski²

¹Faculty of Technical Physics, Poznań University of Technology, Nieszawska 13a, 60-965 Poznań, Poland,

²Institute of Polymer Technology and Dyes, Łódź University of Technology, 91-224 Łódź, Poland

Perylene derivatives are characterized by some fluorescent properties which are highly desirable in many technological applications. These are, in particular, high photostability, great quantum yield, and well defined molecular electronic absorption and emission oscillators. As a rule, perylene derivatives are well soluble in thin homogeneously aligned films of liquid crystals and capable of forming two-dimensional systems (Langmuir – Blodgett films) under certain conditions. The electronic absorption and fluorescence spectra of such systems are very important sources of information about ordering of the dye molecules and the intermolecular interactions leading in some cases to formation of self-aggregates.

As it was reported recently, some *n*-alkoxy-carbonyl-perylenes in LB films could form *J*-aggregates in the ground state [1]. The self-aggregation resulted in a small shift of the absorption maxima towards longer wavelengths and in broadening of the absorption band. Moreover, it was found that the emission of E and Y type excimers had dominating contribution to the fluorescence spectra of the LB films. Similar effects are expected for 3,4,9,10-tetra-(2,2,3,3,4,4,5,5,5-tetrafluoro-1-pentenyl)-perylene for which the hydrogen atoms in the alkoxy chains are replaced with the fluorine ones. The electronic absorption band of this dye dissolved in chloroform shows two maxima at 443 nm and 471 nm (Fig. 1). The respective fluorescence maxima are found at 490 nm and 520 nm. The fluorescence quantum yield in the same solvent is equal to 0.47 ± 0.03 . The basic data quoted here indicate that the tetrafluoro-pentenyl-perylenes are very promising dyes for applications (for example in OLED technology). In the presentation, the effect of self-aggregation of this perylene derivative dissolved in thin layers of 8CB liquid crystal and in LB films will be discussed in detail.

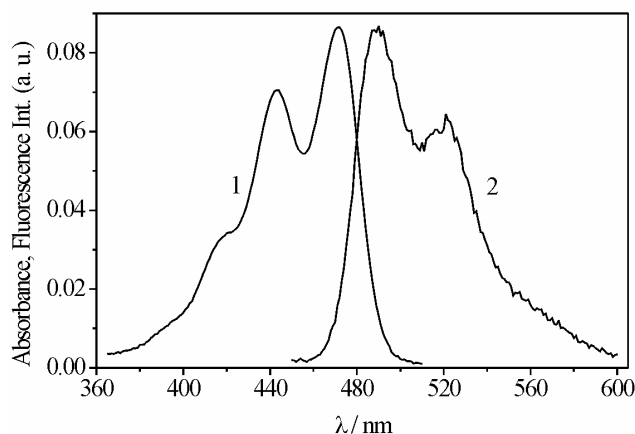


Fig. 1: Electronic absorption (1) and fluorescence (2) spectra of 3,4,9,10-tetra-(2,2,3,3,4,4,5,5,5-tetrafluoro-1-pentenyl)-perylene in chloroform ($x_M = 5 \cdot 10^{-7}$, $d = 1\text{mm}$)

[1] R. Hertmanowski, E. Chrzumnicka, T. Martyński, D. Bauman, J. Luminescence 126 (2007) 323–332.

Acknowledgements

This work was supported by Poznań University of Technology Research Project No. 64-027/2008-BW.

6. SPECTROSCOPY IN CHEMICAL, PHARMACEUTICAL AND ENVIRONMENTAL ANALYSES

Assessment of the Discrimination of Animal Fat by FT-Raman Spectroscopy

O. Abbas¹, R. Codony², C. von Holst³ and V. Baeten¹

¹ *Quality Department of Agro-food Products, Walloon Agricultural Research Centre (CRA-W),
Chaussée de Namur, 24, B-5030 Gembloux, Belgium*

² *Departament de Nutrició i Bromatologia, Facultat de Farmàcia, Av. Joan XXIII, s/n – 08028 Barcelona, Spain*

³ *Joint Research Centre (EC-JRC-IRMM), Retieseweg, 111, B-2440 Geel, Belgium
e-mail: o.abbas@cra.wallonie.be*

Animal fats are important animal by-products and are currently used as ingredient in feeding formulations. However, in the aftermath of the BSE crisis all animal by-products utilised in animal nutrition have been subjected to close scrutiny [1]. Therefore, the majority of European Union Member States have regulated the use of the animal by-products in the animal feeds. Criteria for the safe use of ruminant fat in animal nutrition in Europe are defined by the Regulation 1774/2002 [1] which requires that the material belongs to category of the animal by-products fit for human consumption and the maximum concentration of residual insoluble impurities after purification does not exceed 0.15%.

In the same time, scientists are already working on methods in order to determine and differentiate the fats used in feedstuff formulations in terms of their sources [1], the production technology and from composition data [2]. The objective of our work is to evaluate the suitability of Fourier Transform – Raman spectroscopy for the differentiation of various animal fat origins. This technique is one of the new generation of analytical techniques, fast and non-destructive. Raman spectroscopy is based on the scattering of the light by the molecule.

For this study, we have worked on samples from previous studies [3, 4] which have permitted us to constitute a sample set of 80 fats representative of the major sources of animal fats (fish, poultry, chicken, beef, pig, lamb). Samples were measured by FT-Raman and then treated by chemometric methods to examine the ability of Raman spectroscopy to differentiate the studied animal fats.

Spectra were first treated by Multiplicative Scatter Correction (MSC), followed by a base line correction. We applied a Principle Component Analysis (PCA) on samples corresponding to individual species (in exception of fish oils) to visualize differences between fats and then we have projected samples and mixtures of different fats on the obtained PCA space. Examination of the loadings associated to the principal components informs on the discriminant Raman shift and shows clearly the potential of the methodology proposed.

- [1] EC (1998) Bovine spongiform encephalopathy (BSE), 3rd edn. Vademecum, 16 October 1998. European Community, Brussels.
- [2] EC (2002) Regulation (EC) No 1774/2002 of the European Parliament and of the Council laying down health rules concerning animal by-products not intended for human consumption. Off. J. Europ. Commun., L273:1-95.
- [3] S. Bellorini, S. Strathmann, V. Baeten, O. Fumière, G. Berben, S. Tirendi, C. von Holst *Anal. Bioanal. Chem.* 382 (2005) 1073-1083.
- [4] G. Gasperini, E. Fusari, D.B. Bella, P. Bondioli, *Eur. J. Lipid Sci. Technol.* 109 (2007) 673-681.

Raman and AFM Imaging of Marine Aerosol Particles

J. Barbillat¹, S. Sobanska¹, J. Rimetz¹, S. Scolaro^{1&2}, J. Laureyns¹, D. Petitprez², C. Brémard¹

¹Laboratoire de Spectrochimie Infrarouge et Raman (LASIR UMR CNRS 8516- Bât C5), ²PhysicoChimie des Processus de Combustion et de l'Atmosphère (PC2A UMR CNRS 8522 – Bât C11), CERLA FR-CNRS 2416, Université des Sciences et Technologies de Lille, 59655, Villeneuve d'Ascq Cedex, France

In many environmental applications, the characterization of particulate matter or materials having grain-like structure can be essential to understand the nature of samples. For instance, micrometric size particles in the atmosphere serve as active reaction sites for chemical reactions, thus the characterization of such individual particles can provide much more useful information about the source, reactivity, transport, and removal of atmospheric chemical species than bulk methods. Bulk methods only give the average composition of particulate samples without describing the variability of the individual particles in the sample. Today, the challenge resides in supplying analytical tools able to provide detailed knowledge on the physico-chemical composition (elemental and molecular) and the morphology of individual particles on a micrometer and nanometer scale.

In this work we present results obtained on both environmental and synthetic marine aerosol particles. Complementary to the established automated single particle analysis techniques [1], this study is focused on the use of confocal Raman microspectrometry combined with relevant self-modeling mixture analysis (Multivariate Curve Resolution) providing unique information about the molecular characterization and distribution of species within particles [2]. The atomic force microscopy (AFM) is also used as a complementary technique to describe and compare the morphology of aerosol particles after reactions with high spatial resolution (few tens of nanometers).

Environmental samples have been collected in an industrial/urban atmosphere influenced by marine air masses (trade harbor) [3]. Particles were collected at two sites upwind and downwind of intense industrial activities with PM₁₀ Dekati impactors. Confocal molecular imaging together with AFM studies show a systematic agglomeration of particles emitted by the anthropogenic activities with the long-range transported sea-salt particles. This agglomeration appeared to be the major short term atmospheric event occurring during the transport of sea-salt particles.

Synthetic sea-salt particles were also prepared in laboratory following a well-known atmospheric reaction between gaseous NO₂ and NaCl crystal. The subsequent formation of NaNO₃ at the NaCl (100) surface is studied according to the relative humidity. Raman and AFM imaging show that the size and the morphology of nitrate particles at the NaCl surface mainly depend on the relative humidity and contribute to the knowledge of marine aerosol chemistry in troposphere.

[1] C.-U. Ro, H. Kim, R. Van Grieken, *Anal. Chem* 76 (2004) 1322-1327.

[2] Y. Batonneau, J. Laureyns, J.C. Merlin, C. Brémard, *Analytica Chimica Acta* 446 (2001) 23-37.

[3] Y. Batonneau, S. Sobanska, J. Laureyns, C. Brémard, *Environ. Sci. Technol.* 40 (2006) 1300-1306.

Vibrational Spectroscopic Investigation of Drug-Target-Interactions in Malaria Research

Torsten Frosch¹, Jürgen Popp^{1,2}

¹ Institut für Physikalische Chemie, Universität Jena, Helmholtzweg 4, D-07743 Jena, Germany
e-mail: torsten.frosch@uni-jena.de

² Institut für Photonische Technologien, Albert-Einstein-Straße 9, D-07745 Jena, Germany

Raman and IR spectroscopy was applied an investigation of the molecular mode of action of antimalarial active agents with their biological targets [1-8].

While Malaria is still one of the most devastating infectious diseases on earth [9, 10], resistances against established drugs arise on a global scale [11-13]. However, the molecular mode of action of those key drugs, e.g. chloroquine, is not well understood. It is believed that this class of antimalarials acts in the red blood cell state of the plasmodium's asexual life cycle in the human body. At this stage the drugs interfere with the detoxification process of the hemoglobin digestion by-products [14, 15].

In this contribution we demonstrate the high potential of Raman spectroscopy for a non-invasive, label-free, molecular investigation of important antimalarial active agents [1-5] and the malaria pigment hemozoin [6] as well as their molecular interactions [7, 8]. UV resonance Raman microscopy was applied for a very sensitive and selective investigation of different drugs under physiological conditions [1-4]. The experimental results have been confirmed by means of DFT calculations. Also the biological target hemozoin was localized in the infected cells and structurally investigated [6]. These *in situ* results were compared with spectra of extracted hemozoin as well as with synthesized β -hematin [6] and the Raman spectra of dimeric unit cell of the malaria pigment were calculated for the first time. A new, versatile device for Raman difference spectroscopy was designed and allows for a gentle, sensitive, selective, and precise investigation of drug target interactions [8].

The understanding of molecular vibrations of the active agents and the targets and how they may change upon molecular interactions with each other will inform drug chemistry and help fighting back against Malaria.

- [1] T. Frosch, M. Schmitt, G. Bringmann, W. Kiefer, J. Popp, J. Phys. Chem. B 111 (2007) 1815-1822.
- [2] T. Frosch, M. Schmitt, J. Popp, Anal. Bioanal. Chem. 387 (2007) 1749-1757.
- [3] T. Frosch, M. Schmitt, J. Popp, J. Phys. Chem. B 111 (2007) 4171-4177.
- [4] T. Frosch, M. Schmitt, T. Noll, G. Bringmann, K. Schenzel, J. Popp, Anal. Chem. 79 (2007) 986-993.
- [5] T. Frosch, M. Schmitt, K. Schenzel, J. H. Faber, G. Bringmann, W. Kiefer, J. Popp, J. Biopolymers 82 (2006) 295-300.
- [6] T. Frosch, S. Koncarevic, L. Zedler, M. Schmitt, K. Schenzel, K. Becker, J. Popp, J. Phys. Chem. B 111 (2007) 11047-11056.
- [7] T. Frosch, B. Kuestner, S. Schluecker, A. Szeghalmi, M. Schmitt, W. Kiefer, J. Popp, J. Raman Spectrosc. 35 (2004) 819-821.
- [8] T. Frosch, T. Meyer, M. Schmitt, J. Popp, Anal. Chem. 79 (2007) 6159-6166.
- [9] <http://rbm.who.int/wmr2005>
- [10] J. Sachs, P. Malaney, Nature 415 (2002) 680.
- [11] I.M. Hastings, P.G. Bray, S. A. Ward, Science 298 (2002) 74.
- [12] T.E. Wellems, Science 298 (2002) 124-126.
- [13] R.G. Ridley, Nature 415 (2002) 686-693.
- [14] M. Foley, L. Tilley, Pharmacol. Ther. 79 (1998) 55-87.
- [15] S. Pagola, P.W. Stephens, D.S. Bohle, A.D. Kosar, S.K. Madsen, Nature 404 (2000) 307.

In situ FTIR Spectroelectrochemical Investigations and two-dimensional Correlation Spectroscopy of the Hexacyanoferrate-II/-III Redox Couple

G. Trettenhahn

University of Vienna, Department of Physical Chemistry, Waehringer Street 42,
1090 Vienna, Austria; e-mail: guenter.trettenhahn@univie.ac.at

The electrochemistry of hexacyanoferrate-II and -III has been investigated in a wide range. A variety of opinions for the variation of the heterogeneous rate constant of this system including the adsorption of polymeric hexacyanoferrate complexes, hexacyanoferrate-II and -III on the electrode surface are published. The formation of soluble and insoluble Prussian Blue (PB), of Berlin Green (BG) and of Everitt's salt (ES), which depends on the concentration and composition of the electrolyte, the pH-value, the electrode potential and the cycling time, is also very important due to the wide range of applications of PB, e.g. electrochromic displays, sensors, conducting polymers, clinical applications, batteries and fuel cells.

In this work the electrochemistry of hexacyanoferrate-II and -III is investigated by cyclic voltammetry in combination with time resolved external reflection-absorption in situ FTIR spectroscopy. The influence of electrode material, electrode potential and composition of the electrolyte on the electrode reaction and on the reaction products is discussed. The reversibility of this system is checked by multicycling experiments, which show that there occur some non reversible reaction products which seem to be formed due to an adsorption reaction on the electrode. Further it was found that cyanide ligands in hexacyanoferrate-III can be oxidised to cyanate ions during cyclic voltammetric experiments up to high anodic switching potentials. The stability range of hexacyanoferrate-III with respect to further oxidation depends also on the composition of the electrolyte solution. In situ FTIR spectroelectrochemistry gives direct information about the appearance of electrode surface layers and changes in the interface electrode - electrolyte solution. Two-dimensional correlation analysis of the time resolved FTIR spectra leads to a better understanding of the system. These new results will be discussed with respect to some recent published data.

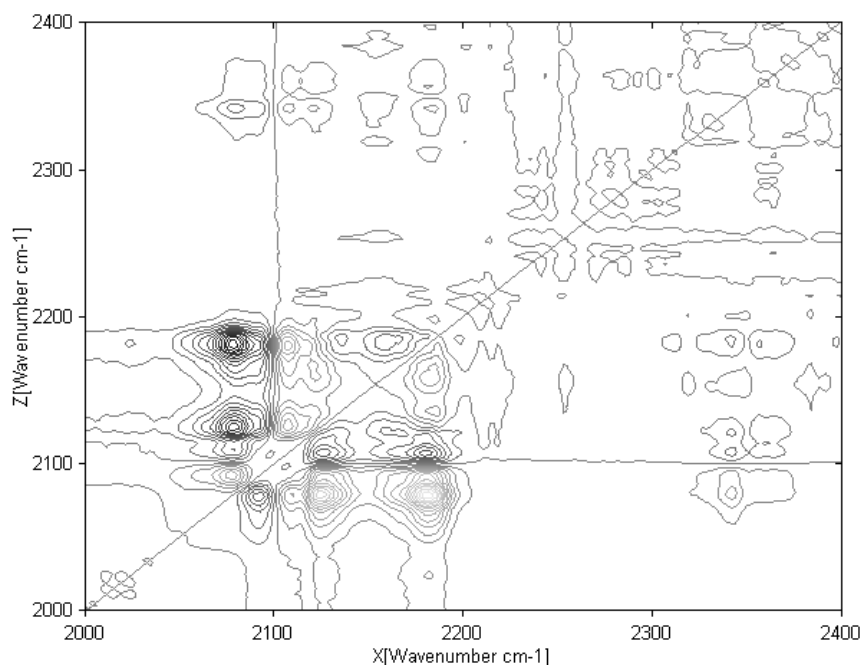


Fig.1: Asynchronous 2D IR correlation spectrum of $[\text{Fe}(\text{CN})_6]^{2-}$ measured at high anodic electrode potentials on gold electrode (from +1900 to +2300 mV vs. Ag/AgCl/KCl (3M) reference electrode).

Significance of Terahertz Spectrometry for Detecting Molecular States of Chemicals

M. Watanabe, T. Kurabayashi, T. Tanno, N. Kikuchi

Terahertz Waves Laboratory, Iwate Prefectural University, Takizawa, Iwate 020-0193, Japan

In 1983, Suto and Nishizawa developed a semiconductor GaP Raman laser and generated a 12 THz wave with a peak power as high as 3W, using a GaP Raman oscillator containing a GaAs mixing crystal. In this experiments, we used Cr:Forsterite lasers for the frequency-tunable and high-power THz wave generation in GaP crystal and pyroelectric deuterium triglycine sulfate as a detector operated at room temperature.

In order to obtain the spectrometric profile of chemicals in aqueous state, we tried to use a membrane filter, such as poly-vinylidene fluoride with 0.22 μm -pore, on which a 1mL solution containing chemical was loaded and dried at 60°C for 12 hours under vacuum and then applied directly for the assay system. The spectrometric profiles of glycine dissolved in deionized water, bovine albumin solution, and serum, respectively, are compared with those of the pellet in solid state mixed with polyethylene powder, as shown in Fig. 1, indicating of partial similarity of the peak profiles among different states of glycine molecule. The utility of the assay system is also shown in the case of L-threonine, L-alanine, L-glutamine and other aminoacids with the concentration dependent profiles.

Furthermore, the spectrometric profiles in the different molecular states of crystal and co-crystal of pharmaceutical drugs were obtained clearly to distinguish them each others. A marked significance to use Terahertz spectroscopy was shown to assay the molecular vibration profiles of chemicals.

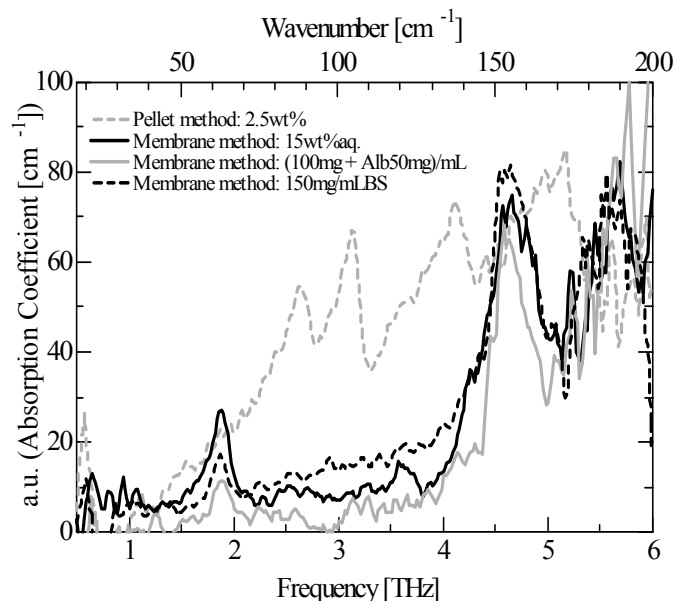


Fig. 1. Comparison of the Terahertz spectrometric profiles of glycine among different assay systems.

[1] K. Suto, J. Nishizawa, IEEE J. Quantum Electron. **QE-17** (1983) 1251-1254.

[2] T. Tanabe, K. Suto, J. Nishizawa, T. Kimura, K. Saito, J. Appl. Phys. **93** (2003) 4610-615.

Acknowledgement : This study was conducted as part of the Terahertz Optics Project for Medical Applications led by J. Nishizawa, organized by the Ministry of Education, Culture, Sports, Science and Technology of Japan, and also supported by Dreamland Iwate Strategic Research Promotions Project of Iwate Prefecture, and by Project Research Fund of Iwate Prefectural University.

IR and Raman and Density Functional Theory Studies on a Non-Steroidal Anti-Inflammatory Drug, Naproxen

Y. Akkaya¹, K. Balci¹, S. Akyuz²

¹Istanbul University, Faculty of Science, Department of Physics, Vezneciler, 34134, Istanbul, Turkey,

²Istanbul Kultur University, Faculty of Science and Letters, Department of Physics, Atakoy Campus, Istanbul, Turkey

Naproxen is a member of the 2-arylpropionic acid family of non-steroidal anti-inflammatory drugs. It has analgesic and anti-inflammatory activity and has been widely used in the treatment of rheumatic diseases. It works by inhibiting both the COX-1 and COX-2 enzymes. In this study, we searched possible stable conformers of free naproxen molecule in electronic ground state by performing a potential energy surface scan calculation performed at B3LYP/3-21G level of theory. The equilibrium geometries of the determined conformers of the free molecule were obtained through geometry optimizations carried out by using B3LYP hybrid DFT and MP2 ab-initio methods with 6-31G(d), 6-31++G(d,p), 6-311++G(d,p), aug-cc-pvTZ basis sets.

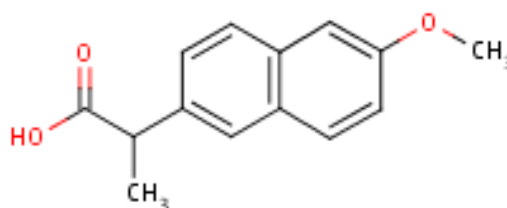


Fig. 1: Chemical structure of naproxen molecule.

For each determined stable conformer of the molecule, vibrational normal modes and corresponding frequencies, IR and Raman intensities were obtained through the frequency calculations performed at the same levels of theory as used in the geometry optimizations, in both harmonic and anharmonic oscillator approaches, separately. In order to fit the calculated harmonic wavenumbers to the experimental ones, two different scaling procedures called “Scaled Quantum Mechanical Force Field (SQM FF) methodology” [1,2] and “Scaling wavenumbers with dual scale factors” [3] were proceeded, independently. Both procedures have yielded results which are in very good agreement with our assignments proposed for the fundamental bands observed in the experimental IR and Raman spectra of the molecule and adequately proved the necessity of proceeding an efficient scaling procedure over the calculated harmonic wavenumbers for a correct vibrational spectroscopic analysis based on frequency calculations performed in harmonic oscillator approach using B3LYP method.

[1] G. Rauhut, P. Pulay, J. Phys. Chem. 99 (1995) 3093.

[2] G. Rauhut, P. Pulay, J. Phys. Chem. 99 (1995) 14572.

[3] M.D. Halls, J. Velkovski, H.B. Schlegel, Theor. Chem. Acc. 105 (2001) 413.

Raman and Infrared Spectroscopic Study of Pharmaceutical Tablets *DIPROL* and *CAFETINE COLD*, Products of *ALKALOID AD SKOPJE* (Republic of Macedonia)

B. Minčeva-Šukarova¹, Liljana Andreeva¹, Olivera Magdenovska¹, Verče Manevska¹,
Nataša Anevaska-Stojanovska²

¹ Institute for Chemistry, Faculty of Natural Sciences & Mathematics, University "Ss Cyril & Methodius",
Arhimedova 5, P.O.Box 162, 1001, Skopje, Republic of Macedonia
e-mail: biljanam@junona.pmf.ukim.edu.mk

² Research & Development Department, *ALKALOID AD Skopje*, Aleksandar Makedonski 12,
1001 Skopje, Republic of Macedonia

Pharmaceutical tablets, *DIPROL* and *CAFETINE COLD*, products of *Alkaloid AD Skopje*, their active components, their excipients and the lubricant have been studied by mid- and near-infrared spectroscopy (in the region 400 to 7000 cm⁻¹) and by micro-Raman spectroscopy (in the region 100 to 4000 cm⁻¹).

The recorded infrared and Raman spectra of *DIPROL* and *CAFETINE COLD* are mainly dominated by the bands due to the vibrations of their active component, paracetamol.

Nevertheless, a detailed vibrational assignment of characteristic frequencies of these tablets and their active component, paracetamol, revealed some differences in the infrared (mid and near) and Raman spectra of the pharmaceutical tablets *DIPROL* and *CAFETINE COLD* compared to the pure paracetamol powder. These differences were mainly observable in the Raman spectra (in the C-H stretching region, from 2800 to 3200 cm⁻¹) but also in the near-infrared spectral region, in the region corresponding to C-H overtones and/or combination bands (at 5775/5790 cm⁻¹ and 4325/4255 cm⁻¹).

According to the literature data, the observed differences in the Raman and infrared spectra could be attributed to possible existence of polymorphism in the paracetamol induced by the pressure used for making the pharmaceutical tablets, but can also be influenced by the effect of the lubricant (magnesium stearate) with the active component (paracetamol)

In order to determine the origin of these effects, Raman microscopic mapping was used to monitor the influence of magnesium stearate as lubricant in powder blends and in commercial tablet *DIPROL* tablets. For this purpose, three artificial mixtures of paracetamol, the excipients and the lubricant were made and were compared with the real tablet sample. The results from the mapping of the artificial mixtures have shown that the presence of the lubricant (magnesium stearate) has the influence on the appearance of the Raman bands in the 2800-3200 cm⁻¹ spectral region.

In addition, near infrared spectroscopy was employed to detect the effect of pressure used for preparing the pharmaceutical tablets *DIPROL* and *CAFETINE COLD*. For this purpose, the possible appearance of polymorphism in paracetamol was examined by comparing the powder blends of tablets *DIPROL* and *CAFETINE COLD* and the corresponding tablets made by high pressure hydraulic press.

Binding Ability of Fosfomycin towards Sodium and Calcium Ions

K. Chruszcz-Lipska¹, M. Baranska¹, L.M. Proniewicz^{1,2}

¹ *Chemical Physics Division, Faculty of Chemistry, Jagiellonian University, 3 Ingardena Str., 30-060 Kraków, Poland*

² *Regional Laboratory of Physicochemical Analysis and Structural Research, Jagiellonian University, 3 Ingardena Str., 30-060 Kraków, Poland*

Fosfomycin ((-)(1*R*,2*S*)-1,2-epoxypropylphosphonic acid) is a clinically important antibiotic used in the treatment of acute lower urinary tract bacterial infections [1,2].

In this work we present experimental as well as theoretical study of fosfomycin sodium and calcium salts at various experimental conditions (pH, temperature). FT-Raman and FT-IR spectra of fosfomycin disodium salt were registered (Fig. 1), compared and analyzed. The assignment of vibrational bands was supported by quantum-chemical calculations (DFT/B3LYP method with 6-311++G** basis set). A special care was devoted to the changes in vibrational modes caused by alterations of the ligand structure upon the formation of new bond to metal ion.

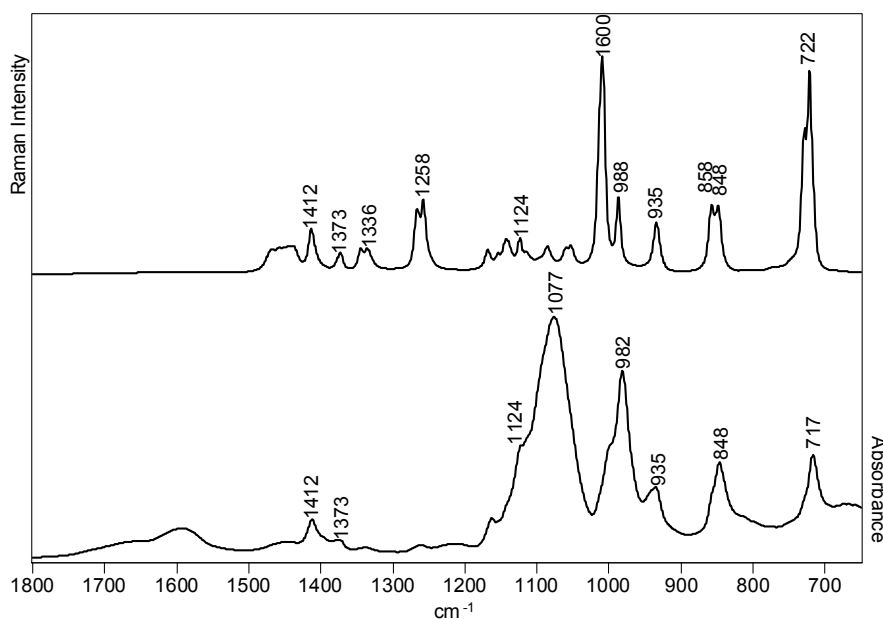


Fig. 1: FT-Raman and FT-IR(ATR) spectra of fosfomycin disodium salt.

[1] P. Liu, A. Liu, F. Yan, M.D. Wolfe, J.D. Lipscomb, H. Liu, *Biochemistry* 42 (2003) 11577-11586.

[2] L.J. Higgins, F. Yan, P. Liu, H. Liu, C.L. Drennan, *Nature* 437 (2005) 837-844.

Acknowledgments

This work was supported by the grant from the Polish State Committee for Scientific Research. The authors are also grateful to the Academic Computer Center "Cyfronet" in Krakow.

Vibrational spectroscopy analysis of the anthraquinone pigment alizarin

A. Baran, M. Baranska

Chemical Physics Division, Faculty of Chemistry, Jagiellonian University, Ingardena 3, 30-060 Kraków, Poland, e-mail: baranska@chemia.uj.edu.pl

Alizarin (1,2-dihydroxyanthraquinone) (Fig.1), is extracted from the roots of madder, *Rubia tinctorum L.*, where it is the main coloring matter [1-3]. Madder has been cultivated as a source of dyestuff since antiquity in central Asia and Egypt to the 19th century when alizarin was synthetically reproduced [2,3]. As a dihydroxyquinone, alizarin belong to a prominent family of pharmaceutically active and biologically relevant chromophores [1].

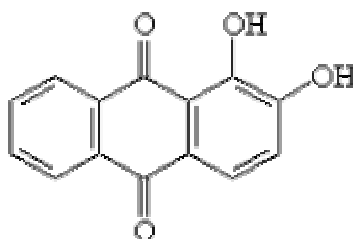


Fig.1: The structure of alizarin.

Alizarin is highly fluorescent and this property seriously limit the application of Raman spectroscopy (RS) to carry out a structural study and detect this molecule in plant or art samples [1, 4]. However, the Fourier transform-RS can be applied since the near-infrared excitation lines lie far from the absorption region of alizarin. The surface enhanced-RS (SERS) technique also makes the fluorescence quenching possible. It is performed by using of rough metal surfaces to enhance the Raman emission [1, 4].

The SERS spectra were collected from methanol solution of alizarin at the concentration of 10^{-5} M on rough Ag electrode with the wavelength excitation of 488 nm, 647 nm and 514.5 nm. Dependent on the excitation line the SERS or SERRS (surface-enhanced resonance Raman scattering) spectra of alizarin were observed. The FTRS spectra of alizarin as well as its complexes with Ag(I), Fe(III), Cr(III) metal ions in the solid state were also recorded. Additionally, alizarin was investigated directly in the roots of *Rubia tinctorum L.* To avoid the fluorescence, the radiation of 1064 nm was used for an excitation. As a complementary method for the investigation of alizarin structure and its interaction with metals FT-IR-ATR spectroscopy was applied. Experimental data were compared with theoretical study of alizarin molecular structure in order to support the assignment of vibrational bands. A quantum-chemical calculations of geometry optimization and vibrational frequencies were performed at DFT level with at least 6-31G** basis set.

- [1] M.V. Cañamares, J.V. Garcia-Ramos, C. Domingo, S. Sanchez-Cortes, *J. Raman Spectrosc.* 35 (2004) 921-927.
- [2] D. De Santis, M. Moresi, *Ind. Crops Prods.* 26 (2007) 151-162.
- [3] H. Schwegge: *Handbuch der Naturfarbstoffe*, Nikol Verlagsgesellschaft, Hamburg, 1993.
- [4] K. Chen, M. Leona, K. Vo-Dinh, F. Yan, M.B. Wabuyele, T. Vo-Dinh, *J. Raman Spectrosc.* 37 (2006) 520-527.

Acknowledgments

The authors gratefully acknowledge Prof. J. Bukowska and Ms. B. Wrzosek from University of Warsaw for their help in collecting SERS spectra of alizarin.

Spectroscopic Study of Humic Substances Extracted From Bottom Sediment and Water

M. Bartoszek, J. Polak, A. Kos, W.W. Sułkowski

*Department of Environmental Chemistry and Technology, Institute of Chemistry, University of Silesia
Szkołna 9, 40-006 Katowice, Poland, e-mail: wsulkows@us.edu.pl*

NMR, EPR and IR spectroscopic studies of humic substances extracted from bottom sediment and water have been applied for characterization of humification processes occurring in the Goczalkowice Reservoir.

Both humic and fulvic acids were extracted from bottom sediment whereas in water only fulvic acids were present.

For the extracted humic substances, the presence of characteristic functional groups was confirmed with IR spectroscopy. Comparison of signal intensity of the main functional groups was conducted by means of ^1H NMR techniques. The concentration of free radicals and g factor was determined with EPR.

It was found that free radical concentration values obtained for fulvic acids extracted from bottom sediment are considerably higher than the values of free radical concentration in humic acids extracted from bottom sediment and fulvic acids extracted from water.

On the basis of the EPR and IR spectra analysis the formation of transition metals complexes with humic substances was confirmed. On the EPR spectra the signals originated from Fe^{3+} , Mn^{2+} and Cu^{2+} ions were observed. Moreover, the enhancement of the absorption band characteristic for ionized carboxylic group can be an evidence of metal binding by humic substances.

^1H NMR and IR analysis of humic and fulvic acids extracted from bottom sediment and water confirms the occurrence of the functional groups, characteristic for humic substances and shows differences in the structure of humic substances extracted from bottom sediment and from water and differences, which appear in the structure of humic and fulvic acids.

Spectroscopic Comparison of the Physico-Chemical Properties of Humic Acids Extracted from Sewage Sludge and Bottom Sediment

J. Polak, M. Bartoszek, M. Kantor, W.W. Sułkowski

*Department of Environmental Chemistry and Technology, Institute of Chemistry,
University of Silesia, Szkolna 9, 40-006 Katowice, Poland
e-mail: wsulkows@us.edu.pl*

Comparison of the physico-chemical properties was carried out for humic acids extracted from sewage sludge and bottom sediment.

The isolated humic acids were investigated by means of EPR, IR, UV/VIS spectroscopic methods and elementary analysis AE.

On the basis of earlier studies it was stated that humic acids extracted from sewage sludge can be divided into humic acids extracted from raw sewage sludge and from sewage sludge after digestion process. The digestion process was found to have the most significant effect on physicochemical properties of humic acids extracted from sludge during sewage treatment [1-3].

Humic acids extracted from sewage sludge had higher free radical concentration than humic acid extracted from bottom sediment. However, g-factor values were similar for all studied samples but it is noteworthy that g-factor values for humic acid extracted from raw sewage sludge and from bottom sediment were lower as compared with humic acid extracted from sewage sludge after fermentation processes.

The IR spectra of all studied humic acids confirmed the presence of functional groups characteristic for humic substances.

It was observed that humic acids extracted from bottom sediment had more aromatic character and contained less carbon, nitrogen and hydrogen than these extracted from sewage sludge.

- [1] J. Pajączkowska, A. Sułkowska, W.W. Sułkowski, M. Jędrzejczyk, J. Mol. Struct. 651-653 (2003) 141.
- [2] J. Polak, W.W. Sułkowski, M. Bartoszek, W. Papież, J. Mol. Struct. 744-747 (2005) 983.
- [3] J. Polak, W.W. Sułkowski, Polish Journal of Environmental Studies 15 (2006) 573-577.

Structural and Vibrational Study of Maprotiline

A.E. Yavuz¹, S. Haman Bayarı², N. Kazancı¹

¹ Ege University, Faculty of Science, Dept. of Physics, Bornova, İzmir, Turkey

² Hacettepe University, Faculty of Education, Dept. of Physics Education, Beytepe Ankara, Turkey

Maprotiline (Ludimil, N-Methyl-9, 10-ethanoanthracene-9(10H)-propanamine) is a tetra cyclic antidepressant (Fig. 1). It is a highly selective inhibitor of norepinephrine reuptake. The solid and solution (CCl₄ and ethanol) infrared spectra of maprotiline have been recorded.

The fully optimized equilibrium structure of maprotiline has been obtained from DFT calculations by using the B3LYP functional in combination with 6-31G and 6-311G (d,p) basis sets. The results of harmonic and anharmonic frequency calculations on maprotiline are presented. The vibrational spectra were interpreted, with the aid of normal coordinate analysis based on a scaled quantum mechanical (SQM) force field [1]. The infrared spectrum was also predicted from the calculated intensities. Vibrational assignment of all the fundamentals was made using the total energy distribution (TED).

The possible interaction between maprotiline and local anesthetic citanest (prilocaine) and neurotransmitter serotonin (5-HT) were investigated.

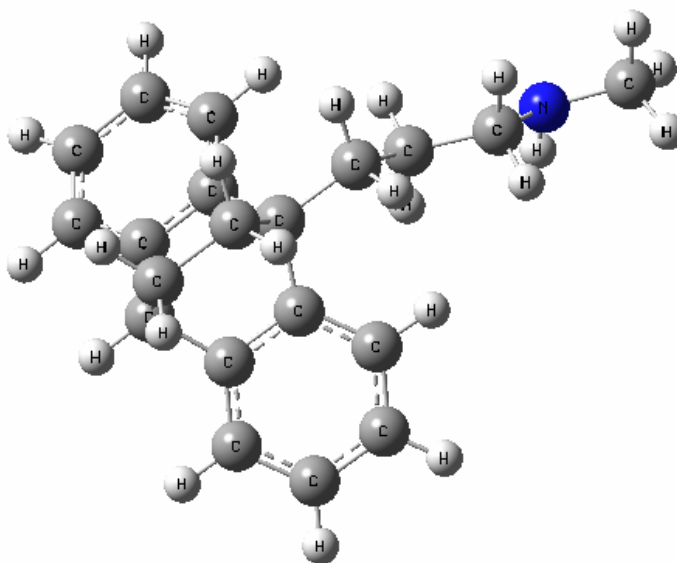


Fig. 1: DFT/6-311G(d,p) structure of maprotiline

[1] J. Baker, A.A. Jarzecki, P. Pulay, J Phys Chem A 102 (1998) 1412–1424.

Structural and Vibrational Study of 4-(2'-Furyl)-1-Methylimidazole

A.E. Ledesma¹, J. Zinzuk², J.J. López González³, A. Ben Altabef¹, S.A. Brandán¹

¹Instituto de Química-Física. Facultad de Bioquímica, Química y Farmacia. Universidad Nacional de Tucumán. Tucumán. R. Argentina, ²Instituto de Química Orgánica de Síntesis (CONICET-UNR), Facultad de Ciencias Bioquímicas y Farmacéuticas, Suipacha 531, 2000 Rosario, Santa Fé. R. Argentina, ³Departamento de Química Física y Analítica, Facultad de Ciencias Experimentales. Universidad de Jaén, 23071 Jaén, España.

The 4-(2'-furyl)-1-methylimidazole (**1**) has been synthesized and its molecular structure is observed in the Figure. The compound was characterized by infrared, Raman, multidimensional nuclear magnetic resonance and mass spectroscopy. The infrared and Raman spectra were registered in solid state, and the RMN ¹H, ¹³C, COSY spectra were registered in a DMSO-d₆ solution. The corresponding geometry for the compound was calculated using the Gaussian 03 [1] program at theory level B3LYP. The harmonic vibrational frequencies for the optimized geometry of the compound were calculated using 6-31G* and 6-311++G** basis sets in the approximation of the isolated molecule. Then, in order to get a good assignment of the IR and Raman spectra in solid phase of (**1**) the best fit possible between the calculated and recorded frequencies was carry out and the corresponding force field was scaled using the Pulay et al. SQMFF methodology.

The force constants were calculated for the compound using the Pulay et al. [2] methodology from the Scaling Quantum Mechanic Force Field (SQM). The assignment of the observed bands in the vibrational spectra was performed. Furthermore, the analysis of the Natural Bond Orbitals (NBO) [3] was carried out to study the charge transference interactions between the furan and imidazole rings of the compound.

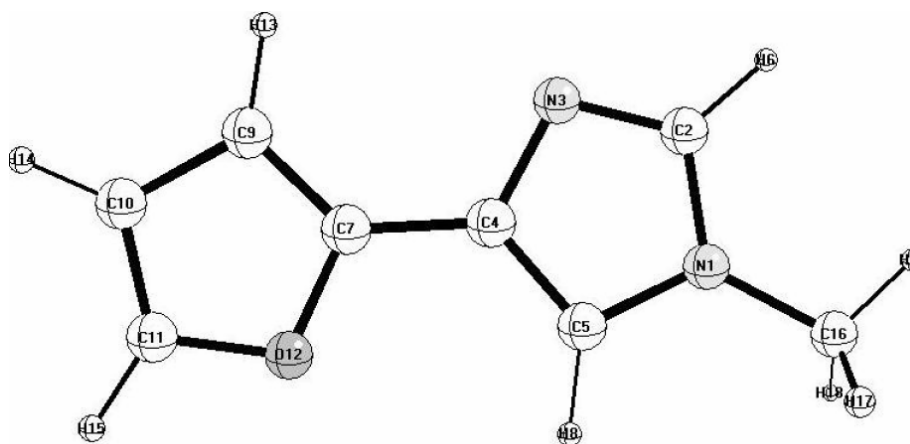


Fig. 1: Structure of 4-(2'-furyl)-1-methylimidazole.

[1] Program Gaussian 03, GAUSSIAN, Inc. Pittsburgh, PAA, USA, 2003.

[2] G. Fogarasi, X. Zhou, P.W. Taylor and P. Pulay, J. Am. Chem. Soc. 105 (1992) 7037.

[3] E.D. Gledening, J.K. Badenhoop, A.D. Reed, J.E. Carpenter, F.F. Weinhold, NBO 3.1; Theoretical Chemistry Institute, University of Wisconsin; Madison, WI, 1998.

Comparison of the Influence of Myristic Acid on Acetaminophen and Acetylsalicylic Acid Binding with Serum Albumin

B. Bojko¹, A. Sułkowska¹, M. Maciążek-Jurczyk¹, J. Równicka¹, D. Pentak²,
W.W. Sułkowski²

¹*Department of Physical Pharmacy, Faculty of Pharmacy, Medical University of Silesia, Sosnowiec, Poland*

²*Department of Environmental Chemistry and Technology, Institute of Chemistry,
University of Silesia, Katowice, Poland
e-mail: bbojko@slam.katowice.pl*

Binding of drugs to serum albumin is one of the main part of their metabolism. Changes of equilibrium between free and bound fraction of drug may significantly affect process of its -distribution and elimination. Fatty acids are one of the ligands which bound with albumin may change the affinity of protein towards the drug.

In our fluorescence studies the influence of increasing concentration of myristic acid (MYR) on binding of acetaminophen (paracetamol, AA) with serum albumin were investigated. The applied concentration ranges of fatty acid relate to the subsequent molecules of MYR associated with the protein [1]. Binding sites of acetaminophen in albumin structure were found. Comparison of association constants calculated by the use of Scatchard and Stern-Volmer method were done for AA-albumin and AA-albumin-MYR complexes. Current results were compared with our previous studies on the influence of myristate on acetylsalicylic acid binding with serum albumin [1].

On the basis on our results we concluded that the competition between acetaminophen and fatty acid depends not only on the competitive binding but also on albumin structure changes induced by fatty acid.

[1] B. Bojko, A. Sułkowska, M. Maciążek, J. Równicka, F. Njau, W.W. Sułkowski, *Int. J. Biol Macromol.* 42 (2008) 314-323.

Transient Absorption, Low-Temperature Raman, Fluorescence Quantum Yield and Stationary Absorption Studies of Various Metal Phthalocyanines and Their Sulfonated Derivatives

P. Ciacka¹, A. Jarota¹, B. Brozek-Pluska¹, H. Abramczyk^{1,2}

¹Laboratory of Laser Molecular Spectroscopy, Institute of Applied Radiation Chemistry, Technical University of Lodz, Wroblewskiego 15 st., 93-590 Lodz, Poland, tel.: (48 42) 631 31 75, 631 31 62, 631 31 88, fax: (48 42) 684 00 43, ²Max-Born-Institut, Max-Born-Str. 2A, 12489 Berlin, Germany, e-mail: abramczy@mbi-berlin.de

Phthalocyanines, well-known dyes, have recently gathered a lot of interest in scientific community. In view of their new and promising applications as PDT photosensitizers, chemical sensors and display and memory devices, determining photochemical properties of phthalocyanines becomes very important. Several important processes, such as aggregation, singlet oxygen generation, intermolecular charge transfer and its dependence on molecular surroundings can be monitored using optical spectroscopy methods, stationary as well as time-resolved ones.

We report recent results for liquid solutions of Al, Fe(II) and Zn phthalocyanines and their sulfonated derivatives obtained by means of femtosecond transient absorption spectroscopy, Raman spectroscopy using cryogenic cooling and stationary absorption.

Raman spectra collected for room as well as low temperatures provide insight into intermolecular charge-transfer process manifesting itself as fluorescence of radicals. The role of structural changes (i.e. phase transitions) in this process is also highlighted.

Femtosecond time-resolved measurements enable us to further elucidate the nature of transient species and provide clear explanations of spectral features. For instance, the technique has given a strong evidence of intramolecular charge-transfer character of fluorescence at 540 nm, in contrast to what has previously been reported in literature.

Stationary absorption and Raman spectra were used to calculate fluorescence quantum yields of compounds in question.

Spectroscopic Investigation of Some Cu(II) Cardiovascular Complexes

O. Cozar¹, F. Drăgan², C. Jelic¹, V. Chiş¹, N. Leopold¹, L. Szabó¹

¹ Babeş-Bolyai University, Faculty of Physics, Kogălniceanu 1, 400084 Cluj-Napoca, Romania,

² University of Oradea, Faculty of Medicine and Pharmacy, Oradea, Romania

e-mail: cozar@phys.ubbcluj.ro

The atenolol (ATE), metoprolol (MET), pindolol (PIN) and verapamil (VER) molecules are most frequently used drugs in the treatment of cardiovascular diseases. They are beta-blocker drugs and reduce the symptoms of angina pectoris (chest pain), decrease the blood pressure of the population with hypertension and are used also in the people treatment after heart attacks. In the last few years, some molecular copper complexes of different drugs (cardiovasculars, antiinflammatories) are used because their activity is enhanced [1-3]. For a better understanding of their activity, structural investigation by different spectroscopic methods (FT-IR, Raman and EPR) and DFT calculations was done.

Molecular complexes with Cu(II) were prepared on going from the starting salts (sodium benzoate and copper sulphate) by co-precipitation procedure. After drying, the powder complexes were analysed by classical KBr pellet technique with an EQUINOX 55 Bruker FT-IR spectrometer in the 400-4000cm⁻¹ spectral domain. FT-Raman spectra were recorded in a backscattering geometry with a Bruker FRA 106/S Raman accessory attached to the FT-IR spectrometer. The EPR spectra of the samples in the powder form were registered in the X band using an ADANI-USA spectrometer.

A comparative study of the FT-IR and Raman spectra of ligands (ATE, MET, PIN and VER) and the corresponding metal complex, allowed us to establish the molecular groups involved in the complexation. In the case of ATE and MET copper compounds, the NH₂ and carboxyl groups are involved in the coordination of the metal ions. Also for PIN and VER compounds the coordination is realized by nitrogen and oxygen atoms from their corresponding molecular groups.

For the assignment of the vibrational bands, density functional theory (DFT) calculations were performed on these molecules. The use of new and rapid instrumentation in IR and Raman spectroscopy has made these techniques suitable for drug process monitoring.

Powder EPR spectra of Cu(II) complexes obtained at room temperature exhibit the absorption signals typical of randomly oriented single state (S=1/2) species having axial symmetry. The ground state for paramagnetic electron is d_{x²-y²} orbital, for ATE, MET and VER compounds. For PIN compound the ground state is d_{z²} orbital. By comparing the shape of these EPR spectra with those obtained for other copper complexes with nitrogen and oxygen ligands we have concluded that the local symmetry around metal ions is of square-planar type with a CuN₂O₂ chromophore in the xOy plane [4].

[1] S.A.C. Wren, P. Tchelitcheff, J. Pharm. Biomed. Analysis 40 (2006) 571.

[2] E. Forizs, L. David, O. Cozar, V. Chiş, G. Damian, Journal of Molecular Structure 482 (1999) 143.

[3] O. Cozar, N. Leopold, C. Jelic, V. Chiş, L. David, A. Mocanu, M. Tomoaia-Cotişel, Journal of Molecular Structure 788 (2006) 1-6.

[4] I. Farias, R. Fernandes, Quim. Nova., São Paulo, 25 (2002) 186.

GC/MS as a Tool for Non-Invasive Diagnosis

M. Culea¹, O. Cozar¹, E. Culea²

¹"Babes-Bolyai" University, Str. M. Kogalniceanu, Nr. 1, Cluj-Napoca, 400084, Romania

²Technical University of Cluj-Napoca, 400020 Cluj-Napoca, Romania

Comparative results for some VOCs in urine or breath by different methods are presented. Organic biomarkers exhaled or present in urine of healthy and patients suffering of diabetes or other diseases were measured by using non-invasive sampling and analysis with gas chromatography-mass spectrometry (GC-MS). Acetone was measured by using halothane as internal standard (Fig. 1). The methods were validated for quantitative determination by studying the parameters of linearity, precision, accuracy, limit of detection [1-3].

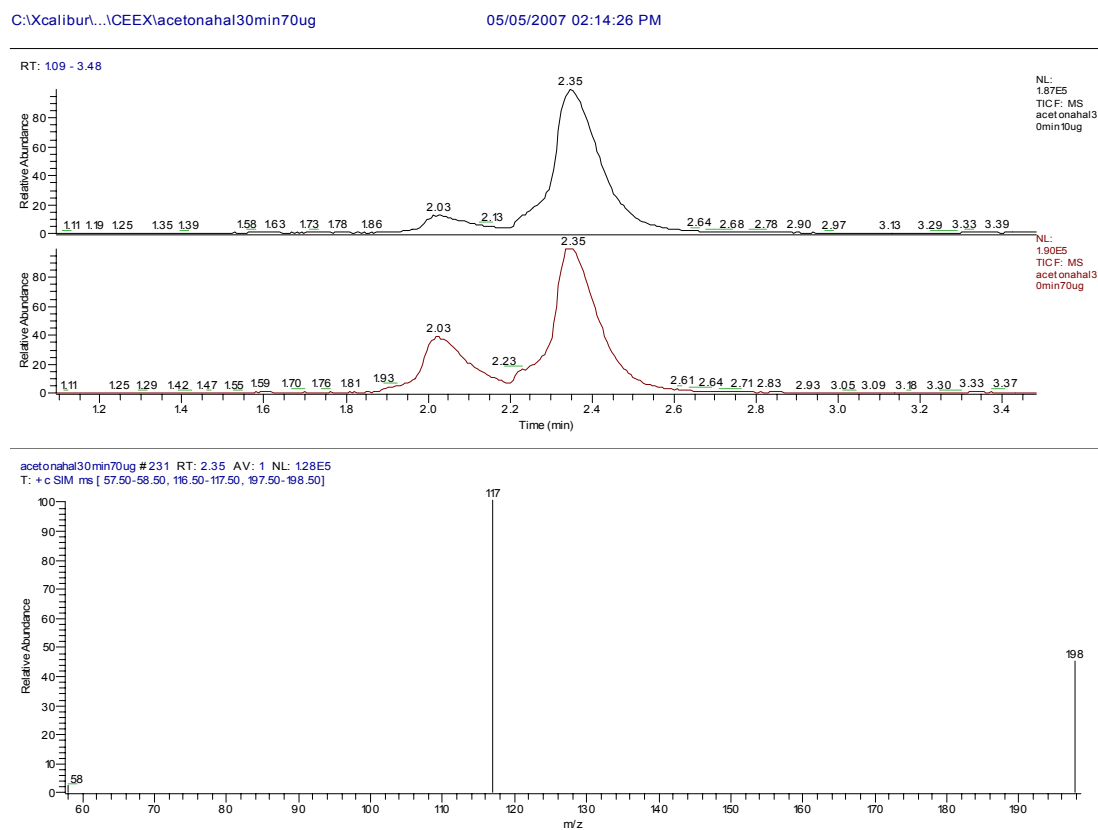


Fig. 1: SIM-GC-MS chromatogram for acetone and halothane, the internal standard: ions m/z 117 and 198, of a urine sample and a standard sample of 10 $\mu\text{g/ml}$ acetone.

- [1] M. Culea, S.Nicoara, A. Nica, C. Gherman, Indoor and Built Environment 12 (2003) 125-129.
 [2] M. Culea, O. Cozar, C. Melian, D. Ristoiu, Indoor and Built Environment 14 (2005) 241-248.
 [3] R.J Delfino, H. Gong, W.S. Linn, Y. Hu, E.D. Pellizzari, J Expo Anal Environ Epidemiol. 13 (2003) 348-363

Study of Amino Acid Transmembranar Transport

M. Culea¹, S. Neamtu²

¹Babes-Bolyai University, Str. Kogalniceanu, nr.1, 400084 Cluj-Napoca, Romania

²INCDTIM Cluj-Napoca, Str. Donath 65-103,400293 Cluj-Napoca, Romania

e-mail: mculea@phys.ubbcluj.ro

A study for amino acid transmembranar transport study in human red cells is presented. The isotope dilution GC/MS technique was used in SIM mode.

Efflux of ¹⁴N labelled amino acid was calculated by using as internal standard the ¹⁵N labelled amino acid. The quantitation of amino acids, as trifluoroacetyl butyl ester derivative, was performed on a chromatographic column coupled to a mass spectrometer (GC-MS). The method was validated in the range 0-100 µg/ml. Small values of the amino acid transmembranar transport were detected for the amino acid studied glycine and leucine.

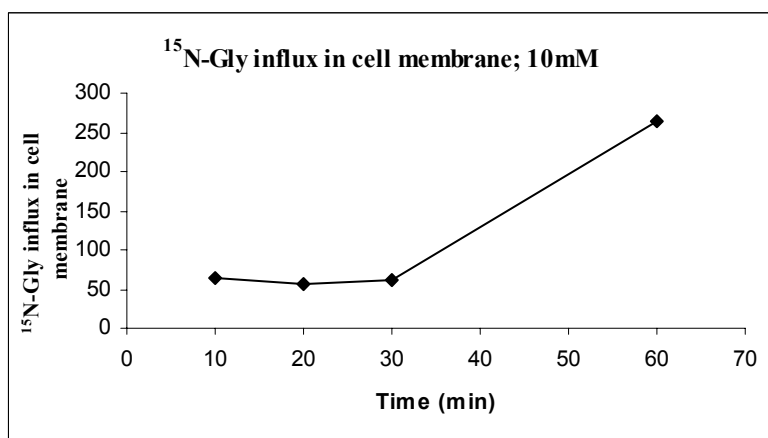


Fig. 1: Glycine influx study versus time of incubation. Gly: 10mM; Time: 0– 60 min.

[1] M. Culea, S. Neamtu, N. Palibroda, M. Borsa, S. Nicoara, J. Molec. Structure 348 (1995) 377-380.

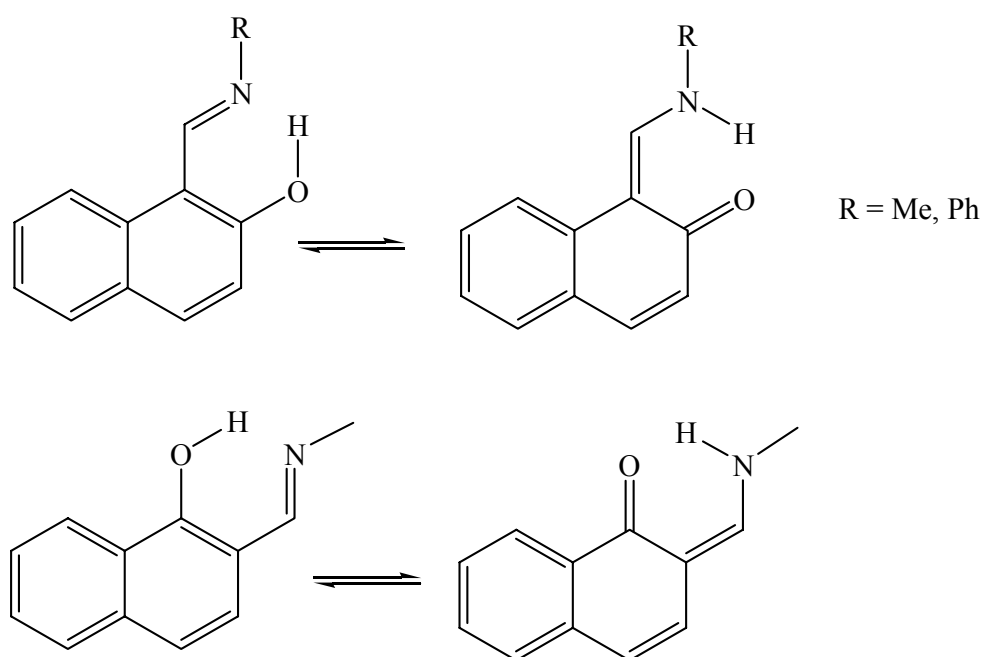
NMR and DFT Study of the Enol Imine \leftrightarrow Enaminone Tautomeric Equilibrium in Schiff Bases in Some Organic Solvents

Teresa Dziembowska¹, Zbigniew Rozwadowski¹, Mirosław Szafran²

¹Institute of Fundamental Chemistry, Technical University of Szczecin, Al. Piastów 42, 71-065 Szczecin, Poland

²Faculty of Chemistry, Adam Mickiewicz University, ul. Grunwaldzka 6, 60-780 Poznań, Poland

The tautomeric enol imine \leftrightarrow enaminone equilibrium of the N-(2-hydroxynaphthylidene)-methylamine, N-(2-hydroxynaphthylidene)-aniline and N-(1-hydroxynaphthylidene)-methylamine have been investigated in carbon tetrachloride, chloroform, acetonitrile, dimethylsulphoxide and methanol by ^1H and ^{13}C NMR spectra and density functional theory (B3LYP/6-31G(d,p) methods using the conductor-like screening continuum solvation model (COSMO). Correlations between the experimental ^1H and ^{13}C NMR chemical shifts of the investigated molecule in solutions and GIAO/B3LYP/6-31G(d,p) calculated magnetic isotropic shielding tensors (σ_{cal}) using the screening solvation model (COSMO), $\delta_{\text{exp}} = a + b \sigma_{\text{cal}}$, are reported.



Single-Molecule Surface Enhanced Raman Scattering on Periodically Nanostructured Gold Films

C. Farcau, S. Astilean

Nanobiophotonics Laboratory, Institute for Interdisciplinary Experimental Research, Babes-Bolyai University, T. Laurian 42, 400271, Cluj-Napoca, Romania

Surface enhanced Raman scattering (SERS) is a spectroscopic technique of great interest in chemistry, biochemistry, and biophysics because vibrational spectra provide characteristic fingerprints of molecular structure and can be used to specifically identify molecules [1]. Several reports have demonstrated the single molecule sensitivity of this technique [2], which opens a new doorway for the analysis of molecular dynamics. In order to achieve such sensitivity noble metal nanostructured surfaces are employed, which can be very effective in localization and enhancement of electromagnetic fields, when illuminated with laser radiation. Up to date most of the single molecule observations were performed by using randomly nanostructured gold or silver surfaces, like dimmers or large clusters of nanoparticles.

Here we report single molecule surface enhanced Raman scattering observations on a gold film patterned with periodic features. The employed SERS substrate consists of a gold film (100 nm thickness) evaporated on top of a regular array of polystyrene microspheres (450 nm diameter), which yields a two-dimensional array of metallic caps. The lateral dimensions of the metallic features exhibited by this type of substrate allow making correlation between topography and local SERS activity. We show by combining atomic force microscopy (AFM) and confocal Raman microscopy, that crevices between adjacent caps, which offer nanometric vicinity of metallic features, are the sites of super-enhanced Raman scattering. In figure 1 we show a typical SERS spectrum and a waterfall plot of SERS spectra recorded as a temporal series, which exhibit hallmarks of single molecule behavior, like fluctuations of the Raman intensity and Raman shift.

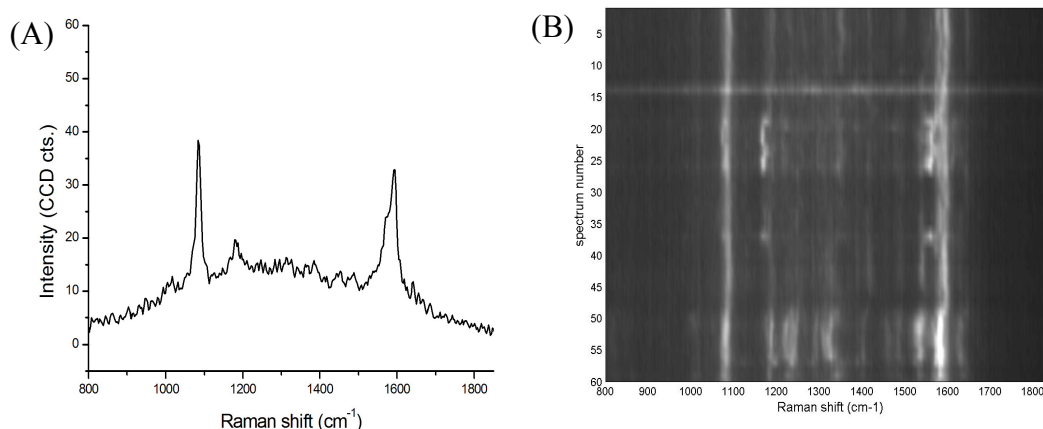


Fig.1: (A) Typical SERS spectrum and (B) Waterfall plot of SERS spectra (0.4 s integration time/spectrum) of p-atp molecules adsorbed on the gold substrate.

[1] T. V. Dinh, *TrAC-Trends Anal. Chem.* 17 (1998) 557-582.

[2] S. Nie, S. R. Emory, *Science* 275 (1997) 1102-1106.

Acknowledgement

This research was supported by the Romanian Agency for Scientific Research (projects CEEX 71/2006 and CNCSIS TD 261/2007).

A Study of the Reduction and Reoxidation of Substoichiometric Magnetite

M. Gotić, G. Koščec, S. Musić

*Division of Materials Chemistry, Ruđer Bošković Institute
PO. Box 180, HR-10002 Zagreb, Croatia*

Magnetite (Fe_3O_4) and maghemite ($\gamma\text{-Fe}_2\text{O}_3$) are ferrimagnetic compounds with unique electric and magnetic properties. They are widely used as material in catalysis, magnetic separation, ceramics processing, energy and magnetic data storage, and as protection from microwave radiation. Moreover, both magnetite and maghemite have been extensively investigated for application in biomedicine. For example, they have been recognised as suitable magnetic materials for MR imaging, drug delivery, drug targeting, cell labelling and magnetic separation, as well as a hyperthermia agent. Magnetite has better magnetic properties than maghemite, however, magnetite tends to oxidise easily due to the presence of Fe^{2+} , whereas maghemite is chemically and physically very stable. The oxidation of magnetite deteriorates its magnetic properties.

In the present work, the substoichiometric magnetite particles ($\text{Fe}_{2.90}\text{O}_4$) of micrometer dimensions were subjected to reduction and reoxidation at a temperature of up to $600\text{ }^\circ\text{C}$. The reduction of substoichiometric magnetite by hydrogen was performed under static conditions, whereas the reoxidation experiments were performed in a stream of oxygen. Samples were characterized by field emission scanning electron microscopy (FE-SEM), XRD, FT-IR and Mössbauer spectroscopy. The experimental condition for stoichiometric magnetite (Fe_3O_4) was obtained. It was found that Mössbauer spectroscopy is a powerful technique for monitoring the stoichiometry of magnetite, but limiting in terms of distinguishing a magnetite-maghemite mixture. FT-IR spectroscopy showed that samples, which by means of Mössbauer spectroscopy were characterised as nonstoichiometric magnetite, contained bands characteristic of magnetite and maghemite. After investigating the micrometer sized particles, all the three peaks present in the XRD patterns of maghemite, but not in the XRD patterns of magnetite, at $2\theta(\text{CuK}\alpha) = 15, 24$ and 26 degrees turned out clearly visible. The magnetite-to-maghemite transition mechanism will be discussed.

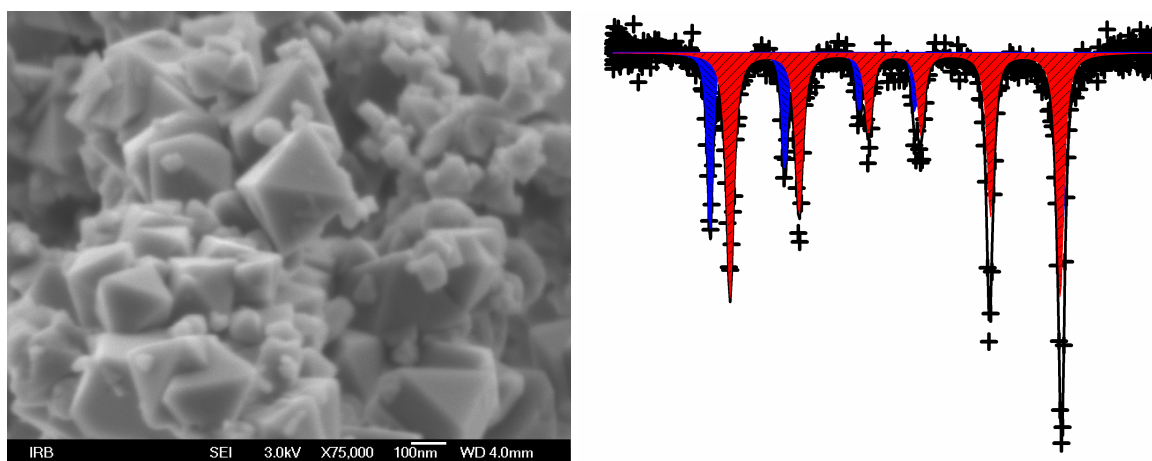


Fig. 1: FE-SEM image (left) and Mössbauer spectrum (right) of stoichiometric magnetite (Fe_3O_4).

Classification of Polish Honeys by Mid-Infrared Spectroscopy and Multivariate Statistical Analysis

A. Hacura¹, M. Jadamus-Hacura²

¹*Institute of Physics, University of Silesia, Uniwersytecka 4, 40-007 Katowice, Poland*

²*Department of Econometrics, University of Economics, Bogucicka 14, 40-226 Katowice, Poland*

There is a great scientific and commercial interest around the world in the characterization of unifloral honeys because of their unique chemical composition and biological properties [1, 2]. Honey is an extremely variable and complex mixture of mono and polysaccharides and other components but consists mostly of glucose and fructose. The actual proportion of these monosaccharides in any particular honey depends largely on the source of the nectar.

Mid-infrared Fourier transform spectroscopy with attenuated total reflection (ATR) sampling and multivariate analysis were used for identification and classification of Polish honey. This method is rapid, non destructive, with high precision and reliable detection. The 65 honey samples from different floral sources (acacia, buckwheat, heather, lime, rope, honey-dew and polyfloral) and from different locations across Poland, were spectrally measured in middle infrared region of 4000-500 cm^{-1} . Spectra were recorded with resolution of 1 cm^{-1} using the Bio-Rad FTS-6000 spectrometer equipped with Pike MIRacle™ ATR accessory.

Partial least squares and principal component regression analysis were used for quantitative analysis of spectral data while linear discriminant analysis, canonical variate analysis and classification tree analysis were used to discriminate honey samples. Classification accuracy near 100% was achieved by discriminant and classification tree analysis.

The use of these good quality spectra of both: honeys and properly prepared sugar samples, together with application of multivariate statistics methods, allowed us to specify among others measurands the glucose/fructose ratios in honey samples.

The obtained results show that mid-infrared spectra contain valuable information on the botanical origin of honey and can be used for qualitative analysis of main components in honey and for their classification as well.

[1] E. Anklam, Food Chemistry 63 (1998) 549-562.

[2] E. Etzold, B. Lichtenberg-Krag, Eur. Food Res. Technol. online 10 October 2007.

IR Spectroscopic Study of the Hydrodechlorination of Chlorobenzenes and Chlorophenols over Nobel Metal Containing Zeolites

I. Hannus, Sz. Mészáros, M. Búza, J. Halász

Department of Applied and Environmental Chemistry, University of Szeged, Rerrich B. tér 1, Szeged, H-6720 Hungary; e-mail: hannus@chem.u-szeged.hu

Halogenated hydrocarbons such as chlorobenzenes and chlorophenols are useful materials for everyday applications. These are used on a large scale in chemical and petrochemical industries, as well as in the agriculture as pesticides or in medical practice as disinfectants. However, most of them are environmental pollutants and the disposal of organic wastes containing halogen has become a major environmental and social problem, while most of them are toxic but stable material, accumulating in the surroundings for long time periods [1]. Thus they are the subject to stringent regulations. Therefore, a lot of effort is devoted in finding proper solutions to detoxifying or to decompose these chemicals in environmentally friendly ways. The Pt- and Pd-containing zeolites could be the real applicants, if the lifetime of the catalyst is acceptable, or the used sample can be regenerated [2].

During the work leading to this contribution we have prepared Pt- and Pd-containing zeolites. NaY-FAU and Na-ZSM-5 were the parent zeolites and ion exchange was carried out in $\text{Pt}(\text{NH}_3)_4\text{Cl}_2$ and $\text{Pd}(\text{NH}_3)_4\text{Cl}_2$ solutions. IR spectroscopic self-supporting wafer technique was employed for adsorption and catalytic measurements. The wafers were prepared from the powdered zeolites and placed into the sample holder of an *in situ* IR cell. During the pretreatment process the $\text{Pt}(\text{NH}_3)_4^{2+}$ and $\text{Pd}(\text{NH}_3)_4^{2+}$ ions were decomposed in oxygen stream, then the wafer was heated to 723 K in oxygen followed by evacuation at the same temperature for two hours. This oxidized sample was reduced in H_2 at 573 K. For hydrodechlorination experiments the pretreated zeolite wafers were loaded with the reactant at room temperature. Both the surface species and the gas-phase products were analysed as the reaction proceeded under various experimental conditions.

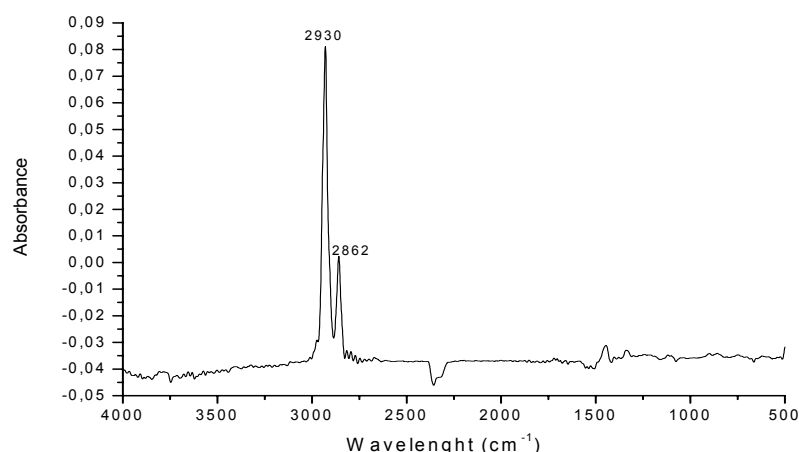


Fig. 1: The gas product of the hydrogenation of 2-chlorophenol on PdY-FAU zeolite at 473 K.

In the case of the hydrogenation of 2-chlorophenol the PdY-FAU zeolite was the most active and the final product was only cyclohexane at 473 K, as Fig. 1 shows. Generally, the Pt-containing zeolite was more selective and the Pd-containing one was more active in the hydrodechlorination.

- [1] J.B. Hoke, G.A. Gramiccioni, E.N. Balko, Appl. Catal. B: Environmental 1 (1992) 63.
[2] I. Hannus, J. Halász, J. Japan Petrol. Inst. 49 (2006) 105.

Catalytic Activity of Bimetallic Gold Containing Nanoparticles on Different Supports Investigated by IR Spectroscopy

I. Hannus¹, M. Búza¹, A. Beck², L. Gucci²

¹Department of Applied and Environmental Chemistry, University of Szeged, Rerrich B. tér 1, Szeged, H-6720 Hungary; e-mail: hannus@chem.u-szeged.hu

²Institute of Isotopes of the Hungarian Academy of Sciences, P.O. Box 77, Budapest, H-1525, Hungary

Bimetallic catalysis has always been a subject of exciting investigations. Gold bimetallic catalysts have been prepared by several methods on different supports. Synergism in bimetallic AuPd catalyst was reported in hydrogenation reactions [1].

Some of the chlorinated organic compounds are widely used commercially, because of their advantageous chemical/physical properties or having toxicity for pestiferous living substances. However, most of them are environmental pollutants. Emitted into the atmosphere they are responsible for diminishing the ozone layer in the stratosphere. Therefore, a lot of effort is devoted in finding proper solutions to decompose these chemicals in environmentally friendly ways. Nobel metals on different carriers play very important role in catalytic hydrodechlorination of these compounds. No such own activity of Au was reported, but improved selectivity and activity could be reached by alloyed type and core/shell supported AuPd bimetallic particles in dichlorodifluoromethane and trichloroethene hydrodechlorination, respectively, compared to the monometallic Pd analogues [2, 3].

During the work leading to this contribution we have prepared SiO₂ and TiO₂ supported bimetallic Au-Pd [4] and Au-Pt samples and the monometallic Au, Pd and Pt analogues by adsorption of the preformed nanoparticles from the corresponding mono- or bimetallic hydrosols. The samples were characterized by X-ray fluorescence spectroscopy (metal content), transmission electron microscopy (metal particle size), X-ray diffraction (crystallinity) and CO chemisorption, oxidation. Catalytic activity of these noble metal nanoparticles was investigated in the hydrodechlorination of CCl₄ as model compound.

IR spectroscopic self-supporting wafer technique was employed for adsorption and catalytic measurements. The wafers were prepared from the solids and placed into the sample holder of an *in situ* IR cell. During the pretreatment process when the wafer was heated at 673 K for 1 h in 20% O₂ in nitrogen stream followed by evacuation at the same temperature the organic compound (remaining reducing and stabilizing agents) were removed. This oxidized sample was reduced in H₂ at 473 K. For hydrodechlorination experiments the pretreated catalyst wafers were loaded with the CCl₄ (carbon tetrachloride) reactant at room temperature. Both the surface species and the gas-phase products were analysed as the reaction proceeded under various experimental conditions by IR spectroscopy.

FT-IR measurements proved that the intermediate product is phosgene (COCl₂) and the final products are CO₂ and HCl. The hydrogen/reactant ratio exerts large influence on the rate of the hydrodechlorination reaction.

- [1] R.W.J. Scott, O.M. Wilson, S.K. Oh, E.A. Kenik, R.M. Crooks, *J. Am. Chem. Soc.* 126 (2004) 15583.
- [2] M. Bonarowska, J. Pielaszek, V.A. Semikolenov, Z. Karpinski, *J. Catal.* 209 (2002) 528.
- [3] M.O. Nutt, K.N. Heck, P. Alvarez, M.S. Wong, *Appl. Catal. B: Environmental* 69 (2006) 115.
- [4] A. Beck, A. Horváth, Z. Schay, Gy. Stefler, Zs. Koppány, I. Sajó, O. Geszti, L. Gucci, *Topics in Catalysis* 44 (2007) 115.

Acknowledgement

This work was performed with the help of grant OTKA K 49564, Hungary.

Characterization of Allergens in Different Perfumes and Herbs

A. Iordache, M. Culea, O. Cozar

*Babeş-Bolyai University, Faculty of Physics, Kogălniceanu 1, RO-400084 Cluj-Napoca, Romania
e-mail: andres_iro2002@yahoo.com*

The allergens in cosmetics products need to be labeled when 0.01 % or 0.001 % values are passed for rinse off and leave on products (7th amendment of European Directive 2003/15/EC, Official Journal of the European Union, L66/26, 11.3.2003). Volatile oils and perfumes (diluted 10:1) were injected directly or by headspace or other extraction methods for shampoos, shower gels and herbs analysis. The samples were analyzed by GC-FID and GC-MS. A HP-5 capillary column, 30mx0.32mm, 0.25 µm film thickness, in a proper temperature program was used. The target analyses followed 26 allergens, but especially limonene was quantitatively determined, by using as internal standard C11:1 ester.

- [1] C. Gherman, M. Culea, O. Cozar, *Talanta* 53 (2000) 253-262.
- [2] T. Hodisan, M. Culea, C. Cimpoiu, A. Cot, *J. Pharm. Biomed. Anal.* 18 (1998) 319-323.
- [3] M. Culea, M. Apetri, C. Gherman, *Roum. J. Physics.* 46 (2001) 451-458.

Clinical Chemistry without Reagents? An Infrared Spectroscopic Technique for Determination of Clinically Relevant Constituents of Body Fluids

O. Klein¹, I. Klein¹, G. Oremek², W. Mäntele¹

¹ *Institut für Biophysik, Max von Laue-Straße 1, 60438 Frankfurt, Germany*

² *Universitätsklinikum, Zentrum der inneren Medizin, Theodor Stern Kai 7, 60590 Frankfurt, Germany*
e-mail: klein@biophysik.org

In the clinical domain it is necessary to determine blood parameters like cholesterol, uric acid, urea, glucose, proteins etc. for a large amount of samples with sufficient precision. At present this is mostly done in the central laboratory, where a time-consuming preparation is needed before the measurement starts. Therefore the time span between the sample drawing and the obtaining of the results often takes too long in case of emergency. Furthermore, multiple instrumentation is needed for several different parameters.

We propose to solve this problem by using a reagent-free method which is able to determine the concentrations of various blood components within one minute [1]. This is done by measuring infrared absorbance spectra with a FTIR spectrometer. To reduce the required amount of blood and to allow fast and easy exchange of the samples, a diamond-ATR-cell was constructed.

Problems which arise due to overlapping bands of different components were solved by using a spectrometric method based on partial-least-squares regression [2]. In the present stage of development we are already able to determine eight relevant parameters in human serum or whole blood [Table 1] and seven parameters in urine. Our method complies with criteria from hospitals for a bedside point-of-care-testing and therefore will minimize the time span between sample drawing and a therapeutical decision.

Table 1: Accuracy and deviation of different parameters of human whole blood

	data set range	RMSECV
total protein	2 – 11 g/dl	± 0,32 g/dl
albumin	1 – 6 g/dl	± 0,15 g/dl
hemoglobin	8 – 17 g/dl	± 0,234 g/dl
immunglobulin g	0,3 – 2,1 g/dl	± 0,12 g/dl
glucose	20 – 340 mg/dl	± 7,5 mg/dl
urea	10 – 220 mg/dl	± 4,4 mg/dl
triglycerides	0 – 1700 mg/dl	± 19,7 mg/dl
cholesterol	35 – 360 mg/dl	± 15 mg/dl

[1] G. Hosafci, O. Klein, G. Oremek, W. Mäntele, *Anal Bioanal Chem* 387 (2007) 1815-22.

[2] T. Næs, T. Isaksson, T. Fearn, T. Davies: *Multivariate Calibration and Classification* (2002); NIR Publications Chichester, UK.

Synthesis, Molecular Structure, IR and Raman Spectra as well as DFT Quantum Chemical Calculations for N-thiocynoacetylpiperidine and its Methyl Derivatives

E. Kucharska¹, W. Szaśiadek¹, H. Ban-Oganowska¹, M. Mączka², J. Hanuza^{1,2}

¹Department of Bioorganic Chemistry, Institute of Chemistry and Food Technology, Faculty of Engineering and Economics, University of Economics, Komandorska 118/120, 53-345 Wrocław, Poland

²Institute of Low Temperature and Structure Research, Polish Academy of Sciences, Okólna 2, 50-950 Wrocław, Poland

The thiocyanate (rhodanide) compounds are used as biocides in the leather making industry. Commercial biocidal formulations form the blend of active ingredients that combine the rapid antimicrobial actions of thiocyanate components with the fungicidal properties of the second component, e.g. thiocyanomethylthiobenzothiazole derivatives [1 and references therein].

Syntheses of N-thiocynoacetylpiperidine and its 2-, 3- and 4-methyl derivatives are described. The following compounds have been studied:

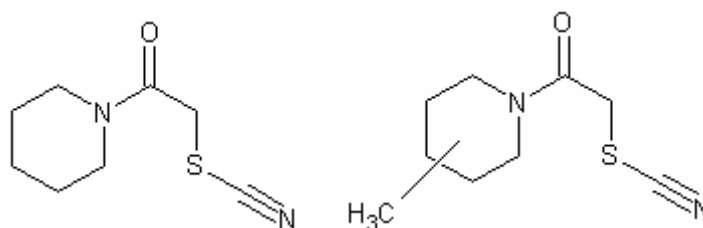


Fig. 1: Structures of N-thiocynoacetylpiperidine and its methyl derivatives

FT-IR and Raman spectra of these compounds have been measured and compared to the spectra of piperidine and alkylamides of thiocynoacetic acid. The 6-31G(d,p) basis set with the B3LYP functional has been used to discuss the structure and vibrational dynamics of the compounds studied. The calculated bond parameters of the optimized structures take the following average values, distances: C≡N 1.167, S-CN 1.700, S-CH₂ 1.856, H₂C-CO 1.534, OC-N 1.367, C=O 1.228 Å and angles: S-C≡N 177.9, H₂C-S-C 100.6, H₂C-CO-N 119.2, N-C=O 123.3°. These data fit well to the X-ray data of similar compounds [2]. The vibrational characteristics of the SCN, CO, CH₂ bridge groups and piperidine ring are reported with their relation to the molecular structures. The most characteristic vibrations have been observed in the following regions: ν(CN): 2156-2149, ν(CO): 1626-1616, ν_{as}(CH₂): 3015-2912, ν_s(CH₂): 2902-2850, ν(S-C): 648-615 and δ(SCN): 475-452 cm⁻¹. The energy of these modes depends on the substitution place of the methyl group. The other normal modes of the SCN, CO, CH₂ groups and piperidine ring with the PED values have been described. The role and influence of the substitution position of the methyl chromophore are discussed.

[1] L. Muthusubramanian, V.S. Sundara Rao, R.B. Mirta, J. Cleaner Production 11 (2003) 695-697.

[2] S. Thamocharan, V. Parthasarathi, R. Malik, D.P. Jindal, P. Piplani, A. Linden, Acta Crystallogr., Sect. C: Cryst. Struct. Commun. 59 (2003) o422-o425.

Kinetic Spectrophotometric Determination of N-(2-Mercaptopropionyl)-glycine in Pharmaceuticals

L. Kukoč Modun, Nj. Radić

*Department of Analytical Chemistry, Faculty of Chemistry and Technology, University of Split,
Teslina 10/V, 21000 Split, Croatia*

N-(2-mercaptopropionyl)-glycine (MPG), also named tiopronin, is a synthetic aminothioliol antioxidant. It is highly desirable to provide a simple, rapid and cost-effective spectrophotometric procedure that is suitable for precise and sensitive determination of MPG in pharmaceutical preparation over a wide analytical range. A few classical (equilibrium) spectrophotometric methods for determination of MPG have been reported, but they lack to fulfill all the abovementioned criteria. Furthermore, to authors' knowledge, there are not any published kinetic spectrophotometric methods for the determination of MPG. Also, none of the cited equilibrium methods for determination of MPG has used Fe(III) and 2,4,6-Trypyridyl-s-triazine (TPTZ) as reagent solution.

In this report a novel, simple and sensitive kinetic spectrophotometric method for the determination of MPG in pharmaceutical preparation is described. The proposed kinetic method has been compared with the equilibrium method. Both methods are based on the coupled redox-complexation reaction whose first part is reduction of Fe(III) by MPG, while second one includes the complexation of Fe(II), resulted from preceding redox reaction, with TPTZ. The stable $\text{Fe}(\text{TPTZ})_2^{2+}$ complex exhibits an absorption maximum at $\lambda = 593 \text{ nm}$. Apparatus used in the kinetic spectrometric measurement was described in our previous publication [1].

MPG can be determined in concentration range from 1.0×10^{-6} to $1.0 \times 10^{-4} \text{ mol L}^{-1}$ using each method. In order to evaluate the potential of the proposed methods to analysis of real sample, both methods were applied to pharmaceutical samples for the determination of MPG. The accuracy of the methods was checked by carrying out recovery studies, when known amounts of the MPG standard were added to the samples before the recommended procedures. There were no significant differences between the labelled contents and those obtained by the two methods. The recoveries were approximately 100% for both methods, indicating that the proposed kinetic method is reliable for the determination of MPG in pharmaceutical preparations.

The proposed kinetic spectrophotometric method can be applied in an analytical laboratory as a simple, sensitive, fast and economical procedure for the determination of MPG in pharmaceuticals.

[1] A. Martinović, L. Kukoč-Modun, N. Radić, *Anal. Lett.* 40 (2007) 805-815.

Rotational Disorder in 2-Piperidyl-5-nitro-6-methylpyridine: Structural Phase Transition and its Vibrational Characteristics

J. Lorenc¹, B. Palasek¹, J. Hanuza^{1,2}, M. Mączka², A. Waśkowska²

¹Department of Bioorganic Chemistry, Institute of Chemistry and Food Technology, Academy of Economics, 118/120 Komandorska Street, 53-345 Wrocław, Poland, ²Institute of Low Temperature and Structure Research, Polish Academy of Sciences, Okólna 2., 50-950 Wrocław, Poland.

2-piperidyl-5-nitro-6-methylpyridine is a novel compound among the pyridine-derivatives that has not yet been studied. The discussion of the vibrational spectra of this material has been based on the structure of this compound and DFT quantum chemical calculations.

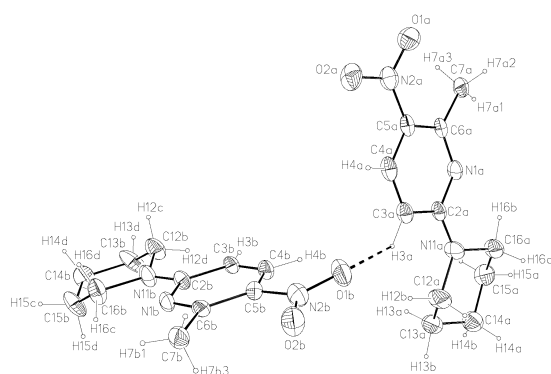


Fig. 1: Asymmetric unit of $C_{11}H_{15}N_3O_2$ in the low temperature phase. Displacement ellipsoids are drawn at the 30% probability level.

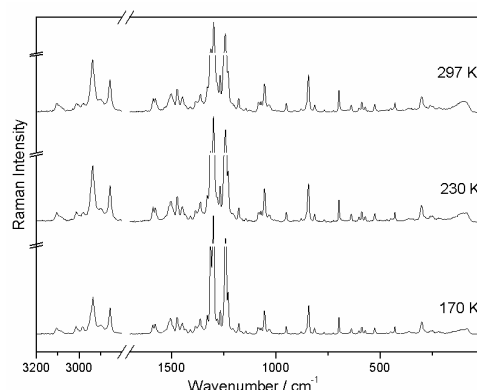


Fig. 2: The Raman spectra of $C_{11}H_{15}N_3O_2$ at 297, 230 and 170 K in the region $3200-30\text{ cm}^{-1}$

X-ray diffraction studies have shown that 2-piperidyl-5-nitro-6-methylpyridine, $C_{11}H_{15}N_3O_2$, undergoes structural phase transition at $T = 240\text{ K}$. The room temperature structure is tetragonal, space group $I4_1/a$, with the unit cell dimensions $a = 13.993(2)$ and $c = 23.585(5)\text{ \AA}$. The pyridine ring takes *trans* conformation with respect to the piperidine unit. While pyridine is well ordered, the piperidine moiety shows apparent disorder resulting from a libration about linking N – C bond. The low temperature phase is monoclinic, space group $I2/a$. Contraction of the unit cell volume by 2.3% at 170 K enables the C – H...O linkage between the molecules of the neighbouring stacks. As result, the asymmetric unit becomes bi-molecular. The thermal librations of the piperidine and methyl groups become considerably reduced at 170 K and nearly fully reduced at about 100 K. The IR spectra and polarised Raman spectra agree with the X-ray structure and confirm the disorder effect on the piperidine ring.

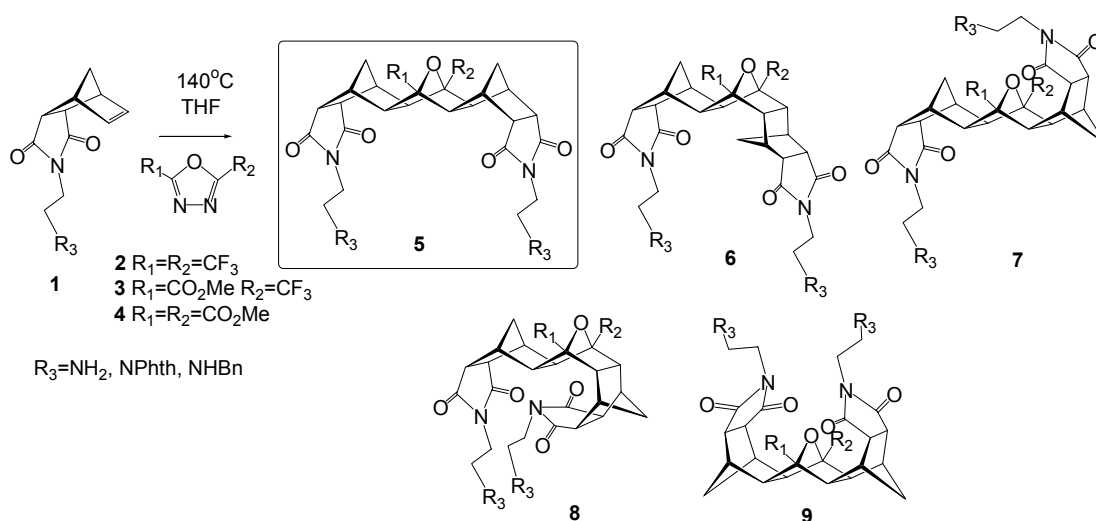
The temperature dependence of IR and Raman modes shows clear changes at about 240, 200 and 100 K. For instance, a clear splitting is observed at 240 K for the following bands: $1472 \rightarrow 1472 + 1467$, $1431 \rightarrow 1434 + 1427$, $1164 \rightarrow 1176 + 1163\text{ cm}^{-1}$. These bands correspond to the vibrations of the methyl group coupled with the pyridine ring. The most pronounced changes are observed, however at about 100 K where the splitting of the following bands is observed: $2945 \rightarrow 2956 + 2944$, $2898 \rightarrow 2912 + 2893$, $1315 \rightarrow 1318 + 1308$, $1055 \rightarrow 1057 + 1052$, $1032 \rightarrow 1034 + 1026$, $907 \rightarrow 911 + 907$, $809 \rightarrow 816 + 812$, $725 \rightarrow 729 + 727$, $587 \rightarrow 588 + 584$, $214 \rightarrow 226 + 218 + 207\text{ cm}^{-1}$. Such effects agree with the structural changes induced by the temperature lowering, i.e. freezing of the methyl and piperidine units librational motions.

Spectroscopic and Quantum-Chemical Assignments of Stereochemistry of Products Obtained by 1,3-dipolar Cycloaddition Reactions of Substituted 1,3,4-oxadiazoles With Norbornenes

Ž. Marinić¹, P. Trošelj², M. Eckert-Maksić², D. Margetić²

¹NMR Centre, Ruđer Bošković Institute, Bijenička cesta 54, 10000 Zagreb, Croatia, ²Laboratory for Physical Organic Chemistry, Division of Organic Chemistry and Biochemistry, Ruđer Bošković Institute, Bijenička cesta 54, 10000 Zagreb, Croatia

The 2-dimensional NMR spectroscopy (COSY, NOESY, ROESY, HMQC, HMBC) was employed to study the stereochemical outcomes of 1,3-dipolar cycloaddition reactions of substituted 1,3,4-oxadiazoles **2-4** with norbornenes [1]. In this reaction five possible products may be formed (**5-9**), while experimentally a single product has been isolated. In conjunction with spectroscopic assignments, density-functional quantum-chemical calculations (GIAO/DFT) were also performed for chemical shift calculations, specifically by GIAO/6-31+G*//B3LYP/6-31G* method [2]. Spectroscopic analysis and calculations have unequivocally proven that synthesized products possess linear (*exo,exo*-:*exo,exo*-) structures **5**.



[1] R.N. Warrener, D. Margetić, E.R.T. Tiekink, R.A. Russell, Synlett (1997) 196-198.

[2] T. Tsuji, M. Ohkita, H. Kawai, Bull. Chem. Soc. Jp. 75 (2002) 415-433.

Entacapone Isomer Quantification Using Raman Spectroscopy

M. Marković, T. Biljan, D. Škalec Šamec

PLIVA Croatia Ltd., Research and Development, Prilaz baruna Filipovića 29, 10 000 Zagreb, Croatia

Raman spectroscopy, due to its non-destructive character and speed, has found widespread use in pharmaceutical applications [1]. It is also being used for quantifying various isomer mixtures, best known being the quantification of xylene isomers [2-3]. We here report quantification of isomer mixture of an active pharmaceutical substance.

Entacapone (2-cyano-3-(5-dihydroxyamino-3,4-dioxo-1-cyclohexa-1,5-dienyl)-N,N-diethyl-prop-2-enamide) is an active substance used in treatment of Parkinson's disease. It can be found in two isomeric forms *Z* and *E*. Isomer *Z* appears as a most common impurity in pharmaceutically more active isomer *E*. For this reason the ability to monitor the quantity of isomer *Z*, in isomer *E* is very important. Both isomers come up with a number of polymorphic forms. The most stable forms of the two isomers have distinct Raman spectra (Fig 1). Based on these distinct spectra the quantification of isomer mixture was performed. Physical mixtures of isomer *Z* in isomer *E* were prepared in range from 0% to 10% (w/w). Quantitative model of the mixture was obtained by Partial Least Square (PLS) Regression. The model performance was improved by applying mathematical pretreatment to the spectral data. In the range from 0% to 10% (w/w), the calibration model was linear.

Raman spectroscopy is a fast, non-destructive and reliable technique for quantification of isomer *Z* in the entacapone isomer mixture.

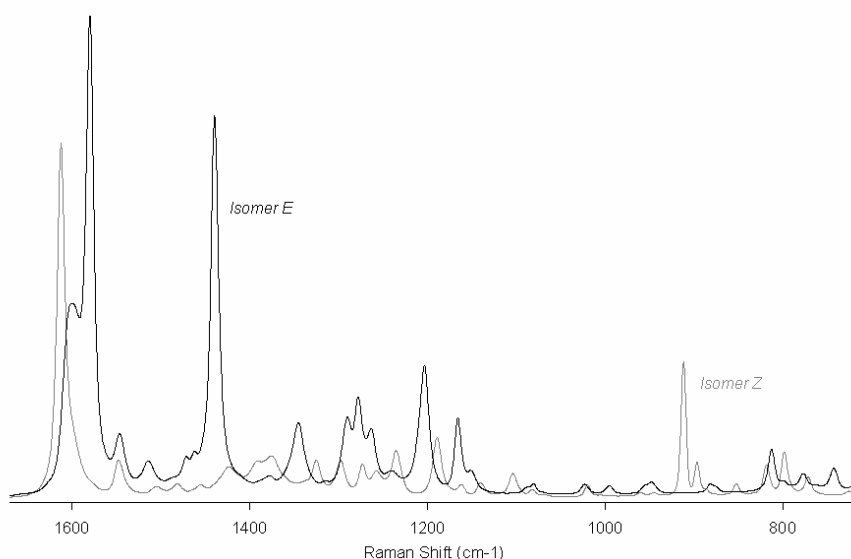


Figure 1: Distinct Raman spectra of entacapone *Z* and *E* isomer.

- [1] S. Cîntă Pînzaru, I. Pavel, N. Leopold, W. Kiefer, J. Raman Spectrosc. 35 (2004) 338-346.
- [2] J. H. Giles, D. A. Gilmore, M. Bonner Denton, J. Raman Spectrosc. 30 (1999) 767-771.
- [3] M. López-Sánchez, M. J. Ruedas-Rama, A. Ruiz-Medina, A. Molina-Díaz, M. J. Ayora-Cañada, Talanta 74 (2008) 1603-1607.

Study of Heparin/Protamine Complexation by Means of Fluorescence Spectroscopy, Light Scattering and Analytical Ultracentrifugation

J. Maurer, V. Vogel, W. Mäntele

*Institute of Biophysics, Johann Wolfgang Goethe-University Frankfurt/Main,
Max-von-Laue-Str. 1, 60438 Frankfurt/Main, Germany*

The administration of heparin, a linear glycosaminoglycan, has been used clinically for many years as the standard procedure for anticoagulation treatment. However, the determination of heparin concentration/activity is more or less empirical and therefore does not assure a precise blood coagulation management for the individual patient. This frequently leads to internal bleeding or local coagulations.

Here we present the approach to investigate the complex formation between heparin and protamine. The binding kinetics of the complex formation was examined by means of light scattering methods and quenching of fluorescence dye labelled protamine. Additionally, both multi-angle light scattering technique and analytical ultracentrifugation were used for characterisation of heparin/protamine complex size distribution.

The observed radius of the heparin/protamine complexes was in the range between 10 nm and 200 nm and the complexation process was completed after a time between 5 min and 15 min. Both parameters depended on the type of solution in which the experiments were carried out (physiological saline solution, model HSA solution and blood plasma).

These results can be used for heparin monitoring. On the basis of light scattering studies, we present a simple, quick and precise quantitative method for heparin concentration measurement which will improve blood coagulation management.

Detection of HEMA in Self-etching Adhesive Systems Using High Performance Liquid Chromatography

V. Pandurić¹, Z. Tarle¹, Z. Hameršak², I. Stipetić², D. Matošević¹, K. Prskalo¹,
V. Negovetić-Mandić¹

¹ Department of Endodontics and Restorative Dentistry, School of Dental Medicine, University of Zagreb, Gundulićeva 5, 10000 Zagreb, Croatia

² Laboratory for Stereoselective Catalysis and Biocatalysis Department for Organic Chemistry and Biochemistry, Institute Rudjer Bošković, Bijenička 54, 10000 Zagreb, Croatia

One of the factors that can decrease hydrolytic stability of self-etching adhesive systems (SEAS) is 2-hydroxyethylmethacrylate (HEMA). Due to hydrolytic instability of acidic methacrylate monomers in SEAS, HEMA can be present even if the manufacturer did not include it in original composition. The aim of the study was to determine the presence of HEMA because of decomposition by hydrolysis of methacrylates during storage, resulting with loss of adhesion strength to hard dental tissues of the tooth crown.

Three most commonly used SEAS were tested: AdheSE ONE, G-bond and iBond under different storage conditions. High performance liquid chromatography (HPLC) analysis was performed on a Nucleosil C₁₈-100 5 μm (250x4.6 mm) column, Knauer K-501 pumps and Wellchrom DAD K-2700 detector at 215 nm. Data were collected and processed by EuroCrom 2000 HPLC software. Samples of adhesives (~70 mg) were dissolved in 2.0 ml of methanol and filtered; 20 μl were injected and isocratically eluted with 20% aqueous methanol for 15 min, followed by gradient to 100% methanol in 5 min. Calibration curves were made related eluted peak area to known concentrations of HEMA (purchased from Fluka). The elution time for HEMA is 12.25 min at flow rate 1.0 ml/min.

Table 1: Tested materials and the HEMA concentration in the study.

Adhesive	Storage	HEMA content (%)
G-bond	New bottle	0.14%
G-bond	Opened bottle, 2 months rt, 3 months 4 °C	0.15%
G-bond	Opened bottle, 5 months rt	0.22%
G-bond	Unopened bottle, 3 months 38 °C	0.31%
iBond	New bottle	0.07%
iBond	Opened bottle, 5 months rt	0.13% (partially polymerized or dried)
iBond	Unopened bottle, 3 months 38 °C	(completely dried or polymerized)

rt - room temperature

Obtained results, shown in table 1 indicate that no HEMA was present in AdheSE ONE because methacrylates are substituted with methacrylamides that seem to be more stable under acidic aqueous conditions. In all other adhesive systems HEMA was detected.

Experimental and Theoretical Investigation of 5-para-nitro-benzylidene-thiazolidine-2-thione-4-one Molecule

A. Pîrnău^{1,2}, V. Chiş¹, L. Szabo¹, O. Cozar¹,
M. Vasilescu¹, O. Oniga³, R.A. Varga⁴

¹Babeş-Bolyai University, Faculty of Physics, Kogălniceanu 1, RO-400084 Cluj-Napoca, Romania

²National Institute for Research and Development of Isotopic and Molecular Technologies, RO-400293, Cluj-Napoca, Romania

³Iuliu Haţieganu University of Medicine and Pharmacy, Department of Pharmaceutical Chemistry, Emil Isac 13, RO-400023 Cluj Napoca, Romania

⁴Babeş-Bolyai University, Faculty of Chemistry and Chemical Engineering, Arany Janos 11, RO-400028 Cluj-Napoca, Romania

Address for correspondence: apirna@phys.ubbcluj.ro

Development of novel therapeutics for the treatment of microbial infections has become a clinical imperative [1,2] and new heterocycle compounds which contain in their structure a series of structural units similar to those of Linezolid are proposed and used to discover new antimicrobial leads. In this connection, thiazolidines derivatives were obtained by replacing the oxygen atom of the oxazolidinone ring with a bulkier sulfur atom.

In this work, experimental methods (FT-IR, Raman and NMR spectroscopies, and X-ray diffraction technique) coupled with quantum chemical calculations based on density functional theory (DFT) are used for structural and electronic characterization of 5-para-nitro-benzylidene-thiazolidine-2-thione-4-one (5p-NBTT), a new synthesized compound with antimicrobial activity.

The molecular vibrations of 5p-NBTT were investigated by FT-IR and FT-Raman spectroscopies. In parallel, quantum chemical calculations based on Density Functional Theory (DFT) are used to determine the geometrical, energetic and vibrational characteristics of the molecule. Different conformers and tautomers of 5p-NBTT have been analyzed by theoretical methods and their relative stability is discussed. The molecular electrostatic potential of this molecule has been calculated and used for predicting site candidates of electrophilic attack.

The ¹H and ¹³C NMR spectra of 5p-NBTT were obtained in DMSO solution and they were also calculated using the GIAO (Gauge-Including Atomic Orbitals) method. Proton NMR spectrum of this molecule in solution shows an unexpected proton chemical shift at 13.0 ppm. This signal is attributed to the proton bound to the nitrogen atom and this very important deshielding can be explained by assuming a relatively strong hydrogen bond of 5p-NBTT with the solvent molecules, realized through NH group [3].

X-ray diffraction technique indicates that 5p-NBTT crystallizes with one tetrahydrofuran (THF) solvent molecule, forming a 1:1 5p-NBTT•THF complex in the monoclinic space group C2/c, with Z = 8 and cell parameters: $a = 29.496 \text{ \AA}$, $b = 7.276 \text{ \AA}$, $c = 14.873 \text{ \AA}$, $\alpha = 90.00^\circ$, $\beta = 95.161^\circ$ and $\gamma = 90.00^\circ$.

[1] C.V. Kavitha, Basappa, S. Nanjunda Swamy, K. Manteligen, S. Doreswamy, M.A. Sridhar, J. Shashidhara Prasad, S. Rangapa, *Bioorg. Med. Chem.* 14 (2006) 2290-2299.

[2] M.L. Cohen, *Nature* 406 (2000) 762-767.

[3] V. Chiş, A. Pîrnău, M. Vasilescu, R. A. Varga, O. Oniga, *J. Mol. Struct. (Theochem)* 851 (2008) 63-74.

Fluorescence Analysis of Sulfasalazine Bound to Defatted Serum Albumin in the Presence of Denaturing Factors

J. Równicka¹, A. Sułkowska¹, M. Maciążek-Jurczyk¹, B. Bojko¹, J. Pożycka¹,
W.W. Sułkowski²

¹Department of Physical Pharmacy, Faculty of Pharmacy, Medical University of Silesia, Sosnowiec, Poland

²Department of Environmental Chemistry and Technology, Institute of Chemistry,

University of Silesia, Katowice, Poland

e-mail: jrownicka@sum.edu.pl

Urea (U) and guanidine hydrochloride (Gu·HCl) - induced destabilization and denaturation of defatted bovine serum albumin (dBSA) and binding of sulfasalazine (SSZ) to dBSA has been studied *in vitro* by the fluorescence spectroscopy.

Disorder of tertiary structure of protein caused by the effect of chemical denaturing agents makes possible a change in binding ability of protein. This results in side-effects.

On the basis on relative fluorescence the binding site of SSZ to dBSA the quenching and the binding constants for complexes dBSA-SSZ, dBSA(U)-SSZ and dBSA(Gu·HCl)-SSZ have been found.

Gu·HCl in concentration higher than 1,8 M causes unfolding of tertiary structure of albumin. Then, on the fluorescence spectrum of dBSA two maxima of fluorescence appeared. The same effect was observed when 5M urea was used as a denaturing factor.

By applying the denaturing coefficient f we indicated concentration of denaturant needed to evoke full denaturation of dBSA.

Fatty acids bound to albumin molecules protect them from denaturing effect of urea and guanidine hydrochloride. Structure of albumin complexed with fatty acids undergoes perturbations in the presence of a higher denaturant concentration than that of the defatted one.

The above empiricism can provide the introduction to clinical trials. Denaturated or destabilized by chemical denaturants albumin *in vitro* probably can be compared *in vivo* with deformed transporting protein molecule or with molecule which passes irregular process of folding.

Fluorescence Analysis of Interaction of Phenylbutazone and Methotrexate in Binding to Serum Albumin in Combination Treatment in Rheumatology

M. Maciążek-Jurczyk¹, A. Sułkowska¹, B. Bojko¹, J. Równicka¹, W.W. Sułkowski²

¹*Department of Physical Pharmacy, Medical University of Silesia, Jagiellońska 4, 41-200 Sosnowiec, POLAND
e-mail: annasulkowska@yahoo.com*

²*Department of Environmental Chemistry and Technology, Institute of Chemistry, University of Silesia, Szkolna 9, 40-006 Katowice, POLAND*

Combination of several drugs is often necessary, especially during long-term therapy. The competition between drugs can cause a decrease of the amount of a drug bound to albumin. This results in an increase of the free, biological active fraction of the drug.

The aim of the presented study was to describe the competition between phenylbutazone (Phe) and methotrexate (MTX), two drugs recommended for the treatment of rheumatology in binding to bovine (BSA) and human (HSA) serum albumin in the high affinity binding site. Fluorescence analysis was used to estimate the effect of drugs on the protein fluorescence and to define the binding and quenching properties of drugs-serum albumin complexes. The effect of the displacement of one drug from the complex of the other with serum albumin has been described on the basis of the comparison of the quenching curves and binding constants for the binary and ternary systems.

2D NMR Study of Media Effects of Ionic Liquids on Hydrogen Bonding

Vytautas Balevicius¹, Zofia Gdaniec², Valdas Sablinskas³

¹ Faculty of Physics, Vilnius University, Sauletekio 9, LT-10222 Vilnius, Lithuania

² Institute of Bioorganic Chemistry, Polish Academy of Sciences, PL-61704 Poznan, Poland

³ Department of General Physics and Spectroscopy, Vilnius University, Universiteto str. 3 Vilnius, LT-01513, Lithuania

Ionic liquids (ILs) are one of the most successful breakthroughs in creating multifunctional materials. ILs have already demonstrated their unique features in many fields of high technology - enzyme catalysis, protein synthesis, membrane technology, battery and fuel cells, nanotechnology, *etc* [1-3 and the references therein]. Nevertheless despite a colossal flux of works on ILs in the last years, certain important gaps remain. The proton sharing and transfer in H-bond systems implanted in various ILs environments and the media (solvent) effects on these processes are among those.

We present some new 2D NMR data obtained using ¹H - ¹³C HSQC (*Heteronuclear Single Quantum Coherence*) on the ionic liquid media effect on the state of the H-bond in the picolinic acid N-oxide (PANO) dissolved in two ammonium based room-temperature ionic liquids (RTILs), namely, in methyltriocetylammmonium trifluoroacetate (**atf4/cqa4**), ethyl-dimethyl-propylammmonium bis (trifluoromethylsulfonyl) imide (**atf1/cqa42**), as well as in one pyrrolidinium based system – in the 1-butyl-1-methylpyrrolidinium trifluoromethanesulfonate (**asu4/cgh3**). PANO as the molecular model system was chosen because of the intramolecular H-bond OH...O←N that cannot be completely destroyed by the solvation of bonding ‘partners’, i.e. –OH and O←N moieties, in ‘aggressive’ ionic environments. Furthermore, derivatives of pyridine and pyridine N-oxide are quite well investigated systems as H-bonds partners (bases). It was found in these studies that the state of H-bond can be very effectively monitored using the ¹³C NMR shifts of the ring carbons [4, 5]. Finally, ¹³C NMR spectra of PANO solutions in chloroform (CHF) and acetonitrile (AN) are known [6].

By their dielectric properties (static dielectric constants of various classes of ILs are spread usually over 11-14 [7, 8]), IL systems are not ‘super-polar’. Their extraordinary action in certain chemical reactions and in other molecular processes is mainly due to supra-molecular structuring in nano-scale effects and possible equilibria within the IL phase [3]. The measured ¹³C NMR shift values are a quite good match for solvents dielectric scheme shows that the state of H-bond in PANO in the studied RTIL solutions is governed in a great deal by the bulk media, except **asu4/cgh3**. This finding can be explained by the extremely strong action of the anion CF₃SO₃⁻ in **asu4/cgh3**. Trifluoromethanesulfonic acid (CF₃SO₃H) is often regarded as one so-called “superacids” (about 1000 times stronger than sulfuric acid).

[1] <http://www.merck.de/servlet/PB/menu/1014040/index.html>

[2] 92nd Bunsen-Colloquium on Physical Chemistry in Ionic Liquids (Clausthal, 2006): <http://www2.imet.tu-clausthal.de/bunsen92>.

[3] D. Bankmann, R. Giernoth, *Progr. Magn. Res. Spectroscopy* 51 (2007) 63-990.

[4] V. Balevicius, H. Fuess, *Lithuanian J. Phys.* 45 (2005) 241-247.

[5] V. Balevicius, J. Tamuliene and D. Hadzi, Abstracts of XVth International Conference on Horizons in Hydrogen Bond Research, September 16-21, 2003, Berlin, 3P19.

[6] J. Stare, A. Jezerska, G. Ambrozic, I. Kosir, J. Kidric, A. Koll, J. Mavri and D. Hadzi, *J. Am. Chem. Soc.* 126 (2004) 4437-4443.

[7] H. Weingaertner, *Z. Phys. Chem.* 220 (2006) 1395-1405.

[8] H. Weingaertner, P. Sasisander, C. Daguene, P. J. Dyson, I. Krossing, J. M. Slattery, T. Schubert, *J. Phys. Chem. B* 111 (2007) 4775-4780.

Structures of 1-Butene and 1-Heptene Primary Ozonides as Studied by Means of Matrix Isolation FTIR Spectroscopy

S. Strazdaite, J. Ceponkus, V. Aleksa, V. Sablinskas

Department of General Physics and Spectroscopy, Vilnius University
Universiteto str. 3 Vilnius, LT-01513, Lithuania

The investigations of chemical reactions between alkenes and ozone have considerable practical importance in modeling of photochemical smog formation. This reaction starts from breaking down C=C bond of alkene and goes through a few steps forming intermediate unstable species- primary ozonide (POZ), secondary ozonide (SOZ) and *Criegee* intermediates (CI), but spatial structures of these species are still unclear. 1-butene and 1-heptene are the ones of the simplest alkenes, which may have conformational diversity due to rotation around aliphatic radical C-C bond closest to the five membered ring. This conformational diversity should persist in primary ozonides, but the precise nature of the conformational equilibrium has not been determined, yet. Primary ozonide is formed together with secondary ozonide. Due to high instability of primary ozonide it's separation from SOZ is not possible, what makes conformational analysis of this molecule difficult. For such analysis, prior information about conformational diversity of secondary ozonide is needed. Such information allows eliminate spectral bands of secondary ozonide from the mixture of the reaction products. Recently, such information became available from work done in our lab [1-2].

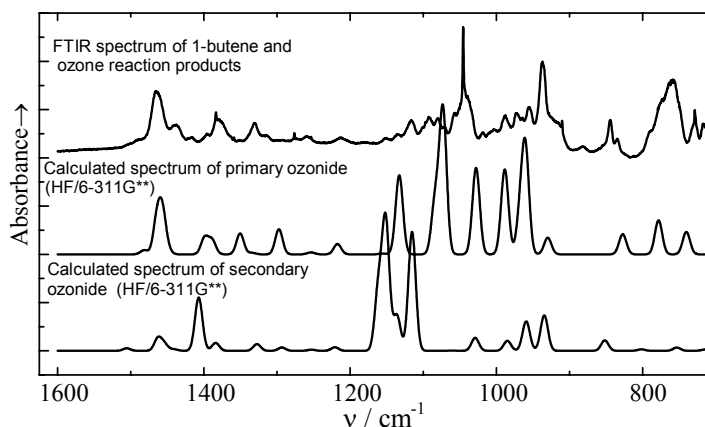


Fig.1: Experimental FTIR spectrum of products of the reaction between 1-butene and ozone in CO₂ matrix and *ab initio* calculated (HF/6-311G**) spectra of *gauche* conformers of primary and secondary ozonides of 1-butene

In this work we obtained FTIR absorption spectra of the ozonization products of 1-butene and 1-heptene, isolated in Xe and CO₂ matrices. Some results for the ozonization products of 1-butene are presented in Fig. 1. From comparison of *ab initio* calculated (HF/6-311G**) and experimental FTIR spectra complete assignment of experimental bands belonging to primary ozonides of 1-butene and 1-heptene was made. It was found that both ozonides preferable exist as *gauche* conformers. Other conformers of the primary ozonides were not found in the mixtures of the reaction product. Contrary, the secondary ozonides of both alkenes exist as mixture of *gauche* and *anti* conformers [1, 2].

[1] R. Bariseviciute, J. Ceponkus, A. Gruodis, V. Sablinskas, Central European Journal of Chemistry 4 (2006) 578-591.

[2] R. Bariseviciute, J. Ceponkus, V. Sablinskas, L. Kimtys, J. Mol. Struct. 844-845 (2007) 186-192.

Vibrational, NMR and DFT Investigations of Amlodipine Molecule

L. Szabó¹, V. Chiş¹, A. Pîrnău^{1,2}, N. Leopold¹, O. Cozar¹, Sz. Orosz³

¹Babeş-Bolyai University, Faculty of Physics, Kogălniceanu 1, RO-400084 Cluj-Napoca, Romania

²National Institute for Research and Development of Isotopic and Molecular Technologies, 71-103 Donath Str., P.O.Box 700, RO-400293 Cluj-Napoca, Romania

³Gedeon Richter LTD., X., Diósgyőri út 21, IO.P.O.B.27.H-1475, Budapest, Hungary

DFT methods are increasingly applied to representative pharmacological compounds aiming to elucidate their molecular structures and electronic properties and to describe the influence of electronic and structural factors on the reactions in which these compounds are involved. These studies contribute to the understanding of the structure-activity relationships and the behavior of the investigated system [1, 2].

The title molecule Amlodipine is used alone or in combination with other medications to treat high blood pressure and chest pain (angina). Amlodipine is in the class of calcium channel blockers and in order to get new insights into its molecular structure and properties, a complete experimental and theoretical study was performed.

The molecular vibrations of Amlodipine were investigated by FT-IR/ATR and FT-Raman spectroscopies. In parallel, quantum chemical calculations based on Density Functional Theory (DFT) are used to determine the geometrical, energetic and vibrational characteristics of the molecule.

The vibrational spectrum of the Amlodipine molecule has been assigned based on DFT calculations at B3LYP level of theory using the standard 6-31G(d) basis set. The experimental vibrational bands were assigned to the calculated normal modes and a very good correlation was achieved between the experimental and theoretical data. The molecular electrostatic potential of the molecule has been calculated and used for predicting site candidates of electrophilic attack.

The ¹H and ¹³C NMR spectra of Amlodipine were obtained in DMSO solution and they were also calculated using the GIAO (Gauge-Including Atomic Orbitals) method implemented in the Gaussian package. The very good correlation found between the experimental and theoretical NMR data allows us to validate the calculated structure and geometrical parameters of this compound.

Solvent effects on the structure and vibrational and NMR spectra were also investigated by using the Onsager and PCM continuum models.

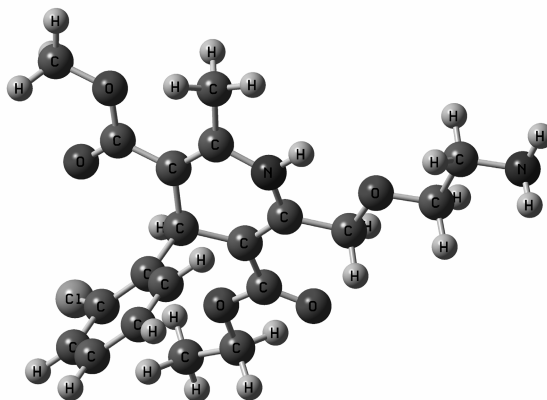


Fig.1: Optimized molecular structure of Amlodipine.

[1] V. Chiş, S. Filip, V. Miclăuş, A. Pîrnău, C. Tănăselia, V. Almăşan, M. Vasilescu, J. Mol. Struct. 363 (2005) 744.

[2] L. Szabó, V. Chiş, A. Pîrnău, B. Simon, O. Cozar, Sz. Orosz, J. Opt. Adv. Mat. 9 (3) (2007) 599.

Vibrational, NMR and DFT Investigations of Ethylenediaminetetraacetic acid

L. Szabó¹, A. Pîrnău^{1,2}, N. Leopold¹, V. Chiş¹, O. Cozar¹

¹Faculty of Physics, Babeş-Bolyai University, Kogălniceanu 1, 400084 Cluj-Napoca, Romania

²National Institute for Research and Development of Isotopic and Molecular Technologies, 71-103 Donath Str., P.O.Box 700, RO-400293 Cluj-Napoca, Romania

Molecular recognition process is the result of several weak noncovalent bonds, due to electrostatic, van der Waals, hydrogen bonding, aromatic π bonds and hydrophobic interactions, having a key role in many important biological reactions. Moreover, the molecular recognition properties exhibited by different molecules can particularly be used for chelation therapy.

Ethylenediaminetetraacetic acid, more commonly known as EDTA, forms complexes with divalent and trivalent metals. The important part of the compound involved in complexing with the metal are the four carboxylic acid groups and the two nitrogens. EDTA is usually administered as a calcium or zinc salt because EDTA has a high affinity for these metals. When EDTA is presented in a Ca or Zn salt form, it not bind these essential metals as highly as when it is administered in the non-salt form. EDTA is also most commonly used for lead poisonings.

The molecular vibrations of EDTA were investigated by ATR FT-IR and FT-Raman spectroscopies. In parallel, quantum chemical calculations based on Density Functional Theory (DFT) are used to determine the geometrical, energetic and vibrational characteristics of the molecule.

The vibrational spectrum of the EDTA has been assigned based on DFT calculations at B3LYP level of theory using the standard 6-31G(d) basis set. The experimental vibrational bands were assigned to the calculated normal modes and a very good correlation was achieved between the experimental and theoretical data. The molecular electrostatic potential of the molecule has been calculated and used for predicting site candidates of electrophilic attack.

The ¹H and ¹³C NMR spectra of EDTA were obtained in DMSO solution and they were also calculated using the GIAO (Gauge-Including Atomic Orbitals) method implemented in the Gaussian package. Again, a very good correlation was found between experimental and theoretical NMR data and this allows us to validate the calculated structure and geometrical parameters of the molecule.

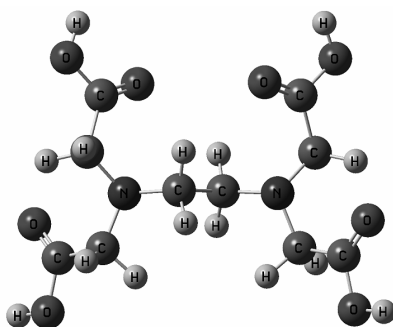


Fig. 1: Optimized molecular structure of EDTA.

The Effect of Silicate Network Modifiers on Colour and Electron Spectra of Transition Metal Ions

A. Terczynska, K. Cholewa-Kowalska, M. Laczka

*AGH University of Science and Technology, Faculty of Materials Science and Ceramics,
Department of Glass Technology and Amorphous Coatings Technology
Ave. Mickiewicza 30, Cracow, Poland*

Glass colour is a very essential factor both in glass making technology and glass state science. Compounds of transition metals and rare earths, where electron mechanism of colouring occurs, are the most often used as a glass dyes. The colour depends both on electron structure of the transition metal ions and chemical composition and structure of base glass, determining the local site of these elements. Knowledge of the influence of the glass matrix on glass colour has both technological and scientific aspect. The UV/VIS spectroscopy is the most often used method allowing to determine the local state of the transition metals in glasses. We use this method to determine influence of the glass matrix on the character of the local state of chosen transition metal ions.

Silicate glasses from oxide systems: R_2O-SiO_2 , (R – K, Na, Li) are used in our examinations as a glass matrix. In order to obtain the colour glass, the compounds of cobalt (Co), nickel (Ni), manganese (Mn) and chromium (Cr) introduced into glass batch in various concentrations. The aim of these examinations was to determine the influence of modifiers (K_2O , Na_2O , Li_2O) of silicate network on the valency and local state of chosen transition metal ions. We also try to confirm UV/VIS spectroscopic results by EPR spectroscopy.

On the base of these examinations complex conclusions are proposed with respect to the influence of inorganic matrix on the coordination state of Ni, Co, Mn, Cr ions in silicate glasses. Particularly, it has been found that Co and Ni ions occur in examined glasses in four and six coordination while Cr occurs only in octahedral coordination.

Conclusions of our research about complexes forming by transition metal ions in glasses and about oxidation state of transition metals were as follows:

- 1) Kind of modifiers of silicate network (Li_2O , Na_2O , K_2O) effects on both the colour of glasses caused to presence of transition metal ions (Ni, Co, Cr, Mn) and the character of electron spectra in visible range.
- 2) Nickel and cobalt occurs in examined silicate glasses as divalent ions in both tetrahedral (LK-4) and octahedral (LK-6) coordination. Coordination equilibrium (LK4/LK6) shifts in direction tetrahedral complex with decreasing of ion potential of modifiers ($Li \rightarrow Na \rightarrow K$).
- 3) Chromium occurs in examined glasses as trivalent ions in octahedral coordination with oxygen but other oxidation state of chromium is also possible. Proportion of Cr(III) ions in K_2O-SiO_2 glasses is lower in comparison with Na_2O-SiO_2 and Li_2O-SiO_2 probably as a result of oxidation of chromium part to higher valence (Cr(VI)).
- 4) Manganese ions occur in examined glasses as trivalent (Mn(III)) but the presence of divalent manganese ions is also possible. Proportion of Mn(III) increases with decreasing of ion potential of silicate network modifiers ($Li \rightarrow Na \rightarrow K$).
- 5) Decrease of ion potential of silicate network modifiers corresponding to increasing of basicity of anion surroundings in glasses. Thus, increasing of oxygen ions basicity favours of both the tetrahedral coordination and higher oxidation state of transition metal ions.

Estimation of the Desulphurization Degree in Light Cycle Oil Using FTIR Spectroscopy

Vesislava Toteva, Anton Georgiev, Liliana Topalova, Sergei Andreev

*University of Chemical Technology and Metallurgy, 8 "St. Kliment Ohridski" Blvd., Sofia 1756, Bulgaria
e-mail: vesislava_t@mail.bg*

One of the world's ecological topics is reducing the sulphur content in the diesel fuels. They are still among the main polluters of the environment with sulphur oxides (SO_x). The current specification in Europe and the USA calls for a maximum sulphur content of 15 ppm, and this level will be reduced to below 10 ppm by the year 2009. In Bulgaria from 01/01/2007 the sulphur in diesel should not exceed 50 ppm.

The aim of the present work was to (i) investigate the possibilities for desulphurization of light cycle oil (component of diesel fuel) by chemical oxidation of sulphur compounds to their respective sulfones, followed by extraction of the oxidized compounds using selective solvents; (ii) determination of the extracted products from the light cycle oil and effectively of desulphurization using FTIR spectral analysis. The suggested method is specific for selective oxidation of sulphur compounds and has no oxidation of aliphatic and aromatic hydrocarbons. By FTIR spectroscopy the quantity and quality of sulfones have been determined at 1304 cm^{-1} . It's was determined ratio between sulfones and sulfoxides $1030\text{-}1060 \text{ cm}^{-1}$ (intermediate product of sulfur compounds oxidation) in the absorbance spectra. Sulfones have a much higher polarity than the parent sulphide molecules, and thus are preferentially extracted from the feed. FTIR analysis allows estimating degree of the oxidation of sulphur compounds, degree of desulphurization by extraction method and registered micro quantity of oxidized products.

Organic Solvents Influence on Electronic Absorption Spectra of 4-R-phenyl-5-carboxyethyl-6-methyl-3,4-dihydropyrimidine-2-tione Derivatives. Ionization Constants Determination

Nada U. Perišić-Janjić¹, Gy.Gy. Vastag¹, J.D. Janjić¹, B.Ž. Jovanović²

¹Department of Chemistry, Faculty of Sciences, Trg D. Obradovića 3, 21000 Novi Sad, Serbia

²Faculty of Technology and Metallurgy, Karnegijeva 4, 11000 Beograd, Serbia

Derivatives of 4-R-phenyl-carboxyethyl-6-methyl-3,4-dihydropyrimidine-2-tione known as “Biginelli compounds” [1] are widely investigated due to their biological activity [2]. For the further application of these biologically active compounds, it is necessary to investigate their physicochemical characteristics. The aim of this work was to study solvents polarity effect and proton-donor ability on electronic absorption spectra of some “Biginelli compounds” and determination of their ionization constants by spectrophotometric method.

Absorption spectra of 4-R-phenyl-carboxyethyl-6-methyl-3, 4-dihydropyrimidine-2-tione derivatives show characteristic absorption maximum at about 302-310 nm in aqueous solutions. A bathochromic shift of absorption maximum and increase of absorption intensity, with decrease of solvent polarity were registered. Absorption spectra recorded in aqueous and alcoholic solution pass through isobestic point at about 290 nm. Changes of absorption maximum position with change of solvent polarity indicate that hydrogen bonds were formed between solvent and investigated compounds. In order to explain the effect of solvent polarity and hydrogen bonding on the absorption spectra, linear solvation energy relationship (LSER) concept developed by Kamlet and Taft [3] was performed.

Ionization constants of “Biginelli compounds” were determined by spectrophotometric method. Effects of chemical structure on ionization constants were investigated. Good correlation was obtained between ionization constants and Hammett substituents constants, σ . Since “Biginelli compounds” are biologically active, correlations between ionization constants, as electronic descriptors, and measure of lipophilicity (log P) of investigated compounds were established. Using computer program “Chemsilico” [4], the biological activity of investigated compounds were determined and correlated with calculated ionization constants. Satisfactory correlation was obtained.

[1] P. Biginelli, Gazz. Chim. Ital. 23, (1993) 360.

[2] C.O. Kappe, Tetrahedron 49 (1993) 6937.

[3] M.J. Kamlet, J.L.M. Abboud, M.H. Abraham, R.W. Taft, J. Org. Chem. 48 (1983) 2877.

[4] <http://www.chemsilico.com/>

Carboxylation Reactions Studied Using *Caged* CO₂

G. Schäfer, W. Mäntele, G. Wille

*Institute of Biophysics, Johann Wolfgang Goethe-University Frankfurt/Main,
Max-von-Laue-Str. 1, 60438 Frankfurt/Main, Germany*

The use of *caged* compounds, i.e. compounds which release a desired effector molecule upon photolytic cleavage, has greatly advanced our understanding of enzymes and their mechanisms. Among other things, they permit the tracking of fast reactions without the need for rapid mixing techniques.

We introduce here the use of “*caged* CO₂” for the study of carboxylation reactions. CO₂ is released from a precursor compound via a laser flash, and its reactions can be observed directly via the strong infrared absorption signal of CO₂ at 2343 cm⁻¹ that is associated with the molecule's stretching mode. Several compounds with different photolytically cleavable protecting groups have been tested; they differ with respect to quantum yield, the rate of CO₂ release and the potentially adverse reactivities of their byproducts.

In subsequent experiments the photolytically triggered CO₂ release was used to monitor the hydration of CO₂ in aqueous solutions of different pH values and their rate increase upon addition of carbonic anhydrase, as well as the formation of carbamates during the reaction of CO₂ with various amines.

Here we report on the photolytically triggered IR difference spectra of the *caged* CO₂ compounds, and the results of *rapid-scan* IR spectroscopy that was employed to monitor the reactions mentioned above.

The ultimate goal of this study will be to use these new tools for the observation of enzymatic carboxylation reactions, namely those carried out by the important class of biotin-dependent carboxylases, and by the most abundant carboxylating enzyme on earth, the plant's Ribulose-1,5-bisphosphatcarboxylase (Rubisco).

Spectrophotometric Studies of the Interaction of Ruthenium with Hesperetin

Krunoslav Vranić, Vlasta Vojković

Laboratory of Analytical Chemistry, Faculty of Science, University of Zagreb, Horvatovac 102a, 10000 Zagreb, Croatia

Hesperetin (5,7,3-trihydroxyl-4-methyl-flavanone) is a kind of flavonoid which occurs ubiquitously in plants, fruits, flowers and foods of plant origin [1]. The interest in the hesperetin is due to its some biological and pharmacological activities, including antioxidant properties [2], inhibition of cancer development [3], etc. Some metal-flavonoides complexes have more antitumor activity [4], so the past few years have seen a remarkable increase in the scientific interest for research of metal-flavonoid complexes. Therefore, in this work, the complexation process of the ruthenium with hesperetin was studied. The investigation was conducted using the spectrophotometric method.

Figure show observation of hesperetin in 50% ethanol aqueous buffer solution (pH 7.5, physiological condition, controlled by phosphate buffer) in absence and presence of Ru(III). In the absorption spectra of hesperetin are absorption band at 328 nm and shoulder at 288 nm. The absorbance value at 328 nm decreased accompanied by the increase of a absorbance at 288 nm and new absorbance around 375 nm gradually with the increase of ruthenium concentration.

The calibration graph is linear in the range from 1 to 8×10^{-5} independent of λ_{\max} used for measurement. The stoichiometric composition of the chelate is Ru(III):hesperetin = 1:1.

According to the obtained results, it can be concluded that the reaction of ruthenium(III) with hesperetin can be applied for the detection of the low Ru(III) concentrations in aqueous solutions. Compared to other methods commonly used for the determination of ruthenium the advantage of present method is that the reaction occurs at room temperature.

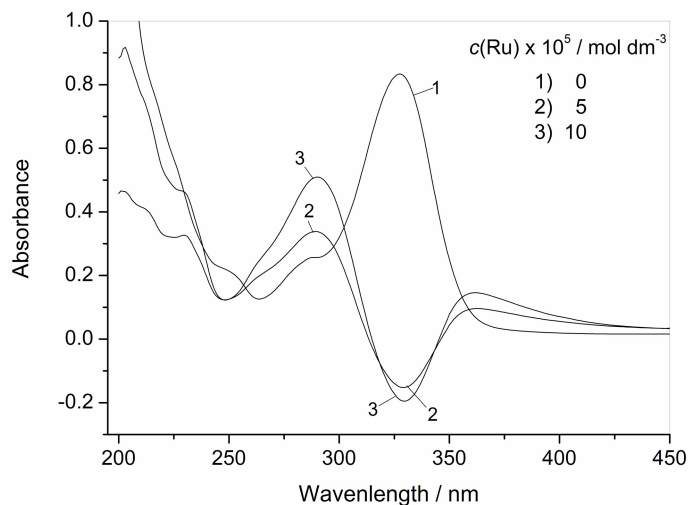


Fig. 1: Electronic absorption spectra of hesperetin in 50 % ethanol in absence (curve 1) and presence of Ru(III) (curves 2,3), at pH 7.5.

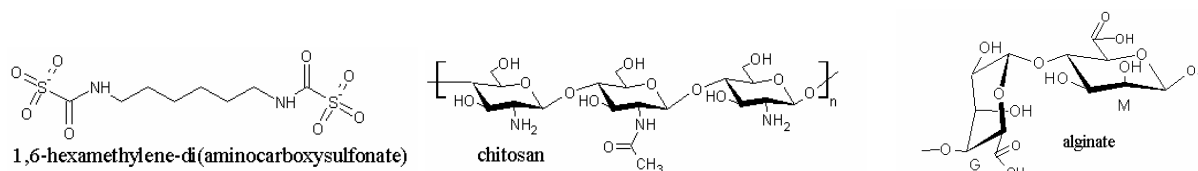
- [1] J.V. Formica, W. Regelson, *Food. Chem. Toxicol.* 33 (1995) 1061–1080.
- [2] M.X. Xie, X.Y. Xu, and Y. D. Wang, *Biochim. Biophys. Acta* 1724 (2005) 215–224.
- [3] A. Hirata, Y. Murakami, Y. Shoji, Y. Kadoma and S. Fujisawa, *Anticancer Res.* 25 (2005) 3367–3374.
- [4] R.M.S. Pereira, N.E.D. Andrades, N. Paulino, A.C.H.F. Sawaya, M.N. Eberlin, M.C. Marcucci, G.M. Favero, E.M. Novak, S.P. Bydlowski, *Molecules* 12 (2007) 1352-1366.

Synthesis, Molecular Structure and Vibrational Spectra of Bioactive Hybrid Materials Composed on Chitosan, Sodium Alginate and 1,6-Hexamethylene-di(aminocarboxysulfonate)

A. Zajac¹, M. Wandas¹, J. Hanuza^{1,2}

¹Department of Bioorganic Chemistry, Institute of Chemistry and Food Technology, Faculty of Engineering and Economics, University of Economics, Komandorska 118/120, 53-345 Wrocław, Poland, ²Institute of Low Temperature and Structure Research, Polish Academy of Sciences, Okólna 2, 50-950 Wrocław, Poland

Bioactive scaffolds are used as biodegradable skeletons inserted into the sites of defective bone for their regeneration. These hybrids can form the ceramics or biopolymers and a number of natural and synthetic materials have been studied for use as scaffolds. Very important direction of these studies is the production of the porous scaffolds made from the natural products, chitosan and alginate [1].



In this study we report synthesis and properties of the scaffold prepared from the chitosan, alginate and 1,6-hexamethylene-di(aminocarboxysulfonate). The thermal and pH conditions have been controlled to obtain the solid product of good microstructure and comprehensive strength. The scanning electron microscopy and mechanical tester have been used to characterise the structure, stability and elasticity of the scaffolds. The formation mechanism of the final product was proposed on the basis of FTIR and FT Raman studies. The changes observed in the spectra during the hybrid formation have been analysed in terms of the possible molecular system produced during syntheses. The chemical quantum calculations with application of the B3LYP/6-311G(2d,2p) basis have been performed to optimise the structure of the substrates and final products. The assignment of the IR and Raman bands to the respective normal modes has been proposed on the results of the DFT calculations. The energy positions of the observed bands have been used in the discussion of the efficiency of cross-linking between the components of the scaffold.

[1] Z. Li, H. R. Ramay, K. D. Hauch, D. Xiao, M. Zhang, *Biomaterials* 26 (2005) 3919 and references therein.

Molecular Spectroscopy in Coke-free Carbon Catalysis

Jian Zhang¹, Andreja Gajović², Dangsheng Su¹, Robert Schlögl¹

¹Department of Inorganic Chemistry, Fritz-Haber Institute of the Max-Planck Society, Berlin, D-14195, Germany

²Molecular Physics Laboratory, Rudjer Boskovic Institute, Bijenicka 54, HR-10002 Zagreb, Croatia

Elemental carbon can catalyze the oxidative dehydrogenation (ODH) of ethylbenzene to styrene, as one of the most important monomers. Compared with the traditional polyvalent metal oxides, carbon-catalyzed ODH reaction is free of coking formation.[1, 2] Herein, we report a combination of molecular spectroscopy (IR, Raman) and electron microscopy (EELS, HRTEM) to identify the coke-free behavior in such a metal-free route.

Nanocarbons (carbon nanotubes, nanodiamonds) can stably catalyze the reaction over a long period of time.[1] After reaction, the used nanocarbons are clean and free of observable coke impurity (Fig. 1a-b), being approved by TPO/EELS results. As revealed in Fig. 1c, major characteristics of nanocarbon remained after a long-time of reaction. No signal corresponding to polymer coke can be found in the infrared spectroscopy of the used sample. To show the unique advantage of nanocarbon, we heated the nanocarbon in a diluted ethylbenzene flow without O₂. As showed in Fig. 1d, the relative ratio of D to G bands ($I_{(D)}/I_{(G)}$) remained almost unchanged, as a direct evidence for the coke-free nature of nanocarbon. Nanocarbon-mediated coke-free ODH represents a significant step to the "green" chemical industries.

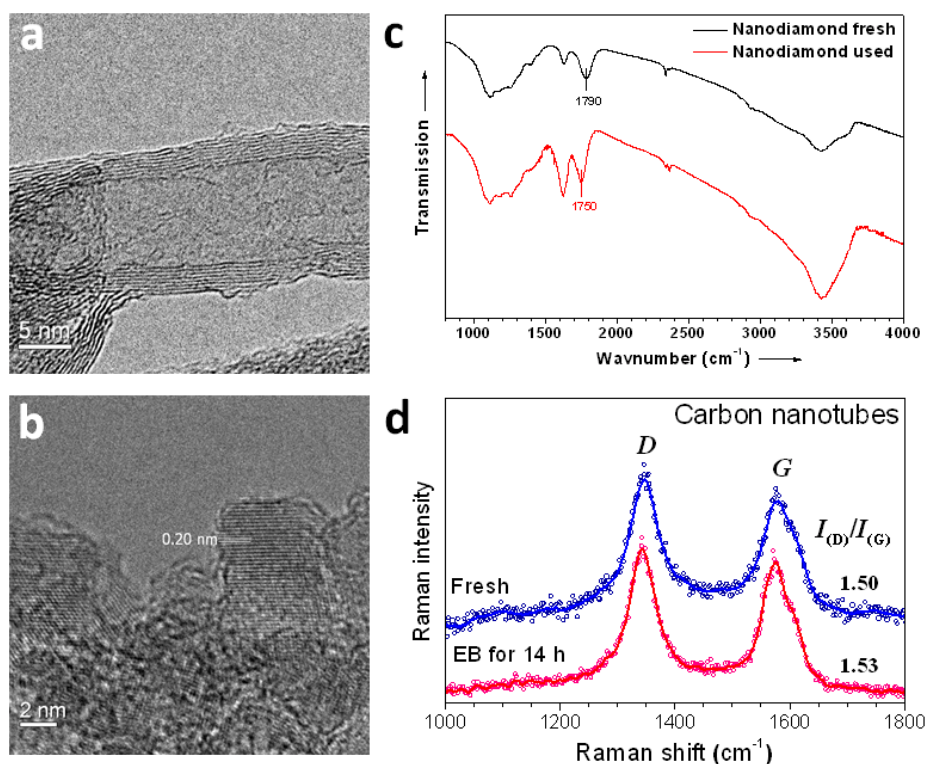


Figure 1: HRTEM images of carbon nanotubes (a) and nanodiamonds (b) after the ODH reaction (2.8% EB, O₂/EB=0.5, $SV_{\text{total}}=150,000 \text{ ml g}^{-1} \text{ h}^{-1}$, 723 K); (c) Infrared spectra of the used nanodiamonds; and, (d) Raman spectra of fresh and used nanotubes after contact with EB for 14 h at 823 K.

- [1] J. Zhang, D.S. Su, A.H. Zhang, D. Wang, R. Schlögl, C. Hébert, *Angew. Chem. Int. Ed.* 46 (2007) 7319-7323.
 [2] D.S. Su, X.W. Chen, X. Liu, J. Delgado, R. Schlögl, A. Gajovic, *Adv. Mater.* in press.

Application of Microspectrometry in Visible Range to Differentiation of Car Solid Paints for Forensic Purposes

B. Trzcińska¹, J. Zięba-Palus¹, P. Kościelniak^{1,2}

¹*Institute of Forensic Research, Westerplatte 9, 31-033 Kraków, Poland*

²*Jagiellonian University, Department of Analytical Chemistry,
ul. R. Ingardena 3, 30-060 Kraków, Poland*

Examination of paint chips found on the car accident place or on victim clothing requires application of optical and spectrometric methods which are non destructive for the sample and provide information about its colour, morphology and chemical composition. Colour is one of the most important characteristics of paint. The determination and comparison of colours are the first step to be taken in forensic investigation. Mikrospectrometers allow an objective measurement of the colour opposed to the subjective results of visual colour comparison. They measure the light energy which is transmitted, absorbed or reflected by a sample at each wavelength of the visible and UV spectrum. As result spectra are obtained and parameters of colour (according to the Commission Internationale de l'Eclairage [CIE] system) are calculated which makes colour comparison of paint samples, much easier [1, 2].

The aim of the paper was to estimate the usefulness of spectral information obtained by Vis microspectrometry in differentiation of small paint coat fragments for criminalistic purposes. The repeatability of the method was also evaluated.

Fragments of red, blue and green solid car paints were chosen for examination. J&M microspectrometer combined to a C. Zeiss Axioplan microscope was used to undertake the measurements in reflectance mode, with Epiplan 50x objective. The spectral range was between 380-780 nm. Samples were measured both, directly on cross section of the paint chip and via the top layer using light beam coming perpendicular to the top surface of the sample. A Tidas program from J&M was used for colour parameters calculation, i.e. tristimulus values, chromacity coordinates and CIELAB units.

It was found that microspectrometry in visible range enabled to distinguish between paint samples of the similar colour and shade but originating from different cars. The results obtained for paint chips measured in cross-section were reproducible. The variation in colour of paint samples measured via top layer was bigger. This seems to be caused by inhomogeneity of paint, defects in top coat originating from weathering process or scratches.

[1] G.J. Chamberlin, D.G. Chamberlin, *Colour, its measurement, computation and application*, Heyden&son Ltd, 1980.

[2] D.R. Cousins, C.R. Platoni, L.W. Russel, *Forens. Sci. Int.* 24 (1984) 183-196.

7. SPECTROSCOPY APPLIED TO ARCHAEOLOGY, ARTS, GEOLOGY AND MINERALOGY

Spectral Characterization of Kolsuz Area (Ulukisla-Nigde) Clays, Central Anatolian Region, Turkey

Burhan Davarcioglu

Department of Physics, Aksaray University, 68100 Aksaray, Turkey

The clay samples taken from Ulukisla-Kolsuz studied area taking place in the northeast part of Nigde province in the Central Anatolian Region-Turkey have been investigated by means of spectroscopic methods. Chemical analyses reveal that the samples chemically consist of SiO₂, TiO₂, Al₂O₃, Fe₂O₃, MnO, MgO, CaO, Na₂O, K₂O, Cr₂O₃ and P₂O₅. DTA (differential thermal analysis) and TGA (thermogravimetric analysis) measurements have been carried out for the determinations of the thermal behaviour of the clay samples.

Firstly, FT-IR (Fourier transform infrared) spectra of the standard clay minerals - "The World Source Clay Minerals" such as illite (IMt-1; Silver Hill, Montana, USA), illite-smectite mixed layer (ISMt-1; Mancos Shale, Ord.), montmorillonite (SCa-3; Otay, San Diego Country California, USA), Ca-montmorillonite (STx; Gonzales Country, Texas, USA), Na-montmorillonite (SWy-1; Crook Country, Wyoming, USA), kaolinite (KGa-1; Washington Country, Georgia, USA), chlorite (ripidolite, CCa-1; Flagstaff Hill, El Dorato Country, California, USA), palygorskite (PFI; Gadsden Country, Florida, USA) were obtained. Then the spectra of anhydrite, gypsum, illite + quartz + feldspar, quartz + feldspar were recorded together with the standard clays. The minerals included in samples taken from Ulukisla-Kolsuz study area were identified by comparing their FT-IR spectra with those of the standard clay minerals and XRD (X-ray diffractometer) analysis results.

The O-H, Al-Al-OH, and Si-O-Si groups in the FT-IR spectrum were detected for the samples belonging to the lower and upper levels of the Ulukisla-Kolsuz stratigraphic field sections (Kk1) and (Kk3) respectively. To see whether any change occur or not in the structure of the clay samples which have been undergone by thermal process, FT-IR spectrum of the sample (Kk1) belonging to the lower level has been taken. The assignments of the vibration frequencies of this spectrum were carried out following the same way applied the spectra of the other samples. In addition, it has been found that Ulukisla-Kolsuz clay samples have included illite, illite-smectite mixed-layer, Na-montmorillonite, chlorite, palygorskite, calcite, feldspar and quartz that silicate has a T-O-T (Tetrahedral-Octahedral-Tetrahedral) smectite structure.

Acknowledgment

This study was fully supported by Turkish Scientific and Technological Research Council (TUBITAK) under project number YDABCAG-2005 (101 Y067).

FT-IR and EDXRF Analysis of Wall Paintings of Ancient Ainos Hagia Sophia Church

S. Akyuz¹, T. Akyuz¹, S. Basaran², I. Kocabas², A. Gulec², H. Cesmeli²

¹*Istanbul Kultur University, Science and Letters Faculty, Physics Department, Atakoy Campus, 34156 Bakirkoy, Istanbul, Turkey*

²*Istanbul University, Letters Faculty, Department of Restoration and Conservation of Artefacts, Vezneciler, 34134, Istanbul, Turkey*

The ancient Ainos was founded at the northern coast of the Aegean Sea and it is one of the most important archaeological sites in Turkey. In this study the wall paintings of ancient Ainos Saint Sophia church were investigated by FT-IR and EDXRF spectroscopy.

The identification of pigments used for archaeological artifacts is important for their restoration, conservation, dating and authentication. The aim of this study is to investigate the chemical composition and manufacture techniques of the wall paintings of ancient Ainos Saint Sophia church dating back to Byzantine age (12. century AC)

Quartz, gypsum and calcite were detected in all the samples. Feldspar phases were inferred from the second derivative profiles of the IR spectra. Black, dark brown and red coloration was due to different concentrations of MnO₂, magnetite and haematite. In the case of black samples, calcium phosphate bands were also observed.



Fig. 1: Ancient Ainos Hagia Sophia Church.

Application of Molecular Spectroscopy to Study the Composition of Prehistoric Pigments from Excavations (Argentina)

L. Darchuk^{1,2}, Z. Tsybriy², E.A. Stefaniak^{1,3}, C. Vazquez^{4,5}, O.M. Palacios⁶, A. Worobiec¹, F. Sizov², and Rene Van Grieken¹

¹*Department of Chemistry, University of Antwerp, Belgium, Universiteitsplein 1, Antwerp, BE-2610, Belgium*

²*Department of IR Devices, Institute of Semiconductor Physics, NASU, Kyiv, Ukraine*

³*Department of Chemistry, Catholic University of Lublin, Poland*

⁴*Department of Chemistry, Buenos Aires University, Argentina*

⁵*Department of Chemistry, Atomic Energy Commission, Buenos Aires, Argentina,*

⁶*CONICET-CIAFIC group, Buenos Aires University, Argentina*

e-mail: Larisa.Darchuk@ua.ac.be

Determination of prehistoric pigments composition was performed by two molecular spectroscopy methods – infrared (IR) and micro-Raman spectrometry (MRS). Infrared spectra were obtained by IR spectrometer Spectrum BX-II (Perkin Elmer). Raman spectrometric measurements were carried out by Renishaw InVia micro-Raman spectrometer with laser excitation at 785 nm.

The objects of investigation were pre-historic pigments from Carriqueo rock shelter (North Patagonia, Argentina). The pigment samples of orange, red and brown shades were collected from archaeological sites.

Usually the natural yellow, orange or red pigments, composed of yellow and red ochres are frequently detected in prehistoric pigments. The main components of ochre are iron (hydro)oxide (haematite or goethite), clay and silica.

Several yellowish, reddish and red-brown pigments demonstrated Raman spectra corresponding to haematite, goethite, gypsum, quartz, oxalates. In some cases huge fluorescence caused by the presence of clay in the pigments disturbed the Raman signal to such an extent that made it not informative. Therefore we used infrared spectrometry to analyse their composition. A thin layer of the pigments was put on BaF₂ substrate and IR absorption was measured. For reddish pigments, we detected absorption bands typical for natural red earth, consisting of iron oxides in hydrated and anhydrous forms. Yellowish pigments consist of amber yellow (a kind of yellow ochre) and satin ochre as main components. Green pigment was recognized as green earth by typical absorption bands.

Towards a Surface-Enhanced Raman Spectra Database of Dyed Textiles

E. del Puerto¹, Z. Jurasekova¹, S. Sánchez-Cortés¹, J.V. García-Ramos¹,
C. Domingo¹, A. Roquero²

¹*Instituto de Estructura de la Materia, CSIC, Serrano 121, 28006 Madrid Spain*

²*Arias Montano 18, 28007 Madrid, Spain*

Historical textiles are a very important type of Cultural Heritage objects, and the correct identification of the organic dyes employed in their fabrication is a real challenge for conservators. The currently analytical methods employed involve chromatography, hence sampling, hence destructiveness. They require taking out some milligrams from the textile, which are afterwards subject to chemical extraction procedures, before carrying out a subsequent HPLC analysis. Then, non-destructive (or micro-destructive) methods would be highly welcome.

Raman spectroscopy has proved to be a very useful non-destructive technique for identification of inorganic materials related to Cultural Heritage. Nevertheless, it is not appropriated for organic dyes, as their own fluorescence normally prevent from taking Raman spectra. Besides, only minute quantities are employed for dyeing the textiles, and the low sensibility of the Raman spectroscopy is unable to detect them. Both drawbacks are overcome when Surface-enhanced Raman Scattering (SERS) is employed.

In this sense, our group has recently reported [1] a new method of production of silver nanoparticles *in situ*, through photoreduction of Ag⁺, to be employed for taking SERS spectra. Applying such method, we have been able to record SERS spectra corresponding to flavonoids molecules (luteolin and apigenin) on silk and wool samples dyed with weld (*Reseda luteola* L.) [2]. For such successful experiment we have only employed a 10 millimetres-long thread taken from the corresponding textiles, and “micro-destroying” only 50 microns of it, where silver nanoparticles are deposited. SERS spectra were recorded from the same 50 microns region. Such reference samples were prepared according old dyeing recipes, for carrying out a pilot study in the frame of the Eu-ARTECH project [3], where HPLC and fluorescence analysis have been performed at different European laboratories.

Employing the same protocol than mentioned above, we are presently carrying out SERS measurements on a unique collection of standards of textiles dyed with natural plants, following original pre-columbian recipes still in use in the central Andean region [4]. The objective is to build up a SERS database of dyed textiles, identifying organic dyes as they really are in the textiles, without pre-treatment of samples. Such library could constitute a useful tool for conservation of historical dyed textiles.

[1] M.V. Cañamares, J.V. García-Ramos, J.D. Gómez-Varga, C. Domingo, S. Sánchez-Cortés, *Langmuir* 23 (2007) 5210-5215.

[2] Z. Jurasekova, C. Domingo, J. V. García-Ramos, S. Sánchez-Cortés, submitted to *J. Raman Spect.*

[3] Eu-ARTECH project (FP6-RII3-CT-2004-506171, 2004-2008), <http://www.eu-artech.org>

[4] *Tintes y tintoreros de América: catálogo de materias primas y registro etnográfico de México, Centro América, Andes Centrales y Selva amazónica*, A. Roquero, Ministerio de Cultura de España, Madrid (2006), ISBN: 848181282X

Acknowledgments

This work has been partially supported by the Ministerio de Educación y Ciencia of Spain (Project FIS2007-63065) and Comunidad de Madrid (S-0505/TIC/0191 MICROSERES). Z.J. acknowledges the European Community's Sixth Framework Programme for Marie Curie Early Stage Research Training Fellowship (Contract MEST-CT-2004-513915). E.d.P. acknowledges CSIC for a JAE-CSIC predoctoral grant.

Comparison between Two Molecular Spectroscopy Techniques as Analytical Tools in the Characterization of Pigments in Southern Spain Cultural Heritage: Micro Raman and Micro-FTIR Spectroscopy

M.L. Franquelo¹, A. Duran^{1,2}, L.K. Herrera¹, M.C. Jimenez de Haro¹, J.L. Perez-Rodriguez¹

¹ *Materials Science Institute of Seville (CSIC-Seville University). c/ Americo Vespucio, 49. 41092 Seville, Spain*

² *Centre de Recherche et de restauration des musées de France –CNRS UMR 171, Palais du Louvre, Porte des Lions, 14 Quai François Mitterrand, 75001 Paris, France*

A general overview about the complementary use of two techniques of molecular spectroscopy in the study of Cultural Heritage is described in this work: micro FT-IR and micro FT-Raman spectroscopy.

Both of them share a series of advantages such as the sensitiveness or spatial refinement (by the incorporation of the microscope); nevertheless, the greater specificity or the possibility of non-destructive (by means of an optical fiber) and on site analysis (by means of a portable equipment) make the Raman spectroscopy a very suitable and powerful technique in Cultural Heritage studies.

On the other hand, Raman spectra are more easily obtained, however difficulties may arise through the scattered signal being obliterated through filters.

A variety of pigments in samples belonging to the Cultural Heritage of Southern Spain are characterized by micro Raman spectroscopy using visible excitation sources and micro FT-IR spectroscopy. Some of the pigments studied comprise blue (azurite, ultramarine blue, Prussian blue), red (vermilion, haematite, red ochre, red lakes), green (copper resinate, verdigris, chromium (III) oxide), orange (realgar), yellow (lead-tin yellow) and white pigments (calcite, gypsum, white lead, titanium white, zinc white, barite, lithopone) among others. A protocol is established for their appropriate characterization.

Some samples have been prepared using the cross-section technique, what involves obviously a destructive study but the total number of samples taken diminishes noticeably due to the combined on site study of the artwork. This technique of preparation provides a wide variety of information: it discloses the stratigraphic succession of the layers in the painting and permits an exact localization of the identified pigment grains. It allows the examination of a quite large portion of a single paint layer in its original condition avoiding any further manipulation. Additionally, the same cross-section sample can be characterized by other techniques of analysis such as energy dispersive X-rays microanalysis coupled to the scanning electron microscopy (SEM-EDX).

Of course, the possibilities of Raman and FT-IR spectroscopies are greatly enhanced if they are used in conjunction with an elementary microanalysis by SEM-EDX. Characterization by micro FT-IR and micro Raman presents difficulties with some pigments. In these cases, analysis by EDX solves most of these arising doubts.

We can conclude that the combined use of both spectroscopic techniques, micro FT-IR and micro Raman together with the SEM-EDX microanalysis, provides a useful method in the characterization (and possible dating) of materials used in Cultural Heritage.

Raman Spectra and Luminescence of the Minerals with Aeschnite and Euxenite Crystal Structure

N. Tomašić¹, A. Gajović², V. Bermanec¹

¹*Institute of Mineralogy and Petrography, Faculty of Science, University of Zagreb, Horvatovac bb, HR-10000 Zagreb, Croatia*

²*Ruder Bošković Institute, POB 180, HR-10002 Zagreb, Croatia, e-mail: gajovic@irb.hr*

Metamict minerals aeschnite-(Y) and polycrase-(Y) showed aeschnite and euxenite structure after recrystallization, respectively. Raman spectra of these minerals show luminescence lines strongly interfering with normal vibration modes (Fig. 1), especially in 200-500 cm^{-1} range (region of Ti/Nb/Ta-O stretching and bending modes). However, their synthetic analogs of REETiTaO₆ composition having single REE content and aeschnite or euxenite structure do not show luminescence lines using 488 and 514.5 nm Ar excitation lines up to 900 cm^{-1} with exception of the Er member [1]. In the case of polycrase-(Y) a separated strong luminescence line is also observed at 684 cm^{-1} . The origin of luminescence in these minerals is discussed in term of the complex REE composition, the crystal field formed in the structure during recrystallization process and its influence on REE in cation sites.

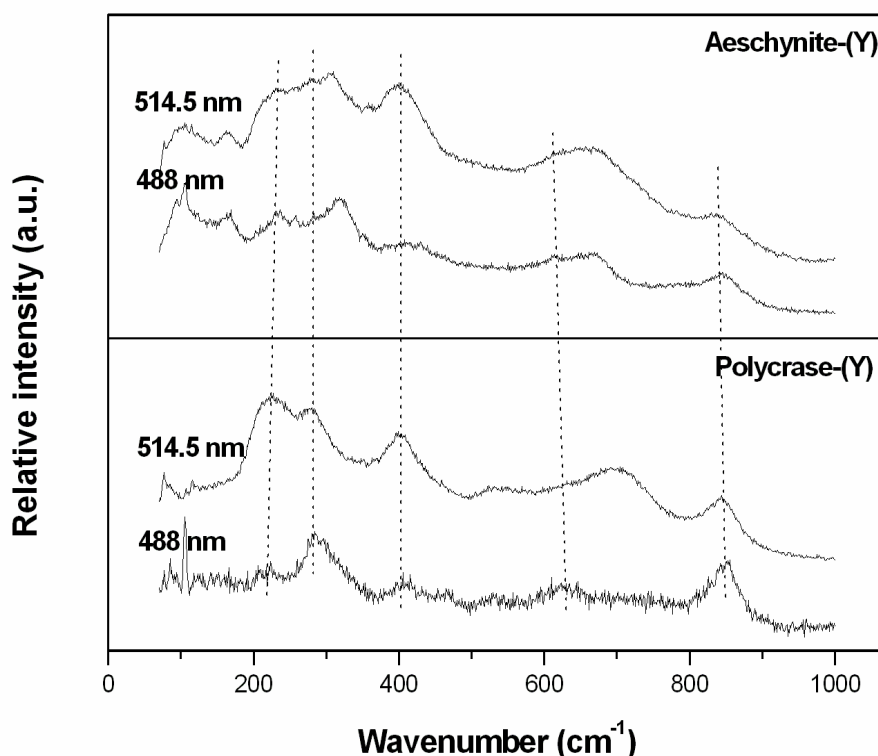


Fig. 1: Raman spectra of aeschnite-(Y) and polycrase-(Y) excited by 488 and 514.5 nm Ar line. Dashed lines indicate the position of Raman modes common for aeschnite and euxenite structure.

[1] C.W.A. Paschoal, R.L. Moreira, C. Fantini, M.A. Pimenta, K.P. Surendran, M.T. Sebastian, J. Eur. Ceram. Soc. 23 (2003) 2661.

Expert Systems Built for the Modeling of Small Molecular Structures Using a Concatenated Spectral Database

S. Gosav¹, M. Praisler¹, D.O. Dorohoi²

¹Department of Physics, "Dunărea de Jos" University, 111 Domneasca St, 800201 Galati, Romania

²Faculty of Physics, "Al.I.Cuza" University, 11 Carol I Bdv, RO 700506, Iași, Romania

e-mail: sgosav@ugal.ro

Gas chromatography-Fourier transform infrared spectrometry (GC-FTIR) and gas chromatography-mass spectrometry (GC-MS) are the two of the most powerful techniques applied for the identification of volatile compounds. GC-FTIR spectra are used for the characterization and identification of compounds because of their remarkable selectivity: especially in the case of small molecules, even a small change in the molecular structure yields significant changes in the form of the spectrum. The utility of GC-MS arises from their sensitivity: the ionization process generally produces a family of particles whose mass distribution is a characteristic of the parent species.

In this paper we are presenting an expert system built for the identification of small molecular structures by using a hybrid spectral database, formed by concatenating the GC-FTIR and GC-MS spectra of three classes of compounds. The expert system was built using Artificial Neural Networks (ANN) and is dedicated to predict the class identity of the modelled compounds. The advantages and limitations of using a hybrid GC-FTIR - GC-MS spectral database are discussed by analysing the performances of the expert system with those obtained for ANN systems built with homogenous databases characterising the same compounds, i.e a GC-FTIR – based expert system and a GC-MS – based expert system.

Optimisation of the Performances of a Hybrid Expert System Designed for the Elucidation of Molecular Structures

S. Gosav, M. Praisler

*Department of Physics, "Dunărea de Jos" University, 111 Domneasca St, 800201 Galati, Romania
e-mail: sgosav@ugal.ro*

An expert system designed for the structure elucidation of volatile compounds having small molecular structures has been built by using a hybrid spectral database, formed by concatenating the GC-FTIR spectra with the GC-MS spectra of the molecules, in the attempt to benefit from both the selectivity of the infrared spectra and of the sensitivity of the mass spectra. On the other hand, characterizing each sample by such a hybrid spectrum has the disadvantage of decreasing the ratio between the number of samples and the number of input variables. In many cases, the number of samples included in the training, test, or validation set cannot be increased, simply because the number of compounds forming the class of substances to be modeled is limited to a relatively small number of analogues. In this case, the challenge in enhancing the performances of the expert system by optimizing the sample/variable ratio is to find efficient selection criteria, which would allow the reduction of the number of input variables without losing the relevant information. In other words, these criteria should allow us to eliminate *only* the redundant information and to maintain into the system (as much as possible) the spectral information needed to obtain a good modeling power.

In this paper we are analyzing two such criteria, i.e. the importance and the sensitivity of the input variables. The advantages and disadvantages of each of these two criteria are also analyzed by comparing the performances of the optimized expert system with those obtained when applied for expert systems built with homogenous spectral data-bases (containing only GC-FTIR or only GC-MS data).

Minerals from Macedonia. XXIV. Spectroscopic and Structural Characterization of Tectosilicates

P. Makreski¹, G. Jovanovski^{1,2}, B. Kaitner³

¹*Institute of Chemistry, Faculty of Science, SS. Cyril and Methodius University, Arhimedova 5, 1000 Skopje, Republic of Macedonia,*

²*Macedonian Academy of Sciences and Arts, Bul. Krste Misirkov 2, 1000 Skopje, Republic of Macedonia*

³*Department of Chemistry, Faculty of Science, Horvatovac 102a, 10000 Zagreb, Croatia*

Continuing the process of systematic spectra-structural studies on the silicate minerals originating from Macedonia [1–6], several representatives from the feldspar species: albite, $\text{NaAlSi}_3\text{O}_8$; microcline, KAlSi_3O_8 ; sanidine, KAlSi_3O_8 ; orthoclase, KAlSi_3O_8 were studied by vibrational spectroscopy and powder X-ray diffraction. Despite the common structural characteristics it was shown that IR ($1300\text{--}370\text{ cm}^{-1}$) and particularly Raman spectroscopy ($1300\text{--}100\text{ cm}^{-1}$) could clearly discriminate between sanidine, albite and orthoclase/microcline. However, since both latter minerals show practically identical IR as well as nearly identical Raman spectra their discrimination and identification was based on the corresponding powder X-ray diagrams. In addition, an attempt to interpret the powder vibrational spectra of rare-occurring zeolite mineral – stilbite-Na, $(\text{NaCa}_2\text{Al}_5\text{Si}_{13}\text{O}_{36}\cdot 14\text{H}_2\text{O})$ was undertaken. The chemical formulas are written according to the results from the X-ray microprobe analysis.

- [1] P. Makreski, G. Jovanovski, S. Stojančeska, *J. Mol. Struct.* 744–747 (2005) 79–92.
- [2] P. Makreski, G. Jovanovski, *J. Raman Spectrosc.* (accepted for publication).
- [3] P. Makreski, G. Jovanovski, B. Kaitner, A. Gajović, T. Biljan, *Vib. Spectrosc.* 44 (2007) 162–170.
- [4] P. Makreski, G. Jovanovski, A. Gajović, *Vib. Spectrosc.* 40 (2006) 98–109.
- [5] P. Makreski, G. Jovanovski, A. Gajović, T. Biljan, D. Angelovski, R. Jaćimović, *J. Mol. Struct.* 788 (2006) 102–114.
- [6] V. Šontevska, G. Jovanovski, P. Makreski, *J. Mol. Struct.* 834–836 (2007) 318–327.

Combined Fluorescence-LIBS and Raman Spectroscopy Setup for Applications in the Field of Cultural Heritage

N.F.C. Mendes¹, I. Osticioli¹, C. Lofrumento¹, A. Zoppi¹, E.M. Castellucci^{1,2}

¹*Department of Chemistry, University of Florence, Polo Scientifico e Tecnologico, via della Lastruccia 3, I-50019, Sesto Fiorentino (FI), Italy*

²*European Laboratory for Non-Linear Spectroscopy (LENS), via Nello Carrara 1, 50019, SestoFiorentino (FI), Italy*

Raman spectroscopy has wide ranging applications for the non-destructive analysis of art and is commonly used for the identification of pigments. Many advantages are provided by this technique in terms of specificity, resolution and sensitivity. In addition, Raman spectroscopy which gives molecular information, can be usefully combined with complementary laser techniques (LIBS) using the same source at different fluences to provide atomic information regarding the composition of materials. Furthermore, by using a laser emission in the UV region at 266 nm it is possible to perform Fluorescence studies of many of the organic materials used by the artists during the creation of the works of art. Organic pigments (dyes), binding media (glues and dairy) and varnishes have indeed chromophores excitable at 266 nm giving intense and different Fluorescence spectra.

This setup for Raman-LIBS and Fluorescence experiments was mounted using the same Nd:YAG pulsed laser, allowing a rapid switch from one technique to the other simply by changing laser wavelength together with the intensity and by inserting or removing the notch filter needed in the Raman mode. For LIBS and Raman experiments the 2nd harmonic emission at 532 nm was used; for Fluorescence studies the UV emission was used.

The purpose of this instrument is to perform fast and reliable analysis of artistic materials with minimum damage done to the samples. The instrument allows time-resolved acquisition which has been used to discriminate Raman signal from background radiation or luminescence contributions, this is of particular interest for measurements done in outdoor environments and to study problematic fluorescent samples.

FTIR and INS Study of Lower Palaeolithic Burned Animal Bones from Vértesszőlős (Hungary)

J. Mihály¹, J. Mink¹, V.T. Dobosi², S.F. Parker³, J. Tomkinson³

¹Chemical Research Center, Hungarian Academy of Sciences, H-1525, Budapest, P.O. Box 17, Hungary,

e-mail: mihaly@chemres.hu; ²Hungarian National Museum, H-1370 Budapest P.O. Box 364

³ISIS Facility, The Rutherford Appleton Laboratory, Chilton, OX11 0QX, UK

The discovery of the Lower Palaeolithic site Vértesszőlős (Hungary) in the 1960s excelled among contemporary finds by various features; i.e., presence of human remains, multiple habitation layers, abundant scientific evidence and last but not least, the presence of fire at a site dated to the second glaciation period (Mindel) [1]. Traces of fire were observed in the form of hearths with radially arrayed, broken long bones (3-5 cm) with visible proofs of burning: intensive black colour.

Archaeological bone samples of burned and unburned appearance from Vértesszőlős excavation were analysed by Fourier transform infrared spectroscopic (FTIR) technique and inelastic neutron spectroscopy (INS) and compared with results of modern bones.

In the FTIR spectrum of bone with the most burned appearance, compared to that of unburned sample, an extra band at 1050 cm⁻¹ (shoulder) starts to grow up. After oven experiment of fresh bone (heated up to 600 °C) a well defined splitting at 1047 and 1038 cm⁻¹ also occurs, presumably due to apatite transformation. The relative intensities of 1102/1043 cm⁻¹ and 604/565 cm⁻¹ are also changed. Crystallinity index (CI) calculation based on FTIR measurements revealed, however, that burnt bones have a lower CI value compared to the 'unburned' one [2].

INS spectra are particularly sensitive to groups associated with hydrogen and relatively insensitive to phosphate and carbonate in bone. No significant difference between spectra of 'burned' and 'unburned' bone samples with near CI values were detected indicating no difference in -OH substitution. However, changes in the phosphate lattice mode vibrations and in the baseline level of the burned bone with the lowest CI value was observed. Detailed FTIR imaging study on the latter sample revealed indeed some traces of degraded humic acid on the bone surface.

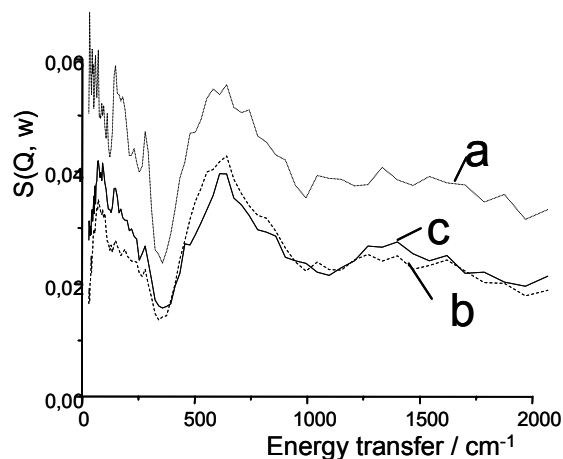


Fig. 1: INS spectra of: 'burned' bone sample with lowest CI (a), 'burned' (b) and 'unburned' (c) bone samples.

[1] M.Kretzoi, V.Dobosi: *Vértesszőlős, Man, Site and Culture*. Budapest, Akadémiai Kiadó 1990.

[2] J.Mihály, J.Mink and L.Hajba, *Archaeometry Workshop*, 2006/3, (URN: urn:nbn:hu-4106, URL:<http://www.ace.hu/am>).

Acknowledgement

The authors gratefully acknowledge financial support from the Hungarian Research Council (OTKA K-61611). J. Mihály thanks for EU funding within NMI3 programme (FP6 EU framework) for performing INS experiment at TOSCA, ISIS Facility.

Vibrational Spectra of β -Cage Units in Different Silicate Structures

W. Mozgawa, W. Jastrzębski

*Faculty of Materials Science and Ceramics, AGH University of Science and Technology
Al. Mickiewicza 30, Kraków, POLAND
e-mail: mozgawa@agh.edu.pl*

This work presents spectroscopic studies of pseudomolecules equivalent to β -cage (sodalite cage) which occur in various aluminosilicate structures. This cage is one of the fundamental structural units occurring in frameworks of zeolites. Studies were carried out for model units in which the K^+ ions were used as terminal charge-compensating cations. The units constituted fragments of structure equivalent to the “isolated” sodalite cage and cages binded with 4- and 6-membered rings. Ab initio calculations were performed using HF method and 6-31dG basis set of functions. As a result of calculations, vibrational spectra and visualizations of individual normal vibrations of the units were obtained. Selection of the calculation method was supported by the analysis of this method influence and the basis set on quality of the findings and time of calculation. The analysis was conducted for $Si_2O(CH_3)_6$ pseudomolecule (siloxane Si-O-Si bridge).

Visualizations of the obtained normal vibrations permitted to identify vibrations characteristic for individual units (especially, the ring vibrations) and to assign them to appropriate bands in the spectra.

The results were compared with those obtained for analogous units containing Al substituted of for Si in tetrahedral positions.

Then the results of the model studies were used to describe experimental vibrational spectra of aluminosilicates (sodalite, LTA and FAU zeolites) containing the units analogous to the model pseudomolecules in their framework.

Application of IR Spectra in the Studies Heavy Metal Cations Immobilization on Natural Sorbents

W. Mozgawa, M. Król

*Faculty of Materials Science and Ceramics, AGH University of Science and Technology
Al. Mickiewicza 30, Kraków, POLAND
e-mail: mozgawa@agh.edu.pl*

This work presents the results of FT-IR spectroscopic studies (MIR) of heavy metal cations (Pb^{2+} , Cd^{2+} , Ag^+ and Cr^{3+}) immobilization from aqueous solutions on various forms of natural sorbents. The sorption has been conducted on natural clinoptilolite-montmorillonite mudstone and on its major components which have been separated from this deposit, i.e. on zeolite and smectite (on their sodium forms).

Based on changes in the spectra due to the immobilization of heavy metal ions, a scale of the sorption and a kind of mechanism in the process (ion exchange and/or chemisorption) can be established. Changes in intensities and positions of the bands corresponding to the characteristic ring vibrations have been observed. These rings occur in pseudomolecular complexes 4-4=1 (built of alumino- and silico-oxygen tetrahedra) which constitute the secondary building units (SBU) and form spatial framework of the zeolite. The most significant changes have been determined in the region of pseudolattice vibrations ($650\text{-}700\text{ cm}^{-1}$). On the other hand, introduction of heavy metal cations into the structure of motmorillonite has caused the modification of band intensities due to stretching vibrations of OH^- groups. In both cases, systematic changes connected with the type of cation (its chemical character) and its concentration in the initial solution have been revealed.

Results of IR-spectroscopic studies have been compared with those obtained by atomic absorption spectroscopy (AAS), from which the proportion of ion exchange to chemisorption in the process and the effective cation exchange capacity of the individual samples have been estimated.

The FTIR Studies of Influence of Different Al₂O₃ and SiO₂ Precursors on Structure of Alumina-Silica Gels and Coatings

A. Adamczyk, W. Mozgawa, M. Handke, E. Długoń, A. Ferensowicz

Faculty of Materials Science and Ceramics, AGH University of Science and Technology,

Al. Mickiewicza 30, Kraków, POLAND

e-mail: aadamcz@agh.edu.pl

The alumina-silica materials were obtained by sol-gel method, using different Al₂O₃ and SiO₂ precursors, what allowed to prepare sols based on water and organic solvents. As SiO₂ precursors, Aerosil 200™ and tetraethoxysilan (TEOS) were chosen, while Disperal™ and aluminium secondary butoxide were used for Al₂O₃ ones. The final suspensions, corresponding to the mullite composition, were prepared by mixing different type sols, based on given above precursors. To obtain bulk samples, gels were then heated in air up to 1150 °C.

The alumina-silica materials were also synthesized as coatings on carbon and steel substrates. The films were deposited by dipping and pulling out the substrates from the sol with a constant speed. Samples obtained in this way were then heated in air (steel) and argon or air (carbon) at 800 °C and 500 °C, respectively.

The FTIR and XRD measurements were taken for the bulk samples annealed at different temperatures to observe the crystallisation and phase transformation processes. The coatings were studied by FTIR spectroscopy (after final annealing) and by XRD diffraction, also using GID configuration.

The comparison of the FTIR spectra of bulk samples and the spectra of pure Disperal™, at the same temperatures annealed, enables to observe the presence of γ -Al₂O₃ and δ -Al₂O₃ in both materials. It is confirmed by the vibrations characteristic for bonds occurring in these phases structure, in the range of 400-900 cm⁻¹, especially bands at about 570 cm⁻¹ and 835 cm⁻¹. In some bulk samples one can also observe the formation of mullite phase, what was confirm by FTIR spectra and XRD measurements. The same phases (γ -Al₂O₃ and δ -Al₂O) are observed in coatings, but the presence of particular ones strongly depends on type of Al₂O₃ and SiO₂ precursors and temperatures of heating. Generally, films synthesized with Disperal™ and Aerosil™ (or TEOS) water and organic solutions, were more crystallized than those based on aluminium secondary butoxide, what was also confirmed by XRD measurements.

The IR Spectroscopy Studies of Alkaline Activated Slag Geopolymers

W. Mozgawa, J. Deja

*Faculty of Materials Science and Ceramics, AGH University of Science and Technology,
Al. Mickiewicza 30, Kraków, POLAND
e-mail: aadamcz@agh.edu.pl*

The geopolymers are considered to be a group of modern aluminosilicate materials of compositions and properties which allow to apply them in many technologies. The possibility of applications of them as alternate binding materials instead of Portland cement occurs to be the most significant fact. In this work, the results of structural studies of different geopolymers, obtained by use of a granulated blast furnace slag, are presented. Slag was subjected to an alkaline activation process. As activators, NaOH, Na₂CO₃ and liquid glass were applied.

As a main investigating method, the IR spectroscopy was used, the results obtained were then compared with the NMR (²⁹Si i ²⁷Al MAS NMR) measurements, the XRD phase analysis and the SEM observations.

In the IR spectra of raw slag as well as in the spectra of products of paste and mortar hydration, bands due to the vibrations characteristic of bonds observed in both types of oxygen bridges: Si-O-Si and Si-O-Al, were assigned. Those bridges make basic structural units, creating then tetrahedral geopolymer chains. It was found, that the slag composition, first of all SiO₂/Al₂O₃ ratio and modifying oxides concentration, influences on the presence of the bands connected with the phases (C-S-H and zeolites, mainly) formed during the hydration, in the IR spectra. Additionally, it was found the essential influence of phases amorphous degree on the spectra shape. It is pointed by the parameters of the component bands, forming the complicated envelopes, during the decomposition process determined.

On the ground of the IR spectra, it was also possible to determine the influence of an activator type, an activation time and hydration conditions, on the products formed. The essential changes were observed for the bands assigned to carbonate and hydroxide groups vibrations. The changes were also noticed in case of bands due to the vibrations of silicate and aluminosilicate bonds vibrations.

Acknowledgment

Financial support for this work was provided by Polish Ministry of Science and Higher Education under special grant HISZPANIA/115/2006.

Study of the Dehydroxylation-Rehydroxylation of Pyrophyllite by Spectrometric and Thermal Analysis Methods

L.A. Pérez-Maqueda¹, A. Duran^{1,2}, P.E. Sánchez Jiménez¹, M.L. Franquelo¹,
J.L. Perez-Rodriguez¹

¹ *Materials Science Institute of Seville (Consejo Superior de Investigaciones Científicas – Universidad de Sevilla). c/ Americo Vespucio, 49, 41092 Seville, Spain.*

² *Centre de Recherche et de restauration des musées de France – CNRS UMR 171, Palais du Louvre, Porte des Lions, 14 Quai François Mitterrand, 75001 Paris, France*

Pyrophyllite is a 2:1 aluminosilicate [Al₂Si₄O₁₀ (OH)₂] clay that has a dioctahedral layer structure with an octahedrally coordinate Al ions sheet in-between two sheets of SiO₄ tetrahedra. The applications of pyrophyllite are due to its good technological properties produced by thermal treatment. Thus, it has been mainly used as a ceramic raw material in refractory industry for applications such as insulating firebrick or foundry specialities and also in various white-ware bodies.

The investigation of the dehydroxylation reaction of clay minerals is important both from theoretical and technical aspects. The dehydroxylation of pyrophyllite has been described as a homogeneous process involving reaction of two cis-OH group with the liberation of water. It has been suggested that the pyrophyllite dehydroxylate consists of 5-coordinate, distorted, trigonal bipyramidal AlO₅ structural units in the aluminium oxide layer sandwiched between two distorted tetrahedral silica layers. ²⁷Al NMR-MAS studies have shown the 6 coordinated Al in pyrophyllite change their structural arrangement to 5 coordinate Al in pyrophyllite dehydroxylated. ²⁹Si MAS-NMR data have confirmed that pyrophyllite dehydroxylate maintains the 2:1 layer structure. The formation of 5-coordinate aluminium sites in pyrophyllite dehydroxylate is consistent with the homogeneous reaction of the adjacent OH groups to liberate water and the formation of a bridging oxide midway between adjacent aluminium atoms. Recently, the dehydroxylation of pyrophyllite has been studied using infrared spectroscopy [1]. Thus, it has been found that the dehydroxylation process is characterized by a decrease in the intensity of the OH signals and phonon bands of pyrophyllite as well as the appearance of two additional signals at 3690 and 3702 cm⁻¹ for samples annealed in the temperature range from 550 to 900 °C. These authors suggested that the dehydroxylation of pyrophyllite is a two-stage process, appearing an unknown intermediate state during the dehydroxylation of pyrophyllite. In this work we have studied the dehydroxylation of pyrophyllite using spectrometric and thermal analysis experimental methods to clarify the mechanism of dehydroxylation, and the possible rehydroxylation, of pyrophyllite.

[1] L. Wang, M. Zheng, S.A.T. Redfern and Z. Zhang, *Clays and Clay Minerals* 50 (2002) 272-283.

Chemical and Spectroscopic Characterization of Some Phosphates Accessory Minerals from Pegmatites of the Sowie Mts (Owles Mts), SW Poland

M. Łodziński¹, M. Sitarz²

¹*Faculty of Geology Geophysics and Environmental Protection;*

²*Faculty of Materials Science and Ceramics;*

AGH University of Science and Technology, Al. Mickiewicza 30, 30-059 Kraków, Poland

Phosphate accessory minerals were found in pegmatite veins and lenses around 15 meters long in Michałkowa near Walim in Sowie Mts gneissic block, Lower Silesia, SW Poland. Pegmatites intersect paragneisses and migmatites and composed mostly of plagioclase, albite, quartz, biotite, chlorites, phosphate minerals and pyrite.

The main primary phosphate aggregates in pegmatite in Michałkowa consist of sarcopside ($\text{Fe}^{2+}, \text{Mn}^{2+}, \text{Mg}$)₃(PO_4)₂ and graftonite ($\text{Fe}^{2+}, \text{Mn}^{2+}, \text{Ca}$)₃(PO_4)₂. The biggest euhedral crystals of sarcopside and graftonite reach up to 2.5 cm in length. Both minerals often contain regularly oriented assemblage of smaller (few to 100 micrometers in diameter) primary and secondary phosphates inclusions of allaudite, apatite, ferrisicklerite, ferroallaudite, ferrowyllieite, hagendorffite, heterosite, kryzhanovskite, maghagendorffite, phosphoferrite, qingheite?, rosemaryite, simferite?, wolfeite and wyllieite. Some minerals are difficult to identify because are strongly altered, oxidized and hydratized.

Samples were investigated in thin sections by means of an OLYMPUS BX-51 polarization microscope in reflected and transmitted light. Chemical composition of samples were analysed by CAMECA SX 100 electron microprobe in the wave-length mode.

Chemical composition of sarcopside vary from grain to grain e.g.: contain 41.23–42.07 wt% of P_2O_5 , 41.45–42.02 wt% of FeO, 10.98–12.78 wt% of MnO, 4.12–5.33 wt% of MgO and traces of F, S and Ca, but are present also variety richer in FeO (up to 43.30 wt%) and MnO (up to 13.67 wt%) and poor in MgO (up to 2.37 wt%). Graftonite also differ in content of FeO, MnO and CaO with average composition: 41.34–41.73 wt% of P_2O_5 , 25.28–27.75 wt% of FeO, 20.44–21.96 wt% of MnO, 8.35–9.95 wt% of CaO, 1.46–1.63 wt% of MgO and traces of F, S and Na.

IR spectroscopic measurements were carried out using a Bio-Rad FTS 60 V and Bio-Rad FTS 165 spectrometers. Monocrystals were studied using Raman micro-spectrometer T-64000 Jobin-Yvon equipped with confocal microscope (OLYMPUS).

Good formed, original crystals of graftonite and sarcopside were selected to the MIR analysis. On the MIR and Raman spectra we can't observe any bands connected with H_2O and OH^- groups. The results confirm that the selected crystals didn't become the alteration process. The previous spectroscopic analysis of isolated $[\text{PO}_4]^{3-}$ tetrahedrons allowed the precise assignation of bands to the corresponding vibration type. The influence of non-tetrahedral cations on the shape of the spectra and the positions of bands has been analysed and the crystalline field splitting effect has been discussed.

Low Temperature Mössbauer Spectra of Rozenite and Szomolnokite

A. Van Alboom^{1,2}, V.G. De Resende², E. De Grave², M.D. Dyar³, J.A.M. Gómez²

¹ Faculty of Applied Engineering Sciences, University College Gent, Schoonmeersstraat 52, 9000 Gent, Belgium, e-mail: toon.vanalboom@hogent.be, ² NUMAT, Department of Subatomic and Radiation Physics, University of Gent, Proeftuinstraat 86, 9000 Gent, Belgium, ³ Department of Earth and Environment, Mount Holyoke College, South Hadley, Massachusetts 01075, USA

In nature rozenite ($\text{FeSO}_4 \cdot 4\text{H}_2\text{O}$) and szomolnokite ($\text{FeSO}_4 \cdot \text{H}_2\text{O}$) are secondary minerals found in the oxidation zones of sulfide deposits. In this study, Mössbauer spectra (MS) at 4.2 K of two natural (S60 and JB626) and two synthetic samples (Mel100 and Mel200) are presented. From the MS and the X-ray diffraction patterns, it is concluded that S60, JB626 and Mel100 are admixtures of two phases (rozenite and szomolnokite), whereas Mel200 is single phased szomolnokite.

At 4.2 K the MS of S60, JB626 and Mel100 consist of a superposition of a ferrous doublet (D1) and a magnetically split component (S2). The hyperfine parameters of D1 are characteristic for Fe^{2+} in rozenite, whereas those of S2 are typical for Fe^{2+} in szomolnokite. The MS at 4.2 K of Mel200 is a single magnetically split ferrous component (S2). The magnetic (sub)spectra were numerically analysed by a model-independent hyperfine field distributed component [1] of which the subcomponents were calculated from the diagonalization of the full nuclear interaction Hamiltonian [2]. The adjusted parameter values (for S2: with highest probability in the B_{hf} distribution) are indicated in Table 1.

Table 1: Mössbauer parameters at 4.2 K for rozenite and szomolnokite phases.

Sample	T K	Spectral component	δ mm s^{-1}	ΔE_Q mm s^{-1}	η	B_{hf} T	Ψ $^\circ$	Ω $^\circ$	Γ mm s^{-1}	Area %	Identification
JB626	4.2	D1	1.38	3.50					0.37	38	rozenite
		S2	1.39	3.09	0.68	32.7	37	63	0.35	62	szomolnokite
S60	4.2	D1	1.40	3.55					0.36	20	rozenite
		S2	1.39	3.13	0.91	32.5	38	65	0.32	75	szomolnokite
Mel100	4.2	D1	1.38	3.48					0.36	73	rozenite
		S2	1.38	3.10	0.94	32.4	38	65	0.26	27	szomolnokite
Mel200	4.2	S2	1.38	3.07	0.59	32.5	37	63	0.30	100	szomolnokite

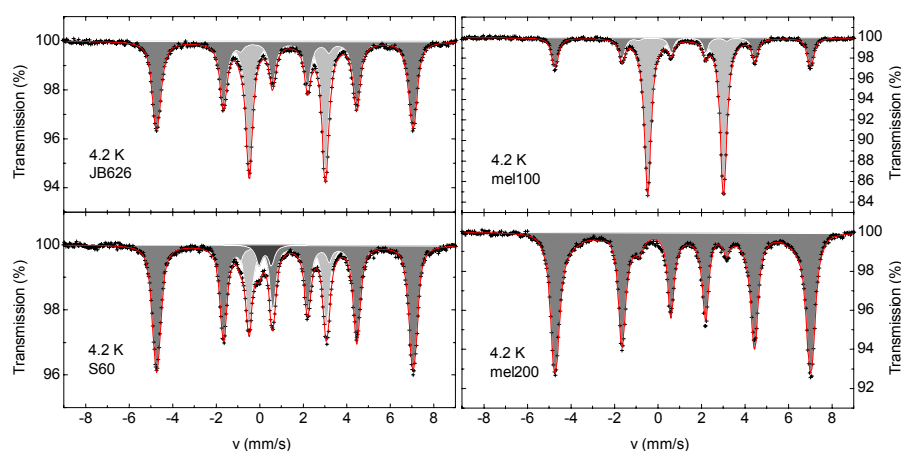


Fig. 1: Mössbauer spectra of the samples at 4.2 K (light gray: D1; gray: S2)

- [1] R.E. Vandenberghe, E. De Grave, P.M.A. de Bakker, *Hyp. Int.* 83 (1994) 29-49.
 [2] G.R. Hoy, S. Chandra, *J. Chem. Phys.* 47 (1967) 961-965.

8. CHEMICAL DYNAMICS

Studies on Microsolvation in the Gas Phase by HR-LIF and REMPI-TOF Spectroscopy

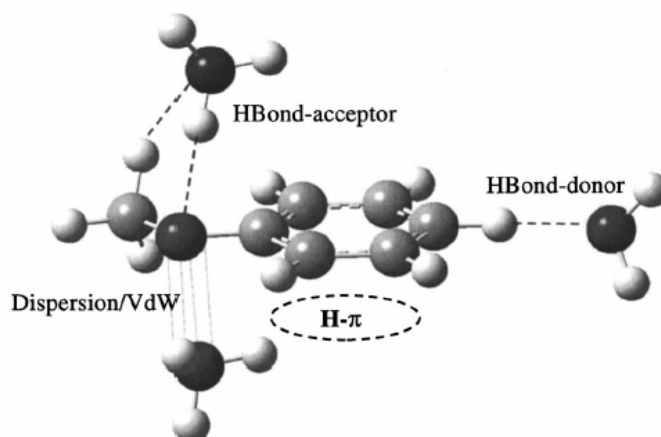
M. Pasquini¹, N. Schiccheri², G. Piani², G. Pietraperzia^{1,2}, E. Castellucci^{1,2}, M. Becucci^{1,2}

¹European Laboratory for Non-Linear Spectroscopy, via N. Carrara 1, 50019 Sesto Fiorentino (FI), Italy,

²Dipartimento di Chimica, Università degli Studi di Firenze, via della Lastruccia 3, 50019 Sesto Fiorentino (FI) Italy

Molecular clusters are quite useful as model systems to learn about the microscopic mechanisms responsible for intermolecular interactions. Clusters of different composition make possible a detailed study of the different binding mechanism related to the existence of van der Waals, hydrogen bond and electrostatic interactions. Knowledge of these processes is of fundamental interest in order to understand the transition from isolated molecules to bulk materials and to validate models for the solvation process.

We are reporting on the spectroscopic study on different 1:1 clusters formed, in supersonic expansions, by anisole with different simple solvents and other aromatic molecules [1-4]. This allows us to probe the nature of the intermolecular bonding when many interaction mechanisms are possibly operative. These clusters have been studied by Resonance Enhanced Multi-Photon Ionization (REMPI) – Time of Flight (TOF) mass spectrometry and by high resolution (rotationally resolved) laser induced fluorescence (HR-LIF) spectroscopy. The spectroscopic parameters we derived (vibrational frequencies, rotational constants in both the ground and the excited state, frequency shift of the $S_1 \leftarrow S_0$ electronic transition with cluster formation) have been modeled with advanced *ab initio* and DFT methods (in collaboration with V. Barone and coworkers, Univ. Napoli, Italy).



- [1] M. Becucci, G. Pietraperzia, M. Pasquini, G. Piani, A. Zoppi, R. Chelli, E. Castellucci, W. Demtroeder, *J. Chem. Phys.* 120 (2004) 5601-5607
- [2] M. Bikzisko, G. Piani, M. Pasquini, N. Schiccheri, G. Pietraperzia, M. Becucci, M. Pavone, V. Barone, *J. Chem. Phys.* 127 (2007) 144303
- [3] M. Pasquini, N. Schiccheri, G. Piani, G. Pietraperzia, M. Becucci, M. Biczysko, M. Pavone, V. Barone, *J. Phys. Chem. B* 111 (2007) 12363-12371

FTIR Study of the Reactivity of Solid CO at High Pressure

M. Ceppatelli^{1,2}, A. Serdyukov³, R. Bini^{1,2}, H.J. Jodl^{1,3}

¹ LENS – European Laboratory for Non-Linear Spectroscopy, Via Nello Carrara 1, 50019 Sesto Fiorentino (FI), Italy. ² Dipartimento di Chimica dell'Università degli Studi di Firenze, Via della Lastruccia 3, 50019 Sesto Fiorentino (FI), Italy, ³ FB Physik, Universität Kaiserslautern, Postfach 3049, D-67653 Kaiserslautern, Germany.

The advent of Diamond Anvil Cell (DAC) has paved the way for the spectroscopic study of matter under extreme conditions of P and T (0.1-500 GPa, 10-5000 K) [1]. In such high density conditions simple molecular systems containing unsaturated bonds typically undergo a redistribution of the electronic density with the formation of reaction products. The reversible formation of extended polymeric solids has been reported for molecular systems like CO₂ and N₂. In other cases, like unsaturated hydrocarbons, the bond reconstruction process is irreversible and allows the recovery of reaction products at ambient conditions. Under suitable reaction conditions, such processes may show high yields and selectivity in total absence of solvent, catalysts and radical initiators, leading to the synthesis of new classes of materials with advanced optical, mechanical and energetic properties, while fulfilling the requirements for a green chemistry [2, 3]. CO is a challenging molecular system both from a theoretical and applicative point of view. The phase diagram of CO shows very strong analogies with that of nitrogen in the low P-T region. Nevertheless with increasing pressure, despite being isoelectronic, the two molecules show a very different behaviour. As a matter of fact, while the transformation of N₂ to a non-molecular solid occurs above 110 GPa and 2000 K [4], CO reacts in much milder conditions at 5.5 GPa and 300 K. The high pressure reactivity of solid CO has been investigated in several experimental and theoretical studies [5], nevertheless up to now many aspects of this subject remain unclear. These aspects, mainly related to the employment of laser light to probe the sample, concerns the PT stability region of CO, the identification of the reaction mechanism and the characterization of the reaction products. Here we report the results of a FTIR study on the high pressure reactivity of solid CO at different temperatures avoiding any exposition of the sample to laser light. The pressure was measured by means of the IR active band of a vibrational pressure sensor calibrated with respect to the ruby fluorescence scale. The reaction pressure threshold has been individuated for every investigated temperature and for each P-T point in the phase diagram we monitored the reaction kinetics in constant thermodynamic conditions until the achievement of the equilibrium. Different behaviours have been observed at 300 K and 400 K, with different reaction mechanisms and products. In both cases a bright orange solid sample is recovered at ambient conditions, but while at 300 K this is the main reaction product, at 400 K CO₂ massively forms together with the solid product. The FTIR spectra show a clear evidence of the formation of CO₂ and provide a fine insight in the different composition of the solid products.

- [1] V. Schettino, R. Bini, M. Ceppatelli, L. Ciabini, and M. Citroni, *Chemical reactions at very high pressure* in *Advances in Chemical Physics*, Vol. 131, pp. 105-242 (Ed. Stuart A. Rice), John Wiley & Sons Interscience (2005).
- [2] M. Citroni, M. Ceppatelli, R. Bini, V. Schettino, *Laser-Induced Selectivity for Dimerization Versus Polymerization of Butadiene Under Pressure*, *Science* 295 (2002) 2058-2060.
- [3] D. Chelazzi, M. Ceppatelli, M. Santoro, R. Bini and V. Schettino, *High-pressure synthesis of crystalline polyethylene using optical catalysis*, *Nat. Materials* 3 (2004) 470-475.
- [4] M.I. Eremets et al., *Single bonded cubic form of nitrogen*, *Nat. Materials* 3 (2004) 558-563.
- [5] W.J. Evans et al., *Pressure-Induced Polymerization of Carbon Monoxide : Disproportionation and Synthesis of an Energetic Lactonic Polymer*, *Chem. Mater.* 18 (2006) 2520-2531.

ESIPT from the S₂ Singlet State in the 3-Hydroxyflavone

V.I. Tomin, R. Jaworski

*Institute of Physics, Pomeranian University in Slupsk, ul. Arciszewskiego, 22b, Slupsk, 76-200, POLAND
e-mail: tomin@apsl.edu.pl*

The proton transfer in the excited state of organic molecules and their complexes belongs to the most frequently occurred primary photoreactions. The study and understanding of such processes is of a fundamental importance for chemistry and Life Sciences as they play a key role in the main photosynthesis reactions of plants and for functioning of various biological organisms.

Spectra of the dual fluorescence of 3-hydroxyflavone, the archetype molecule appearing in ESIPT state, in ethyl acetate with picosecond time resolution were obtained at excitation within S₁ and S₂ singlet bands of absorption by 44 ps pulses of the optical parametric generator. The detection part consists of the spectrograph 2501S (Bruker Optics, USA) and the streak camera C4334-01 (Hamamatsu, Japan). The spectrograph insures spatial resolution of the analyzed light (wavelength axes), whereas the streak camera allows for temporal resolution of the light beam coming out of the spectrograph.

Spectra dynamics reveals time development of the internal proton transfer in the excited state (ESIPT) of molecule from the hydroxyl to the carbonyl group, stable ratio intensities of the normal and the tautomer bands of fluorescence is accomplished for 210 ps at excitation in the first singlet band (wavelength 340 nm). At the same time excitation in the S₂ band gives stable value of the same ratio faster, for time 170 ps, besides, the relative contribution of the tautomer form to the integral emission remains higher during all interval of emission observation. For the first time the obtained data directly evidence an additional channel of ESIPT from the S₂ singlet state of 3-hydroxyflavone, the estimates show that the probability of this process k_{n2} is very high and amounts $0.84 \cdot 10^{12} \text{ s}^{-1}$ if the value of nonradiative transitions S₂→S₁ probability in the 3HF molecule p_{n2} is equal 10^{12} s^{-1} . For estimates of k_{n2} we used the expression

$$\frac{(I_N / I_P)_{S_2}}{(I_N / I_P)_{S_1}} = \frac{p_{n2}}{p_{n2} + k_{n2}},$$

where $(I_N / I_P)_{S_2}$ and $(I_N / I_P)_{S_1}$ are the relative intensities of fluorescence emission in maxima of the normal form and the tautomer at excitation in the S₂ and S₁ bands, respectively. The relative intensities should be taken after establishing the equilibrium between both forms of the luminophor in the excited states.

The obtained results may be applied for other chemical compound appearing in the ESIPT states, some of them are specially synthesised and tested as multiparametric sensors and possess by unique properties in determination of polarity of environment, local electric fields, detection of single molecules of water in membranes and vesicles, various properties of H-bonds [1, 2]. We think that registered process of creation of photoreaction products through the S_n^N states may be concerned and other primary photoreactions, such as redistribution of the electronic density (charge transfer) in the excited state, the protolytic reactions, the intramolecular proton transfer (phototautomerization), the creation of H-bonds, excimer and exciplexes.

[1] D. Altschul, S. Oncul, A.P. Demchenko, J. Mol. Recognit. 19 (2006) 459-477.

[2] A.P. Demchenko, Analytical Biochemistry 343 (2005) 1-22.

Kinetics and Mechanistic Studies of the Dissociation of Anthranilic-diacetato-2,2'-dipyridyl Chromium (III) Dihydrated in Acidic Media

A.S. Bali¹, Ajit Viridi²

¹*Department of Engineering Chemistry, Model Institute of Engineering & Technology, Jammu, India*

²*Department of Engineering Physics, Model Institute of Engineering & Technology, Jammu, India*

Acid catalysed dissociation of anthranilic-diacetato-2,2'-dipyridyl chromium (III) dihydrated [Cr(atda)(dipyridyl)] hydrate has been studied kinetically in aqueous perchloric media over a temperature range 50-70 °C, under these experimental conditions, the reaction occurs by acid assisted path only. According to the rate law: Rate = k_H^+ [Complex][H⁺], where k_H^+ is the rate constant for acid assisted path. Analysis of the rate data corresponding to k_H^+ path suggests that the reaction is first order in [HClO₄] for the title complex and the chelate ring in 2,2'-dipyridyl complex suffers one ended dissociation accompanied by protonation of the released end of the basic ligand which leads to a faster rupture of the remaining metal ligand bond leading to the complex loss of the ligand.

Vibrational Spectra of the 2-, 4-Bromo- and 4,4'-Chlorobenzophenones and Their Interpretation Using Structural-dynamical Models

L.M. Babkov¹, N.A. Davydova², K.E. Uspenskiy¹

¹Saratov State University, Moskovskaya st, 155, Saratov, 410012, Russia

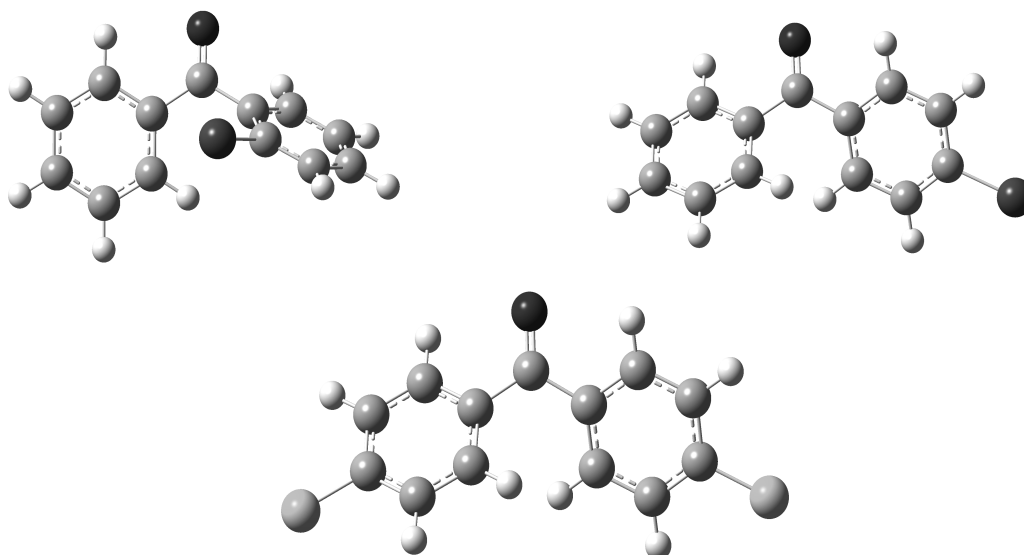
E-mail: babkov@sgu.ru

²Institute of Physics of NAS of Ukraine, 46 Nauki prosp., Kyiv, 03022, Ukraine

E-mail: davydova@iop.kiev.ua

In the last time to the investigation of physcal-chemistry properties and the structure of haloido-substituted benzophenones is paid a lot of attention. Between of the investigation methods of these compounds the theoretical and experimental methods of the molecular spectroscopy and quantum chemistry are useful.

Using density functional method (B3LYP/6-31G) [1] the energies, structures, dipole moments and polarizabilities of the 2-, 4-bromo- (2BrBP, 4BrBP) and 4,4'-chlorobenzophenones (4,4'-CIBP) molecules were calculated. In harmonic and anharmonic approximation the force fields of the mentioned above molecules were built and the frequencies of the fundamental normal modes, their forms and intensities in the vibrational spectra together with overtones and combinational frequencies were computed. The comparison of the calculated and measured frequencies pointed to the significant improvement of the modeling results at the transition from harmonic approximation to the anharmonic one. It has been found that it is possible to avoid the scaling procedure for the calculated force fields and vibrational frequencies. On the basis of the modeling results a full interpretation of the measured spectra of the crystalline samples of investigated compounds was given.



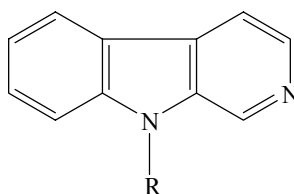
[1] J. Frisch, G.W. Trucks, H.B. Schlegel et al., Gaussian03, Revision B.03; Gaussian, Inc., Pittsburgh PA, 2003.

Betacarboline Tautomerism Induced by Temperature. Dual Emission of Betacarboline Self-Associated Hydrogen Bond Aggregates.

C. Carmona, J. Hidalgo, A. Sánchez-Coronilla, M.A. Muñoz, M. Balón

Departamento de Química Física, Facultad de Farmacia, Universidad de Sevilla, 41012 Sevilla, Spain

A systematic study of the influence of the gradual decrease of temperature, from room temperature up to 118 K, on the UV-vis absorption and fluorescence emission spectra of betacarboline, 9H-pyrido[3,4-b]indole, BC, has been carried out in 2-methylbutane, 2MB. For the sake of comparison, the effect of the decreasing temperature on the behavior of other model systems, such as BC plus N₉-methyl-9H-pyrido[3,4-b]indole, MBC, and BC plus pyridine, PY, has also been analyzed.



R = H **BC**

R = CH₃ **MBC**

These studies have allowed concluding that the observed spectral changes are due to the formation of hydrogen bonded self-associated BC aggregates. Initially, up to ~ 208K, red shifts, around 20 nm, are observed in the absorption and emission spectra. The emission shift is accompanied by a strong fluorescence quenching of the structured emission at 342 nm and 358 nm. These changes have been ascribed to the formation of a hydrogen bond BC dimer with a proton transfer structure, PTC, the fluorescence quenching being due to an electron-driven proton-transfer in the PTC which leads to an ultra fast internal conversion.

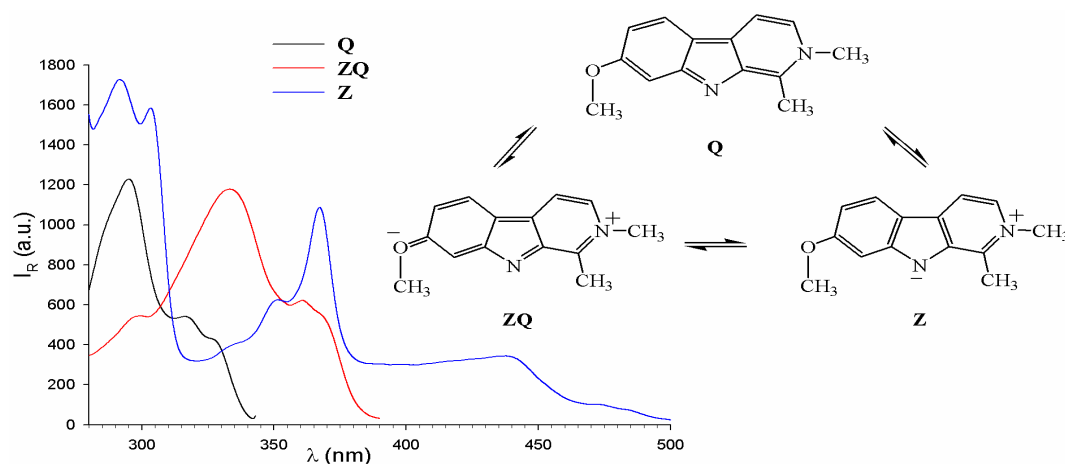
At lower temperatures, the quenching is non-operative and the emission intensity increases up to 178 K. Further, from 178 K to 118 K, and only for BC in 2MB, dual emission is observed. The emission at low wavelength decreases and, concomitantly, the typical BC large Stokes shifted emission, around 500 nm, appears. Isoemissive points are observed in the spectra. These last changes are ascribed to the formation of ground state cyclic tetrameric BC hydrogen bond aggregates. In these complexes, the tautomeric form that emits dual fluorescence, from its locally excited state, LE, and its intramolecular charge transfer state, ICT, is generated by a quadruple proton transfer in the hydrogen bonded tetramer.

Ground state Isomerism and Dual Fluorescence of 2-Methylharmine Anhydronium Base (7-Methoxy-1, 2-dimethyl-2H-pyrido[3,4-b]indole) in Aprotic Solvents

Emilio García-Fernández, María A. Muñoz, Carmen Carmona and Manuel Balón

Departamento de Química Física, Facultad de Farmacia, Universidad de Sevilla, 41012 Sevilla, Spain

Ground state isomerism and dual fluorescence of 2-methylharmine anhydronium base (7-methoxy-1, 2-dimethyl-2H-pyrido[3,4-b]indole), HIAB, in aprotic solvents have been studied using electronic absorption, steady state and time resolved fluorescence spectroscopic techniques. The solvent polarity and the emission wavelength dependence of the fluorescence excitation spectra conclusively show the existence of ground state equilibria between three HIAB isomeric species, namely Q, Z and ZQ.



The solvent polarity and the excitation wavelength dependence of the steady state and time resolved fluorescence decays reveal that the HIAB isomers can emit dual fluorescence from a locally, LE, and an intra molecular charge transfer, ICT, excited states. According to the proposed mechanism, the ZQ isomer simultaneously emits from its LE and ICT states, while Q and Z exclusively emit from their LE and ICT states, respectively.

Phase Transition and NH₃ Motions in Polycrystalline [Ca(NH₃)₆](ClO₄)₂ Studied by Infrared Spectroscopy and Inelastic/Quasielastic Incoherent Neutron Scattering

J. Hetmańczyk, Ł. Hetmańczyk, E. Mikuli and A. Migdał-Mikuli

*Department of Chemical Physics, Faculty of Chemistry, Jagiellonian University,
ul. Ingardena 3, 30-060 Kraków, Poland*

The examined compound [Ca(NH₃)₆](ClO₄)₂ was obtained from tetraaquacalcium chlorate(VII) according to the method proposed by Smith and Koch [1]. [Ca(NH₃)₆](ClO₄)₂ has two solid phases between 95 and 295 K: low-temperature phase (phase II) and high-temperature phase (phase I). The phase transition temperature at $T_C^h = 123.3$ K (on heating) and at $T_C^c = 122.0$ K (on cooling) was determined by means of differential scanning calorimetry (DSC), by extrapolating the T_{peak}^h and T_{peak}^c vs. rate of sample heating and cooling to the scanning rate value of 0 K·min⁻¹, respectively. The following thermodynamic parameters for phase I ↔ phase II transition were obtained: $\Delta H = 1.95 \pm 0.22$ kJ·mol⁻¹ and $\Delta S = 15.8 \pm 0.3$ J·mol⁻¹·K⁻¹. The large transition entropy indicates considerable configurational disordering in the high temperature phase (so called ODIC crystals). The thermal hysteresis of the phase transition temperature at T_c equal to ca. 1.3 K and the heat flow anomaly sharpness suggest that the detected phase transition is a first-order one. Room-temperature phase of this compound was analyzed by means of X-ray powder diffraction. Heksaamminecalcium chlorate (VII) crystallizes in the cubic system (Fm3m space group) with cell parameter: $a = 11.685$ Å and four molecules per unit cell. The crystal structure consist of octahedral [Ca(NH₃)₆]²⁺ cations and tetrahedral ClO₄⁻ anions. Therefore, the results of X-ray diffraction are very similar to those obtained earlier for [Ni(NH₃)₆](ClO₄)₂ and especially for [Mg(NH₃)₆](ClO₄)₂ [2,3]. Fourier transform middle infrared (FT-MIR) spectra were measured during cooling of the sample at temperatures ranging from 290 to 20 K. The appearing of two new bands in the wavenumber range of 3100 cm⁻¹ and 3200 cm⁻¹ at the vicinity of T_c , suggests that during phase transition crystal structure changes. The QENS and IINS spectra for [Ca(NH₃)₆](ClO₄)₂ were measured with NERA (Dubna in Russia) time of flight spectrometer at the following temperatures: 20, 110, 131 and 220 K. Neutron scattering elastic peak, registered at 110 K (low-temperature phase-II) and also at higher temperatures (high-temperature phase-I), shows distinct broadening, which is typical for dynamically, orientationally disordered crystals (ODIC). Fast reorientational motion of NH₃ ligands in [Ca(NH₃)₆]²⁺ can be pretty good described by a simple model of 120° instantaneous jumps around 3-fold axis on a picoseconds correlation time scale. The NH₃ ligands suddenly change neither the velocity nor the character of their reorientational motion at detected by DSC phase transition at T_c . The dynamical, orientational disorder is also confirmed by very much diffused spectra of the phonon density of states $G(\nu)$ for all temperatures higher than 20 K. It is due to great disorder connected with fast molecular motions, especially to the disorder of hydrogen atoms. Just the $G(\nu)$ spectra obtained for the low temperature phase at temperature 20 K show some peaks characteristic for ordered phase. Concluding the NH₃ groups perform fast stochastic reorientation below and above the phase transition.

[1] G.F. Smith, E.G. Koch, *Z. anorg. Chem.* 223 (1935) 17.

[2] A. Migdał-Mikuli, E. Mikuli, M. Rachwalska, S. Hodorowicz, *Phys. Stat. Sol. (a)* 47 (1978) 57.

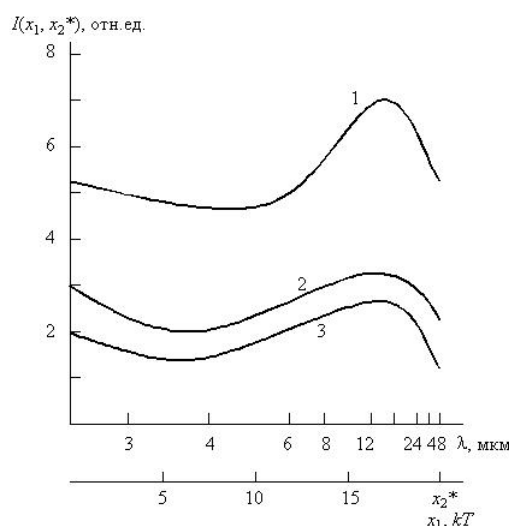
[3] S. Hodorowicz, M. Ciechanowicz-Rutkowska, J.M. Janik, J.A. Janik, *Phys. Stat. Sol. (a)* 43 (1977) 53.

Laser Photo-Ionization (Dissociation) of Molecules in the Isotopes Separation and Relativistic Calculating the Hyperfine Structure Parameters in Heavy-Element Chemistry and Spectroscopy

O.Yu. Khetselius

Odessa University, P.O. Box 24a, Odessa-9, 65009, South-East, Ukraine

Relativistic calculation of spectra and hyperfine structure (hfs) parameters for heavy elements (^{133}Cs , ^{201}Hg , ^{223}Ra , ^{252}Cf) is carried out. Calculation scheme is based on the relativistic perturbation theory [1]. The contribution due to inter electron correlations to hfs constants is about 120-1200 MHz for different states, contribution due to the finite size of a nucleus and radiative contribution is till 2 dozens MHz. Obtained data for hfs parameters are used in further in laser photo-ionization (dissociation) detecting the isotopes. We propose the new optimal schemes of laser photo-ionization method in the isotopes and nuclear reactions products detecting. As example, it's studied the reaction of spontaneous ^{252}Cf isotope fission on non-symmetric fragments, one of that is Cs. Resonant excitation of Cs is realized by the dye laser pulse, the spectrum of which includes the wavelengths of two transitions $6^2\text{S}_{1/2}-7^2\text{P}_{3/2}$ (4555Å) and $6^2\text{S}_{1/2}-7^2\text{P}_{1/2}$ (4593Å). The corresponding optimal parameters of laser and electric fields, quantum transitions etc are given. We present a new multi-level optimized model for definition of the optimal real form of laser pulse to reach maximal effectiveness of laser action in process of laser ionization (dissociation) of molecules too. Model is based on differential equation of the Focker-Plank type for density of molecules with the vibration energy x on some vibration level and operators, describing RT relaxation and laser filed [2]. The conditions and parameters for optimal excitation for molecules of HCl (PH_3 , CF_3Br , SiH_4) are given. In fig. we give a dependence (of number of particles) of functional: $I(u) = \text{Int} f(x_1, t_1; x_2, t_2) h(x) dx$ in the interval $x_1 \sim \{15, 21\}$ on x_1 and laser wavelength, corresponding to rotational transition x_1-x_2 ($T = 300 \text{ K}$). Here $h(x)$ is the function, corresponding to required form of the final distribution $f(x, t, u)$, i.e. density of molecules with vibration energy x at moment $t \sim [0, R]$.



- [1] A.Glushkov, O.Khetselius et al., Nucl. Ph. A 734 (2004) 21-28; J. Phys. CS 35 (2006) 425-430.
 [2] O. Khetselius, Photoelectronics 15 (2006) 101-108; Mol. Phys., Europ. Phys. J. (2008).

PEP Vibrations from DFT

M. Rudbeck¹, S. Kumar¹, M. Blomberg², M-A. Mroginski³, A. Barth¹

¹*Department of Biochemistry and Biophysics, The Arrhenius Laboratories for Natural Sciences, Stockholm University, SE-106 91 Stockholm, Sweden*

²*Department of Physics, Albanova, and Department of Biochemistry and Biophysics, The Arrhenius Laboratories for Natural Sciences, Stockholm University, SE-106 91 Stockholm, Sweden*

³*Institut für Chemie, Max-Volmer-Laboratorium, TU Berlin, PC 14, Straße des 17. Juni 135, D-10623 Berlin, Germany*

Phosphoenol pyruvate (PEP) was studied as fully ionized, singly protonated and doubly protonated in gas-, H₂O- and D₂O-phase using density functional theory (DFT) with the B3LYP functional and with the 6-31++G(d,p) basis set. All computations except the gas-phase were compared with experimental Fourier transform infrared (FTIR) results in solution and were in good agreement. The P-O stretching is of specific importance since phosphate is transferred from PEP to adenosine diphosphate (ADP) in the glycolytic pathway. The computational assignments of these specific frequencies are provided.

Dynamic Quenching as a Simple Test for the Mechanism of Excited-State Reaction

Vladimir I. Tomin¹, Sule Oncul², Grzegorz Smolarczyk¹,
Alexander P. Demchenko³

¹*Institute of Physics, Pomeranian University, 76-200 Słupsk, Arciszewskiego str. 22B, Poland*

²*Department of Biophysics, Marmara University, Istanbul, Turkey*

³*Palladin Institute of Biochemistry, 01030, Kyiv, Ukraine*

We report on comparative studies of dynamic fluorescence quenching of 3-hydroxyflavone (**3HF**) and of its novel analogs by nitric oxide spin compound TEMPO. These dyes exhibit the excited-state intramolecular proton transfer (ESIPT) reaction that allows observation of two separate bands in fluorescence emission - of initially excited form and of the product of ESIPT reaction. In the frame of two-state excited-state reaction formalism we develop the theory predicting different dependence of intensities at two bands in steady-state spectra in the cases of thermodynamic and kinetic control of ESIPT. In line with these predictions, the quenching changes strongly the distribution of intensities between these bands for **3HF** but does not change it for the novel compounds whose excited states exhibit strong charge transfer character. Based on these findings we suggest that the quenching of fluorescence by an efficient collisional quencher can be a simple and convenient method using only the steady-state experiment for distinguishing the excited-state reactions occurring under thermodynamic or under kinetic controls. This method can be used for large-scale screening of a series of compounds – potential candidates for application in fluorescence sensor and biosensor technologies.

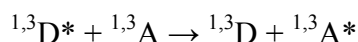
9. THEORETICAL SPECTROSCOPY AND COMPUTER METHODS

New Features in Theoretical Description of Electronic Energy Transfer: Mechanisms and Matrix Element Calculation

E. Benassi

Dipartimento di Chimica, Università di Modena e Reggio Emilia, Modena, Italy
e-mail: enrico.benassi@libero.it

We are introducing a new general theoretical model for the description of electronic energy transfer (eet) mechanisms which is discussed in the framework of non-radiative transition theory referring to the standard Born-Oppenheimer and Condon approximations. Despite of using the model to describe eet processes between an excited donor (D^*) and an acceptor (A)



the theory is also fully capable to take into account the presence of a third body B (bridge, spacer,...). The electronic transition matrix element between initial ($|e's'\rangle = |D^* A\rangle$) and final ($|e''s''\rangle = |D A^*\rangle$) states is given by

$$T_{e''s'',e's'} = V_{e''s'',e's'} + \sum_{es(\neq e's')} \frac{V_{e''s'',es} V_{es,e's'}}{E_{e's'} - E_{es}} + \dots$$

This equation allows us to separate the eet into a *direct process*, linked to the first order term ($V_{e''s'',e's'}$), and into an *indirect process*, due to higher orders and involving intermediate states ($|es\rangle$).

The attention will be focused on both direct and indirect electronic mechanisms considering the singlet-singlet eet as well as the triplet-triplet eet of the Scheme. At first, a simplified model was used to describe eet considering only two MOs (HOMO and LUMO) and two electrons for each monomers. Then this model was extended considering a more expanded MOs space and evaluating the importance of core MOs. At short ranges, for T - T eet, in addition to the usual exchange term, it was necessary to take into account the penetration terms (overlap-dependent contributions), because of the non-orthogonal MOs base. It was also evaluated for the first time the role of the overlap-dependent normalization factor on the electronic coupling promoting the eet.

First computational results were obtained considering both the electronic direct and indirect mechanisms for both S - S and T - T eet. All the different electronic contributions were calculated and analyzed for different model arrangements of ethylene and formaldehyde dimers. The comparison between results achieved in this work and previously obtained ones in the framework of the VB model [1] is also discussed.

[1] R.D. Harcourt, G.D. Scholes, K.P. Ghiggino, J. Chem. Phys. 101 (1994) 10521.

[2] G.D. Scholes, Ann Rev. Phys. Chem. 54 (2003) 57.

***Ab initio* Molecular Orbital Calculations of the Structures and Vibrational Spectra of Some Molecular Complexes Containing Sulphur Dioxide**

T.A. Ford

*Centre for Theoretical and Computational Chemistry, School of Chemistry,
University of KwaZulu-Natal, Westville Campus, Private Bag X54001,
Durban 4000, South Africa*

Recent *ab initio* calculations on the complexes formed between boron trifluoride and some common Lewis bases, such as ammonia [1], water [2], phosphine [3] and hydrogen sulphide [2], have revealed a pattern of behaviour in the values of some of the computed properties governed by the position of the heavy atom of the base in the periodic table. These properties are the molecular structures, interaction energies and vibrational spectra. In order to determine whether these patterns were also present in the properties of the corresponding complexes with another Lewis acid, sulphur dioxide, the calculations have been extended to cover these four complexes as well.

Although complexes of boron trifluoride with hydrogen fluoride and hydrogen chloride were found to be preferentially of the donor-acceptor type [4], the analogous complexes with sulphur dioxide optimized as conventionally hydrogen-bonded species.

The similarities and contrasts between the natures of the two families of aggregates are discussed and rationalized.

- [1] F. Gaffoor and T.A. Ford, *Spectrochim. Acta* in press (2008).
- [2] G.A. Yeo and T.A. Ford, *S. Afr. J. Chem.* 59 (2006) 129-134.
- [3] T.A. Ford, to be published.
- [4] G.A. Yeo and T.A. Ford, *J. Mol. Structure (Theochem)* 771 (2006) 157-164.

Raman Scattering of the Light on Metastable Levels of Diatomics: Consistent Energy Approach

A.V. Glushkov^{1,2}

¹*Odessa University, P.O.Box 24a, Odessa-9, 65009, South-East, Ukraine*

²*Institute of Spectroscopy, Russian Acad.Sci., Troitsk-Moscow, 142090, Russia*

Laser action on molecules leads to different non-linear processes, including multi-photon ionization, excitation and dissociation, Raman scattering. The elementary two-photon processes are linear coherent and combinational scattering. The intensities and polarization of lines in these spectra are defined by polarizability and derivative on inter-nuclear distance. In this paper it is considered a process of Relay and Raman vibration scattering of the light on metastable levels of molecules (H_2 , HD, D_2 , Li_2 , Rb_2 , Cs_2 , Fr_2). On the example of polarizability of metastable molecules it has been studied an effect of nuclear motion in processes of the second order of the perturbation theory. New numerical method for construction of the Green electron functions for optical electrons and electron wave functions is developed within the pseudo-potential approach in the spheroid coordinates system that allows to take into account non-spherical character of molecular field.

We have carried out the calculations of molecular polarizability, its derivative on inter-nuclear distance, depolarization degree under Relay and Raman light scattering on the frequencies of the Rb, Nd lasers. Relativistic generalization of proposed approach is carried out within QED perturbation theory with account of relativistic, correlation effects (the Superatom [1, 2] and Dirac packages (DP) [3] are used; the DP using in a progress). Our calculation scheme is based on gauge-invariant QED perturbation theory and generalized dynamical nuclear model with using the optimized one-quasiparticle representation at first in the theory of light scattering [1, 2].

Analysis of results of the calculation of a polarizability, its derivative on inter-nuclear distance, for example, for excited triple metastable $c^3\Pi_n$, states of the H_2 , HD, D_2 molecules on the frequencies of the Rb (1,78eV) and Nd (1,18eV) lasers shows that the main contribution into polarization of the cited metastable molecules is provided by changing the electron shell under action of the external electromagnetic field. An influence of the nuclear motion terms is quite little.

- [1] A.V. Glushkov, JETP Lett. 55 (1992) 99-103, A.V. Glushkov, L.N. Ivanov, Phys. Lett. A 170 (1992) 22-28, A.V. Glushkov, In: Low Energy Antiproton Phys., AIP Serie. 796 (2005) 201-205.
 [2] A.V. Glushkov et al, Nucl. Phys. A 734S (2004) 21-28; Int. Journ. Quant.Chem. 99 (2004) 879-886; 99 (2004) 936-942; J. Phys. CS. 11 (2005) 188-198; 178 (2005) 199-208; Recent Advances in Theory of Phys. and Chem. Systems (Springer) 15 (2006) 185-300; Ibid. 15 (2006) 301-308.

Single-centre Molecular Orbital Theory of Transition Metal Complexes

S. Lebernegg, G. Amthauer, M. Grodzicki

*Dept. of Materials Research and Physics, Institute of Mineralogy,
University of Salzburg, A-5020 Salzburg*

Most of the optical and magnetic properties of transition metal compounds are determined by the splitting pattern of the partially filled d-orbitals. Theoretical methods for calculating this splitting pattern range from simple empirical methods as ligand field theory (LFT) up to first principle approaches as molecular orbital (MO) theories and beyond. Whereas the latter solve the full multi-centre problem numerically, LFT constitutes a single-centre, essentially atomic-like problem that can, in principle, be solved analytically, albeit only by using empirically adjusted parameters.

In order to bridge the gap between both levels of description and to maintain the atomic-like structure of LFT, a single-centre representation of the MO-Hamiltonian is derived based on ligand-orthogonalized d-orbitals that explicitly account for overlap and covalency effects. The metal-ligand orbital interactions are transformed into a "ligand-field" that can be interpreted as a repulsive pseudopotential and is roughly proportional to the square of the overlap matrix between metal and ligand orbitals. The reliability of this single-centre representation is confirmed by comparing the calculated d-orbital energies for several Cu^{II}-fluoride model complexes with results from fully numerical MO-calculations in the local density approximation by the SCC-X α method [1] that are in quantitative agreement with each other. Moreover, the detailed analysis of the results demonstrates that by far the largest part, viz. about 90%, of the ligand-field splitting arises from the metal-ligand orbital interactions.

In the second part the single-centre MO-approach will be compared with LFT, still being widely used for interpreting the optical spectra of transition metal compounds. Separation of the overlap integrals into radial and angular parts [2] shows that the repulsive pseudopotential exhibits the same angular dependence as the electrostatic ligand-field of LFT. Since the symmetry of the systems is exclusively contained in the angular part, this result elucidates why, on one side, LFT generally leads to the qualitatively correct splitting pattern of the d-orbitals. On the other hand, the essential difference consists in the radial parts. Whereas LFT gives, for cubic systems, the well-known R^5 -dependence, the single-centre MO-approach yields basically an exponential dependence of the ligand-field splitting on the metal-ligand distance R . Accordingly, the widespread claim that the ligand-field splitting is proportional to R^5 is merely based on the fact that any exponential can locally be approximated by an appropriate R^n but is devoid of any physical basis. In summary, this analysis facilitates the understanding of both the merits and the limitations of LFT.

Finally, the versatility of this approach is demonstrated by calculating the d-orbital splitting pattern of some known iron-bearing complexes without using empirically adjusted parameters. Since, in addition, the single-centre MO-Hamiltonian bears the same conceptual simplicity as the LFT-Hamiltonian, the explicit inclusion of multiplet splittings via the Racah parameters, as well as spin-orbit interactions is easily possible in exactly the same fashion as in LFT. Consequently, such a scheme offers a more consistent and reliable means for evaluating and interpreting optical and NIR spectra of transition metal compounds.

[1] M. Grodzicki, J. Phys. B13 (1980) 2683-2691

[2] M. Grodzicki, Croat. Chem. Acta 60 (1987) 263-268

FTIR and Raman Spectra of Some Tetra Substituted Benzenes

V. Mukherjee¹, N.P. Singh^{1,*}, R.A. Yadav²

¹Department of Physics, Udai Pratap Autonomous College, Varanasi-221002, India

²Department of Physics, Banaras Hindu University, Varanasi-221005, India

* email: nps_physics@rediffmail.com

FTIR and Raman spectra of the 2,3,6-trifluoro-benzonitrile, 2,3,6-trifluoro-aniline and 2,3,6-trifluoro-benzoic acid molecules have been recorded in the spectral ranges 400-4000 cm^{-1} and 50-4000 cm^{-1} respectively. Conventional Hartree-Fock *ab initio* and Density Functional method have been employed to optimize geometries and calculate vibrational frequencies with their IR and Raman intensities and depolarization ratios for the Raman lines. Normal coordinate analysis method has also been set up to carry out the potential energy distributions (PEDs) in that despite, the great utility of *ab initio* over NCA method, assignment of vibrational frequencies to normal mode vibrations with the help of PEDs is more feasible. The influences of presence of fluorine atoms to the normal mode of benzonitrile, aniline and benzoic acid have been discussed.

Theoretical Study of a Combined Electronic + Vibrational Relaxation Process in Thiophosgene SCCl_2

Svetoslav Rashev¹, David C. Moule²

¹*Institute of Solid State Physics, Bulg. Acad. Sci., Tsarigradsko chaussee 72, 1784 Sofia, Bulgaria.*

²*Department of Chemistry, Brock University, St. Catharines, Ontario L2S3A1, Canada*

Nonradiative relaxation processes are extremely important for the fluorescent and phosphorescent properties of most materials, in particular for those, explored as perspective laser media. Such processes are capable of suppressing or completely extinguishing radiative emission from a certain material, by redistributing the absorbed excitation energy among the vibrational degrees of freedom (phonos, etc.). Theoretical exploration of relaxation processes is a difficult task, that often has to be carried out on simple model systems, in order to understand the basic mechanisms involved.

Thiophosgene is a four-atomic symmetric molecule with the structure of formaldehyde that serves as a very suitable model case for exploration of various photophysical and photochemical phenomena, taking place in molecules in general. Thiophosgene has been widely studied spectroscopically both in its ground as well as in the lower excited electronic states [1, 2]. It is noteworthy, that the molecule exhibits strong fluorescence from its second excited electronic state $S_0 \leftarrow S_2$, in addition to that from the first $S_0 \leftarrow S_1$ (in violation of Kasha's rule) but no phosphorescence from its first triplet $S_0 \leftarrow T_1$. All these peculiarities can be rationalized on the basis of the theory of radiationless transitions in polyatomic molecules [2-4].

We have performed a computational study of the electronic nonradiative transition from the first excited triplet state T_1 to the ground electronic state S_0 in thiophosgene (CSCl_2). This process is responsible for a strong reduction in the phosphorescence quantum yield from the T_1 state. Our results demonstrate that for the correct description of the electronic relaxation process it is necessary to take explicitly into account the vibrational redistribution among highly excited vibrational levels in S_0 .

The obtained theoretical results lead to the conclusion, that the explored nonradiative process is not a true irreversible decay, because of the insufficient vibrational level density involved. On this basis we predict, that the phosphorescence intensity from T_1 should exhibit violent quantum beats, with a period of about 100-200 ps, that could be observed experimentally.

[1] A. Maciejewski, R.P. Steer, *Chem. Revs.* 93 (1993) 67-98.

[2] T. Fujiwara, E.C. Lim, R. H. Judge, D.C. Moule, *J. Chem. Phys.* 124 (2006) 124301.

[3] S. Rashev, D.C. Moule, S.T. Djambova, *Chem. Phys. Lett.* 441 (2007) 43-47.

[4] S. Rashev, D.C. Moule, *J. Chem. Phys.* 128 (2008) 31295391.

Vibrational Isotope Effect by the Low Rank Perturbation Method

T.P. Živković

Institute Rudjer Bošković, Bijenička cesta 54, Zagreb, CROATIA
e-mail: zivkovic@irb.hr

Mathematical formalism of the Low Rank Perturbation (LRP) method is applied to the vibrational isotope effect. A pair of two n -atom isotopic molecules **A** and **B** which are identical except for isotopic substitutions at ρ atoms is considered. Vibrational isotope effect is treated within the harmonic approximation and under assumption (consistent with the Born-Oppenheimer approximation) that force field does not change due to isotopic substitutions. Within those approximations LRP is exact.

LRP replaces standard treatment of this effect which involves the solution of the $3n \times 3n$ matrix eigenvalue equation with a solution of a much smaller $3\rho \times 3\rho$ matrix equation. This reduction of dimensionality results in the improved computational efficiency. In addition, LRP provides a new conceptual insight into the regularities of the vibrational isotope effect. Within the LRP formalism one finds that vibrational frequencies ω_k and normal modes $|\Psi_k\rangle$ of the isotopomer **B** depend mainly on local properties involving region subject to the isotopic substitution. The only global properties needed to obtain frequencies and normal modes of the isotopomer **B** are frequencies ν_i of the parent molecule **A**. Vibrational isotope effect does not depend on any fine details outside the region subject to the isotopic substitutions (such as force constants in this region, detailed geometry, atomic masses, etc).

In the case of planar molecules LRP applies separately to in-plane and to out-of-plane vibrations. Particularly simple is LRP treatment of out-of-plane vibrations. Several examples of out-of-plane vibrations of planar molecules will be given. In the case of out-of-plane vibrations of benzene (H,D)-isotopomers one finds that LRP frequencies reproduce available experimental frequencies better than highly sophisticated DFT frequencies improved with scaling technique.

- [1] T.P. Živković: *Solution of the generalized eigenvalue equation perturbed by a generalized low rank perturbation*. Theor. Chim. Acta 76 (1989) 331-351.
- [2] T.P. Živković: *Vibrational isotope effect by the low rank perturbation method*. J. Math. Chem. 28 (2000) 267-285.
- [3] T.P. Živković: *Vibrational isotope effect of linear and planar molecules: Deuterated bromoethenes*. J. Math. Chem. 28 (2000) 287-312.
- [4] T.P. Živković: *On the vibrational interlacing rule in deuterated benzenes: I Out-of-plane vibrations*. Croat. Chem. Acta. 80 (2007) 547-555.

Molecular Mechanics Study of Antihypertensive Val-Tyr Dipeptide

G.A. Akverdieva¹, N.M. Godjajev^{1,2}, S. Akyuz³, N.E. Dogan³, T. Akyuz³

¹Institute for Physical Problems, Baku State University, Z.Khalilov st.23, AZ-1148, Baku, Azerbaijan, ²Qafqaz University, Baku-Sumqayit Road, 16 km, Khirdalan, AZ-0101, Baku, Azerbaijan, ³Istanbul Kultur University, Science and Letters Faculty, Physics Department, Atakoy Campus, 34156 Bakirkoy, Istanbul, Turkey

Antihypertensive peptides received much interest over the last decade. Val-Tyr dipeptide is known to be angiotensin converting enzyme (ACE) inhibitory peptide in vitro [1]. In order to understand the mechanism of the activity of a drug it is necessary explore its conformational possibilities and determine physiologically active conformations.

In this study conformational behavior of antihypertensive dipeptide Val-Tyr has been investigated by molecular mechanics. The analysis of dipeptide is based on universal sets of low-energy conformational states of free amino acids. For χ_1 of the side chains of both Val and Tyr, all three values of torsion minima 60, 180, -60° were considered. The value 180° for χ_2 and χ_3 of Val and the values 90° and 180° for χ_2 and χ_3 of Tyr, which correspond to stable states of side chains of these residues, were taken. Thus, 72 conformations, belonging to the folded and extended shapes of backbone were calculated. Calculation results reveal that 20% of the examined conformations have the relative energy up to 2 kcal/mol and both shapes are equally probable for this dipeptide. The optimal conformations of folded ($E_{rel.} = 0.0$ kcal/mol) and extended ($E_{rel.} = 0.5$ kcal/mol) backbone shapes are illustrated in Figure 1. Massivity of side chains of amino acid residues is an important factor, which form the stabilizing forces-dispersion interactions of side chains of Val and Tyr. The energy of dipeptide is very sensitive to positions of the side chains of the amino acid residues. Though the extended shape of this dipeptide is the best, from the point of view of mono-peptide energy, in the conformations with the folded backbone, the side chains are more close to each other and form effective dispersion contacts. In addition, the folded structures are also favourable as regards dispersion contacts of the backbone elements, which result in the density packing of mono-peptide links. So, the distance from atom CG1 of side chain of Val to atom O of side chain of Tyr is 4.1 and 7.7 Å, the distance from atom CG2 of side chain of Val to atom O of side chain of Tyr is 6.3 and 8.6 Å and the distance between N and C atoms of the opposite terminals of the molecule is 4.7 and 6.0 Å in the mentioned optimal folded and extended structures, respectively.

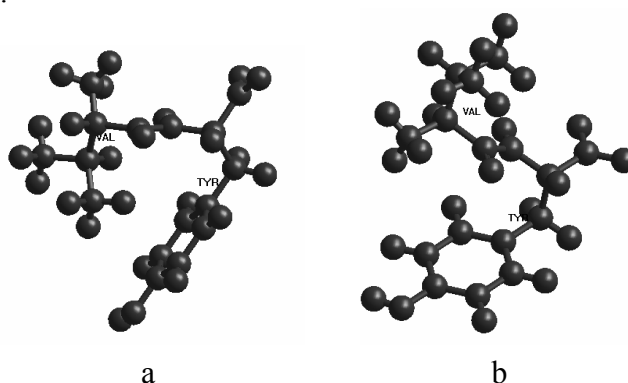


Fig. 1: The optimal folded (a) and extended (b) structures of Val-Tyr dipeptide

- [1] T. Matsui, X. L. Zhu, K. Watanabe, K. Tanaka, Y. Kusano, K. Matsumoto, Life Sciences 79 (2006) 2492-2498.
[2] L. Vercruyssen, N. Morel, J. Van Camp, J. Szust, G. Smaghe, Peptides 29 (2008) 261-267.

Ab Initio Calculations of pK_a Values for Some 6-Methyl-2-Pyridine Carboxaldehyde Derivatives

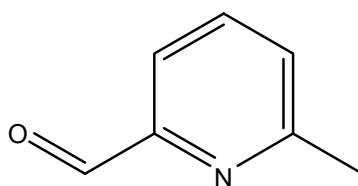
Sinem Aydemir¹, Murat Duran², Erol Tasal¹, Halil Berber³, Cemil Öğretir², M. Selami Kılıckaya¹

¹Department of Physics, Faculty of Arts & Sciences, Eskişehir Osmangazi University, 26480 Eskişehir, Turkey

²Department of Chemistry, Faculty of Arts & Sciences, Eskişehir Osmangazi University, 26480 Eskişehir, Turkey

³Department of Chemistry, Faculty of Arts & Sciences, Anadolu University, 26470 Eskişehir, Turkey

In this study, *ab initio* calculations on 6-Methyl-2-Pyridine Carboxaldehyde acid and its deprotonation mechanism was evaluated by theoretical calculations. The acidity constants, pK_a values have been determined by using B3LYP/6-31G(d) basis sets of density functional theory (DFT) along with physical and thermodynamic parameters. The geometries of all the structures have been fully optimized with the Gaussian-03 programme using the hybrid B3LYP method with a 6-31G* basis set. The *ab initio* geometries have been used in calculating the solvation free energies carried out using at the B3LYP/6-31G(d). The conversion factor of 1 Hartree = 627.5095 kcal mol⁻¹ was used since the total energies were given in Hartree.



6-methyl-2-pyridine carboxaldehyde

Fig. 1: The molecular structure of 6-methyl-2-pyridine carboxaldehyde.

[1] T. Güray, E. Açikkalp, C. Öğretir, S. Yarlıgan, J. Mol. Graphics Modell. 26 (2007) 154-165.

[2] K. Gemma, R. Fernando, W. Graeme, R. Isabel, Bioorg. Med. Chem. 15 (2007) 2850–2855.

Acknowledgements

We are grateful to ESOGU for financial support through Research Project No: 200519010 and ESOGU Research Project No: 200819015.

Ab Initio Calculations of pK_a Values for 7-Acetoxy coumarin-3-Carboxylic Acid

Sinem Aydemir¹, Murat Duran², Erol Tasaş¹, Halil Berber³, Cemil Öğretir², M. Selami Kılıçkaya¹

¹Department of Physics, Faculty of Arts & Sciences, Eskişehir Osmangazi University, 26480 Eskişehir, Turkey

²Department of Chemistry, Eskişehir Osmangazi University, 26480 Eskişehir, Turkey

³Department of Chemistry, Faculty of Arts & Sciences, Anadolu University, 26470 Eskişehir, Turkey

In our study, *ab initio* calculations on 7-Acetoxy coumarin-3-Carboxylic Acid and its deprotonation mechanism was evaluated by theoretical calculations. The acidity constants, pK_a values have been determined by using B3LYP/6-31G(d) basis sets of density functional theory (DFT) along with physical and thermodynamic parameters. The geometries of all the structures have been fully optimized with the Gaussian-03 programme using the hybrid B3LYP method with a 6-31G* basis set. The *ab initio* geometries have been used in calculating the solvation free energies carried out using at he B3LYP/6-31G(d). The conversion factor of 1 Hartree = 627.5095 kcal mol⁻¹ was used since the total energies were given in Hartree.

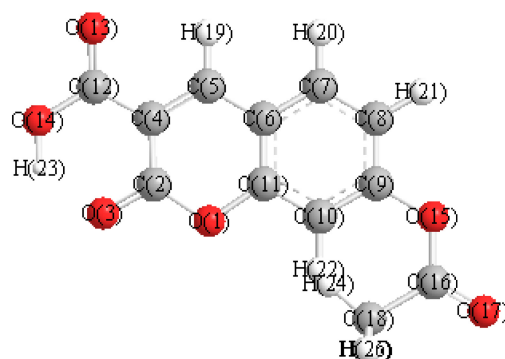


Fig. 1: The molecular structure of 7-Acetoxy coumarin-3-carboxylic acid.

[1] T. Güray, E. Açikkalp, C. Öğretir, S. Yarlıgan, J. Mol. Graphics Modell. 26 (2007) 154-165.

[2] K. Gemma, R. Fernando, W. Graeme, R. Isabel, Bioorg. Med. Chem. 15 (2007) 2850–2855.

Acknowledgements

We are grateful to ESOGU for financial support through Research Project No: 200519010 and ESOGU Research Project No: 200819015.

An Effective Scaling Frequency Factor Method (ESFF) for Scaling of Harmonic Vibrational Frequencies

Piotr Borowski¹, Manuel Fernández-Gómez²,
Maria-Paz Fernández-Liencrez², Tomás Peña Ruiz²

¹*Faculty of Chemistry, Maria Curie-Skłodowska University, pl. Marii Curie-Skłodowskiej 3,
20-031 Lublin, Poland*

²*Department of Physical and Analytical Chemistry, University of Jaén, 23071 Jaén, Spain*

A novel method for scaling of harmonic vibrational frequencies that follow from the solution of Wilson-Decius-Cross equations, named the ESFF method, was proposed [1]. The basic assumption of the method is construction of the so-called effective scaling factor for each normal mode, which takes into account contributions from local modes to that normal mode. The contributions are established from the diagonal elements of the potential energy distribution (PED) matrix. Then given the set of scaling factors for local modes, effective scaling factors for normal modes are obtained as their PED-weighted sums. The determination of local scaling factors can be done by means of the least-squares fitting method, i.e. we search for the local factors that minimize the least-squares merit functional for a given set of well assigned experimental vibrational bands of a given set of molecules.

The ESFF method at the DFT/B3LYP/6-311G** level was initially applied to toluene molecule [1] and the results were compared to these obtained with the well-established SQM (Scaled Quantum Mechanical) method [2]. Substantial reduction of the RMS value for 19 assigned frequencies in the range of 3000-400 cm⁻¹ (3.29 vs. 2.48 cm⁻¹ in favor of the ESFF method) was observed in this case. This improvement was achieved with the aid of 5 (!) rather than 8 (like in the case of the SQM approach) local scaling factors.

A number of tests of the ESFF approach have been carried out since then. Each time the ESFF results (scaled frequencies) were somewhat or even significantly better than the corresponding SQM results. For example, the set consisting of three related, but with different structural motifs, molecules, i.e. toluene, styrene and 4-methylstyrene, was considered. Careful selection of bands in the range of 3000-400 cm⁻¹ resulted in the set of 66 wavenumbers. Different statistical experiments clearly show superiority of the ESFF approach over the SQM method. In particular, the reduction of the RMS value from 4.69 cm⁻¹ for SQM down to 3.32 cm⁻¹ for ESFF with the same number of local scaling factors was observed. In addition, initial tests of the factors' transferability problem were also carried out. First, the local scaling factors were calculated on the basis of "pure" vibrational modes that appear in the selected set, i.e. modes for which the contribution of one of the local modes was found to be higher than 60%. However, the effective scaling factors were calculated for all 66 modes. Scaled frequencies, both for "pure" and delocalized modes, turned out to be of basically the same quality as previously (an increase of the RMS value by 0.06 cm⁻¹ was obtained). Second, the local scaling factors found from the set of bands of three considered molecules gave the scaled frequencies for toluene which are of comparable quality as these obtained with the aid of local factors optimized for toluene itself.

The ESFF method is now tested using the training set of molecules proposed by Baker and coworkers [2] and the results are again very promising.

[1]Piotr Borowski, Manuel Fernández-Gómez, Maria-Paz Fernández-Liencrez, Tomás Peña Ruiz, Chem. Phys. Lett. 446 (2007) 191-198.

[2] Jon Baker, Andrzej A. Jarzecki, Peter Pulay, J. Phys. Chem. 102 (1998) 1412-1424.

Analysis of the Vibrational Spectrum of P-Methyl Styrene Based on IR, Raman and INS Data and *Ab Initio* and DFT Calculations

Manuel Quesada Rincón¹, Manuel Fernández-Gómez¹, M^a Paz Fernández-Liencre¹,
Tomás Peña Ruiz¹, Piotr Borowski²

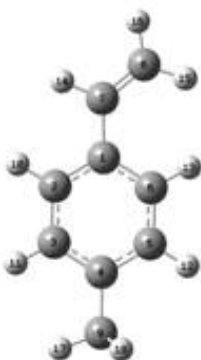
¹Department of Physical and Analytical Chemistry, University of Jaén, Campus "Las Lagunillas", sn.
E-23071 Jaén, Spain

²Faculty of Chemistry, Maria Curie-Skłodowska University, pl. Marii Curie-Skłodowskiej 3,
20-031 Lublin, Poland

An investigation of the geometric structure, force field and fundamental vibration wavenumbers of p-methylstyrene molecule (Fig.) has been carried out by using *ab initio* and density functional theory (DFT) and scaling methods. The experimental data used as reference in the scaled force field have been those from IR, Raman and Inelastic Neutron Scattering (INS) spectra recorded by us.

In the harmonic oscillator approach, the fundamental vibrational wavenumbers, IR intensities and thus the predicted IR spectra of the p-methylstyrene were calculated by using DFT/B3LYP method with 6-31G* and 6-311++G** basis set. The vibrational wavenumbers calculated with DFT/B3LYP were scaled by using two different methods: 1) The SQM method developed by Pulay et al. [1, 2] 2) The wavenumber-linear scaling method (WLS) proposed by Yoshida et al. [3] This all has allowed us to propose a new assignment which checks and extends the existing one [4, 5].

The WLS method uses linear relationships between the scaling factor, defined as the ratio between observed and calculated frequencies, and the calculated ones. This method turns out to be a very useful tool for a fast approach to the assignment of the vibrational spectrum of p-methylstyrene. As for SQM method, the scaling procedure has been carried out in different steps. First a unique scale factor, 0.928 as recommended for B3LYP/6-31G* level was used regardless of the internal natural coordinates. Then this unique factor was refined in order to fit the experimental frequencies. Afterward, a set of 9 independent scale factors associated with the natural internal coordinates was used; and finally this set was also refined in order to reproduce the experimental frequencies.



- [1] P. Pulay, G. Fogarasi, G. Pongor, J.E. Boggs, J.A. Varga, *J. Am. Chem. Soc.* 105 (1983) 7037.
- [2] G. Fogarasi, X. Zhou, P.W. Taylor, P. Pulay, *J. Am. Chem. Soc.* 114 (1992) 8191.
- [3] A. Yoshida, A. Ehara, H. Matsuura, *Chem. Phys. Lett.* 325 (2000) 477.
- [4] B.J. Ansari, *Indian J. Pure Appl. Phys.* 8 (1979) 725
- [5] P.P. Garg, R.M.P. Jaiswal, *Indian J. Pure Appl. Phys.* 27 (1989) 75.

Denoising Raman Spectra of Biological Samples Using Wavelets

O. Gamulin¹, M. Kosović¹, M. Balarin¹, D. Krilov¹, J. Brnjas-Kraljević¹

University of Zagreb, Medical school, Department of Physics and Biophysics, Šalata 3, Zagreb, Croatia

A range of applications of Raman spectroscopy in investigations of biological systems is emerging rapidly. The spectral analysis of these systems is difficult because of their complexity, and the noise superimposed on Raman signals.

Increasing the laser power and increasing the number of co-added scans are two standard methods to improve signal to noise (S/N) ratio. However, they are often counter productive. The former destroys the sample, and the latter changes sample properties because of drying.

In this work, we use wavelet transform to improve S/N ratio [1]. We apply different wavelet denoising methods [2] (fixed form threshold, SURE, Minimax, Penalize, Wavelet packet) to Raman spectra with different levels of S/N ratio, and analyze their efficiency. Two efficiency criterions were defined. One is the number of preserved vibrational bands in the denoised spectrum in comparison to the referent spectrum. The second criterion is the preservation of relative intensities of vibrational bands in the denoised spectrum. For this purpose, the series of Raman spectra was recorded from the same sample of rat skull bone. Different levels of S/N ratio in the recorded spectra were achieved by varying the number of scans and the laser power. The spectrum with the best S/N ratio was selected as the reference, and its vibrational bands were assigned using second derivatives. Spectra with smaller S/N ratios were denoised with wavelet transformations and their vibrational bands were assigned and compared with the reference. To check the first efficiency criterion we counted how many vibrational bands assigned to the referent spectrum were preserved in the denoised spectra. For second criterion the ratio of integral intensities of PO₄ and amid I band was compared between denoised and referent spectra. The efficiency of wavelet denoising was also tested for different wavelet families (Haar, Daubechies, Symlets, Coiflets, BiorSplines, ReverseBior, DMeyer), and compared with standard smoothing methods such as Block Averaging and Savitsky-Golay.

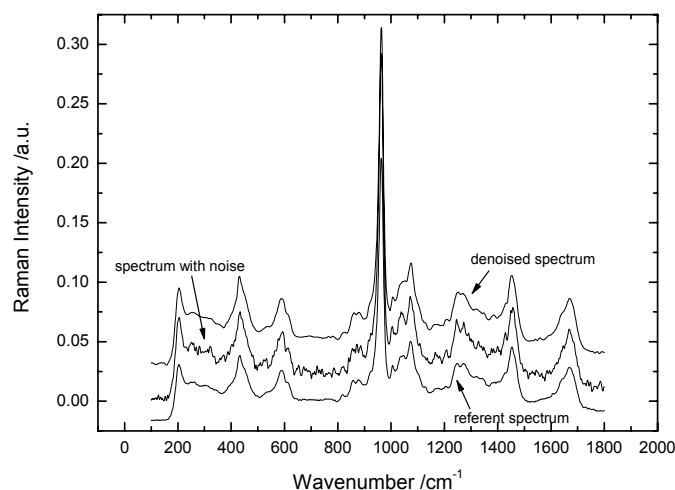


Fig. 1: Comparison of original, denoised and referent spectrum

- [1] C.R. Mittermayr, S.G. Nikolov, H. Hutter, M. Grasserbauer, *Chemometrics and intelligent laboratory systems* 34 (1996) 187-202
- [2] B.K. Alsberg, A.M. Woodward, M.K. Winson, J. Rowland, D.B. Kell, *The Analyst* 122 (1997) 645-652.

New Laser-Electron Nuclear Effects in the Nuclear γ Transition Spectra of Molecular Systems

A.V. Glushkov^{1,2}, S.V. Malinovskaya¹, O.Yu. Khetselius¹

¹Odessa University, P.O.Box 24a, Odessa-9, 65009, South-East, Ukraine

²Institute of Spectroscopy, Russian Acad.Sci., Troitsk-Moscow, 142090, Russia

A new class of problems has been arisen in the modern quantum optics and spectroscopy and connected with modelling of the co-operative laser-electron-nuclear phenomena in molecular systems [1]. It includes a calculation of the probabilities and energies of the mixed γ -optical quantum transitions in atoms and molecules, intensities of the complicated γ -transitions due to the changing of the molecular excited states population under action of laser radiation, quantum chemical calculation of the complex "laser-nuclear-molecule" systems. Due to the emission or adsorption of the nuclear γ -quantum in molecules there is changing the electron vibration-rotation states. As result, general energetic and spectral properties of system are changed. We at first develop a new, consistent, quantum-mechanical approach to calculation of the electron-nuclear γ transition spectra (set of vibration satellites in molecule) of nucleus in molecule, based on the relativistic density functional (DF) formalism and energy approach (S-matrix formalism of Gell-Mann and Low) [1,2]. Decay and excitation probability are linked with imaginary part of the molecule - field system. Calculation results of electron-nuclear γ -transition spectra of the nucleus in some atomic and multiatomic systems are given. As illustration in fig. 1 a spectrum of emission and adsorption of nucleus ^{127}I ($E_\gamma = 203$ keV) in molecule of H^{127}I is presented (the initial state of molecule: $\nu_a = 0, J_a = 0$). Estimates are made for vibration-nuclear transition probabilities for number of molecules: diatomics, three-atomic XY_2 ($D_{\infty h}$), four-atomic XY_3 (D_{3h}), five-atomic XY_4 (T_d), six-atomic XY_3Y_2 (D_{3h}), seven-atomic XY_6 (O_h) ones.

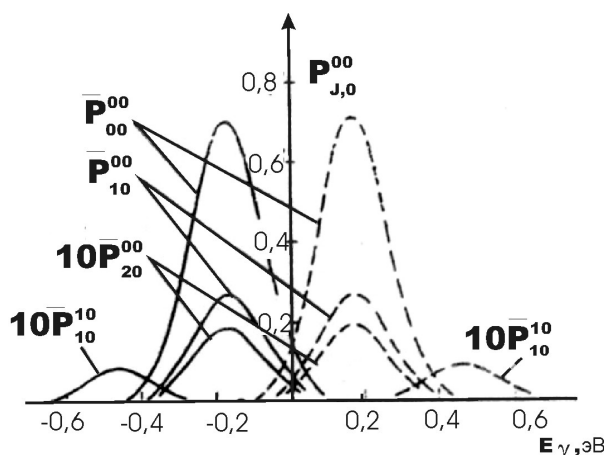


Fig. 1: Spectrum of emission and adsorption of nucleus ^{127}I ($E_\gamma = 203$ keV) in molecule of H^{127}I .

- [1] L.N. Ivanov, V.S. Letokhov, JETP 93 (1987) 396-404; V. Letokhov, V. Minogin, JETP 69 (1975) 1369-1376; A.V. Glushkov, L. Ivanov, Phys. Lett. A 170 (1992) 33-38.
 [2] A.V. Glushkov, S.V. Malinovskaya, Int. Journ.Quant.Chem. 99 (2004) 889-936; 104 (2005) 496-500; 104 (2005) 512-562; J.Phys.CS, 188 (2005) 199-208.

Spectroscopy of Hadronic Molecules and Molecules with Superheavy Elements: Spectra, Energy Shifts and Widths for Different Nuclear Models

O.Yu. Khetselius¹, A.V. Glushkov^{1,2}, E.P. Gurnitskaya¹, A.V. Loboda¹

¹*Odessa University, P.O.Box 24a, Odessa-9, 65009, South-East, Ukraine*

²*Institute for Spectroscopy, Russian Acad. Sci., Troitsk, Moscow reg., 142090, Russia*
e-mail: glushkov@paco.net

A great interest to studying the superheavy elements and their molecular compounds has been stimulated by inaugurating the heavy-ion synchrotron storage cooler ring combination SIS/ESR at GSI. With this facility, which allows to produce, store and cool fully stripped heavy ions beams up to U^{92+} and to create the superheavy molecules [1], new ways are opened in the field of molecular and nuclear spectroscopy from this side. Paper is devoted to studying the spectra, potential curves, radiative corrections for hadronic molecules and molecules with superheavy elements X113, X114 with account of the definite nucleus structure modelling. One of the main purposes is establishment a quantitative link between quality of the nucleus structure modelling and accuracy of calculating energy and spectral properties of the molecular systems. We apply our numerical code [2] to calculating spectra of the hadronic (pion, kaon, hyperon) molecules. A new ab initio approach [2] to relativistic calculation of the spectra for superheavy molecules (XH) with an account of relativistic, correlation, nuclear, radiative effects on the basis of gauge-invariant QED perturbation theory is proposed. Zeroth approximation is generated by the effective ab initio model functional, constructed on the basis of the comprehensive gauge invariance procedure [2]. The wave functions zeroth basis is found from the Klein-Gordon (pion atom) or Dirac (kaon, hyperon) equation. The potential includes the core ab initio potential, the electric and polarization potentials of a nucleus (the Fermi and Gauss models and the uniformly charged sphere model are considered). For low orbits there are important effects due to the strong hadron-nuclear interaction (pion system. The energy shift is connected with length of the hadron-nuclear scattering (scattering amplitude under zeroth energy). For superheavy elements the correlation corrections of high orders are accounted within the Green functions method. The magnetic inter-electron interaction is accounted in the lowest order, the Lamb shift polarization part – in the Uhling-Serber approximation, self-energy part – within the Green functions method. We are carrying out the calculation of the following systems :1).energy levels, hfs parameters for superheavy X113, X114 atoms and one-centre studying the spectra and potential energies for the XH molecules for different models of charge distribution in a nucleus; 2). Shifts and widths of transitions (2p-1s,3d-2p, 4f-3d) in some exotic pionic and kaonic molecules with ^{18}O , ^{24}Mg etc. and also $K^{-4}He$.

- [1] C. Betty, E. Friedman, A. Gal et al., Phys. Rep. 287 (1997) 385-470; A.V. Glushkov et al., In: New Projects and New lines of research in Nuclear Physics, eds. G. Fazio, F. Hanappe, World Sci., Singapore (2003) 142-158.
- [2] A.V. Glushkov, L.N. Ivanov, Phys. Lett. A. 170 (1992) 33-38; A.V. Glushkov, E.P. Ivanova, J. Quant. Spectr. Rad. Tr. (US) 36 (1986) 127-148; Preprint ISAN N3, Moscow (1992); A.V. Glushkov et al., In: Low Energy Antiproton Phys., AIP Series 796 (2005) 211-215. Recent Advances in Theory of Phys. and Chem. Systems (Springer) 15 (2006) 185-300; Ibid. 15 (2006) 301-308.

Density Functional Calculation of Raman Intensity in High Pressure Phases of TiO₂ crystal

D. Kirin¹, I. Lukačević³, S.K. Gupta², P.K. Jha²

¹ *Ruder Bošković Institute, Bijenička c. 54, 10002 Zagreb, Croatia*

² *Department of Physics, University of Bhavnagar, Bhavnagar, India*

³ *Department of Physics, J.J Strossmayer University, 31000 Osijek, Croatia*

Intensity of Raman lines are important part of the information contained in the vibrational spectra of crystals. Due to the changes in the crystal structure as a response to external perturbation (pressure, temperature) the frequencies, as well as, intensities of Raman active modes change.

We have calculated Raman spectra of different crystal forms of TiO₂ crystal [1] as a function of pressure. The ABINIT density functional program package [2] are used for the calculation of vibrational frequencies and intensities of Raman bands. The values given by calculations are in a fair agreement with the observed positions of phonons as a function of pressure. The possibility to use Raman intensities as additional tool in the study of phase transitions is discussed.

[1] K. Legarec and S. Desgreniers, *Solid State Comm.* 94 (1995) 519–524.

[2] The ABINIT code is a common project of Universite Catholique de Louvain, Corning, Incorporated and other contributors (www.abinit.org).

Computer Analysis of ATR-FTIR Spectra of Paint Samples for Forensic purposes

Małgorzata Szafarska¹, Michał Woźniakiewicz¹, Mariusz Pilch¹,
Janina Zięba-Palus², Paweł Kościelniak^{1,2}

¹ Jagiellonian University, Faculty of Chemistry, R. Ingardena Str. 3, 30-060 Kraków, Poland

² Institute of Forensic Research, Westerplatte Str. 9, 31-033 Kraków, Poland

Infrared spectrometry is the method commonly applied to analytical examination of different materials for forensic purposes [1]. The advantage of this method is its non-destructive character as well as the possibility of identifying the main functional groups and structural elements of samples examined. However, IR investigations of such physical evidences as paint samples (microchips, smears on fabric), inks (on documents) and fibres are especially difficult. The reason is that the samples are often very small and, in addition, it is not usually possible to separate them entirely from the base.

An analytical tool offering quite unusually the possibility to examine the criminalistic traces without their prior separation from base is Attenuated Total Reflectance Fourier Transform Infrared (ATR-FTIR) technique. However, in case of ATR analysis of paints coats the influence of the base is usually significant hence the bands of not only a paint but also of the base are present in the reflection spectra. As a consequence, identification of the paint is very difficult or even impossible in practice. Therefore, this study was aimed to develop a mathematical approach allowing the undesired bands to be effectively eliminated from the paint spectra.

The Method of Subtraction and Normalization of IR Spectra (MSN-IR) was developed and successfully applied to extract the pure paint spectrum from the spectrum of paint coat on different bases acquired by the ATR-FTIR technique. The examined spectra (pure base and sample spectrum) were normalized in an iterative manner by the division by every each point of the calculated spectra. Number of obtained normalized spectra was equal with number of original spectrum points. Then, every normalized pure base spectrum were subtracted from every spectrum of the paint on foil (fabric). The subtractive results and the standard (pure paint) spectra were also normalized and after repeated process of comparison the final spectrum with the highest 'similarity' to the standard spectrum was found. The best subtraction was obtained when the value of correlation factor endeavored to zero.

The utility of the MSN-IR has been confirmed by analyses of several different paints sprayed on plastic (polyester) foil and fabric materials (cotton). A few examples of paint spectra obtained by the computer calculation were compared with those acquired from pure paints. It was found that proposed numerical algorithm allowed – in contrast to other mathematical approaches conventionally used for this aim – a pure paint IR spectrum to be effectively extracted without a loss of chemical information provided. Moreover, this approach is able to reduce the time consumption and to improve the reproducibility of spectral subtraction. The results obtained prove that the proposed procedure is a useful tool which could be applied in forensic discrimination and group identification of paints.

[1] J. Zięba-Palus, *J. Mol. Struct.* 511/512 (1999) 327–335.

Comparison of Theoretical Intensity Calculations and Experimental Intensities Measurements for Non Linear Triatomic Molecules

J. Lamouroux¹, V.I.G. Tyuterev¹, L. Régalia-Jarlot¹, S.A. Tashkun²

¹Université de Reims, G.S.M.A (U.M.R 6089), Campus du Moulin de la Housse, B.P. 1039, 51067 Reims Cedex 2, France

²Laboratory of Theoretical Spectroscopy, Institute of Atmospheric Optics, SB RAS, 1, Akademicheskii av., 634055 TOMSK, Russia

The knowledge of the infrared spectra of the atmospheric molecules is of the first importance for the atmospheric and metrological applications. Both measurements and calculations of lines intensities are necessary to complete spectroscopic databases.

Intensity calculations can be performed in different ways : one employs variational [1, 2] or DVR [3] methods using *ab initio* dipole moment functions, another one relies on effective spectroscopic models involving empirically determined *transition moment parameters* [4-6] specific for individual rovibrational bands. We report recent results based on a synthetic approach [7, 8] that allows a derivation of accurate values of transition moment parameters for ro-vibrational bands from molecular potential energy surface and dipole moment functions for non-linear triatomic molecule of the C_{2v} and C_s symmetry groups. Predictions of transition moment band parameters in case of isotopic substitutions including a symmetry breaking one: $C_{2v} \rightarrow C_s$ will be discussed.

Comparisons between the theoretical intensity calculations and the experimental measurements for non-linear triatomic molecule of the C_{2v} and C_s symmetry groups as the water molecule H_2O and the deuterated sulphide hydrogen isotopologues D_2S and HDS will be presented. For the water molecule, these comparisons are possible as a lot of intensity data are available in the literature. Concerning the $D_2^{32}S$ and $HD^{32}S$ isotopologues, no intensity data were available, so we performed the first intensities measurement for the first and second triad bands [9]. The experimental intensities measurements were carried out by multispectrum fitting procedure [10] using the high resolution infrared spectra recorded with the Fourier transform spectrometer of Reims University. Comparisons between variational and algebraic methods of calculations are also discussed.

- [1] H. Partridge, D.W. Schwenke, J. Chem. Phys. 106 (1997) 4618; 113 (2000) 6592.
- [2] W. Gabriel, E.-A. Reinsch, P. Rosmus et al., J. Chem. Phys. 99 (1993) 897.
- [3] J. Tennyson (and references therein), in Jensen P. Bunker P.R.(Eds.), Computational Molecular Spectroscopy, Wiley & Sons, Chichester, 2000, p305.
- [4] C. Camy-Peyret, J.M. Flaud, Molecular Spectroscopy: Modern Research III (1985), Ed. K.N. Rao, p69; M.R. Aliev, J.K.G. Watson, *ibid*, p1.
- [5] O.N. Sulakshina, Yu. Borkov, V.I.G. Tyuterev and A. Barbe, J. Chem. Phys. 113 (2000) 10572.
- [6] S. Kassi, A. Campargue, M.-R. De Backer-Barilly and A. Barbe, J. Mol. Spectrosc. 244 (2007) 122-129.
- [7] J. Lamouroux, Thesis, Université de Reims (2007)
- [8] J. Lamouroux, S.A. Tashkun and V.I.G. Tyuterev, Chem. Phys. Lett. 452 (2008) 225.
- [9] J. Lamouroux, L. Régalia-Jarlot, V.I.G. Tyuterev, X. Thomas, P. Von der Heyden, S.A. Tashkun and Yu. Borkov, J. Mol. Spectrosc. in press.
- [10] J.J. Plateaux, L. Régalia, C. Boussin and A. Barbe, J. Quant. Spectrosc. Radiat. Transfer 68 (2001) 507-520.

Correlating the Force Fields of Methylpyrazines: Vibrational Spectrum of Tetramethylpyrazine

I. López-Tocón, J.F. Arenas, S.P. Centeno, D. Pelaez and J.C. Otero

Department of Physical Chemistry, Faculty of Science, University of Málaga, E-29071 Málaga, Spain.

Raman and Infrared spectra of tetramethylpyrazine (tetra-MPz) have been recorded and the *ab initio* calculated force field has been refined following the scaled quantum mechanical force field (SQMFF) methodology by Pulay [1]. It is well-known that the *ab initio* quantum chemical calculations overestimate the vibrational wavenumbers and then, scale factors are usually employed to fit the calculated frequencies to experimental ones. Moreover, this method allows us to transfer the scale factors among structurally related molecules yielding a priori estimation of the fundamental vibrational frequencies. In this case, the scale factors are directly transferred from 2-methylpyrazine [2]. The scaled frequencies of tetra-MPz agree quite well with the experimental ones in the whole spectral range.

In addition, the assignment of the vibrational spectrum of tetra-MPz has been compared with that of pyrazine and other methylpyrazines in order to determine how affects the substitution of the aromatic ring on the vibrational frequencies and to check the transferability of the scale factors. It is demonstrated that the scaled force fields of the methylpyrazine series obtained by transferring the scale factor reproduce the experimental frequency shifts as happen in substituted benzene derivatives.

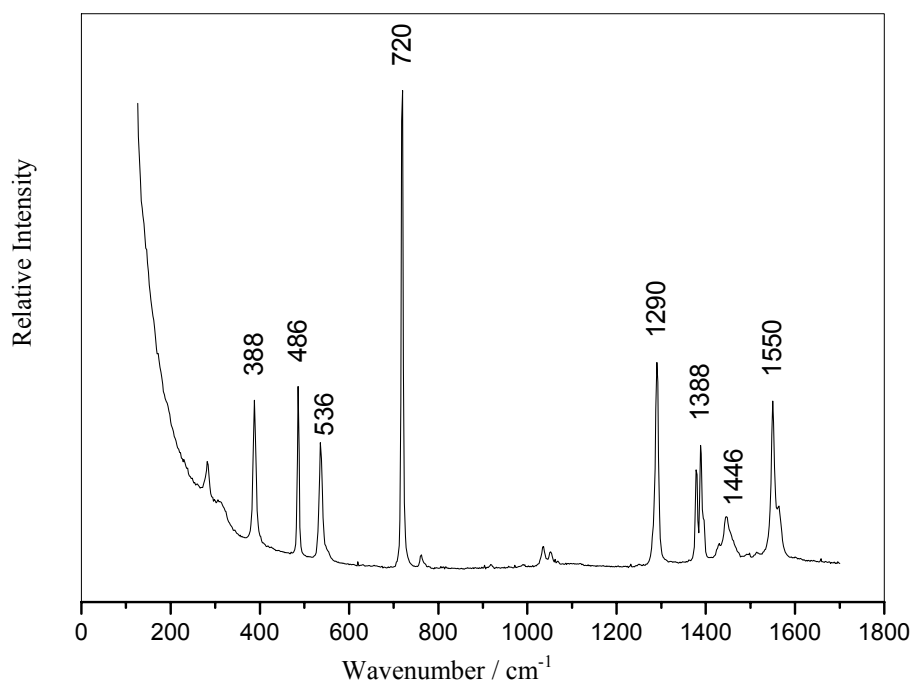


Figure 1: Raman spectrum of a 1M aqueous solution of tetra-MPz.

[1] P. Pulay, G. Fogarasi, J.E. Boggs, J. Chem. Phys. 74 (1981) 3999.

[2] J.F. Arenas, I. López-Tocón, J.C. Otero, J.I. Marcos, Vibr. Spectrosc. 19 (1999) 213.

Matrix Isolation FTIR Spectroscopic and Theoretical Study of Dimethyl 2,2-Dioxo-1*H*,3*H*-Pyrazolo[1,5-*c*][1,3]Thiazole-6,7-Dicarboxylate

C.M. Nunes, S. Lopes, T.M.V.D. Pinho e Melo, R. Fausto

Department of Chemistry, University of Coimbra, P-3004-535 Coimbra, Portugal.

Heterocyclic compounds play a central role in chemistry. They have a wide range of applications and represent about half of the known organic compounds. The discovery of new heterocyclic systems and the understanding of their properties and structure are important research topics. Our efforts have been focussed on the study of pericyclic reactions of extended dipoles such as azafulvenium methides and diazafulvenium methides in order to develop new routes to heterocyclic compounds [1, 2]. The diazafulvenium methides can be generated from the thermal extrusion of sulfur dioxide from 2,2-dioxo-1*H*,3*H*-pyrazolo[1,5-*c*][1,3]thiazoles making relevant the gathering of information on the chemistry and structure of 2,2-dioxo-1*H*,3*H*-pyrazolo[1,5-*c*][1,3]thiazoles.

In this study, dimethyl 2,2-dioxo-1*H*,3*H*-pyrazolo[1,5-*c*][1,3]thiazole-6,7-dicarboxylate (DPTD) has been synthesized and its monomeric structure studied by DFT calculations. A systematic search of the preferred conformations of DPTD on the ground state potential energy surface and their vibrational spectra was performed using the Gaussian 03 program at the DFT(B3LYP)/6-31+G(p) and DFT(B3LYP)/6-311++G(p,d) levels of theory.

The compound has also been studied by Matrix Isolation FTIR spectroscopy (in both argon and xenon matrices) and in the condensed phases: neat amorphous and crystalline solid states. Finally, the photochemical behaviour of the matrix isolated DPTD monomer was investigated through *in situ* broadband irradiation using a standard Hg(Xe) lamp as UV-light ($\lambda > 235$ nm) source.

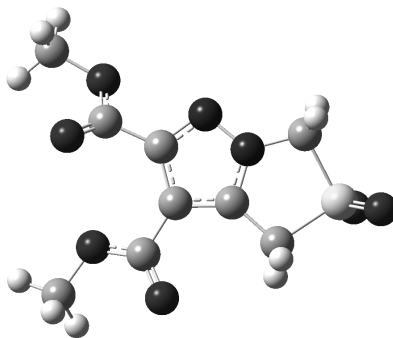


Fig. 1: Structure of the most stable conformer of DPTD.

- [1] (a) T.M.V.D. Pinho e Melo, M.I.L. Soares, A.M.d'A. Rocha Gonsalves, H. McNab, *Tetrahedron Lett.* 45 (2004) 3889-3893; (b) T.M.V.D. Pinho e Melo, M.I.L. Soares, A.M.d'A. Rocha Gonsalves, J.A. Paixão, A. Matos Beja, M. Ramos Silva, *J. Org. Chem.* 70 (2005) 6629-6638; (c) T.M.V.D. Pinho e Melo, M.I.L. Soares, C.M. Nunes, *Tetrahedron* 63 (2007) 1833-1841; (d) A. Kaczor, T.M.V.D. Pinho e Melo, M.I.L. Soares, R. Fausto, *J. Phys. Chem. A* 110 (2006) 6531-6539.
- [2] (a) T.M.V.D. Pinho e Melo, M.I.L. Soares, A.M.d'A. Rocha Gonsalves, *Tetrahedron Lett.* 47 (2006) 791-794; (b) T.M.V.D. Pinho e Melo, M.I.L. Soares, C.M. Nunes, J.A. Paixão, A. Matos Beja, M. Ramos Silva, *J. Org. Chem.* 72 (2007) 4406-4415.

Acknowledgements

This work was funded by FCT (Projects POCTI/QUI/58937/2004 and POCTI/QUI/59019/2004), and the Instituto de Investigação Interdisciplinar of the University of Coimbra (Project III/BIO/40/2005). C.M. Nunes acknowledges FCT the Ph.D. grant (SFRH/BD/28844/2006).

Experimental, Ab Initio and Density Functional Theory Studies on Sulfadiazine

Gulce Ogruc-Ildiz¹, Sevim Akyuz¹, Aysen E. Ozel²

¹Istanbul Kultur University, Science and Letters Faculty, Physics Department, Atakoy Campus, 34156 Bakirkoy, Istanbul, Turkey

²Istanbul University, Science Faculty, Physics Department, Vezneciler 34134, Istanbul, Turkey

Sulfadiazine is a member of the sulfonamides or sulfa drugs and widely used as antibacterial agents. It is used for the treatment of a variety of infections, including toxoplasmosis, an infection of the brain. It can also be used to prevent certain types of meningococcal disease.

In this study combined experimental and computational study on molecular vibrations of free sulfadiazine has been reported. Harmonic and anharmonic wavenumbers of the molecule have been calculated by the aid of Gaussian03 program package and by ab initio HF and DFT methods at B3LYP/6-31++G(d,p) levels of theory. The theoretically possible stable conformers of free sulfadiazine molecule in electronically ground state were searched by means of torsion potential energy surfaces scan studies at both semi-empirical PM3 and B3LYP/3-21G levels of theory. The possible conformers of the molecule were determined by varying the dihedral angles C1-C7-S8-N9, C7-S9-N9-C10 and S8-N9-C10-N11. The geometry optimizations of the stable conformers were performed. The vibrational normal modes of each conformer and associated wavenumbers, IR intensities and Raman activities were calculated and the results were compared with those of experimental findings. The fundamental vibrational modes were assigned depending on their total energy distribution. The theoretically constructed spectra coincide satisfactorily with those of experimental spectra.

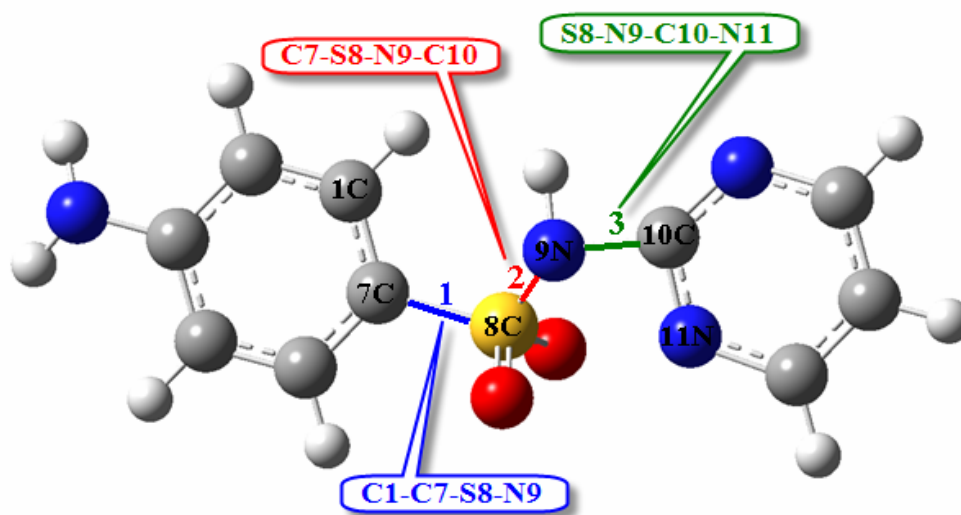


Fig. 1: The model of sulfadiazine molecule

New Spectroscopic Studies of the Fourth-Positive ($A^1\Pi \rightarrow X^1\Sigma^+$) System Bands in $^{13}\text{C}^{16}\text{O}$

R. Kępa, M. Ostrowska-Kopec

*Atomic and Molecular Physics Laboratory, Institute of Physics,
University of Rzeszów, 35-959 Rzeszów, Poland*

The present work puts forward the results of the observation carried out under high resolution by conventional, photographic spectroscopy and modern analysis of thirteen bands with $v' = 7-12$ and $v'' = 16-24$ of the fourth-positive ($A^1\Pi \rightarrow X^1\Sigma^+$) band system.

The current investigations include much greater than until now [1-3] region of the observed $^{13}\text{C}^{16}\text{O}$ molecule spectrum. Especially, new transitions connected with not hitherto observed $v' = 12$ vibrational level of $A^1\Pi$ state were recorded and studied. Otherwise, the region of perturbations observed in the first excited state of the fourth-positive system was significantly enlarged. The observed perturbations were confronted with those predicted from the theoretical calculations.

- [1] S.G. Tilford and J.D. Simmons, *J. Phys. Chem. Ref. Data* 1 (1972) 147-188.
- [2] J. Domin, *Acta Phys. Hung.* 60(1-2) (1986) 43-47.
- [3] C. Haridass and K.P. Huber, *ApJ* 420 (1994) 433-438.

Vibrational Spectroscopic Investigation of Free and Coordinated 5-Aminoquinoline: The IR, Raman and DFT Studies

Aysen E. Ozel¹, Sefa Celik¹, Sevim Akyuz²

¹*Istanbul University, Science Faculty, Physics Department, Vezneciler 34134, Istanbul Turkey*

²*Istanbul Kultur University, Science and Letters Faculty, Physics Department, Atakoy Campus, 34156 Bakirkoy, Istanbul, Turkey*

Quinoline family compounds are of great interest in pharmacy and widely used as a parent compound to make drugs. In this study experimental IR and Raman spectra of 5-aminoquinoline (5-AQ) and its zinc halide complex $\{Zn(5-AQ)_2Cl_2\}$, together with the computational results of free AQ and its hydrogen bonded complex $\{H_2O-5AQ\}$ have been reported. For computational studies Gaussian 03 program package were used. The geometry of the free 5-AQ and 5-AQ interacting with H_2O through the ring nitrogen, were optimized using both ab initio HF and DFT methods at B3LYP/6-31++G(d,p) levels of theory. Harmonic and anharmonic vibrational frequencies and infrared intensities were calculated at the same level of theory. The Total Energy Distribution (TED) of the vibrational modes of the molecules was calculated with the Scaled Quantum Mechanics (SQM) method by using Parallel Quantum Mechanics Solutions (PQS) program and the fundamental vibrational modes were characterized by their total energy distribution. Experimental and theoretical results allowed us to determine the presence of intra and inter-molecular interactions and to discuss their strengths.

Hindered Rotation in the Infrared Spectra of HCl in Liquefied Rare Gases

A. Padilla, J. Pérez

Departamento de Física Fundamental y Experimental, Electrónica y Sistemas. Facultad de Física, Universidad de La Laguna. 38205, La Laguna, Tenerife, Spain

Infrared spectra of hydrogen halides in non polar solutions have been widely analyzed as a prototype of changes in the spectra of molecules in solution.

The more intriguing fact is that together with the P and R branches, which correspond to the envelopes of the low density gas spectra, it appears a central prominent resonance (Q branch) in the region where absorption is forbidden by the rotational selection rules for the isolated molecule.

The nature of the Q branch has been object of discussion along the last decades, and a large list of both theoretical and experimental works have been developed around this matter.

In a recent work [1] it has been proved that this Q branch is shifted from the vibrational fundamental frequency, being this shift correlated with that of the stretching mode of the $\text{HX}\cdots\text{solvent}$ Van der Waals complex.

A second effect discussed in that work is that the intensity of the Q branch is correlated with the loss of intensity of the region corresponding to transitions between the lower energy rotational states, and a simplified model was developed to reproduce the corresponding profiles.

In this model it is assumed that the solute molecule is able to rotate freely in the liquid, only when the sum of its translational and rotational energy is greater than the potential barrier corresponding to the anisotropic interaction between the solvent and the solute molecules.

The objective of this work is to show how this effect can also be seen in the far infrared spectra, comparing those of the HCl in Ar, Kr and Xe at different temperatures, and to analyze the comparative results between the pure rotational and vibration-rotation spectra.

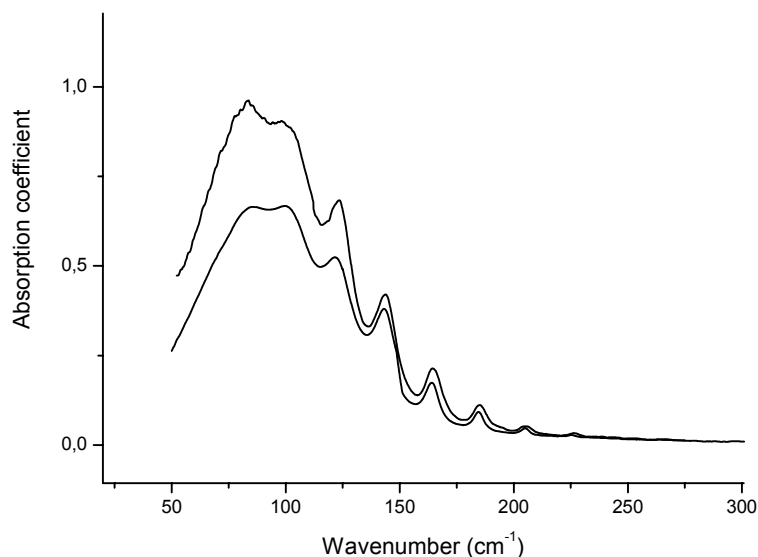


Fig. 1: Far infrared spectra of HCl in liquid Kr (top) and Xe (bottom) at $T = 165$ K [2].

[1] J. Pérez, A. Padilla, W.A. Herrebout, B.J. Van der Veken, A. Calvo Hernández and M.O. Bulanin. *J. Chem. Phys.* 122 (2005) 194507.

[2] W. Herrebout, B.J. Van der Veken, A. Medina, A. Calvo Hernández and M.O. Bulanin. *Mol. Phys.* 96 (1999) 1115.

New Analysis of the Comet–Tail ($A^2\Pi_i \rightarrow X^2\Sigma^+$) System Bands in $^{12}\text{C}^{18}\text{O}^+$

R. Kepa, I. Piotrowska

*Atomic and Molecular Physics Laboratory, Institute of Physics,
University of Rzeszów, 35-959 Rzeszów, Poland*

Four bands (with $v' = 2-5$ and common $v'' = 0$) of the comet–tail ($A^2\Pi_i \rightarrow X^2\Sigma^+$) band system were recorded under high resolution by conventional, photographic spectroscopy and modern analysis of them was carried out. The current investigations include much greater than until now [1, 2] region of the observed $^{12}\text{C}^{18}\text{O}^+$ molecule spectrum. In particular, the 5-0 band were recorded and studied for the first time.

Thanks to application of high resolution it was possible to record the complete set of twelve branches in all studied bands. The great precise of the measurements and use of commonly accepted theoretical model allowed us to obtain full spectroscopic characteristic of analyzed excited vibrational levels $v' = 2-5$ of the upper $A^2\Pi_i$ state. Especially, the values of A_D , p and q molecular constants for the $v' = 2, 3, 4$ and all rotational parameters for $v' = 5$ were extracted for the first time. Otherwise, the first values of the numerous equilibrium constants, as well as RKR parameters and experimental term values were calculated. Finally, Franck–Condon factors and r–centroids for the comet–tail bands were provided.

[1] R.K. Dhumwad, A.B. Patwardhan and V.T. Kulkarni, *J. Mol. Spectrosc.* 78 (1979) 341–343.

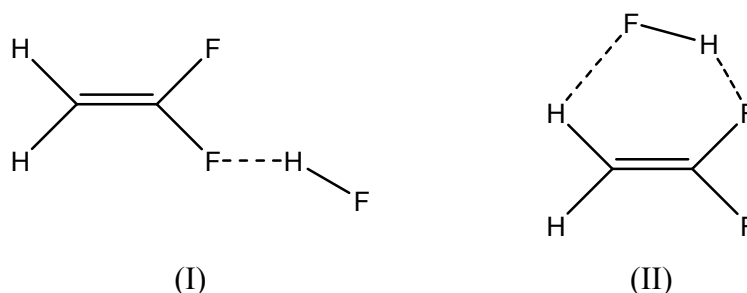
[2] B.R. Vujisić and D.S. Pešić, *J. Mol. Spectrosc.* 128 (1988) 334–349.

A Theoretical Study of the Hydrogen Bonding between vic-, cis- and trans-C₂H₂F₂ Isomers and Hydrogen Fluoride

Victor H. Rusu, João Bosco P. da Silva, Mozart N. Ramos

Departamento de Química Fundamental, Universidade Federal de Pernambuco, 50.670-901, Recife (PE), Brasil

MP2/6-31++G(d,p) and B3LYP/6-31++G(d,p) theoretical calculations have been used to investigate the hydrogen bonding formation involving vic-, cis- and trans-C₂H₂F₂ isomers and hydrogen fluoride. Our calculations have revealed the existence of two possible hydrogen complexes. In both cases, hydrogen fluoride acts as a proton donor, as shown below to cis-C₂H₂F₂⋯HF:



where their binding energies including BSSE and ZPE corrections are 8.7 kJ.mol⁻¹ and 9.0 kJ.mol⁻¹, respectively, using B3LYP calculations. In all the three isomers for both MP2 and B3LYP calculations, the binding energies for the non-cyclic and cyclic hydrogen complexes are essentially equal, being the cyclic structure slightly more stable. The cyclic complex formation reduces the polarity, in contrast to what occurs with the non-cyclic complex. This result is more accentuated in vic-C₂H₂F₂⋯HF, where Δμ(cyclic) is -3.07D, whereas Δμ(non-cyclic) is +1.92D using B3LYP calculations. The corresponding MP2 values are -1.89D and +0.44D, respectively.

As expected, the complexation produces an H-F stretching frequency downward shift, whereas its IR intensity is enhanced, as it can be seen below:

Complex	Level of Calculation	Δν _{HF} (cm ⁻¹)		A ^C _{HF} /A ^{is} _{HF}	
		(I)	(II)	(I)	(II)
vic-C ₂ H ₂ F ₂ ⋯HF	MP2	-51	-65	3.2	1.8
	B3LYP	-66	-84	3.9	2.4
cis-C ₂ H ₂ F ₂ ⋯HF	MP2	-70	-103	2.9	2.8
	B3LYP	-89	-130	3.7	4.1
trans-C ₂ H ₂ F ₂ ⋯HF	MP2	-98	-107	2.9	2.2
	B3LYP	-127	-136	4.4	2.9

On the other hand, the vibrational modes of vic-, cis- and trans-C₂H₂F₂ isomers are little affected by complexation. The new vibrational modes due to hydrogen bonding formation show several interesting features, in particular the HF bending modes, which are pure rotations in free molecule.

Effects of Wave Function Modifications on Calculated HC and CC Stretching Frequencies in $\text{H}_2\text{C}=\text{CHX}$ and $\text{HC}\equiv\text{CHX}$ Molecules

Mozart N. Ramos¹, Kelson C. Lopes², Victor H. Rusu¹, Regiane C.M.U. Araújo²

¹*Departamento de Química Fundamental, Universidade Federal de Pernambuco (UFPE), 50739-901, Recife (PE), Brasil,*

²*Departamento de Química, Universidade Federal da Paraíba (UFPB), 58036-300, João Pessoa (PB), Brasil*

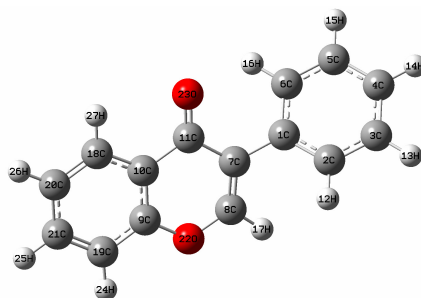
Two-level factorial designs (FD) have been used to determine the effects of wave function modifications on calculated CH and CC harmonic stretching frequencies of the $\text{H}_2\text{C}=\text{CHX}$ and $\text{HC}\equiv\text{CHX}$ molecules with X= H, CH_3 , F, Cl and CN. These modifications were treated at two levels, which consists in: (I) using either a double- or a triple-zeta valence basis set; (II) including or not diffuse functions in basis set, (III) including or not polarization functions in basis set, and (IV) performing a calculation with or without electron correlation beyond the Hartree-Fock level, i.e., MP2 or B3LYP. Our results have shown that valence (VAL), diffuse (DIF), polarization (POL) and electron correlation (CORR) principal effects as well as some second-order interaction effects are significant to build factorial models for these vibrational modes. When valence and diffuse functions are introduced in the basis set, the calculated HC and CC stretching frequencies are decreased in both the $\text{HC}\equiv\text{CHX}$ and $\text{H}_2\text{C}=\text{CHX}$ molecules. For instance, when diffuse functions are used in the basis set, the reductions in ν_{HC} and ν_{CC} are -9.0 cm^{-1} and -13.2 cm^{-1} in $\text{HC}\equiv\text{CHX}$, whereas their corresponding values in $\text{H}_2\text{C}=\text{CHX}$ are -4.1 cm^{-1} and -13.8 cm^{-1} , respectively. However, these reductions are much more accentuated when the electron correlation effect is introduced in the Hartree-Fock wave functions. As expected, by far the correlation principal effect is the most important on the frequency values. This effect provokes a decrease of -281.4 cm^{-1} and -153.5 cm^{-1} in the $\text{C}\equiv\text{C}$ and $\text{C}=\text{C}$ vibrational frequencies, respectively, using the MP2 calculations, whereas this decrease for the H-C oscillator is -156.1 cm^{-1} and -116.1 cm^{-1} in $\text{HC}\equiv\text{CHX}$ and $\text{H}_2\text{C}=\text{CHX}$ respectively. This same effect produces an important POL-CORR interaction effect on HC and CC stretching frequencies, increasing their values by $+45.3 \text{ cm}^{-1}$ and $+18.4 \text{ cm}^{-1}$ in $\text{HC}\equiv\text{CHX}$, respectively, whereas their corresponding values in $\text{H}_2\text{C}=\text{CHX}$ are $+43.9 \text{ cm}^{-1}$ and $+11.0 \text{ cm}^{-1}$, respectively. Finally, algebraic models were then established to explain how calculated HC and CC stretching frequencies in $\text{HC}\equiv\text{CHX}$ and $\text{H}_2\text{C}=\text{CHX}$ depend on the characteristics of the molecular orbital wave functions.

Vibrational Spectroscopic Investigation on Vitamin P Using *Ab Initio* and DFT Method: Theoretical Study

P. Singh, S. Jaiswal, G. Srivastav, R.A.Yadav

*Laser and Spectroscopy Lab, Department of Physics,
Banaras Hindu University, Varanasi-221005, India
e-mail: priyankasingh1097@gmail.com*

Vitamin P (Bioflavonoid), 2-Phenyl-1, 4-benzopyrone, are natural drugs. It has antioxidant, anti-inflammatory, antiallergenic, antiviral, and anti-carcinogenic properties. *Ab initio* calculation have been performed using Gaussian 03 program to compute its optimized geometry, harmonic vibrational frequencies along with intensities in IR and Raman spectra and atomic charges at RHF/6-31+g*, B3LYP/6-31+g* and B3LYP/6-311++g** levels. To make vibrational analysis Gaussian View software was used. The optimized molecular structure is found to possess C_1 point group symmetry. The Vitamin P is a non-planar molecule, while the benzopyronone moiety is nearly planar. Since Vitamin P contains 27 numbers of atoms, it possesses 75 normal modes of vibrations. Raman activities calculated by quantum chemical methods have been converted to Raman intensities using Raman scattering theory. Eleven vibrational frequencies have been assigned in narrow spectra range $1000-1200\text{ cm}^{-1}$. The band having frequency 3385 cm^{-1} is calculated to appear with strong intensity in Raman spectrum. Most of the vibrational frequencies are very weak in Raman spectrum. Calculations have been made keeping minimum energy conformations. The atomic numbering and rotatable bond C_1-C_7 of Vitamin P are given in Figure .1. It is expected that the present calculations should be useful for the further investigations of the important biological derivatives both from experiment and theory.



- [1] G.J. Kapadia, V. Balasubramanian, H. Tokuda, A. Iwashima, H. Nishino, *Cancer Lett.* 115 (1997) 173–178.
 [2] Bandyukova et al., *Rastit. Resur.* 23 (1987) 607–612.
 [3] Pelzer et al., *Farmaco* 53 (1998) 421–424.
 [4] Ren-Wang Jianga et al., *J. Mol. Struct.* 642 (2002) 77–84.

Experimental and Theoretical Studies on ^{13}C and ^1H NMR Spectra of 6-(2-fluorobenzoyl)-3-(2-(4-(4-fluorophenyl) piperazin-1-yl)-2-oxoethyl)benzo[d]thiazol-2(3H)-one

Erol Taşal¹, Yadiğar Gülseven¹, İsa Sıdır¹, Tijen Önkol², Cemil Öğretir³,
M. Selami Kılıçkaya¹

¹Department of Physics, Faculty of Arts & Sciences, Eskişehir Osmangazi University, 26480 Eskişehir, Turkey

²Department of Pharmaceutical Chemistry, Department of Pharmacy, Gazi University, 06330 Ankara, Turkey

³Department of Chemistry, Faculty of Arts & Sciences, Eskişehir Osmangazi University, 26480 Eskişehir, Turkey

^1H NMR spectra of 6-(2-fluorobenzoyl)-3-(2-(4-(4-fluorophenyl)piperazin-1-yl)-2-oxoethyl)benzo[d]thiazol-2(3H)-one molecule have determined experimentally. ^1H and ^{13}C was studied theoretically. ^1H and ^{13}C NMR chemical shifts of title compound have been calculated by means of Hartree-Fock (HF), Becke-1-Lee-Yang-Parr (B1LYP) and Becke-3-Lee-Yang-Parr (B3LYP) methods with 6-31G(d,p) basis set. The comparison of the experimental and the theoretical results has indicated that HF method with 6-31G(d,p) basis set found to be superior to the scaled B1LYP and B3LYP approach for predicting ^1H NMR chemical shifts.

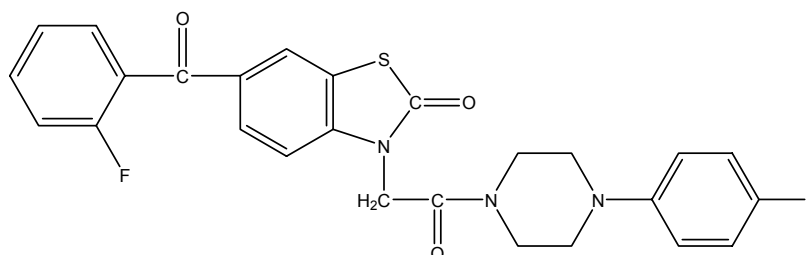


Fig. 1: Molecular structure of 6-(2-fluorobenzoyl)-3-(2-(4-(4-fluorophenyl)piperazin-1-yl)-2-oxoethyl)benzo[d]thiazol-2(3H)-one.

- [1] T.Önkol, E. Yıldırım, K. Erol, S. Ito, M.F. Şahin, *Arch. der Pharm.* 334 (2001) 17-20.
[2] R.M. Silverstein, Clayton G. Bossler, Terence C. Morrini: *Spectrometric identification of organic compounds*. John Wiley & Sons. Inc. 1991.
[3] K. Wolinski, J.F. Hinton, P. Pulay, *J. Am. Chem. Soc.* 112 (1990) 8251-8260.

Acknowledgements

We are grateful to ESOGU for financial support through Research Project No: 200519010 and ESOGU Research Project No: 200819XXX.

Theoretical Studies on Molecular Structure and Some Molecular Properties of 6-(2-fluorobenzoyl)-3-(2-(4-(4-fluorophenyl)piperazin-1-yl)-2-oxoethyl)benzo[d]thiazol-2(3H)-one

Erol Taşal¹, Yadiğar Gülseven¹, İsa Sıdır¹, Tijen Önkol²

¹Department of Physics, Faculty of Arts & Sciences, Eskişehir Osmangazi University, 26480 Eskişehir, Turkey

²Department of Pharmaceutical Chemistry, Faculty of Pharmacy, Gazi University, 06330 Ankara, Turkey

The values of some thermodynamic parameters (such as zero-point vibrational energy, sum of electronic and zero point energy, thermal correction to energy, etc.) and frontier molecular orbitals highest occupied molecular orbital (HOMO), lowest unoccupied molecular orbital (LUMO) along with geometric properties of the title compound were studied to enlighten the molecular structure. The calculations were carried out by means of Hartree-Fock (HF), Becke-Lee-Yang-Parr (B1LYP) and Becke-3-Lee-Yang-Parr (B3LYP) density functional methods with 6-31G(d) basis set, respectively.

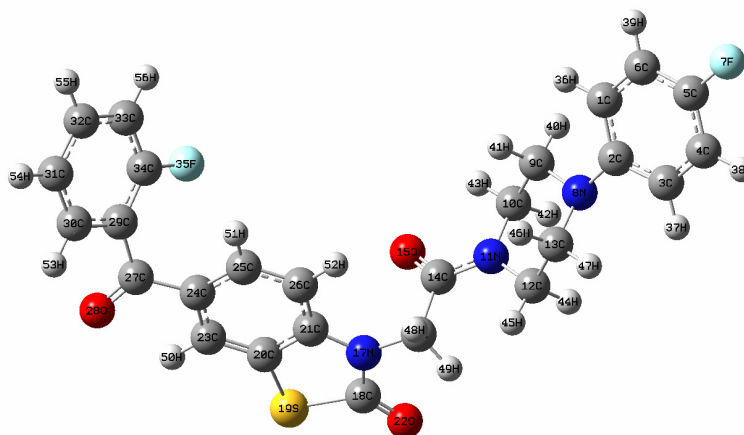


Fig. 1: Molecular structure of 6-(2-fluorobenzoyl)-3-(2-(4-(4-fluorophenyl)piperazin-1-yl)-2-oxoethyl)benzo[d]thiazol-2(3H)-one.

[1] T. Önkol, E. Yıldırım, K. Erol, S. Ito, M.F. Şahin, *Arch. der Pharm.* 334 (2001) 17-20.

Acknowledgements

We are grateful to ESOGU for financial support through Research Project No: 200519010 and ESOGU Research Project No: 200819XXX.

Quantum Chemical Studies on Tautomerism and Acidity-Basicity Behaviours of Some 1,2,4-triazole Derivates

Yadigar Gülseven¹, Erol Taşal¹, İsa Sıdır¹, Cemil Öğretir²

¹Department of Physics, Faculty of Arts & Sciences, Eskişehir Osmangazi University, 26480 Eskişehir, Turkey

²Department of Chemistry, Faculty of Arts & Sciences, Eskişehir Osmangazi University, 26480 Eskişehir, Turkey

The gas and liquid phase acidity-basicity behaviours of some 1,2,4-triazole derivates [1] were investigated using DFT (Density Functional Theory) calculation method. The preferred tautomeric forms were predicted using the DFT calculated acidity constants and physical parameters. The correlation attempt between the experimental and calculated acidity constants, pK_a values, revealed that the B3LYP/6-311G(d,p) calculated pK_a values are closer to the experimental values with a regression of almost unity ($R^2 = 0.99$).

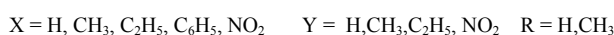
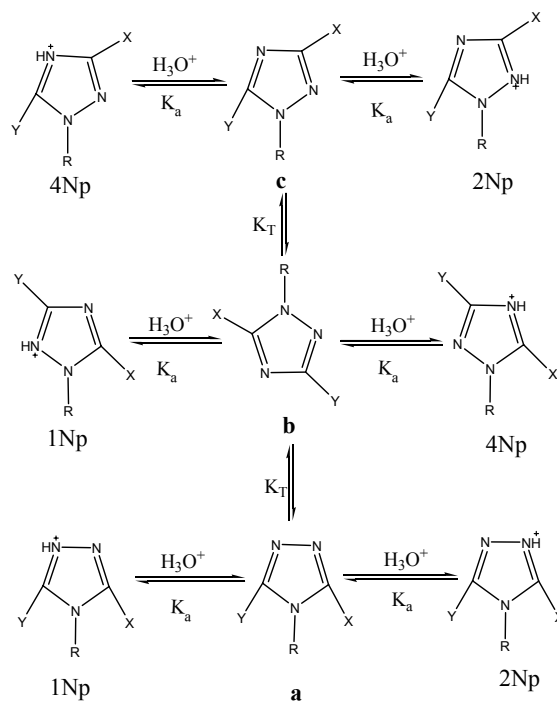


Fig. 1: Prototropic annular tautomerization and protonation patterns for c-substituted 1,2,4- triazole derivatives.

[1] J. Catalan, J. Luis, M. Abboud, J. Elguero: *Basicity and Acidity of Azoles*, Copyright© by Academic Pres, Inc. 1987.

Acknowledgement

We are grateful to ESOGU for financial support through Research Project No: 200519010 and ESOGU Research Project No: 200819XXX.

DFT and Ab Initio Computational Study of Structural Properties and Vibrational Spectra for Protonated Water Clusters

T. Wróblewski

*Institute of Physics, Pomeranian University in Slupsk,
Arciszewskiego 22, 76-200 Slupsk, Poland*

Protonated water clusters are the subjects of increasing interest, both experimental [1-3] and theoretical [4-6]. Ionized water clusters constitute the most abundant ionic species in the low stratosphere [7]; water ions are important in atmospheric nucleation and chemical reactions.

The geometrical parameters and spectral properties of different conformers of protonated water clusters $H^+(H_2O)_{n=1-4}$ are investigated with Density Functional Theory and ab initio methods. Results of Hartree-Fock and hybrid DFT methods: BVP86, B3LYP, PBEPBE, MPW1PW91, HTCH and THCTH with 6-311G++(2d,2p) and 6-311G++(3df,3pd) basis sets and high levels of ab initio computational studies with the quadratic complete basis set (CBS-Q) were compared with experimental data of vibrational modes. Some differences in spectral features between Eigen (H_3O^+) and Zundel ($H_5O_2^+$) conformers among different experiments as well as between experiments and theory are denoted.

- [1] A.W. Castleman, Jr. and R.G. Keesee, *Science* 241 (1988) 36-42.
- [2] K. Honma, L.S. Sunderlin and A.W. Castelman, Jr., *J. Chem. Phys.* 99 (1993) 1623-1632.
- [3] T. Wróblewski, E. Gazda, J. Mechlinska-Drewko, G.P. Karwasz, *Int. J. Mass Spectrom.* 207 (2001) 97-110.
- [4] H.-P. Cheng, *J. Phys. Chem. A* 102 (1998) 6201-6204.
- [5] M.P. Hodges and D.J. Wales, *Chem. Phys. Lett.* 324 (2000) 279-288.
- [6] T. Wróblewski, L. Ziemczonek, E. Gazda, G.P. Karwasz, *Rad. Phys. Chem.* 68 (2003) 313-318.
- [7] G. Hauck and F. Arnold, *Nature* 311 (1984) 547-550.

A Theoretical IR and Raman Spectroscopic Study on 1,2-Bis(o-carboxyphenoxy) ethane molecule

G. Yapar¹, K. Balci²

¹Istanbul University, Faculty of Science, Department of Physics, Vezneciler, 34134, Istanbul, Turkey

²Istanbul Technical University, Faculty of Science, Department of Chemistry, Ayazaga Campus, Istanbul, Turkey

Salicylic acid is a key molecule in producing of many skin-care products used in the treatment of acne, psoriasis, calluses, corns, keratosis pilaris, and warts. Due to its effect on skin cells, salicylic acid is used in several shampoos used to treat dandruff. Salicylic acid is also used as an active ingredient in gels which remove warts. In our this study subjected to 1,2-Bis(o-carboxyphenoxy) ethane which is a member of the compound group called “Glycol Podands with salicylic acid end”, theoretically possible stable conformers of the molecule in electronic ground state were searched by means of molecular dynamics calculations. The equilibrium geometrical parameters for the determined 19 stable conformers of the free molecule were obtained through geometry optimizations carried out using B3LYP hybrid DFT method with 6-31G(d). The vibrational normal modes and corresponding wavenumbers, IR and Raman intensities for the most stable three conformers of the molecule were obtained by means of frequency calculations performed in “harmonic oscillator” approach at 6-31G(d), 6-31++G(d,p) and aug-cc-pvTZ basis sets.

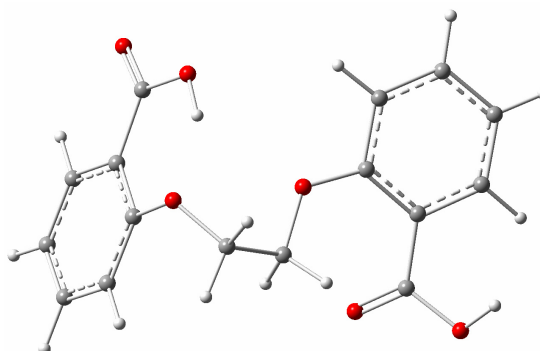


Fig. 1: 1,2-Bis(o-carboxyphenoxy) ethane molecule.

In order to reduce systematical overestimations at the calculated harmonic wavenumbers and thus to fit them to the corresponding experimental wavenumbers, two different scaling procedures referred to as “Scaled Quantum Mechanical Force Field (SQM FF) methodology” [1, 2] and “Scaling wavenumbers with dual scale factors” [3] were proceeded, independently. The obtained scaled wavenumbers have been found to be in good agreement with our assignments proposed for the fundamental bands observed in the recorded experimental IR and Raman spectra of the molecule.

[1] G. Rauhut, P. Pulay, J. Phys. Chem. 99 (1995) 3093.

[2] G. Rauhut, P. Pulay, J. Phys. Chem. 99 (1995) 14572.

[3] M.D. Halls, J. Velkovski, H.B. Schlegel, Theor. Chem. Acc. 105 (2001) 413.

Pippard Relations Modified by the Raman Frequency Shifts for the Phases I and II in NH₄I

H. Yurtseven

Department of Physics, Middle East Technical University, Ankara 06531, Turkey

Pippard relations in terms of the frequency shifts of the ν_7 (40 cm⁻¹) lattice mode, are established here for the phases I and II in NH₄I. The temperature-induced frequency shift, $(1/\nu)(\partial\nu/\partial T)_P$ is calculated through the isobaric mode Grüneisen parameter γ_P using the lattice parameter data at zero pressure for the phases I and II in NH₄I. From the frequency shifts, the specific heat C_p is calculated for the phases studied at zero pressure. Also, the pressure-induced frequency shift, $(1/\nu)(\partial\nu/\partial P)_T$ is calculated through the isothermal mode Grüneisen parameter γ_T at 250 K and it is related to the thermal expansivity α_P for the phases I and II in NH₄I.

Linear variation of C_p with the $(1/\nu)(\partial\nu/\partial T)_P$ and also a linear variation of α_P with the $(1/\nu)(\partial\nu/\partial P)_T$, indicate that the frequency shifts obtained for the ν_7 (40 cm⁻¹) lattice mode exhibit similar critical behaviour as C_p and α_P close to the I-II phase transition in NH₄I.



Calculation of the Raman Frequencies Using Volume Data Close to the Tricritical and Second Order Phase Transitions in NH_4Cl

H. Yurtseven

Department of Physics, Middle East Technical University, Ankara 06531, Turkey

We calculate here the Raman frequencies of the ν_5 TO (174 cm^{-1}) and ν_2 (1708 cm^{-1}) modes as a function of temperature in the region of the tricritical ($p = 1.6 \text{ kbar}$) and the second order ($p = 2.8 \text{ kbar}$) phase transitions in NH_4Cl . This calculation of the Raman frequencies is performed through the mode Grüneisen parameter by using the experimental length-change data obtained at zero pressure where the NH_4Cl crystal exhibits a first order phase transition ($T_\lambda = 242 \text{ K}$). The predicted Raman frequencies of the modes studied here, agree with our observed frequencies for the tricritical ($T_c = 257 \text{ K}$) and second order ($T_c = 268 \text{ K}$) transitions in NH_4Cl .

This indicates that the Raman frequencies can be predicted from the measurements of the crystal volume close to phase transitions by the method given here.

10. SURFACE SPECTROSCOPIES

Multifunctional Plasmonic Nanostructures for Surface-Enhanced Spectroscopies

S. Astilean, M. Baia, D. Maniu, F. Toderas, C. Farcau, M. Iosin, V. Canpean

*Faculty of Physics, Babes-Bolyai University, Str. M. Kogalniceanu 1,
400084 Cluj-Napoca, Romania*

Noble-metal nanostructures exhibit an enhanced optical interaction with visible light due to the resonant excitation of localized surface plasmons [1-2]. As result, dramatic changes are observed in the optical properties of molecules when adsorbed on metallic nanoparticles. The best-known example is surface enhanced Raman scattering (SERS). A closely related and complementary surface enhanced spectroscopy, surface enhanced infrared absorption (SEIRA), can also be performed on metal structures. Single metal nanoparticles have been reported to decisively influence the molecular fluorescence as well.

Here, we report the fabrication of nanoparticle arrays *via* nanosphere lithography, chemical synthesis and self-assembling routes. In the first procedure self-assembled polystyrene nanospheres are used as lithographic masks to deposit metal and generate periodic arrays of nanoparticles or nanoholes. The second procedure of fabrication involves chemical synthesis of nanoparticles and subsequent attachment of as synthesized nanoparticles onto solid surfaces via amine-terminated molecular layer. Scanning and transmission electron microscopy, atomic force microscopy, and optical transmission and reflectivity measurements have been employed to correlate the nanometer-scale morphology and topography of fabricated nanostructures with their optical properties.

The fabricated plasmonic nanostructures have been investigated as unique multifunctional platforms for spectroscopic detection of low-concentration analytes [3-5]. The SERS efficiency was evaluated with p-aminothiophenol as probe molecule at different excitation laser lines. Both FT-SERS and SEIRA spectra of p-aminothiophenol absorbed onto nanoparticle gold films were successfully recorded from the same metallic substrate. Moreover, morphological changes induced in the initial assemblies of gold nanoparticles by annealing allowed us to convert the SERS substrate into a sensitive sensor based on local surface plasmon resonance (LSPR). We also examined the fluorescence of Eosin Y – protein (BSA) in the presence on gold colloidal nanoparticles immobilized on glass substrate in comparison with the emission of Eosin Y – BSA deposited on bare glass.

The potential use of fabricated plasmonic nanostructures as highly SERS and SEIRA-active substrates as well as LSPR-based and metal-enhanced fluorescence sensors for biomolecules detection can foster many exciting applications, from biology, biochemistry and DNA sequencing to detection and identification of single molecules.

- [1] D.A. Stuart, A.J. Haes, C.R. Yonzon, E.M. Hicks and R.P. Van Duyne, *Nanobiotech.* 152 (2005) 13.
- [2] B. J. Wiley, S. H. Im, Z.-Y. and Y. Xia, *J. Phys. Chem. B* 110 (2006) 15666.
- [3] M. Baia, L. Baia, J. Popp, S. Astilean, *Appl. Phys. Lett.* 88 (2006) 143121.
- [4] S. Astilean, *Radiation Physics and Chemistry* 76 (2007) 436.
- [5] F. Toderas, M. Baia, L. Baia, S. Astilean, *Nanotechnology* 18 (2007) 255702.

Acknowledgement

We acknowledge the financial support from the ANCS Project CEEX No 71/2006 (Matnantech).

Structural Studies of Lipid Bilayers on Titania Surfaces by Means of Polarization Modulation Infrared Reflection Absorption Spectroscopy

M. Nullmeier¹, I. Zawisza¹, S.E. Pust¹, R. Boukherroub², S. Szunerits^{2,3}, G. Wittstock¹

¹Carl von Ossietzky University of Oldenburg, Center of Interface Science (CIS), Department of Pure and Applied Chemistry and Institute of Chemistry and Biology of the Marine Environment, D-26111 Oldenburg, Germany

²Institut de Recherche Interdisciplinaire (IRI) USR CNRS-3078, Institut d'Electronique, de Microélectronique et de Nanotechnologie (IEMN), CNRS UMR-8520 Cité Scientifique, Avenue Poincaré - BP. 60069, 59625 Villeneuve d'Ascq, France

³Laboratoire d'Electrochimie et de Physicochimie des Matériaux et des Interfaces (LEPMI), CNRS-INPG-UJF, 1130 rue de la piscine, B.P. 75, St. Marin d'Hères Cedex, France

Titanium and titanium-based materials are used and tested as implants due to their high biocompatibility. The native oxide layer which grows on titanium surfaces is of great biomedical importance, since pure metallic surfaces are often toxic for a biological medium interacting with the implant surface. In a living organism the implant material is exposed to electrolytes, lipid cell membranes and proteins. The initial stages of adsorption are crucial for the biocompatibility of the implant.

For a detailed structural, conformational and hydrational analysis of an adsorbed or adsorbing organic layer on surfaces the polarization modulation infrared reflection absorption spectroscopy (PM IRRAS) can be used. This method requires a highly reflecting surface, limiting the application of metal oxides and semiconductors. Calculations of the reflectivity, the phase shift and the mean square electric field (MSEF) of the *p*- and *s*-polarized IR radiation show that some ultra thin metal oxide and semiconductor layers when deposited on a gold surface can be successfully applied for PM IRRAS. It was shown that the reflectivity, the phase shift and the MSEF in up to 20 nm thick titanium layers with its 3-4 nm thick native oxide layer are comparable to that on pure gold. The surface selection rule is fulfilled.

A lipid bilayer of 1,2-dimyristoyl-*sn*-glycero-3-phosphocholine (DMPC), serving as a model lipid membrane, was deposited using the Langmuir-Blodgett- and Langmuir-Schaeffer techniques on a titania surface. The transfer was done in liquid expanded (LE) and liquid condensed (LC) state and the structure of both lipid bilayers was compared. The structure of the bilayer in LE state is dominated by the interactions between the zwitterionic phosphatidylcholine polar head group and the titania surface. Due to the low surface coverage the intermolecular distances are large and provide much space for water of hydration. The positively charged choline group is tilted by 70° toward the surface and the negatively charged phosphate group has a small tilt of 15° to the surface normal. This opened structure corresponds to the B crystal structure of DMPC. In LC state, the intermolecular distances in the bilayer are reduced. The polar head group is weaker hydrated, the choline group has a smaller tilt (55°) and the phosphate group a larger tilt of 30° to the surface normal. This structure corresponds to the crystal structure A of DMPC.

Vibrational Study on the Bioactivity of Portland Cement-Based Materials for Endodontic Use

P. Taddei¹, A. Tinti¹, M.G. Gandolfi², F. Siboni³, C. Prati³

¹Biochemistry Department, University of Bologna, Italy

²Center of Biomineralogy, Crystallography and Biomaterials, University of Bologna, Italy

³Department of Odontostomatological Sciences, University of Bologna, Italy

In the last decade, white Portland cement was developed as endodontic sealer and root-end filling material. This new material was investigated because it sets in the presence of water, an important property for dental materials. One of the main disadvantages when using white Portland cement is its extended setting time and difficult handling.

This study was aimed at investigating modified Portland cement-based materials with regard to their bioactivity (i.e. the capability of forming a calcium phosphate layer in physiological fluids) after treatment for different times (from 1 to 90 days), at 37°C, in Dulbecco's Phosphate buffered saline (DPBS) and Hank's balanced salt solution (HBSS).

To evaluate the influence of a calcium phosphate on bioactivity, two cements were investigated: wTC 1% (derived from white Portland cement) and wTC-TCP (wTC 1% added with tricalcium phosphate). ATR/FT-IR and micro-Raman spectroscopy were used to investigate the presence of deposits on the surface of the cements and the composition changes of the cement as a function of storage time.

Micro-Raman and ATR-FTIR analyses of the wTC-TCP cement treated with DPBS revealed the presence of a calcium phosphate deposit already after one day of storage, as suggested by the presence of the IR bands at about 1025 cm⁻¹ (asymmetrical stretching of phosphate group), 600 and 560 cm⁻¹ (bending of phosphate group) and of the Raman band at 963 cm⁻¹ (symmetrical stretching of phosphate group). At the same storage time, wTC1% showed a thinner deposit. The thickness of the deposit was evaluated by the analysis of the micro-Raman spectra recorded in the section of the samples and by the $I_{960(\text{phosphate})}/I_{990(\text{cement})}$ (Raman) and $I_{1030(\text{phosphate})}/I_{950(\text{cement})}$ (IR) ratios obtained on the surfaces of the samples.

At increasing storage times in DPBS, the thickness of the deposit increased as well as its crystallinity and the bands of carbonated apatites appeared at 1460-1415, 1025, 960, 600-560 cm⁻¹ (IR, carbonate ion in a B-type carbonated apatite, asymmetrical stretching, symmetrical stretching and bending of phosphate, respectively) and 1074, 1050, 965, 606-595-436 cm⁻¹ (Raman, carbonate stretching, asymmetrical stretching, symmetrical stretching and bending of phosphate, respectively). After 60 and 90 days of treatment with DPBS, the bands of the cement were no longer observable for wTC-TCP, while they were detectable for wTC 1%. This result indicated a better bioactivity for the former than for the latter.

The composition changes of the cement (ettringite/silicate ratio) were evaluated on the surface and in the interior of the samples by the I_{990}/I_{860} (Raman) and I_{1110}/I_{950} (IR) ratios.

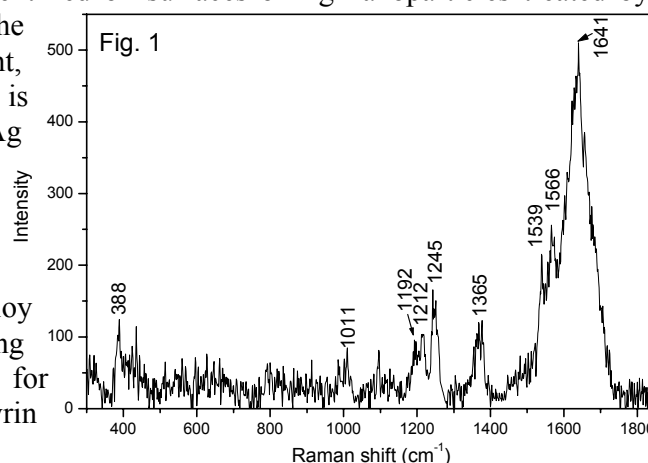
Bands at 3640 cm⁻¹ (IR) and 360 cm⁻¹ (Raman), attributable to Ca(OH)₂, were observable in the interior of all the samples, but not on their surface. This result indicated a Ca(OH)₂ release in the storage medium, which appeared slightly more pronounced for wTC-TCP. This behaviour, confirmed by pH measurements of the storage fluids, is known to render the material biocompatible. The samples treated with HBSS showed analogous trends; however, bioactivity was noticeably less pronounced than in DPBS, according to the lower phosphate concentration in the former than in the latter. Ca(OH)₂ release was less significant as well.

Surface-enhanced Resonance Raman Scattering of Free-base Porphyrins for Ultrasensitive Spectral Detection and Surface Probing

B. Vlckova¹, K. Siskova^{1,3}, M. Prochazka², J. Stepanek², P. Smejkal¹, P.-Y. Turpin³

¹Dept. of Physical and Macromol. Chemistry, Charles University in Prague, Hlavova 8/2030, 128 40 Prague 2, Czech Republic, ² Institute of Physics, Charles University in Prague, Ke Karlovu 5, 121 16 Prague 2, Czech Republic, ³ BIOMoCeTi, Université P. et M. Curie ParisVI, GENOPOLE Campus 1, 91030 Evry, France

Recent development of SERS and SERRS (surface-enhanced /resonance/ Raman scattering) spectroscopies is strongly stimulated by their ultrasensitivity currently achieving a single molecule detection level, as well as by their recent incorporation into the expanding field of plasmonics [1]. Free-base (f.b.) porphyrins, a class of biologically important chromophores, have been the subject of interest as target adsorbates for both sensitive and selective SERRS spectral detection [2]. In this brief overview we demonstrate that, due to their unique molecular structure and reactivity towards plasmonic metal nanoparticle surfaces, f.b. porphyrins can also be employed as surface probes. Using a cationic f.b. 5,10,15,20-tetrakis (1-methyl-4-pyridiniumyl)porphine (H₂TMPyP) as an example, we show that after identification of all observable SERRS spectral forms with help of factor analysis [3] and their assignment to the corresponding surface species, we obtain a tool for probing the impact of chemical modifications of Ag nanoparticle surfaces. Treatment of Ag nanoparticles by various selected ions has been performed (i) after the Ag nanoparticle preparation by a chemical procedure and/or by laser ablation (LA) of a Ag target in the aqueous ambient, or, alternatively, (ii) in the course of their preparation by LA. On Ag nanoparticle surfaces stabilized by weakly adsorbed anions, the porphyrin becomes readily metallated yielding Ag⁺-TMPyP surface species. By contrast, the native structure of the cationic f.b. porphyrin molecules becomes preserved in the case of their electrostatic bonding to molecular anions strongly bond to Ag nanoparticle surface. Finally, Ag(0)-TMPyP surface species have been identified on surfaces of Ag nanoparticles treated by chloride or thiosulphate anions. In the particular case of chloride-treatment, formation of Ag(0) adsorption sites is accompanied by formation of compact Ag nanoparticle aggregates with numerous “hot spots” [4]. In accord with our expectations, the SERRS spectral detection limit of Ag(0)-TMPyP in such a system is as low as 1×10^{-11} M (Fig. 1). The possibilities to employ the results of the surface probing for tailoring the Ag nanoparticle surface modifications for ultrasensitive detection of specific porphyrin surface species will be discussed.



[1] G.A. Baker, D.S. Moore, *Anal. Bioanal. Chem.* 382 (2005) 1751-1770.

[2] B. Vlckova, P. Smejkal, M. Michl, M. Prochazka, P. Mojzes, F. Lednicky, J. Pflieger, J. Inorg. Biochem. 79 (2000) 295-300.

[3] M. Prochazka, B. Vlckova, J. Stepanek, P.-Y. Turpin, *Langmuir* 21 (2005) 2956-2962.

[4] I. Sloufova, K. Siskova, B. Vlckova, J. Stepanek *Phys. Chem. Chem. Phys.* (2008) doi:10.1039/b718178g.

Acknowledgment

Financial support by the 203/07/0717 grant awarded by GACR, by the MSM 0021620857 long term research program and by KAN100500652 awarded by AVCR is gratefully acknowledged. Present address of KS: Institute of Macromolecular Chemistry, ASCR, Heyrovsky Square 2, Prague 6, CR.

Adsorption of Isoniazid onto Sepiolite-Palygorskite Group of Clays: An IR and DFT Study

Elif Akalin¹, Sevim Akyuz², Tanil Akyuz²

¹*Istanbul University, Science Faculty, Department of Physics, Vezneciler 34134 Istanbul, Turkey*

²*Istanbul Kultur University, Science and Letters Faculty, Department of Physics, Atakoy Campus, 34156 Istanbul, Turkey*

Isoniazid (abbreviated as INH) is the most widely used drug in the treatment of tuberculosis. It also seems to be effective in the treatment of extrapulmonary illnesses such as meningitis and genito-urinary infections. In this study adsorption of isoniazid on sepiolite, loughlinitite (natural Na-sepiolite) and palygorskite from Anatolia were investigated by FT-IR spectroscopy. Sepiolite and palygorskite form an important group of clay minerals which have many industrial, catalytic and environmental applications. INH molecule can form complexes through its nitrogens and oxygen as a ligand. The NH₂ group hydrogens behave as donors and nitrogen and oxygen behave as acceptors. In order to investigate the interaction mechanism of isonizid with the clay framework, harmonic and anharmonic vibrational spectra of INH interacting with Al(OH)₃ through the ring nitrogen have been calculated and compared with the IR spectra of adsorbed INH. The vibrational wavenumber calculations of free and coordinated INH were carried out with the Gaussian 03 package. DFT/B3LYP level of theory with 6-31++G(d,p) basis set has been used. IR spectroscopy indicates that molecules adsorbed on sepiolite-palygorskite group of clays are coordinated to Lewis acidic sites and/or surface hydroxyls by H-bonding interaction through pyridine ring nitrogen lone pairs.

FT-IR and FT-Raman Spectra of SnS Film Deposited by Chemical Bath Deposition Method

Sabiha Aksay¹, Güneş Süheyla Kürkçüoğlu², A. Şenol Aybek¹, Metin Kul¹, Evren Turan¹, Tülay Özer¹, Hüseyin Berber³, Halil Berber³, Muhsin Zor¹

¹Department of Physics, Anadolu University, TR-26470, Eskisehir, Turkey

²Department of Physics, EskisehirOsmangazi University, TR- 26480 Eskisehir, Turkey

³Department of Chemistry, Anadolu University, TR-26470, Eskisehir, Turkey

SnS semiconductor films using as a absorber layer for solar cells have been deposited onto microscope slides by chemical bath deposition method at room temperature. The crystal structure of the sample has been determined by using X-ray diffraction. X-ray diffraction pattern of the SnS film is given in Fig. 1. It showed that the sample was polycrystalline with orthorhombic structure. FT-IR spectrum of the sample has been investigated in 4000-400 cm^{-1} region. FT-Raman spectrum of the sample is given in Fig. 2. It can be seen that six Raman peaks are clearly observed at 970.14, 609.34, 303.90, 239.23, 106.47 and 64.32 cm^{-1} for SnS.

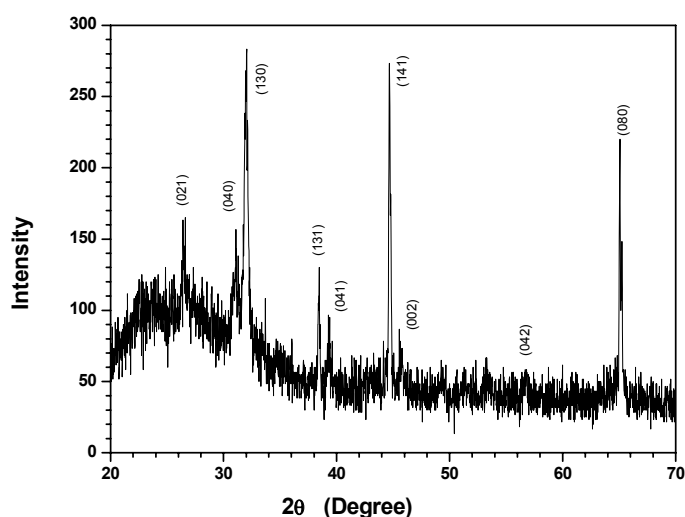


Fig. 1: X-ray diffraction of the SnS sample.

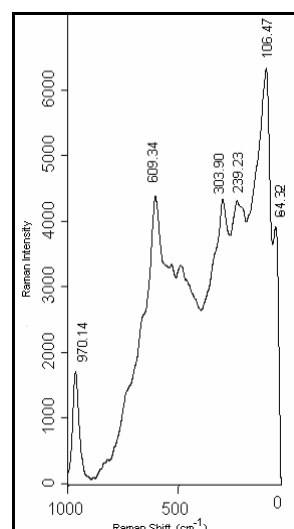


Fig. 2: FT-Raman spectrum of the SnS sample.

[1] A. Tanusevski, *Semicond. Sci. Technol.* 18 (2003) 501-505.

[2] X.L. Gou, J. Chen, P.W. Shen, *Matter Chem. and Phys.* 93 (2005) 557-566.

Surface Enhanced Raman Spectroscopy (SERS) Study of Diluted Solutions of Cimetidine and Some of its Metallocomplexes

S. Bonora¹, M. Di Foggia¹, A. Maris²

¹Department of Biochemistry 'G. Moruzzi', University of Bologna,
Via Belmeloro 8-2, I-40126 Bologna, Italy

²Department of Chemistry 'G. Ciamician', University of Bologna,
Via Selmi 2, I-40126 Bologna, Italy

Cimetidine (**cim**) is a drug used in the treatment of peptic ulcer, and acts as a powerful histamine H₂-receptor antagonist. **Cim** is able to coordinate transition metal ions, and some clinical studies supported the hypothesis that the interaction with metals may play an important role *in vivo* [1]. SERS technique offers the suitable sensitivity to study these interactions at physiological concentrations.

Figure 1 shows the 300–1800 cm⁻¹ spectral region of SERS spectra of **cim** and of **cim**:Me 1:1 complexes. Noticeable differences are observed in the presence of divalent cations, mainly in the 600–1100 cm⁻¹ spectral region, particularly in the case of Cu⁺⁺ ions (d). Also the relative intensity of the bands near 1300 cm⁻¹ changes, with the appearance, in the **cim**:Cu⁺⁺ system, of a new component at 1320 cm⁻¹. Moreover, the ν_{CN} stretching band at about 2200 cm⁻¹ shifts to higher frequency in the presence of copper ions. An *ab initio* calculation with the HF/6-31G** basis set was performed to estimate the energetic stability consequent to the binding of the different groups of **cim** with Ag surface and used to determine the optimized geometry of **cim** and of **cim**:Me 1:1 complexes adsorbed on the colloid. The SERS and DFT results suggest that the site of adsorption changes. Moreover, they differs noticeably from the Raman spectra of the pure solid crystalline **cim** and of some solid **cim**-Me complexes [2], confirming the great ability of SERS technique to deal with problems related to the biomedical field. Moreover, they support the hypothesis that the copper ion plays an important role in increasing the pharmacological efficacy of **cim**.

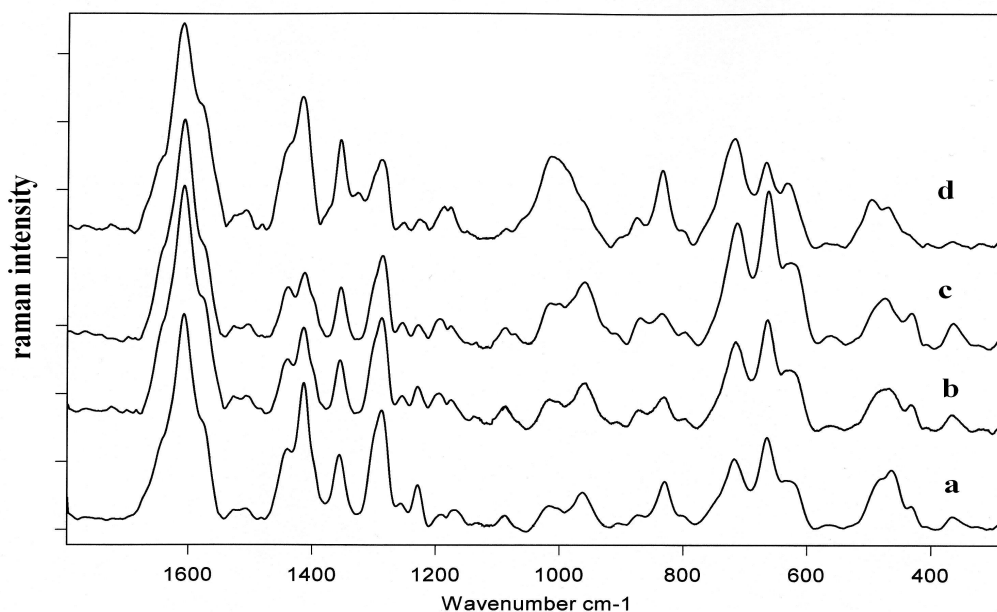


Fig. 1: 300–1800 cm⁻¹ spectral region of SERS spectra of **cim** 0.05 % (a) and of its metallocomplexes (**cim**:Me 1:1) with Ca (b); Cd (c) and Cu (d).

[1] M. Kirkova, M. Atanassova, E. Russanov, *Gen. Pharmacol.* 33 (1999) 271.

[2] M. Barańska, L.M. Proniewicz, *J. Mol. Struct.* 511-512 (1999) 153.

Fabrication and Functionalization of Core-Shell Au/Ag Nanoparticles with Advanced Physico-Chemical Properties: Application to the Detection of Pollutants by Surface-Enhanced Raman Scattering

C. Domingo, L. Guerrini, S. Sánchez-Cortés, J.V. García-Ramos

Instituto de Estructura de la Materia, CSIC, Serrano 121, 28006 Madrid Spain

Au and Ag colloids are metallic systems largely employed in Surface-enhanced Raman spectroscopy (SERS) [1-4]. Despite of their easy preparation, these systems are rather difficult to control and characterize because of the enormous range of nanoparticle (NP) sizes and shapes. Although the Au surface shows a lower enhancement factor in the visible in comparison to that of Ag one, colloids of this metal have many advantages, including an easier preparation and a higher homogeneity as the dispersion of diameters concerns. For this reason, many attempts to obtain composite particles by depositing Ag on preformed Au NPs have been carried out in order to induce a higher homogeneity in the Ag surfaces [5, 6] as well as to induce a greater SERS enhancement of the Au colloid. Au NPs may act as seed to induce the Ag grown by chemical reduction of Ag^+ in the presence of preformed colloidal Au [7]. These composite Au/Ag core-shell nanoparticles have received enormous attention in the fields of surface chemistry and electrochemistry [8, 9]. The Ag and Au colloids display different optical and surface chemical properties. The former have to be considered from the point of view of the electromagnetic mechanism associated with the SERS effect; the latter from the point of view of the direct metal-analyte interaction, which may be strongly dependent on the surface composition. Even small surface composition differences have to be carefully considered, especially when fabricating NPs-based sensors [10].

We report an easy method for the self-deposition of Ag^+ on gold NP surfaces. By using SERS, we demonstrated the progressive Ag enrichment of the outer part of the gold NPs in the colloidal suspension, employing luteolin, thiophenol and lucigenin as probe molecules. These molecules are characterized by their different spectral pattern on both metals. In fact, the SERS technique is an extremely powerful tool for the identification of structural changes in the adsorbate when interacting with different substrates, as gold or silver.

- [1] J.A. Creighton, C.G. Blatchford, M.G. Albrecht, *J. Chem. Soc., Faraday Trans.* 75 (1979) 790.
- [2] M. Moskovits, *Rev. Mod. Phys.* 57 (1985) 783.
- [3] S. Sanchez-Cortes, J.V. Garcia-Ramos, G. Morcillo, *J. Colloid Interface Sci.* 167 (1994) 428.
- [4] C.G. Blatchford, J.R. Campbell, J.A. Creighton, *Surf. Sci.* 120 (1982) 435.
- [5] R.G. Freeman, M.B. Hommer, K.C. Grabar, M.A. Jackson, M.J. Natan, *J. Phys. Chem.* 100 (1996) 718.
- [6] N. Felidj, G. Levi, J. Pantigny, J. Aubard, *New J. Chem.* (1998) 725.
- [7] M.A. Hayat, *Colloidal Gold: Principles, Methods, and Applications*; Academic Press: San Diego, 1989.
- [8] M.G. Mason, J.C. Hansen, *J. Vac. Sci. Technol. A* 12 (1994) 2023.
- [9] S.G. Corcoran, G.S. Chakarova, K Sieredski, *J. Electroanal. Chem.* 377 (1994) 85.
- [10] K. Kim, K.L. Kim, S.J. Lee, *J. Chem. Phys. Lett.* 403 (2005) 77.

Acknowledgment

This work has been partially supported by the Ministerio de Educación y Ciencia of Spain (Project FIS2007-63065) and Comunidad de Madrid (S-0505/TIC/0191 MICROSERES). L. G. acknowledges an I3P fellowship from CSIC.

Building Highly Selective Hot Spots in Ag Nanoparticles Using Bifunctional Diamines with Variable Length: Application to the Detection of Pollutants by Surface-Enhanced Raman Scattering

J.V. García-Ramos, L. Guerrini, I. Izquierdo, C. Domingo, S. Sánchez-Cortés

Instituto de Estructura de la Materia, CSIC, Serrano 121, 28006 Madrid, Spain

Surface-enhanced optical techniques are extremely high sensitive analytical techniques mainly based on the giant electromagnetic (EM) enhancement induced by nanostructured noble metal surfaces and associated to their localized plasmon resonance (LPR) [1, 2]. It is widely accepted that the main part of the electromagnetic field intensification occurs in special regions of the metallic surface called hot spots (HS) [5]. Among these HS, interparticle junctions or gaps existing between metal nanoparticles (NPs) are points where the EM intensification seems to take place in a greater extent [6]. In the last time there has been a renewed interest in the fabrication and theoretical study of such systems [7-9]. Metal NPs in suspension seem to be the best substrate to induce a high EM intensification [12], but the fabrication of such HS escapes to the experimental control in macro conditions resulting in the lack of reproducibility, both in the distribution and density of these interstitial sites. Moskovits et al. [10, 11] recently demonstrated that, by using bifunctional thiol-containing adsorbates as linker molecules, it is possible to produce chemically driven SERS active systems consisting of assemblies of strongly interacting NPs.

We have employed α,ω -diamines of different chain lengths as HS formation inducers, by virtue of their bifunctional nature and affinity to interact strongly with the silver surface. At the same time, they act as molecular hosts for SERS detection of analytes presenting low affinity for the metal surface, specifically cyclodiene-type chlorinated insecticides. In fact, the self-assembled monolayers formed on the metal surface by α,ω -diamines may mimic the lipid bilayer of the cell membrane, where these insecticides mainly develop their toxicity.

- [1] M. Moskovits, *Rev. Mod. Phys.* 57 (1985) 783.
- [2] R. Aroca, *Surface-enhanced Vibrational Spectroscopy*, John Wiley & Sons, Chichester, 2006
- [3] S. Nie, S.R. Emory, *Science* 275 (1997) 1102.
- [4] K. Kneipp, Y. Wang, H. Kneipp, L.T. Perelman, I. Itzkan, R.R. Dasari, M.S. Feld, *Phys. Rev. Lett.* 78 (1997) 1667.
- [5] A. Otto, *J. Raman Spectrosc.* 37 (2006) 937.
- [6] M. Futamata, *Faraday Discuss.* 132 (2006) 45.
- [7] E.C. Le Ru, P.G. Etchegoin, M.J. Meyer, *J. Chem. Phys.* 125 (2006) 204701.
- [8] M. Käll, H. Xu, P. Johansson, *J. Raman Spectrosc.* 36 (2006) 510.
- [9] P. Olk, J. Renger, T. Härtling, M.T. Wenzel, L.M. Eng, *Nano Lett.* 7 (2007) 1736.
- [10] D.J. Anderson, M. Moskovits, *J. Phys. Chem.* 110 (2006) 13722.
- [11] S.J. Lee, A.R. Morrill, M. Moskovits, *J. Am. Chem. Soc.* 128 (2006) 2200.
- [12] R.F Aroca, R. Alvarez-Puebla, N. Pieczonka, S. Sanchez-Cortes, J.V. Garcia-Ramos, *Adv. Coll. Interface Sci.* 116 (2005) 45.

Acknowledgment

This work has been partially supported by the Ministerio de Educación y Ciencia of Spain (Project FIS2007-63065) and Comunidad de Madrid (S-0505/TIC/0191 MICROSERES). L.G. acknowledges an I3P fellowship from CSIC. I. I. acknowledges CSIC for a JAE-CSIC predoctoral grant.

SERS Analysis of Herbicide Diquat on Nanostructured Metal Electrodes

M.R. Lopez-Ramirez¹, L. Roldán², J.V. Garcia-Ramos², S. Sanchez-Cortes²

¹Department of Physical Chemistry (Associate Unit of Instituto de Estructura de la Materia (CSIC)), Faculty of Sciences, University of Málaga, E-29071 Málaga, Spain

²Instituto de Estructura de la Materia, CSIC, E-28006 Madrid, Spain

The combination of electrochemical techniques with SERS spectroscopy allows us to record *in situ* Raman spectrum of an adsorbed species on the metal electrode surface. Therefore we are able to obtain both structural and conformational information associated to the interaction of the molecule on a metal-electrolyte interface.

SERS spectra are very sensitive to potential shifts in this metal-electrolyte interface leading not only to an overall enhancement of the spectra but also to an enhancement of the relative intensities of the SERS spectra bands. Consequently there is a fundamental difference between the electrodes and colloids substrates: while in the first case, we are able to easily modify the potential range, in a colloid aggregates the potential of the interface is not uniform throughout the sample, changing with the time of the system.

In this work we have studied the behaviour of different reduced species of Diquat (DQ) investigated by means of SERS spectroscopy on silver and copper electrodes. This research was aimed to complete the information obtained in a previous SERS study of this molecule on silver colloids [1]. We have interpreted the SERS spectra of DQ under different experimental conditions due to the special properties of this molecule, which is a dication species belonging to the viologens family with very interesting redox behavior.

The analysis of these SERS spectra show that the absorption mechanism of DQ on metal electrodes depends on several factors such as the potential range, the herbicide concentration, the excitation wavelength or the metal electrode used in the SERS experiment. An additional disadvantage which difficult the study of DQ is its ability to form dimmers in the proximity of the metal surface, which is also analysed in this work.

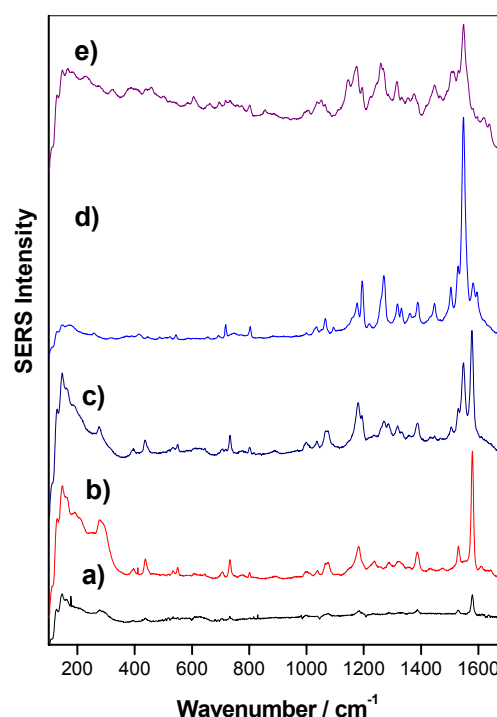


Fig. 1: SERS spectra of DQ (10^{-3} M) in Cl^- 0.1 M on Cu electrode by excitation at 785 nm at the following electrode potential: a) 0.00 V, b) -0.25 V, c) -0.50 V, d) -0.75 V, e) -1.00 V.

[1] M.R. Lopez-Ramirez, L. Guerrini, J.V. Garcia-Ramos, S. Sanchez-Cortes, *Vibrational Spectroscopy* (2008) in press.

Acknowledgment

This work has been partially supported by the Ministerio de Educación y Ciencia of Spain (Project FIS2007-63065) and Comunidad de Madrid (S-0505/TIC/0191 MICROSERES).

SERS Study of Self-Assembled Carbazolyl-Diacetylene Monolayers Chemisorbed on Gold Surfaces

M. Muniz-Miranda¹, E. Giorgetti², G. Margheri², S. Sottini², A. Giusti³, G. Dellepiane³

¹ Dipartimento di Chimica, Università di Firenze, Via della Lastruccia 3, 50019 Sesto Fiorentino, Italy
e-mail: muniz@chim.unifi.it

² Istituto dei Sistemi Complessi – CNR, Via Madonna del Piano 10, 50019 Sesto Fiorentino, Italy

³ Dipartimento di Chimica e Chimica Industriale, Università di Genova, Via Dodecaneso 31, 16146 Genova, Italy

Surface Enhanced Raman Scattering (SERS) was employed for studying the polymerization of self-assembled carbazolyl-diacetylene (CDS9) monolayers chemisorbed on smooth gold substrates by depositing silver colloidal nanoparticles. The formation of two polymer forms of CDS9 is expected by UV irradiation, a red phase and a blue phase [1], which is characterized by a higher structural order in the polymer chain. SERS measurements have been here performed to obtain information on the predominance of one of these forms and on the structural arrangement. For obtaining a suitable SERS response from CDS9 chemisorbed on smooth gold surfaces, a large increase of the surface roughness has been ensured by depositing a silver colloidal layer, as shown in Figure 1. The SERS spectra (Figure 2) obtained with different exciting lines (514.5 nm and 647.1 nm) show the predominance of the red phase, denoted by the occurrence of the C=C stretching mode around 1500 cm^{-1} , with respect to the presence of the blue form, characterized by the C=C stretching mode around 1450 cm^{-1} . This fact can be related to the presence of the carbazolyl groups, which introduce a larger disorder in the polymer arrangement with respect to polymers of conventional diacetylenes.

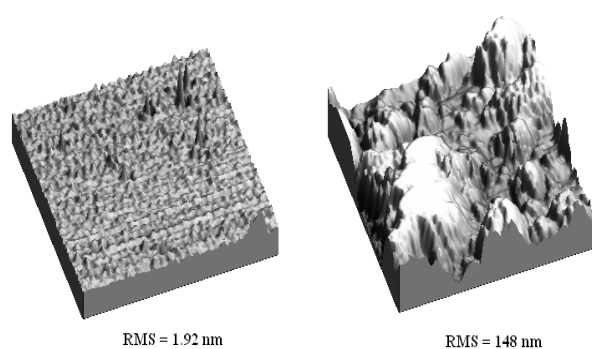


Fig. 1: AFM images of Au surfaces in the absence (left) and in the presence (right) of Ag particles.

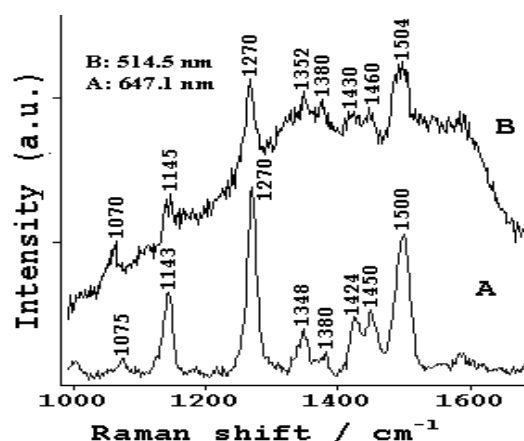


Fig. 2: SERS spectra of CDS9 polymer adsorbed on Au surfaces after doping with Ag particles.

[1] M.D. Mowery, C.E. Evans, J. Phys. Chem. B 101 (1997) 8513-8519.

Study of the Adsorption of 2-Mercaptobenzoxazole on Gold Colloidal Nanoparticles by Means of Surface Enhanced Raman Scattering

M. Muniz-Miranda¹, B. Pergolese², A. Bigotto²

¹*Department of Chemistry, University of Florence, Via della Lastruccia 3, 50019 Sesto Fiorentino, Italy
e-mail: muniz.unifi.it*

²*Department of Chemical Sciences, University of Trieste, Via L. Giorgieri 1, 34127 Trieste, Italy*

Thiolic/thionic derivatives of benzazoles have widespread applications in the field of the corrosion protection of metals. Among these, 2-mercaptobenzoxazole (MBO) is an extremely efficient corrosion inhibitor for many metals and their alloys, and a large number of investigations were carried out in order to clarify the interaction mechanism between this compound and metal surfaces. SERS investigations on MBO adsorbed on different metal substrates, as copper electrodes [1], silver sols [2] and smooth copper surfaces doped with silver colloidal nanoparticles [3] were carried out. In order to gain further information on how the adsorption of MBO is affected by the nature of metal, a SERS investigation of MBO adsorbed on gold colloidal nanoparticles was planned and the results of this study are here reported. SERS spectra were interpreted with the help of DFT calculations on MBO/Au surface complex models (see Figure 1).

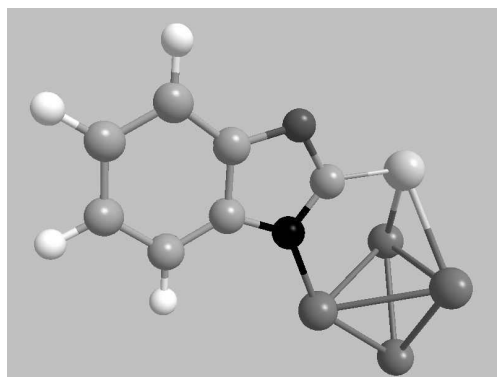


Fig. 1: Optimized structure for one model of MBO/Au surface complex.

The adsorption of MBO on Au colloids is analogous to that observed on silver colloids and on smooth copper surfaces doped with Ag colloidal nanoparticles: the ligand adsorbs in its ionized thiolic form through the nitrogen and sulphur atoms. The molecular orientation adopted by MBO is tilted with respect to the gold surface, as observed in all the other cases. Therefore, it can be concluded that the nature of metal has a negligible influence on the adsorption mechanism of this important corrosion inhibitor. By means of this investigation we have also elucidated that the use of DFT calculations of surface complex models with mixed basis sets is a very promising tool for the assignment of SERS spectra of strongly adsorbed organic compounds.

[1] M. Fleishmann, I.R. Hill, G. Mengoli, M.M. Musiani, J. Akhavan, *Electrochim. Acta* 30 (1985) 879-888.

[2] A. Bigotto, B. Pergolese, *J. Raman Spectrosc.* 32 (2001) 953-959.

[3] B. Pergolese, M. Muniz-Miranda, A. Bigotto, *J. Phys. Chem. B* 110 (2006) 9241-9245.

***In vitro* Biofilms Formation on Polymer Matrix Composites**

E. Stodolak¹, C. Paluszkiwicz², M. Błażewicz¹

¹AGH – University of Science and Technology, Faculty of Materials Science and Ceramics,
Department of Biomaterials, Al. Mickiewicza 30, 30-059 Krakow, Poland

²AGH – University of Science and Technology, Faculty of Materials Science and Ceramics,
Department of Silicate Chemistry, Al. Mickiewicza 30, 30-059 Krakow, Poland

Non-metallic materials, particularly those based on various polymeric compositions, are achieving considerable acceptance as biomaterials for the fabrication of implants. However, in order to obtain a proper *in vivo* acceptance of an implant with improved biocompatibility, its surface properties require to be matched depending on the desired medical use.

A novel approach of the surface modification is fabrication of polymer composite materials with fibrous components. Modification of polymer matrix with fibrous components changes the volume properties of the resulting composite material (e.g. mechanical parameters) and simultaneously influences its surface physical and chemical state. It is known, that biomaterial surface with a particular degree of roughness favours adhesion of bone cells. Another important factor determining the cellular response is the surface energy of biomaterial. Problem of correlation between the surface parameters of biomaterial and cellular response is not still well recognized.

The work reports the effects of modification of biostable polymer matrix (PTFE-PVDF-PP) by means of fibrous components. Two types of chopped fibers were used for modification of polymeric matrix, namely carbon fibers and bio-polymer fibres (sodium alginate, NaAlg). As a result of the presence of fibrous phase, the composite specimens differing in the surface roughness were obtained. The specimens containing alginate fibers revealed significant changes in wettability and surface energy in comparison to pure polymer.

The biopolymer fibres (NaAlg) degraded during *in vitro* incubation covering the surface of the material with the bio-polymer layer (bio-film) which lowered its wettability and increased the surface energy.

Formation of the biofilm was study by FTIR-ATR spectroscopy. The measurements were carried in the mid-infrared range (600–4000 cm⁻¹). The spectra were collected with 4 cm⁻¹ resolution.

New bands observed in 1600-1654 cm⁻¹ range corresponded to stretching vibrations of carbonyl bond related to methylene group (–CH₂–CO), which confirmed that the newly formed surface is similar to the pure bio-polymer.

- [1] A.S. Hoffman, J.A. Hubbell; *Surface-immobilized biomolecules. Biomaterials Science*, An Introduction to Materials in Medicine, Elsevier Inc 2004, 225-232.
- [2] S. Wu, *Polimer interface and adhesion*, Introduction 13-45, Marcel Dekker, New York 1982.
- [3] M. Lampin, R. Warocquier-Clerout, C. Legris, M. Degrange, *Correlation between substratum roughness and wettability, cell adhesion, and cell migration*, J Biomed Mater Res 36 (1997) 99-108

IR Mapping of Bio-Ceramic Layers on Titanium Substrate

C. Paluszkiwicz¹, W.M. Kwiatek², E. Długon¹, A. Weselucha-Birczyńska³, M. Piccinini⁴

¹AGH - University of Science and Technology, Faculty of Materials Science and Ceramics,
Al. Mickiewicza 30, 30-059 Kraków, Poland

²Institute of Nuclear Physics PAN, ul. Radzikowskiego 152, 31-342 Kraków, Poland

³Jagiellonian University, Faculty of Chemistry, ul. Ingardena 3, 30-060 Kraków, Poland

⁴INFN - Laboratori Nazionali di Frascati, Via E. Fermi 40, I-00044 Frascati (Rome), Italy

Modern medicine requires high quality implant materials. Bio-ceramics have revolutionized orthopedic and dental repair of damaged parts of the bone system. Some of biomaterials due to their biocompatibility allow manipulation and adaptation to the shape and dimensions of bone defects.

Titanium and its alloys are widely used in bio-implant applications. The nature of their surfaces can directly influence cellular response, ultimately affecting the rate and quality of new tissue formation. In order to improve titanium implants properties, they are usually covered with various kinds of layers. The bio-inert ceramic materials have attractive properties, such as strength and fracture for medical applications. For example ceramics containing zirconia (ZrO_2) are attractive materials because of chemical durability and ionic conductivity. Consequently, ZrO_2 has various applications in engineering and as biomaterial.

Vibrational spectroscopy has been extensively used for in vitro and in vivo investigations of degradation mechanism and kinetics of different biomedical devices as well as it has been used to characterize the crystalline and amorphous domains in biomineralization process. Infrared and Raman spectroscopy methods are valuable tools in the biomaterials engineering allowing the study of the processes occurring during their preparation.

In vitro tests, where the materials immersed in simulated body fluids and/or artificial saliva, have been used to evaluate the biocompatibility of biomaterials. This kind of tests are a wide range of repeatable and reproducible methods, which are regulated by international standards for commercial use and scientific development of new materials and products.

The aim of this work has been to examine zirconia silicate coatings obtained by sol-gel method on titanium and its alloys. The bioactivity of the composite films was studied by immersing the coatings in synthetic body fluids (SBF).

The changes in phase composition of biomaterials were determined by FTIR reflection technique based on focal plane array (FPA) detection system. Raman micro-spectroscopy was used as the complementary measurements. The study of the interaction of components of artificial body fluids with biomaterials being subjected to different environmental conditions by FTIR imaging is shown.

Acknowledgment

This work has been partly supported by Laboratori Nazionali di Frascati (Italy) under project TARI No. 67 contract No. RII3-CT-2004-506078.

Surface-Enhanced Raman Scattering from a Single Molecularly-bridged Silver Nanoparticle Aggregate

M. Sladkova¹, B. Vlckova¹, K. Siskova¹, I. Pavel², M. Moskovits², M. Slouf³

¹Department of Physical and Macromolecular Chemistry, Charles University, Hlavova 2030, 12840 Prague 2, Czech Republic; ² Department of Chemistry and Biochemistry, University of California at Santa Barbara, Santa Barbara, CA 93106 USA; ³ Institute of Macromolecular Chemistry ASCR, Heyrovsky Sq.2, 16206 Prague 6, Czech Republic

SERS (Surface-enhanced Raman Scattering) spectroscopy in systems with Ag nanoparticles has recently become a subject of reinforced interest stemming from achievement of single molecule level of detection. While the most efficient amplifiers have been proposed and proven to be Ag nanoparticle dimers [2,3], the frequently encountered small aggregates of Ag nanoparticles with several „hot spots“ are of interest from both the theoretical [4] and experimental point of view as well.

In this contribution, we report temporally fluctuating SERS signals originating from a particular small aggregate of 4,4'-diaminoterphenyl (DATP)-bridged Ag nanoparticles. An unequivocal correspondence between the morphology of the nanoobject and SERS signal obtained from it with a confocal Raman micro-spectrometer was ensured by assembling samples of widely spaced small Ag nanoparticle aggregates on chemically functionalized, SiO_x coated finder grids for TEM, and by determination of the selected aggregate position with respect to the markers of a particular mesh of the finder grid. Samples were assembled on 3-aminopropyltrimethoxysilane (APTMS)-derivatized, SiO_x coated Cu grids by a three step procedure involving (i) Ag nanoparticle attachment to APTMS-derivatized grids, (ii) attachment of DATP linkers to Ag nanoparticles by one terminal amine group, (iii) attachment of Ag nanoparticles to the second terminal amine group of the linker. TEM image

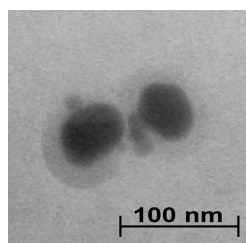


Fig. 1

of a selected single aggregate of DATP-bridged Ag nanoparticles and the temporally fluctuating SERS signal obtained from it at 514.5 nm excitation are shown in Figs. 1 and 2, respectively. The aggregate is constituted by a trimer of small particles interlocked between two larger particles (Fig. 1). Time-evolution of SERS-signal measured from this aggregate shows temporal fluctuations, in which the signal of DATP alternates with that of graphitic carbon, represented by two distinct, rather broad bands (Fig.2). The time-evolution of the SERS signal indicates that the bridging diaminoterphenyl molecule decomposes to graphitic carbon in at least one of the "hot spots" within the aggregate.

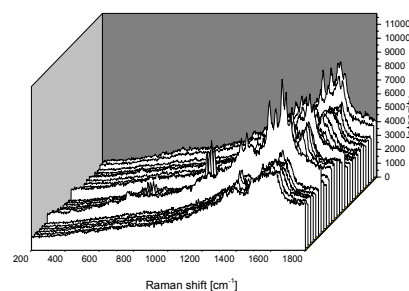


Fig. 2

- [1] K. Kneipp, et al, Phys. Rev. Lett. 78 (1997) 1667-1670.
 [2] H. Xu, J. Aizpurua, M. Kall, P. Apell, Phys. Rev. E 62 (2000) 4318-4324.
 [3] B. Vlcková, M. Moskovits, I. Pavel, K. Siskova, M. Sladkova, M. Slouf, Chem. Phys. Lett. (2008), doi:10.1016/j.cplett.2008.02.078.
 [4] M. Käll, H. Xu, P. Johansson, J.Raman Spectr. 36 (2005) 510.

Acknowledgment

Financial support by the 203/07/0717 and 203/05H001 grants awarded by GACR and by the MSM0021620857 long term research program are gratefully acknowledged. Present address of KS: Institute of Macromolecular Chemistry, ASCR, Heyrovsky Square 2, Prague 6, CR.

11. TIME RESOLVED SPECTROSCOPY

Ultrafast Conformational Dynamics of (R) - 1,1'-Bi-2-naphthol Measured with Time-Resolved Circular Dichroism

Claire Niezborala, François Hache

Laboratoire d'Optique et Biosciences, Ecole Polytechnique, CNRS, INSERM, 91128 Palaiseau, France

Circular dichroism (CD) is known to be a sensitive probe of molecular conformations. The idea of using CD in a pump-probe configuration in order to study the dynamics of structural changes occurring in molecules or in biomolecules is therefore quite natural [1]. In this context, we have recently developed a new technique which allows measurements of time-resolved CD in a user-friendly and artefact-free way. We will present and apply it to the study of the conformational dynamics of the excited state of 1,1'-Bi-2-naphthol.

CD can be obtained either with modulated circular polarizations or through ellipticity measurements. To get rid of the artefacts induced by the first technique, we have developed the second one which only involves non-modulated, linearly-polarized beams. The sample is placed between crossed polarizer and analyzer. The probe ellipticity is measured through a Babinet-Soleil compensator (BS) by recording the transmitted intensity (the "PM" signal) as a function of the BS retardation. A mechanical chopper is inserted on the pump optical path and a lock-in amplifier allows us to measure the modulated part of the PM signal (the "LI" signal). When measuring simultaneously the PM and the LI signals for small BS retardations, we obtain two parabolas [2]. Comparing both quadratic coefficients of the PM and LI parabolas directly yields the change in absorption whereas the shift between the LI and PM parabolas yields the change in CD (see figure 1d,e).

Experiments have been performed in the UV to investigate the dihedral angle changes in photoexcited (R)-1,1'-Bi-2-naphthol. Pump pulses are obtained after frequency tripling the output of a 150 fs, 1 kHz Titanium-Sapphire laser. Pulse energy is about 200 nJ. A tunable probe was obtained through several stages of optical parametric amplification. Results for two solvents are given in figure 1c ($c = 2.2 \cdot 10^{-4}$ M) for a probe wavelength of 237 nm. The pump-induced CD is plotted as a function of the pump-probe delay. The dots are obtained for Ethanol whereas the squares are for Ethylene Glycol. Pump-induced absorption changes are plotted in figure 1b. It is important to note that the absorption change is the same for both solvents and that there is no noticeable dynamics on the 400 psec timescale. On the contrary, we observe a quite different behaviour for the CD curves: a large difference is obtained for the two solvents and a 100 psec dynamics is measured for Ethanol. These differences prove that we observe true changes in the molecule conformation and not just an electronic relaxation or a reorientation effect. These conformational changes are clearly solvent dependent: the higher the viscosity, the longer the relaxation time. We assign this dynamics to a dihedral angle variation [3, 4].

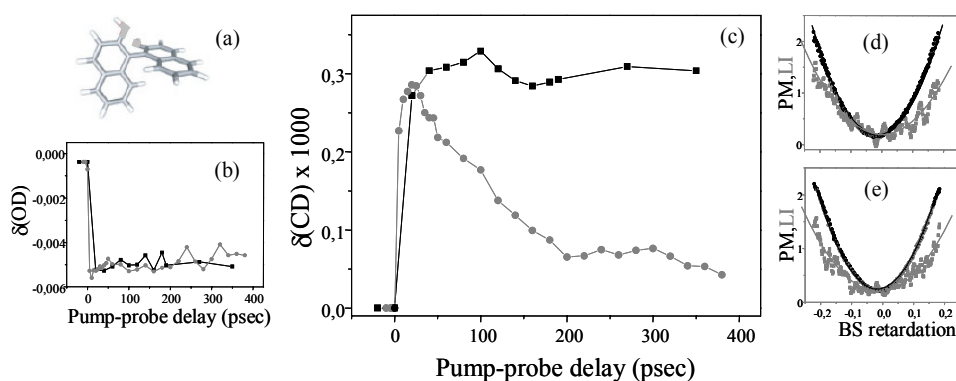


Fig. 1: (a) Structure of 1,1'-Bi-2-naphthol. (b,c) Time-resolved absorption and CD of 1,1'-Bi-2-naphthol in Ethanol (dots) and in Ethylene Glycol (squares). (d,e) Raw PM and LI parabolas at delays 40 and 375 psec in Ethanol.

We have also performed this experiment at 245 nm where we observe induced absorption. In that case, we observe the onset of a CD signal. The rise time is about 25 ± 10 psec in Cyclohexane (a value in agreement with previous estimations performed in 1,1'-Binaphthyl [3, 4]) whereas it is 80 ± 20 psec in Ethanol. This difference is attributed to the formation of hydrogen bonds between the hydroxy groups and the solvent in the latter case.

- [1] J. W. Lewis, R. A. Golbeck, D. S. Kliger, X. Xie, R. C. Dunn and J. D. Simon, *J. Phys. Chem.* 96 (1992) 5243.
 [2] C. Niezborala and F. Hache, *J. Opt. Soc. Am. B* 23 (2006) 2418.
 [3] D. P. Millar and K. B. Eisenthal, *J. Chem. Phys.* 86 (1985) 5076.
 [4] S. Fujiyoshi, S. Takeuchi and T. Tahara, *J. Phys. Chem. A* 108 (2004) 5938.

Site-Specific Folding Dynamics of Peptides Studied by Time-Resolved Infrared-Spectroscopy

C. Krejtschi¹, O. Ridderbusch¹, R. Huang², T.A. Keiderling², K. Hauser¹

¹*Institut für Biophysik, University of Frankfurt, Max-von-Laue-Str. 1, 60438 Frankfurt, Germany*

²*Department of Chemistry, University of Illinois at Chicago, 845 W. Taylor St. Chicago, Illinois 60607-7061, USA*

Peptides with well-defined secondary structure are ideal model systems to study protein folding mechanisms by infrared spectroscopy. IR-techniques provide both, the necessary time resolution as well as the structural sensitivity. The amide I' region, mainly the C=O stretching vibrations of the polypeptide backbone, is a marker band for secondary structure. However, vibrational transitions of individual amide groups are not resolved. Isotopic labeling of individual amide ¹³C=O groups induce site-specific frequency shifts and thus enhance localized structural information. We initiate thermal unfolding by a nanosecond laser-excited temperature jump (~10 °C) and probe amide I' absorption changes at single wavelengths. The alpha-helix to random coil transition of polyglutamic acid has been studied under reversible folding/refolding pHconditions [1]. The observed relaxation kinetics indicate a 2-state folding process and time constants for folding and unfolding could be extracted using complementary equilibrium measurements. Site-specific dynamics have been monitored for the thermal unfolding of an isotopically labeled β-hairpin peptide, a 12-mer tryptophan zipper peptide whose conformation is stabilized by a hydrophobic core formed by four tryptophan residues. Various single and crossstrand ¹³C=O isotopically labeled peptide variants have been studied by probing the relaxation kinetics at individual amide I' components. Differences in kinetic behavior have been found for the loss of beta-strand and the gain of disordered structure. The isotope-edited kinetics show variations in local structural stability of the hairpin backbone. Our data supports a multistate dynamic behavior that prevents clear determination of folding and unfolding time constants. Nonetheless, the site-specific kinetics are consistent with a hydrophobic collapse hypothesis for hairpin folding [2].

[1] C. Krejtschi, R. Huang, T.A. Keiderling, K. Hauser, *Vibrational Spectroscopy* (2008), in press.

[2] K. Hauser, C. Krejtschi, R. Huang, L. Wu, T.A. Keiderling, *J. Am. Chem. Soc.* 130 (2008) 2984-2992.

Time-Resolved Study of Photophysics of SAD (Salicylic Acid Derivatives) in Aqueous Solution

I.P. Pozdnyakov¹, A. Pigliucci², N. Tkachenko³, V.F. Plyusnin¹, E. Vauthey²,
H. Lemmetyinen³

¹*Institute of Chemical Kinetics and Combustion, Institutskaya 3, 630090 Novosibirsk, Russia*

²*Laboratory of Ultrafast Spectroscopy, University of Geneva, Ernest Ansermet 30, 1211 Geneva, Switzerland*

³*Institute of Materials Chemistry, Tampere University of Technology, 33101 Korkeakoulunkatu 8, Tampere, Finland*

Salicylic acid derivatives (SAD) are among the simplest systems which exhibit excited singlet state intramolecular proton transfer (ESIPT). In last two decades photophysics of SAD was intensively investigated in gas phase, non-polar and aprotic polar solvents [1, 2], but information about photoprocesses in aqueous media was scarce.

In this work up-conversion ($\lambda_{\text{ex}} = 266 \text{ nm}$, $\tau_{\text{resp}} = 280 \text{ fs}$), single-photon counting ($\lambda_{\text{ex}} = 340 \text{ nm}$, $\tau_{\text{resp}} = 300 \text{ fs}$) and steady-state techniques were used to investigate photophysics of several SAD (salicylic (H_2SA), 5-sulfosalicylic (H_3SSA), 2-methoxybenzoic (HMBA) and 2-aminobenzoic acids (HABA)) in aqueous solution in wide pH range. Series of important spectral and kinetic properties of the ground and excited (S_1) states of individual forms of SAD was defined (Table 1) including acid-base equilibrium constants (pK_a and pK_a^*), time constants of vibrational cooling of the S_1 states (τ_{VR}), fluorescence quantum yields (ϕ_f) and lifetimes (τ_{fl}), rate constants of fluorescence (k_{fl}) and quenching of the S_1 states by H^+ ($k_{\text{q}}(\text{H}^+)$).

Table 1: Main spectral and kinetic parameters of ground and excited states of different forms of SAD

Species	$\lambda_{\text{abs}} / \text{nm}$	$\lambda_{\text{em}} / \text{nm}$	ϕ_f	$\tau_{\text{VR}} / \text{ps}$	$\tau_{\text{fl}} / \text{ns}$	$k_{\text{fl}} \times 10^{-7} / \text{s}^{-1}$	$k_{\text{q}}(\text{H}^+) \times 10^{-10} / \text{M}^{-1}\text{s}^{-1}$
H_2SA	303	450	$\approx 4 \times 10^{-3}$	2.3	0.1	4.0	-
HSA^-	296	408	0.36	1.5	4.05	8.9	5.3
H_2SSA^-	302	440	0.01	1.0	0.17	5.9	-
HSSA^{2-}	298	403	0.43	0.7	5.9	7.3	3.4
HMBA	296	365	0.22	0.6	1.3	17	3.5
MBA^-	280	340	0.011	1.1	0.13	8.5	-
HABA	326	420	0.21	0.9	3.65	5.7	1.6
ABA^-	310	395	0.64	1.4	8.75	7.3	-

All forms of SAD exhibits large Stokes shift of fluorescence ($(6-11) \times 10^3 \text{ cm}^{-1}$) indicating serious reorganization of SAD molecules in the excited state. It was found also that anionic forms of SAD have the biggest quantum yields and lifetimes of luminescence, although k_{fl} values don't change significantly. These facts were explained well by the model of H-chelate ring reorganization in excited S_1 state of SAD [1, 2]. Indeed, according to this model decreasing of the distance between negatively charged COO^- group and proton of $\text{OH}(\text{NH}_2)$ group should take place in the excited state of SAD resulting in increasing of columbic interaction between these groups and stabilization of excited state of anionic forms.

[1] H.-C. Ludemann, F. Hillenkamp, R.W. Redmond, J. Phys. Chem. A 104 (2000) 3884-93.

[2] J.L. Herek, S. Pedersen, L. Banares, A.H. Zewail, J. Chem. Phys. 97 (1992) 9046-61.

Acknowledgment

This work was supported by RFBR (grants 05-03-32474, 06-03-32110, 06-03-90890, 05-03-39007GFEN) and Program of integration projects of SB RAS-2006 (grants № 4.16).

Pore Size Distribution of NF/RO Composite Membranes by Positron Annihilation Lifetime Spectroscopy

V. Dananić¹, K. Košutić¹, B. Kunst¹, D. Bosnar²

¹*Faculty of Chemical Engineering and Technology, University of Zagreb,
Marulićev trg 19, Zagreb, Croatia*

²*Department of Physics, Faculty of Science, University of Zagreb,
Bijenička 32, Zagreb, Croatia
e-mail: vdanan@fkit.hr*

The nanofiltration/reverse osmosis (NF/RO) composite membranes have widespread use in the processes of removal of water pollutants and desalinization. These devices usually operate under significant mechanical pressure (0.8–4 MPa) during long time. The membrane's pores are thus exposed to significant mechanical stresses and chemical interactions with solvent/solute. Basically there are three retention mechanisms: size exclusion, charge exclusion (NF charged membranes) and physicochemical interactions between membrane and solvent/solute. Which of these mechanisms is a dominant one it depends on a variety of requirements and environmental settings. Whenever the first mechanism - size exclusion - is a dominant one, it is vitally important to describe and understand the pore size distribution within the membrane [1]. The aim and purpose of this work is to experimentally probe for membrane's free volume by positron annihilation lifetime technique and subsequently reveal the pore size distribution from the distribution of positron lifetime [2].

The relevant theoretical models which presuppose the pore size distribution to be unimodal or bimodal are briefly discussed.

[1] K. Košutić, D. Dolar, B. Kunst, *J. Memb. Sci.* 282 (2006) 109-114.

[2] D. Bosnar, Zs. Kajcsos, L. Liskay, L. Lohonyai, P. Major, S. Bosnar, C. Kosanović, B. Subotić, *Nucl. Instr. and Meth. A* 581 (2007) 91-93.

The Temporal Dipole Moment of the Solutes Undergoing Charge Transfer in the Excited State

A. Krzysztofowicz, V.I. Tomin

Institute of Physics, Pomeranian University, Arciszewskiego 22B, 76-200 Slupsk, Poland

Important conclusions about a geometrical transformation of molecular structure of quantum systems with charge transfer in the excited state could be obtained from the knowledge of its dipole moment change in time. Unfortunately, until now, available experimental methods allow us to obtain only stationary values of the dipole moments for both the local excited and the charge transfer states.

On the basis of the theory of solvatochromism the time dependence of the dipole moment on the correlation function for the instant spectra kinetics and some other solution parameters has been deduced [1,2]. The time-resolved fluorescence spectra of the 6-propionyl-2-dimethylaminonaphthalene (Prodan) in glycerol solution were measured by means of the apparatus consisting of the solid state Nd:YAG laser with the optical parametric generator as the excitation part, and the spectrograph 2501S (Bruker Optics, USA) jointed with the streak camera C4334-01 (Hamamatsu, Japan) as the detection part [3]. The spectrograph insures spatial resolution of the analyzed light (wavelength axes), whereas the streak camera allows for temporal resolution of the light beam coming out of the spectrograph.

Using the fast Fourier transform and the Debye's equation we obtained for our solution the time dependent dielectric relaxation function [4] which was used for the calculation of the time dependence of the Stokes shift and the electric dipole value of the Prodan in polar solvents. The initial and the final values of dipole moments are close to ones obtained by means of the steady-state spectroscopy methods.

[1] V.I. Tomin, A. Krzysztofowicz, *Z. Naturforsch* 59a (2004) 476.

[2] A. Krzysztofowicz, V.I. Tomin, *Optica Applicata* 36 (2006) 483-487.

[3] A..A. Kubicki, P. Bojarski, M. Grinberg, M. Sadownik, B. Kukliński, *Optics Communications* 263 (2006) 275–280.

[4] Ch-P. Hsu, X. Song, R.A. Marcus, *J. Phys. Chem.* 101 (1997) 2546-2551.

12. NEW INSTRUMENTATION

Raman Spectroscopic Analysis in Acoustically Levitated Drops

Don McNaughton¹, Rudolf Tuckermann², Ljiljana Puskar¹, Bayden Wood¹, Jurgen Popp³,
Torsten Frosch³

¹Monash University, School of Chemistry, Centre of Biospectroscopy, Wellington Rd.,
Clayton, Victoria 3800, Australia

²University of Göttingen, Institute of Physical Chemistry, Göttingen, Germany

³Institute of Physical Chemistry, Friedrich-Schiller-University, Jena, Germany

Acoustic levitation has been shown to be a useful technique for contact-less handling of small solid and liquid samples in a gaseous environment with sample sizes typically of diameter 0.2–2 mm. Because of the lack of containment acoustic levitation inhibits wall effects and offers a contact-less handling medium for micro-sized samples. The combination of Raman spectroscopy with acoustic levitation, Raman Acoustic Levitation Spectroscopy (RALS), first coupled to Raman spectroscopy by Biswas¹, enables a time-resolved, contact-less monitoring of in-situ chemical reactions and physical and biological processes in a single drop suspended in a gaseous environment.

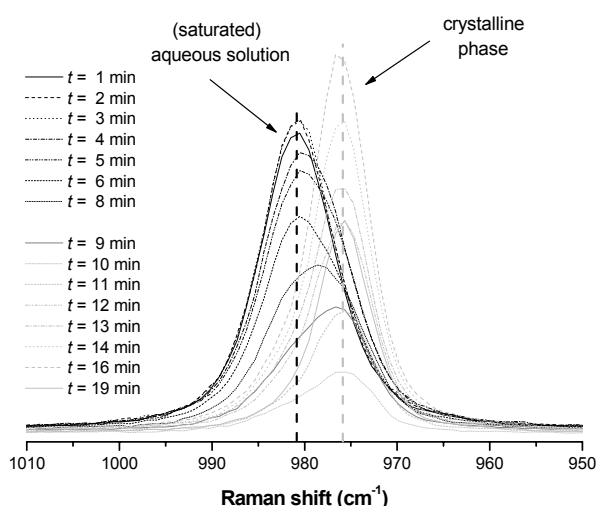


Figure 1: Raman spectra of evaporation and crystallization of a saturated aqueous solution of an acoustically levitated drop of $(\text{NH}_4)_2\text{SO}_4$ in ambient air at $T = 20\text{ }^\circ\text{C}$ and $\text{RH} = 39\%$ (sampling every 30 s)

The main focus of this work has been to probe the utilization of RALS in quantitative analytical chemistry. The apparatus consists of an acoustic levitation device (Dantec/Invent) mounted on an x,y,z translation stage and coupled to a Renishaw micro Raman spectrometer. After carrying out some systematic tests to probe the sensitivity of the technique to drop size, shape and position, RALS has been successfully applied in monitoring sample dilution and pre-concentration, evaporation, crystallization, and an acid-base reaction. The spectra obtained through an experiment monitoring the crystallization of ammonium sulphate is shown in figure 1.

We have also applied the RALS technique to the field of biospectroscopy, recently in monitoring the malarial pigment, hemozoin in live malarial infected levitated red blood cells². Live red blood cells, 5 μL , in phosphate buffered saline were levitated in the acoustic levitator and the heme dynamics monitored through the exchange of oxygen. Raman spectra of levitated malarial infected red blood cells showed the distinct signature of the malarial pigment hemozoin.

- [1] A. Biswas: *Thermal processing of o-terphenyl: A Raman study*. Appl. Spectrosc. 47 (1993) 458.
[2] L. Puskar, R. Tuckermann, T. Frosch, J. Popp, V Ly, D. McNaughton and B.R. Wood: *Raman acoustic levitation spectroscopy of red blood cells and Plasmodium falciparum trophozoites*. Lab on a Chip 7 (2007) 1125–1131.

New Application of Infrared Microscopy and Imaging in Difficult Sample Analysis

J. Mink^{1,2}, J. Mihály¹, Z. Bacsik¹, V. Gombás², X. Zhou³

¹Chemical Research Center, Hungarian Academy of Sciences, H-1525, Budapest, P.O. Box 17, Hungary E-mail: jmink@chemres.hu, ²Faculty of Information Technology, Research Institute of Chemical and Process Engineering, University of Pannonia, Egyetem u. 10, Veszprém H-8200 Hungary, ³Department of Physical, Inorganic and Structural Chemistry, Stockholm University, SE-106 91 Stockholm, Sweden

Structural study of complex samples (e.g. microcrystals of zeolites, aerosol particles, archeological materials and biological tissues) using Fourier transform infrared (FTIR) microscopy and imaging will be discussed.

FTIR microscopic study of zeolites with chiral and achiral structures has been performed. Thermal decomposition of organic amines (templates) was monitored on 50-100 μm diameter single crystal particles up to 400 $^{\circ}\text{C}$ by heated sample stage FTIR microscope. The complete removal temperatures have been determined for several $\text{Ge}_x\text{Si}_{10-x}\text{O}_{20}$ zeolite crystals [1].

FTIR microscopy has several advantages compared to traditional analytical methods used in analysis of aerosol samples (no sample preparation need, some 10^{-11} g samples can be investigated non-destructively in a short measurement time). Inorganic ions (SO_4^{2-} , HSO_4^- , NH_4^+ , NO_3^-) and even ionic compounds have been determined. The submicron particles contained mostly acetone soluble organic compounds (aliphatic hydrocarbons, organonitrates, carbonyl compounds) and inorganic ions (mostly ammonium sulphate), while the supermicron particles consisted of insoluble bioaerosol (amide, carbohydrate, phosphate) and traces of soil (SiO_2 , kaolinite) [2].

FTIR microscopy, due to high lateral resolution ($\sim 5 \mu\text{m}$) is suitable for homogeneity studies of art objects. Late Neolithic painted ceramics were studied: as red colouring pigment cinnabar was identified for the first time, mixed homogeneously with purified kaolinite [3].

It was firstly demonstrated in our laboratory, that IR spectra of human hair can be correlated with general physiological condition of human body [4]. The strong degradation of hair surface due to UV-irradiation, bleaching agents, etc. cause difficulties in spectral evaluation. Therefore FTIR imaging of cross-section of human hair was carried out. The spatial resolution ($\sim 5 \mu\text{m}$) will provide several hundreds of spectra characteristic to medulla, cortex and cuticle. We have developed a special program system based on cluster analysis to select important spectra of microtomed hair. The multispectral approach with combination of statistical data processing will provide new and sensitive diagnostic opportunities based on spectral features of non-degraded cortex and medulla.

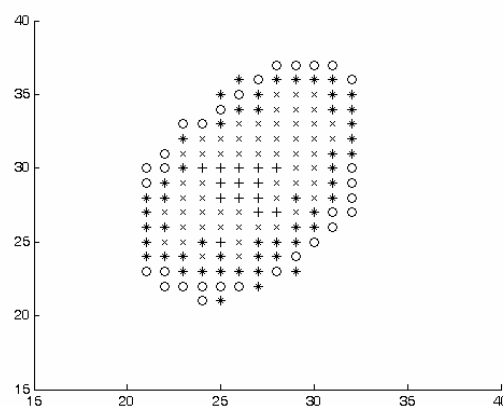


Fig. 1: Transmission FTIR imaging of human hair ($4\mu\text{m}$).
+ - medulla, x - cortex, * - slightly degraded cuticle, o - strongly degraded cuticle.

- [1] L. Tang, L. Shi, C. Bonneau, J. Sun, A. Ojuva, M. Kritikos, R.G. Bell, Z. Bacsik, J. Mink and X. Zhou, *Nature Materials* (accepted for publication)
- [2] Z. Bacsik, I.S. Butler, A. Gelencsér, A. Hoffer, G. Kiss, J. Mink and V. Velekey, *Appl. Spectr. Rev.* (under preparation)
- [3] J. Mihály, V. Komlósi, A. Tóth, Zs. Tóth and G. Ilon, *Proceeding of 9th European Meeting on Ancient Ceramics (EMAC)*, 24-27 Oct. 2007, Budapest, Hungary
- [4] An European Patent application procedure is under progress

Acknowledgement

The authors gratefully acknowledge financial support from the Hungarian Research Council (OTKA K-61611) and from the Children Cancer Foundation, Hungary.

Employing Polyethylene as Contacting Agent Between ATR-crystals and Solid Samples with Hard Surfaces

Vladimir Ivanovski¹, Thomas G. Mayerhöfer^{2,3}, Jürgen Popp^{2,3}

¹*University of Sts. Cyril and Methodius, Faculty of Natural Sciences and Mathematics, Institute of Chemistry, Arhimedova 5, 1000 Skopje, Republic of Macedonia*

²*Institut für Physikalische Chemie, Friedrich-Schiller-Universität, Lessingstraße 10, D-07743 Jena, Germany*

³*Institut für Photonische Technologien e.V., Albert-Einstein-Str. 9, D-07745 Jena, Germany*

Modern attenuated total reflection (ATR)-spectroscopy appeared at the end of the 5th decade and the beginning of the 6th decade of the previous century. Since then it has found widespread use for the structural investigation especially of liquids and soft solids like polymers etc. For samples with hard surfaces, e.g. most of the inorganic single crystals, ATR-spectroscopy has a shadowy existence due to the need of establishing an intimate contact between the incidence medium (i.e. the ATR-crystal) and the medium under investigation.

All proper techniques presented so far, however, show either the disadvantage of being comparably complicated to use or of employing toxic and volatile liquids. The aim of this work is therefore to introduce a technique that is easy to apply and assures optical contact using a non-toxic and easily removable coupling agent.

To assess the quality of polyethylene as contacting agent we conducted IR-ATR experiments employing an ATR-ZnSe semi-sphere as ATR-crystal and an optically polished (001)-cut of a fresnoite ($\text{Ba}_2\text{TiSiO}_8$, optically uniaxial) single crystal. Both s- and p-polarized infrared spectra were recorded at different angles of incidence ranging from 10° to 80°. These spectra were compared with a second series of spectra where we employed CS_2 as immersion liquid, which is the reference material known from literature [1], and with artificial spectra modelled from previously obtained single crystal data [2]. Since the employment of polyethylene results in a superior resemblance between measured and modelled spectra and is much easier and safer to apply, we expect this technique to open up the way for a routine application of IR-ATR spectroscopy to materials with hard surfaces.

[1] G. Kortüm, *Reflectance Spectroscopy: Principles, Methods, Applications*, Springer-Verlag, Berlin-Heidelberg-New York, 1969.

[2] T.G. Mayerhöfer, H.H. Dunken, *Vibrat. Spectr.* 25 (2001) 185.

WORKSHOP & EXHIBITION

Latest Innovations in Raman Microscopy for Ultra Fast Raman Imaging and Macro-mapping

Horiba Jobin Yvon S.A.S.

Raman microscopy has become an important tool for the analysis of materials on the micron scale, providing crucial information to experimentalists working in the fields of pharmaceutical research, semiconductors, geology, etc.

The unique confocal and spatial resolution of micro-Raman systems has enabled optical far field resolution to be pushed to its limits with often sub-micron resolution achievable for chemical imaging of small structures or isolated objects. The non destructive and non contact aspects of this technique, plus the fact that it requires no sample preparation, makes it an ideal analytical tool, which is more and more acknowledged by the research and industrial communities.

Although Raman Imaging is widely used already, it is sometimes seen as rather slow in comparison to other imaging techniques such as NIR or fluorescence microscopy. With the patented LineScan technique where the laser beam is raster-scanned along a line, one could already produce faster acquisition times as all spectra along the line are taken simultaneously.

Now, things have evolved much further, pushing the limits of systems to obtain high quality Raman images with unprecedented speeds of acquisition. Now, we have taken things much further, pushing the limits of our systems to obtain high quality Raman images with unprecedented speeds of acquisition. Indeed, with point-by-point Raman mapping, a lot of the acquisition time is wasted in communication between the hardware and the software.

Recent advances in detection and hardware communication have enabled us to reach measurement times as low as a few ms/point, opening the door to quasi-instantaneous chemical imaging. This revolution has a name: SWIFT™ mapping.

In addition, HORIBA Jobin Yvon has launched a new imaging mode, the revolutionary DuoScan™ (patent pending), which offers the best of both the micro and the macro world, as it generates Raman maps across both μm -scale and cm-scale areas with FULL coverage of your sample. When looking at large sample surfaces, whether it is to measure component distribution or to search for contaminants, it often comes down to finding a needle in a haystack. The DuoScan allows you to vary the spot size from 1 μm to 300 μm to match your image pixel size, ensuring that you don't miss a spot even on very large sample areas. The images produced are fully confocal, to better reject fluorescence or signals coming from beneath the analyzed surface.

Discussions around the state of the art and new trends for Raman Imaging will be made, illustrated by application examples and demonstration measurements that emphasize the real interest in Raman Imaging, pushing further the limits in either spatial resolution or mapping speed.

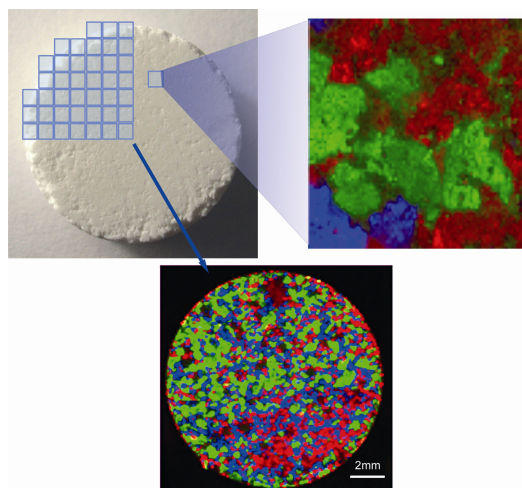


Figure 1:

(a) White light image of a Pharmaceutical tablet.

(b) DuoScan™ large area mapping on a full tablet. 100% of this 12.5 mm diameter tablet was imaged in about 10 minutes.

(c) DuoScan™ point-by-point mapping on a region of interest for finer analysis, pixel size: 1 μm .

The New Vacuum FT-IR Spectrometer: Design Advances and Research Application

J. Sikola¹, G. Zachmann², M. Huber²

¹Optik Instruments sro., 592 61 Doubravnik 187, Czech Republic, e-mail: jiri.sikola@vol.cz

²Bruker Optik GmbH, Rudolf-Plank-Str. 27, Ettlingen, 76275, Germany
e-mail: Guenter.Zachmann@brukeroptics.de, Michael.Huber@brukeroptics.de

When the bar for research FT-IR spectrometers was set, we knew that some day we would feel obliged to raise it. For the new VERTEX 80 series Bruker Optics provides an innovative interferometer concept and a very flexible vacuum optics layout, which is the culmination of everything that have been pioneered and developed in over 30 years. The new research FT-IR spectrometer is based on the true-aligned UltraScan™ interferometer (see fig. 1), which provides the highest spectral resolution achievable on a bench top FT-IR spectrometer. The precise linear air bearing scanner and high quality optics guarantees the ultimate sensitivity and stability.

The rugged and stable cast aluminium vacuum optics bench enables demanding experiments such as high spectral resolution (0.060 cm^{-1}), ultra fast time resolved spectroscopy (ms down to few ns temporal resolution), or ultra-violet spectral range (up to $50,000\text{ cm}^{-1}$) measurements. The two optional external detector ports accommodate liquid He dewars of bolometer and/or hot electron-detectors (see beam exits OUT 2 and OUT 5 in fig.1). In combination with the external water cooled high power Hg-arc source, the recently rediscovered terahertz spectral range is accessible (down to less than 5 cm^{-1}). The evacuated optics bench eliminates atmospheric moisture absorptions and provides extreme sensitivity and stability, especially in the far IR spectral regions. All these features make the VERTEX 80v also an ideal instrument to be adapted to a synchrotron light source with its highly brilliant infrared beam.

In this contribution we will prove the instruments resolving power $\nu/\Delta\nu$ of better than 300.000:1 on iodine vapour absorption lines in the visible spectral range and demonstrate its excellent measurement sensitivity and stability. Furthermore, based on FT-IR-microscopy data measured with the VERTEX 80 series spectrometer and an adapted HYPERION infrared microscope, we show that the achievable lateral resolution of such a system is practically only limited by Abbe's diffraction barrier.

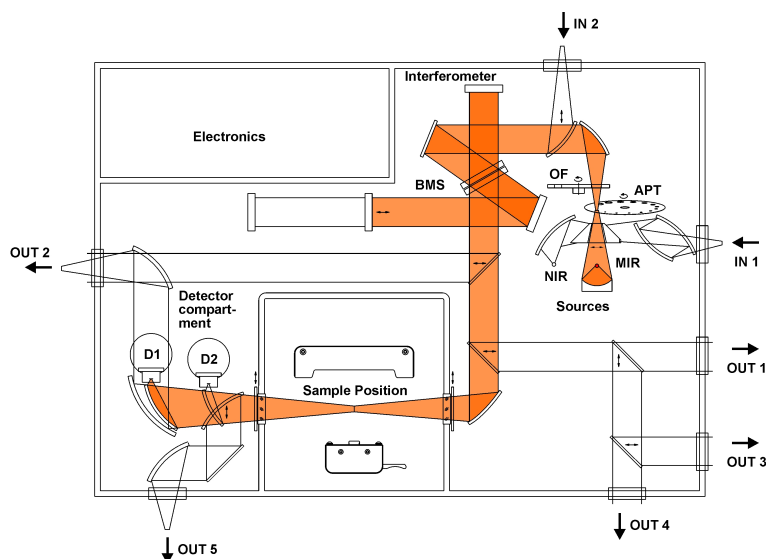


Fig. 1: Optics layout of the vacuum research FT-IR spectrometer VERTEX 80v.

“State of the Art” Spectroscopy in Food Analysis

Marion Egelkraut-Holtus, Uwe Oppermann

*Shimadzu Europa GmbH, Albert Hahn Str. 6-10, 47269 Duisburg, Germany
e-mail: meh@shimadzu.de*

A wealth of spectroscopic methods exists for residue analysis and quality control. The method and type of instrumentation employed are dictated by the composition and formulation of the samples to be measured. Spectroscopy is the method of choice if quick and simple information about the sample material is required, both qualitatively and quantitatively. The optimum spectroscopic method is determined by the sample characteristics.

The widest application range is covered by the UV-VIS spectrometers, which are ideal for the quantitative and qualitative analysis of samples in absorption, transmission and reflection measurement modes. In food laboratories, routine instruments like the new UV-1800 with a small footprint are required for routine applications such as the Casein determination. The optical system shows the highest level of resolution in this class at 1 nm.

FTIR Spectrometers, from the near to the far IR region, allow specific identification of substances. They can be used in combination with a range of accessories, including microscope, each accessory being selected according to the sample material and properties. The latest development in this segment is the IRAffinity-1 with an extraordinary signal-noise-ratio of 30,000:1 and a high resolution of 0.5 cm^{-1} .

Fluorescence spectrometers that are capable of highly sensitive quantitative analyses complete the range of spectroscopic methods suitable for the analysis of food stuffs.

Even though quantitation of substances in food is a typical spectroscopic application, the determination of trace elements is the favourite subject of atomic absorption- and ICP-OES spectrometers. The drinking water as one of the most important ingredients of all foodstuffs has to be strictly controlled according to the paragraphs 5 to 7 of the new European drinking water regulations (2003). The concentration levels of the essential and toxic elements are tightly controlled so that a constant water quality can be maintained. Elements like mercury, cadmium and lead are included in the list of contaminants and must not exceed their maximum contaminant levels according to EPA. Other elements, like platinum, palladium and rhodium actually are not straight in the focus of the public interest, even though, these platinum elements, through the liberation of very fine particles from the catalytic converters are accumulated in our environment and found in significant concentrations in our food chain.

Analytical procedures for the determination of substances in food are described using a wide variety of different system configurations. In recent laboratory requirements these “state of the art” tools allowing a high sample throughput and guaranteeing the highest level of quality.

PerkinElmer

LAST MINUTE ABSTRACTS

Molecular Structure and Vibrational Spectroscopy investigation of Secnidazole using Density-Functional Theory

Soni Mishra¹, Deepika Chaturvedi¹, Poonam Tandon¹, V.P. Gupta¹, A.P. Ayala²,
S.B. Honorato², H.W. Siesler³

¹Physics Department, University of Lucknow, Lucknow 226007, India
e-mail: poonam_tandon@hotmail.com

²Departamento de Física, Universidade Federal do Ceará, C. P. 6030, 60.455-900 Fortaleza, CE, Brazil

³Department of Physical Chemistry, University of Duisburg-Essen, Essen D45117, Germany

Secnidazole (α , 2-dimethyl-5-nitro-1H-imidazole-1-ethanol) is an antimicrobial drug and is particularly effective in the treatment of amebiasis, giardiasis, trichomoniasis and bacterial vaginosis. Secnidazole crystallizes as a hemihydrate, which belongs to a monoclinic system, space group $P2_1/c$, $a = 12.424 \text{ \AA}$, $b = 12.187 \text{ \AA}$, $c = 6.662 \text{ \AA}$, $\beta = 100.9^\circ$. The optimized geometry of Secnidazole molecule has been determined by Density Functional Theory (DFT) method. Energies have been obtained using DFT method with B3LYP functionals with extended basis sets 4-31G, 6-31G and 6-311++G(d,p) for the three stable conformers of secnidazole. Using the optimized structure, we have determined the infrared and Raman frequencies for the molecule using DFT method. In this work, we also present a detailed vibrational spectroscopy investigation of secnidazole by using infrared and Raman spectroscopies. Based on these results, we discuss the correlation between the vibrational modes and the crystalline structure of the most stable conformer of secnidazole. The resulting frequencies are in excellent agreement with experiment. A complete assignment is provided the fundamental vibrational bands in terms of frequency and potential energy distribution. The calculated Raman spectrum is compared with experimental data obtained in the hemihydrate (30 °C) and anhydrous (90 °C) forms.

INDEX

- | | | | | | |
|----------------------------|----------|--------------------------------|--------------------------|---------|--------------------------|
| Abbas | O. | 214 | Barnes | A. | 1 |
| Abramczyk | H. | 8, 139, 227 | Barth | A. | 98, 129, 289 |
| Adameczyk | A. | 275 | Bartoszak-Adamska | E. | 34 |
| Akalin | E. | 330 | Bartoszek | M. | 223, 224 |
| Akkaya | Y. | 41, 219 | Basar | Gonul | 42 |
| Aksay | S. | 26, 205, 331 | Basar | Gunay | 42, 118 |
| Akverdieva | G.A. | 298 | Basaran | S. | 263 |
| Akyuz | S. | 36, 41, 42, 118, 219, | Baumann | S. | 20, 49 |
| | | 263, 298, 311, 313, 330 | Bayarı | S.H. | 90, 188, 225 |
| Akyuz | T. | 36, 263, 298, 330 | Bayrak | C. | 43 |
| Aleksa | V. | 251 | Beck | A. | 237 |
| Alieva | R.R. | 119 | Becucci | M. | 280 |
| Alikhani | E. | 25 | Bellanato | J. | 44 |
| Almeida | R. | 125 | Belogurova | N.V. | 106, 119 |
| Altiokka | B. | 205 | Ben Altabef | A. | 45, 226 |
| Ambrosov | S.V. | 123, 162 | Benassi | E. | 46, 47, 291 |
| Amthauer | G. | 294 | Berber | Halil | 299, 300, 331 |
| Anashkin | A. | 184, 190 | Berber | Hüseyin | 331 |
| Andreev | S. | 255 | Bercean | V. | 62 |
| Andreeva | Lj. | 37, 220 | Bermanec | V. | 267 |
| Andrushchenko | V. | 109, 117 | Bernhard | U. | 114 |
| Anevska-Stojanovska | N. | 220 | Bernstorff | S. | 153 |
| Aranyi | A. | 133 | Bhaktha | S.N.B. | 152 |
| Araújo | R.C.M.U. | 317 | Bigotto | A. | 337 |
| Ardelean | I. | 211, 212 | Biliškov | N. | 19 |
| Arenas | J.F. | 309 | Biljan | T. | 244 |
| Arığ | A.B. | 188 | Bini | R. | 281 |
| Arslan | T. | 209 | Bistričić | L. | 77, 155, 189, 202 |
| Ashall | B. | 144 | Bitenc | M. | 5 |
| Astilean | S. | 156, 164, 179, 233, 326 | Blazewicz | M. | 167, 168, 338 |
| Atrian | S. | 141 | Blazewicz | S. | 160, 163, 169 |
| Ayala | A.P. | 353 | Blomberg | M. | 289 |
| Aybek | A.Ş. | 331 | Boehlig | H. | 109 |
| Aydemir | S. | 299, 300 | Bogun | M. | 168 |
| Baban | A. | 89 | Bojko | B. | 227, 248, 249 |
| Babkov | L.M. | 38, 39, 40, 284 | Bonora | S. | 332 |
| Bacsik | Z. | 347 | Boopalachandran | P. | 27 |
| Baeten | V. | 214 | Borba | A. | 48 |
| Baia | L. | 179 | Borodi | G. | 170 |
| Baia | M. | 179, 326 | Borowski | P. | 301, 302 |
| Balarin | M. | 195, 206, 303 | Bosca | M. | 157, 170 |
| Balci | K. | 41, 219, 323 | Bosnar | D. | 344 |
| Baldeck | P. | 149, 164 | Bouazaoui | M. | 149, 150, 152 |
| Balevicius | V. | 250 | Boukherroub | R. | 327 |
| Bali | A.S. | 283 | Bouř | P. | 109, 117 |
| Bally | T. | 10 | Bramble | A. | 114 |
| Balón | M. | 285, 286 | Brandán | S.A. | 226 |
| Ban-Oganowska | H. | 240 | Breda | S. | 69 |
| Banica | F. | 121 | Brehm | G. | 20, 49, 50 |
| Baraldi | I. | 46 | Breitinger | D.K. | 20, 49, 50 |
| Baran | A. | 222 | Brémard | C. | 215 |
| Baranović | G. | 19, 95, 97, 155 | Brkic | G. | 115 |
| Baranska | M. | 221, 222 | Brnjas-Kraljević | J. | 195, 206, 303 |
| Barbillat | J. | 215 | Brožek-Pluska | B. | 8, 139, 227 |
| Barczak | M. | 154 | Bruker Optik GmbH | | 350 |
| Barlea | M. | 86 | Burova | T. | 184, 190 |
| | | | Búza | M. | 236, 237 |

- | | | | | | |
|-------------------------|--------|---|--------------------------|--------|--------------------------------|
| Cahil | A. | 97b | Dellepiane | G. | 336 |
| Cakić | M. | 197 | Demchenko | A.P. | 290 |
| Camaiti | M. | 200 | Despotović | I. | 57 |
| Canpean | V. | 156 , 326 | Dettin | M. | 99 |
| Capdevila | M. | 141 | Di Foggia | M. | 99 , 332 |
| Capoen | B. | 149, 150, 152 | Didović | M. | 159 |
| Capozzi | V. | 134 | Długoń | E. | 275, 339 |
| Carmona | C. | 285 , 286 | Dobosi | V.T. | 272 |
| Carmona | P. | 120 | Dobrowolski | J.Cz. | 58 , 88 |
| Castellano | G. | 201 | Dogan | N.E. | 298 |
| Castellucci | E.M. | 200, 271, 280 | Dombi | G. | 79 |
| Cavalu | S. | 121 | Domènech | J. | 141 |
| Čeh | M. | 153, 161, 181 | Domingo | C. | 265, 333 , 334 |
| Çelik | Ö. | 188, 313 | Dorohoi | D.O. | 268 |
| Centeno | S.P. | 309 | Došlić | N. | 14 |
| Ceponkus | J. | 51 , 251 | Doyle | G. | 122 , 144 |
| Ceppatelli | M. | 281 | Dozova | N. | 25 |
| Cesmeli | H. | 263 | Drăgan | F. | 229 |
| Chaturvedi | D. | 353 | Drożdżewski | P. | 21 |
| Chenenko | T. | 114 | Dubček | P. | 153 |
| Chicea | D. | 86 | Dubey | I. | 136 |
| Chiş | V. | 52 , 229, 247, 252, 253 | Dubey | L. | 136 |
| Chisaera | A. | 5 | Duran | A. | 266, 277 |
| Cholewa-Kowalska | K. | 53 , 254 | Duran | M. | 299, 300 |
| Chruszcz-Lipska | K. | 221 | Durig | D.T. | 96 |
| Ciačka | P. | 228 | Durig | J.R. | 96 |
| Cindrić | M. | 78, 83 | Dyar | M.D. | 279 |
| Ciorba | S. | 46 | Džafić | E. | 191 |
| Codony | R. | 214 | Dziembowska | T. | 232 |
| Cordier | A. | 158 | Eckert-Maksić | M. | 243 |
| Cozar | O. | 211, 212, 229 , 230, 238,
247, 252, 253 | Egelkraut-Holtus | M. | 351 |
| Cristiano | M.L.S. | 125 | Elefanty | A. | 103 |
| Cristini | O. | 149 | Ellmerer | M. | 102 |
| Crnjak Orel | Z. | 5 | Engelen | B. | 97b |
| Csendes | Z. | 133 | Estronca | T.M.R. | 69 |
| Culea | E. | 85, 86, 97a, 157 , 170,
230, 238 | Eusébio | E.M.S. | 69 |
| Culea | M. | 97a, 230 , 231 | Fabian | H. | 9 |
| D'Auria | S. | 186 | Fagnano | C. | 99 |
| da Silva | J.B.P. | 316 | Fahmy | K. | 100 |
| Dąbrowski | A. | 154 | Farcau | C. | 233 , 326 |
| Damm | U. | 102 | Fausto | R. | 7, 48, 69, 70, 94, 125,
310 |
| Dananić | V. | 77, 189, 344 | Feichtner | F. | 102 |
| Darányi | M. | 142 | Felföldi | K. | 30, 79 |
| Darchuk | L. | 264 | Ferensowicz | A. | 275 |
| Davarcioglu | B. | 262 | Fernández-Gómez | M. | 301, 302 |
| David | L. | 62, 89 | Fernández-Lienres | M.-P. | 301, 302 |
| Davidović | E. | 54 | Ferrari | M. | 5 |
| Davydova | N.A. | 38, 284 | Fojud | Z. | 92 |
| De Grave | E. | 4 , 158, 279 | Ford | T.A. | 292 |
| de Resende | V.G. | 4 , 158 , 279 | Forgó | P. | 79 |
| deCruz | A. | 200 | Fraczek | A. | 160 |
| Dědic | R. | 126 | Franquelo | M.L. | 266 , 277 |
| Defonsi Lestard | M.E. | 45 | Fridrichova | M. | 207 |
| Dega-Szafran | Z. | 34, 55 , 56 | Friščić | I. | 143 |
| Deja | J. | 276 | Frosch | T. | 103, 216, 346 |
| del Puerto | E. | 265 | Furić | K. | 5, 59 , 202, 206, 210 |
| Delgado | J. | 178 | | | |

- | | | | | | |
|-------------------------|--------|---|---------------------------------|------|------------------------------------|
| Gajović | A. | 143 , 153, 161 , 178, 181, 260, 267 | Hannus | I. | 236 , 237 |
| Galabov | B. | 11 | Hanuza | J. | 71, 240, 242, 259 |
| Gálvez | E. | 44 | Hashimoto | E. | 127 |
| Galvin | M. | 144 | Hauer | I. | 89 |
| Gamulin | O. | 195, 206, 303 | Hauser | K. | 342 |
| Gandolfi | M.G. | 328 | Heise | H.M. | 102 |
| García-Fernández | E. | 286 | Henry | M. | 107 |
| García-Ramos | J.V. | 265, 333, 334 , 335 | Heraud | P. | 103 , 110 |
| Gatjal | A. | 60 , 62, 63 | Hernik | K. | 28 |
| Gauger | D.R. | 109, 135 | Herrera | L.K. | 266 |
| Gawel | B. | 73 | Hetmańczyk | J. | 64, 287 |
| Gdaniec | Z. | 250 | Hetmańczyk | Ł. | 64 , 287 |
| Gellini | C. | 65 | Hidalgo | J. | 285 |
| Georgiev | A. | 255 | Hirota | E. | 22 |
| Giorgetti | E. | 336 | Hobza | P. | 135 |
| Giusti | A. | 336 | Holomb | R. | 148 |
| Glamazda | A. | 171 | Holzer | M. | 180 |
| Glaubitz | C. | 111 | Honorato | S.B. | 353 |
| Glushkov | A.V. | 123 , 162 , 293 , 304 , 305 | <i>Horiba Jobin Yvon S.A.S.</i> | | 349 |
| Gnatyuk | I.I. | 39, 40 | Hrenar | T. | 13, 78, 83 |
| Gocan | I. | 62 | Huang | R. | 342 |
| Godjajev | N.M. | 298 | Huber | M. | 350 |
| Gojlo | E. | 138 | Íde | S. | 188 |
| Golec | B. | 91 | Ike | Y. | 104 , 127 |
| Gombás | V. | 124 , 347 | Ilić | Lj. | 197 |
| Gómez | J.A.M. | 279 | Ilie | S. | 194 |
| Gómez-Zavaglia | A. | 48, 70, 125 | Ionete | R. | 140 |
| Gopas | J. | 115 | Iordache | A. | 238 |
| Gosav | S. | 268 , 269 | Iosin | M. | 164 , 326 |
| Gotić | M. | 5, 234 | Iriepa | I. | 44 |
| Govorčin Bajsić | E. | 155 | Ivanda | M. | 5 , 147, 174, 177, 206, 210 |
| Gracin | D. | 153 | Ivanovski | V. | 348 |
| Grandidier | B. | 152 | Iveković | D. | 143, 176 |
| Granozzi | G. | 16 | Izquierdo | I. | 334 |
| Grdadolnik | J. | 101 , 132 | Jadamus-Hacura | M. | 235 |
| Grodzicki | M. | 294 | Jaiswal | S. | 318 |
| Gróf | M. | 60, 62 , 63 | Jakšić | M. | 198 |
| Guczi | L. | 237 | Jamróz | M.E. | 58 |
| Guerrini | L. | 333, 334 | Jamróz | M.H. | 58, 88 |
| Gulec | A. | 263 | Jančar | B. | 161 |
| Gülseven | Y. | 94, 319, 320, 321 | Janjić | J.D. | 256 |
| Gumula | T. | 163 , 169 | Jarota | A. | 228 |
| Gunel | T. | 118 | Jastrzębski | W. | 273 |
| Gupta | S.K. | 145, 306 | Jaworski | R. | 282 |
| Gupta | V.P. | 353 | Jayne | C. | 114 |
| Gurnitskaya | E.P. | 305 | Jednačak | T. | 83 |
| Gütlich | P. | 3 | Jelic | C. | 229 |
| Győri | Z. | 203 | Jelovica Badovinac | I. | 65 |
| Habinshuti | J. | 152 | Jestin | Y. | 5 |
| Hache | F. | 341 | Jha | P.K. | 145 , 306 |
| Hacura | A. | 235 | Jimenez de Haro | M.C. | 266 |
| Hadži | D. | 132 | Jodl | H.J. | 281 |
| Hala | J. | 126 | Jovanović | B.Ž. | 256 |
| Halász | J. | 236 | Jovanovski | G. | 82, 270 |
| Hamaguchi | H. | 6 | Jović | B. | 54 |
| Hameršak | Z. | 246 | Jovtiuk | O.V. | 165 |
| Hammad | T.M. | 208 | Juraić | K. | 153 |
| Handke | M. | 192 , 193 , 275 | Jurasekova | Z. | 265 |

Juribašić	M.	66	Kucharska	E.	240
Jurić	M.	67	Kudryasheva	N.S.	106, 119
Jurkin	T.	199	Kukoč Modun	L.	241
Kaczor	A.	75, 125	Kukovec	B.-M.	59
Kaitner	B.	270	Kukovecz	Á.	142, 172, 203, 204
Kaminskii	A.A.	71	Kul	M.	331
Kamnev	A.A.	105	Kumar	M.	33
Kandemirli	F.	90	Kumar	S.	129, 289
Kantor	M.	224	Kunst	B.	344
Karachevtsev	V.	146, 171	Kurabayashi	T.	218
Karpenko	E.	171	Kürkçüoğlu	G.S.	26, 205, 209, 331
Katrusiak	A.	56	Kus	N.	69
Kavлак	İ.	26, 209	Kuznetsova	I.M.	185, 186
Kawashima	Y.	22	Kwiatek	W.M.	339
Kazancı	N.	225	L'Abbate	N.	134
Keiderling	T.A.	342	Laane	J.	27
Keça	R.	312, 315	Lacham-Kaplan	O.	114
Keresztury	G.	23, 76, 128	Lacome	N.	25
Khalavka	Yu.B.	165	Laczka	M.	53, 254
Khetselius	O.Yu.	123, 162, 288, 304, 305	Lamouroux	J.	308
Kikuchi	N.	218	Langer	K.	180
Kılıckaya	M.S.	299, 300, 319	Lasalvia	M.	134
Kin	S.	118	Lasch	P.	9
Kinowski	C.	152	Lasocha	W.	73
Kiricsi	I.	142, 172, 203	Laurent	C.	4, 158
Kirin	D.	306	Laureyns	J.	215
Kiss	J.T.	30, 133	Lebernegg	S.	294
Klein	I.	239	Ledesma	A.E.	226
Klein	O.	191, 239	Lemmetynen	H.	343
Kleinpeter	E.	24	Leopold	N.	52, 229, 252, 253
Klepac	D.	159	Lesciute	D.	51
Knežević	A.	130	Leskovac	M.	155, 189
Kocabas	I.	263	Ličina	V.	147
Koch	A.	24	Liu	X.	178
Kocot	A.	68, 131	Loboda	A.V.	305
Kojima	S.	104, 127	Łodziński	M.	278
Köksoy	B.	90	Lofrumento	C.	271
Koleva	V.	97b	Lopes	K.C.	317
Kolos	R.	88	Lopes	S.	70, 310
Kondepati	V.R.	102	López González	J.J.	226
Kónya	Z.	142, 172, 203, 204	Lopez-Ramirez	M.R.	335
Korovyanko	O.O.	165	López-Tocón	I.	309
Kos	A.	223	Lóránd	T.	128
Košćec	G.	234	Lorenc	J.	242
Kościelniak	P.	261, 307	Lukačević	I.	306
Kosović	M.	195, 206, 303	Lutz	H.D.	97b
Košutić	K.	344	Macalik	L.	71
Kowalczyk	I.	34	Maciążek-Jurczyk	M.	227, 248, 249
Kowalewska	A.	192, 193	Mączka	M.	71, 240, 242
Kožišek	J.	60, 62, 63	Madathil	S.	100
Kozma	G.	204	Mader	J.K.	102
Krehula	S.	166	Madrid	A.I.	44
Krejtšchi	C.	342	Magdas	D.A.	211, 212
Krilov	D.	195, 206, 303	Magdenovska	O.	220
Krim	L.	25	Makowski	M.	74
Kröger	S.	42	Makreski	P.	270
Król	M.	274	Maksić	Z.B.	57, 81
Kruglova	E.B.	196	Maksimov	Yu.V.	151
Krzysztofowicz	A.	345	Makulski	W.	72
Kubiak	M.	21			

Malek	K.	73, 74, 75	Mrazkova	E.	135
Malinovskaya	S.V.	123, 162, 304	Mrnka	L.	116
Manevska	V.	220	Mroginski	M-A.	289
Maniu	D.	326	Mukherjee	V.	32, 295
Mäntele	W.	111, 180, 191, 239, 245, 257	Muniz-Miranda	M.	336, 337
Mantsch	H.H.	12	Muñoz	M.A.	285, 286
Margetić	D.	243	Musić	S.	5, 130, 147, 166, 173, 174, 177, 182, 206, 234
Margheri	G.	336	Mykowska	E.	213
Marinić	Ž.	66, 243	Nagy	C.	62
Maris	A.	332	Najdoski	M.	97b
Marković	M.	244	Naumann	D.	9
Martyński	T.	213	Naumov	P.	82
Marzec	K.M.	73, 75	Neamtu	S.	231
Mašić	L.	108	Negovetić Mandić	V.	246
Matějka	P.	60, 62, 63, 116	Němec	I.	207
Maties	V.	85	Němec	P.	207
Matošević	D.	130, 246	Ng	E.	103
Maurer	J.	245	Niezborala	C.	341
Mayerhöfer	T.G.	348	Nikolić	A.	54
McCann	K.	27	Nikolić	G.S.	197
McNaughton	D.	103, 114, 346	Novak	P.	78, 83, 93
Meera	A.P.	159	Novikov	E.G.	17
Mehulić	K.	84	Nullmeier	M.	327
Meić	Z.	13, 76, 93	Nunes	C.M.	70, 310
Meljanac	D.	153	Öğretir	C.	29, 299, 300, 319, 321
Mendes	N.F.C.	271	Ogruc-Ildiz	G.	311
Mergen	O.	188	Olejniczak	Z.	53, 92
Merkel	K.	68, 131	Oncul	S.	290
Mészáros	Sz.	236	Oniga	O.	247
Mezzenga	E.	134	Önkol	T.	94, 319, 320
Michalowski	J.	169	Oppermann	U.	351
Michalska	D.	28	Oremek	G.	239
Mielke	Z.	91	Orlić	N.	65
Migdal-Mikuli	A.	64, 287	Orosz	Sz.	252
Mihaljević	B.	198	Oshtrakh	M.	17
Mihaly	J.	272, 347	Osticioli	I.	271
Mikociak	D.	167, 169	Ostrowska-Kopeć	M.	312
Mikuli	E.	64, 287	Otero	J.C.	309
Milata	V.	60, 62, 63	Ozel	A.E.	311, 313
Milder	O.B.	17	Özer	T.	331
Miljanić	S.	76	Padilla	A.	314
Minakova	E.A.	196	Palacios	O.M.	264
Minčeva-Šukarova	B.	220	Palasek	B.	242
Mink	J.	80, 124, 272, 347	Pálinkó	I.	30, 79, 80, 133
Mitić	Ž.	197	Palmer	R.	200
Mishra	S.	353	Paluszkiewicz	C.	160, 163, 167, 168, 169, 338, 339
Mitsa	V.	148	Pandurić	V.	246
Moguš-Milanković	A.	147	Parker	S.F.	272
Mohaček Grošev	V.	132	Pascuta	P.	97a, 170
Molina	M.	120	Pashynska	V.	171
Moll	M.	50	Pasquini	M.	280
Montagna	M.	5	Patonay	G.	107
Morawiec	Z.	8, 139	Pavel	I.	340
Mordechai	S.	115	Peigney	A.	158
Moroni	L.	65	Pelaez	D.	309
Moskovits	M.	340	Pentak	D.	227
Moule	D.C.	296			
Movre Šapić	I.	77, 189			
Mozgawa	W.	192, 273, 274, 275, 276			

- | | | | | | |
|-----------------|----------|----------------------|-------------------|--------|------------------------------|
| Petitprez | D. | 215 | Rada | M. | 85 |
| Peran | N. | 81 | Rada | S. | 85, 86, 97a, 170 |
| Pérez | J. | 314 | Radić | Nj. | 241 |
| Pérez-Maqueda | L.A. | 277 | Rakvin | B. | 67 |
| Perez-Rodriguez | J.L. | 266, 277 | Ramos | M.N. | 316, 317 |
| Pergolese | B. | 337 | Randić | M. | 84 |
| Perišić-Janjić | N.U. | 256 | Rankin | D.W.H. | 45 |
| PerkinElmer | | 352 | Räsänen | M. | 18 |
| Perna | G. | 134 | Rashev | S. | 296 |
| Petreska | J. | 37 | Raškovska | A. | 87 |
| Petrović | S. | 54 | Raulin | K. | 149, 150, 152 |
| Petruševski | G. | 82, 87 | Régalia-Jarlot | L. | 308 |
| Philis | J.G. | 31 | Rémiás | R. | 172 |
| Piani | G. | 280 | Ridderbusch | O. | 342 |
| Piantanida | I. | 108 | Rimetz | J. | 215 |
| Pica | M. | 97a | Rincón | M.Q. | 302 |
| Piccinini | M. | 339 | Ristić | D. | 5, 206, 210 |
| Pičuljan | K. | 78, 83 | Ristić | M. | 5, 130, 173, 182, 206 |
| Pietraperzia | G. | 280 | Ristova | M. | 87 |
| Pietraszko | A. | 28 | Robbe-Cristini | O. | 150, 152 |
| Pigliucci | A. | 343 | Robertson | H.E. | 45 |
| Pilch | M. | 307 | Rode | J.E. | 58, 88 |
| Pinho e Melo | T.M.V.D. | 70, 310 | Rodríguez-Casado | A. | 120 |
| Piotrowska | I. | 315 | Rogojerov | M. | 23 |
| Pírňau | A. | 247, 252, 253 | Rokita | M. | 137 |
| Pisanski | T. | 84 | Roldán | L. | 335 |
| Pisternik | T. | 180 | Roquero | A. | 265 |
| Placek | I. | 8 | Równicka | J. | 227, 248, 249 |
| Planinić | P. | 67 | Rozwadowski | Z. | 232 |
| Plavšić | D. | 84 | Rubčić | M. | 78 |
| Plodinec | M. | 143 | Rudbeck | M. | 289 |
| Plokhotnichenko | A. | 171 | Ruiz | T.P. | 301, 302 |
| Pluskiewicz | W. | 131 | Rusak | G. | 108 |
| Plyusnin | V.F. | 343 | Rusu | D. | 89 |
| Pohle | W. | 109, 135 | Rusu | M. | 89 |
| Pokynbroda | T. | 171 | Rusu | V.H. | 316, 317 |
| Polak | J. | 223, 224 | Ryazanova | O. | 136 |
| Polovková | J. | 60 | Sablinskas | V. | 51, 250, 251 |
| Pop | L. | 85, 157, 170 | Sadlej | J. | 88 |
| Popović | S. | 173, 174, 175 | Sagdinc | S.G. | 90 |
| Popović | Z. | 59 | Saldyka | M. | 91 |
| Popp | J. | 216, 346, 348 | Salvi | P.R. | 65 |
| Pozdnyakov | I.P. | 343 | Sánchez-Coronilla | A. | 285 |
| Požycka | J. | 248 | Sánchez-Cortés | S. | 99, 265, 333, 334, 335 |
| Praisler | M. | 268, 269 | Sánchez Jiménez | P.E. | 277 |
| Prati | C. | 328 | Şansonetti | A. | 200 |
| Premović | P. | 197 | Šarić | A. | 174 |
| Presmanes | L. | 4 | Sarlós | F. | 203 |
| Prochazka | M. | 329 | Şasiadek | W. | 240 |
| Prónayová | N. | 60 | Sato | A. | 22 |
| Proniewicz | L.M. | 73, 74, 75, 221 | Schäfer | G. | 111, 257 |
| Prskalo | K. | 130, 246 | Schettino | V. | 2 |
| Prugovečki | B. | 67 | Schiccheri | N. | 280 |
| Puchkovska | G.A. | 39 | Schlögl | R. | 260 |
| Puchkovska | G.O. | 40 | Scognamiglio | V. | 186 |
| Pucić | I. | 198, 199 | Scolaro | S. | 215 |
| Puskar | L. | 110, 346 | Semionkin | V.A. | 17 |
| Pust | S.E. | 327 | Seok | J.-K. | 107 |
| Pyrkosz | A. | 131 | Serdyukov | A. | 281 |

Seshimo	Y.	104	Strekowski	L.	107
Setnescu	R.	194	Striova	J.	200
Shastri	S.	111	Šturm	S.	161, 181
Sherin	P.S.	47, 112	Su	D.S.	178 , 260
<i>Shimadzu</i>		351	Sulkowska	A.	227, 248, 249
Siboni	F.	328	Sulkowski	W.W.	223, 224, 227, 248, 249
Sidr	İ.	94, 318, 319, 321	Sundius	T.	23, 128
Siesler	H.W.	353	Surmacki	J.	8, 139
Signorell	R.	15	Suzdalev	I.	151
Sikola	J.	350	Svoboda	A.	126
Simon	V.	121	Sytnyk	M.S.	165
Šindler-Kulyk	M.	46	Szabó	G.	203
Singh	A.K.	32	Szabó	L.	229, 247, 252 , 253
Singh	A.N.	32	Szafarska	M.	307
Singh	B.	32	Szafran	M.	34 , 55, 56, 232
Singh	N.P.	295	Szunerits	S.	327
Singh	P.	318	T addei	P.	99, 328
Singh	R.	33	Tamaian	R.	140
Singh	V.B.	32	Tanaka	Y.	22
Siskova	K.	329, 340	Tandon	P.	353
Sitarz	M.	92 , 137 , 278	Tanno	T.	218
Sizov	F.	264	Tanno	Z.	130, 246
Sizykh	A.G.	119	Taşal	E.	94 , 299, 300, 319 , 320 , 321
Škalec Šamec	D.	244	Tashkun	S.A.	308
Skoko	Ž.	147, 175	Tátrai	D.	203
Škorić	I.	46	Tazbir	M.	8, 139
Škrtić	D.	130	Temizkan	G.	118
Sladkova	M.	340	Ten	G.	184, 190
Slouf	M.	340	Terczynska	A.	254
Słowiak	R.	167	Thomas	S.	159
Smejkal	P.	329	Tinti	A.	99, 141 , 328
Smiechowski	M.	138	Tkachenko	N.	343
Smolarczyk	G.	290	Tobin	M.	110
Smrečki	V.	93	Toderas	F.	164, 179 , 326
Snytnikova	O.A.	112	Tokárová	H.	116
Sobanska	S.	215	Tolnai	B.	30
Šoptrajanov	B.	87, 97b	Tomašić	N.	267
Sottini	S.	336	Tomin	V.I.	282 , 290 , 345
Sović	D.	176	Tomkinson	K.	272
Spalletti	A.	46	Topalova	L.	255
Spirovski	F.	97b	Torreggiani	A.	99, 141
Srivastav	G.	318	Torrens	F.	201
Staiano	M.	186	Toteva	V.	255
Stangret	J.	138	Trajkovic	F.	37
Stanley	E.	103	Trettenhahn	G.	217
Stare	J.	132	Trošelj	P.	243
Stavrov	S.S.	113	Trounson	A.O.	114
Ștefănescu	I.	140	Truckhachev	S.V.	39
Stefaniak	E.A.	264	Trzińska	B.	261
Štefanić	G.	5, 175, 177	Tsentalovich	Yu.P.	112
Stefov	V.	97b	Tsybriy	Z.	264
Stella	L.	66	Tuckermann	R.	346
Stepanek	J.	329	Turan	E.	331
Stepanenko	Olesya	185	Türkeş	T.	188
Stepanenko	Olga	186	Turoverov	K.K.	185, 186
Stipetić	I.	246	Turpin	P.-Y.	329
Știufiuc	R.	52	Turrell	S.	149, 150, 152
Stodolak	E.	168, 338	Tušek-Božić	Lj.	66
Stolarski	R.	213	Tuttolomondo	M.E.	45
Strazdaite	S.	251			

Tyuterev	VI.G.	308	Zachmann	G.	350
Uspenskiy	K.E.	38, 40, 284	Žagar	K.	181
Uversky	V.N.	185	Zajac	A.	259
Užarević	K.	83	Zawisza	I.	327
Valić	S.	159	Zerulla	D.	122, 144
van Alboom	A.	279	Zhang	J.	178, 260
Van Cromphaut	C.	4	Zhou	S.X.	96
Van Grieken	R.	264	Zhou	X.	347
Vandenberghe	R.E.	4	Žic	M.	182
Varetti	E.L.	45	Zięba-Palus	J.	261, 307
Varga	R.A.	247	Zierkiewicz	W.	28
Vasilescu	M.	247	Žilić	D.	67
Vastag	Gy.Gy.	256	Zimmermann	B.	97, 176
Vauthey	E.	112, 343	Zinczuk	J.	226
Vazquez	C.	264	Ziolo	J.	68
Vedeanu	N.	211, 212	Živković	T.P.	297
Venter	M.M.	62	Zoppi	A.	271
Verhoefen	M.-K.	111	Zor	M.	331
Verkhusha	V.V.	185	Zozulya	V.	136
Vikić-Topić	D.	84, 93	Zürbig	J.	49
Vinković	M.	66	Zwielly	A.	115
Virdi	A.	35, 283			
Vlckova	B.	329, 340			
Vogel	V.	180, 245			
Vojković	V.	258			
Vojta	D.	95, 97			
Volka	K.	116			
Voloshin	I.	136			
Volovšek	V.	77, 189, 202			
von Holst	C.	214			
Vorob'ev	M.	187			
Vosátka	M.	116			
Vranić	K.	258			
Vukičević	D.	84			
Vyklický	V.	126			
Wachtveitl	J.	111			
Wagner	M.	27			
Wandas	M.	259			
Wann	D.A.	45			
Waškowska	A.	242			
Watanabe	M.	218			
Weber	I.	111			
Weibel	A.	158			
Weil	M.	20, 49			
Weselucha-Birczynska	A.	160, 339			
Wikiel	A.	72			
Wille	G.	257			
Wittstock	G.	327			
Wolarz	E.	213			
Wood	B.	103, 110, 114, 346			
Worobiec	A.	264			
Woźniakiewicz	M.	307			
Wroblewski	T.	322			
Wysokiński	R.	28			
Yadav	R.A.	33, 295, 318			
Yapar	G.	323			
Yavuz	A.E.	225			
Yurtseven	H.	324, 325			